

MULTIPLE POLLUTANT REMOVAL USING THE CONDENSING HEAT EXCHANGER

Phase I Final Report

Start Date: October, 1995

End Date: July, 1997

Issue Date: June, 1998

This report contains no trade secret information

Principal Authors

R. T. Bailey

B. J. Jankura

G. A. Kudlac

McDermott Technology, Inc.

1562 Beeson Street

Alliance, Ohio 44601

This project was sponsored by the U. S. Department of Energy,
the Ohio Coal Development Office (Department of Development, State of Ohio),
the Electric Power Research Institute, and Babcock & Wilcox

US DOE-FETC Contract:

DE-AC22-95PC95255-06

Ralph T. Bailey

OCDO Grant Agreement:

CDO/D-94-1

FAX: 330-829-7283

McDermott Technology, Inc. Contract: CRD 1337

Phone: 330-829-7353

Disclaimer

“This report was prepared as an account of work sponsored by the United States Government and the Ohio Coal Development Office (OCDO). Neither the United States, any agency thereof, the State of Ohio, any agency thereof, or Babcock & Wilcox, nor any of their employees, makes any warranty, express or implied, or assumes any legal liabilities or responsibility for the accuracy, completeness or usefulness of any information, apparatus, product, or process disclosed, or represents that its use would not infringe privately owned rights. Reference herein to any specific commercial product, process, or service, by trade name, mark, manufacturer, or otherwise, does not necessarily constitute or imply its endorsement, recommendation, or favoring by the United States, the State of Ohio, or any agency thereof. The views and opinions of authors expressed herein do not necessarily state or reflect those of the United States Government or any agency thereof.”

ABSTRACT

The Integrated Flue Gas Treatment (IFGT) system is a new concept whereby a Teflon[®] covered condensing heat exchanger is adapted to remove certain flue gas constituents, both particulate and gaseous, while recovering low level heat. The pollutant removal performance and durability of this device is the subject of a USDOE sponsored program to develop this technology. The program was conducted under contract to the United States Department of Energy's Fossil Energy Technology Center (DOE-FETC) and was supported by the Ohio Coal Development Office (OCDO) within the Ohio Department of Development, the Electric Power Research Institute's Environmental Control Technology Center (EPRI-ECTC) and Babcock and Wilcox - a McDermott Company (B&W).

This report covers the results of the first phase of this program. This Phase I project has been a two year effort. Phase I includes two experimental tasks. One task dealt principally with the pollutant removal capabilities of the IFGT at a scale of about 1.2MW_e. The other task studied the durability of the Teflon[®] covering to withstand the rigors of abrasive wear by fly ash emitted as a result of coal combustion.

The pollutant removal characteristics of the IFGT system were measured over a wide range of operating conditions. The coals tested included high, medium and low-sulfur coals. The flue gas pollutants studied included ammonia, hydrogen chloride, hydrogen fluoride, particulate, sulfur dioxide, gas phase and particle phase mercury and gas phase and particle phase trace elements. The particulate removal efficiency and size distribution was investigated. These test results demonstrated that the IFGT system is an effective device for both acid gas absorption and fine particulate collection. Although soda ash was shown to be the most effective reagent for acid gas absorption, comparative cost analyses suggested that magnesium enhanced lime was the most promising avenue for future study.

The durability of the Teflon[®] covered heat exchanger tubes was studied on a pilot-scale single-stage condensing heat exchanger (CHX[®]). This device was operated under typical coal-fired flue gas conditions on a continuous basis for a period of approximately 10 months. Data from the test indicate that virtually no decrease in Teflon[®] thickness was observed for the coating on the first two rows of heat exchanger tubes, even at high inlet particulate loadings. Evidence of wear was present only at the microscopic level, and even then was very minor in severity.

TABLE OF CONTENTS

<u>Section</u>	<u>Page</u>
Executive Summary.	vii
1.0 INTRODUCTION	1-1
1.1 Background	1-1
1.1.1 Commercial Condensing Heat Exchanger	1-1
1.1.2 Integrated Flue Gas Treatment System	1-3
1.2 Phase I Technical Program	1-3
1.3 Preliminary Economic Comparison	1-5
2.0 FACILITIES	2-1
2.1 Integrated Flue Gas Treatment System	2-1
2.2 SBS/IFGT Pilot Plant Facility	2-3
2.3 ECTC/CHX [®] Pilot Plant Facility	2-5
3.0 TEST DESCRIPTION	3-1
3.1 Pollutant Abatement	3-1
3.1.1 Acid Gas Absorption	3-2
3.1.2 Mercury and Heavy Metals Removal	3-6
3.1.3 Ammonia Removal	3-7
3.1.4 Particulate Removal	3-7
3.1.5 Heat Recovery	3-8
3.1.6 Calcium Reagents	3-8
3.1.7 Reporting Basis	3-9
3.2 Wear Assessment	3-9
3.2.1 Unit Operation	3-9
3.2.2 Inspection Measurements	3-10
4.0 RESULTS AND DISCUSSION	4-1
4.1 Heat Recovery	4-1
4.1.1 Measured Heat Recovery	4-1
4.1.2 Predictions of Heat Recovery and Gas Side Pressure Drop	4-2

TABLE OF CONTENTS (Cont'd)

<u>Section</u>	<u>Page</u>
4.2 SO ₂ Removal	4-6
4.2.1 Test Repeatability	4-6
4.2.2 Sodium Reagent Test Results	4-7
4.2.3 Lime Reagent	4-13
4.3 Chloride/Fluoride Removal	4-15
4.4 Ammonia Removal	4-18
4.5 Particulate Removal	4-21
4.5.1 Particle Removal Efficiency as a Function of Particle Size	4-22
4.5.2 Total Particle Removal	4-26
4.6 Mercury Removal	4-29
4.6.1 Measurement Methods and Detection Limits	4-29
4.6.2 Mercury Concentration in the Coal	4-30
4.6.3 Comparison of Gas Phase Mercury Speciation from Method 29 and the Ontario Hydro Method	4-30
4.6.4 Mercury Partitioning	4-32
4.6.5 Vapor Phase Mercury Removal	4-34
4.6.6 Particle Phase Mercury Removal	4-36
4.7 Trace Element Removal	4-37
4.7.1 Trace Element Measurement and Detection Limits	4-37
4.7.2 Vapor Phase Trace Element Removal	4-38
4.7.3 Particle Phase Trace Element Removal	4-39
4.8 NO _x Removal	4-42
4.9 Wear Tests at ECTC	4-43
4.9.1 Operation Summary and Discussion	4-43
4.9.2 Wear Performance Discussion	4-48

TABLE OF CONTENTS (Cont'd)

<u>Section</u>	<u>Page</u>
5.0 ECONOMIC ANALYSIS OF FGD TECHNOLOGIES	5-1
6.0 CONCLUSIONS	6-1
7.0 REFERENCES	7-1
8.0 BIBLIOGRAPHY	8-1
9.0 LIST OF ACRONYMS AND ABBREVIATIONS	9-1

LIST OF FIGURES

<u>Figure</u>	<u>Page</u>
1.1 Condensing Heat Exchanger of the CHX [®] Design	1-2
2.1 Schematic of an Integrated Flue Gas Treatment System	2-1
2.2 SBS/IFGT Pilot Plant Facility	2-4
2.3 Gas Flow Schematic of the ECTC Facility	2-5
2.4 CHX [®] Pilot Unit at the ECTC	2-6
3.1 Location of Film Thickness and Surface Replication Measurements	3-11
4.1 Components of Heat Recovery in the IFGT Process	4-2
4.2 Percent Difference Between the Measured and Predicted Heat Recovery for the Five Heat Transfer Tests	4-4
4.3 Comparison of Measured and Predicted Condensate Flow Rates	4-4
4.4 Measured and Predicted Pressure Drop Across the First Heat Exchanger Stage as a Function of Air Flow Rate	4-5
4.5 Effect of L/G at High pH	4-8
4.6 Effect of pH on SO ₂ Absorption	4-9
4.7 Effect of Load on SO ₂ Removal	4-10
4.8 Effect of Outlet Temperature on SO ₂ Removal	4-11
4.9 Effect of Inlet SO ₂ Concentration on SO ₂ Removal	4-12
4.10 Effect of Inlet SO ₂ Concentration on SO ₂ Removal at Half Load	4-13
4.11 Effect of Reagent Type on SO ₂ Removal	4-14
4.12 Fly Ash Particle Size Distribution at the IFGT Inlet for Each Coal Tested	4-22
4.13 Fly Ash Particle Size Distribution at the Inlet and Outlet of the IFGT System for Test I-14M	4-24
4.14 Particle Removal Efficiency by Particle Size for the Data in Figure 4.13	4-24

TABLE OF CONTENTS (Cont'd)

<u>LIST OF FIGURES</u>	
<u>Figure</u>	<u>Page</u>
4.15	Particle Removal Efficiency by Particle Size for All Full Load Tests 4-25
4.16	Particle Removal Efficiency by Particle Size for Partial Load Tests 4-26
4.17	Flue Gas Mercury Concentration Resulting from 100% Release of Mercury in the Coal. 4-31
4.18	Comparison of Vapor Phase Ionic Mercury Measured Using Method 29 and Ontario Hydro (OH) Sample Trains 4-31
4.19	Comparison of Vapor Phase Elemental Mercury Measured Using Method 29 and Ontario Hydro Sample Trains 4-33
4.20	Vapor Phase and Particle Phase Concentrations of Mercury in the Flue Gas 4-33
4.21	IFGT Removal Efficiency for Ionic Mercury (Left y-axis) and Ionic Mercury Concentration (Right y-axis) 4-35
4.22	IFGT Removal Efficiency for Elemental Mercury (Left y-axis) and Elemental Mercury Concentration (Right y-axis) 4-35
4.23	Removal Efficiency for Particle Phase Mercury 4-36
4.24	IFGT Removal Efficiency for Vapor Phase Arsenic (Left y-axis) and the Inlet Concentration (Right y-axis) 4-38
4.25	IFGT Removal Efficiency for Vapor Phase Selenium (Left y-axis) and the Inlet Concentration (Right y-axis) 4-39
4.26	Particle Phase Elemental Concentration at the IFGT Inlet 4-40
4.27	Particle Phase Trace Element Removal Efficiency 4-41
4.28	Ratio of Element Concentration in the Fly Ash at the IFGT Outlet to the Inlet 4-41
4.29	Measured NO _x Removal as a Function of L/G for Test Series I 4-42
4.30	P-5A Measurements of Particulate Concentration During the One Year Wear Test 4-44
4.31	Top of CHX [®] Heat Exchanger Prior to Washing 4-45
4.32	Top of CHX [®] Heat Exchanger After Washing 4-45
4.33	Fly Ash Deposits on the Tubes in the CHX [®] Heat Exchanger 4-46
4.34	Wash Water Solids Concentration 4-47
4.35	Differential Pressure Across the CHX [®] Unit as a Function of Time 4-48
4.36	Cumulative Change in Teflon [®] Film Thickness as a Function of Time for Tubes 1 through 6 4-49
4.37	Cumulative Change in Teflon [®] Film Thickness as a Function of Time for Tubes 7 through 12 4-49
4.38	Cumulative Change in Teflon [®] Film Thickness as a Function of Time and Angular Position -- Tube 1 4-50
4.39	Cumulative Change in Teflon [®] Film Thickness as a Function of Time and Angular Position -- Tube 5 4-51
4.40	Microphotograph of Clean Tube Surface 4-52
4.41	Microphotograph of Tube 1 -- End of Test 4-52
4.42	Microphotograph of Tube 6 - End of Test 4-53

TABLE OF CONTENTS (Cont'd)

<u>LIST OF TABLES</u>	
<u>Table</u>	<u>Page</u>
3.1	Coal Analyses 3-1
3.2	Test Series I Completed Test Matrix 3-3
3.3	Test Series II Completed Test Matrix 3-4
3.4	Test Series III Completed Test Series 3-5
3.5	Test Series IV Completed Test Matrix 3-6
3.6	Design Operating Conditions for the CHX [®] Pilot Unit -- One Year Wear Test 3-10
4.1	Summary Operating Conditions and Comparison to Predicted Heat Recovery for the Five Heat Transfer Tests 4-3
4.2	Repeatability of SO ₂ Removal Measurements 4-7
4.3	Vapor and Particle Phase Chloride Concentration and Removal Efficiencies 4-15
4.4	Vapor and Particle Phase Fluoride Concentration and Removal Efficiencies 4-17
4.5	Summary of Ammonia Removal Measurements 4-20
4.6	List of Cascade Impactor Tests 4-23
4.7	Overall Particulate Removal Data 4-27
4.8	Mercury Detection Limits and the Minimum Reportable Concentrations 4-29
4.9	Detection and Reporting Limits for Trace Elements 4-37
4.10	Summary of CHX [®] Operating Conditions at the ECTC 4-43
5.1	Preliminary Economic Comparison 5-4

EXECUTIVE SUMMARY

McDermott Technology Inc., Research and Development Division entered into contract with the United States Department of Energy (DOE) in September 1995 to study "Multiple Pollutant Removal Using the Condensing Heat Exchanger" under Contract DE-AC22-95PC95255. The program was conducted under contract to the United States Department of Energy's Fossil Energy Technology Center (DOE-FETC) and was supported by the Ohio Coal Development Office (OCDO) within the Ohio Department of Development, the Electric Power Research Institute's Environmental Control Technology Center (EPRI-ECTC) and Babcock and Wilcox - a McDermott Company (B&W). The guidance and support of the project managers from the sponsoring organizations, Thomas J. Feeley III of DOE-FETC, Richard Chu of the OCDO, and Gerry B. Maybach of the EPRI-ECTC, is gratefully acknowledged.

This contract includes two phases with the second phase to be proposed after completing the first phase. Phase I testing was completed at a scale of about 1.3 MW_r. By comparison, the Phase II work will be proposed at a scale of about 10 MW_r. The purpose of this report is to present the results of the Phase I tests.

The purpose of Phase I of this contract was to determine the pollutant removal performance and the anticipated wear life of an Integrated Flue Gas Treatment (IFGT) system using flue gas from coal combustion. The project was divided into four tasks. These included:

- Task 1: Project Management,
- Task 2: Pollutant Removal tests at ARC
- Task 3: Wear tests at ECTC
- Task 4: Reporting

Two topical reports have been prepared for this project. The topical reports cover Tasks 2 and 3. The Task 2 Topical Report covers the pollutant removal portion of Phase I. The Task 3 Topical Report covers the wear life segment of this Phase I. The two topical reports will be issued under separate cover. However, since these reports include details that are not present in the main body of this Final report, the technical content of the two topical reports are also included as addenda to the Final report.

In addition to these planned activities, a preliminary economic comparison was made of two versions of the IFGT system versus a conventional limestone forced oxidation scrubbing process that dominates the flue gas desulfurization market. The results of that activity are also reported here.

Integrated Flue Gas Treatment uses two Condensing Heat Exchangers (CHX[®]) to recover waste heat from the flue gas and remove a variety of pollutants from combustion flue gas. The Teflon[®] covered internals of the CHX[®] permits heat recovery at temperatures below the sulfuric acid dew point of the flue gas.

Condensing Heat Exchangers using Teflon[®] covered heat exchanger tubes are used in the industrial market to recover energy from flue gas, thereby improving the overall thermal efficiency of the combustion process. More than 110 commercial units are in service, with

operating life up to 14 years. These industrial installations have been exclusively gas and oil-fired. Prior to this work, only limited data existed on the pollutant removal efficiency of the IFGT process. Also, the effects of long-term exposure to abrasive fly ash on the integrity of the Teflon[®] covered heat exchanger tubes was unknown.

Task 2 Overview

Task 2 of this contract was conducted at McDermott Technology's Research Center in Alliance, Ohio. Flue gas was generated using a 1.75 MW_t (6 million Btu/hr) coal-fired Small Boiler Simulator (SBS) combustor. A pilot Integrated Flue Gas Treatment System rated at 1.2 MW_t (4 million Btu/hr) was located downstream of the SBS. The pollutant removal characteristics of the IFGT system were measured over a wide range of operating conditions in four series of tests. Flue gas pollutants of interest included:

- particulate
- sulfur dioxide, chlorides and fluorides
- gas phase mercury, arsenic, and selenium
- particle phase mercury and other particle phase trace elements
- ammonia

The four test series investigated pollutant removal performance using three different coals and three different sulfur scrubbing reagents. The coals tested included a high sulfur coal (Ohio), a medium sulfur coal (Pittsburgh #8) and a low sulfur coal (Powder River Basin). The first three series of tests used sodium carbonate (soda ash) as the scrubbing reagent for each of the three different coals. The fourth test used high sulfur Ohio coal with soda ash, lime and magnesium-lime as the scrubbing reagents.

Lime and magnesium-lime scrubbing reagents were investigated as possible alternatives to sodium carbonate. Soda ash is significantly more expensive than lime per pound of SO₂ removed and can pose a difficult disposal problem if not reclaimed or recycled. Limestone was not tested because a more reactive reagent is needed for the IFGT process to achieve high SO₂ removal with low liquid-to-gas ratios.

Pollutant removal efficiencies were determined by simultaneous measurements of concentration at the inlet and outlet of the IFGT system. The test program investigated the effect of various operating conditions and coal type on pollutant removal. IFGT operating conditions that were varied during the tests included:

- Reagent liquid-to-gas ratio
- Reagent pH
- Flue gas flow rate and outlet temperature
- Fly ash concentration in the flue gas

Comparison of Measured Data to Target Goals

In the Phase I Management Plan, pollutant removal goals were established for the IFGT system to provide a basis for comparison to actual measurements. The goals established in the Management Plan are presented below along with a summary of actual achievements.

SO₂ Removal

Goal	Actual (soda ash)	Actual (mag-lime)
> 95% with a liquid-to-gas ratio (L/G) < 1.34 l/m ³ (10 gal/1000 ft ³)	97% at L/G = 0.60 l/m ³ (4.5 gal/1000 ft ³)	88% at L/G = 0.88 l/m ³ (6.6 gal/1000 ft ³)

The SO₂ removal goal was easily achieved at the targeted test conditions using sodium carbonate reagent. As indicated in the table, the target SO₂ removal was also achieved at a lower L/G than originally specified. This is significant since operation at a lower L/G represents a less costly operating condition in terms of pump power and gas-side pressure drop. Using a mag/lime reagent, an SO₂ removal of 88% was achieved at a low L/G. This is sufficiently high to be considered promising. An SO₂ removal of 95% could be achieved with an increase in L/G or by allowing more time for the buildup of magnesium salts in the recirculating liquid.

Particulate Removal

Particle Size Range	Removal Efficiency Goal (%)	Actual Removal Efficiency (%) (100% Load)	Actual Removal Efficiency (%) (65% Load)
>10 μm	90%	98.7%	97.6%
5 μm to 10 μm	80%	98.8%	96.0%
2 μm to 5 μm	60%	97.1%	79.7%
< 2 μm	25%	76.4%	51.9%

The IFGT system, while not designed to be a primary particulate removal device, does provide substantial particle removal. The targeted particulate removal efficiency is based on a range of particle size, rather than an average over all particle sizes so that the comparisons are not biased by the effect of particle size distribution. At full load, the actual particle removal efficiency exceeded the goal in each of the targeted size fractions. As indicated in the table, the particle removal efficiency decreased with load, as expected, but still exceeded the targeted removal efficiencies.

Chloride and Fluoride Removal

Removal Goal	Actual
> 95% with a liquid-to-gas ratio < 1.34 l/m ³ (10 gal/1000 ft ³)	Chloride: ~98% at L/G= 0.67 l/m ³ (5 gal/1000 ft ³) Fluoride: 83%-99% at L/G = 0.67 l/m ³ (5 gal/1000 ft ³)

As was expected, the removal of chlorides and fluorides with soda ash was as great or greater than the SO₂ removal at similar operating conditions. Hydrogen chloride and hydrogen fluoride are generally more soluble in aqueous solutions than SO₂, and so are preferentially absorbed. This is in agreement with historical performance of wet scrubbers using limestone, lime, or soda ash.

Gas Phase Mercury Removal

Mercury Form	Removal Goal	Actual
Ionic	> 95% for a liquid-to-gas ratio of 1.34 l/m ³ (10 gal/1000 ft ³)	Averaged about 80%
Elemental	+50%	Averaged -23.3% with wide variations

The measured average removal efficiencies for three of four test series show that the goals for gas phase elemental and ionic mercury removal were not achieved. Ionic mercury removal averaged about 80% for the three test series. This is consistent with ionic mercury removal efficiencies measured by others.* Rather than removing any elemental mercury, these tests indicated in most cases that some of the ionic mercury was being reduced to elemental mercury in the IFGT. Whether this phenomenon is actually occurring in the IFGT is uncertain. This trend was consistent in all of the tests during which two different sampling procedures were employed. There exists some concern that this phenomenon is an artifact of the sampling techniques. Regardless, the goal for elemental mercury removal was not achieved. This indicates that the lower operating temperature does not appreciably enhance elemental mercury removal and may, in fact, enhance the reduction of oxidized mercury in the liquid phase.

* Noblett, J.G., "Control of Air Toxics from Coal-Fired Power Plants Using FGD Technology," EPRI Second International Conference on Managing Hazardous Air Pollutants, Washington, D.C., July 13-15, 1993.

Particle Phase Mercury Removal

Goal	Measured Total Particulate Removal (%)	Measured Particulate Mercury Removal (%)
Same total removal as particulate	Pitt #8 coal* : 94.9% PRB coal : 88.9% Ohio coal : 94.1%	Pitt #8 coal : 73.6 ±11.1% PRB coal : 43.8 ±28.2% Ohio coal : 80.0 ±11.0%

As indicated, the removal efficiency for particulate mercury was less than the removal efficiency for the total particulate. The reason for this anomaly is that the particulate mercury is concentrated in the smallest particles (< 2 μm), which are less effectively removed by the IFGT process than the larger particles (> 2 μm). Typically, the mercury concentration in the fly ash at the outlet of the IFGT system was 5 to 10 times greater than the concentration of mercury in the fly ash at the inlet to the IFGT.

For the tests with Pittsburgh #8 and the Ohio #6/#5 coals, the particulate mercury removal averaged about 75%, while the measured removal efficiency for particulate less than 2 micrometers was 76.4%. This indicates that essentially all of the particulate mercury may be contained in the particulate that is less than 2 micrometers.

Vapor Phase Trace Element Removal

No goal was specified for trace element removal other than for mercury, since few of these elements exist in the vapor state in significant quantities. Measurements showed significant vapor phase concentrations of arsenic and selenium for the Ohio and Pittsburgh coals. For these coals, the removal efficiency for vapor phase selenium ranged from 50% to 98%, and the arsenic removal efficiency was greater than 98%. These are significant reductions in the concentrations of these elements.

Particle Phase Trace Element Removal

A goal was not established for particle phase trace elements other than mercury, since these other elements are not at this time considered for regulation. On average, the removal of particle phase trace elements followed the same pattern as for particle phase mercury. The trace elements were concentrated in the fine particulate, and the total particle phase element removal averaged about 80%.

Ammonia and Oxides of Nitrogen Removal

A goal was not established for ammonia (NH₃) and nitrogen oxides (NO_x) removal. For ammonia, the objectives were to evaluate the potential of operating an IFGT in conjunction with an SCR or SNCR system to achieve higher NO_x removal rates by addressing the problem of

* Pitt #8 = Pittsburgh #8; PRB = Powder River Basin; Ohio = 80% Ohio #6 and 20% Ohio #5

ammonia slip. Therefore, tests were conducted to measure ammonia removal through the IFGT system, and estimate the amount of ammonia that reacts with SO₃ before the IFGT system. The inlet ammonia concentration ranged from 31 ppm to 94 ppm and removal efficiency ranged from 57% to 93%. All ammonia tests were conducted at full load. The amount of ammonia that reacts with SO₃ before the IFGT system was estimated by comparing the measured and calculated ammonia concentration at the IFGT inlet based on the ammonia injection rate. The ammonia reduction attributable to ammonia-sulfur reactions ranged from 27% to 45%, and averaged 36%.

The absorption of NO_x as expected, was not significant. The initial measurements of NO_x at the inlet and outlet of the IFGT indicated that NO_x removals were too small to quantify.

Task 3 Overview

Task 3 of this contract was conducted at the Electric Power Research Institute's (EPRI) Environmental Control Technology Center (ECTC) near Barker, New York. A single-stage CHX[®] unit was installed downstream of the ECTC electrostatic precipitator. The unit was operated as a heat recovery unit to determine the effects of long-term exposure to fly ash under typical flue gas conditions.

Standard operating parameters (flue gas flows and temperatures, cooling water temperatures, etc.) were monitored and recorded by the ECTC data acquisition system over the course of the program. In addition, periodic visual inspections and Teflon[®] film thickness measurements were performed to determine the amount of wear. Finally, replications of the Teflon[®] film surface were made to both document the general physical condition of the Teflon[®] surface and allow for detection of wear at the microscopic level. Surface replications are made by moistening a strip of cellulosic film in acetone, laying the strip on the tube surface, and allowing to dry. The physical characteristics of the tube surface are thus exactly duplicated on the cellulosic film.

The wear test unit was operated for over 6,200 hours during the test program. A summary of the operating conditions is shown in the table below.

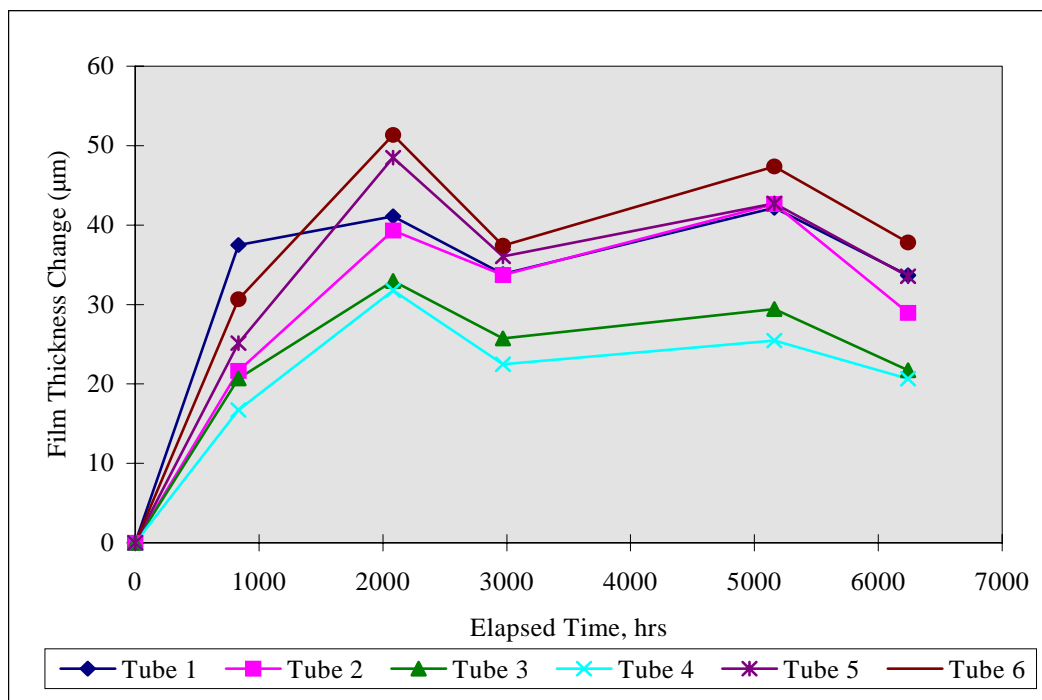
Summary of CHX[®] Operating Conditions at the ECTC

Time of Operation	6,240 hours
Inlet Gas Flow	1,275 scmh (750 scfm)
Inlet Gas Temperature	150°C (300°F)
Inlet Water Temperature	55 to 60°C (130 to 140°F)
Outlet Gas Temperature	82 to 93°C (180 to 200°F)
Outlet Water Temperature	76 to 80°C (170 to 175°F)
Inlet Particulate Loading (average)	25 mg/dscm (0.02 lb/10 ⁶ Btu) 2,060 hours 400 mg/dscm (0.35 lb/10 ⁶ Btu) 4,180 hours
Tube Wash Cycle	20 minutes every 8 hours

Five inspection trips were made over the course of the test program. During each trip, visual inspections, Teflon[®] thickness measurements and surface replications were performed.

No visible signs of wear were evident over the course of the test program. Minor amounts of fly ash deposition, not removed by the normal wash cycle, were detected after 5,000 hours of operation. These deposits were located several rows down from the top of the tube manifold and were attributed to inadequate wash water flow rates. A new wash nozzle manifold (3 nozzles vs. 1 nozzle) was installed following the 5,000 hour inspection. The end of test inspection revealed virtually no ash deposition.

Data from the Teflon[®] thickness measurements indicated no significant decrease in the tube film thickness. Measurements were made at several locations on each of the tubes in the top two rows of the tube bank. Over the course of the test program, the Teflon[®] film thickness increased approximately 7-10% (30.5 to 50.8 μm [0.0012 to 0.002 inch] of a nominal 508 μm [0.020 inch] film) after roughly 2,000 hours of operation then showed no subsequent signs of decrease. This initial thickness increase has been attributed to a relaxation of surface stresses in the Teflon[®]. These surface stresses are a result of the manufacturing process, and stress relaxation occurs when the Teflon[®] film is heated. A graphical summary of the Teflon[®] thickness measurements is given for the first row of tube in the figure below.



Cumulative Change in Teflon[®] Film Thickness as a Function of Time for Tubes 1 through 6

Evaluation of the film surface replications revealed no significant wear damage to the Teflon[®] covering. Very minor wear damage was visible on tube 6, which was subject to the highest flue gas flow rate. This damage, however, was on the μm scale and is of the same magnitude as the

surface striations created during manufacture and should pose no problems for extended operation.

Preliminary Comparative Economic Analysis

A comparative economic analysis was performed of the IFGT system against the conventional limestone forced oxidation (LSFO) system. Two versions of the IFGT system were considered. The first employed soda ash as the reagent and the second used magnesium promoted lime. The analysis was based on a plant life of 30 years, a 70% load factor and a capital levelization factor of 15.2%. The analysis was based on a plant size of 100 MW_e. The comparative annualized costs are presented here as follows:

Limestone Forced Oxidation:	\$3,620,000
Soda Ash based IFGT:	\$3,635,000
Mg Lime based IFGT:	\$2,689,000

While the comparative costs of the soda ash based IFGT are essentially equivalent to the conventional LSFO system, the mag-lime based IFGT compares very favorably. This economic advantage, though based on many assumptions and of a very preliminary nature, offers sufficient advantage to warrant further detailed study.

Conclusions

Task 2

The Task 2 goals for the project were met or exceeded in all cases except for vapor phase mercury removal. The goals for mercury removal were based, in part, on the relatively high gas-liquid contact area of the condensing heat exchanger, the high reactivity of the sodium reagent, and the relatively lower operating temperature of the IFGT process compared with other flue gas clean-up technologies. That this goal - for vapor phase mercury removal - was not realized indicates that temperature and surface area by themselves will not provide reductions in elemental mercury at typical flue gas concentrations. Other methods of promoting elemental mercury capture were beyond the scope of work for this project.

The Task 2 results show that the IFGT process is an effective multiple pollutant removal system that can also provide an improvement in thermal efficiency. The data measured in this Task provides the basis for predictions of the performance of an IFGT system for both utility and industrial applications. This data is needed to provide performance guarantees as well as to evaluate the economic cost and benefit of an IFGT system.

Task 3

Based on the operational and inspection data collected over the course of the test program, the following conclusions are drawn:

- No significant wear was observed for any of the Teflon[®] tube coverings. Minor microscopic wear detected on some tubes is insignificant and should pose no problems for extended operation.
- Particulate deposition can be a problem, especially at higher particulate loadings and insufficient wash water flows. Increasing the wash water flow rate by modifying the wash nozzle manifold essentially eliminated particulate deposition.
- Teflon[®] life expectancy should be greater than 10 years. Tube replacement will more likely be required due to operational problems other than abrasive wear.

Economic Comparison

The IFGT system offers sufficient economic advantage to warrant further experimental and engineering study, especially with respect to the mag-lime based system.

1.0 INTRODUCTION

1.1 Background

The 1990 Clean Air Act Amendments address the need to reduce the quantity of pollutants released to the atmosphere. Some pollutants are currently regulated and additional species are targeted for control in the near future. The emission of SO₂ and particulate from electric utilities is currently regulated under the Phase I and Phase II requirements defined in Title IV. An additional 189 substances, classified as hazardous air pollutants, have been identified for regulation under Title III of the Clean Air Act Amendments. The Title III requirements will be imposed across approximately 750 source categories. Cluster rules are also being established to set emission standards for specific industries. Many state and local agencies are already imposing stringent regulations on hazardous pollutants, such as mercury. There is a need for equipment to remove the pollutants of concern in a cost-effective manner. Most of the commercial pollutant removal equipment suffers from three major drawbacks:

- 1) Commercially available pollution removal equipment is parasitic, that is, they consume energy during operation. A typical coal-fired power plant will have a 2-4% or more reduction in power generation capacity when commercial SO₂ and particulate removal equipment is added for gas clean up.
- 2) Commercially available flue gas clean up equipment generally treats only one pollutant at a time. Separate units are installed for each pollutant to be removed.
- 3) Most of the commercial flue gas clean up equipment used in the electric utility industry cannot be economically scaled down for industrial coal-fired applications. Capital cost and operating cost of these units are often prohibitive for the smaller energy producer.

1.1.1 Commercial Condensing Heat Exchanger

An untapped source of energy from coal-fired units is the waste heat in the flue gas released to the stack. The efficiency of a boiler can be significantly increased by decreasing the flue gas exit temperature. One means of lowering the exit temperature is to use a condensing heat exchanger to recover both sensible and latent heat from the flue gas. Condensing Heat Exchangers (CHX[®]) using Teflon[®]-covered internals are widely used to recover waste heat from flue gases. The Teflon[®] covering protects the heat exchanger components from corrosion as the temperature of the flue gas drops below the acid dew point. The most common applications to date, are boilers firing oil or natural gas. Single-stage commercial condensing heat exchangers have provided satisfactory performance and lifetimes for more than one hundred industrial installations for the past fourteen years.

Commercial condensing heat exchangers remove both sensible and latent heat from the flue gas in a single unit. Figure 1.1 is a drawing of a typical condensing heat exchanger application. It shows the heat exchanger along with the support equipment provided for a retrofit application.

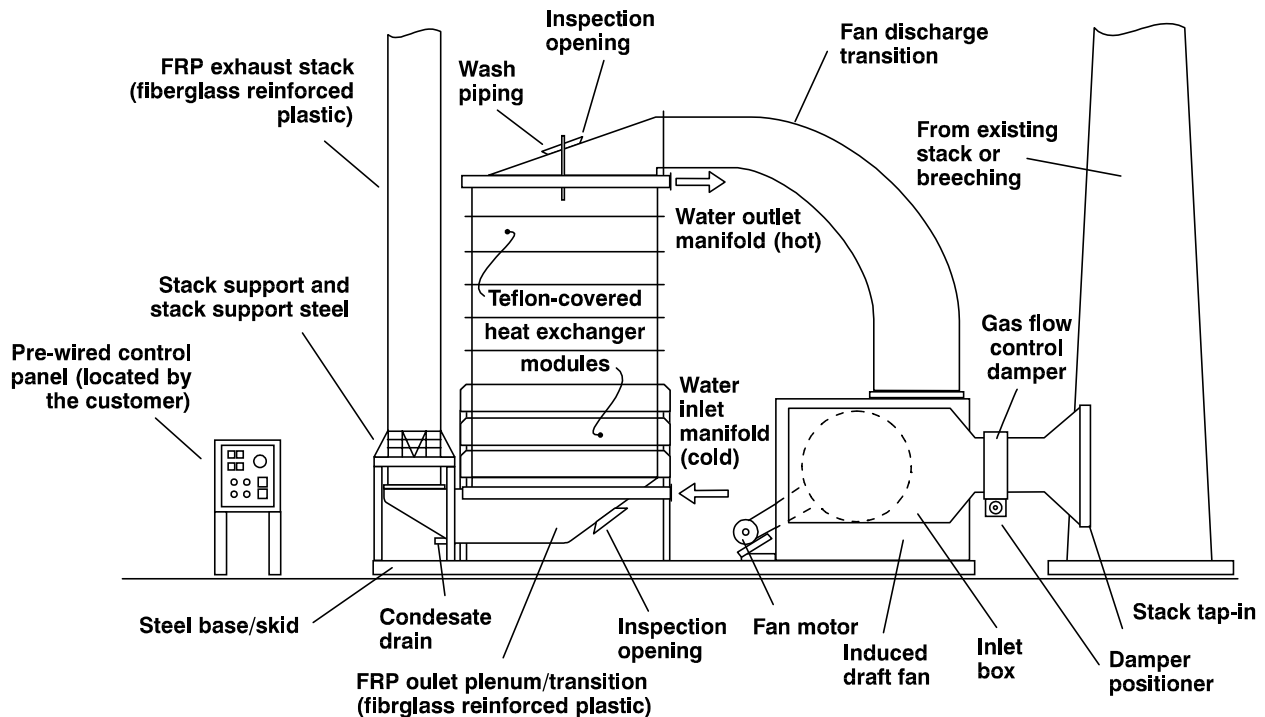


Figure 1.1 Condensing Heat Exchanger of the CHX[®] Design

The flue gas passes down through the heat exchanger while the water passes upward in a serpentine path through the tubes. Condensation occurs within the heat exchanger as the gas temperature at the tube surface is brought below the dew point. The condensate falls as a constant rain over the tube array and is drained at the bottom. Some cleaning of the gas can occur within the heat exchanger as the particulate impact the tubes and acid gas condensation occurs.

Commercial designs are optimized for removing heat and ensuring adequate lifetime of the unit. Heat exchanger tubes are made of Alloy 706 (10% nickel and 90% copper), a material commonly used in boiler water applications. Each tube is covered with Teflon[®] extruded over the outside of the tube. Since Teflon[®] is hydrophobic, condensation on the surface of the tube occurs in drops rather than in a film. This allows continuous exposure of most of the surface and improves heat transfer.

Teflon[®] is also durable and resistant to abrasion by solid particles in the gas. Fly ash will not stick to the Teflon[®] tubes. The inside surfaces of the heat exchanger shell are covered with Teflon[®] sheets. During fabrication, the Teflon[®]-covered tubes are pushed through the Teflon[®] tube sheet lining to form a Teflon[®]/Teflon[®] seal, ensuring that all heat exchanger surfaces exposed to the flue gas are protected against acid corrosion. Interconnections between the heat exchanger tubes are made outside the tube sheet and are not exposed to the corrosive flue gas stream.

A commercial condensing heat exchanger is made up of heat exchanger modules that can be stacked in series in the gas stream. This modular design allows the size of the unit to be optimized for each application at minimum cost. To ensure the lifetime of the Teflon[®] covering

on the tubes, the inlet gas temperature is limited to 260°C (500°F), a condition easily satisfied in most flue gas waste heat recovery applications.

1.1.2 Integrated Flue Gas Treatment System

A recent innovation to the commercial condensing heat exchanger design, called the Integrated Flue Gas Treatment (IFGT) system, exhibits improved pollutant removal from the flue gas while recovering waste heat. The IFGT system is a two-stage condensing heat exchanger. Most of the sensible heat is removed from the gas in the first heat exchanger stage. The second heat exchanger stage can be operated in a condensing mode, recovering latent heat from the gas while removing pollutants. The top of the second heat exchanger stage is equipped with an alkali reagent spray system to enhance SO₂ and particulate removal. Pollutant removal mechanisms in the IFGT include condensing (for water, some organic compounds, and some acid gases and trace metals), impaction (for particulate), and gas absorption (for removal of SO₂ and other acid gases). In an IFGT, several pollutants are treated using a single device - while recovering waste heat. Because of its modular design, it can be easily built for a wide range of applications. An additional benefit realized by using the IFGT system is the proportional reduction in carbon dioxide released per MW of generated electricity because of the increase in plant efficiency.

The IFGT condensing heat exchanger is expected to effectively remove air toxics still present in the flue gas that penetrate upstream pollution removal devices (i.e., baghouse or electrostatic precipitator). The vapor phase air toxics that routinely pass through these removal devices include mercury, selenium and arsenic. Low temperature operation and gas-liquid contact inherent to the IFGT promotes the removal of air toxics in the gas phase and present on the fine particulate.

It has been proposed to use an IFGT system downstream of a selective catalytic reduction (SCR) or selective non-catalytic reduction (SNCR) unit to remove the remaining ammonia in the flue gas. SCR and SNCR devices utilize the injection of ammonia into the flue gas upstream of the SCR/SNCR zones. The ammonia is the reducing agent. Invariably, excess ammonia is injected. The excess that remains in the flue gas is referred to as ammonia slip. NO_x removal can be increased by increasing the ammonia injected into the flue gas, but because of ammonia slip, local atmospheric emission limits may be exceeded for ammonia. By capturing the excess ammonia in the IFGT, higher concentrations of ammonia can be injected upstream of the SCR thereby increasing NO_x removal without increasing ammonia emissions to the atmosphere.

1.2 Phase I Technical Program

In the Phase I Proposal, two primary technical issues were identified that needed to be resolved to bring the IFGT Process to commercial practice for coal-fired applications;

- 1) The pollutant removal performance of the IFGT system, and
- 2) The expected lifetime for the Teflon[®]-covered tubes that comprise the heat exchanger surface when exposed to flue gas containing fly ash from coal combustion.

Item 1 has been addressed in Phase I and is reported in the Task 2 Topical Report for this project. The Task 2 Topical Report provides the results of pollutant removal tests conducted at McDermott Technology Inc.'s, Alliance Research Center. Task 2 investigated the removal performance of the IFGT process for a variety of flue gas pollutants. These included SO₂, NO_x, particulate, mercury and other trace elements, chloride and fluoride compounds, and ammonia.

Four series of tests (series I through IV) were conducted using four coals and three reagents. The coals included two blends of Ohio #5 and Ohio #6 coals, a Powder River Basin coal, and a Pittsburgh #8 coal. The different coals were selected to represent high, medium, and low sulfur content and also represent several different classifications of coal used by the utility industry. The Pittsburgh coal was selected for its sulfur content and also because this coal is used at the Kintigh Station, the site of the Environmental Control Technology Center (ECTC) and the planned location for Phase II testing.

The reagents tested included sodium carbonate, lime and magnesium enhanced lime (mag-lime*). The IFGT process was originally designed for the industrial market, and the sodium-based reagent provided a highly reactive reagent that required a minimum of preparation before use. For utility applications, sodium reagents are costly and represent a significant disposal problem if not reclaimed or recycled. Although sodium-based regenerable scrubbing systems have been used in the utility industry (Wellman Lord and dual alkali systems) they are not widely accepted. Lime and magnesium-lime reagents are typically less reactive than sodium, but are less costly and pose a much simpler disposal problem.

The goal of Task 2 was to determine the pollutant removal efficiencies of the IFGT process and the functional dependence on process parameters so that reliable predictions of performance can be made for commercial coal-fired applications.

The Task 3 Topical Report deals primarily with erosive wear. One of the major questions that must be addressed before the IFGT can be considered viable for coal-fired applications is the expected material lifetime for the Teflon[®] covering on the tubes. Commercial condensing heat exchangers with Teflon[®]-covered parts have exhibited lifetimes of over 14 years, but these have been clean fuel (oil or natural gas) applications. Tests on coal-fired units have been limited in duration.

To address the material lifetime issue for coal-fired applications, a long-term wear test was included in Phase I of this project as Task 3 -- "Long-Term Wear Testing". The specific goal of this task is to determine the amount of wear, if any, on the Teflon[®]-covered internals of the heat exchanger. The location of maximum material wear in an IFGT will be at the inlet of the first heat exchanger stage. This is where the flue gas and Teflon[®] coverings are the hottest, the flue gas velocity and particulate loading the highest, and where the particulates first impact the Teflon[®]-covered tubes. It is expected that the top rows of tubes in an IFGT will experience the maximum wear due to fly ash abrasion. A single-stage condensing heat exchanger unit was used for the material lifetime demonstration since the inlet conditions will be the same as for an IFGT.

* Mag lime is a physical mixture of magnesium oxide and calcium oxide. It is typically manufactured from Dolomite. The MgO is usually less than 6% by weight of the total.

Visual and physical examinations were performed on the top rows of tubes at periodic intervals during the one-year demonstration.

1.3 Preliminary Economic Comparison

To provide guidance for the continued development of the IFGT system, an economic comparison was made with the base technology used in the Flue Gas Desulfurization (FGD) industry on utility scale boilers. That base technology is "Limestone Forced Oxidation Wet Scrubbing (LSFO)". The comparative cost analysis was performed by the B&W Company, the Company's manufacturer of LSFO systems. The cost comparison was made with two versions of the IFGT system. The first uses soda ash and the second uses mag-lime. The results of this analysis are presented here as part of the section titled Results and Discussion.

2.0 FACILITIES

2.1 Integrated Flue Gas Treatment System

The IFGT condensing heat exchanger, shown schematically in Figure 2.1 is designed to enhance the removal of pollutants from the flue gas stream. The IFGT design uses many of the same heat exchanger components found in the commercial CHX[®] design, so unit lifetimes are expected to be comparable to current commercial units. The pilot facility at B&W's Alliance Research Center is essentially full scale in the vertical direction, with a stack of seven heat exchanger modules in the first stage and a stack of eight modules in the second heat exchanger stage. The cross-sectional area of the heat exchanger shell is 0.3 m by 0.46 m (1 ft. X 1.5 ft).

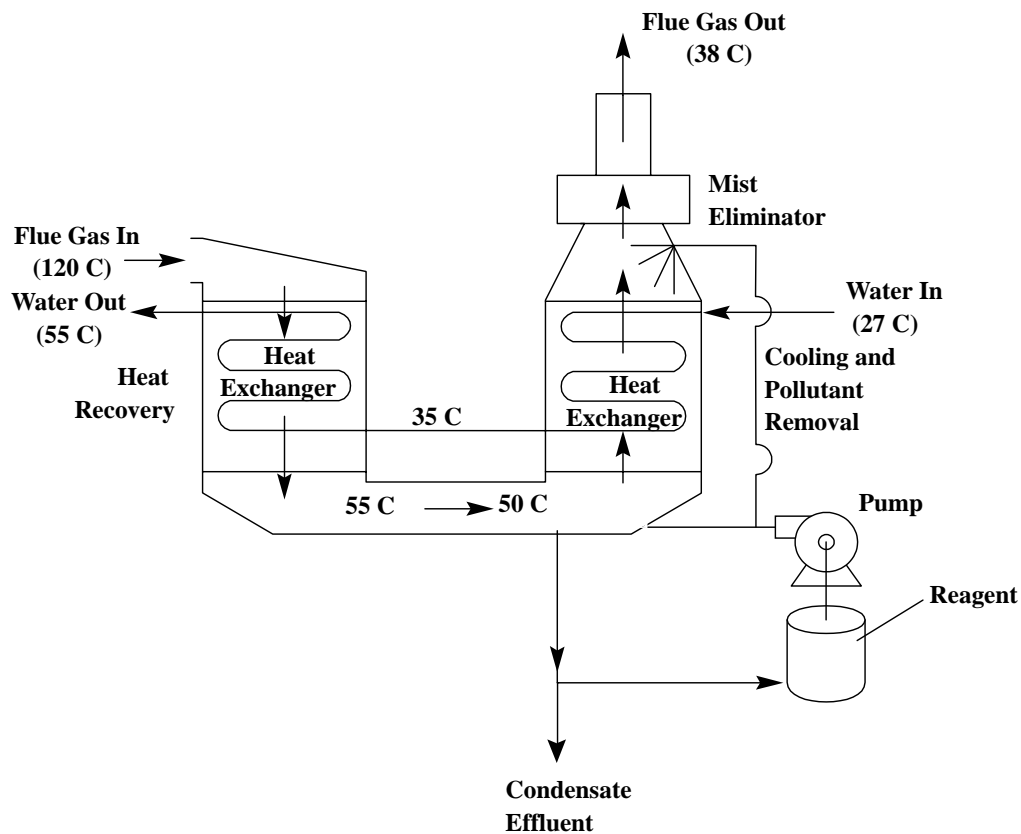


Figure 2.1 Schematic of an Integrated Flue Gas Treatment System

The IFGT system consists of four sections: the first heat exchanger stage, the interstage transition region, the second heat exchanger stage, and the mist eliminator. The major differences between the integrated flue gas treatment design and the conventional condensing heat exchanger design are:

- 1) the integrated flue gas treatment design uses two heat exchanger stages instead of one,
- 2) the interstage transition region, located between the two heat exchanger stages, is used to direct the gas to the second heat exchanger stage, acts as a collection tank, and allows treatment of the gas between the stages,
- 3) the gas flow in the second heat exchanger stage is upward, rather than downward,
- 4) the top of the second heat exchanger stage is equipped with an alkali reagent spray system, and
- 5) the mist eliminator is used to remove any alkali spray and condensed droplets from the flue gas.

Most of the sensible heat is removed from the gas in the first heat exchanger stage of an IFGT system. The transition region can be equipped with water or alkali sprays to saturate the flue gas with moisture and assist removal of pollutants and particulate from the gas. The inter-stage transition piece is made of corrosion resistant fiberglass-reinforced plastic. Usually, the second heat exchanger stage is operated in the condensing mode, removing latent heat from the gas along with pollutants. The gas in this module flows upward and countercurrent to the liquid. This provides a scrubbing mechanism that enhances particulate impaction and gas absorption. The dimensions and spacings of the heat exchanger tubes ensures that the particulate impact wet tubes where droplet condensation is taking place. Sub-micron size particles act as condensation sites in the gas. This enhances collection by impaction. These small particles also come into contact with the wetted tubes by Brownian diffusion.

The mechanisms described above primarily address the removals of particulate and condensable vapors. Additional flue gas processing is still needed, however, to provide adequate removal of SO₂ from the flue gas. To achieve this, the top of the second heat exchanger module is equipped with an alkaline spray system. The condensed gases, particulate, and alkaline spray are collected at the bottom of the transition section. The condensate from the flue gas provides a portion of the water requirements for the spray system. In some applications, all of the water requirements can be met with condensate, thereby reducing or eliminating fresh water demands. This improves the attractiveness of the process by reducing the fresh water requirements. A condensate/reagent blow down stream is used to maintain the process chemistry.

The spray/disengagement region consists of three plastic sections installed above the second heat exchanger stage. Each section is about 0.46 m (1.5 ft) in height. The three plastic sections contain the second-stage reagent spray nozzles and two sets of chevron style mist eliminators. They also provide a disengagement zone for liquid drops entrained in the flue gas as it exits the second heat exchanger stage. The mist eliminators are designed to capture any droplets entrained by the flue gas as it passes upwards through the counter flowing liquid.

An alkali reagent tank is used to mix fresh reagent with the recirculating solution/slurry. For example, sodium carbonate is added to the solution in the tank with a pH controlled variable speed screw feeder. A mixer stirs the solution in the tank to dissolve the sodium carbonate. The scrubbing solution and condensate collected at the bottom of the interstage transition during operation is gravity fed to the reagent tank. As originally constructed, and during initial testing, the reagent tank was equipped with an overflow drain to remove accumulated water and dissolved solids inventory due to condensation, makeup water addition, and the accumulated reaction products. To improve reagent utilization, the overflow connection was later moved - after Test Series I - to the reagent return line from the interstage transition.

The scrubbing solution can be directed to the top of the second stage heat exchanger or to the transition section. The fiberglass interstage transition located between the two heat exchanger stages is equipped with six spray nozzles.

2.2 SBS/IFGT Pilot Plant Facility

Flue gas for the pollutant removal test was provided by a pilot scale furnace designated as the Small Boiler Simulator (SBS). This 1.75 MW_t (six million Btu/hr) combustion research facility includes fuel preparation and handling equipment, a furnace and convection pass that provided a typical flue gas time-temperature history, a heat exchanger, dry scrubber module and a bag house. Figure 2.2 shows an isometric view of the major components of the SBS facility and how they are connected to the pilot IFGT condensing heat exchanger. The IFGT facility is in a bypass loop downstream of the SBS induced draft fan.

The coal burner used for these tests is a low NO_x burner equipped with dual air zones. The same burner with the same nominal air register settings was used for all of the test coals. Although designed as a Low NO_x burner, it was not operated as such during these tests. NO_x concentrations typically ranged from 300 ppm to 400 ppm. The furnace load was set to provide the required flue gas flow rate and was essentially constant at 1.3 MW_t (4.4 million Btu/hr) for all tests.

The heat exchanger downstream of the SBS convection pass is a two-pass shell and tube construction with cooling water in the shell and flue gas passing through the tubes. The heat exchanger is used to reduce the flue gas temperature at the outlet of the SBS convection pass from a temperature of about 370°C (700°F) to a temperature of about 150°C (300°F). The 150°C flue gas temperature is an upper limit for the bag house, and is also the typical operating temperature of the dry scrubber when in service.

The SBS bag house typically removes 99.9+% of the particulate from the flue gas leaving the furnace. For these tests a measurable particle loading at the IFGT unit was needed to characterize the particle removal efficiency of the IFGT system. To provide a measurable particle loading at the CHX[®] facility, approximately 10% to 20% of the flue gas from the SBS

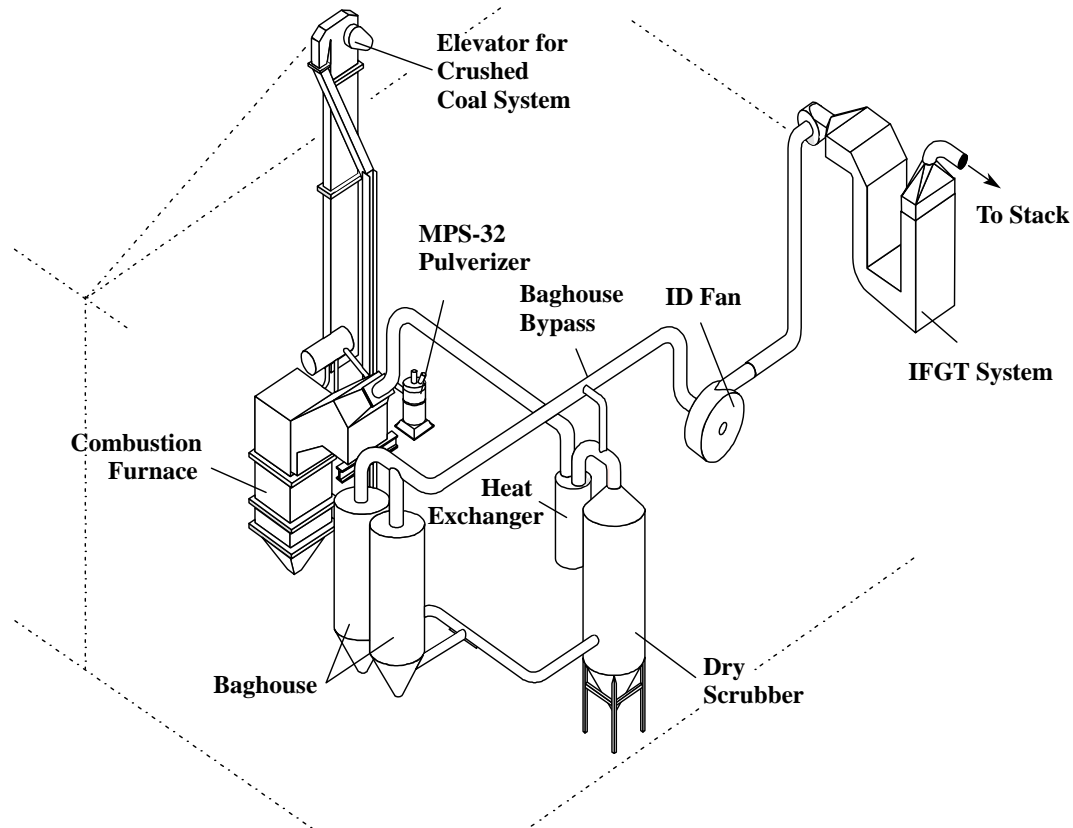


Figure 2.2 SBS/IFGT Pilot Plant Facility

furnace was bypassed around the bag house. The dry scrubber module was not used for these tests, but provided the gas path from the heat exchanger to the bag house. Heat loss and air infiltration downstream of the bag house limited the flue gas temperature at the inlet of the IFGT system to about 120°C (250°F).

Flue work brings the exhaust gas from the SBS to the pilot IFGT. The 305 mm (12 inch) insulated flue is tied into the exhaust of the SBS downstream of the baghouse and I.D. fan. The flue gas enters at the top of the first heat exchanger stage and exits out the top of the second heat exchanger stage. A 305 mm non-insulated PVC flue is installed at the exit of the pilot IFGT to an exhaust stack placed outside the building.

Gas sampling lines and 102 mm (4 inch) ports for in-situ sampling are located at the inlet and outlet of the IFGT facility. The heated gas sample lines provide a continuous flow of flue gas for the on-line gas analyzers. One gas sample line is in the inlet duct just upstream of the first heat exchanger stage. The other gas sample line is in the PVC outlet duct. Heat-traced lines are used to transport the flue gas samples from the ducts to the gas analyzers. Two 102 mm (4-inch) ports are installed both in the inlet and in the outlet flue gas ducts for particulate sampling and other gas sampling as required by the test program.

The facility is equipped with instrumentation to measure the flow rate and temperatures of the IFGT process streams, including the flue gas, cooling water, reagent flow rate to the nozzles, blowdown stream and make up water.

2.3 ECTC/CHX[®] Pilot Plant Facility

The Environmental Control Technology Center (ECTC) was used to provide the flue gas to the wear test CHX[®] unit for this test program. The ECTC is a comprehensive test facility for evaluating advanced emissions control technologies applied to high sulfur coals. The test facility utilizes about one percent of the flue gas available from the 662 MW Kintigh Station, a pulverized coal boiler operated by the New York State Electric and Gas Corporation (NYSEG) near Barker, New York.

A flow schematic of the ECTC facility is shown in Figure 2.3. The facility is operated 24 hours a day, allowing long-term continuous tests to be performed. The pilot CHX[®] unit was installed in

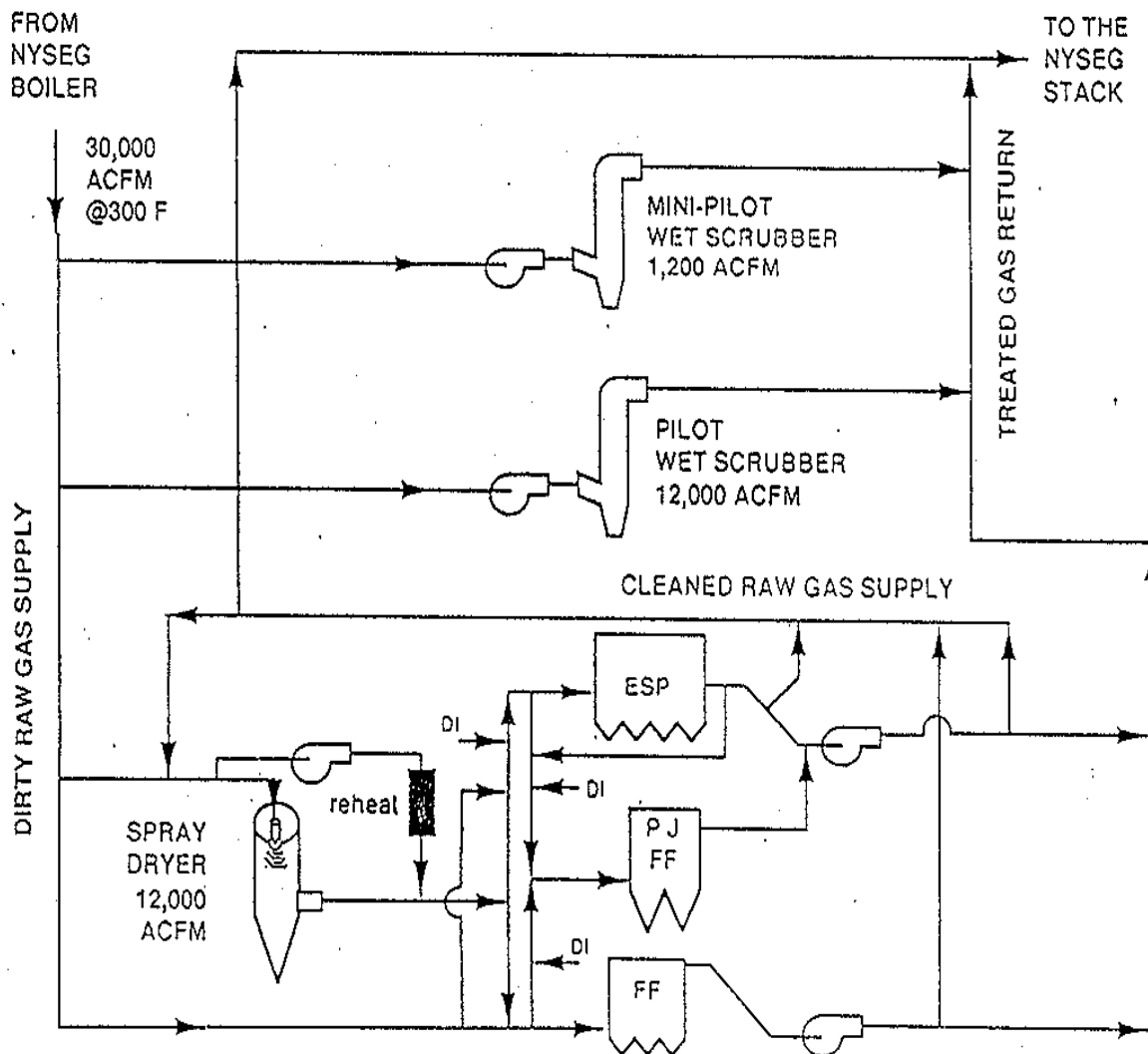


Figure 2.3 Gas Flow Schematic of the ECTC Facility

the mini-pilot wet scrubber sub-loop of the ECTC. This loop has a flue gas flow capacity of 2040-2550 acmh (1200-1500 acfm), sufficient to provide the "design" flue gas velocity of 12.2 m/sec (40 ft/sec) between the tubes at the inlet of the heat exchanger. To reproduce expected commercial conditions, the unit used a slipstream from the flue gas after it exits the electrostatic precipitator (ESP). The pilot CHX[®] test unit was located downstream of the ESP in place of the mini-pilot wet scrubber.

The CHX[®] unit used for the wear test is a skid-mounted, single-stage unit as shown in Figure 2.4. In addition to the heat exchanger, the unit is also equipped with a flue gas inlet control damper, water pump, and water circulation tank. The internal dimensions of the heat exchanger are 30.87 cm by 36.51 cm (12 5/32 inches by 14 3/8 inches). There are six heat exchanger tubes in each

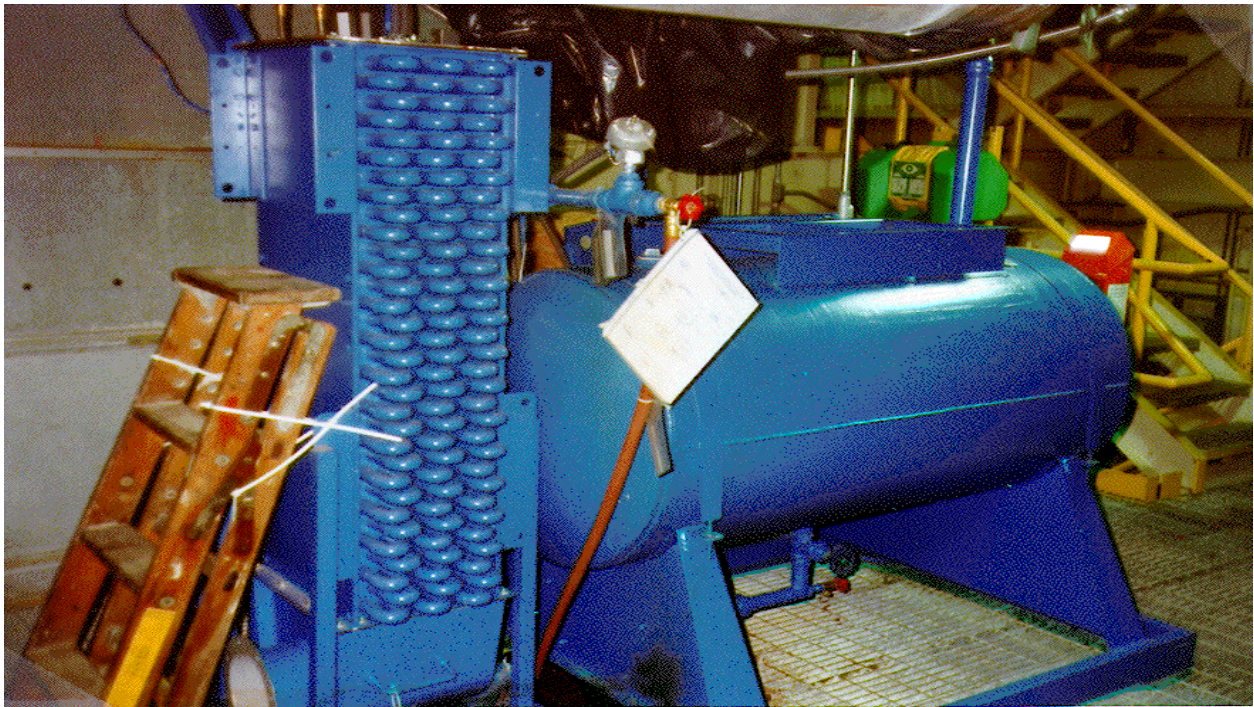


Figure 2.4 CHX[®] Pilot Unit at the ECTC

row and 32 rows of tubes. The heat exchanger tube rows are staggered from each other (triangular pitch) so that there is no open line of sight from the top to the bottom of the heat exchanger. The CHX[®] pilot test unit heat exchanger is operated with countercurrent flow, with the flue gas entering the top of the heat exchanger and exiting at the bottom, and the cooling water entering the bottom row of tubes and exiting the top row. The flue gas inlet plenum is removable, allowing access to the top of the heat exchanger for inspection of the Teflon[®] film on the top rows of tubes.

Data from the CHX[®] pilot test unit and ECTC equipment was collected and recorded by the ECTC data acquisition system. In addition, ECTC personnel maintained an hourly log of the major test parameters, including gas and water flows and temperatures, and ESP operating conditions.

3.0 TEST DESCRIPTION

3.1 Pollutant Abatement

The experimental test program completed for the SBS/IFGT facilities was designed to investigate the effect of the primary system operating parameters on pollutant removal and is discussed below. The SBS/IFGT facilities were operated from 5 to 12 days on each coal to characterize the performance of the IFGT system. Four coals were tested. These coals are described in Table 3.1. The Pittsburgh #8 coal was also used at the ECTC for the wear tests. Tests using that coal will provide a link to the 5.0 MW IFGT tests at the ECTC scheduled for Phase II.

Table 3.1 Coal Analyses

Coal		80% Ohio #5 20% Ohio #6 Test Series I	Pittsburgh # 8 Test Series II	Powder River Basin Test Series III	80% Ohio #6 20% Ohio #5 Test Series IV
C	% by wt.	69.15	75.08	58.74	75.58
H ₂	% by wt.	5.03	5.09	4.05	5.24
S	% by wt.	3.85	2.58	0.44	3.07
O ₂	% by wt.	7.01	5.45	14.48	8.79
N ₂	% by wt.	1.37	1.5	0.96	1.41
H ₂ O	% by wt.	6.93	0.92	15.12	2.83
Ash	% by wt.	6.66	9.38	6.21	5.08
Heating Value - wet basis (Btu/lb)		12538	13438	10049	13320
Arsenic	ppm _m	12.43	7.92	1.59	7.47
Barium	ppm _m	3.24	25.26	493.50	3.85
Beryllium	ppm _m	0.15	0.63	0.11	0.83
Cadmium	ppm _m	0.70	0.05	0.09	0.19
Cobalt	ppm _m	0.78	0.91	1.43	0.53
Chromium	ppm _m	46.58	0.34	9.26	1.23
Manganese	ppm _m	15.75	9.29	28.20	6.19
Nickel	ppm _m	22.11	18.93	13.14	42.70
Lead	ppm _m	5.71	2.58	3.05	6.01
Selenium	ppm _m	1.56	1.17	0.12	1.90
Mercury	ppm _m	0.43	0.10	0.41	0.13
Chlorides	ppm _m	2200	123	134	1900
Fluorides	ppm _m	25.8	<11	46	25.6

Tables 3.2 through 3.5 summarize the completed test matrix for test series I, II, III, and IV. Each matrix is grouped according to the different types of pollutant removal under study. The first three test series evaluated removal efficiencies for various gas phase, and particulate phase species with different coals and soda ash. The fourth test series evaluated the ability of the soda ash, lime and mag-lime to capture SO_2 , mercury, and heavy metals, and investigated the use of mesh pads for providing fine particulate control. The HCl and HF measurements conducted in test series IV repeated measurements that were made earlier in the program and showed relatively poor HCl removal efficiencies compared to all other test data. Mesh pads were also used in test series IV for assisting fine (submicron) particulate removal. The mesh pads were positioned in the interstage of the IFGT system. Particle loading and size distribution measurements were made at the inlet and outlet of the IFGT system.

During each test series, several large samples of blowdown waste water were collected in 35 gallon drums. This condensate waste will be used to evaluate disposal methods in Phase II of the program. Additionally, smaller samples of the blowdown were collected to determine the chemistry of the waste water and to test for mercury, particulate, and other heavy metals.

3.1.1 Acid Gas Absorption

In these tests, SO_2 and NO_x removal, and HCl and HF removal were evaluated. SO_2 , HCl, and HF removal was evaluated during all four test series. Numerous tests were conducted on each coal so that sufficient data was collected to determine the removal characteristics of the IFGT for these gas phase pollutants.

At high pH with Na_2CO_3 , or $\text{Ca}(\text{OH})_2$, the rate controlling resistance to mass transfer of SO_2 is from the gas phase to the liquid surface. Above a pH of about 6.5, the vapor pressure of SO_2 in the liquid is negligible. Under these conditions, the major factors for SO_2 removal performance are the amount of gas-liquid surface area in the 2nd stage of the IFGT and flue gas velocity. When the pH of the absorbing solution falls below about 6.5, the liquid phase SO_2 vapor pressure increases which contributes to a measurable reduction in the absorption of SO_2 . To investigate these effects, the test matrix included conditions at a variety of pH, flue gas inlet velocity, and liquid-to gas ratio (L/G). The SO_2 tests were conducted with continuous gas concentration monitors at the IFGT inlet and outlet. Therefore, the test durations were relatively short. Once the inlet and outlet SO_2 levels stabilized, approximately 10 to 20 minutes was required to collect operating data from the Data Acquisition System and other instruments, and to collect process stream samples.

The absorption of NO_x occurs by mechanisms similar to SO_2 . However, approximately 95% of NO_x is in the form of NO with the remaining being principally NO_2 . The solubility of NO is less SO_2 by a factor of about 1300. As will be described later, NO_x absorption proved at the outset of testing to be negligible and testing for NO_x absorption was curtailed for subsequent tests.

The test matrix for each test series included one test to investigate HCl and HF removal. The HCl and HF removal efficiency was quantified across the IFGT utilizing EPA methods and required approximately two hours to complete a single test.

Table 3.2 Test Series I Completed Test Matrix.

Test ID	pH	Flue Gas Outlet Temperature (°C)	Flue Gas Inlet Velocity (m/s)	Stage 2 L/G Ratio (l/m ³)	Particulate Loading (mg/dscm)	IFGT Inlet NH3 Concentration (ppm _v)	Stage 2 Steam Injection (kg/hr)
---------	----	----------------------------------	-------------------------------	---------------------------------------	-------------------------------	--	---------------------------------

SO₂ and NO_x Removal and Heat Recovery

1	8	Dewpoint	12	0.07	<14 to 420
2	8	Dewpoint	12	0.13	<14 to 420
3	8	Dewpoint	12	0.27	<14 to 420
4	8	Dewpoint	12	0.67	<14 to 420
5	8	Dewpoint	12	1.07	<14 to 420
7	8	Dewpoint	6	2.14	<14 to 420
8	8	Dewpoint	6	0.27	<14 to 420
9	8	Dewpoint	6	0.67	<14 to 420
10	8	Dewpoint	6	1.07	<14 to 420
11	8	Dewpoint - 11	12	0.07	<14 to 420
12	8	Dewpoint - 11	12	0.13	<14 to 420
13	8	Dewpoint - 11	12	0.27	<14 to 420
14	8	Dewpoint - 11	12	0.67	<14 to 420
15	8	Dewpoint - 11	12	1.07	<14 to 420
16	7	Dewpoint	12	0.07	<14 to 420
17	7	Dewpoint	12	0.27	<14 to 420
18	7	Dewpoint	12	1.07	<14 to 420
19	6	Dewpoint	6	0.07	<14 to 420
20	6	Dewpoint	6	0.27	<14 to 420
21	6	Dewpoint	6	1.07	<14 to 420
22	7	Dewpoint - 11	6	1.88	<14 to 420
23	7	Dewpoint - 11	6	1.34	<14 to 420
24	7	Dewpoint - 11	6	0.40	<14 to 420
25	7	Dewpoint - 11	6	0.67	<14 to 420
26	7	Dewpoint - 11	6	1.07	<14 to 420

HCl and HF Removal

4A	8	Dewpoint	12	0.67	420
----	---	----------	----	------	-----

Hg and Heavy Metals Metals Removal

4B	8	Dewpoint	12	0.67	420
4C	8	Dewpoint	12	0.67	<14
14D	8	Dewpoint - 11	6	0.67	420

Ammonia Removal

4	8	Dewpoint	12	0.67	420	50
4F	8	Dewpoint	12	0.67	420	10
14G	8	Dewpoint - 11	12	0.67	420	50

Particulate Removal

4J	8	Dewpoint	12	0.67	0.3	----	45.3
----	---	----------	----	------	-----	------	------

Particulate Removal - Cascade Impactor

4L	8	Dewpoint	12	0.67	0.3	----	0
14M	8	Dewpoint - 11	12	0.67	0.3	----	0
4N	8	Dewpoint	12	0.67	0.3	----	45.3

Table 3.3 Test Series II Completed Test Matrix

Test ID	pH	Flue Gas Outlet Temperature (°C)	Flue Gas Inlet Velocity (m/s)	Stage 2 L/G Ratio (l/m ³)	Particulate Loading (mg/dscm)	IFGT Inlet NH ₃ Concentration (ppm _v)
---------	----	----------------------------------	-------------------------------	---------------------------------------	-------------------------------	--

SO₂ Removal and Heat Recovery

1	8	Dewpoint	12	0.07	<14 to 28
2	8	Dewpoint	12	0.13	<14 to 28
3	8	Dewpoint	12	0.27	<14 to 28
4	8	Dewpoint	12	0.67	<14 to 28
5	8	Dewpoint	12	1.07	<14 to 28
6	8	Dewpoint	6	0.27	<14 to 28
7	8	Dewpoint	6	0.67	<14 to 28
8	8	Dewpoint	6	1.07	<14 to 28
9	6	Dewpoint	12	0.07	<14 to 28
10	6	Dewpoint	12	0.27	<14 to 28
11	6	Dewpoint	12	0.67	<14 to 28
12	7	Dewpoint	12	0.07	<14 to 28
13	7	Dewpoint	12	0.27	<14 to 28
14	7	Dewpoint	12	0.67	<14 to 28
16	6	Dewpoint	6	0.67	<14 to 28
17	6	Dewpoint	6	0.27	<14 to 28
18	6	Dewpoint	6	1.07	<14 to 28
19	6	Dewpoint	6	0.80	<14 to 28
20	7	Dewpoint	6	0.27	<14 to 28
21	7	Dewpoint	6	0.67	<14 to 28
22	7	Dewpoint	6	1.07	<14 to 28
23	7	Dewpoint - 11	6	0.47	<14 to 28
24	7	Dewpoint - 11	6	1.27	<14 to 28
25	7	Dewpoint - 11	6	0.27	<14 to 28
26	7	Dewpoint - 11	6	0.67	<14 to 28
27	7	Dewpoint - 11	6	1.07	<14 to 28

HCl and HF Removal

4B	8	Dewpoint	12	0.67	<14 to 28
----	---	----------	----	------	-----------

Hg and Heavy Metals Metals Removal

4A	8	Dewpoint	12	0.67	<14 to 28
4C	8	Dewpoint	12	0.67	42 to 420

Ammonia Removal

4D	8	Dewpoint	12	0.67	<14 to 28	50
4E	8	Dewpoint	12	0.67	<14 to 28	20
4F	8	Dewpoint - 11	12	0.67	<14 to 28	50

Particulate Removal

4F	8	Dewpoint - 11	12	0.67	<14 to 28	50
----	---	---------------	----	------	-----------	----

Particulate Removal - Cascade Impactor

4G	8	Dewpoint	12	0.67	42 to 420	----
----	---	----------	----	------	-----------	------

Table 3.4 Test Series III Completed Test Series

Test ID	pH	Flue Gas Outlet Temperature (°C)	Flue Gas Inlet Velocity (m/s)	Stage 2 L/G Ratio (l/m ³)	Particulate Loading (mg/dscm)	IFGT Inlet NH3 Concentration (ppm _v)
---------	----	----------------------------------	-------------------------------	---------------------------------------	-------------------------------	--

SO₂ Removal and Heat Recovery

1	NC	Dewpoint	12	0.00	420 to 830
2	NC	Dewpoint	12	0.40	420 to 830
3	4	Dewpoint	12	0.40	420 to 830
4	4	Dewpoint	12	0.20	420 to 830
5	5	Dewpoint	12	0.40	420 to 830
6	5	Dewpoint	12	0.20	420 to 830
7	6.5	Dewpoint	12	0.40	420 to 830
8	6.5	Dewpoint	12	0.20	420 to 830
9	8	Dewpoint	12	0.40	420 to 830
10	8	Dewpoint	12	0.20	420 to 830
11	8	Dewpoint	6	0.80	420 to 830
12	8	Dewpoint	6	0.40	420 to 830
13	5	Dewpoint	6	0.80	420 to 830
14	6.5	Dewpoint	6	0.40	420 to 830
15	nc	Dewpoint - 11	12	0.40	420 to 830
16	6.5	Dewpoint - 11	12	0.40	420 to 830
17	6.5	Dewpoint - 11	12	0.20	420 to 830
15R	NC	Dewpoint - 11	12	0.20	420 to 830

HCl and HF Removal

7A	6.5	Dewpoint	12	0.40	420 to 830
----	-----	----------	----	------	------------

Hg and Heavy Metals Metals Removal (See Note 1)

9A	8	Dewpoint	12	0.40	420 to 830
12A	8	Dewpoint	6	0.40	420 to 830

Ammonia Removal

7B	6.5	Dewpoint	12	0.40	420 to 830	20
9B	8	Dewpoint	12	0.40	420 to 830	50
18	8	Dewpoint - 11	12	0.40	420 to 830	50

Particulate Removal

9B	8	Dewpoint	12	0.40	420 to 830	20
12C	8	Dewpoint	6	0.40	420 to 830	----

Particulate Removal - Cascade Impactor

12B	8	Dewpoint	6	0.40	420 to 830	----
12D	8	Dewpoint	6	0.40	420 to 830	----

Table 3.5 Test Series IV Completed Test Matrix

Test ID	Feed pH	Return pH	Flue Gas Outlet Temperature (°C)	Flue Gas Inlet Velocity (m/s)	Stage 2 L/G Ratio (l/m ³)	Particulate Loading (mg/dscm)	Reagent	Mesh Pad
---------	---------	-----------	----------------------------------	-------------------------------	---------------------------------------	-------------------------------	---------	----------

SO₂ Removal and Heat Recovery

1	8	--	Dewpoint	12	0.53	420 to 830	Sodium Carbonate	
2	8	--	Dewpoint	6	0.53	420 to 830	Sodium Carbonate	
3	8	--	Dewpoint	12	0.80	420 to 830	Hydrated Lime	
4	10	--	Dewpoint	12	1.07	420 to 830	Hydrated Lime	
5	10	--	Dewpoint	12	0.53	420 to 830	Hydrated Lime	
6	8	--	Dewpoint	12	0.53	420 to 830	Hydrated Lime	
7	8	--	Dewpoint	12	1.07	420 to 830	Hydrated Lime	
8	6	--	Dewpoint	12	0.80	420 to 830	Hydrated Lime	
9	6	--	Dewpoint	12	0.53	420 to 830	Hydrated Lime	
10	6	--	Dewpoint	12	1.07	420 to 830	Hydrated Lime	
12	--	8	Dewpoint	12	0.13	420 to 830	Mag-Hydrated Lime	
13	--	8	Dewpoint	12	0.27	420 to 830	Mag-Hydrated Lime	
14	--	7	Dewpoint	12	0.53	420 to 830	Mag-Hydrated Lime	
14R1	--	6	Dewpoint	12	0.53	420 to 830	Mag-Hydrated Lime	
15	--	7	Dewpoint	12	1.07	420 to 830	Mag-Hydrated Lime	
16	--	6	Dewpoint	12	0.27	420 to 830	Mag-Hydrated Lime	

HCl and HF Removal

1A	8	--	Dewpoint	40	0.53	420 to 830	Sodium Carbonate	
----	---	----	----------	----	------	------------	------------------	--

Hg and Heavy Metals Removal

14A	8	7	Dewpoint	12	0.53	420 to 830	Mag-Hydrated Lime	
-----	---	---	----------	----	------	------------	-------------------	--

Particulate Removal

2A	8	--	Dewpoint	6	0.53	420 to 830	Sodium Carbonate	None
----	---	----	----------	---	------	------------	------------------	------

Particulate Removal - Cascade Impactor

1B	8	--	Dewpoint	12	0.53	420 to 830	Sodium Carbonate	Interstage
2B	8	--	Dewpoint	6	0.53	420 to 830	Sodium Carbonate	None

3.1.2 Mercury and Heavy Metals Removal

The ability of the IFGT to remove mercury and heavy metals from the flue gas and the fate of the mercury was also determined. A total of eight test conditions were completed. Mercury speciation measurements were conducted at both the inlet and outlet of the IFGT to quantify total, elemental, and oxidized mercury removal for each of the coals evaluated. Quantifying the individual specie is important since each species has different chemical and physical properties. The main forms of mercury emitted in flue gas are elemental (Hg⁰) and oxidized (Hg⁺⁺). Previous SBS measurements indicate that the total mercury emissions were within the expected range of 1-10 µg/m³ (0.7 to 7 lb/trillion Btu) for coal-fired boilers.

Mercury species are removed from the flue gas by either condensation of Hg⁰ or absorption of Hg⁺⁺ into the liquid. Condensation of Hg⁰ is usually not complete as the trace metal

concentration is relatively low. However, this test series was based on the hope that the lower outlet flue gas temperature of the IFGT (35°C, 90°F) compared to a commercial wet scrubber (50°C, 122°F) may provide for higher levels of elemental mercury condensation.

Mercury concentration measurements were conducted on the following process streams:

- coal feed
- IFGT inlet and outlet gas flows and particulate
- IFGT condensate/blowdown
- baghouse ash

Under steady-state operating condition, measurements were conducted in triplicate for all eight test conditions to determine the repeatability of the data. Each test required approximately two hours of sample time. Blanks were also run in order to assess the uncertainty in the measurements and to detect unknown sources of contamination.

3.1.3 Ammonia Removal

During ammonia removal tests ammonia was injected upstream of the IFGT system at a constant measured flow rate. Below 230°C (450°F) ammonia reacts with sulfur trioxide (SO₃) in the flue gas, so that some of the ammonia may be removed from the flue gas upstream of the IFGT. Ammonia removal tests were conducted only during the first three test series. A matrix of 3 tests was completed during each test phase for a total of nine tests. For all of these tests, removal efficiency was based on measurements at the inlet and outlet of the IFGT. A Severn Sciences continuous ammonia analyzer was used to sequentially measure the ammonia concentration upstream and downstream of the IFGT. Differences between the measured and calculated concentration based on the injection rate of ammonia at the IFGT inlet were used as a measure of the ammonia-sulfur reactions.

3.1.4 Particulate Removal

These tests determined the overall particulate removal efficiency of the IFGT facility and the removal efficiency as a function of particle size. The particulate loading to the IFGT facility consisted of the fugitive emissions from the SBS baghouse, and a portion of the flue gas from the SBS that was diverted around the baghouse and fed directly to the IFGT. Approximately 20% of the flue gas bypassed the SBS baghouse.

A total of eight cascade impactor tests were completed to measure the particulate size distribution. Andersen Mark III cascade plate impactors were utilized for all particulate sizing tests. Additional total particulate measurements were obtained as part of the sampling for mercury and acid gases. For those measurements, the sampling technique requires collection of particulate as well as the gas sample. Thirty-one total particulate concentration measurements were completed.

The effect of steam injection on particulate removal was investigated in this test program. It has been postulated that the addition of steam to flue gas can enhance the removal of fine particulate. Supersaturating the flue gas causes condensation to occur on particulate, resulting in particle

growth. As the smaller submicron size particles increase in diameter they may become easier to remove from the flue gas stream. Saturated plant steam was injected between the first and second stage of the IFGT and particulate loading measurements were conducted at the inlet and outlet to the IFGT.

The effect of mesh pads on particulate removal was investigated. Several layers of mesh pads were placed in the horizontal transition just before entering the second stage. The particulate removal efficiency was measured by cascade impactor tests at the 1st stage inlet and outlet. Mesh pads provide a target surface for impaction of fine particulate that passes through the first stage.

3.1.5 Heat Recovery

The heat recovery provided by the IFGT was an integral part of the standard data acquisition, and was recorded continuously for all of the tests. In addition to this standard data, the following tests were conducted to investigate specific heat transfer mechanisms.

- *Onset of 1st Stage Condensation* - For this test, cooling water passed only through the 1st stage heat exchanger. The cooling water flow rate was increased until condensate initially formed on the tubes. The data was compared to heat transfer models to better understand the conditions that initiate condensation.
- *Onset of 1st Stage Measurable Condensate Flow* - This was an extension of the previous test, where the cooling water flow rate is sufficient to produce a continuous flow of condensate that can be collected and weighed. The data was compared to heat transfer models to better understand the conditions that initiate condensation.

3.1.6 Calcium Reagents

After a preliminary analysis of the data collected through the third test phase, the database for a sodium carbonate reagent was deemed sufficient to meet the project goals and objectives. The remaining tests conditions for the fourth test phase were modified to include reagents other than sodium carbonate.

Effective reagents for the fourth test series must supply a source of alkalinity in the liquid phase that can then readily react with the SO₂ absorbed from the flue gas. The dissolved alkalinity produced by the reagent defines the SO₂ absorption capacity of the liquor, and includes all dissolved species more alkaline than the bisulfite ion (HSO₃⁻). Flue Gas Desulfurization (FGD) systems have primarily relied on highly soluble reagents containing sodium carbonate and slurry reagents containing calcium hydroxide and magnesium hydroxide, or calcium carbonate that slowly dissolve into alkaline anions. The two additional reagents selected for the fourth test series derive their alkalinity from calcium and magnesium hydroxide compounds. The first reagent, calcium hydroxide is widely used in commercial FGD systems and dissolves into highly alkaline hydroxide (OH⁻) anions. The second reagent, magnesium promoted calcium hydroxide is also widely used in commercial FGD systems and in addition to (OH⁻) anions also produces high dissolved concentrations of alkaline sulfite (SO₃⁼) anions. The SO₂ removal performance of the these reagents was expected to be sufficient enough to justify their use in commercial

applications. The calcium hydroxide reagent was expected to have lower SO₂ removal capabilities as the reagent does not produce as high dissolved alkalinity as sodium carbonate or magnesium promoted calcium hydroxide.

3.1.7 Reporting Basis

The concentration of compounds, elements, and particulate in the flue gas are on a dry basis, corrected to 3% excess oxygen. The units used in this report are micrograms per dry standard cubic meter (µg/dscm),* milligrams per dry standard cubic meter (mg/dscm), and parts per million on a volume basis (ppm_v). The concentration of compounds and elements in the solid phase are reported as parts per million on a mass basis (ppm_m).

3.2 Wear Assessment

3.2.1 Unit Operation

The ECTC pilot facility and the pilot condensing heat exchanger were operated so that the wear test was conducted under conditions representative of commercial operation at the flue gas inlet of an IFGT condensing heat exchanger. Specifically, this required:

- A flue gas with a representative particulate loading, temperature, and flow for a commercial coal-fired application. For example, the inlet particulate loading was to be maintained at 34 mg/dscm (0.03 lbs/10⁶ Btu) or greater during the test period.
- Controlling the temperature and flow rate of the cooling water for the condensing heat exchanger to provide the Teflon[®] film temperature expected at the flue gas inlet of a full-scale IFGT unit.
- Operation of the CHX[®] unit on a continuous basis, whenever possible, to maximize the Teflon[®] exposure to flue gas.

The design operating conditions used as a basis for operation of the CHX[®] pilot unit are shown in Table 3.6. All major operating parameters were monitored by ECTC personnel (and recorded by the ECTC data acquisition system) to ensure that the CHX[®] test unit was operating within the desired conditions.

To achieve the desired particulate loading at the inlet to the condensing heat exchanger, the test unit was located downstream of the ECTC ESP. An opacity meter was used to monitor the flue gas particulate loading downstream of the ESP. In addition to the opacity meter, an Environmental Systems P-5A *in-situ* particulate monitor was used as a qualitative indicator for the particulate loading level to aid ECTC personnel in maintaining a steady particulate loading. Finally, EPA Method 5 particulate loading measurements were made at various times during the test to confirm the opacity readings and the particulate loading to the unit.

* Standard conditions are 20 C and 1 atm.

Table 3.6 Design Operating Conditions for the CHX[®] Pilot Unit -- One Year Wear Test

Parameter	Nominal Value	Range
Inlet Flue Gas Temperature	160 °C (320 °F)	+/- 17 °C (30 °F)
Outlet Water Temperature	77 °C (170 °F)	+/- 11 °C (20 °F)
Cooling Water Supply	11.4 lpm {3.0 gpm (est.)}	---
Flue Gas Velocity, between tubes	12.2 m/sec (40 ft/sec)	+/- 1.5 m/sec (5 ft/sec)
Inlet Flue Gas Flow	1,275 scmh (750 scfm)	+85 -0 scmh (+50 -0 scfm)
Inlet Particulate Loading	representative of poor to good particulate cleanup from a commercial cleanup device.	34 to 340 mg/dscm (0.03 to 0.30 lbs/10 ⁶ Btu)

3.2.2 Inspection Measurements

In order to determine the amount of wear, if any, on the Teflon[®] covered internals of the heat exchanger, and specifically the tubes, three types of measurements, in addition to a visual inspection, were performed during each of the five inspection trips conducted during the course of the test program. These measurements included:

- Vertical and horizontal tube dimensions
- Eddy current Teflon[®] film thickness determination
- Teflon[®] film surface replications

A fourth type of surface measurement utilizing a surface profilometer, which was originally specified as a test program measurement, was not used due to damage to the Teflon[®] film caused by the profilometer probe during use.

Each measurement was performed at several locations on the top two rows of tubes. A graphical representation of the measurement locations is shown in Figure 3.1. Tubes 1 through 6 are located in the top row of the heat exchanger and tubes 7 through 12 in the second row. Flue gas flow with respect to the diagram is from the left and then into the page. Each of the dimensional measurements (horizontal, vertical, and film thickness) were performed in triplicate at each location and the values averaged. These location values were then averaged to obtain an average tube value. Single surface replications were made at each of the indicated locations. Three replications were performed on tube 6 since the greatest potential for abrasive wear was expected on this tube. Descriptive summaries of each of the three measurement techniques may be found in the following paragraphs:

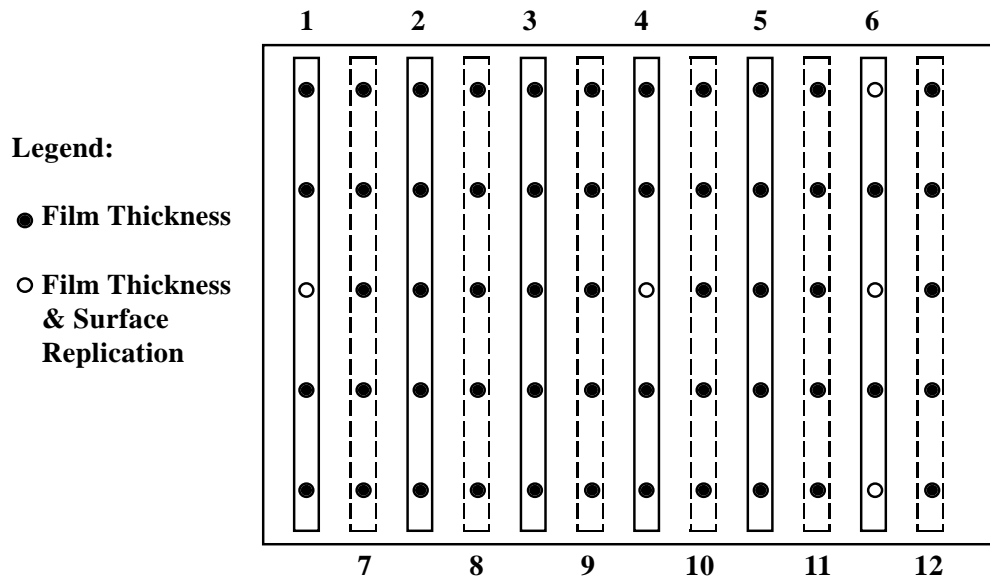


Figure 3.1 Location of Film Thickness and Surface Replication Measurements

Tube Dimensions: Micrometers were used to measure the top-to-bottom and side-to-side dimensions of the top row of tubes at each of the locations shown in Figure 3.1 (locations labeled "Film Thickness" on tubes 1 through 6). A digital caliper micrometer was used for the horizontal diameter measurements and a standard micrometer was used for the vertical diameter measurements. The overall accuracy of the horizontal diameter measurement was $25.4\ \mu\text{m}$ (0.001 inches) and the overall accuracy of the vertical diameter measurement was $12.7\ \mu\text{m}$ (0.0005 inches). After two sets of dimensional measurements were obtained, it was discovered that the Teflon[®] tube surfaces were being damaged by the micrometers. This was most likely due to the tight tube spacing, which complicated the insertion and removal of the calipers. Evaluation of the two sets of measurements indicated that any change in film thickness would be more evident from the eddy current measurements, so this procedure was dropped from subsequent inspection trips.

Film Thickness: An Elcometer 300 Coating Thickness Gage, which uses an eddy current measurement principle, was used to make the film thickness measurements. The instrument has a range of 25.4 to $1,016\ \mu\text{m}$ {0.001 to 0.040 inches (1 to 40 mils)} and an accuracy of $\pm 1\%$ of its reading. Teflon[®] thickness measurements were made for the top surface of the first and second row of heat exchanger tubes. Thickness measurements were also made at specified angles from vertical ($0 + 45$ and $0 - 45$ degrees) for the top row of tubes. In relation to the diagram in Figure 3.1, "vertical" may be thought of as a line coming straight out of the paper, "+45" angled towards tube 1 and "-45" angled towards tube 6. Thickness measurements could not be made for these angles for the second row of tubes because of the staggered array (overlap of the tubes for adjacent rows) of the tubes. Measurements were made at the locations indicated in Figure 3.1. As mentioned above, these measurements were made in triplicate at each location and angle and then averaged. These location average values were then averaged for each tube to obtain a tube average. Each data set was then normalized based on 1) the calibration data for that particular set, and 2) the film thickness data from a "reference" tube measured at the same time using the same calibration as the inspection.

Surface Roughness: A cellulosic film surface replication technique was used to obtain a physical replicate of the Teflon[®] tube surfaces. The goal of making the surface replications was to record and observe any microscopic changes to the Teflon[®] tube surface. The replications were made during each inspection trip at the locations indicated in Figure 3.1. After cleaning the Teflon[®] tube surfaces, a strip of cellulosic film tape was moistened with acetone and laid on the surface of the tube. Upon drying, the tape was lifted from the tube and mounted on a glass slide, replicate side up. This procedure was then repeated for the remaining sample locations. The tapes were then viewed under a microscope and photographed at magnifications of 25X and 200X for comparison with the replications made prior to exposing the heat exchanger to flue gas.

4.0 RESULTS AND DISCUSSION

4.1 Heat Recovery

One principal benefit of the IFGT process compared with other gas clean up technologies is the capability to recover waste heat from the flue gas. The heat recovery capability can be a substantial benefit provided there is a use for the recovered heat. The quantity of heat that can be recovered from the flue gas is dependent on several factors including the temperature of the flue gas, the sink temperature for the cooling water, and the flue gas water vapor dew point. In an open cycle industrial system the heat recovery can amount to 10% to 12% of the furnace heat release.

For coal combustion, the flue gas dew point is typically about 38°C (100°F), which is substantially less than for oil and gas combustion. In addition, the sink temperature at electric utility generating plants that use a closed steam cycle is typically higher than the sink temperature associated with open cycle processes. The combination of low dew point temperature and high sink temperature reduces the quantity of heat than can be recovered, but this heat can still have a significant impact on the cost of operation.

4.1.1 Measured Heat Recovery

Temperatures and flows of cooling water and flue gas were monitored continuously during these tests, primarily as a means to control the operating conditions of the IFGT. The flue gas inlet temperature was maintained at 120°C (250°F) for all tests. Flue gas outlet temperature was maintained either at the water vapor dew point, or 8°C to 12°C (14°F to 22°F) below the dew point. The 120°C inlet temperature is lower than the 150°C (300°F) that is typical of the inlet temperature to most flue gas desulfurization systems. At the ARC pilot IFGT, the baghouse is limited to a 150°C temperature, and heat loss and air infiltration reduces the temperature to well below 150°C. A 120°C inlet temperature was selected because it was quickly attainable at startup, and could be controlled regardless of the gas flow or ambient conditions.

Since the water and gas-side temperatures and flows were nearly the same for all tests, the heat recovery (as a percentage of furnace heat release) was also nearly the same. Figure 4.1 shows the components of heat recovery expressed as a percentage of the furnace heat release for an outlet flue gas temperature at the dew point (Test I-5) and 10°C (18°F) below the dew point (Test I-14D). For a condensing mode of operation, the heat recovery is equally split between the first and second heat exchanger stages, and the latent heat recovery (2%) accounts for about 1/3 of the total heat recovery (6%). In Test I-5 (non-condensing) the stage 1 heat recovery is nearly the same as for test I-14D, while the second stage heat recovery is less, because of the absence of condensation.

Although net condensation does not occur in Test I-5, both evaporation and condensation occur in the second heat exchanger stage. The flue gas enters the second stage at a temperature greater than the dew point by about 17°C (30°F). The flue gas is then evaporatively cooled to the adiabatic saturation temperature. As the flue gas moves through the second stage, the water initially evaporated to cool the flue gas is condensed as the flue gas temperature is reduced to the

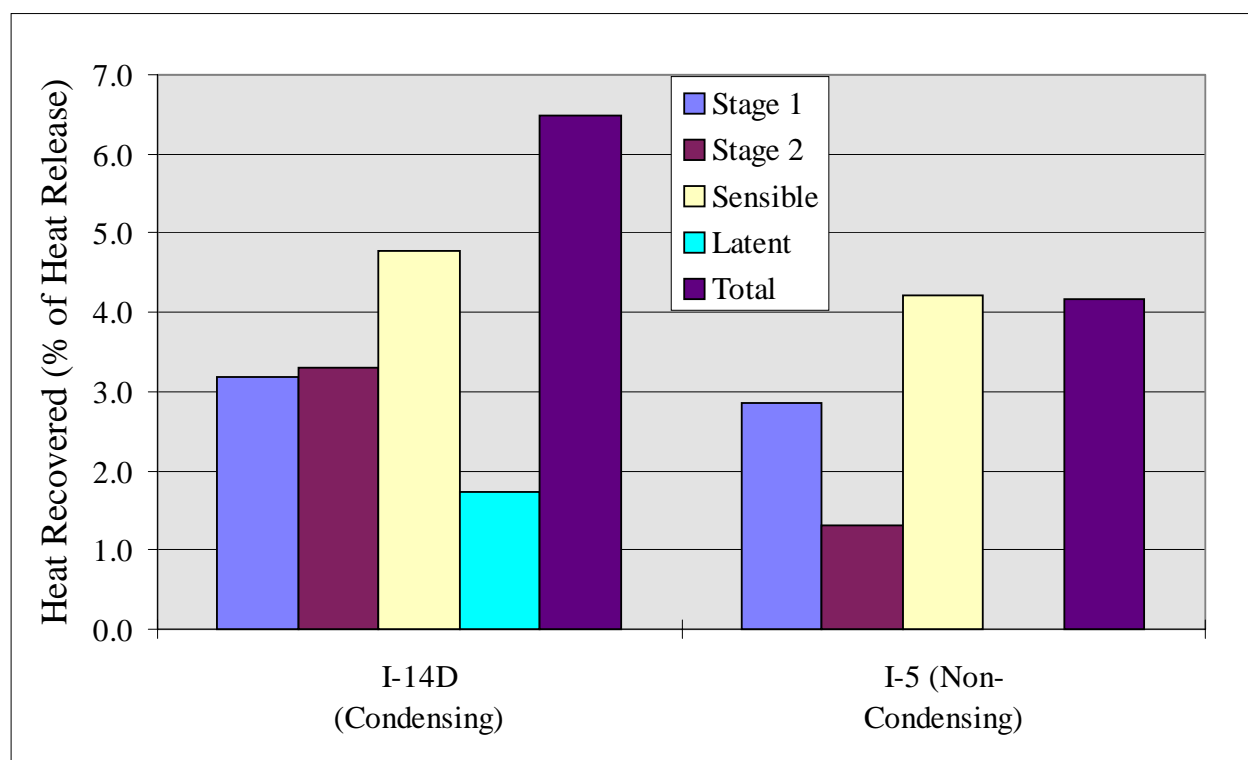


Figure 4.1 Components of Heat Recovery in the IFGT Process

original dew point temperature. This reflux process does not affect the net heat transfer, but it may influence the removal of pollutants.

4.1.2 Predictions of Heat Recovery and Gas Side Pressure Drop

CHX's[®] are sized with the assistance of a computer program that determines the physical size of the heat exchanger for the required gas flow and predicts heat recovery and gas side pressure drop through the unit. Several tests were conducted to determine the accuracy of these predictions.

Heat Recovery - Heat transfer tests were conducted using only the first heat exchanger stage so that the effect of water flow rate and water temperature could be closely controlled, and condensate flow rates could be accurately measured. Table 4.1 lists the operating conditions for these tests, which were designed to vary the condensation in the heat exchanger in a step wise fashion. As shown in Table 4.1, the energy balance for the measured data varied between about $\pm 5\%$.

Figure 4.2 shows the percent error between the measured and predicted heat recovery for the five tests. As shown, the errors are all negative indicating that the model consistently predicts a slightly greater energy recovery than was measured.

Figure 4.3 is a comparison of measured and predicted condensate flows for the five tests. As expected, based on the energy balance error, the program predicts a slightly greater condensate flow rate than was measured. Although the predictions show a fixed bias, the difference between

Table 4.1 Summary Operating Conditions and Comparison to Predicted Heat Recovery for the Five Heat Transfer Tests

	<u>CASE 1</u> II-HX1	<u>CASE 2</u> II-HX2	<u>CASE 3</u> II-HX3	<u>CASE 4</u> II-HX4	<u>CASE 5</u> II-HX5
Cooling Water Flow Rate (Corr) (kg/min)	15.7	15.3	22.6	22.9	21.8
Cooling Water Inlet Temperature (°C)	18.1	12.3	11.3	22.4	11.4
Cooling Water Outlet Temperature (°C)	62.1	60.0	47.9	54.2	43.6
Water Energy Gain, Stage 1 (kw)	48.3	50.9	57.6	50.9	48.9
Flue Gas Flow (Wet) (kg/min)	39.2	39.0	39.1	38.8	27.7
Gas Temperature @ Module 1 Inlet (°C)	120.7	123.3	123.7	124.1	120.9
Inlet Dew Point Temperature (°C)	35.5	35.3	36.1	36.0	34.5
Humidity at CHX inlet (gm/gm)	0.036	0.036	0.038	0.037	0.035
Flue Gas Flow (dry) (kg/min)	37.9	37.6	37.7	37.4	26.8
Gas Temperature @ Module 1 Outlet (°C)	53.0	51.3	47.7	52.8	41.7
Flue Gas Total Energy Loss (kw)	48.4	54.4	60.9	49.7	49.6
Condensate Flow Rate (gm/min)	85.4	165.0	249.9	71.5	293.8
Condensation Heat to Water (kw)	3.5	6.8	10.3	2.9	12.1
Fraction of Water Energy Gain (%)	7.3%	13.3%	17.8%	5.8%	24.7%
Overall Water/Gas Energy Balance (%)	-3.3%	3.6%	2.9%	-5.9%	-1.7%
PREDICTIONS					
Predicted Water Energy Gain, Stage 1 (kw)	49.1	53.4	60.7	51.6	50.1
Measured - Predicted (kw)	-0.8	-2.5	-3.0	-0.7	-1.2
Measured - Predicted (%)	-1.65%	-4.89%	-5.29%	-1.39%	-2.42%
Predicted condensate flow (gm/min)	165.7	202.2	300.8	183.9	312.3
Measured - Predicted (gm/min)	-80.3	-37.2	-51.0	-112.3	-18.5
Predicted flue gas outlet temperature (°C)	56.2	53.9	49.6	56.0	40.3
Measured - Predicted (°C)	-3.2	-2.6	-1.9	-3.3	1.4
Predicted water outlet temperature (°C)	62.8	62.3	49.8	54.6	44.3
Measured - Predicted (°C)	-0.7	-2.3	-1.9	-0.4	-0.8

measured and predicted energy recovery are quite small. Likewise, the differences between measured and predicted condensate flows and water and gas temperatures are all on the order of experimental error.

Gas Side Pressure Drop - The gas side pressure drop through the first heat exchanger stage was measured as a function of air flow rate for isothermal operation and is shown in Figure 4.4. Also shown in this figure, is the predicted gas side pressure drop for the first stage. The predicted pressure drop is less than the measured pressure drop by about 8% over the entire range of flows.

Part of the error in the predicted pressure drop is likely due to differences in the geometry of the pilot CHX[®] unit compared with a full scale unit. The “near wall” area in the pilot unit represents a larger fraction of the total flow area than a commercial sized unit. Pressure drop predictions are based on data for commercial sized units that closely simulate an infinite array of tubes.

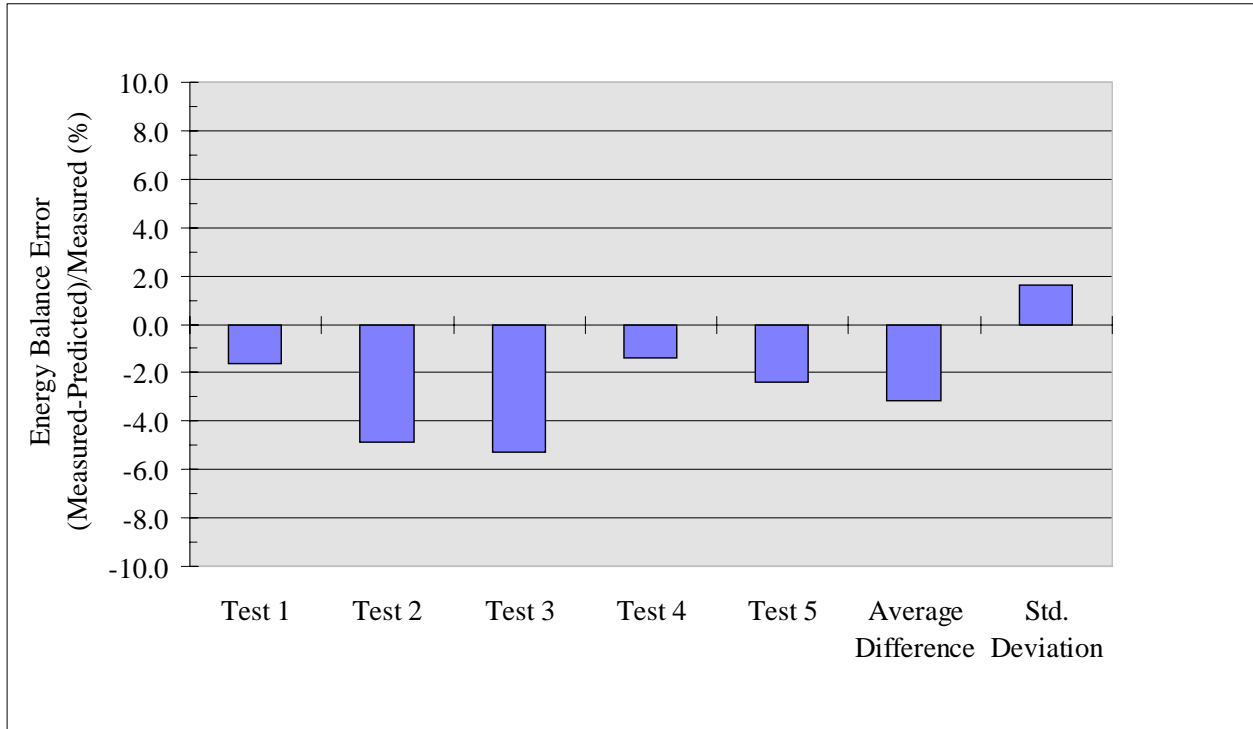


Figure 4.2 Percent Difference Between the Measured and Predicted Heat Recovery for the Five Heat Transfer Tests

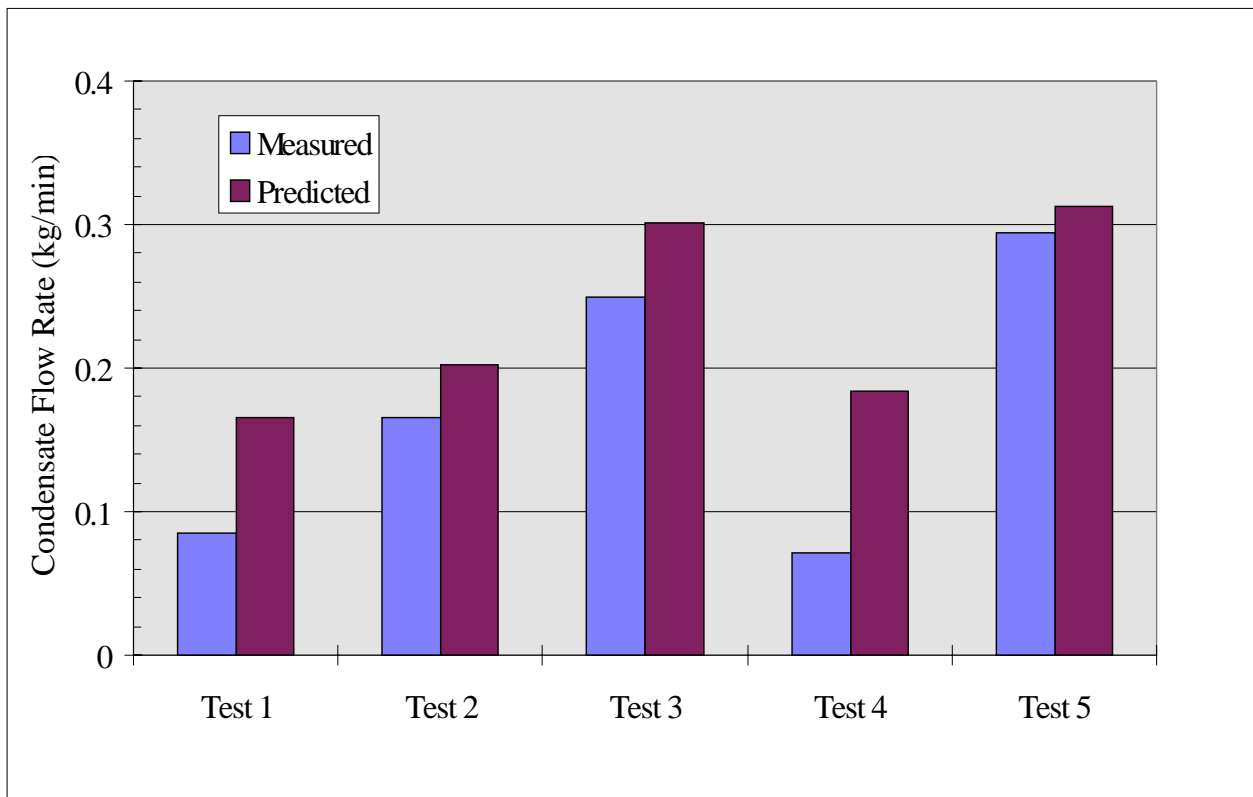


Figure 4.3 Comparison of Measured and Predicted Condensate Flow Rates

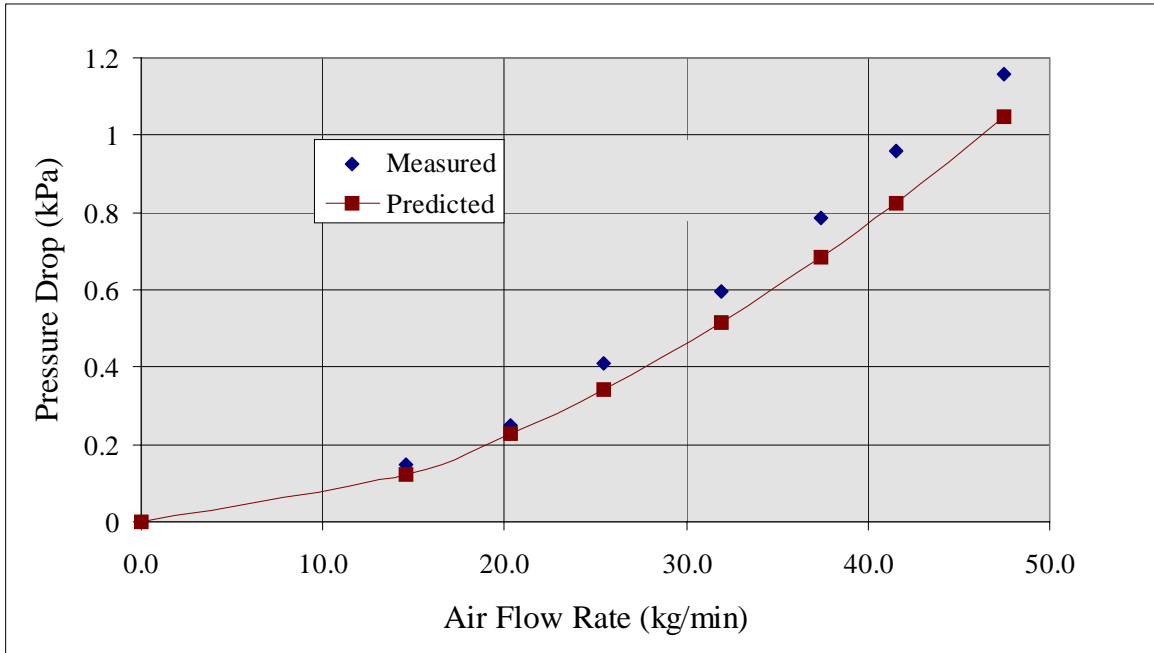


Figure 4.4 Measured and Predicted Pressure Drop Across the First Heat Exchanger Stage as a Function of Air Flow Rate

4.2 SO₂ Removal

SO₂ absorption in the IFGT was studied as a function of L/G, pH, load, reagent type, outlet temperature, and coal type. Overall SO₂ removal performance can be expressed in terms of percent removal or in terms of “number of transfer units”. Although in chemical engineering parlance N_g is defined rigorously as $dN_g = dy/(y-y_i)$, it has become common practice in the FGD industry to define N_g as follows:

$$N_g = -\ln(1-\epsilon) \quad (1)$$

where:

$$\epsilon = 100(1 - y_{outlet}/y_{inlet}) \quad (2)$$

ϵ = SO₂ removal efficiency, %

y_{inlet} = Inlet SO₂ concentration (ppm_v)

y_{outlet} = Outlet SO₂ concentration (ppm_v)

y_i = SO₂ vapor pressure at the gas-liquid interface (ppm_v)

Expressing performance in terms of transfer units has two advantages. First, N_g has greater sensitivity to incremental changes than removal percentage when the SO₂ removal efficiency approaches 100%. The effect of operating parameters are more easily visualized in graphical form. Second, transfer units usually produce more linear relationships between SO₂ removal and system parameters. For the plots shown in this section, the left y-axis is given in transfer units and the right y-axis shows the equivalent percent removal.

4.2.1 Test Repeatability

Soda ash reagent testing was carried out for the four test series with 118 individual tests. For selected tests, system operating conditions were repeated to determine the repeatability of SO₂ performance data. A comparison of the repeatability data for all coals is shown in Table 4.2 below. The measure of repeatability used in Table 4.2 is the standard deviation of the SO₂ removal. Overall, the repeatability was good. The average standard deviation in the measurements was $\pm 0.6\%$, and ranged from 0.2% to 1.4%.

Table 4.2 Repeatability of SO₂ Removal Measurements

Test ID ¹	Number of Measurements	Average SO ₂ Removal (%)	Standard Deviation (% of Removal)
I-4	7	97.2	0.5
II-4	5	98.3	0.2
III-7	3	97.1	0.5
IV-2	4	87.2	1.4

⁽¹⁾ "I-4" denotes test series I, test condition 4.

4.2.2 Sodium Reagent Test Results

Effect of L/G

The recirculated liquid flow rate is one of the major process operating factors affecting the SO₂ removal efficiency. For all of the figures that follow, the recirculated liquid flow rate is expressed as the ratio of liquid (or slurry) flowing to the top of the 2nd stage of the IFGT to the flue gas flow leaving the top of the 2nd stage. This quantity is generally referred to as the "Liquid-To-Gas Ratio" (L/G) and is considered one of the major process operating factors specified by Flue Gas Desulfurization (FGD) system designers. When the L/G increases, the qualitative effect is to increase the liquid (or dissolved) alkalinity per unit volume of treated gas. When the gas flow is constant and the reagent flow rate is increased, there is usually an increase in the liquid surface area per unit volume of treated gas, an increase in the amount of liquid in the IFGT system (commonly called the "liquid holdup"), and an increase in the turbulence (or agitation) between the gas and liquid. These effects improve the mass transfer characteristics of SO₂ removal.

The major effect of increasing L/G under typical constant load conditions is to increase the exposed surface area for gas absorption, and to increase the rate of absorption by reducing the resistance for SO₂ transport into the liquid. The SO₂ removal efficiency data shown in Figure 4.5 for Test series I, shows the quantitative effect of L/G at full load. At low L/G in the range of 0.07 to 0.27 l/m³ (0.5 to 2.0 gal/1000 ft³), the SO₂ removal efficiency increases rapidly, and reflects the generation of additional surface area from partial to complete liquid coverage of the internal tubes and walls, and an increase in the capacity of the reagent for SO₂ absorption. As the L/G increases above 0.27 l/m³, more surface area is generated by increasing the number of liquid droplets flowing downward between the tubes. The incremental surface area generated for an L/G > 0.27 l/m³ is significantly less, and the SO₂ removal efficiency increases only moderately. The qualitative effect of L/G measured for test series I was consistently evident for all of the coals tested.

The data shown in Figure 4.5 for Test Series I, a high-sulfur Ohio Coal, show that 95% SO₂ removal efficiency can be obtained at an L/G between 0.13 and 0.2 l/m³ (1.0 and 1.5 gal/1000 ft³). Increasing the L/G by a factor of 4 from 0.27 to 1.07 l/m³ (2.0 to 8.0 gal/1000 ft³) only

moderately increases the SO₂ removal efficiency from approximately 96.5% to 98.5%. However, this represents a significant increase in the transfer units from 3.3 N_g to 4.3 N_g .

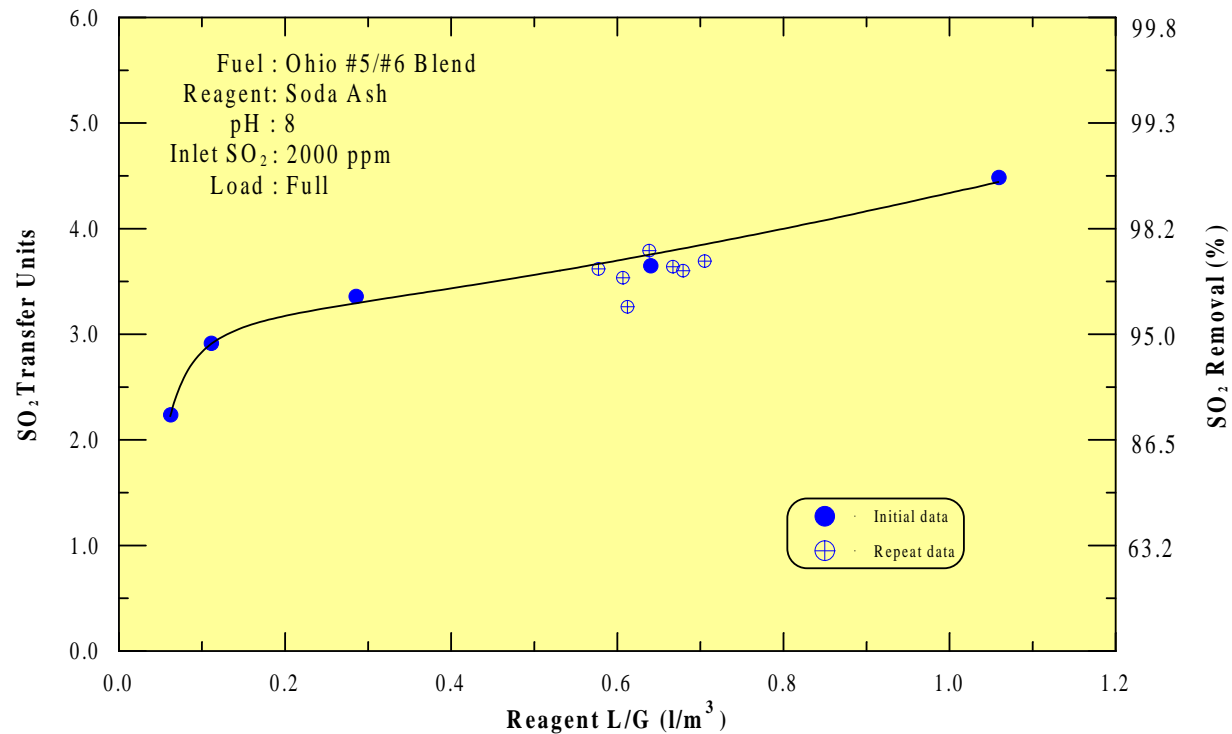


Figure 4.5 Effect of L/G at High pH

Effect of pH

The pH of the recirculating liquid entering the top of the second stage can affect the SO₂ removal efficiency. The effect will only be significant when the pH is sufficiently low that for the specific test conditions, the composition of the liquid flowing down through the IFGT second stage changes significantly. A significant composition change will be evident when the pH of the liquid leaving the bottom of the IFGT is low enough to create significant SO₂ vapor pressure at the gas-liquid interface. When this condition occurs, a sufficient excess of dissolved alkalinity is not present to absorb SO₂ and still maintain the pH at the gas-liquid interface above approximately six. For typical IFGT operating conditions with sodium reagent, operation at a recirculated solution pH greater than approximately 8.0 will usually ensure that the liquid pH leaving the IFGT is above 7.0, with no significant SO₂ vapor pressure.

The SO₂ removal efficiency at a pH of 8 and 7 for Test Series I is shown in Figure 4.6. The SO₂ removal efficiency at a pH of 7 is somewhat lower than with a pH of 8 with good agreement on the incremental effect of L/G. At similar L/Gs, reducing the pH from 8 to 7 lowered the SO₂ removal efficiency by approximately 0.5 transfer units. At the lower pH of 7, the reduced SO₂ removal efficiency reflects sufficient changes in the liquid composition for the generation of a significant SO₂ vapor pressure.

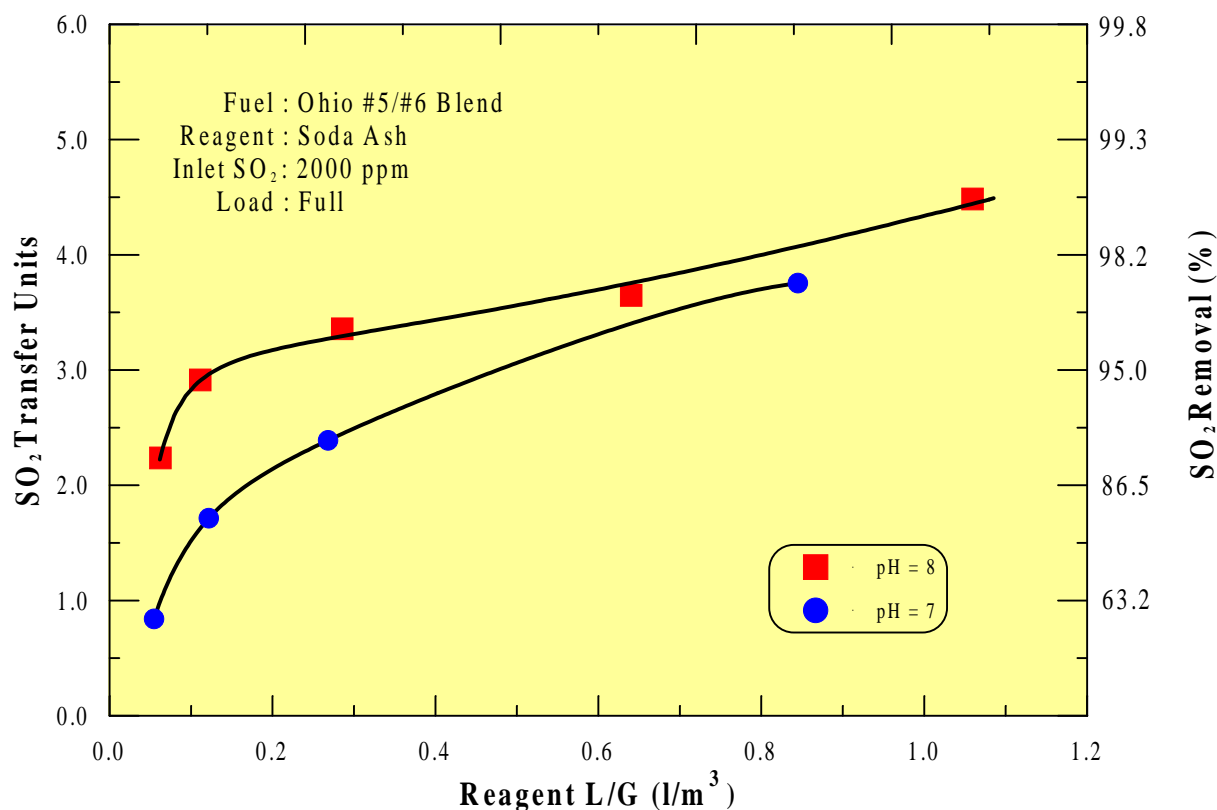


Figure 4.6 Effect of pH on SO₂ Absorption

Effect of Load

The effect of the load on SO₂ removal efficiency is shown in Figure 4.7 along with the effects of L/G and pH. For operation at half load, the SO₂ removal efficiency is significantly less by approximately 1.5 N_g . Two factors are contributing to the reduction in SO₂ removal efficiency at reduced load. First, the reduced load decreases the liquid holdup and its contribution to exposed surface area for gas absorption from droplets traveling downward from tube to tube. Second, is the reduction in turbulence between the liquid and gas. The reduced turbulence decreases the rate of absorption by increasing the resistance in the gas phase for SO₂ transport into the liquid surface.

Effect of Outlet Temperature

The outlet flue gas temperature of the IFGT second-stage is typically adjusted for operation at temperatures ranging from slightly above to several degrees below the dewpoint. The flue gas temperature throughout the IFGT second stage is relatively constant when operating at or below the dewpoint. When the operating temperature of the flue gas within the IFGT second stage changes, physical and mass transfer properties of the flue gas, SO₂, and liquid may also change. The overall effect on the rate of mass transfer is complex, but the net effect on the mass transfer rate may be estimated by combining the individual temperature effects.

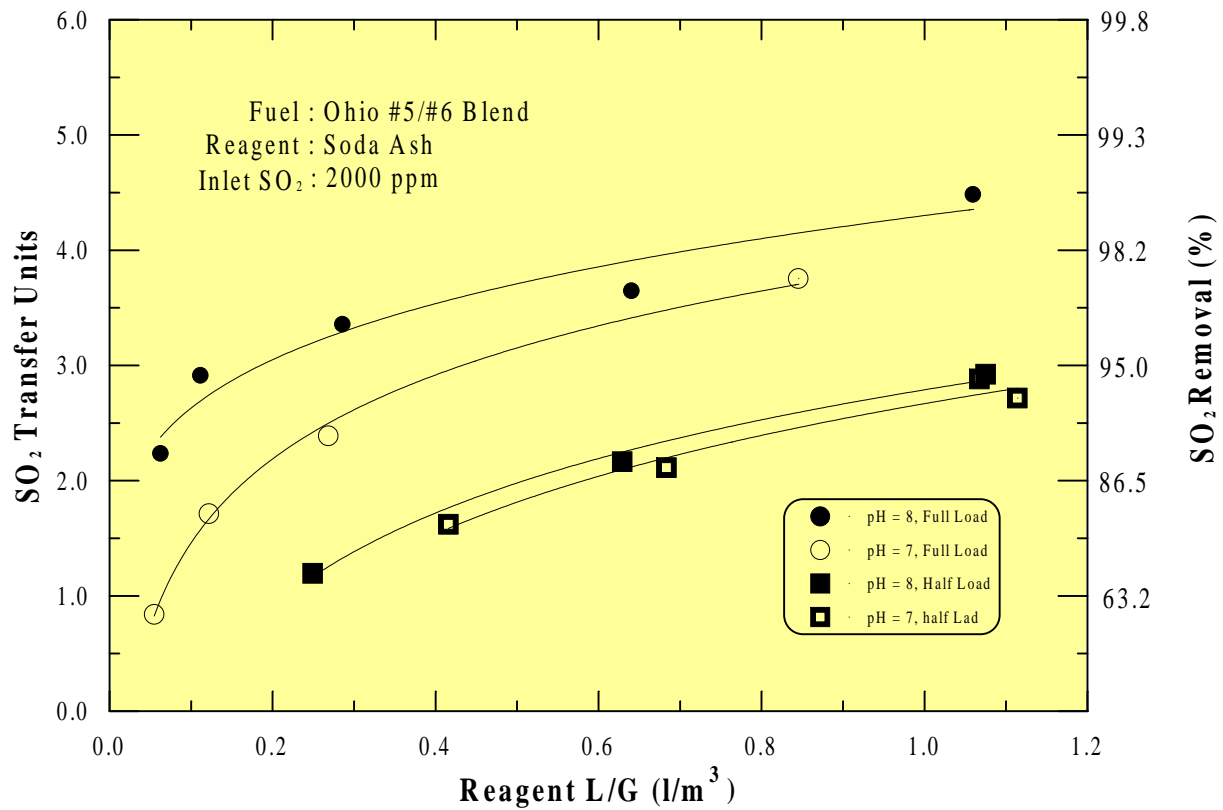


Figure 4.7 Effect of Load on SO₂ Removal

The effect of temperature on the mass transfer rate was measured during Test Series I at a pH of 8 at full load and is shown in Figure 4.8. The data suggests that reducing the operating temperature by 9°C (16°F) reduces the mass transfer rate by approximately 3 to 5%. To estimate the observed effect of temperature, dimensionless empirical power law mass transfer correlations for droplets and cylindrical tubes were evaluated for the effect of temperature dependency. In an attempt to simplify the estimate, the analysis was conducted assuming a high pH in which the liquid phase resistance to mass transfer could be considered insignificant. This was confirmed experimentally as increasing the pH above 8 did not change the difference between the reagent feed pH and the pH at the exit of the IFGT second stage. For the droplets falling between the tubes, the following expression for turbulent mass transfer around a sphere applies.⁽¹⁾

$$N_{sh} = 2.0 + 0.55N_{re}^{1/2}N_{sc}^{1/3} \tag{3}$$

where:

- N_{sh} = Sherwood No.
- N_{re} = Reynold's No.
- N_{sc} = Schmidt No.

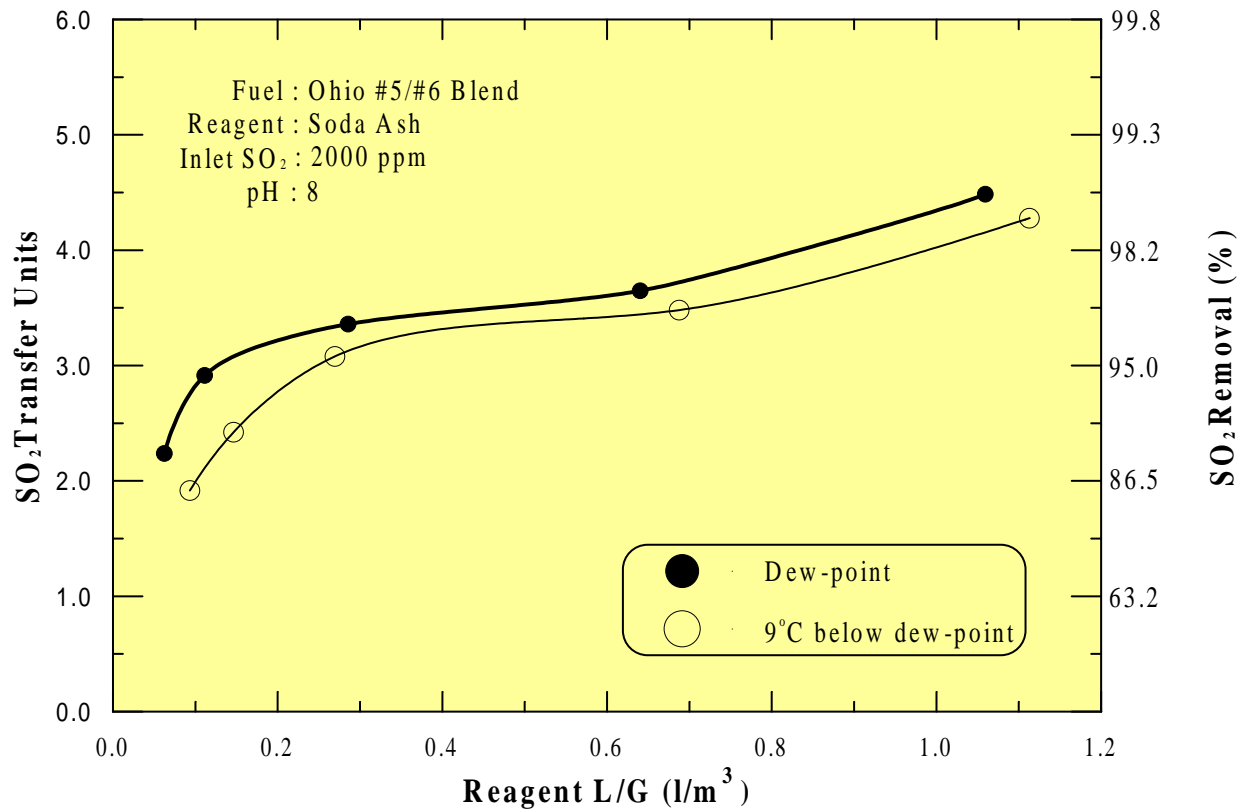


Figure 4.8 - Effect of Outlet Temperature on SO₂ Removal.

For the liquid flowing over the tubes the expression for turbulent mass transfer is⁽²⁾

$$N_{sh} = 0.25N_{re}^{0.6}N_{pr}^{0.38} \tag{4}$$

For both expressions, the factors that are temperature dependant are the flue gas density, flue gas viscosity, and binary diffusion coefficient for SO₂ in flue gas. The dependency of these parameters on temperature was used in Equations 3 and 4, to determine the overall effect of a 9°C (16°F) temperature decrease on the mass transfer rate. For the droplets, the net effect was a decrease in mass transfer rate of approximately 9%. For the tubes, the net effect was a decrease in mass transfer rate of approximately 10%. The total mass transfer in the IFGT second stage is some combination from the droplets and tubes. As the estimated effect of temperature is essentially identical for both the droplets and tubes, the estimated effect of the temperature reduction is approximately 9%. This is consistent with the measured reduction in transfer units of approximately 3% to 5%.

Effect of Coal Type

The primary effect of the coal type is the variation in the coal sulfur content. The coal ash content and coal ash alkali composition have an insignificant effect as essentially all of the fly ash is

collected in the upstream baghouse. For the four coals tested, the flue gas SO₂ concentration ranged from approximately 300 ppm_v to 2000 ppm_v. The SO₂ removal efficiency at full load and solution pH of 8 for various L/Gs is shown in Figure 4.9. At these conditions, no clear effect of the coal sulfur content on SO₂ removal efficiency is evident. This is consistent with operation under gas phase mass transfer limited conditions where the SO₂ removal efficiency is unaffected by variations in the inlet SO₂ concentration.

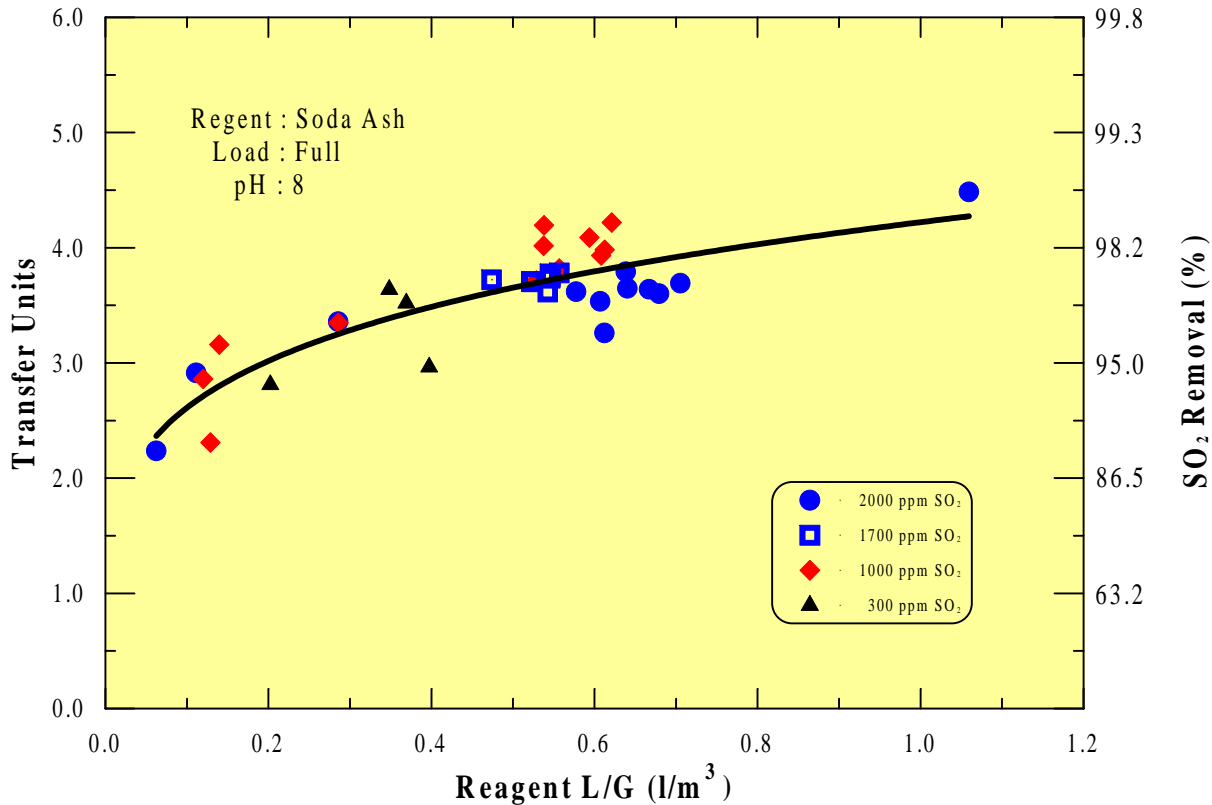


Figure 4.9 Effect of Inlet SO₂ Concentration on SO₂ Removal

As an example, if the inlet SO₂ concentration is reduced by a factor of 2, the SO₂ absorbed will likewise decrease by a factor of 2 and the SO₂ removal efficiency will remain the same. The SO₂ removal efficiency at half load and reagent feed pH of 7 for various L/Gs is shown in Figure 4.10. At these conditions, there was a noticeable effect of the coal sulfur content on SO₂ removal efficiency. It is generally assumed that at pH of 7 or less there will be significant SO₂ back pressure at the gas-liquid interface, causing some liquid phase mass transfer resistance. Under these conditions, reducing the flue gas SO₂ concentration will contribute to higher SO₂ removal efficiency.

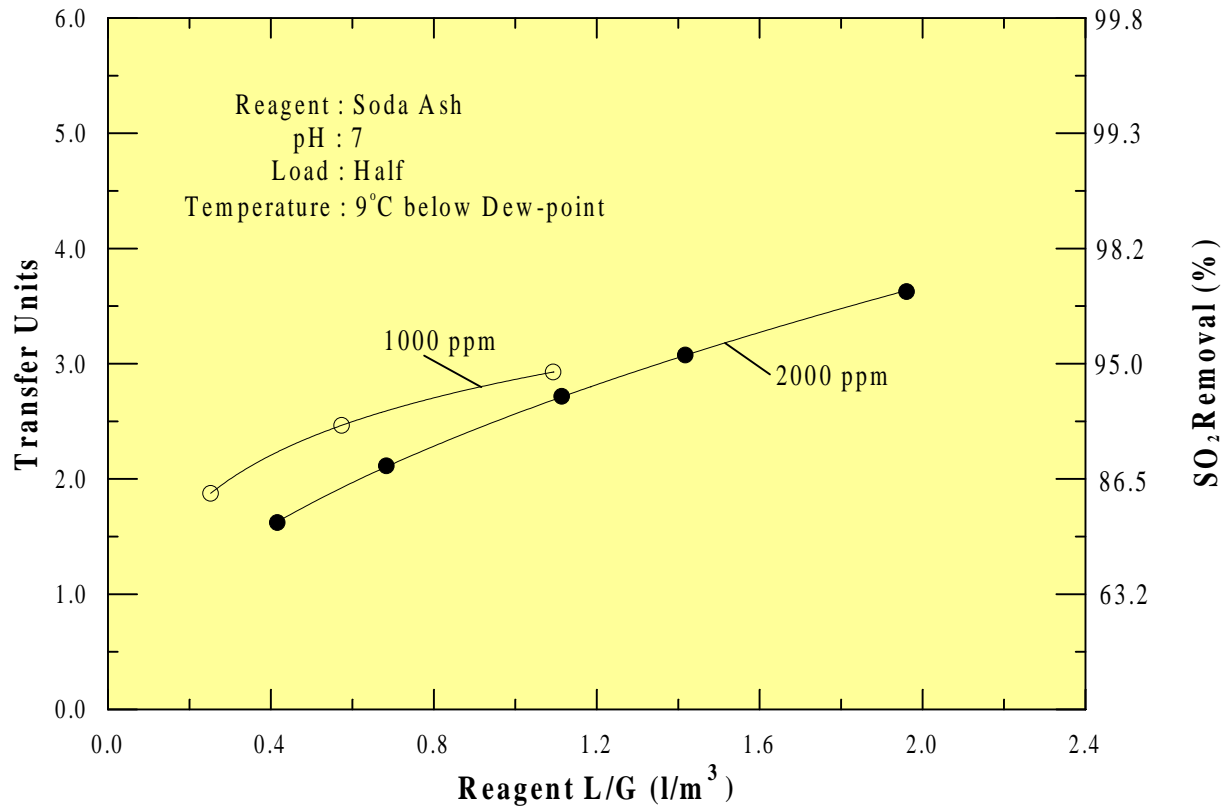


Figure 4.10 Effect of Inlet SO₂ Concentration on SO₂ Removal at Half Load

4.2.3 Lime Reagent

A lime-based reagent differs from soda ash reagent in both the type of alkaline species they generate, and in the amount of dissolved alkaline species produced. With soda ash reagent, the active alkaline species is highly soluble sodium sulfite and bicarbonate. A lime reagent produces relatively low dissolved levels of hydroxide. In a 5% magnesium-95% lime reagent, approximately 5% of the total alkali comes from magnesium sulfite. While the magnesium sulfite is low in total concentration, it is highly soluble and can deliver 10 to 15 times as much dissolved alkalinity as a calcium-based lime reagent.

The effect of reagent type on SO₂ removal efficiency is shown in Figure 4.11 for full load conditions. At an L/G of 0.8 l/m³ (6 gal/1000ft³), the SO₂ removal efficiency for the sodium reagent was 98%, and for the mag-lime reagent was 83%. For both reagents the pH measured in the scrubbing solution return line was approximately 7.5. While there was a small reduction in reagent pH of 0.5 across the second stage for the sodium reagent, the mag-lime reagent scrubbing solution pH dropped by approximately four. This is consistent with the lower SO₂ removal

efficiency, and suggests that the mag-lime has insufficient dissolved alkalinity at an L/G of 0.8 l/m³ to absorb the available SO₂.

When planning the mag-lime tests, it was anticipated that a 5% mag-95% lime reagent would give only slightly less SO₂ removal efficiency than soda ash. The results showed a significant drop in SO₂ removal efficiency. Post test analysis indicated that the actual composition of the mag-lime reagent was 12% magnesium hydroxide and 88% calcium hydroxide. The high magnesium concentration should have allowed sufficient buildup of dissolved magnesium sulfite. However, the dissolved solids for the mag-lime test was unexpectedly low, about 0.4 %, and is the cause for the lower than anticipated removal. Allowing more operation time for the magnesium sulfite to dissolve or, higher L/G will be required to approach the performance of a sodium reagent.

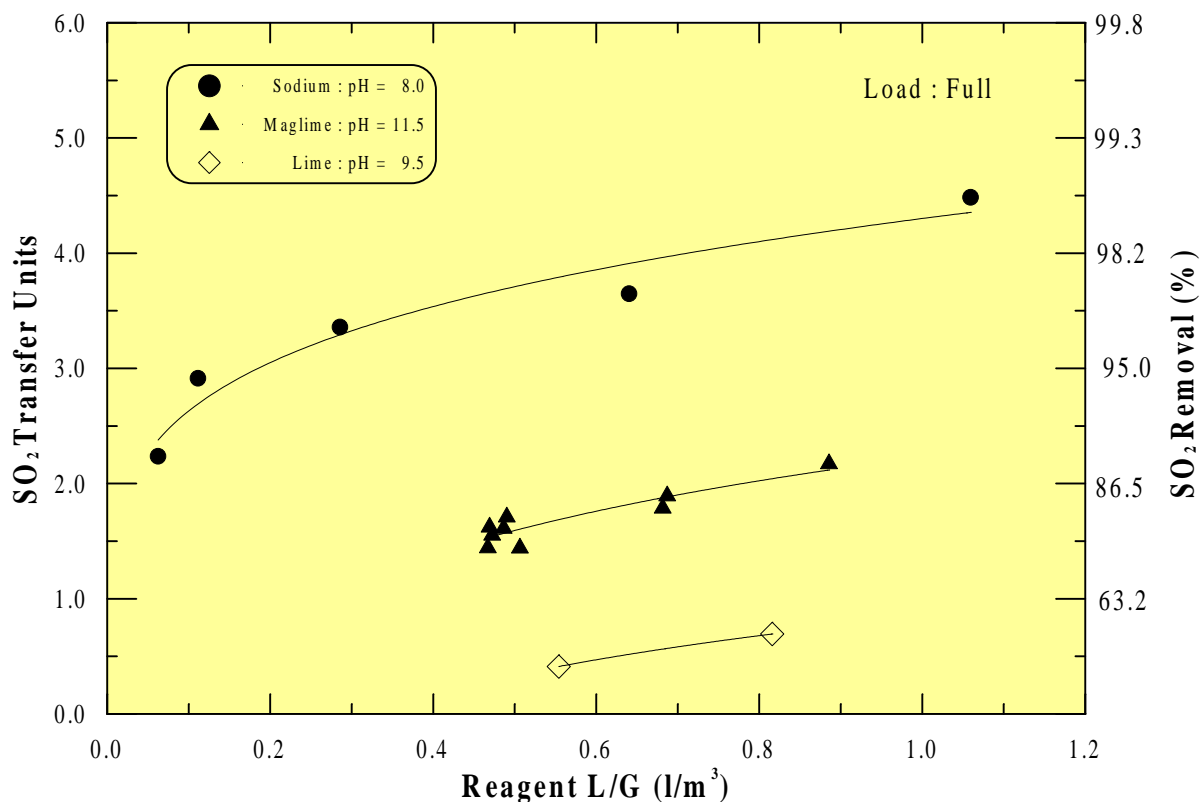


Figure 4.11 Effect of Reagent Type on SO₂ Removal

For the lime reagent, significantly lower SO₂ removal efficiency was anticipated. At an L/G of 0.8 l/m³ (6 gal/1000 ft³), the SO₂ removal efficiency for the sodium reagent was 98% for a feed pH of 8.0. For the lime reagent at the same L/G, the SO₂ removal efficiency was approximately 50%, for a feed pH of 9.5. There was a significant reduction in the pH of the scrubbing solution (~5.5 pH units) across the second stage. This was expected, as the lime reagent produces very low dissolved alkalinity in the lime slurry.

4.3 Chloride/Fluoride Removal

Chlorine and fluorine are halogens present in coal and released from combustion as the acid gases hydrogen chloride (HCl) and hydrogen fluoride (HF). Of the four halogens - fluorine (F), chlorine (Cl), bromine (Br), and iodine (I) present in coal, chlorine and fluorine are the most abundant and are present in sufficiently high concentrations to be of concern. Some countries currently require emissions control of these halogens, and new regulations are pending in others. The IFGT system has the capability to absorb these acid gases by mechanisms similar to the capture of SO₂. Generally, HCl and HF will be absorbed at levels equal to or greater than SO₂. This section reports the removal efficiencies of HCl and HF measured across the IFGT for various coals for a wide range of combustion emission concentrations. Although some data are inconsistent, high removals were generally obtained for both HCl and HF.

Chlorine

Chloride emissions are a major contributor to man-made atmospheric acidity. Most of the chloride in coal is in the form of NaCl, which is converted essentially 100% to HCl in the combustion process. The HCl passes completely through the combustion process and particulate collection devices as there is little interaction between the HCl and fly ash. Generally, deposition will only occur in the particulate collection device if the flue gas temperature is below the acid dew point for HCl of 60°C (140°F). While SO₂ and NO_x emissions are greater than emissions of HCl, both the absorption rate and solubility of HCl in water is much higher.

The HCl concentration was measured at the inlet and outlet of the IFGT for each coal. Table 4.3 lists the test conditions and indicates how HCl partitioned to the vapor and particulate phases and the removal efficiency for the particulate and gas phases. More than 99.9% of the HCl entering the IFGT was in the vapor phase with concentrations ranging from 22 mg/dscm to 134 mg/dscm. The HCl concentration in the particle phase was generally much lower than in the vapor phase. As shown in Table 4.3, the HCl concentration in the particulate was generally less than 400

Table 4.3 Vapor and Particle Phase Chloride Concentration and Removal Efficiencies

Test	Scrubbing Solution pH	Location	Conc. in Particulate (ppm _v)	Unit Concentrations			Removal Efficiency			on Filter (%)	Percent in Vapor (%)
				Vapor (ug/dscm)	Particulate (ug/dscm)	Total (ug/dscm)	Vapor (%)	Particulate (%)	Total (%)		
I-4A	7.9	Inlet	134	134430	97	134527				0.07	99.9
		Outlet	8080	44709	209	44919	66.7	-116.3	66.6	0.47	99.5
II-4B	8.3	Inlet	16600	184429	26	184455				0.01	100.0
		Outlet	---	1150	---	1207	99.4	---	99.4	0.00	100.0
III-7A	6.5	Inlet	0.26	21997	0.01	21997				0.00	100.0
		Outlet	0.31	551	0.00	551	97.5	90.3	97.5	0.00	100.0
IV-1A	8.0	Inlet	396	156951	15	156966				0.01	100.0
		Outlet	18600	3628	44	3672	97.7	-184.5	97.7	1.20	98.8

ppm_m. However, for test series II, the HCl concentration in the particulate was very high - 16,600 ppm_m. For test series II, the SBS carbon carryover was also very high, and the baghouse was operated without bypass. The relatively high HCl concentration measured in the

particulate could be due to either excessive carbon carryover from the furnace adsorbing HCl, or HCl being concentrated in the particulate fines that pass through the baghouse. The overall effect indicated an 40-fold increase in the particulate's chloride concentration compared to the other tests.

The HCl removal efficiency for tests I, II, and III, were 66.7%, 99.4%, and 97.5%, respectively. The results for test I, were much lower than anticipated. A review of the analytical methods and procedures followed did not explain the results. The test was repeated in test series IV and the removal efficiency was measured at 97.7%. For test III, the effect of reagent feed pH on HCl removal efficiency was measured by reducing the reagent feed pH from approximately 8.0 to 6.5. The HCl removal efficiency was not significantly reduced and measured 97.5%.

The HCl removal efficiency for the particulate phase indicates large negative efficiencies. This is primarily due to the relatively large measurement uncertainty associated with the small measured concentrations for chloride in the particulate.

Fluorine

Fluoride emissions are a relatively minor component of the acid gases from coal combustion. For the four test series, the concentration of HCl in the flue gas was 40 to 87 times greater than the concentration of HF. Like HCl, the absorption rate and solubility of HF in water is much higher than SO₂ or NO_x. Most of the HF in coal is in the form of the mineral fluorapatite [Ca₅(PO₄)₃(OH,F,Cl)], fluorite (CaF₂), and biotite [K(Mg,Fe)₃(AlSi₃)O₁₀(OH,F)₂]. These fluoride compounds are converted essentially 100% to HF in the combustion process. Like HCl, HF also passes completely through the combustion process and particulate collection devices as there is little interaction between the HF and fly ash.

The HF removal efficiency was measured at the inlet and outlet of the IFGT for each coal with sodium reagent. Table 4.4 lists the test conditions and the vapor and particulate phase concentration and removal efficiency. More than 98% of the HF entering the IFGT was in the vapor phase with concentrations ranging from 0.43 mg/dscm to 4.3 mg/dscm. The HF concentration in the particulate was generally less than 700 ppm_m. However, for test series II, the HF concentration in the particulate was relatively high and measured 49,000 ppm_m. For test series II, the SBS carbon carryover was also very high, and the baghouse was operated without bypass. The relatively high HF concentration measured in the particulate could be due to either excessive carbon carryover from the furnace adsorbing HF, or HF being concentrated in the particulate fines that pass through the baghouse. The overall effect indicated an 80-fold increase in the particulate's fluoride concentration compared to the other tests.

Table 4.4 Vapor and Particle Phase Fluoride Concentration and Removal Efficiencies

Test	Scrubbing Solution pH	Location	Conc. in Particulate (ppm _v)	Unit Concentrations			Removal Efficiency			Percent on Filter (%)	Percent in Vapor (%)
				Vapor (ug/dscm)	Particulate (ug/dscm)	Total (ug/dscm)	Vapor (%)	Particulate (%)	Total (%)		
I-4A	7.9	Inlet	37	1655	14	1669				0.87	99.1
		Outlet	560	60	2	62	96.4	85.6	96.3	3.35	96.7
II-4B	8.3	Inlet	48800	4184	65	4249				1.52	98.5
		Outlet	---	22	---	22	99.5	---	99.5	0.00	100.0
III-7A	6.5	Inlet	22	431	1	432				0.24	99.8
		Outlet	241	74	1	75	82.8	9.5	82.7	1.25	98.7
IV-1A	8.0	Inlet	610	1859	24	1883				1.27	98.7
		Outlet	2535	42	6	48	97.8	74.8	97.5	12.62	87.4

As shown in Table 4.3, the HCl concentration in the particulate was generally less than 400 ppm_m. However, for test series II, the HCl concentration in the particulate was very high - 16,600 ppm_m. For test series II, the SBS carbon carryover was also very high, and the baghouse was operated without bypass. The relatively high HCl concentration measured in the particulate could be due to either excessive carbon carryover from the furnace adsorbing HCl, or HCl being concentrated in the particulate fines that pass through the baghouse. The overall effect indicated an 40-fold increase in the particulate's chloride concentration compared to the other tests.

The HF removal efficiency for tests I, II, III, and IV, were 96.3%, 99.2%, 82.7%, and 97.5%, respectively. The results were generally as expected. The HF removal for test III was lower than the other three tests and may be due to the lower reagent pH for this test, or may be due to uncertainty arising from the low concentrations of HF for this test.

4.4 Ammonia Removal

Ammonia has been used extensively in electric utility and industrial catalytic systems to control NO_x emissions. A concern in the operation of these systems is how much ammonia passes through unreacted and is emitted to the atmosphere. These ammonia emissions are commonly referred to as "Ammonia Slip". Currently, the USEPA has not imposed limits on ammonia slip. However, ammonia emission limits have been established by state and local agencies. In California, NO_x emission limits generally range from 2 ppm to 10 ppm. Operators of NO_x control systems must balance between using sufficient ammonia to meet NO_x emissions without exceeding the ammonia slip limits. Excessive ammonia use can also cause ammonia salt formation, which can cause fouling in air heaters and catalyst deactivation in the NO_x control equipment. The ammonia salts are formed by the reaction of ammonia with SO₃ in the flue gas to form ammonium sulfate compounds (NH₄HSO₄ and (NH₄)₂SO₄). With these concerns in mind, operators of ammonia based NO_x control systems could benefit from an IFGT system if the IFGT could demonstrate the ability to absorb a large amount of ammonia. The NO_x system could then be operated at higher ammonia to NO_x ratios without increasing ammonia slip.

One objective for ammonia testing for Task 2 was to measure ammonia removal through the IFGT system. Ammonia removal was based on measurements at the inlet and outlet of the IFGT. Ammonia was injected at a constant measured flow rate upstream of the IFGT inlet, at the inlet to the SBS system ID fan. The ammonia flow rate was measured by a certified rotameter and manually controlled at the rotameter. A continuous ammonia analyzer (Severn Science Instruments Ammonia Analyzer) was then used to sequentially measure the ammonia concentration upstream and downstream of the IFGT. For selected tests, the measurements of the continuous analyzer were verified using USEPA Method 206.

During each of the first three test series, three ammonia removal tests were conducted. Table 4.5, Section A, summarizes the results for all nine test conditions. The inlet ammonia concentration ranged from 31 ppm_v to 94 ppm_v and removal efficiency ranged from 57% to 93%. All ammonia tests were conducted at full load. For test III-9B, the measured inlet ammonia concentration was inconsistent with previous data and was estimated from the rotameter settings and previously measured reductions from ammonia-sulfur reactions. The ammonia removal efficiency for test III-9B was subsequently adjusted from 24% to 57%. The IFGT system outlet flue gas temperature for tests I-14G, II-4F, III-18 were planned to be at 9°C (20°F) below the water vapor dewpoint. However, due to seasonal variations in the process cooling water temperature, the actual outlet temperatures achieved were 9°C (16°F), 7°C (13°F), and 4°C (7°F), respectively, below the water vapor dewpoint.

The ammonia removal data in Table 4.5 indicates that the major factors effecting ammonia removal include the IFGT outlet temperature, L/G, the level of dissolved solids in the recirculating liquid, and liquid pH. The effect of outlet temperature is shown for three pair of data sets in Table 4.5, Section B. As with SO₂, the solubility of ammonia in aqueous solution is strongly affected by temperature. The solubility of ammonia increases as the temperature of the liquid decreases. The equilibrium solubility of ammonia in contact with air containing 100 ppm ammonia is approximately 65 mg/l at 38°C (100°F) and increases to 100 mg/l at 27°C (80°F). On average, the data suggests that the ammonia removal efficiency improved by approximately 0.75 N_g for a 6°C (11°F) reduction in outlet temperature.

The effect of inlet ammonia concentration is shown for two pair of data sets in Table 4.5, Section C. There was essentially no measured improvement in ammonia removal efficiency in Test Phase I, when the inlet ammonia concentration was reduced from 94 ppm_v to 68 ppm_v. In Test Phase II the ammonia removal efficiency improved somewhat from 73% to 83% when the inlet ammonia concentration was reduced by almost half from 68 ppm_v to 31 ppm_v.

In the third test phase, the reagent feed total dissolved solids, or “TDS”, was reduced from approximately 12% to 4% to reflect the relatively low sulfur content of powder river basin coal. Reducing the TDS reduces the ionic strength in the reagent feed and increases the solubility of ammonia in the liquid. For Test Phase III, the lower TDS enhanced the ammonia solubility by approximately 30%. As shown in Table 4.5, Section D, high TDS test (I-4F) is compared to a low TDS test (III-18). The measured ammonia removal efficiency for both tests was 76%. As previously discussed, the slightly lower flue gas ammonia concentration will not significantly affect the ammonia removal efficiency. Therefore, the data suggests that the ammonia removal efficiency can be held constant while reducing the L/G from 0.67 l/m³ (5.0 gal/1000 ft³) to 0.39 l/m³ (2.9 gal/1000 ft³) by lowering the TDS from approximately 12% to 4%.

Ammonia, being an alkaline gas, is better absorbed by liquids with lower pH. The effect of pH on ammonia removal efficiency was investigated in Test Phase III, see Table 4.5, Section E. For the indicated tests, two factors were varied. The inlet ammonia concentration was reduced from 70 pm to 31 ppm, and the reagent feed pH was reduced from 8.2 to 6.8. Based on the previous data, the estimated effect of lowering the inlet ammonia concentration would be a reduction in ammonia removal efficiency of approximately 0.4 N_g. However, by also reducing the pH from 8.2 to 6.8, the ammonia removal efficiency **increased** from 57% to 87%, or a net increase of 1.1 TU. These results suggest that for the operating conditions used in test phase III, reducing the liquid pH from 8.2 to 6.8 improved the ammonia removal efficiency by approximately 1.5 N_g.

Another objective for ammonia testing for Task 2 was to estimate the amount of ammonia that reacts with SO₃ before the IFGT system. Below 230°C (450°F), ammonia reacts with sulfur trioxide (SO₃) in the flue gas, so that some of the gaseous ammonia will be removed from the flue gas upstream of the IFGT. Differences between the measured and calculated ammonia concentration at the IFGT inlet based on the ammonia injection rate determined the amount of the ammonia-sulfur reactions. For the nine completed ammonia tests, the ammonia reduction attributable to ammonia-sulfur reactions ranged from 27% to 45%, and averaged 36%. The ammonia reduction for test III-9B was measured at 75%, and was considered inconsistent with the other test results.

Table 4.5 Summary of Ammonia Removal Measurements

Section A - Data Summary						
Test	NH ₃ At CHX Inlet (ppm _v , wet)	NH ₃ At CHX Outlet (ppm _v , wet)	NH ₃ Removal (%) / (TU)	Outlet Gas Temp. (°C)	Feed pH	L/G l/m ³
I - 4G	70	5	93 / 2.69	27.2	7.9	0.67
I - 4F	94	22	76 / 1.43	36.1	7.9	0.67
I - 4E	68	16	76 / 1.42	36.1	7.9	0.68
II - 4D	68	12	83 / 1.76	36.0	8.2	0.66
II - 4F	64	7	88 / 2.16	29.3	8.2	0.64
II - 4E	31	8	73 / 1.30	36.3	8.2	0.64
III - 18	84	20	76 / 1.45	38.0	7.9	0.39
III - 9B	70	30	57 / 0.86	42.3	8.2	0.35
III - 7B	31	4	87 / 2.02	42.3	6.8	0.34
Section B - Effect of Lower Outlet Temperature.						
I - 4E	68	16	76 / 1.42	36.1	7.9	0.68
I - 14G	70	5	93 / 2.69	27.2	7.9	0.67
II - 4D	68	12	83 / 1.76	36.0	8.2	0.66
II - 4F	64	7	88 / 2.16	29.3	8.2	0.64
III - 9B	70	30	57 / 0.86	42.3	8.2	0.35
III - 18	84	20	76 / 1.45	38.0	7.9	0.39
Section C - Effect of Lower Inlet NH ₃ Concentration.						
I - 4F	94	22	76 / 1.43	36.1	7.9	0.67
I - 4E	68	16	76 / 1.42	36.1	7.9	0.68
II - 4D	68	12	83 / 1.76	36.0	8.2	0.66
II - 4E	31	8	73 / 1.30	36.3	8.2	0.64
Section D - Effect of Reduced L/G and Total Dissolved Solids.						
I - 4F	94	22	76 / 1.43	36.1	7.9	0.67
III - 18	84	20	76 / 1.45	38.0	7.9	0.39
Section E - Effect of pH.						
III - 9B	70	30	57 / 0.86	42.3	8.2	0.35
III - 7B	31	4	87 / 2.02	42.3	6.8	0.34

4.5 Particulate Removal

The IFGT system is effective at removing particulate from a flue gas stream because of the serpentine gas flow path around the Teflon[®]-covered tubes in the heat exchangers. The primary removal mechanism is inertial impaction of the larger particles on the tube surface. Previous testing conducted using oil-fired flue gas indicated that removal extends to smaller particles in which inertial effects are minimal.

Although effective at removing particulate, the CHX[®] design is not intended to handle the full particle load from a coal-fired boiler. Collected particulate must be rinsed from the tubes and flushed from the system at regular intervals to prevent plugging between tubes. However, since the measurement of particle loading, particle removal efficiency, and trace element concentrations in particulate are all more easily made if the particle loading to the IFGT inlet is relatively large, the particle loading to the IFGT system inlet was set to about 500 to 900 mg/dscm (0.4 to 0.6 lb/MBtu) for most of the tests. This particle loading represents about 10% of the ash in the coal. In the SBS combustor about 50% of the fly ash is retained in the furnace/convection pass as bottom ash and ash deposits and so the loading to the IFGT system was about 20% of the normal ash loading to the baghouse.

To achieve the targeted particle loading, the baghouse bypass valve was opened so that the baghouse pressure drop was reduced about 20%, indicating a bypass gas flow of about 20%. Once set, the valve position was maintained for the duration of a test. The normal bag cleaning cycle based on baghouse pressure drop was suspended during a test day. Likewise, soot blowing of the convection pass tubes was delayed until the end of a test day. These precautions prevented upsets in the particle loading at the IFGT during testing. Soot blowing and bag cleaning was performed at the end of a test day. Similarly, particulate was permitted to accumulate in the first stage of the IFGT system during a test day and was rinsed after daily testing was completed.

Using this procedure, the particle loading to the IFGT system was lowest at the start of the day when the baghouse pressure drop was lowest. Later in the day, as the filter cake on the bags caused the baghouse pressure drop to increase, a larger fraction of the gas flow was bypassed and so the particle loading at the IFGT system inlet increased. These mild changes in particle loading did not influence the results as the particle loading changed only slowly with time, and removal efficiencies were always based on simultaneous measurements at the inlet and outlet of the IFGT system.

Raw coal for the SBS furnace was crushed, dried and stored in a bunker. The crushed coal was then ground in an MPS pulverizer and stored in a second bunker. All of the coals used on these tests was ground to the same nominal coal fineness of 70% through a 200 mesh screen (70% < 75 micrometers).

The particle size distributions of the fly ash at the inlet to the IFGT system for the four test series are shown in Figure 4.12. The cumulative percent of the mass is shown as a function of the flyash aerodynamic particle size. These size distributions were measured with the cascade

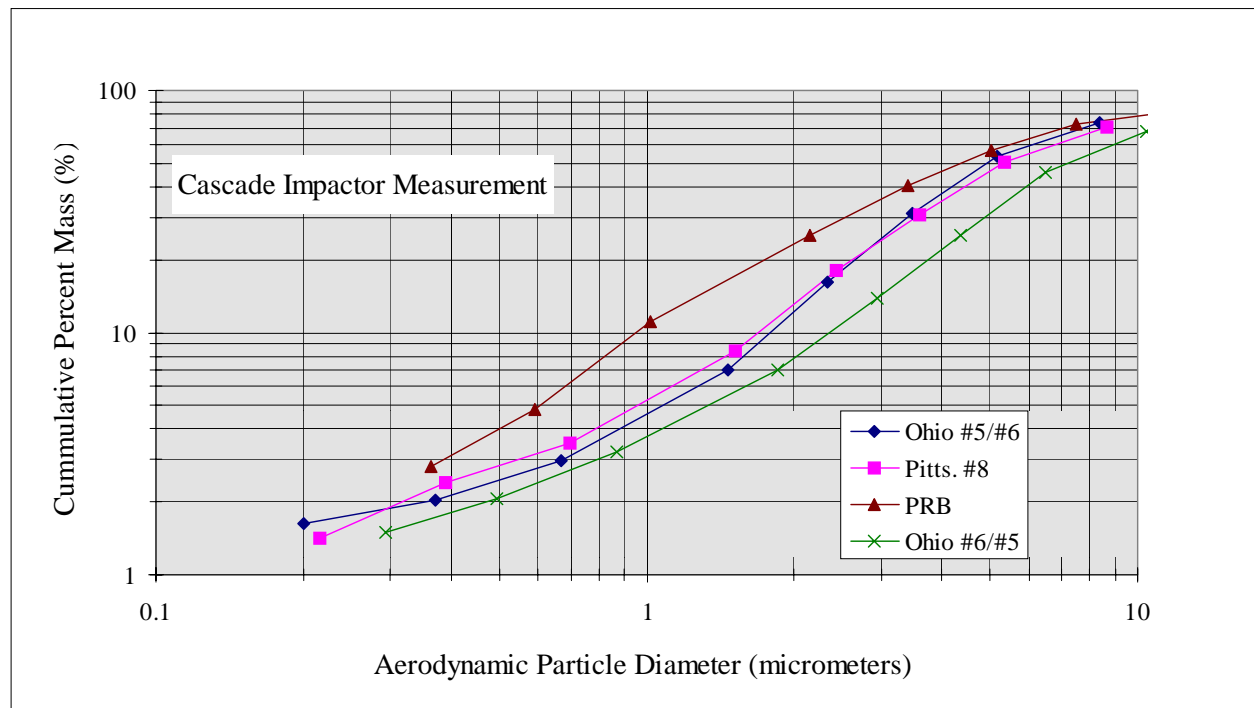


Figure 4.12 Fly Ash Particle Size Distribution at the IFGT Inlet for Each Coal Tested

impactor at the inlet to the IFGT system. As shown in the figure, the flyash size distribution for test series I and II (Ohio 5/6 and Pittsburgh coals) are nearly identical. The size distribution for test series IV (Ohio 6/5) is slightly larger, and the size distribution for test series III, Powder River Basin coal, is smaller. The mass median diameters for the four test series range from 4 μm to about 7 μm , which is in the range of that for coal-fired utility power plants.

4.5.1 Particle Removal Efficiency as a Function of Particle Size

Cascade impactor measurements were made for selected tests to determine the fly ash particle size distribution measurements at the inlet and outlet of the IFGT system. The particle size distribution combined with the measured particle loading at the inlet and outlet was used to determine the particle removal efficiency as a function of particle size.

Removal efficiencies calculated in this manner are subject to errors because of the small amount of mass collected on some of the filters (< 1 mg), and because the different flue gas conditions at the inlet and outlet flues result in slightly different cut sizes for the impactor plates. To minimize these errors, the following approach was used to determine removal efficiencies:

- The aerodynamic particle diameter cut size of the cascade impactor stages were calculated based on the flue gas properties, temperature and sample flow rate through the cascade impactor. The procedure followed was that recommended by Southern Research Institute⁽³⁾:

- The cumulative percent of mass and the particle loading were used along with the calculated particle diameter cut sizes to determine the cumulative mass loading (mg/dscm) as a function of particle size at the inlet and outlet.
- Linear interpolation of the cumulative mass loading data was used to determine the slope of the curve ($dm/d\log[D]$) at a set of diameters, D. Removal efficiency was calculated at each D as the percent change in ($dm/d\log[D]$) from the inlet to the outlet.

Cascade impactor measurements were made for seven different tests which spanned the four test series and included two different inlet gas velocities (loads). Table 4.6 provides a listing of the cascade impactor tests cross referenced to the test at which total removal measurements were also made. Five tests were conducted at full load and two tests were conducted at partial load.

Table 4.6 List of Cascade Impactor Tests

Cascade Impactor Test ID	Total Removal Test ID	Inlet Gas Velocity (m/s)	L/G (l/m³)	Gas Outlet Temperature Difference From Dew-Point (°C)	Comments
I-4L	I-4B	11.77	0.64	0.0	
I-14M	I-14D	12.05	0.70	-9.0	
I-4N	I-4J	11.79	0.64	1.0	Inter-stage Steam Injection
II-4G	II-4C	11.78	0.63	0.0	
III-12B	III-12A	7.10	0.36	0.0	Partial Load
IV-1B	IV-1A	11.14	0.52	0.0	Mesh Pad
IV-2B	IV-2A	7.02	0.47	0.0	Partial Load

Figure 4.13 shows the cumulative mass distribution at the inlet and outlet of the IFGT for test I-14. The data is presented as the cumulative mass as a function of fly ash aerodynamic particle size. The data in this figure shows that the mass median diameter (50% mass) at the inlet to the IFGT is about 5 μm , and is about 1 μm at the outlet.

Figure 4.14 shows the particle removal efficiency as a function of particle size calculated from the data presented in Figure 4.13. This curve has several general characteristics that are evident in all of the data:

- The removal efficiency is greatest at the largest particle size and then decreases rapidly with particle size below 3 μm .
- The removal efficiency decreases to a minimum value at about 0.6 μm .

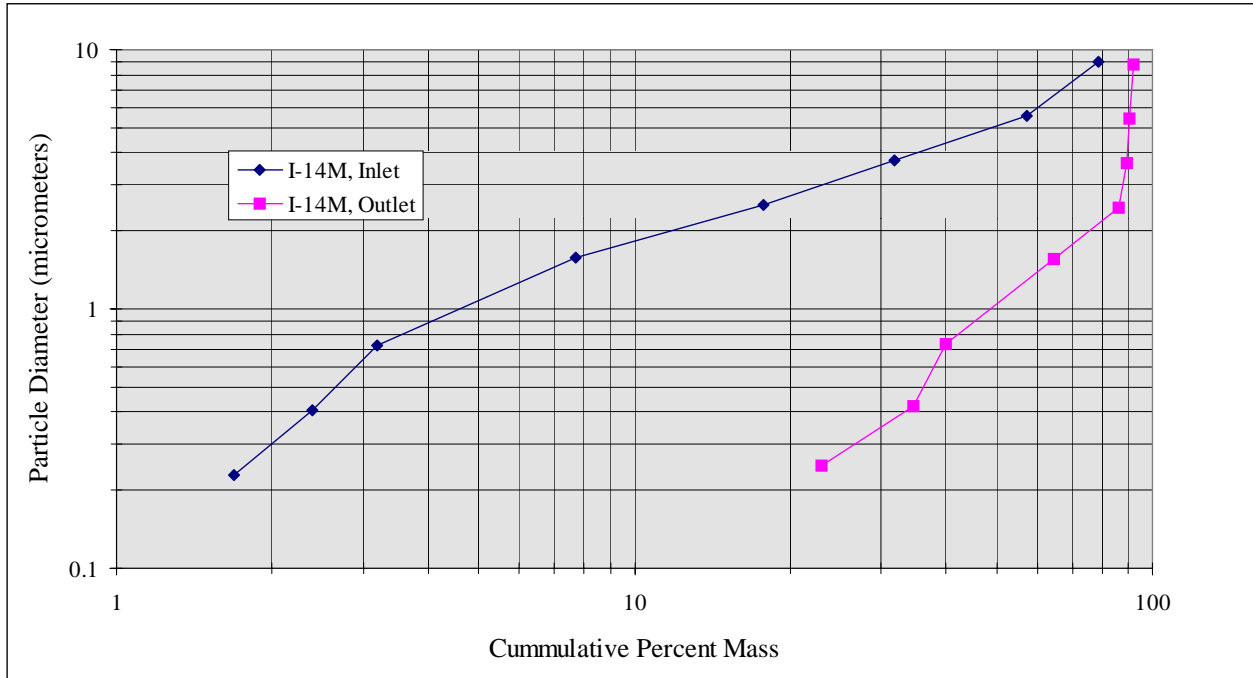


Figure 4.13 Fly Ash Particle Size Distribution at the Inlet and Outlet of the IFGT System for Test I-14M

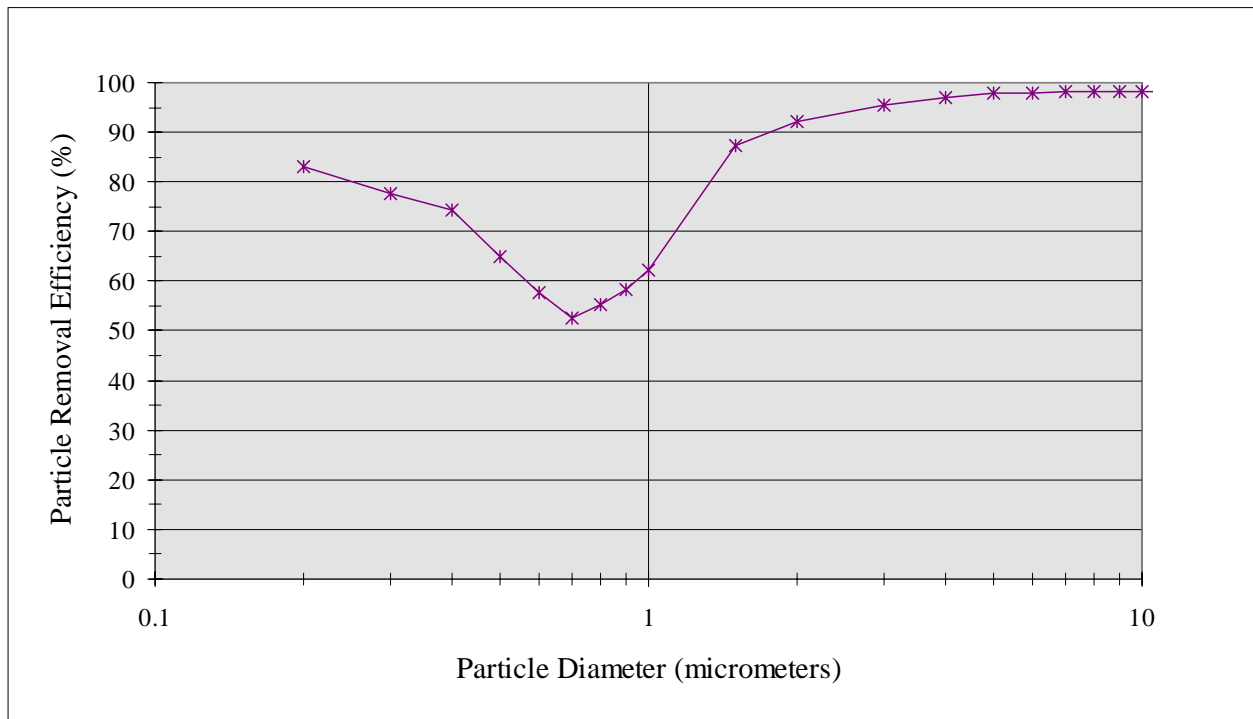


Figure 4.14 Particle Removal Efficiency by Particle Size for the Data in Figure 4.13

- the removal efficiency increases as particle diameter decreases for diameters below about 0.6 μm .

The removal efficiencies for particle sizes greater than 1 μm have the least uncertainty because they represent the greatest amount of mass collected on the filters. Similarly, the removal efficiencies for particulate less than 1 μm have the greatest uncertainty because they represent only a small fraction of the mass collected. Typically, the mass collected on the filters in this size range was less than .5 mg, and represented less than 5% of the total mass collected.

The decrease in removal efficiency with particle size is expected since the primary particle removal mechanism is inertial impaction, which is less effective as particle size decreases. The cause for the increase in removal efficiency for diameters less than $\sim 0.5\mu\text{m}$ is not known. In this size range diffusion and thermophoresis may become important mechanisms and enhance particle removal.

Figure 4.15 shows the removal efficiency as a function of particle size for the five full-load tests, and the average for the five tests. The data show that the average removal efficiency for particles greater than 1 μm is in excess of 90%, while the average removal for particles smaller than 1 μm is about 60%.

The removal efficiency as a function of particle size for the two partial load tests are shown in Figure 4.16. The two data curves have the same general shape as the data for full load, but with lower overall removal efficiencies. This again is not unexpected since the effect of inertial impaction is diminished as gas velocity is decreased.

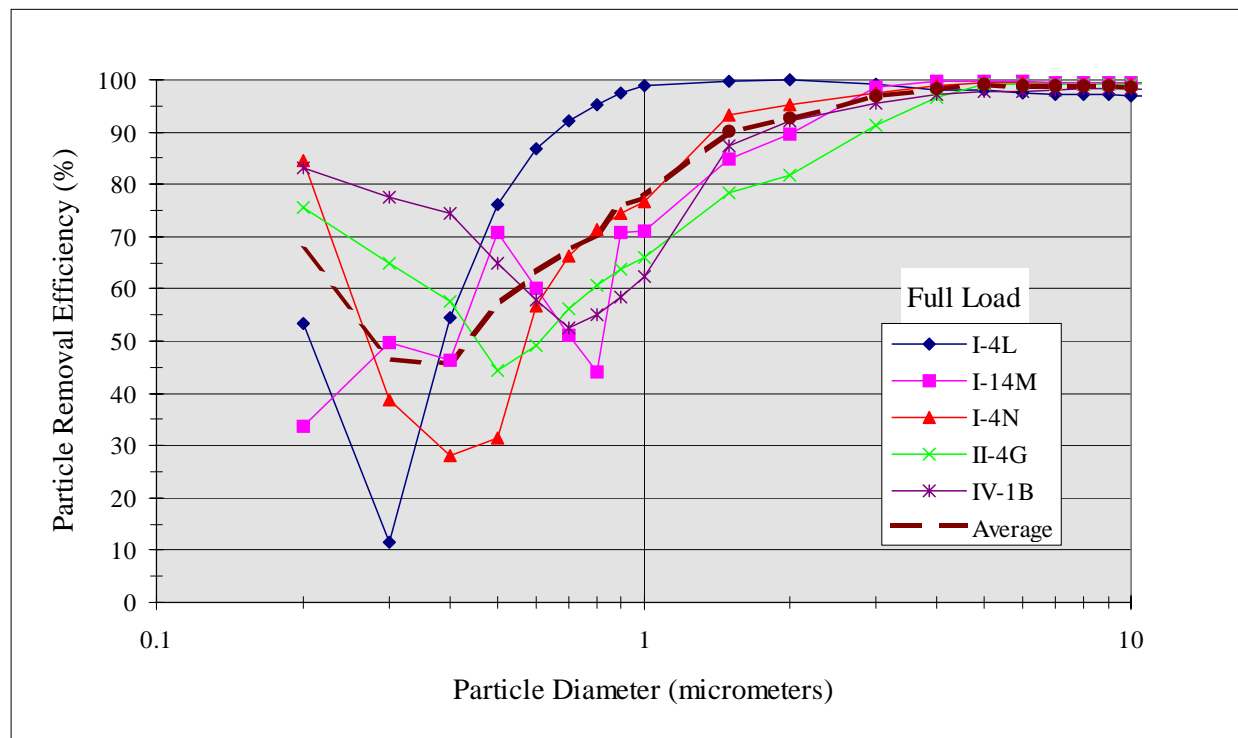


Figure 4.15 Particle Removal Efficiency by Particle Size for All Full Load Tests

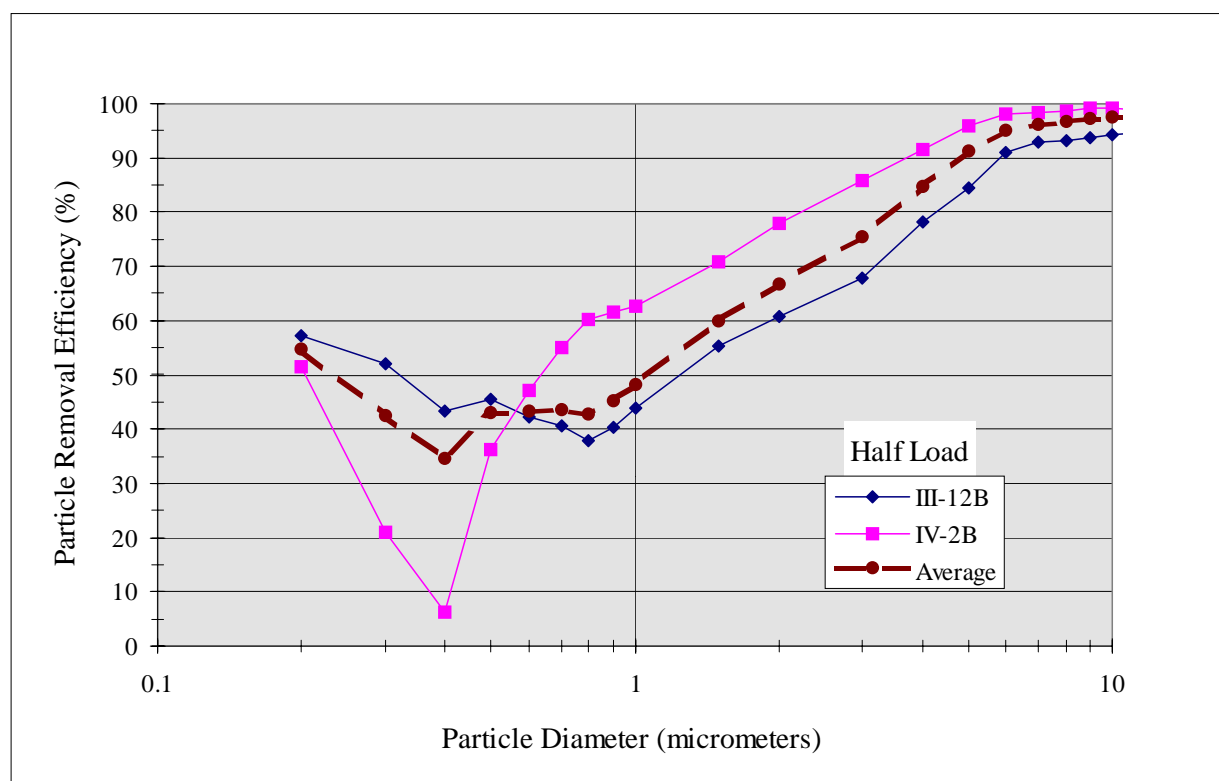


Figure 4.16 Particle Removal Efficiency by Particle Size For Partial Load Tests

4.5.2 Total Particle Removal

Particle loading at the inlet and outlet of the IFGT facility was made during all of the sampling for mercury/trace metals, chloride/fluoride, and ammonia, along with several dedicated Method 5 samples.

The only abnormal occurrence in the particle loading data occurred in test series II using the Pittsburgh #8 coal. With Method 5 sampling, the total collected particulate consists of the fly ash collected on a filter (filter particulate) and the fly ash that deposits on the sampling probe surfaces and is collected in a rinse (probe rinse particulate). In test series II, the probe rinse particulate was weighed with a scale of insufficient accuracy and resolution. For the test series II tests, particle removal efficiency was calculated based on the filter weights only. This is a conservative approach since for all tests, the probe rinse is a greater fraction of the total particulate collected at the inlet to the IFGT facility than at the outlet.

The particle removal data are shown in Table 4.7. Along with the particle loading and removal efficiency, this table also provides the type of test, sampling time, gas velocity at the CHX[®] inlet and the reagent liquid-to-gas ratio. For test series I, the particle loading exceeded 400 mg/dscm, and the particle removal efficiency exceeded 95%. For test series II, the inlet particle loading varied from about 0.7 to 400 mg/dscm, and the removal efficiency ranged from 23% to 94%. For tests II-4A and II-4F all of the flue gas was routed through the baghouse. The low inlet particle

loadings of 3.6 and 0.7 mg/dscm are the fugitive baghouse emissions and are well below the NSPS limit of 42 mg/dscm (0.03 lb/million Btu).

Table 4.7 Overall Particulate Removal Data

Test Number	Test Type	Total Sample Time (hrs)	Inlet Gas Velocity (m/s)	Outlet Gas Temperature (°C) ¹	L/G (l/m ³)	Inlet Particle Loading (mg/dscm)	Particle Removal Efficiency (%)
I-14D	M-29 Avg.	6.0	12.05	-9.0	0.70	842.	96.5
I-4A ²	M-26	1.7	11.87	0.0	0.67	722.	96.4
I-4J ³	M-5	2.0	11.79	1.0	0.64	711.	95.2
I-4F	M-5/NH ₃	2.0	11.95	0.0	0.65	644.	95.6
I-4B	M-29 Avg.	6.0	11.77	0.0	0.64	642.	97.2
I-4C	M-29 Avg.	6.0	11.78	0.0	0.63	401.	95.9
II-4C	M-29 Avg.	6.0	11.87	0.0	0.53	655.	93.9
III-7A	M-26	2.0	11.70	0.0	0.38	482.	88.7
III-9B	M-5NH ₃	1.3	11.60	1.0	0.35	480.	89.7
III-9A	M-29/OH Avg.	6.0	11.53	0.0	0.36	478.	88.4
IV-14A	M-29/OH Avg.	6.0	11.42	-1.0	0.49	296.	95.1
IV-1A	M-26	2.0	11.14	0.0	0.52	40.2	94.3
II-4A	M-29 Avg.	6.0	11.77	0.0	0.61	3.6	71.9
II-4F	M-5/NH ₃	2.0	11.94	-8.0	0.64	0.7	23.6
IV-2A	M-5	1.3	7.02	0.0	0.47	444.	93.0
III-12A	M-29/OH Avg.	6.0	7.10	0.0	0.36	384.	77.6

1) Gas Temperature Relative to The Water Vapor Dew Point Temperature

2) Woven Mesh Pad Located in the IFGT Interstage

3) Interstage Steam Injection

The removal efficiency for tests III-9A, -9B and -7A averaged about 89%, which is less than other data at comparable particle loadings. The lower overall removal efficiency for these tests is due to the finer fly ash particle size distribution for the Powder River Basin coal and the lower removal efficiency for the fine particulate.

From the data in the table, it is evident that the particle removal efficiency decreases as the particle loading to the CHX[®] is reduced. This is due to the size distribution of the particulate. The other trend in evidence in Table 4.7 is shown by tests III-9B and III-12A which show a decrease in removal efficiency as the gas velocity (i.e., load) is decreased.

In Test IV-2A, the use of wire mesh pads was investigated as a means of fine particulate removal. For this test four layers of mesh pad were located in the interstage between the first and second heat exchanger stages. The measured removal efficiency of 93% is substantially greater than the 77.5% removal efficiency for test III-12A which was also conducted at partial load, but without the use of a mesh pad. Although this is a substantial difference, most of the difference may be attributable to differences in the inlet particle size distribution.

With the exception of load (gas velocity) and particle loading, the removal efficiency is insensitive to other operating conditions over the range tested.

4.6 Mercury Removal

4.6.1 Measurement Methods and Detection Limits

The mercury content of the vapor and particle phases entering the IFGT facility were measured in each of the four test series. Triplicate two hour tests were conducted at each test condition. In the first two test series, mercury concentrations were measured exclusively using EPA Method 29 sample trains. During the third and fourth test series the triplicate measurements consisted of two Ontario Hydro sample trains bracketing a single Method 29 sample train. The sample time for the mercury measurements were two hours for each triplicate test.

The measurement accuracy of speciated forms of mercury using Method 29 and the Ontario Hydro method have not been resolved, and this issue is beyond the scope of this work. Rather, the concentrations of the speciated forms and the total mercury as determined using the Method 29 and Ontario Hydro are presented in this report with the caution that the absolute accuracy of the speciated concentrations are in question.

The concentration of mercury in the recovered impingers (vapor phase) and the concentration of mercury in the digested particulate samples (particle phase) was measured using Cold Vapor Atomic Absorption (CVAA). The detection for mercury measurements in the laboratory using CVAA is 0.1 parts per billion (ppb) for ionic mercury and 0.5 ppb for elemental mercury when measured in a prepared solution. The solution analyzed in the laboratory is prepared from the impinger and washing solutions gathered from the Method 29 and Ontario Hydro sampling trains. Mercury emissions are normally expressed on terms of micrograms per dry standard cubic meter, (ug/dscm). If the laboratory detection limits of 0.1 to 0.5 ppb are transformed to ug/dscm using typical Method 29 and Ontario Hydro sampling rates and impinger volumes, the detection limits can be compared to actual measurements to insure that these measurements are sufficiently above the detection limits to be meaningful. The estimated detection limits for mercury are summarized in Table 4.8. Also listed in Table 4.8 are the minimum reportable

Table 4.8 Mercury Detection Limits and the Minimum Reportable Concentrations

Mercury Form	Detection Limit in the Flue Gas (ug/dscm)	Minimum Reportable Concentration (ug/dscm)
Ionic Vapor Phase	0.02	0.5
Elemental Vapor Phase	0.20	1.0
Total Vapor Phase	0.22	1.0
Particle Phase	0.01	0.2
Total mercury	0.23	1.0
Mercury in the Coal	2.66	(-)

concentrations that have been used in this report. These minimum reportable concentrations take into account the detector's limits as well as triplicate test repeatability.

4.6.2 Mercury Concentration in the Coal

Typically, the concentration of mercury in the coal was determined from grab samples of the pulverized coal in the coal pipe just upstream of the burner. Grab samples were obtained at the start, middle, and end of a two-hour test period. A composite of the grab samples from the triplicate tests was used to obtain a test average coal sample for analysis.

Not all of the collected samples were analyzed for mercury. Rather, the mercury concentration in the coal provided measurement redundancy and a cross check by which the reasonableness of gas and particle phase measurements could be evaluated.

Figure 4.17 shows the concentration of mercury in the flue gas that would result from 100% emission of the mercury contained in the coal for each coal in the four test series. The error bars indicate the range of multiple measurements. The mercury level from the Ohio #5/#6 coal (Test Series I) and the PRB coal are relatively high, while the Pittsburgh #8 and Ohio #6/#5 coal are relatively low*. The coals selected for the pollutant removal tests were based primarily on sulfur content and origin. Within those parameters, coals with high mercury concentrations were desired in order to provide increased measurement accuracy associated with the absolute concentrations and mercury removal. The mercury concentration in the Ohio and Pittsburgh coals are within ranges generally reported in the literature.⁴ The concentration of mercury in the PRB coal is higher than typically reported in the literature.

4.6.3 Comparison of Gas Phase Mercury Speciation from Method 29 and the Ontario Hydro Method

Mercury vapor in the flue gas exists in both elemental (Hg^0) and ionic (Hg^{++}) forms. The ionic form is the more reactive of the two, so that ionic mercury is more readily removed in sulfur scrubbing systems. EPA Method 29 sampling has been validated for measuring metals concentration, including mercury, in the vapor state. With this technique, the metal vapors are trapped by the chemical solutions in the sample impinger bottles. The ability of Method 29 to distinguish between the different forms of mercury in the vapor state has been under question, and alternate methodologies (Ontario Hydro, for example) have been proposed to more accurately assess the concentration of the two forms of mercury.

In test series III and IV, triplicate measurements consisted of an EPA Method 29 sample train bracketed by two Ontario Hydro (OH) sample trains. A comparison of the ionic mercury concentration measured with the two techniques at the inlet and outlet of the IFGT facility are shown in Figure 4.18. The OH data are the average of two measurements and the uncertainty bars indicate the data range.

* Ohio #5/#6 denotes a blend of 80% Ohio #5 and 20% Ohio #6. The Ohio #6/#5 contained 80% #6 and 20% #5.

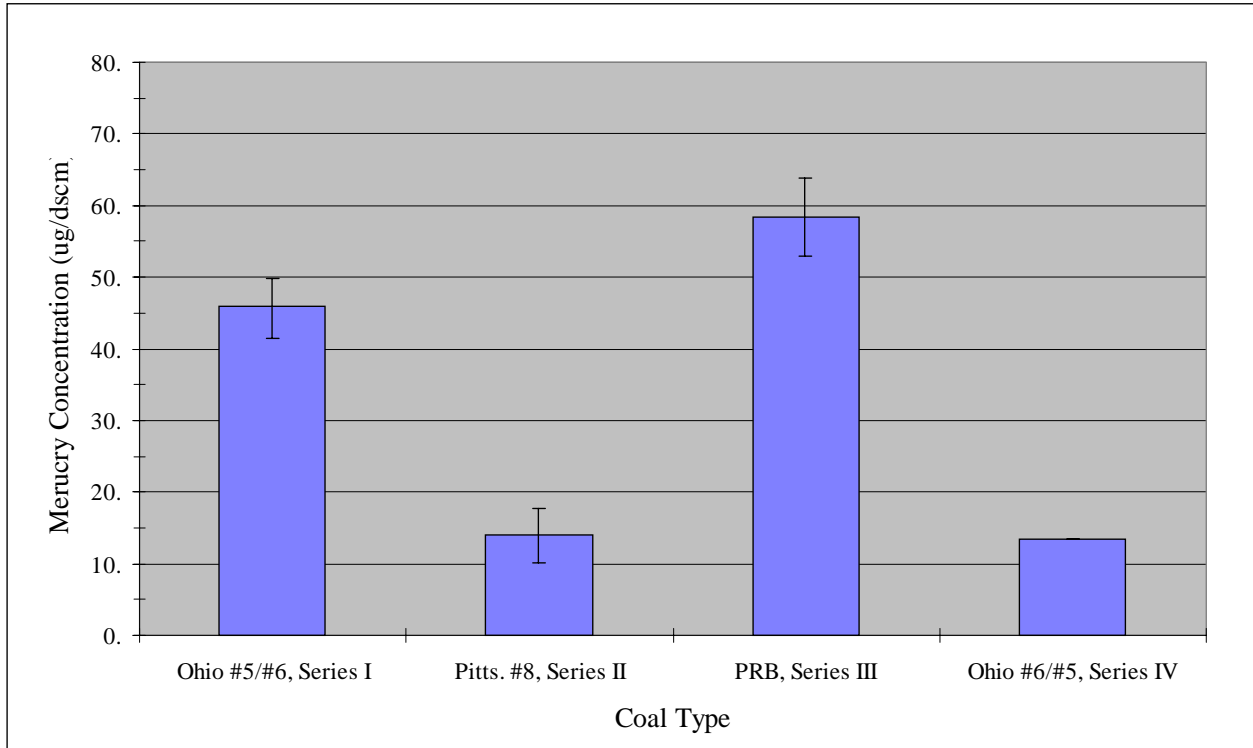


Figure 4.17 Flue Gas Mercury Concentration Resulting from 100% Release of Mercury in the Coal

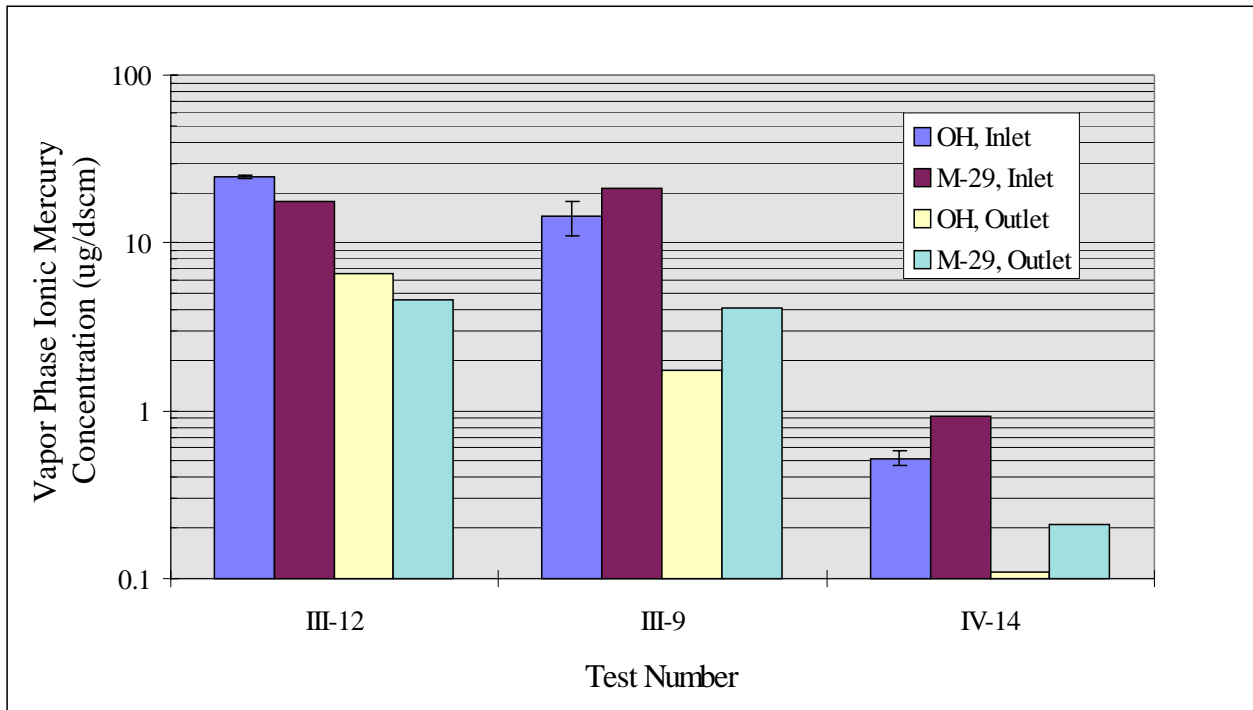


Figure 4.18 Comparison of Vapor Phase Ionic Mercury Measured Using Method 29 and Ontario Hydro (OH) Sample Trains

Figure 4.18 shows that at the inlet to the IFGT facility, the OH measurement of Hg^{++} exceeded the M-29 measurement of Hg^{++} in test III-12, while in test III-9 and IV-14, the M-29 measurement exceeded the OH measurement. In all three tests, the M-29 measurement is outside the range of the OH measurements.

Comparison of the OH and M-29 data at the outlet of the IFGT indicate the same trend, so that the relative change in Hg^{++} across the IFGT system is nearly the same for either technique. This indicates that the difference between the two measurement techniques may have been due to a real variation in Hg^{++} concentration in the flue gas over the six hour duration of the triplicate tests. The difference in the average ionic mercury concentration between tests series III and IV is due to the coal used for each test. Test III used a PRB coal while test IV used an Ohio coal.

Figure 4.19, is a corresponding comparison of the two measurement techniques for elemental mercury at the inlet and outlet of the IFGT facility. For tests III-12 and III-9 the elemental mercury concentration was quite high and the difference in concentration between the two measurement techniques at the inlet and outlet location are quite small. For test IV-14 the concentration of Hg° was very low. The OH method provides a slightly larger measured value of Hg° at both the inlet and outlet of the IFGT. The relative difference between the two techniques for this test is greater than for test series III, but the absolute difference is again very small.

Comparison of the OH and M-29 measurements of elemental and ionic mercury show only relatively small differences, and the difference is consistent at the inlet and outlet measurement locations. For this reason, no further distinction will be made between the two techniques with respect to the total concentration of mercury or the speciated forms of mercury. The data from the two measurement techniques were averaged to determine test average mercury concentrations and removal efficiencies.

4.6.4 Mercury Partitioning

Mercury is a relatively volatile element that can exist in the flue gas as a vapor and can also be attached to particulate carried by the flue gas. Figure 4.20 shows the concentration of mercury in the flue gas at the inlet to the IFGT facility as vapor, and that contained on the particulate, for all of the tests. The particulate and vapor forms are both in the common basis of $\mu\text{g}/\text{dscm}$. Expressed in this form, it is understood that the particle phase mercury concentration in the flue gas depends not only on the mercury concentration in the fly ash, but also the fly ash concentration in the flue gas.

Figure 4.20 shows that for test series I and III most of the mercury is partitioned to the vapor phase and is very repeatable from test to test. In test series II the total vapor phase concentration was below reportable limits, while in test II-4C the particulate concentration is larger than for any other test. In test IV-14 the vapor phase concentration is about the same as the particulate phase. For the data shown in Figure 4.20, the particle loading to the IFGT facility was about the same for all tests.

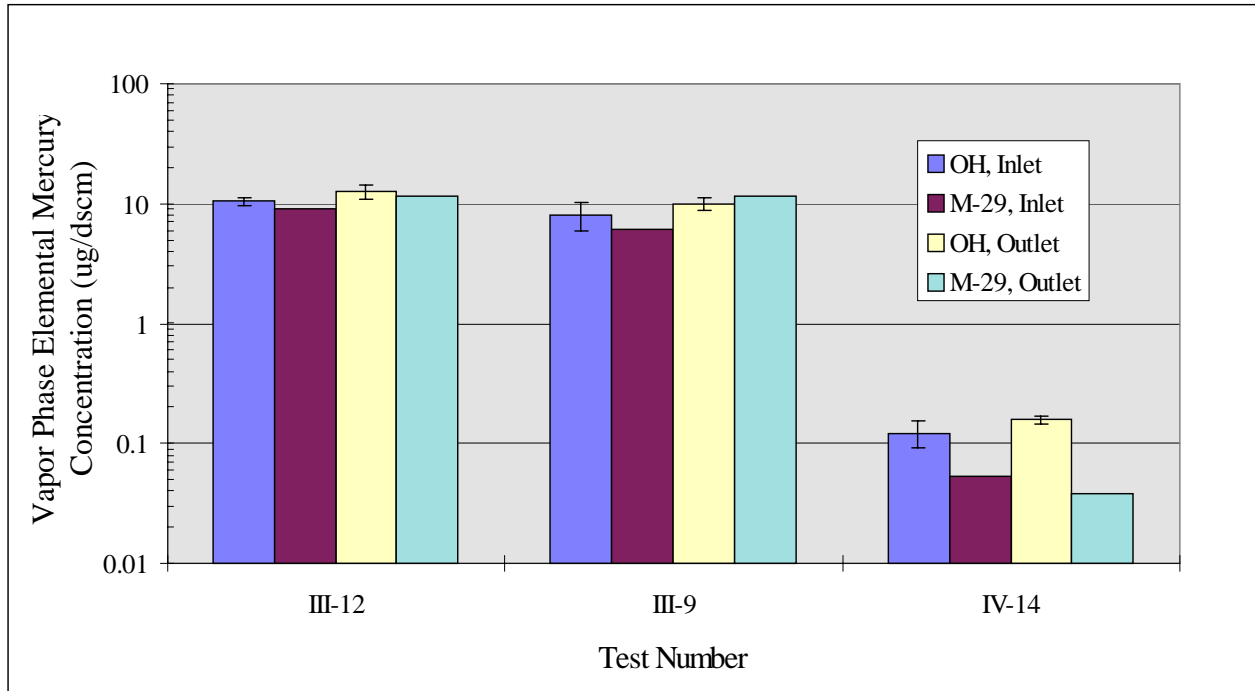


Figure 4.19 Comparison of Vapor Phase Elemental Mercury Measured Using Method 29 and Ontario Hydro Sample Trains

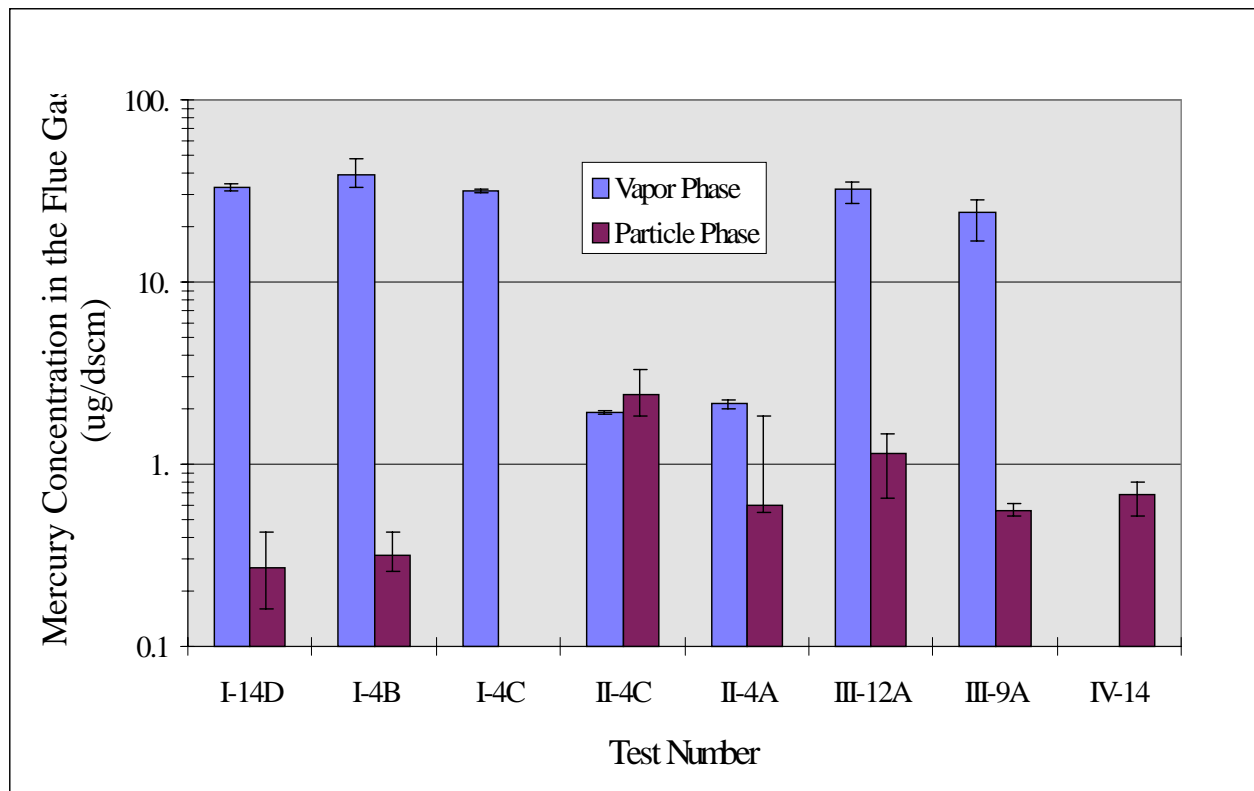


Figure 4.20 Vapor Phase and Particle Phase Concentrations of Mercury in the Flue Gas

The differences in particle phase concentration shown in Figure 4.20 is primarily due to differences in mercury concentration in the fly ash, and not particle loading. The cause of the variation from one test series to the next is not known, but is likely dependent on the coal type. Field measurements of mercury concentrations at utility power plants have traditionally shown wide variation.⁽⁵⁾ Precautions were taken during the tests to ensure that combustion conditions were duplicated for each of the four tests. This included the same burner, excess air, load, primary and secondary air temperatures, coal grind (fineness), downstream equipment and operating procedure.

4.6.5 Vapor Phase Mercury Removal

Figure 4.21 shows the triplicate average ionic mercury concentration at the inlet to the IFGT facility and the calculated removal efficiency for each test. The vertical bars on the concentration data indicate the range of the triplicate measurements. The vertical bars on the removal efficiency is the estimated uncertainty based on the standard deviation in the triplicate measurements.

For test series I, III, and IV the ionic mercury removal efficiencies ranged from 75% to 85%, while for test series II the removal efficiency averaged less than 0%. Removal efficiencies on the order of 70% to 90% for ionic mercury are to be expected.⁽⁶⁾ The measured concentrations for test II are just above reportable limits, and so may be subject to relatively large error. However, the measured concentrations for test IV-14 are similarly low, and are in agreement with the data for test series I and III. The data and analysis procedures from test series II have been reviewed and a cause for the abnormal results could not be found. However, the data are not in agreement with that from the other three test series and are not in agreement with data reported in the literature, and so should be considered questionable.

Figure 4.22 shows the average concentration and removal efficiency of elemental mercury for each test. The removal data averages from about 0% to -35% and is independent of mercury concentration or coal type. Elemental mercury removal data is not presented for test series II as the concentrations were below reportable limits.

The indicated increase in elemental concentration across the IFGT facility was not limited to triplicate averages at the inlet and outlet. Essentially all paired inlet/outlet measurement of elemental mercury indicated some increase in concentration. This effect may be real, if captured ionic mercury is reduced to elemental mercury and subsequently evolved from the scrubbing solution. This effect may also be an artifact of the sample trains used to measure ionic and elemental mercury.

Removal efficiencies of about 0% for elemental mercury are in general agreement with published data for other flue gas treatment equipment, primarily wet scrubbers.⁽⁷⁾ An anticipated benefit from low temperature operation of the IFGT facility was not realized. The outlet flue gas temperatures for the data in Figure 4.22 ranged from about 27°C to 37°C (80°F to 98°F), which is well below the normal operating temperature for wet scrubbers.

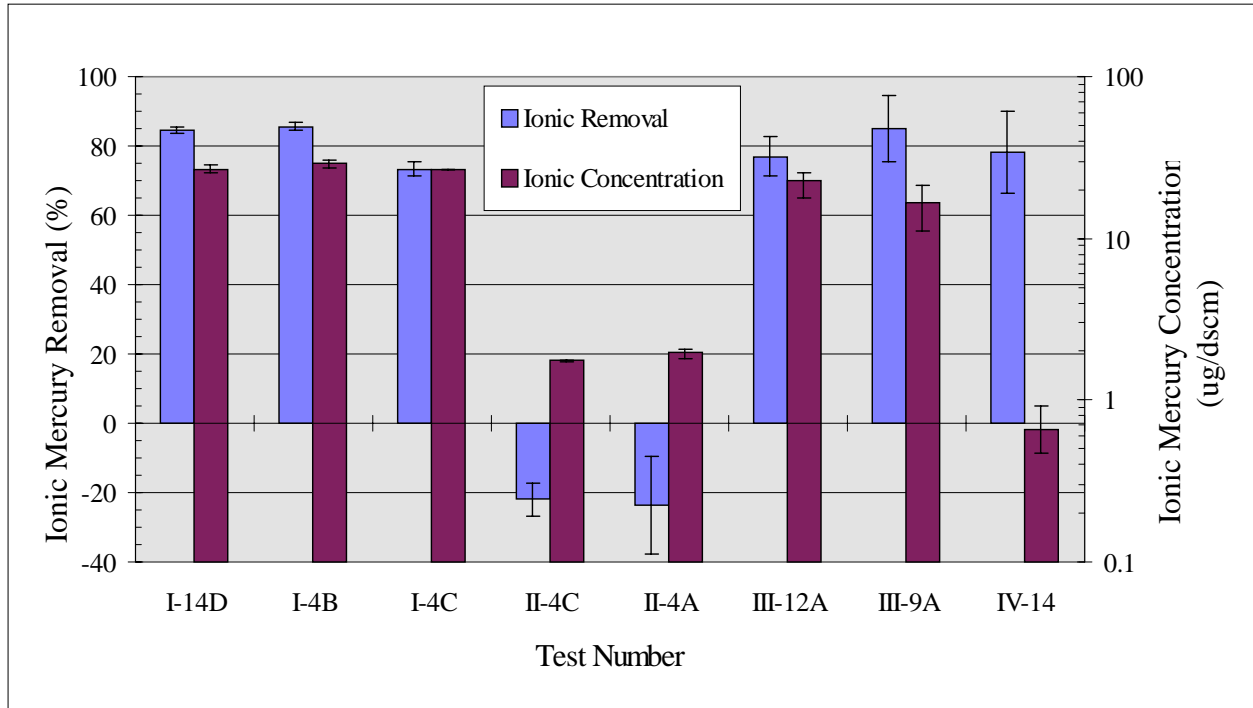


Figure 4.21 IFGT Removal Efficiency for Ionic Mercury (Left y-axis) and Ionic Mercury Concentration (Right y-axis)

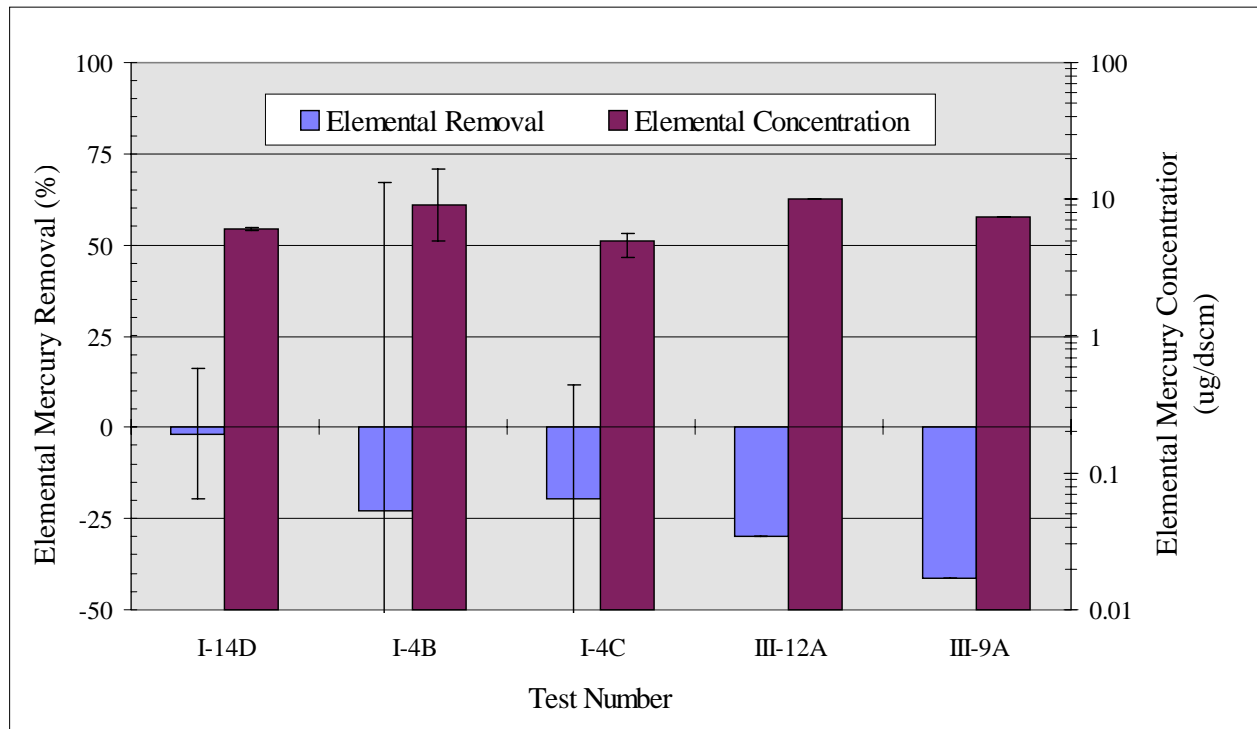


Figure 4.22 IFGT Removal Efficiency for Elemental Mercury (Left y-axis) and Elemental Mercury Concentration (Right y-axis)

4.6.6 Particle Phase Mercury Removal

The particle phase mercury concentration and removal efficiency for each of the tests are shown in Figure 4.23. Data are shown only for those tests in which the mercury concentration was above reportable limits. Three of the tests show an average removal efficiency of about 75%. Of the two tests that have lower removal efficiencies, test III-12A was conducted at partial load, and the lower mercury removal (42%) was due to a lower particulate removal efficiency (77%). The cause of the low removal efficiency of test III-9A is unknown. As indicated by the uncertainty limits, the measured concentrations of particulate mercury in the triplicate tests varied significantly.

The particle phase mercury removal is less than the overall particulate removal because the mercury concentration in the particulate at the outlet of the IFGT facility averaged 3 to 5 times greater than at the inlet. This indicates that the mercury tends to be concentrated in the sub-micron particulate, which is less effectively removed by the IFGT process.

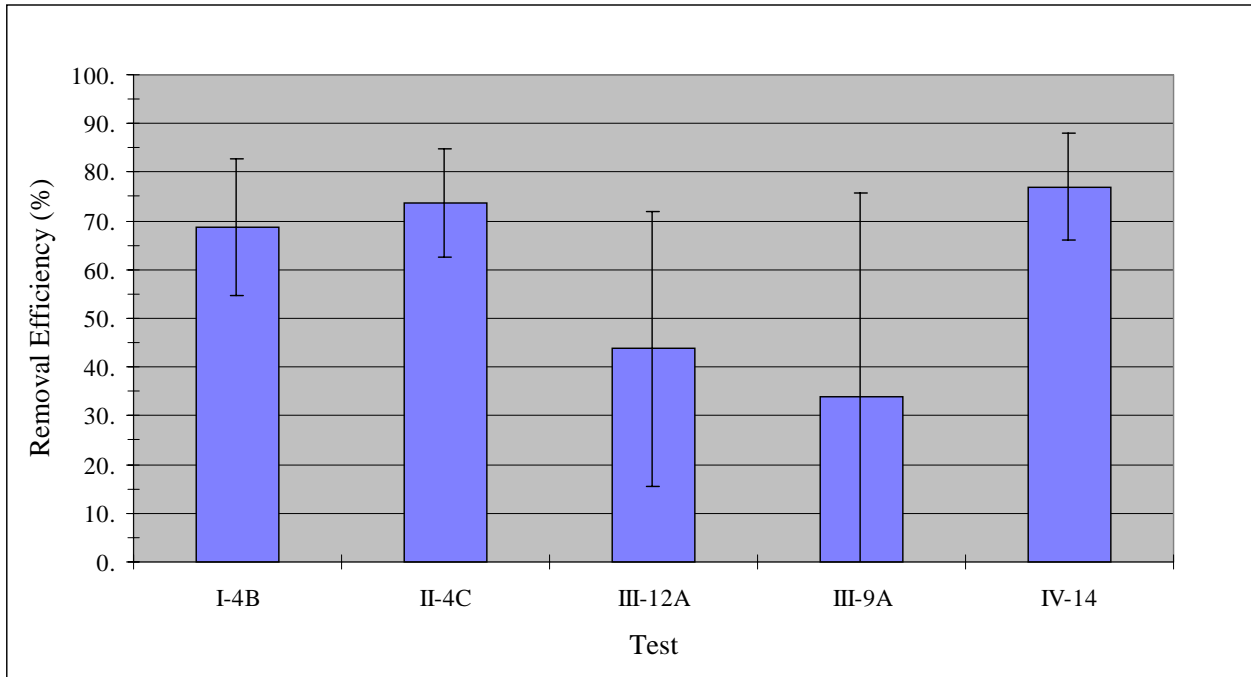


Figure 4.23 Removal Efficiency for Particle Phase Mercury

4.7 Trace Element Removal

4.7.1 Trace Element Measurement and Detection Limits

The trace element content of the vapor and particle phases entering the CHX[®] were measured in each of the four test series. Triplicate two hour tests were conducted at each test condition. In the first two test series, element concentrations were measured exclusively using EPA Method 29 sample trains. During the third and fourth test series the triplicate measurements consisted of two Ontario Hydro sample trains bracketing a single Method 29 sample train. The sample time for the Method 29 and Ontario Hydro trains were two hours for each of the triplicate tests. The Ontario Hydro sample trains were used primarily to obtain comparative mercury speciation data.

The concentration of trace elements in the recovered impingers and the concentration of trace elements in digested particulate samples were measured using graphite furnace atomic absorption (GFAA). Table 4.9 lists the limits of detection of the trace elements for the gas phase, fly ash, and coal samples that are typical for the four test series for the M-29 sample train. Also shown are the minimum reportable detection limits which have been defined as 10 times the detectable limit or 1.0 ug/dscm, whichever is greater for gas phase concentrations.

Table 4.9 Detection and Reporting Limits for Trace Elements

Element	Vapor Phase Limits		Particle Phase Limits		Coal
	Detection Limit (ug/dscm)	Reporting Limit (ug/dscm)	Detection Limit (ug/dscm)	Reporting Limit (ug/dscm)	Detection Limit (ppm)
Arsenic	0.117	1.2	0.064	1.0	0.20
Barium	1.173	11.7	0.643	6.4	2.00
Beryllium	0.059	1.0	0.439	4.4	0.10
Cadmium	0.012	1.0	0.026	1.0	0.02
Chromium	0.117	1.2	0.064	1.0	0.40
Cobalt	0.235	2.4	0.161	1.6	0.20
Lead	0.117	1.2	0.142	1.4	0.20
Manganese	0.117	1.2	0.101	1.0	0.40
Nickel	0.235	2.4	0.161	1.6	0.20
Selenium	0.117	1.2	0.142	1.4	0.20

Although Ontario Hydro trains have not been validated for trace elements other than mercury at this time, vapor phase trace elements were also measured in the Ontario Hydro impingers for test series III. The detection limits for vapor phase metals from OH sample trains are about 5 times

greater than for the M-29 sample trains shown in Table 4.9. For test series III and IV the vapor phase concentration of all trace elements except mercury were below reportable values for both the OH sampling methods, so that an accurate comparison of the two techniques using this data cannot be made.

4.7.2 Vapor Phase Trace Element Removal

Most of the trace elements are non-volatile and condense to a solid state at relatively high temperatures. Generally, trace elements measured in the vapor phase were below the reportable limits of detection at the inlet to the CHX[®]. This was especially true for the Pittsburgh and PRB coals for which gas phase concentrations of trace elements was very low. The exceptions are arsenic and selenium which occurred in fairly high concentration for several of the coals tested. Significant quantities of lead, nickel, and manganese were occasionally measured, but the repeatability of the concentration data as determined by the triplicate measurements was poor.

Figure 4.24 shows the concentrations and removal efficiency for arsenic for test series I and IV that used the Ohio coals. The uncertainty bars on the concentration represent the range of triplicate measurements, while the uncertainty bars on removal efficiency represents a root mean square (rms) uncertainty based on triplicate concentration measurements. The concentration of arsenic for the Pittsburgh and PRB coals were below reportable limits, and are not shown. For the tests shown in Figure 4.24, the arsenic concentration varied from 20 to 70 ug/dscm, and the removal efficiency was greater than 95%. The removal efficiency for test IV-14A with a mag-lime reagent is no different than for the other tests in which soda ash reagent was used.

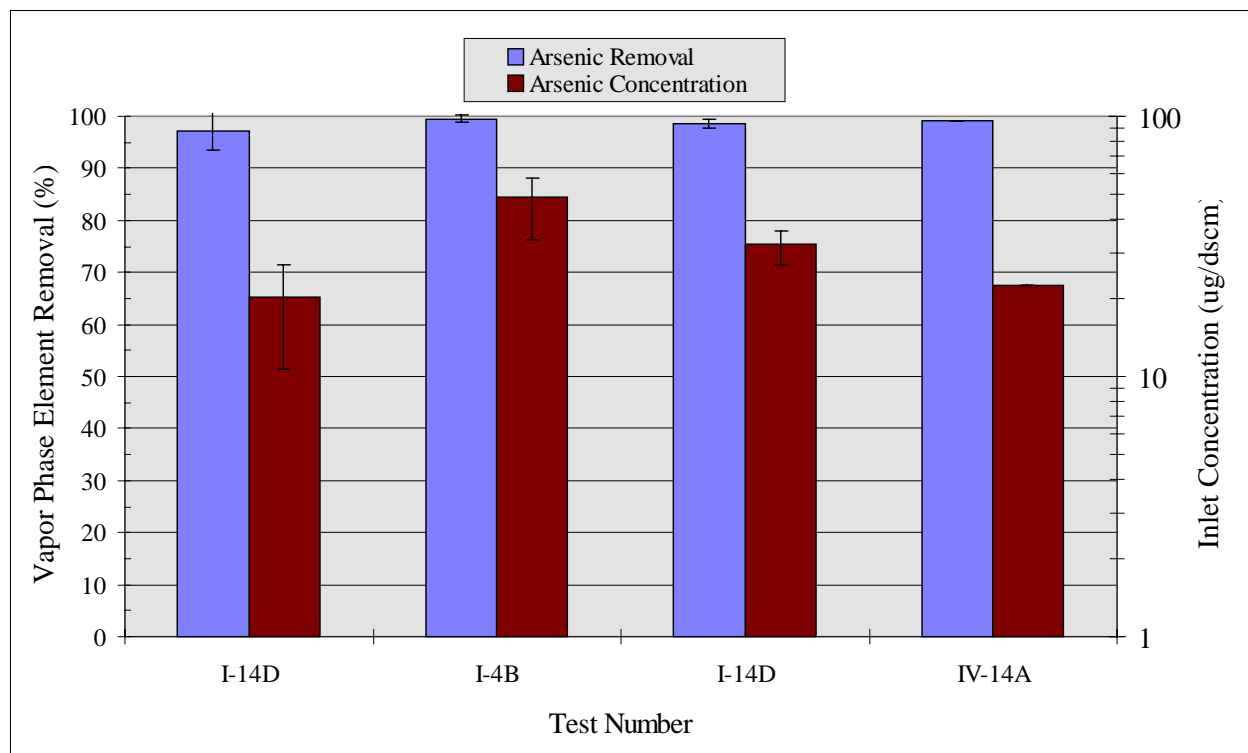


Figure 4.24 IFGT Removal Efficiency for Vapor Phase Arsenic (Left y-axis) and the Inlet Concentration (Right y-axis)

Figure 4.25 is a similar figure showing the concentration and removal efficiency for vapor phase selenium. Reportable quantities of selenium were measured in the Pittsburgh coal (series II) as well as for the Ohio coals (series I and IV). For test series I and test II-4C the selenium concentration and removal efficiency are both quite high. For test II-4A, the removal efficiency is about 50%, but the concentration is just above the reportable limit, and the uncertainty in the removal efficiency is quite large.

Test IV-14A represents a single Method 29 sample. The removal efficiency is lower than for tests with comparable concentrations. The lower removal efficiency for this test may be due to the mag-lime reagent that was used. All other tests were conducted with sodium based reagent.

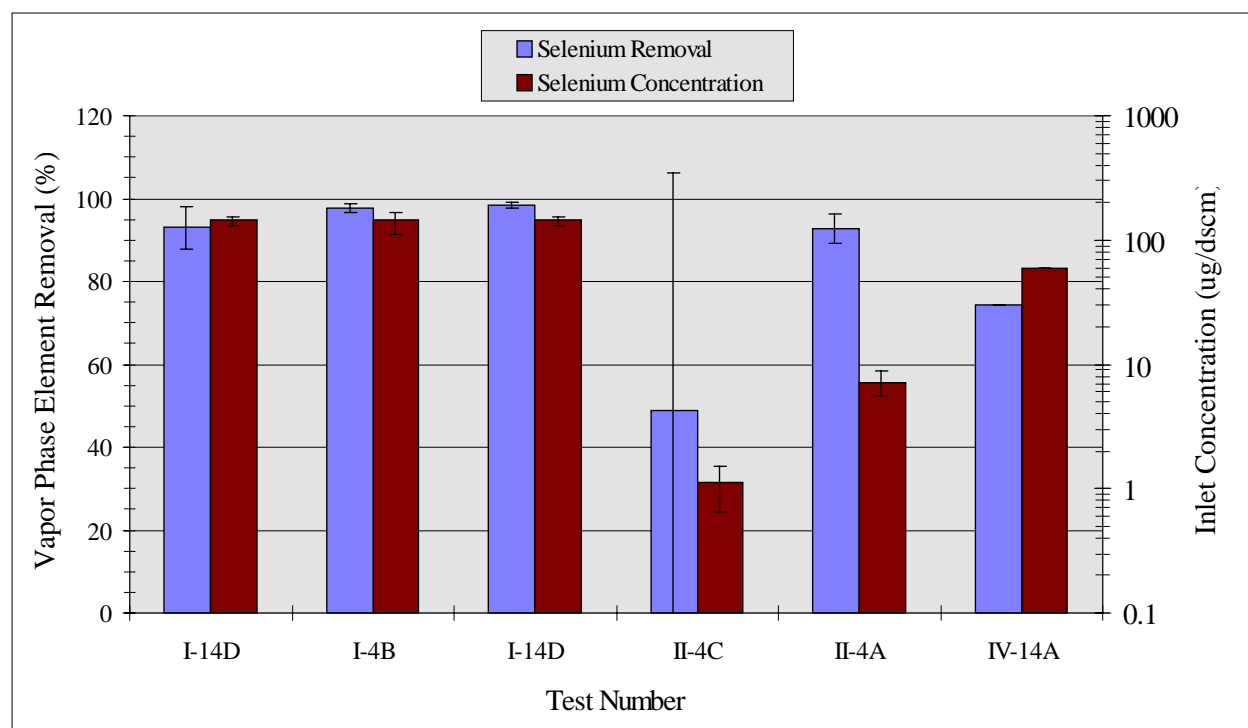


Figure 4.25 IFGT Removal Efficiency for Vapor Phase Selenium (Left y-axis) and the Inlet Concentration (Right y-axis)

4.7.3 Particle Phase Trace Element Removal

When expressed on a gas phase basis, the concentration of an element contained on particulate depends on both particulate concentration in the flue gas and the element concentration in the particulate. It is the product of these two numbers which represents the total quantity of the element in the flue gas.

Figure 4.26 shows the particle phase concentration of the elements in the flue gas at the inlet for three tests that represent the three different coals. For these three tests the particle loading at the inlet to the CHX[®] was relatively constant, so most of the test to test variation shown in the figure is due to variation of the elemental concentration in the particulate.

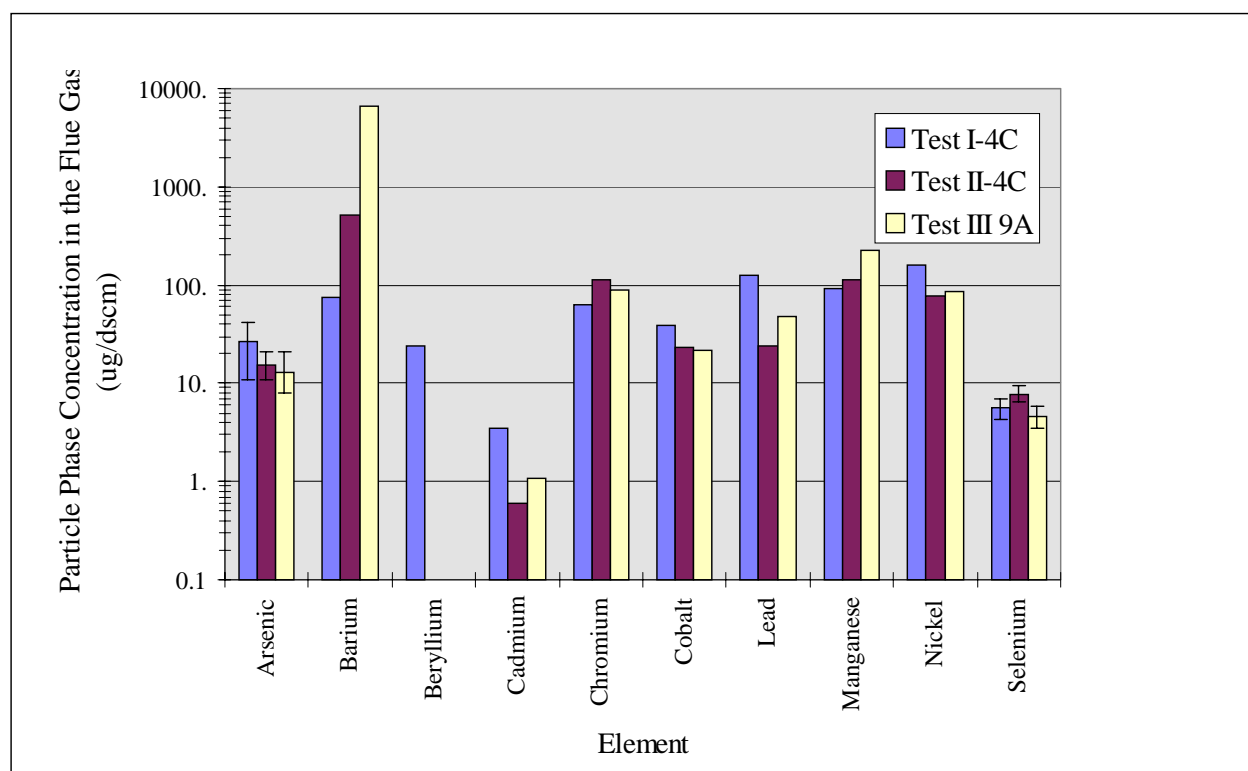


Figure 4.26 Particle Phase Elemental Concentration at the IFGT Inlet

Chromium has the lowest concentration of all of the elements measured, and is just above reportable limits. For most of the elements the variability with coal type (Ohio, Pittsburgh and PRB) is less than the variability from element to element. The exception is barium which had a very high concentration for test series III (PRB coal).

Figure 4.27 shows the element removal efficiency for the particle phase data. Measured data from all full-load tests are included in this figure. The particle phase removal efficiencies range from about 20% for cadmium to 100% for Beryllium. In general, although the concentration of cadmium in the particulate was above reportable limits, the triplicate measurements indicated a large variability.

For all elements except beryllium, the removal efficiency for the element is less than the removal efficiency measured for the particulate. For the tests shown in Figure 4.27, particle removal efficiencies ranged from 87% to 96%. The reduced efficiency for the removal of these elements compared to removal of the total particulate is caused by enrichment in the fine particulate.

With the exception of beryllium, all elements indicated a higher concentration in the fly ash at the outlet of the IFGT system than at the inlet to the IFGT system. This is illustrated by Figure 4.28 which shows the ratio of the element concentration in the particulate at the inlet of the CHX[®] to that at the outlet. As shown, the element concentration in the fly ash at the outlet is generally 2 to 10 times that at the inlet. Since the median particle size of the flyash at the outlet is about one-fifth of that at the inlet (1 micron vs 5 microns) this indicates that the fine

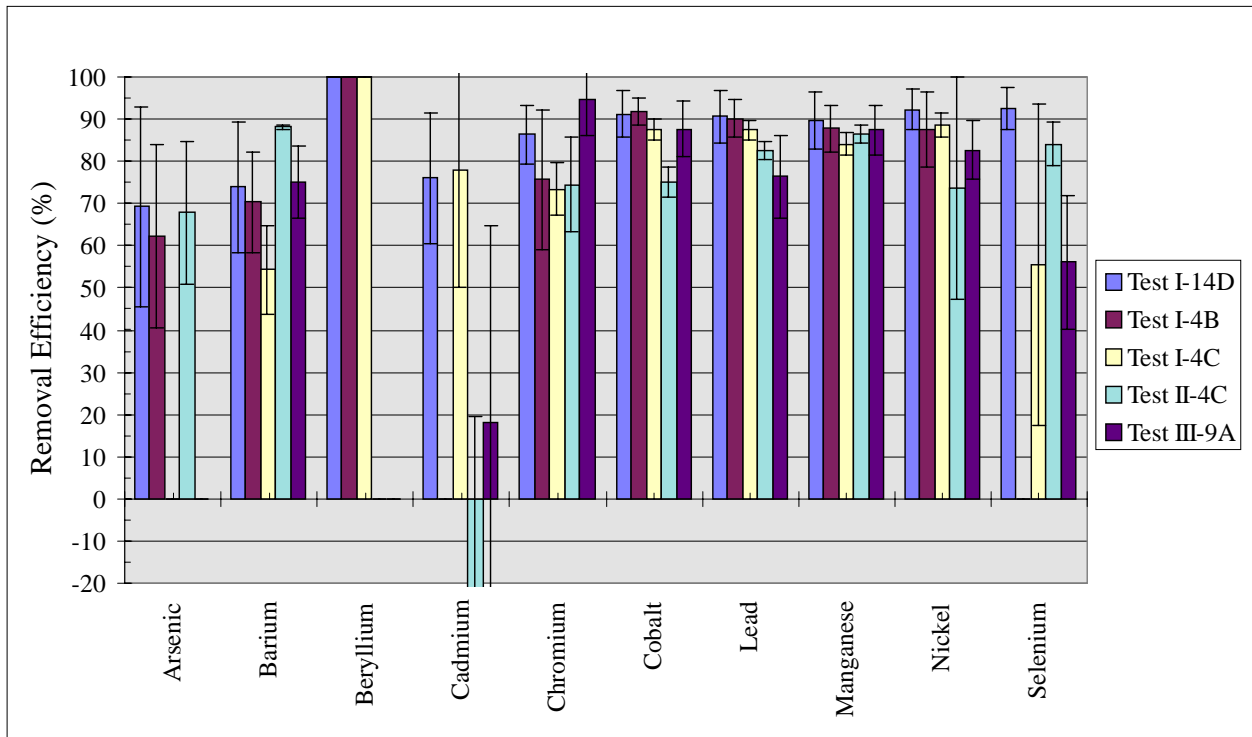


Figure 4.27 Particle Phase Trace Element Removal Efficiency

particulate contain proportionately higher concentrations of these elements. The removal of the element is less than the removal of the total particulate because the fine particulate, of which only 60% is removed, contains a disproportionate amount of the element.

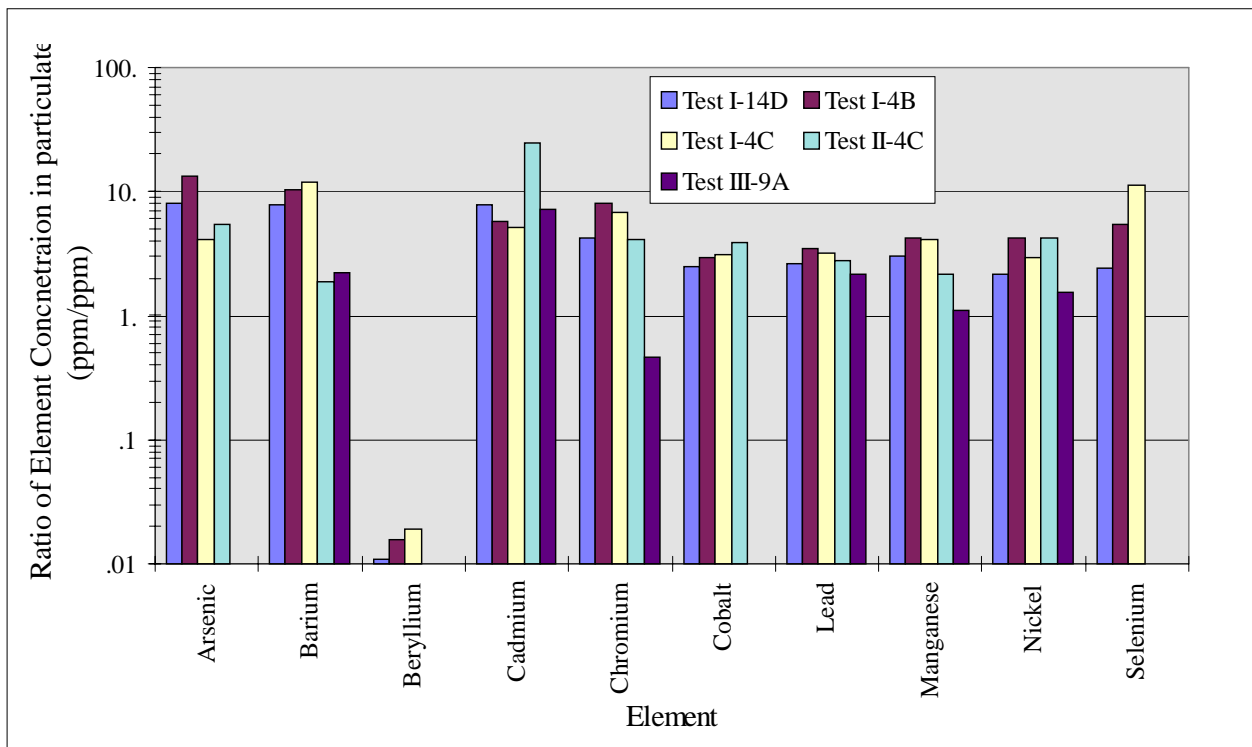


Figure 4.28 Ratio of Element Concentration in the Fly Ash at the IFGT Outlet to the Inlet

4.8 NO_x Removal

NO_x concentrations at the inlet and outlet of the IFGT facility were measured during test series I. Although removal of NO was not anticipated, NO₂ removal with the sodium based reagent was possible. The NO_x measurements in Test Series I were performed to determine if any measurable reduction in NO_x occurred in the IFGT process.

Figure 4.29 shows the calculated NO_x removal efficiencies for all of measured data. Within the experimental error of the measurements, NO_x removal averaged 0% for all of the tests. Based on these results, NO_x measurements were suspended for the remaining tests.

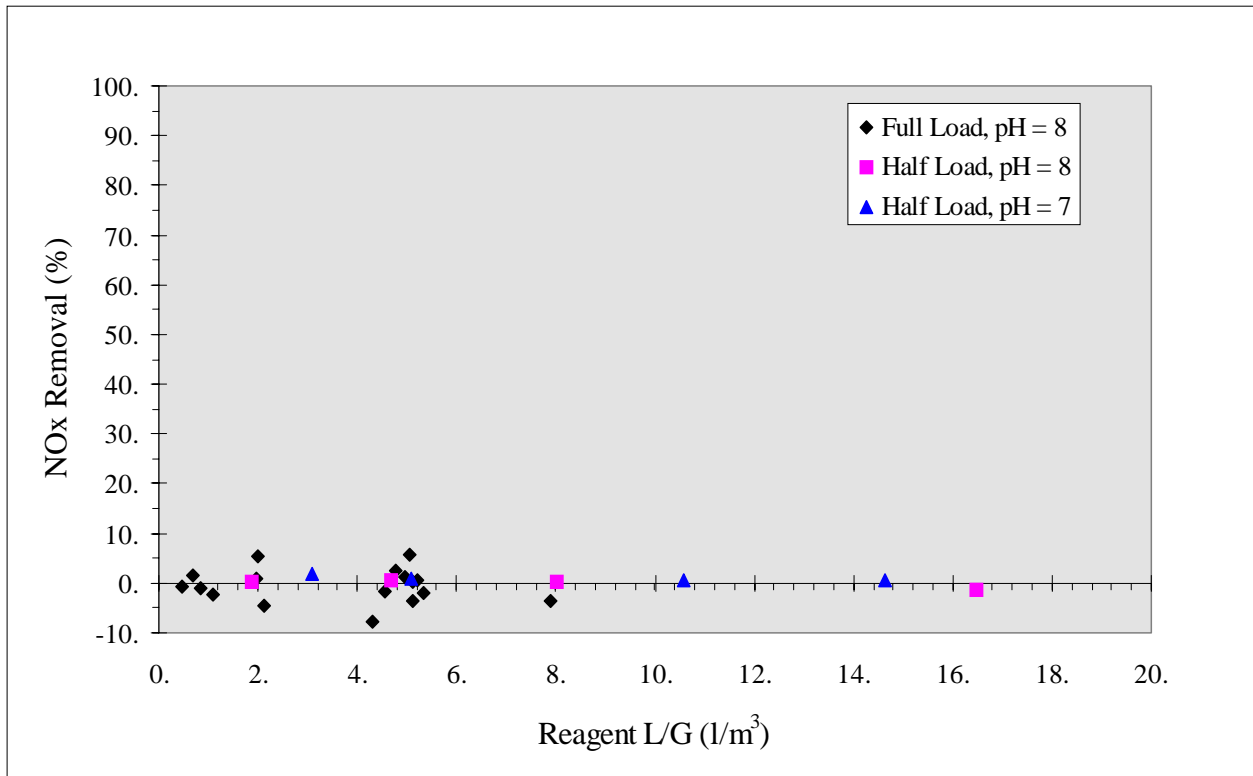


Figure 4.29 Measured NO_x Removal as a Function of L/G for Test Series I

4.9 Wear Tests at ECTC

4.9.1 Operation Summary and Discussion

Over the course of the wear tests, the CHX[®] pilot test unit was operated "at conditions" for 6,240 hours. During this time, all major design conditions operating ranges were met and maintained. A summary of the major operating conditions and the actual operating ranges is given in Table 4.10.

Table 4.10 Summary of CHX[®] Operating Conditions at the ECTC

Operating Parameter	Range or Value
Inlet Gas Flow	1275 scmh (750 scfm)
Inlet Gas Temperature	150°C (300°F)
Inlet Water Temperature	55 to 60°C (130 to 140°F)
Outlet Gas Temperature	82 to 93°C (180 to 200°F)
Outlet Water Temperature	76 to 80°C (170 to 175°F)
Inlet Particulate Loading (EPA M5 average)	25 mg/dscm (0.022 lb/10 ⁶ Btu) 2,060 hours 400 mg/dscm (0.35 lb/10 ⁶ Btu) 4,180 hours
Tube Wash Cycle	20 minutes every 8 hours

The particulate loading to the inlet of the CHX[®] test unit is reported as an average unit because the loading was increased partway through the test. The above value represents an average of the measured values after the change in particulate loading. A graphical summary of the CHX[®] inlet particulate loading over the course of the test program is shown in Figure 4.30. The particulate loading data presented in Figure 4.30 was obtained using an Environmental Systems P-5A *in situ* particulate monitor. The P-5A monitor was operated on a continuous basis and served as a qualitative indicator for the particulate loading level to aid ECTC personnel in maintaining a steady particulate loading to the CHX[®]. EPA Method 5 particulate sample trains were performed periodically to confirm the particulate loading. Particulate loadings from the EPA Method 5 sample trains are considered to be the official particulate loading data for Task 3.

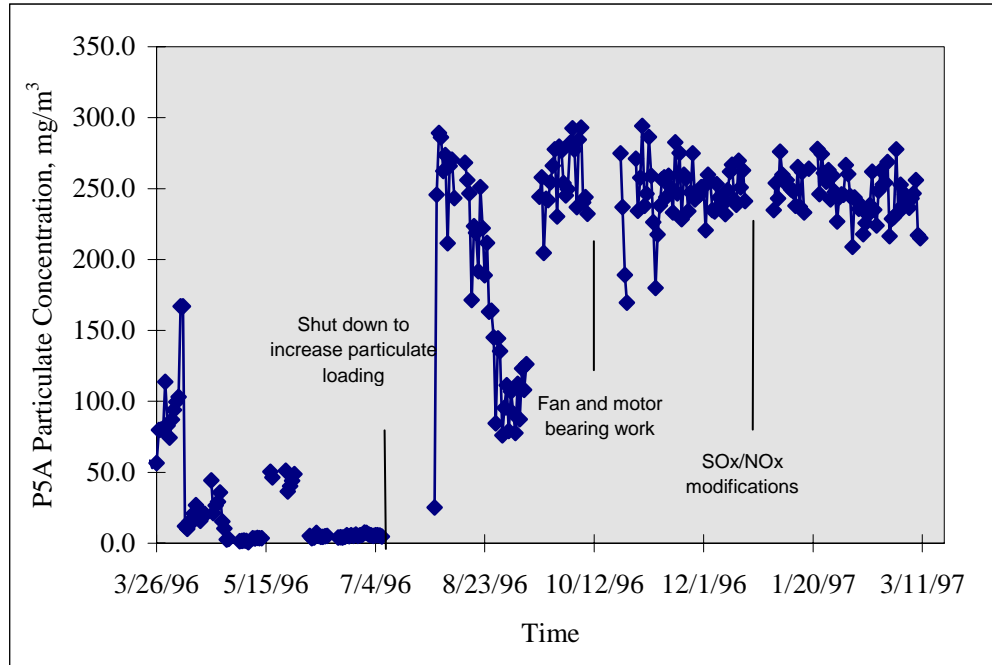


Figure 4.30 P-5A Measurements of Particulate Concentration During the One Year Wear Test

Visual inspections of the top surface of the CHX[®] heat exchanger were made both before and after scheduled tube washings during each inspection trip. In every case, the "dirty" inspection revealed a uniform coating of fly ash on each tube with no apparent bias from one tube to another. This coating covered the top (leading) half of each tube. Minimal fly ash was found on the bottom (trailing) half. After washing, the "clean" inspection revealed essentially complete removal of the fly ash coating, with only isolated areas (<5% total visible surface area) retaining some of the fly ash. Photographs of typical "dirty" and "clean" tubes may be found in Figures 4.31 and 4.32, respectively. The clean area in the center of Figure 4.31 is due to inadvertent contact with the tube surface prior to being photographed.

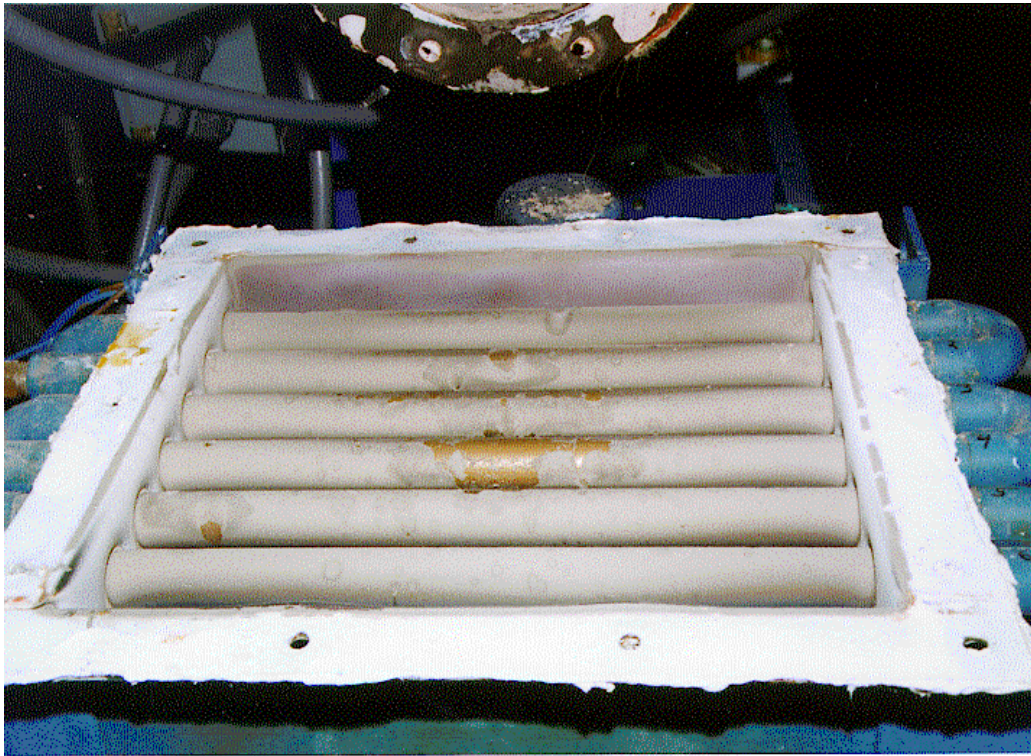


Figure 4.31 Top of CHX[®] Heat Exchanger Prior to Washing



Figure 4.32 Top of CHX[®] Heat Exchanger After Washing

After approximately 5,000 hours of operation, several fly ash deposits were found in the heat exchanger which were unaffected by the wash cycle. These deposits began approximately halfway down the heat exchanger, on the tubes closest to the walls, and continued to the bottom of the heat exchanger. These deposits can be seen in Figure 4.33. The most likely cause for these deposits is inadequate wash water flow rate. The initial wash water setup consisted of one

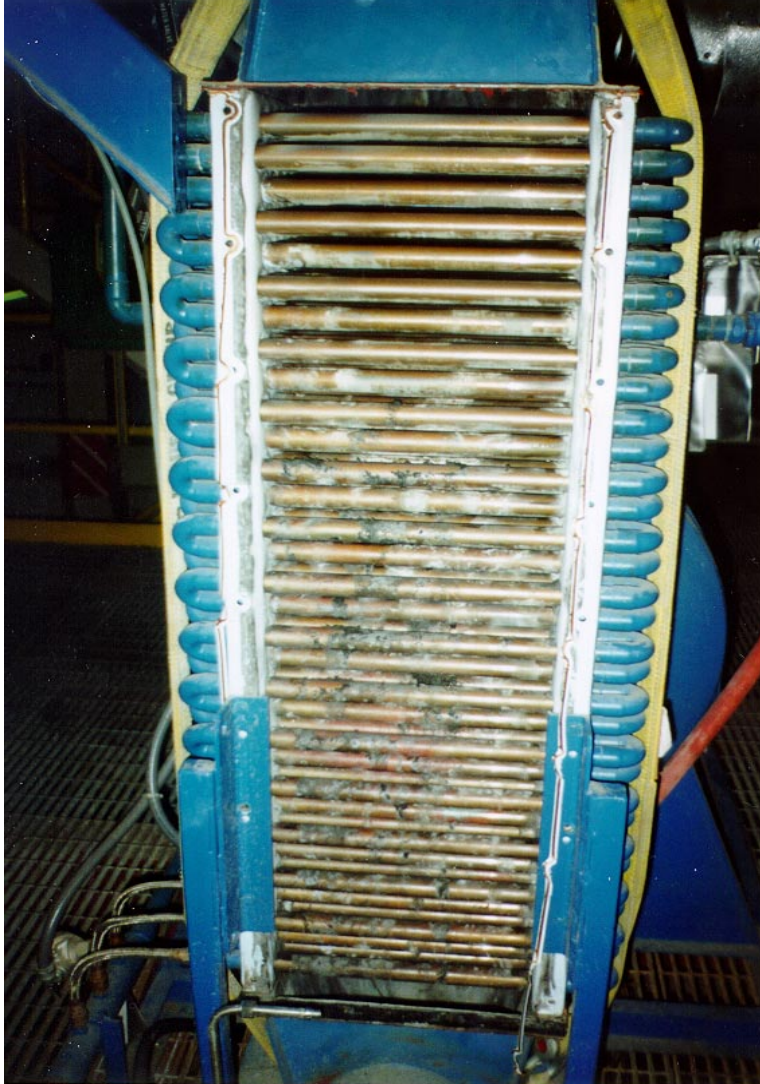


Figure 4.33 Fly Ash Deposits on the Tubes in the CHX® Heat Exchanger

(1) spray nozzle with a nominal flow rate of 3.8 lpm (1 gpm) which operated for 20 minutes every 8 hours. This is the standard wash cycle for oil-fired applications. While the top few rows of tubes were effectively cleaned, being subjected to the most energetic cleaning, the tubes further down in the heat exchanger were essentially cleaned by wash water dripping from the tubes above. Any deposits which were not removed, but only wetted, then served as sites for additional fly ash deposition. Based on these findings, a new wash nozzle manifold, consisting of three (3) equally spaced 3.8 lpm (1 gpm) nozzles, was installed for the remainder of the test. This new manifold was also operated for 20 minutes, effectively tripling the wash water flow rate.

The effect of the modified wash water manifold can be seen in Figures 4.34 and 4.35. In Figure 4.34, the percent solids of the wash water effluent is shown for the two manifold setups. For the original setup (1 nozzle), it can be seen that the percent solids concentration levels off at the end of the wash cycle, indicating that less than complete solids removal is occurring. With the modified manifold (3 nozzles), not only is the percent solids concentration continually decreasing, the initial and final concentrations are higher (and lower, respectively), indicating more complete solids removal.

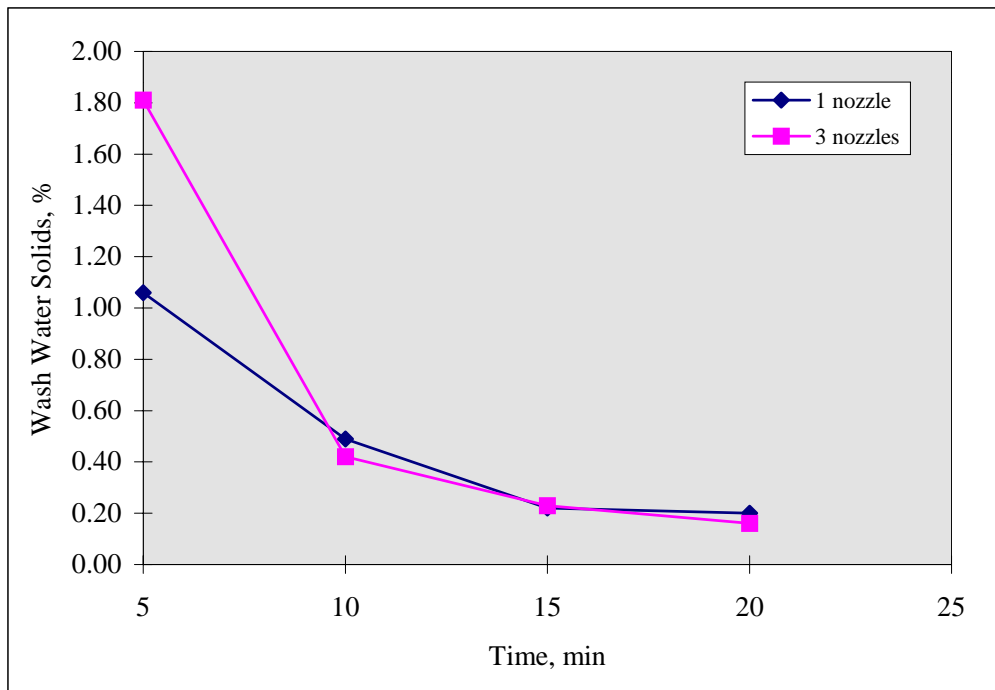


Figure 4.34 Wash Water Solids Concentration

In Figure 4.35, the heat exchanger differential pressure drop is shown as a function of time for the last four extended operating periods. The first three periods were conducted with one wash nozzle in service, the last with the three-nozzle manifold. In each of the first three operating periods, the differential pressure drop increased by approximately 100 Pa (0.4 in. H₂O) and was increasing, while the pressure drop increase for the last period was approximately 50 Pa (0.2 in. H₂O) and essentially steady.

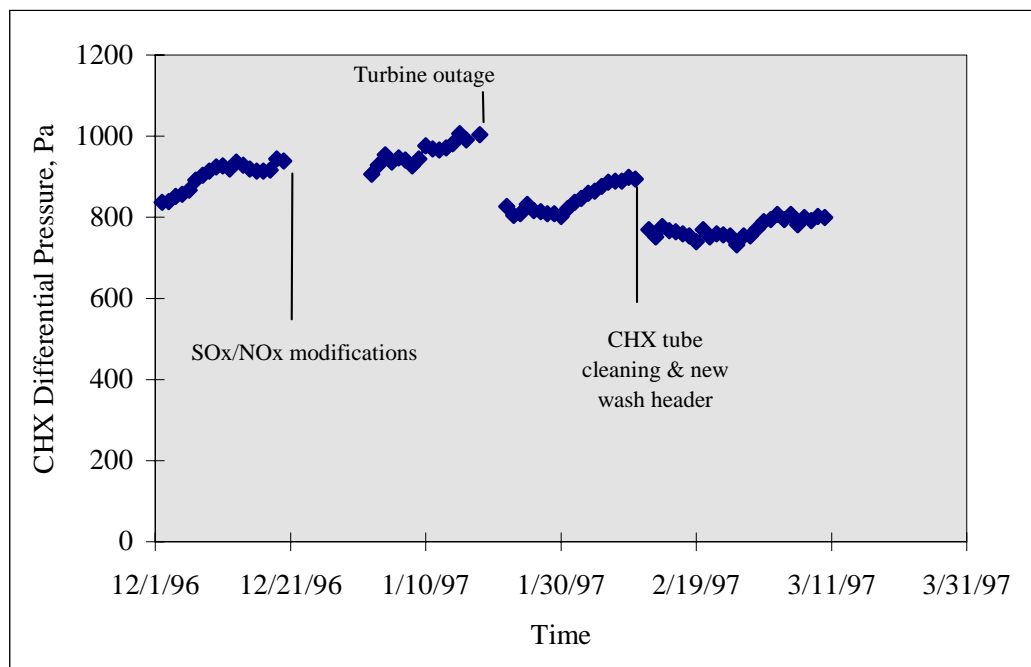


Figure 4.35 Differential Pressure Across the CHX[®] Unit as a Function of Time

4.9.2 Wear Performance Discussion

The primary goal of Task 3 was to determine the amount of wear, if any, incurred by the Teflon[®] internals of the CHX[®] pilot unit's heat exchanger (specifically the heat exchanger tube surfaces), while operating under typical flue gas conditions. As mentioned in Section 4.2, three measurement techniques were employed in an effort to determine the amount and type of wear. This section will focus on the results from two of the techniques (eddy current film thickness and surface replication). The third technique (vertical and horizontal tube dimensions) is not included in this discussion for the reasons outlined in Section 4.2.

Teflon[®] Film Thickness Measurements

Six complete sets (including measurements taken prior to flue gas exposure) of film thickness measurements were obtained during the course of the test program. Each set consists of 90 data points for the top row of tubes (3 angles * 6 tubes * 5 locations) and 30 data points for the second row of tubes (1 angle * 6 tubes * 5 locations). Tabular summaries of each of the data sets are located in Appendix A of Addendum II. All film thickness data presented in the tables and in graphical form have been normalized.

Results of the film thickness measurements indicated that no significant reduction in tube film thickness occurred during the course of the test program. Figures 4.36 and 4.37 illustrate this finding. The data presented in Figures 4.36 and 4.37 represent the average tube values for measurements taken in the vertical position for tubes 1 through 6 and tubes 7 through 12, respectively.

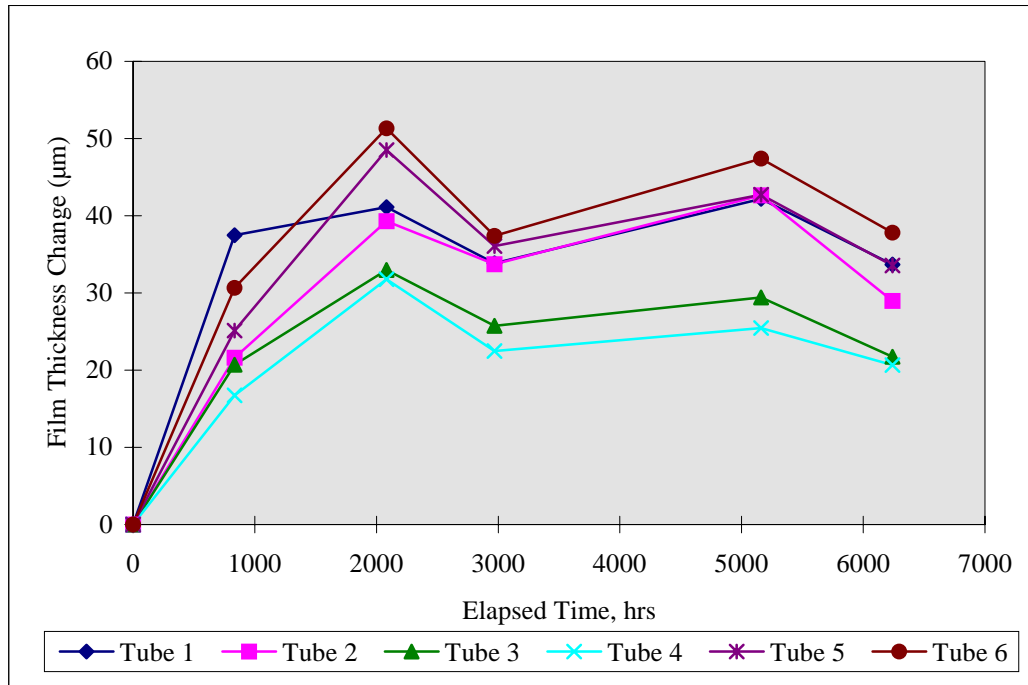


Figure 4.36 Cumulative Change in Teflon® Film Thickness as a Function of Time for Tubes 1 through 6

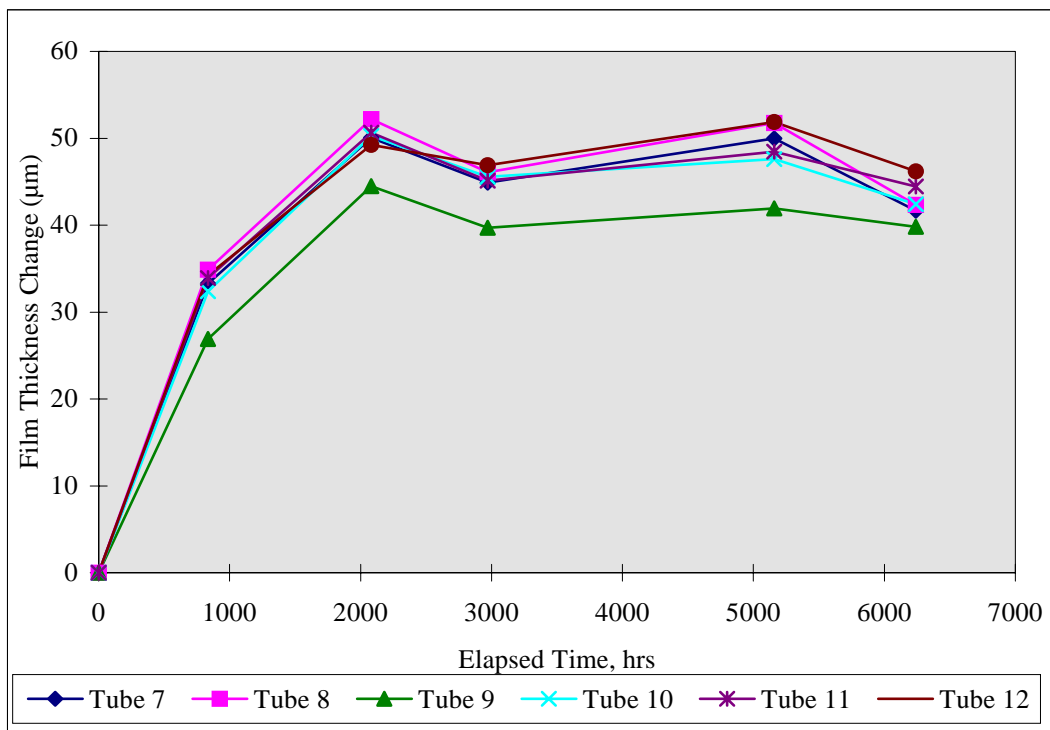


Figure 4.37 Cumulative Change in Teflon® Film Thickness as a Function of Time for Tubes 7 through 12

As illustrated in the two figures, after an initial increase in film thickness, no significant decrease was observed for any of the measured tubes. The increase in film thickness observed during the first two inspection trips is most likely due to the relaxation of surface stresses in the Teflon[®] film. These surface stresses result from the manufacturing process, and stress relaxation occurs when the Teflon[®] film is heated. The amount of increase ranged from 30.5 to 50.8 μm (1.2 to 2.0 mils), representing a 7 to 10% increase for a nominal 508 micron (20 mil) film.

As mentioned in Section 4.2, thickness measurements were also obtained for angles of +45° and -45° from the vertical at each of the measurement locations. These off-angle measurements were conducted to expand the amount of film surface being inspected and thus offer a more complete picture of any potential wear patterns and tendencies. In addition, the flue gas velocity at these locations was higher, creating the potential for greater abrasive wear than on the top surface of the tubes. In Figures 4.38 and 4.39, film thickness data is plotted as a function of both time and measurement angle for tubes 1 and 5, respectively. Due to the flue gas flow pattern from the inlet plenum to the first row of tubes, tubes 1 and 5, respectively, were chosen as representative of minimal and maximal potential wear sites. Tube 6, having the greatest potential for wear in the top row, was not chosen for this comparison due to instrument positioning problems during inspection, resulting in greater measurement variation. Plots for the other 4 tubes from the top row may be found in Appendix G of Addendum II.

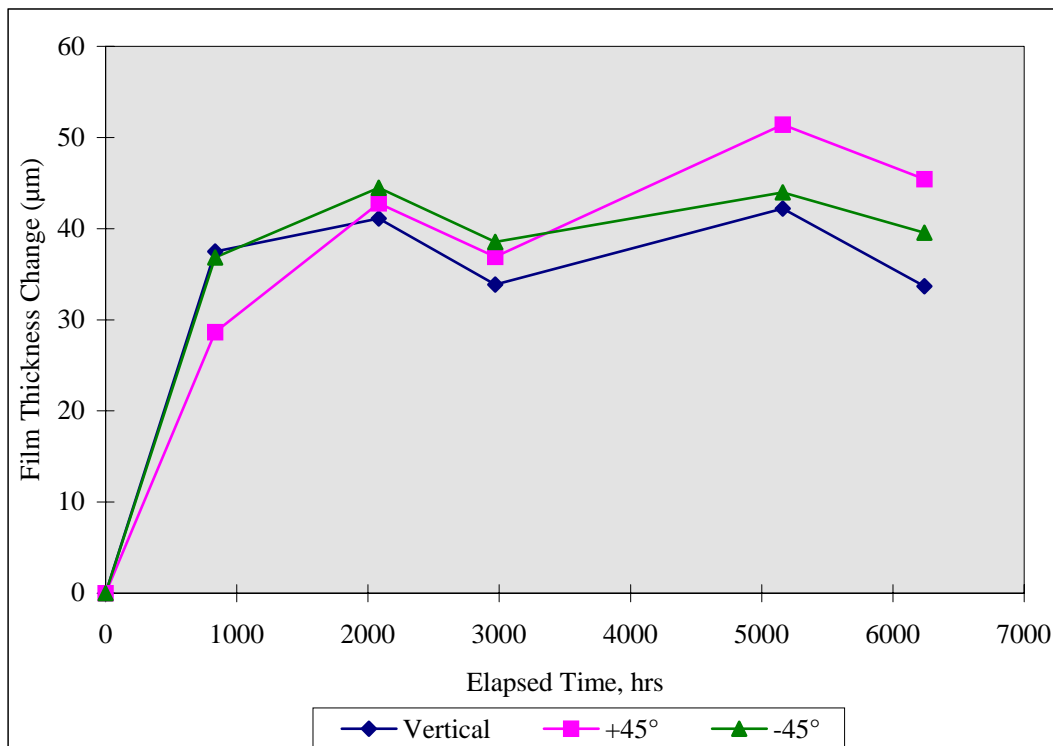


Figure 4.38 Cumulative Change in Teflon[®] Film Thickness as a Function of Time and Angular Position -- Tube 1

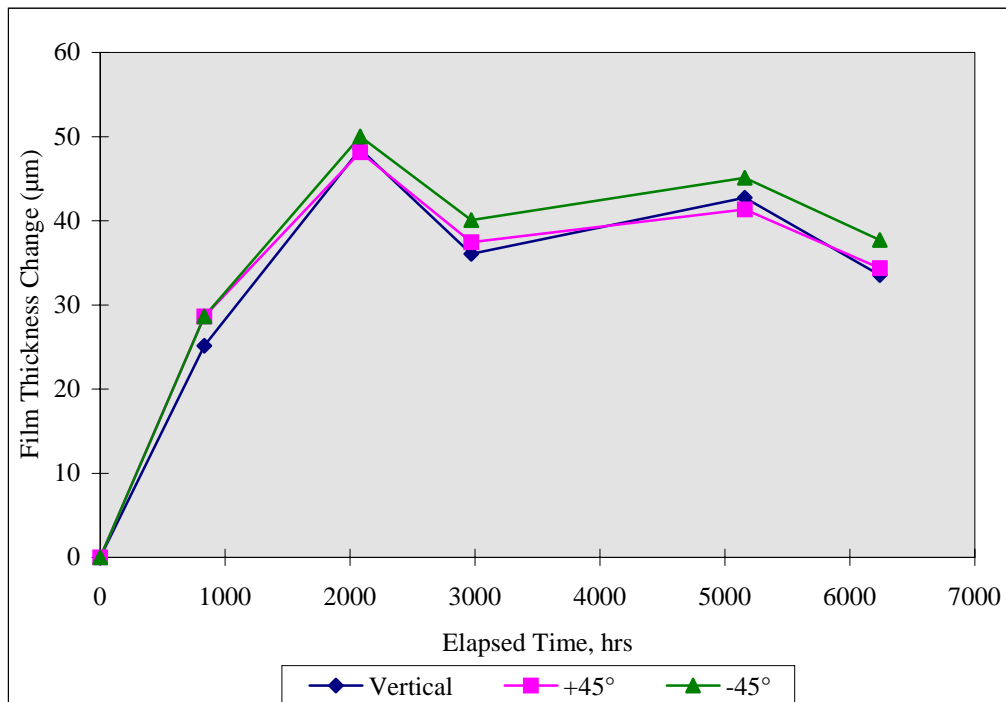


Figure 4.39 Cumulative Change in Teflon® Film Thickness as a Function of Time and Angular Position -- Tube 5

In each of the figures it can be seen that there were no significant differences in film thickness changes as a function of angular position, suggesting that high flue gas velocity areas, such as those between tubes, do not incur increased amounts of abrasive wear. Similar results were observed for the other 4 tubes in the top row of the heat exchanger. Although there appears to be a slight (10.2 µm [0.4 mil]) decrease in film thickness for tube 5, this amount is within the absolute accuracy range (+/- 1% of reading) of the thickness gage for a nominal 508 µm (20 mil) film.

Teflon® Surface Replications

Six sets (including replications made prior to flue gas exposure) of film surface replications were obtained during the course of the test program. Each set consists of 5 film replications made in the locations shown in Figure 3.1. The goal of making the surface replications was to record and observe any microscopic changes to the Teflon® tube surface which may not be evident to the naked eye or detected with the eddy current film thickness technique. As mentioned in Section 4.2, each replication was inspected under a microscope and then photographed at two different magnifications (25X and 200X). Comparisons were then made between the pre-test, intermediate and post-test replications to determine the location and amount of microscopic surface wear. Representative examples of the surface replications are shown in Figures 4.40 through 4.42. Figure 4.40 represents a typical tube surface prior to exposure to flue gas, Figure 4.41 shows the surface of tube 1, and Figure 4.42 the surface of tube 6, both at the conclusion of the test program. The microphotographs in each of the three figures were taken at a magnification of 200X.

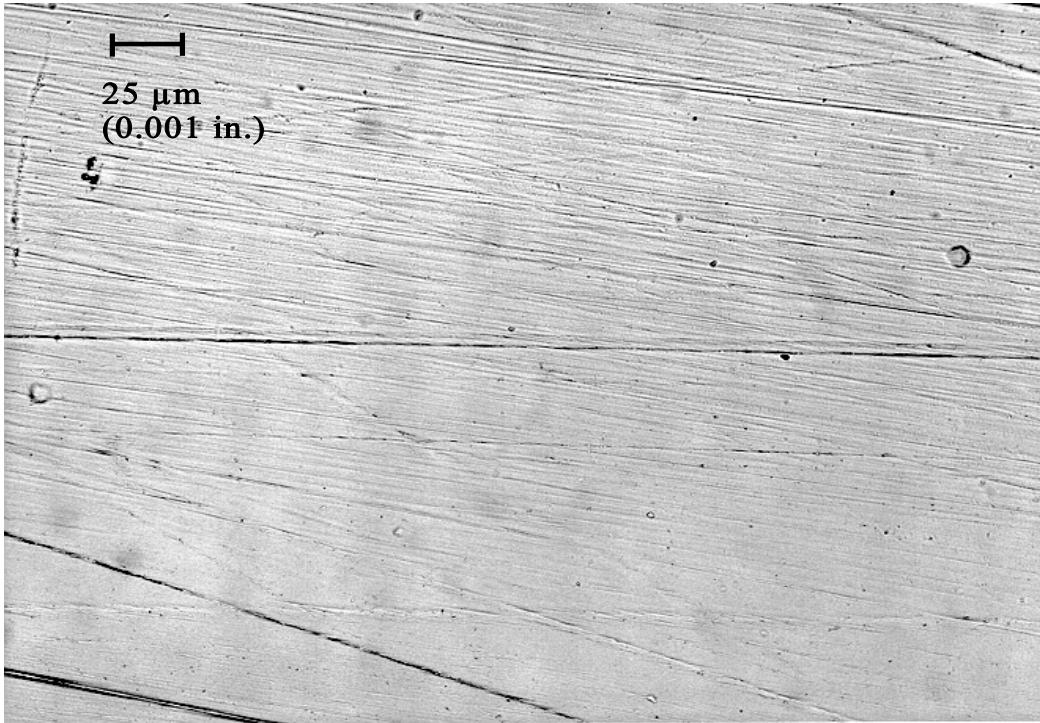


Figure 4.40 Microphotograph of Clean Tube Surface

In Figure 4.40 the surface of the Teflon[®] film is extremely smooth, with only minor striations running axially (lengthwise). These striations result from the manufacturing process. In Figure 4.41 (tube 1), minimal surface damage is visible. This is not unexpected in that the predicted flue gas flow pattern to the top row of tubes has a region of low flow at this tube. The vertical

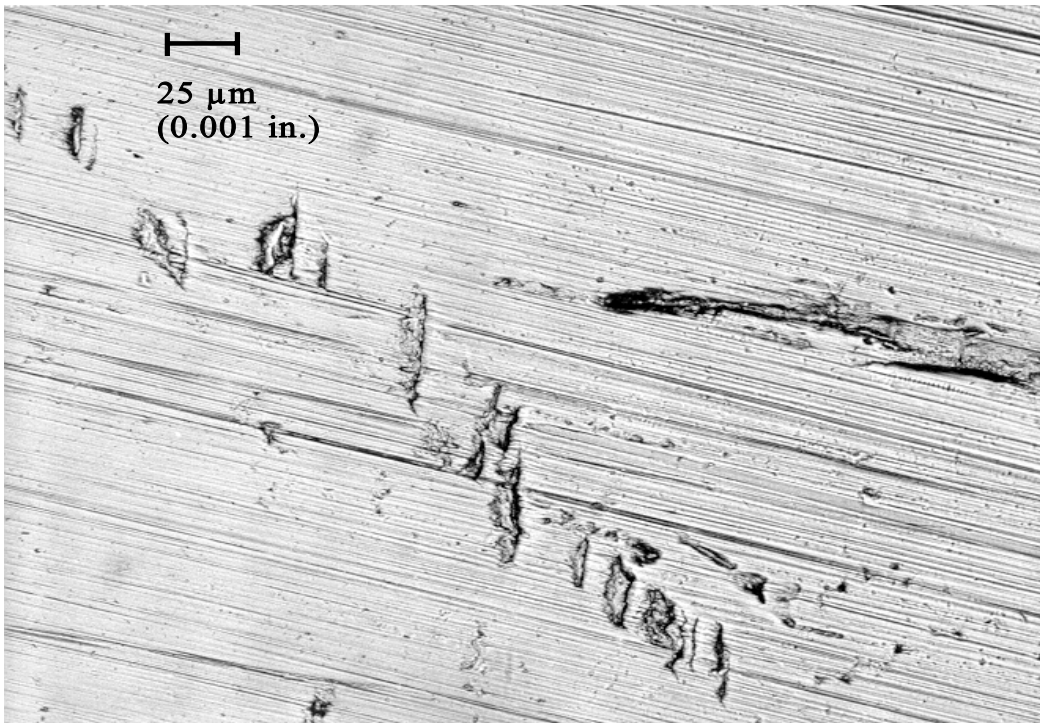


Figure 4.41 Microphotograph of Tube 1 -- End of Test

marks running from the lower right to upper left are cuts in the surface made by the calipers used to make the tube dimensional measurements (see Section 4.2). In Figure 4.42 (tube 6) some minor wear damage is visible. This also is not unexpected, since this tube was expected to see the most flue gas (and fly ash). The wear damage appears to be very fine and uniform, but very small (μm range), resembling small, circular depressions. Typically, details for any given object are visible to the naked eye down to about $200\ \mu\text{m}$ (8 mils). At a magnification of 200X, this translates to a size of approximately 38.1 mm (1.5 inches) on the microphotograph. For comparison, the dark oval in the center of the Figure 4.42 is approximately $12.7\ \text{mm}$ (0.5 inches) long, or approximately $63\ \mu\text{m}$ (2.5 mils).

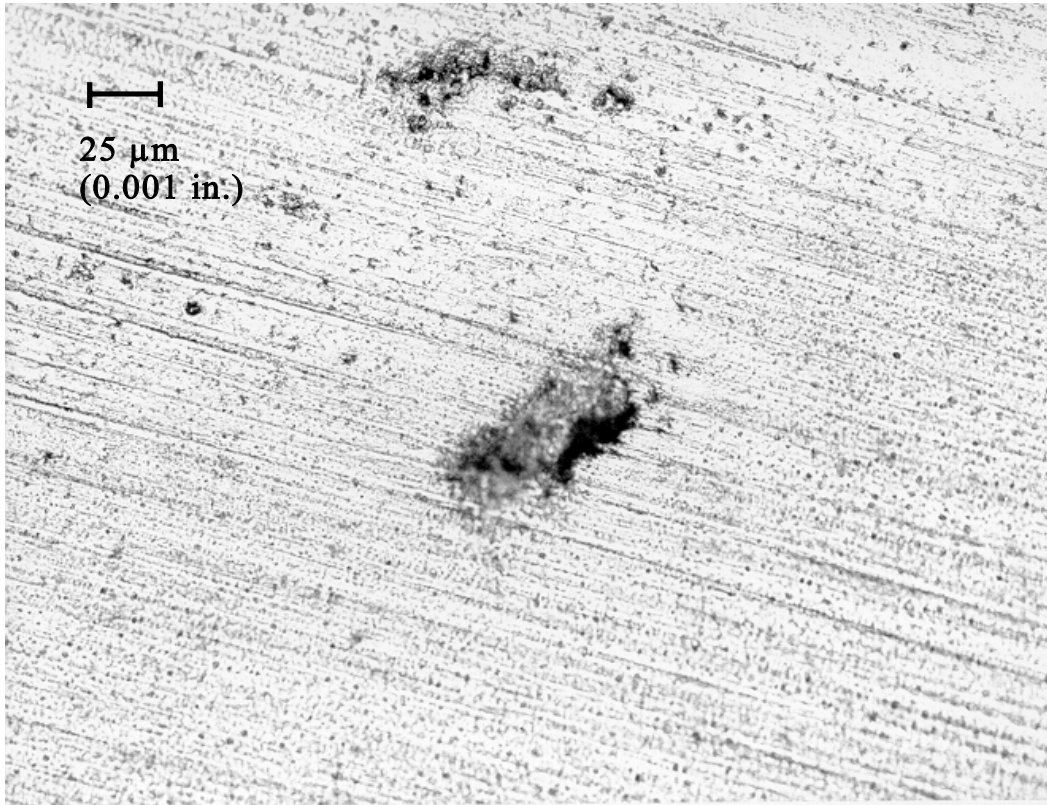


Figure 4.42 Microphotograph of Tube 6 -- End of Test

5.0 ECONOMIC ANALYSIS OF FGD TECHNOLOGIES

For the IFGT technology to be commercially viable, its effective pollution removal capability must be achieved at a competitive cost. A cost analysis of an IFGT system was developed based on the results of the pilot IFGT tests conducted in Task 2. The results of the analysis are presented in Table 5.1. This report summarizes the economic analysis methodology and discusses the results for a limestone based wet Flue Gas Desulfurization (LWFGD) system, the sodium-based IFGT system, and a mag-lime-based IFGT system.

The IFGT system used in this analysis consists of eight modules in both the first and second heat exchanger stages. One-half of the first heat exchanger consists of the standard copper-nickel and Teflon[®] coated water heating tubes. One-half of the first stage heat exchanger and all of the second stage consists of Teflon[®]-covered aluminum tubes that are open to the atmosphere. The capital, design, erection and operation costs of two IFGT systems were compared to the cost of a LWFGD system. The IFGT systems are with a soda ash reagent and mag-lime reagent.

Although the IFGT system can remove several pollutants, the analysis assumes the equipment is installed only for SO₂ removal. Credit is not taken for removal of particulate, other acid gases, ammonia, or trace elements. Credit is taken for heat recovery by the IFGT system. For this analysis it is assumed that the IFGT recovers 3% of the furnace heat release and that this heat can be returned to the power cycle, providing a 1% improvement in cycle efficiency. Credit is not taken for the reduction in emissions that result from the increase in cycle efficiency and are based on the amount of emissions per unit of electrical energy generated.

Economic analyses are sensitive to the assumptions that are used as a basis for comparison. Because the IFGT system design is based on industrial size, the capacity of the largest single unit at this time, is smaller than nearly all utility power plant scrubbers. However, for this analysis a 100 MW_e plant was assumed, requiring three IFGT units in parallel. This was compared to a single LWFGD system of the same flue gas capacity. In addition to plant size, the economic comparison assumes the plant burns a 1.5% sulfur coal, the plant thermal efficiency is 33%, and that the flue gas enters the FGD equipment at 300 F and 6% excess oxygen.

The cost components that were evaluated and the basis of the evaluation is as follows:

Capital – the cost of all equipment required to operate the units, gas flange to gas flange, and from receipt of the reagent to the discharge of the byproduct effluent. It includes the increase in the cost of the fan and motor required to offset the pressure drop through the FGD equipment. Capital cost also includes all wiring, instrumentation and controls required to operate the equipment. For each of the three FGD scenarios, B&W Inc. estimated these costs using the same procedures that are used to cost commercial offerings.

Design and Erection (D/E) - the design and erection costs were estimated at 55% of the capital cost.

Operating Power – This includes the power required to operate all the FGD auxiliary equipment.

Fan Power – The increase in fan power (kW/in W.G.) required to overcome the pressure loss through the FGD system.

Reagent – The reagent cost is sensitive to geographic location in the United States. For this estimate a representative reagent cost was used excluding shipping. The molar calcium-to-sulfur ratio used for the limestone system evaluation was 1.08. For the sodium-based IFGT system, the sodium-to-sulfur ratio used was 2.2. For the mag-lime-based IFGT the (calcium + magnesium)-to-sulfur ratio used was 1.05

By-Product Disposal – For limestone reagent it is assumed that the byproduct is dewatered and disposed in a lined landfill. The cost per pound is based on the cost of the landfill sufficient for the estimated plant life. Credit is not taken for a gypsum grade byproduct sold to wallboard manufacturers. For soda ash and mag-lime, the disposal cost represents the cost of an evaporation pond to handle the effluent for the same time period.

Heat Recovery – It is assumed that 3% of the furnace heat release is removed from the flue gas and is recovered into the plant steam cycle, resulting in a 1% improvement in cycle efficiency.

Electricity cost – Electricity is evaluated at \$0.055/kW for both electricity consumed and electricity saved.

The annualized and life cycle costs associated with these components for the three FGD scenarios are shown in Table 5.1. All costs shown in the Table including the annualized and life cycle costs are in current dollars.

Comparison of the costs for the three scenarios shows the following:

Capital cost - the IFGT system is less costly than the LWFGD system by about \$5 million and the total installed cost is less costly by about \$7.5 million. This is due to the very few auxiliary systems required by soda ash and mag-lime systems compared to limestone systems that require a large amount of auxiliary equipment.

Power Consumption – The power consumption by the IFGT auxiliary systems is one tenth to one-fifth of that required by the LWFGD auxiliary equipment. This is entirely offset by the increase in fan power required by the higher pressure drop of the IFGT system. The total power consumption of the soda ash IFGT is slightly less than the limestone process while the mag-lime IFGT is slightly greater.

Reagent cost – the annualized cost of soda ash is nearly \$2 million more than limestone, while mag-lime is about \$0.4 million more. The reagent cost is a significant portion of the total annualized operating cost for the IFGT systems.

Byproduct disposal – soda ash and mag-lime disposal costs are both about \$.13 million greater than the limestone process wastes. LWFGD. This is due entirely to limestone dewatering which reduces the byproduct volume by about 50%.

Annual operating cost – The annual operating cost for the soda ash exceeds the limestone process \$2 million, while mag-lime costs are \$0.65 million more. The cost differential is almost entirely due to reagent cost.

Heat Recovery – The annual cost recovery for a 1% improvement in cycle efficiency achieved with the IFGT is \$0.48 million.

Total Annual Cost – the total annual cost of the mag-lime IFGT (operating, annualized D/E and heat recovery) is about \$.22 million less than LWFGD, while the soda ash IFGT is about \$1.1 million more.

Life Cycle Cost – The total life cycle cost of the mag-lime IFGT is \$4.4 million less than for LWFGD. This represents about a 10% savings. The slightly greater operating cost associated with mag-lime IFGT is offset by the much lower D/E cost. The life cycle cost of the soda-ash IFGT is \$23 million greater than LWFGD. All of the greater cost is attributable to the cost of the reagent.

As shown by the above analysis, a mag-lime IFGT system can provide a less expensive alternative to sulfur removal than LWFGD at a 100 MW scale. The power cost for both systems is about the same, while the higher cost of the mag-lime is nearly offset by heat recovery. What could be the most attractive feature of the mag-lime system is the relatively low initial cost of the system. The total D/E cost for LWFGD is equivalent to \$212/kW, while the mag-lime system is equivalent to \$136/kW, installed. As the plant size increases, the cost per installed kW decreases for LWFGD so that for a 1200 MW plant the cost of installed LWFGD is about \$90/kW. IFGT units larger than 35 MW have not yet been designed. Some reduction in installed kW is expected with increased size, but the magnitude is not known. Based on past analyses of LWFGD, the installed cost of the two units will be about equivalent for a plant size of about 400 MW.

Table 5.1 provides a comparison of three scenarios for flue gas desulfurization. This is the first rigorous evaluation of the cost of IFGT compared to LWFGD. In addition to providing cost comparison Table 5.1 also indicates the costly components of the IFGT system, indicating areas of improvement. For the IFGT systems, fan power to overcome gas side pressure drop is the most expensive component of operating power. The pressure loss in an IFGT can be easily reduced by reducing the surface area of the tubes in the first or second stage. This is equivalent to reducing the number of heat exchanger modules in each stage from the standard eight to seven or six. In this analysis, the surface area is not required for heat transfer. This surface may be required to maintain effective particulate removal (if needed) or SO₂ removal, and this will have to be determined.

Table 5.1 Preliminary Economic Comparison

COMPARISON VARIABLES	LIMESTONE WET FGD SYSTEM	SODA ASH BASED IFGT SYSTEM	MAG-LIME BASED IFGT SYSTEM
COST (U.S. Dollars)			
Capital Cost	\$13,671,269	\$8,745,157	\$8,773,721
Erection Cost	\$7,519,198	\$4,809,836	\$4,825,547
Total Design & Erection (D/E Cost)	\$21,190,467	\$13,554,993	\$13,599,268
POWER			
Gas Side Pressure Drop (in. WG)	8.86	11.00	12.20
ID Fan Power (kW/in WG)	200	200	200
Increased ID Fan Electricity (kW)	1772	2200	2440
Auxiliary Power Consumption (kW)	657	49	129
Total Power Consumption (kW)	2429	2249	2569
Annual Cost (\$/Year)	\$819,205	\$758,498	\$866,421
REAGENTS			
Consumption (lb/hr)	4,335	4,262	2,187
\$ / ton	\$5.44	\$110.00	\$57.00
Annual Cost (\$/YR)	\$72,304	\$1,437,402	\$382,204
BY-PRODUCT DISPOSAL			
Product (Lb/Hr)	9,244	20,554	20,069
Disposal Cost (\$/lb)		\$0.0014	\$0.0014
Operating - hours per year	6132	6132	6132
Annual Cost (\$/YR)	\$0	\$175,192	\$171,058
ANNUAL OPERATING COST			
Reagent	\$72,304	\$1,437,402	\$382,204
Power	\$819,205	\$758,498	\$866,421
By-Product Disposal	\$0	\$175,192	\$171,058
Annual Cost (\$/YR)	\$891,508	\$2,371,091	\$1,419,683
HEAT RECOVERY			
Annual Heat Recovery	\$0	\$481,800	\$481,800
TOTAL COSTS (Annual)			
Heat Recovery	\$0	(\$481,800)	(\$481,800)
Operating Cost	\$891,508	\$2,371,091	\$1,419,683
D/E Cost (Annualized at 15.2%)	\$2,728,488	\$1,745,343	\$1,751,044
Total Cost (Annual)	\$3,619,996	\$3,634,635	\$2,688,927

Basis

Plant Load Factor = 70%
 Plant Life = 30 years
 Capital Levelization Factor = 15.2%
 Cost of Electricity = \$0.055/kW

6.0 CONCLUSIONS

The work performed under Tasks 2 and 3 of this Phase I contract have shown the IFGT to be a potentially viable new technology for the abatement of both major and minor gaseous and particulate pollutants from fossil fired boilers. The Task 2 tests demonstrated that the IFGT was capable of removing several pollutants in an efficient and low cost manner. The wear tests conducted in Task 3 showed that no significant wear problems were implicit with the use of Teflon[®] covered heat exchanger tubes. The preliminary economic comparison of the IFGT when compared to the dominant commercial FGD LSFO process compared very favorably. Some of the more important conclusions drawn from this work are summarized below.

SO₂ Removal

The IFGT process has exceeded the goal for SO₂ removal, providing greater SO₂ removal than a conventional wet scrubber operating at similar L/G. The sodium carbonate reagent is highly reactive and has sufficient dissolved alkalinity to remove all of the SO₂ in high sulfur flue gas even at very low liquid-to-gas ratios. Greater than 95% removal of SO₂ at L/Gs less than one tenth of that required by conventional LSFO systems shows that the surface area of the tubes in the second stage provides more than adequate gas-liquid contact for SO₂ absorption.

The 50% SO₂ removal using lime slurry and the 88% removal efficiency of the mag-lime slurry reflects the diminished absorption capacity of these reagents. The estimated removal efficiencies for a 0.75% sulfur coal are estimated to be approximately 70% for lime and 95% with mag-lime.

The SO₂ removal tests using calcium based reagents confirm that they are potentially acceptable alternatives to the sodium based reagents. This is significant from the standpoint of operation costs, disposal costs, and environmental issues. Calcium based byproducts are environmentally benign and are potentially saleable.

Particle Removal

At full load, the particle removal efficiency of the IFGT process exceeded goals. The overall removal efficiency depends on the particle size distribution of the fly ash entering the IFGT system. Removal efficiency for particulate greater than 2.5 microns averaged 98%. More significantly, the removal efficiency for particulate smaller than 2.5 microns averaged 76%. These fine particulate, referred to as PM_{2.5}, will be regulated in the near future, and while the exact nature of the regulations are not yet defined, the IFGT process provides the capability to address these forthcoming regulations. The test data show that while the removal efficiency is dependent on the size distribution of the coal, it is otherwise independent of coal type.

Particle removal was achieved at an inlet particle loading up to 800 mg/dscm. For a typical utility coal-fired boiler this represents about 10% to 15% of the fly ash removed by particulate clean-up devices. Higher particulate loading is possible, but the point at which high particle loading affects the performance (removal efficiency or cleaning) of the IFGT has not been determined. Although the IFGT process may not be capable of handling the full particulate loading from a boiler, it can provide relief from operational problems and upsets associated with particle removal devices. In the case of an ESP, the IFGT could augment or replace some of the

particulate removal capability of the ESP. In the case of a baghouse, an IFGT could accommodate an increase in particulate loading due to damaged bags, providing more flexibility to plant operation.

The IFGT system was operated at particle loading up to 800 mg/dscm without problems in handling or disposing of the particulate from the system. The fly ash retained on the heat exchanger tubes was easily rinsed by increasing the flow rate of rinse water above the design value of about 60 liters per minute per square meter (1.5 gpm/ft²). The design value is based on experience with oil and gas-fired units, and the increase in flow needed for the higher loading of coal fly ash is expected.

Mercury

The goal for vapor phase mercury removal of 90% was not achieved. Measured removal efficiencies for vapor phase mercury ranged from +69% to -23% and was significantly dependent on relative amounts of ionic and elemental mercury. Ionic mercury removal ranged from 75 to 85%. There was no measurable removal of elemental mercury. In fact, some tests indicated an increase in elemental mercury across the IFGT. This result could be an artifact of sampling techniques or could be caused by reduction of ionic mercury in the aqueous phase and subsequent evolution of elemental mercury.

The inability to remove elemental mercury in the IFGT system indicates that flue gas temperature is not a significant factor in the removal of this specie. The flue gas temperatures in the IFGT were about 15°C (27°F) cooler than in wet FGD systems, while the measured removal efficiencies closely parallel results obtained in other studies.

Ionic mercury removal was essentially the same for all tests, and no clear trend with operating condition over the range tested was evident. If the effects of operating condition are small, they could easily be masked by the overall accuracy of the measurements. The removal efficiency for ionic mercury parallels that obtained in conventional wet FGD systems that operate with different scrubbing chemistry, pH and L/G.

Full-load particulate mercury removal ranged from 55% to 80%. This is less than the total particle removal efficiency. The cause of the difference is the enrichment of mercury in the fine particulate and the fact that the fine particulate removal for the IFGT is less than the overall removal.

Chloride and Fluoride

The goals for chloride and fluoride removal from the flue gas were met with the IFGT system. Except for one outlier (Test I-4A) the chloride removal averaged 98.2% over all tests. Fluoride removal ranged from 83% to 99% for the coals and operating conditions tested. Many chloride and fluoride compounds tend to be highly soluble in aqueous solutions and the high measured removal efficiencies were expected.

NO_x

NO_x removal measured in test series I averaged essentially 0%, and so these measurements were suspended for the balance of the tests. Either the sodium reagent was not effective at removing the NO₂, or the NO₂ component of total NO_x was too small to detect any change in concentration of total NO_x.

Ammonia

Ammonia removal ranged from 50% to 90% depending primarily on the scrubbing solution pH, dissolved solids, and the flue gas outlet temperature. Although there are no Federal regulations for ammonia removal, state and local emissions limits typically range from 2 to 10 ppm. The IFGT can effectively remove ammonia to these concentrations, thereby providing the means to more completely remove NO_x with SCR and SNCR systems.

Trace Elements

The test data showed that arsenic and selenium were the only vapor phase trace metals that were consistently detected. Other elements were occasionally detected in reportable quantities but measurement repeatability was poor. The removal efficiencies for arsenic and selenium averaged greater than 95%.

Heat Recovery

Heat recovery averaged 5.0% of furnace heat release with an inlet flue gas temperature of 120°C (250°F), an outlet flue gas temperature of 35°C (95°F) and a cooling water inlet temperature of 30°C (86°F). At these conditions the outlet flue gas temperature is at or above the water vapor dew point and all of the heat recovery is in the form of sensible heat. For inlet flue gas temperatures of 150°C (300°F), which is more typical for back-end gas cleanup, the heat recovery would increase to 6% of the furnace heat release.

For utility power plants, the amount of useable heat that can be recovered from the flue gas will depend on the temperature at which heat is rejected in the power cycle. Typically, this is higher than the 30°C used in this test, and is closer to 60°C (140°F). With this restriction the energy that can be recovered into the power cycle is reduced to about 3% of the furnace heat release.

This energy recovery is significantly less than the 8% to 12% that can be recovered in gas-fired industrial processes. In industrial processes the cooling water temperature can be as low as 10°C (50°F), the flue gas temperature in excess of 175°C (350°F) and the water vapor dew point near 60°C (140°F). Still, a 3% energy recovery can provide a 1% increase in generated electricity. For a 100 MW plant this is equivalent to approximately \$.5 million per year. This improvement in efficiency can partially offset the operating cost of the IFGT equipment.

Wear

The single-stage pilot CHX[®] unit installed at the ECTC operated for over 6,200 hours. Visual inspections, film thickness measurements, and film surface replications were performed at various times during the test program. No significant wear was detected on any of the tube surfaces. Specific conclusions about the wear test results include the following:

Particulate Deposition: At higher particulate loadings, deposition can be a problem, particularly if inadequate wash water flow rates are used. Wetted ash surfaces which are not removed during washing become sites for additional ash deposition, resulting in increases in heat exchanger pressure drop. Installation of the modified, 3-nozzle manifold (and subsequent increase in flow rate) seemed to alleviate this problem. For oil applications, the "design" wash schedule is 40.75 l/min/m² (1 gpm/ft²) for 10 minutes. Based on the results from this test program, this rate will need to be increased for higher particulate loadings such as coal-fired utility applications.

Film Thickness: No significant decrease in film thickness was detected during the course of the test program. After an initial increase in film thickness resulting from surface stress relaxation during heating, film thicknesses remained essentially constant. Some locations exhibited a slight decrease (0.4 mils) in thickness, but this amount is within the absolute accuracy range (+/- 1% of reading) of the thickness gage. Measurements at various angular positions around the circumference of the tubes also showed no significant wear, even in areas of high flue gas velocity.

Film Surface: Surface replications taken during the course of the test program revealed only minor, microscopic wear damage to the surface of the Teflon[®] film, and only on tubes subjected to the highest flue gas flow rates. The wear damage appeared to be on the m. level and was very fine and uniform, resembling round depressions in the film surface. At this scale, this type of wear damage should pose no problems for long-term operation of a large-scale unit.

Predicted Teflon[®] Film Life: Based on the measurement data, the Teflon[®] coating on the heat exchanger tubes should have a life expectancy of greater than 10 years. If the 0.4 mil decrease observed for some tube locations is correct, 10 years of operation would yield an approximate decrease in film thickness of 4 mils from a nominal film thickness of 20 mils. It would be more probable that any tube replacement would be due to other operational problems (e.g., scale buildup, temperature excursions due to cooling water failure, etc.). For comparison, operation at a particulate loading of 400 mg/dscm (0.35 lb/10⁶ Btu) for 6 months is equivalent to 10 years at 20 mg/dscm (0.017 lb/10⁶ Btu).

Comparative Economic Analysis

The comparative economic analysis performed as part of this program is sufficiently promising to give encouragement for the continued pursuit if the development of the IFGT concept to commercial reality.

Based on the results of Phase I testing we can conclude that the overall objectives of Phase I, have been met. Specifically,

- The pollutant removal performance of the IFGT process for pollutants that are currently regulated, or for which regulations are being considered, have been characterized for a range of operating conditions and for a range of coal types.

- Most of the pollutant removal goals for the IFGT process were demonstrated. Removal of vapor phase mercury, and the elemental form of mercury in particular was less than originally expected, but in general agreement with data for other types of flue gas treatment equipment.
- Tests with calcium-based reagents have shown that they are a feasible alternative to sodium reagent for low sulfur coals. Process modifications to permit higher L/Gs or greater dissolved alkalinity in the reagent will likely provide 90%+ SO₂ removal for higher sulfur coals.
- The increase in SO₂ transfer units with L/G for both soda ash and calcium reagents was less than expected, and indicates a possible mal-distribution between the liquid scrubbing solution and the flue gas. This mal-distribution is most likely associated with the region near the walls of the second-stage heat exchanger. This type of wall effect is common in small pilot-scale facilities. Larger test facilities provide performance results more representative of commercial scale equipment.
- The IFGT is an effective particulate removal device, removing over 98% of particulate greater than 2.5 microns and 76% of particulate smaller than 2.5 microns. The removal of the fine particulate is especially important in view of impending regulations on PM 2.5.
- The IFGT is effective at removing vapor phase selenium and arsenic, the only trace elements that were repeatably measured in significant quantities in the flue gas.
- The operating temperatures and water vapor content of the flue gas for utility power boilers will typically limit heat recovery to about 3% of the boiler heat release. This heat recovery can increase plant efficiency, providing a substantial economic benefit and reducing emission of pollutants on the basis of energy produced.
- The Integrated Flue Gas Treatment process successfully removes multiple pollutants (SO₂, HCl, HF, particulate, ammonia, arsenic, selenium, and mercury) in a single device.
- At least ten year life of the Teflon[®] covering of the heat transfer surface is achievable.
- Magnesium enhanced lime is more cost effective than soda ash for use with the IFGT.

7.0 REFERENCES

1. Fogiel, M., "The Essentials of Transport Phenomena II," The Research and Education Association, 1987.
2. Holman, J.P., "Heat Transfer - Fourth Edition," McGraw Hill, 1976.
3. Johnson, J.W., "A Computer-Based Cascade Impactor Data Reduction System," Southern Research Institute, March 1978, EPA-600/7-78-042.
4. U.S. Geological Survey Coal Quality (COALQUAL) Database: Version 1.3, OPEN FILE-REPORT 94-205, 1994.
5. EPRI, "Electric Utility Trace Substances Synthesis Report - Volume 3," EPRI TR-104614-V3, 1994.
6. Peterson, J.R., et al, "Mercury Emissions Control By Wet FGD Systems: EPRI Pilot-Scale Results," EPRI, DOE, EPA 1995 SO₂ Control Symposium.
7. Sloss, L.L., "Mercury Emissions and Effects - The Role of Coal," IEA Coal Research Report ISBN 92-9029-258-X, 1995.

8.0 BIBLIOGRAPHY

P.V Danckwerts., "Gas-Liquid Reactions," McGraw-Hill, 1970.

J.B. Jarvis, et al, " The Effect of High Total Dissolved Solids on Wet Lime-Limestone Flue Gas Desulfurization Systems," EPRI TR-100242, 1991.

J.F. Zemaitis, et al, " Handbook of Aqueous Electrolyte Thermodynamics," AICHE, 1986.

9.0 LIST OF ACRONYMS AND ABBREVIATIONS

ARC	Alliance Research Center
B&W Inc.	Babcock and Wilcox Inc.
CHX [®]	Condensing Heat Exchanger (trademarked product name)
ECTC	Environmental Control Technology Center
EPRI	Electric Power Research Institute
FGD	Flue gas desulfurization
IFGT	Integrated flue gas treatment (trademarked product name)
MTI	McDermott Technology Inc.
PRB	Powder River Basin
USDOE	United States Department of Energy
USEPA	United States Environmental Protection Agency

MULTIPLE POLLUTANT REMOVAL USING THE CONDENSING HEAT EXCHANGER

Phase I Final Report

Addendum I

Task 2 Topical Report: Pollutant Removal Tests

Start Date: November, 1995

End Date: May, 1997

Issue Date: June, 1998

This report contains no trade secret information

Principal Authors

R. T. Bailey

B. J. Jankura

McDermott Technology, Inc.

1562 Beeson Street

Alliance, Ohio 44601

This project was sponsored by the U. S. Department of Energy,
the Ohio Coal Development Office (Department of Development, State of Ohio),
the Electric Power Research Institute, and Babcock & Wilcox

US DOE-FETC Contract:

DE-AC22-95PC95255

Ralph T. Bailey

OCDO Grant Agreement:

CDO/D-94-1

FAX: 330-829-7283

McDermott Technology, Inc. Contract: CRD 1337

Phone: 330-829-7353

Disclaimer

“This report was prepared as an account of work sponsored by the United States Government and the Ohio Coal Development Office (OCDO). Neither the United States, any agency thereof, the State of Ohio, any agency thereof, or Babcock & Wilcox, nor any of their employees, makes any warranty, express or implied, or assumes any legal liabilities or responsibility for the accuracy, completeness or usefulness of any information, apparatus, product, or process disclosed, or represents that its use would not infringe privately owned rights. Reference herein to any specific commercial product, process, or service, by trade name, mark, manufacturer, or otherwise, does not necessarily constitute or imply its endorsement, recommendation, or favoring by the United States, the State of Ohio, or any agency thereof, The views and opinions of authors expressed herein do not necessarily state or reflect those of the United States Government or any agency thereof.”

ABSTRACT

The pollutant removal performance of an Integrated Flue Gas Treatment (IFGT) system using flue gas from coal combustion was investigated in Phase I, Task 2 of the "Multiple Pollutant Removal Using the Condensing Heat Exchanger" test program. The program was conducted under contract to the United States Department of Energy's Fossil Energy Technology Center (DOE-FETC) and was supported by the Ohio Coal Development Office (OCDO) within the Ohio Department of Development, the Electric Power Research Institute's Environmental Control Technology Center (EPRI-ECTC) and Babcock and Wilcox - a McDermott Company (B&W).

Integrated Flue Gas Treatment (IFGT) uses two Condensing Heat Exchangers (CHX's[®]) in series to recover waste heat from the flue gas and remove a variety of pollutants from the flue gas. The Teflon[®]-covered internals of the condensing heat exchanger permit heat recovery at temperatures below the acid dew-point of the flue gas. Prior to this work, only limited data existed on the pollutant removal efficiency of the IFGT process.

The pollutant removal characteristics of the IFGT system were measured over a wide range of operating conditions in a pilot Integrated Flue Gas Treatment System rated at 1.2 MW_t (4 million Btu/hr) using a wide range of coals. The coals tested included a high-sulfur coal, a medium-sulfur coal and a low-sulfur coal. The flue gas pollutants investigated included ammonia, hydrogen chloride, hydrogen fluoride, particulate, sulfur dioxide, gas phase and particle phase mercury and gas phase and particle phase trace elements. The particulate removal efficiency and size distribution was also investigated. Pollutant removal efficiencies were determined by simultaneous measurements of concentrations at the inlet and outlet of the IFGT system as a function of the coal type, scrubbing liquid, liquid-to-gas ratio and pH, flue gas flow rate and flue gas outlet temperature, and fly ash concentration in the flue gas. Soda ash, lime and magnesium-lime scrubbing reagents were investigated.

The test results show that the IFGT system can remove greater than 95% removal of acid gases with a liquid-to-gas ratio less than 1.34 l/m³ (10 gal/1000 ft³), and that lime reagents show promise as a substitute for soda ash. Particulate and ammonia gas removal was also very high. Ionic mercury removal averaged 80%, while elemental mercury removal was very low. Trace metals were found to be concentrated in the fine particulate with removal efficiencies in the range of 50% to 80%. The data measured in this task provides the basis for predictions of the performance of an IFGT system for both utility and industrial applications.

TABLE OF CONTENTS

<u>Section</u>	<u>Page</u>
1.0 EXECUTIVE SUMMARY	1-1
2.0 INTRODUCTION	2-1
2.1 Background	2-1
2.1.1 Commercial Condensing Heat Exchanger Design	2-2
2.1.2 Integrated Flue Gas Treatment (IFGT) Condensing Heat Exchanger Design	2-3
2.2 Phase I Technical Program	2-5
3.0 FACILITIES AND EQUIPMENT	3-1
3.1 Small Boiler Simulator (SBS) Furnace	3-1
3.2 Integrated Flue Gas Treatment System	3-1
3.3 IFGT Removal Mechanisms	3-4
4.0 TEST DESCRIPTION	4-1
4.1 Test Conditions	4-1
4.1.1 Acid Gas Pollutant Removal	4-2
4.1.2 Mercury and Heavy Metals Removal	4-7
4.1.3 Ammonia Removal	4-7
4.1.4 Particulate Removal	4-8
4.1.5 Heat Recovery	4-8
4.1.6 Calcium Reagents	4-9
4.2 Sampling	4-9
4.3 Reporting Basis	4-11
5.0 RESULTS AND DISCUSSION	5-1
5.1 Heat Recovery	5-1
5.1.1 Measured Heat Recovery	5-1
5.1.2 Predictions of Heat Recovery and Gas Side Pressure Drop	5-2
5.2 SO ₂ Removal	5-6
5.2.1 Test Repeatability	5-6
5.2.2 Sodium Reagent Test Results	5-7
5.2.3 Lime Reagent	5-13

TABLE OF CONTENTS (Cont'd)

<u>Section</u>	<u>Page</u>
5.3 Chloride/Fluoride Removal	5-15
5.4 Ammonia Removal	5-18
5.5 Particulate Removal	5-21
5.5.1 Particle Removal Efficiency as a Function of Particle Size	5-22
5.5.2 Total Particle Removal	5-25
5.6 Mercury Removal	5-29
5.6.1 Measurement Methods and Detection Limits	5-29
5.6.2 Mercury Concentration in the Coal	5-30
5.6.3 Comparison of Gas Phase Mercury Speciation from Method 29 and the Ontario Hydro Method	5-30
5.6.4 Mercury Partitioning	5-33
5.6.5 Vapor Phase Mercury Removal	5-34
5.6.6 Particle Phase Mercury Removal	5-35
5.7 Trace Element Removal	5-37
5.7.1 Trace Element Measurement and Detection Limits	5-37
5.7.2 Vapor Phase Trace Element Removal	5-38
5.7.3 Particle Phase Trace Element Removal	5-39
5.8 NO _x Removal	5-42
6.0 CONCLUSIONS AND RECOMMENDATIONS	6-1
7.0 REFERENCES	7-1
8.0 BIBLIOGRAPHY	8-1
9.0 LIST OF ACRONYMS AND ABBREVIATIONS	9-1

TABLE OF CONTENTS (Cont'd)**APPENDICES**

APPENDIX

- A. DETAILED FACILITY AND INSTRUMENTATION
- B. DETAILED ANALYSIS METHODS
- C. TABULATED DATA FOR TEST SERIES I, OHIO #5/#6 COAL
- D. TABULETED DATA FOR TEST SERIES II, PITTSBURGH #8 COAL
- E. TABULATED DATA FOR TEST SERIES III, POWDER RIVER BASIN COAL
- F. TABULATED DATA FOR TEST SERIES IV, OHIO #6/#5 COAL

LIST OF FIGURES

<u>Figure</u>	<u>Page</u>
2.1 Drawing of a Typical Condensing Heat Exchanger Application	2-3
2.2 Schematic of the IFGT Condensing Heat Exchanger	2-4
3.1 Equipment Arrangement and Gas Flow Path for the Small Boiler Simulator and Condensing Heat Exchanger Test Facilities	3-2
3.2 Distribution of Total Liquid Phase Sulfite as a Function of pH	3-7
5.1 Components of Heat Recovery in the IFGT Process	5-3
5.2 Percent Difference Between the Measured and Predicted Heat Recovery for the Five Heat Transfer Tests	5-3
5.3 Comparison of Measured and Predicted Condensate Flow Rates	5-5
5.4 Measured and Predicted Pressure Drop Across the First Heat Exchanger Stage as a Function of Air Flow Rate	5-5
5.5 Effect of L/G at High pH	5-8
5.6 SO ₂ Removal as a Function of L/G at Two Levels of pH	5-9
5.7 Effect of Load on SO ₂ Removal	5-10
5.8 Effect of Outlet Temperature on SO ₂ Removal	5-11
5.9 Effect of Inlet SO ₂ Concentration on SO ₂ Removal	5-12
5.10 Effect of Inlet SO ₂ Concentration on SO ₂ Removal at Half Load	5-13
5.11 Effect of Reagent Type on SO ₂ Removal	5-14
5.12 Fly Ash Particle Size Distribution at the IFGT Inlet for Each Coal Tested	5-22
5.13 Fly Ash Particle Size Distribution at the Inlet and Outlet of the IFGT System for Test I-14M.	5-24
5.14 Particle Removal Efficiency by Particle Size for the Data in Figure 5.13	5-24
5.15 Particle Removal Efficiency by Particle Size for All Full Load Tests	5-26
5.16 Particle Removal Efficiency by Particle Size for Partial Load Tests	5-26
5.17 Flue Gas Mercury Concentration Resulting From 100% Release of Mercury in the Coal.	5-31
5.18 Comparison of Vapor Phase Ionic Mercury Measured Using Method 29 (M-29) and Ontario Hydro (OH) Sample Trains	5-31

TABLE OF CONTENTS (Cont'd)
LIST OF FIGURES

<u>Figure</u>	<u>Page</u>
5.19 Comparison of Vapor Phase Elemental Mercury Measured Using Method 29 and Ontario Hydro Sample Trains	5-32
5.20 Vapor Phase and Particle Phase Concentrations of Mercury in the Flue Gas	5-33
5.21 IFGT Removal Efficiency for Ionic Mercury (Left y-axis) and Ionic Mercury Concentration (Right y-axis)	5-34
5.22 IFGT Removal Efficiency for Elemental Mercury (Left y-axis) and Elemental Mercury Concentration (Right y-axis)	5-35
5.23 Removal Efficiency for Particle Phase Mercury	5-36
5.24 IFGT Removal Efficiency for Vapor Phase Arsenic (Left y-axis) and the Inlet Concentration (Right y-axis)	5-38
5.25 IFGT Removal Efficiency for Vapor Phase Selenium (Left y-axis) and the Inlet Concentration (Right y-axis)	5-39
5.26 Particle Phase Elemental Concentration at the IFGT Inlet	5-40
5.27 Particle Phase Trace Element Removal Efficiency	5-41
5.28 Ratio of Element Concentration in the Fly Ash at the IFGT Outlet to the Inlet	5-41
5.29 Measured NO _x Removal as a Function of L/G for Test Series I	5-42

LIST OF TABLES

<u>Table</u>	<u>Page</u>
4.1 Coal Analyses	4-1
4.2 Test Series I Completed Test Matrix	4-3
4.3 Test Series II Completed Test Matrix	4-4
4.4 Test Series III Completed Test Matrix	4-5
4.5 Test Series IV Completed Test Matrix	4-6
5.1 Summary Operating Conditions and Comparison to Predicted Heat Recovery for the Five Heat Transfer Tests	5-4
5.2 Repeatability of SO ₂ Removal Measurements	5-7
5.3 Vapor and Particle Phase Chloride Concentrations and Removal Efficiencies	5-15
5.4 Vapor and Particle Phase Fluoride Concentrations and Removal Efficiencies	5-17
5.5 Summary of Ammonia Removal Measurements	5-19
5.6 List of Cascade Impactor Tests	5-23
5.7 Overall Particulate Removal Data	5-28
5.8 Mercury Detection Limits and the Minimum Reportable Concentrations	5-29
5.9 Limits of Detection of the Trace Elements	5-37

1.0 EXECUTIVE SUMMARY

This is the Task 2 Topical Report for “Multiple Pollutant Removal Using the Condensing Heat Exchanger,” conducted by McDermott Technology, Inc., Research & Development Division under contract to the United States Department of Energy. This work was jointly sponsored by the Department of Energy’s Fossil Energy Technology Center (DOE-FETC), the Ohio Coal Development Office (OCDO) within the Ohio Department of Development, the Electric Power Research Institute’s Environmental Control Technology Center (EPRI-ECTC), and Babcock & Wilcox - a McDermott Company (B&W). The guidance and support of the project managers from the sponsoring organizations, Thomas J. Feeley III of DOE-FETC, Richard Chu of the OCDO, and Gerry B. Maybach of the EPRI-ECTC, is gratefully acknowledged.

The purpose of Phase I of this contract was to determine the pollutant removal performance and the anticipated wear life of an Integrated Flue Gas Treatment (IFGT) system using flue gas from coal combustion. This Task 2 Topical Report covers the pollutant removal portion of Phase I. A separate Task 3 Topical Report covers the wear life segment of this Phase I. Integrated Flue Gas Treatment uses two Condensing Heat Exchangers (CHX’s[®]) to recover waste heat from the flue gas and remove a variety of pollutants from combustion flue gas. The Teflon[®]-covered internals of the CHX[®] permits heat recovery at temperatures below the acid dew point of the flue gas.

Condensing Heat Exchangers using Teflon[®]-covered heat exchanger tubes are used in the industrial market to recover energy from flue gas, thereby improving the overall thermal efficiency of the combustion process. More than 110 commercial units are in service, with operating lifetimes up to 14 years. These industrial installations have been exclusively gas and oil-fired. Prior to this work, only limited data existed on the pollutant removal efficiency of the IFGT process. Also, the effects of long-term exposure to abrasive fly ash on the integrity of the Teflon[®]-covered heat exchanger tubes was unknown.

Task 2 Overview

Task 2 of this contract was conducted at McDermott Technology’s Research Center in Alliance, Ohio. Flue gas was generated using a 1.75 MW_t (6 million Btu/hr) coal-fired Small Boiler Simulator (SBS) combustor. A pilot Integrated Flue Gas Treatment System rated at 1.2 MW_t (4 million Btu/hr) was located downstream of the SBS. The pollutant removal characteristics of the IFGT system were measured over a wide range of operating conditions in four series of tests. Flue gas pollutants of interest included:

- particulate
- sulfur dioxide, chlorides and fluorides
- gas phase mercury, selenium and arsenic
- particle phase mercury and other particle phase trace elements
- ammonia

The four test series investigated pollutant removal performance using three different coals and three different sulfur scrubbing reagents. The coals tested included a high sulfur coal (Ohio), a medium sulfur coal (Pittsburgh #8) and a low sulfur coal (Powder River Basin). The first three series of tests used sodium carbonate - known commercially as soda ash - as the scrubbing reagent for each of the three different coals. The fourth test used high sulfur Ohio coal with soda ash, lime and magnesium-lime as the scrubbing reagents.

Lime and magnesium-lime scrubbing reagents were investigated as possible alternatives to sodium carbonate. Soda ash is significantly more expensive than lime per pound of SO₂ removed and can pose a difficult disposal problem if not reclaimed or recycled. Limestone was not tested because a more reactive reagent is needed for the IFGT process to achieve high SO₂ removal with low liquid-to-gas ratios.

Pollutant removal efficiencies were determined by simultaneous measurements of concentration at the inlet and outlet of the IFGT system. The test program investigated the effect of various operating conditions and coal type on pollutant removal. IFGT operating conditions that were varied during the tests included:

- Reagent liquid-to-gas ratio
- Reagent pH
- Flue gas flow rate
- Flue gas outlet temperature
- Fly ash concentration in the flue gas

Comparison of Measured Data to Target Goals

In the Phase I Management Plan, pollutant removal goals were established for the IFGT system to provide a basis for comparison to actual measurements. The goals established in the Management Plan are presented below along with a summary of actual achievements.

SO₂ Removal

Goal	Actual (soda ash)	Actual (mag-lime)
> 95% with a liquid-to-gas ratio (L/G) < 1.34 l/m ³ (10 gal/1000 ft ³)	97% at L/G = 0.60 l/m ³ (4.5 gal/1000 ft ³)	88% at L/G = 0.88 l/m ³ (6.6 gal/1000 ft ³)

The SO₂ removal goal was easily achieved at the targeted test conditions using sodium carbonate reagent. As indicated in the table, the target SO₂ removal was also achieved at a lower L/G than originally specified. This is significant since operation at a lower L/G represents a less costly operating condition in terms of pump power and gas-side pressure drop. Using a mag/lime reagent, an SO₂ removal of 88% was achieved at a low L/G. This is sufficiently high to be

considered promising. An SO₂ removal of 95% could be achieved with an increase in L/G or by allowing more time for the buildup of magnesium salts in the recirculating liquid.

Particulate Removal

Particle Size Range (micrometers, μm)	Removal Efficiency Goal (%)	Actual Removal Efficiency (%) (100% Load)	Actual Removal Efficiency (%) (65% Load)
>10 μm	90%	98.7%	97.6%
5 μm to 10 μm	80%	98.8%	96.0%
2 μm to 5 μm	60%	97.1%	79.7%
< 2 μm	25%	76.4%	51.9%

The IFGT system, while not designed to be a primary particulate removal device, does provide substantial particle removal. The targeted particulate removal efficiency is based on a range of particle size, rather than an average over all particle sizes so that the comparisons are not biased by the effect of particle size distribution. At full load, the actual particle removal efficiency exceeded the goal in each of the targeted size fractions. As indicated in the table, the particle removal efficiency decreased with load, as expected, but still exceeded the targeted removal efficiencies.

Chloride and Fluoride Removal

Removal Goal	Actual
> 95% with a liquid-to-gas ratio < 1.34 l/m ³ (10 gal/1000 ft ³)	Chloride: ~98% at L/G= 0.67 l/m ³ (5 gal/1000 ft ³) Fluoride: 83%-99% at L/G = 0.67 l/m ³ (5 gal/1000 ft ³)

As was expected, the removal of chlorides and fluorides with soda ash was as great or greater than the SO₂ removal at similar operating conditions. Hydrogen chloride (HCl) and hydrogen fluoride are generally more soluble in aqueous solutions than SO₂, and so are preferentially absorbed. This is in agreement with historical performance of wet scrubbers using limestone, lime, or soda ash.

Gas Phase Mercury Removal

Mercury Form	Removal Goal	Actual
Ionic	> 95% for a liquid-to-gas ratio of 1.34 l/m ³ (10 gal/1000 ft ³)	Test I: 81.4 ±1.6 % Test III: 80.4 ±7.6 % Test IV: 78.2 ±6.9 %
Elemental	50%	Test I: -15.9 ±68.8 % Test III: -34.6 ±34.2 % Test IV: -19.4 ±93.9 %

The measured average removal efficiencies for three of the four test series show that the goals for gas phase elemental and ionic mercury removal were not achieved. Ionic mercury removal averaged about 80% for the three test series. This is consistent with ionic mercury removal efficiencies measured by others.¹ The elemental mercury removal averaged less than 0%, and although the uncertainty is high, this trend was consistent in all of the tests and using two different sampling procedures. This could be a real effect, or possibly an artifact of the sampling technique. Regardless, the goal for elemental mercury removal was not achieved. This indicates that the lower operating temperature, and the large low temperature surface area of the IFGT system does not appreciably enhance elemental mercury removal, and may enhance the reduction of oxidized mercury in the liquid phase.

Particle Phase Mercury Removal

Goal	Measured Particulate Removal (%)	Measured Particulate Mercury Removal (%)
Same total removal as particulate	Test II : 94.9% Test III : 88.9% Test IV : 94.1%	Test II : 73.6 ±11.1% Test III : 43.8 ±28.2% Test IV : 80.0 ±11.0%

As indicated, the removal efficiency for particulate mercury was less than the removal efficiency for the total particulate. The reason for this anomaly is that the particulate mercury is concentrated in the smallest particles (< 2 μm), which are less effectively removed by the IFGT process than the larger particles (> 2 μm). Typically, the mercury concentration in the fly ash at the outlet of the IFGT system was 5 to 10 times greater than the concentration of mercury in the fly ash at the inlet to the IFGT.

For tests II and IV the particulate mercury removal averaged about 75%, while the measured removal efficiency for particulate less than 2 micrometers was 76.4%. This indicates that

¹ Noblett, J.G., "Control of Air Toxics from Coal-Fired Power Plants Using FGD Technology," EPRI Second International Conference on Managing Hazardous Air Pollutants, Washington, D.C., July 13-15, 1993.

essentially all of the particulate mercury is contained in the particulate that is less than 2 micrometers. Although the stated goal was not achieved, the distribution of mercury with particle size precluded removal performance any better than was measured.

Vapor Phase Trace Element Removal

A goal was not specified for trace element removal other than for mercury, since few of these elements exist in the vapor state in significant quantities. Measurements showed significant vapor phase concentrations of arsenic and selenium for the Ohio and Pittsburgh coals. For these coals, the removal efficiency for vapor phase selenium ranged from 50% to 98%, and the arsenic removal efficiency was greater than 98%. These are significant reductions in the concentrations of these elements.

Particle Phase Trace Element Removal

A goal was not established for particle phase trace elements other than mercury, since these other elements are not at this time considered for regulation. On average, the removal of particle phase trace elements followed the same pattern as for particle phase mercury. The trace elements were concentrated in the fine particulate, and the total particle phase element removal averaged about 80%.

Ammonia and Oxides of Nitrogen Removal

A goal was not established for ammonia (NH₃) and nitrogen oxides (NO_x) removal. For ammonia, the objectives were to evaluate the potential of operating an IFGT in conjunction with an SCR or SNCR to achieve higher NO_x removal rates by addressing the problem of ammonia slip. Therefore, tests were conducted to measure ammonia removal through the IFGT system, and estimate the amount of ammonia that reacts with SO₃ before the IFGT system. The inlet ammonia concentration ranged from 31 ppm to 94 ppm and removal efficiency ranged from 57% to 93%. All ammonia tests were conducted at full load. The amount of ammonia that reacts with SO₃ before the IFGT system was estimated by comparing the measured and calculated ammonia concentration at the IFGT inlet based on the ammonia injection rate. The ammonia reduction attributable to ammonia-sulfur reactions ranged from 27% to 45%, and averaged 36%.

The absorption of NO_x as expected, was not significant. The initial measurements of NO_x at the inlet and outlet of the IFGT indicated NO_x removals were too small to quantify.

Conclusions

The Task 2 goals for the project were met or exceeded in all cases except for vapor phase mercury removal. The goals for mercury removal were based, in part, on the relatively high gas-liquid contact area of the condensing heat exchanger, the high reactivity of the sodium reagent, and the relatively lower operating temperature of the IFGT process compared with other flue gas clean-up technologies. That this goal - for vapor phase mercury removal - was not realized indicates that temperature and surface area by themselves will not provide reductions in

elemental mercury at typical flue gas concentrations. Other methods of promoting elemental mercury capture were beyond the scope of work for this project.

The Task 2 results show that the IFGT process is an effective multiple pollutant removal system that can also provide an improvement in thermal efficiency. The data measured in this Task provides the basis for predictions of the performance of an IFGT system for both utility and industrial applications. This data is needed to provide performance guarantees as well as to evaluate the economic cost and benefit of an IFGT system.

2.0 INTRODUCTION

2.1 Background

The 1990 Clean Air Act Amendments address the need to reduce the quantity of pollutants released to the atmosphere. Some pollutants are currently regulated and additional species are targeted for control in the near future. The emission of SO₂ and particulate from electric utilities is currently regulated under the Phase I and Phase II requirements defined in Title IV. An additional 189 substances, classified as hazardous air pollutants, have been identified for regulation under Title III of the Clean Air Act Amendments. The Title III requirements will be imposed across approximately 750 source categories. Cluster rules are also being established to set emission standards for specific industries. Many state and local agencies are already imposing stringent regulations on hazardous pollutants, such as mercury. There is a need for equipment to remove the pollutants of concern in a cost-effective manner. Most of the commercial pollutant removal equipment suffers from three major drawbacks:

- 1) Commercially available pollution removal equipment is parasitic, that is, it consumes energy during operation. A typical coal-fired power plant will have a 2-4% or more reduction in power generation capacity when commercial SO₂ and particulate removal equipment is added for gas clean up.
- 2) Commercially available flue gas clean up equipment generally treats only one pollutant at a time. Separate units are installed for each pollutant to be removed.
- 3) Most of the commercial flue gas clean up equipment used in the electric utility industry cannot be economically scaled down for industrial coal-fired applications. Capital cost and operating cost of these units are often prohibitive for the smaller energy producer.

An untapped source of energy from coal-fired units is the waste heat in the flue gas released to the stack. The efficiency of a boiler can be significantly increased by decreasing the flue gas exit temperature. One means of lowering the exit temperature is to use a condensing heat exchanger to recover both sensible and latent heat from the flue gas. Condensing Heat Exchangers (CHX[®]) using Teflon[®]-covered internals are widely used to recover waste heat from flue gases. The Teflon[®] covering protects the heat exchanger components from corrosion as the temperature of the flue gas drops below the acid dew point. The most common applications to date, are boilers firing oil or natural gas. Single-stage commercial condensing heat exchangers have provided satisfactory performance and lifetimes for more than one hundred industrial installations for the past fourteen years.

A recent innovation to the commercial condensing heat exchanger design, called the Integrated Flue Gas Treatment (IFGT) system, exhibits improved pollutant removal from the flue gas while recovering waste heat. The IFGT system is a two-stage condensing heat exchanger. Most of the sensible heat is removed from the gas in the first heat exchanger stage. The second heat exchanger stage can be operated in a condensing mode, recovering latent heat from the gas while removing pollutants. The top of the second heat exchanger stage is equipped with an alkali

reagent spray system to enhance SO₂ and particulate removal. Pollutant removal mechanisms in the IFGT include condensing (for water, some organic compounds, and some acid gases and trace metals), impaction (for particulate), and gas absorption (for removal of SO₂ and other acid gases). In an IFGT, several pollutants are treated using a single device - while recovering waste heat. Because of its modular design, it can be easily built for a wide range of applications. An additional benefit realized by using the IFGT system is the proportional reduction in carbon dioxide released per MW of generated electricity because of the increase in plant efficiency.

The IFGT condensing heat exchanger is expected to effectively remove air toxics still present in the flue gas that penetrate upstream pollution removal devices (i.e., bag house or electrostatic precipitator). The vapor phase air toxics that routinely pass through these removal devices include mercury, selenium and arsenic. Low temperature operation and gas-liquid contact inherent to the IFGT promotes the removal of air toxics in the gas phase and present on the fine particulate.

It has been proposed to use an IFGT system downstream of a selective catalytic reduction (SCR) or selective non-catalytic reduction (SNCR) unit to remove the remaining ammonia in the flue gas. SCR and SNCR devices utilize the injection of ammonia into the flue gas upstream of the SCR/SNCR zones. The ammonia is the reducing agent. Invariably, excess ammonia is injected. The excess that remains in the flue gas is referred to as ammonia slip. NO_x removal can be increased by increasing the ammonia injected into the flue gas, but because of ammonia slip, local atmospheric emission limits may be exceeded for ammonia. By capturing the excess ammonia in the IFGT, higher concentrations of ammonia can be injected upstream of the SCR thereby increasing NO_x removal without increasing ammonia emissions to the atmosphere.

2.1.1 Commercial Condensing Heat Exchanger Design

Commercial condensing heat exchangers remove both sensible and latent heat from the flue gas in a single unit. Figure 2.1 is a drawing of a typical condensing heat exchanger application. It shows the heat exchanger along with the support equipment provided for a retrofit application. The flue gas passes down through the heat exchanger while the water passes upward in a serpentine path through the tubes. Condensation occurs within the heat exchanger as the gas temperature at the tube surface is brought below the dew point. The condensate falls as a constant rain over the tube array and is drained at the bottom. Some cleaning of the gas can occur within the heat exchanger as the particulate impact the tubes and acid gas condensation occurs.

Commercial designs are optimized for removing heat and ensuring adequate lifetime of the unit. Heat exchanger tubes are made of Alloy 706 (10% nickel and 90% copper), a material commonly used in boiler water applications. Each tube is covered with Teflon[®] extruded over the outside of the tube. Since Teflon[®] is hydrophobic, condensation on the surface of the tube occurs in drops rather than in a film. This allows continuous exposure of most of the surface and improves heat transfer.

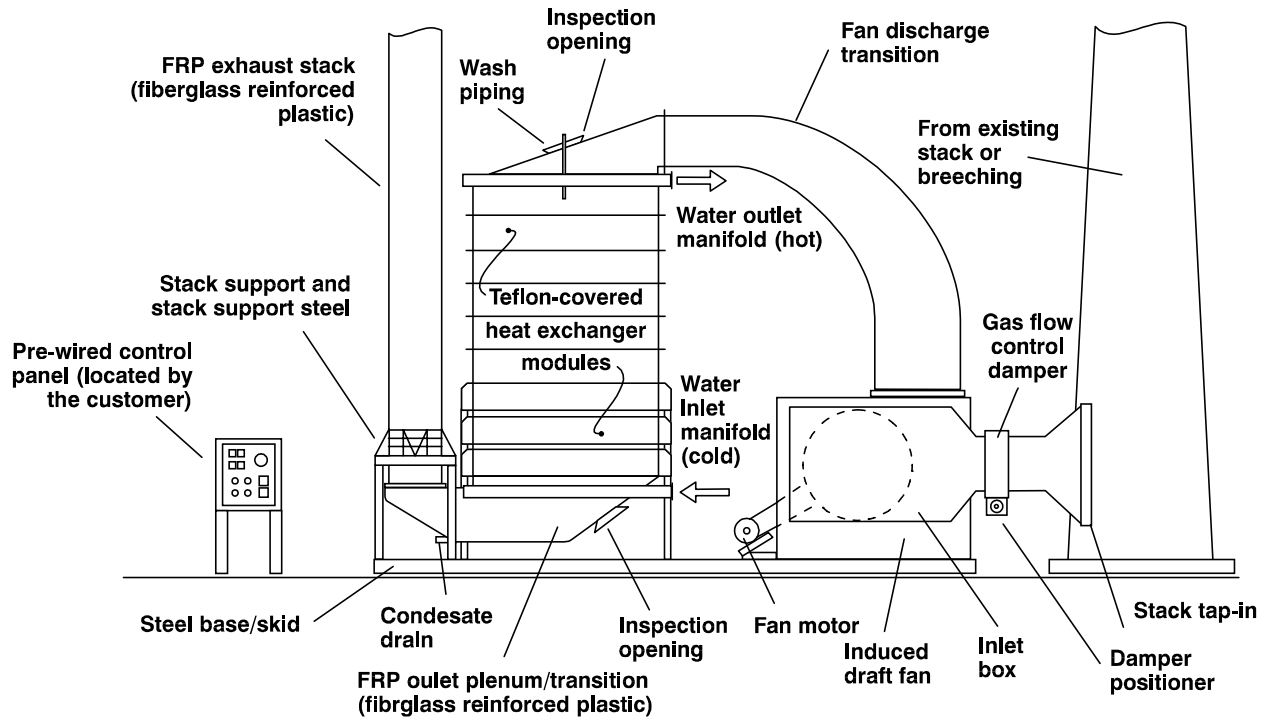


Figure 2.1 Drawing of a Typical Condensing Heat Exchanger Application

Teflon[®] is also durable and resistant to abrasion by solid particles in the gas. Fly ash will not stick to the Teflon[®] tubes. The inside surfaces of the heat exchanger shell are covered with Teflon[®] sheets. During fabrication, the Teflon[®]-covered tubes are pushed through the Teflon[®] tube sheet lining to form a Teflon[®]/Teflon[®] seal, ensuring that all heat exchanger surfaces exposed to the flue gas are protected against acid corrosion. Interconnections between the heat exchanger tubes are made outside the tube sheet and are not exposed to the corrosive flue gas stream.

A commercial condensing heat exchanger is made up of heat exchanger modules that can be stacked in series in the gas stream. This modular design allows the size of the unit to be optimized for each application at minimum cost. To ensure the lifetime of the Teflon[®] covering on the tubes, the inlet gas temperature is limited to 260°C (500°F), a condition easily satisfied in most flue gas waste heat recovery applications.

2.1.2 Integrated Flue Gas Treatment (IFGT) Condensing Heat Exchanger Design

The IFGT condensing heat exchanger, shown schematically in Figure 2.2, is designed to enhance the removal of pollutants from the flue gas stream compared to a commercial CHX[®]. The IFGT design uses many of the same heat exchanger components found in the proven commercial design, so unit lifetimes will be comparable to current commercial units.

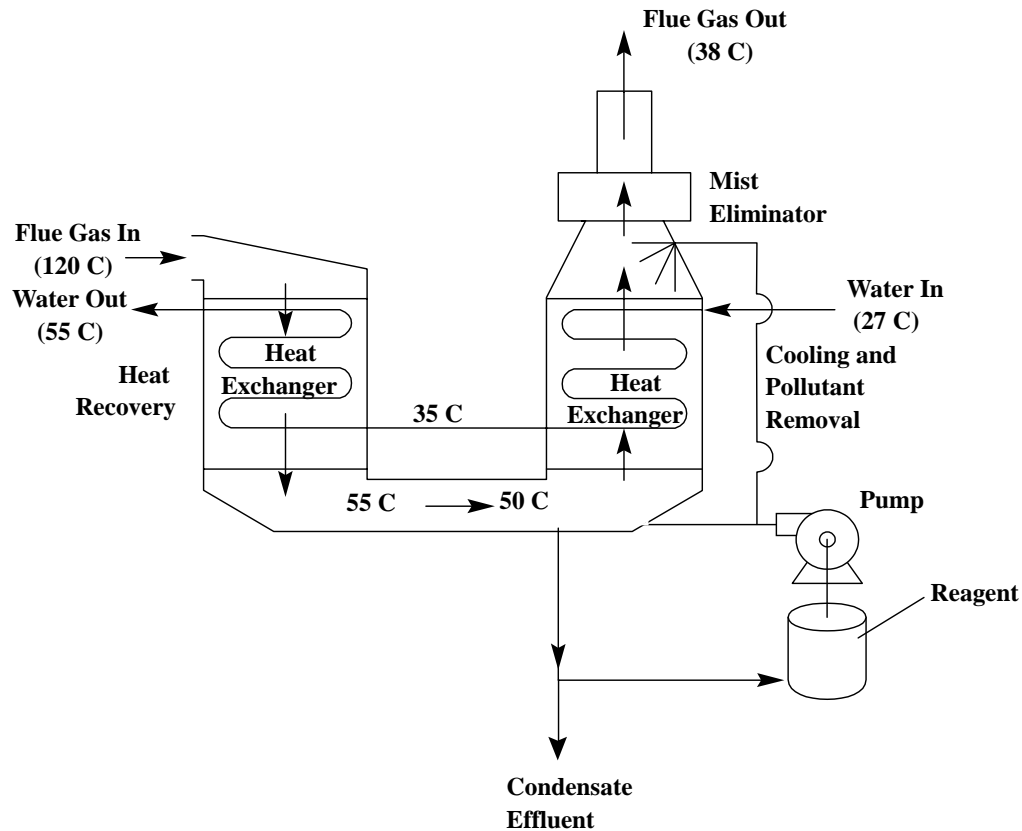


Figure 2.2 Schematic of the IFGT Condensing Heat Exchanger

An IFGT system consists of four sections: the first heat exchanger stage, the inter-stage transition region, the second heat exchanger stage, and the mist eliminator. The major differences between the integrated flue gas treatment design and the conventional condensing heat exchanger design are:

- 1) the integrated flue gas treatment design uses two heat exchanger stages instead of one,
- 2) the inter-stage transition region, located between the two heat exchanger stages, is used to direct the gas to the second heat exchanger stage, acts as a collection tank, and allows treatment of the gas between the stages,
- 3) the gas flow in the second heat exchanger stage is upward, rather than downward,

- 4) the top of the second heat exchanger stage is equipped with an alkali reagent spray system, and
- 5) the mist eliminator is used to remove any alkali spray and condensed droplets from the flue gas.

Most of the sensible heat is removed from the gas in the first heat exchanger stage of an IFGT system. The transition region can be equipped with water or alkali sprays to saturate the flue gas with moisture and assist removal of pollutants and particulate from the gas. The inter-stage transition is made of corrosion resistant fiberglass-reinforced plastic. Usually, the second heat exchanger stage is operated in the condensing mode, removing latent heat from the gas along with pollutants. The gas in this module is flowing upward while droplets fall downward. This provides a scrubbing mechanism that enhances particulate and pollutant capture. The dimensions and spacings of the heat exchanger tubes ensures that the larger particulate impact the wet tubes where droplet condensation is taking place. Sub-micron size particles can be collected by impaction with the tubes or droplets, or can be collected by diffusion.

The mechanisms described above primarily address the removals of particulate, highly water soluble pollutants and condensible pollutants. Additional flue gas processing is still needed, however, to provide adequate removal of SO₂ from the flue gas. To achieve this, the top of the second heat exchanger module is equipped with an alkali reagent spray system. The condensed gases, particulate, and alkali reagent are collected at the bottom of the transition section. The condensate from the flue gas can provide a portion or all of the water requirements for the alkali reagent spray system. This improves the attractiveness of the process by reducing the fresh water requirements. A condensate/reagent blow down stream is used to maintain the reagent chemistry.

The flue gas outlet of the IFGT system is equipped with a mist eliminator to reduce the moisture carryover and ensure that local environmental requirements are satisfied.

2.2 Phase I Technical Program

In the Phase I Proposal, two primary technical issues were identified that needed to be resolved to bring the IFGT Process to commercial practice for coal-fired applications;

- 1) The expected lifetime for the Teflon[®]-covered tubes that comprise the heat exchanger surface when exposed to flue gas containing fly ash from coal combustion.
- 2) The pollutant removal performance of the IFGT system

Item 1 has been addressed in Phase I and is reported in the Task 3 Topical Report for this project. Item 2 is addressed by this report, which provides the results of pollutant removal tests conducted at McDermott Technology Inc.'s, Alliance Research Center.

Task 2 investigated the removal performance of the IFGT process for a variety of flue gas pollutants. These included SO₂, NO_x, particulate, mercury and other trace elements, chloride and fluoride compounds, and ammonia.

Four series of tests (series I through IV) were conducted using four coals and three reagents. The coals included two blends of Ohio #5 and Ohio #6 coals, a Powder River Basin coal, and a Pittsburgh #8 coal. The different coals were selected to represent high, medium, and low sulfur content and also represent several different classifications of coal used by the utility industry. The Pittsburgh coal was selected for its sulfur content and also because this coal is used at the Kintigh Station, the site of the ECTC and the planned location for Phase II testing.

The reagents tested included sodium carbonate, lime and magnesium enhanced lime (mag-lime). The IFGT process was originally designed for the industrial market, and the sodium-based reagent provided a highly reactive reagent that required a minimum of preparation before use. For utility applications, sodium reagents are costly and represent a significant disposal problem if not reclaimed or recycled. Although sodium-based regenerable scrubbing systems have been used in the utility industry (Wellman Lord and dual alkali systems) they are not widely accepted. Lime and magnesium-lime reagents are typically less reactive than sodium, but are less costly and pose a much simpler disposal problem.

The goal of Task 2 was to determine the pollutant removal efficiencies of the IFGT process and the functional dependence on process parameters so that reliable predictions of performance can be made for commercial coal-fired applications.

3.0 FACILITIES AND EQUIPMENT

3.1 Small Boiler Simulator (SBS) Furnace

Flue gas for the pollutant removal test was provided by a pilot scale furnace designated as the Small Boiler Simulator (SBS). This 1.75 MW_t (six million Btu/hr) combustion research facility includes fuel preparation and handling equipment, a furnace and convection pass that provided a typical flue gas time-temperature history, a heat exchanger, dry scrubber module and a bag house. Figure 3.1 shows an isometric view of the major components of the SBS facility and how they are connected to the pilot IFGT condensing heat exchanger. The IFGT facility is in a bypass loop downstream of the SBS induced draft fan.

The coal burner used for these tests is a low NO_x burner equipped with dual air zones. The same burner with the same nominal air register settings was used for all of the test coals. Although designed as a Low NO_x burner, it was not operated as such during these tests. NO_x concentrations typically ranged from 300 ppm_v to 400 ppm_v. The furnace load was set to provide the required flue gas flow rate and was essentially constant at 1.3 MW_t (4.4 million Btu/hr) for all tests.

The heat exchanger downstream of the SBS convection pass is a two-pass shell and tube construction with cooling water in the shell and flue gas passing through the tubes. The heat exchanger is used to reduce the flue gas temperature at the outlet of the SBS convection pass from a temperature of about 370°C (700°F) to a temperature of about 150°C (300°F). The 150°C flue gas temperature is an upper limit for the bag house, and is also the typical operating temperature of the dry scrubber when in service.

The SBS bag house typically removes 99.9+% of the particulate from the flue gas leaving the furnace. For these tests a measurable particle loading at the IFGT unit was needed to characterize the particle removal efficiency of the IFGT system. To provide a measurable particle loading at the CHX[®] facility, approximately 10% to 20% of the flue gas from the SBS furnace was bypassed around the bag house. The dry scrubber module was not used for these tests, but provided the gas path from the heat exchanger to the bag house. Heat loss and air infiltration downstream of the bag house limited the flue gas temperature at the inlet of the IFGT system to about 120°C (250°F).

3.2 Integrated Flue Gas Treatment System

Integrated Flue Gas Treatment is an extension of the CHX[®] condensing heat exchanger technology. The standard CHX[®] design for heat recovery consists of eight tube modules stacked vertically. Each module consists of eight rows of tubes positioned in a triangular pitch. The cross section of the heat exchanger is then adjusted to accommodate the full load gas flow. The pilot facility at B&W's Alliance Research Center is essentially full scale in the vertical direction, with a stack of seven heat exchanger modules in the first stage and a stack of eight modules in the second heat exchanger stage. The cross-sectional area of the heat exchanger shell is 0.3 m X 0.46 m (1 ft. X 1.5 ft.).

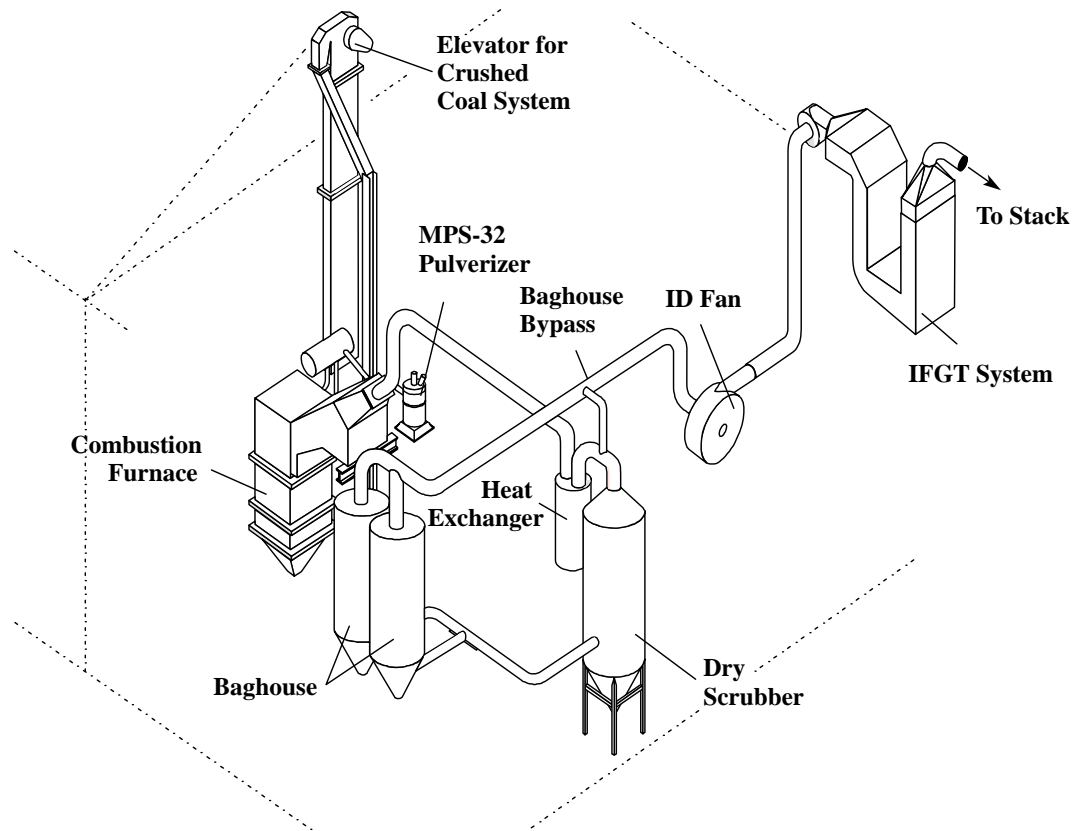


Figure 3.1 Equipment Arrangement and Gas Flow Path for the Small Boiler Simulator and Condensing Heat Exchanger Test Facilities

Referring to Figure 2.2, the four major sections of the IFGT are the first heat exchanger stage, the inter-stage transition region, the second heat exchanger stage, and the spray/disengagement region. The flue gas flow path is down flow through the first stage and up flow through the second stage.

Most of the sensible heat is removed from the flue gas in the first heat exchanger stage of the IFGT. Condensation can occur within the first heat exchanger stage if the gas temperature at the tube surface is below the water vapor dew point. Some flue gas pollutant removal also occurs within the first heat exchanger as particulate impact the tubes and acid gas condensation and absorption occurs.

The inter-stage transition provides a gas flow path between the two heat exchanger stages and acts as a collection sump for reagent/condensate. The transition is equipped with spray nozzles that can be used to assist in removing pollutants from the flue gas. The transition piece is made of corrosion resistant fiberglass-reinforced plastic.

The second heat exchanger stage can be operated in the condensing mode, removing both latent and sensible heat from the gas along with pollutants. Flue gas in this stage flows upward while the liquid droplets in the gas fall downward. This provides a scrubbing mechanism that enhances particulate and pollutant capture.

The spray/disengagement region consists of three plastic sections installed above the second heat exchanger stage. Each section is about 0.46 m (1.5 ft) in height. The three plastic sections contain the second-stage reagent spray nozzles and two sets of chevron style mist eliminators. They also provide a disengagement zone for liquid drops entrained in the flue gas as it exits the second heat exchanger stage.

An alkali reagent tank is used to mix fresh reagent with the recirculating solution/slurry. For example, sodium carbonate is added to the solution in the tank with a pH controlled variable speed screw feeder. A mixer stirs the solution in the tank to dissolve and react the sodium carbonate. The scrubbing solution and condensate collected at the bottom of the inter-stage transition during operation is gravity fed to the reagent tank. As originally constructed, and during initial testing, the reagent tank was equipped with an overflow drain to remove accumulated water and dissolved solids inventory due to condensation, makeup water addition, and the accumulated reaction products. To improve reagent utilization, the overflow connection was later moved - after test series I - to the reagent return line from the inter-stage transition.

The scrubbing solution can be directed to the top of the second stage heat exchanger or to the transition section. The fiberglass inter-stage transition located between the two heat exchanger stages is equipped with six spray nozzles.

Flue work is installed to bring the exhaust gas from the SBS to the pilot IFGT. The 305 mm (12 inch) insulated flue is tied into the exhaust of the SBS downstream of the bag house and I.D. fan. The flue gas enters at the top of the first heat exchanger stage and exits out the top of the second heat exchanger stage. A 305 mm non-insulated PVC flue is installed at the exit of the pilot IFGT to an exhaust stack placed outside the building.

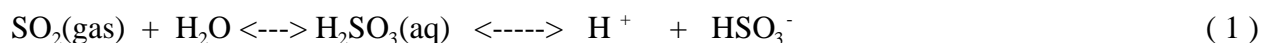
Gas sampling lines and 102 mm (4 inch) ports for in-situ sampling are located at the inlet and outlet of the IFGT facility. The heated gas sample lines provide a continuous flow of flue gas for the on-line gas analyzers. One gas sample line is in the inlet duct just upstream of the first heat exchanger stage. The other gas sample line is in the PVC outlet duct. Heat-traced lines are used to transport the flue gas samples from the ducts to the gas analyzers. Two 102 mm (4 inch) ports are installed both in the inlet and in the outlet flue gas ducts for particulate sampling and other gas sampling as required by the test program.

The facility is equipped with instrumentation to measure the flow rate and temperatures of the IFGT process streams, including the flue gas, cooling water, reagent flow rate to the nozzles, blowdown stream and make up water. A detailed description of the facility and instrumentation is contained in Appendix A.

3.3 IFGT Removal Mechanisms

System Chemistry - In the IFGT process, SO₂ is absorbed and neutralized by chemical reaction with an alkaline reagent in the second stage. The process uses gas absorption and liquid phase acid-base reactions of sulfur and sodium species. The chemistry for the absorption of SO₂ and chemical reaction with a sodium carbonate reagent in the IFGT system can be described by a complex set of reactions. Most of these reactions take place in the absorber section where the exposure time between the flue gas and scrubbing liquid is very short - on the order of 1.5 seconds. The following subsections provide an overview of the system chemistry and summarize relevant aspects of the limiting steps to mass transfer in the second stage.

Sulfur Dioxide Absorption - The absorption of SO₂ from the flue gas with a sodium reagent depends on a gas-liquid mass transfer process where the SO₂ is transferred into the scrubbing liquor and neutralized by dissolved alkaline species. SO₂ is physically absorbed very rapidly into water to form sulfurous acid that further dissociates into aqueous ions. A simplified equilibrium reaction describing the chemical sequence is shown in equation 1.



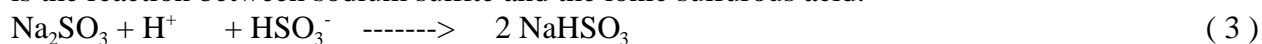
The ability of SO₂ to dissolve in water is limited. At typical IFGT system operating conditions, and with flue gas SO₂ concentration of 2000 ppm, the solubility of SO₂ in water is approximately 540 mg/liter. Approximately 70% of the dissolved SO₂ is dissociated, while 30% remains in the undissociated form as H₂SO₃ (aq). When operating at liquid-to-gas ratio (L/G) of 0.27 l/m³ (2.0 gal/1000 ft³), the SO₂ removal efficiency attributable to physical absorption and dissolution *without chemical reaction* is approximately 3.5 %. If dissolved alkaline species that can neutralize the H⁺ are in the bulk liquid entering the second stage, then more SO₂ can be absorbed, and the SO₂ removal efficiency is enhanced.

Sodium Carbonate Make-up - Sodium carbonate is used to maintain the process liquor pH at a level appropriate for SO₂ removal in the second stage. Bulk soda ash is stored in a hopper as a dry powder. The soda ash is added to the reagent tank, where sodium carbonate immediately dissolves and reacts with sodium bisulfite to form sodium sulfite, water, and carbon dioxide gas.



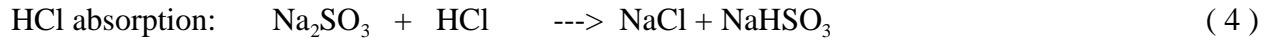
Sodium carbonate is very soluble in water. When added in powder form, the dissolution is very rapid and no solid sodium carbonate is present in the scrubbing liquid when sprayed into the IFGT system.

Sulfite Neutralization - The primary chemical reaction for the neutralization of the absorbed SO₂ is the reaction between sodium sulfite and the ionic sulfurous acid.



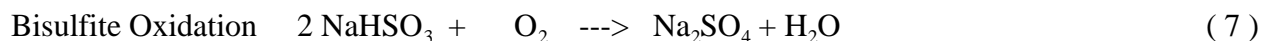
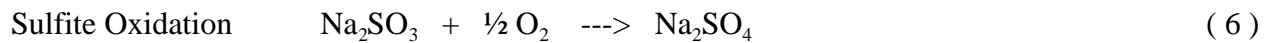
While the type of alkali added to the process is sodium carbonate, sodium carbonate does not directly react with the absorbed SO₂, the "active" alkali that reacts with the absorbed SO₂ is sodium sulfite.

Halide Acid Gas Neutralization - In addition to the reactions discussed above, trace amounts of hydrogen chloride and hydrogen fluoride acid gases in the flue gas are also absorbed by the liquid.



These acid gases are extremely soluble; they completely dissociate in the aqueous solution, and are absorbed to a very high extent.

Sodium Oxidation - The oxidation of sodium compounds to sodium sulfate occurs because of the excess oxygen in the flue gas that dissolved into the liquid



The sulfite oxidation depletes sodium sulfite and competes with the sulfite neutralization of absorbed SO_2 . The sulfite oxidation reaction is, therefore, considered an undesirable reaction. Essentially all of the oxygen dissolved in the scrubbing liquid from the flue gas will be consumed through these sodium oxidation reactions. Fortunately, oxygen has a relatively low solubility in aqueous liquids and reasonable efforts to minimize the flue gas oxygen concentration such as minimizing combustion excess air and duct air infiltration can be used.

SO_2 Absorption Limitations - Gas absorption is one of the most common industrial mass transfer unit operations and is the process where one or more soluble components of a gas mixture are absorbed in a liquid. The absorption into the liquid can be purely physical absorption or as with the IFGT process, can involve chemical enhancement through a chemical reaction in the liquid phase. The extent of physical absorption depends on the solubility of the substance absorbed. Chemical absorption involves chemical reactions between the absorbed gas and other constituents in the absorbing medium. In the IFGT process, if the chemical reactions in the liquid instantaneously consume all the SO_2 absorbed, then the limiting factors for the rate of mass transfer are amount the gas-liquid surface area, and the ability of SO_2 to diffuse through the flue gas to the liquid surface.

To instantaneously consume all the SO_2 absorbed, the scrubbing liquid must contain sufficient dissolved alkalinity so that no finite SO_2 liquid vapor pressure exists at any location in the absorber section. Dissolved alkalinity is a measure of the capacity of the scrubbing liquor to absorb SO_2 . Any dissolved ion that is more alkaline than the bisulfite ion (HSO_3^-) formed by the dissolution of SO_2 from the gas into the liquid contributes to the dissolved alkalinity. The pertinent ion for a sodium reagent is the sulfite ion (SO_3^-) formed by the neutralization of the sodium carbonate reagent with sodium bisulfite (Equation 2).

The equilibrium SO₂ vapor pressure over the liquid, the theoretical limit that the IFGT system can only approach, generally depends on the liquor's temperature, pH, relative concentration of sulfite and bisulfite species, and the liquid ionic strength. For test series I, the distribution of liquid phase sulfite and its effect on pH and SO₂ liquid vapor pressure is shown in Figure 3.2. At a liquid pH above 6.5, most of the dissolved sulfur is in the form SO₃⁼ and the SO₂ liquid vapor pressure is essentially zero (<1 ppm). If the liquid pH at the gas-liquid interface is below approximately 6.0, the SO₂ liquid vapor pressure increases dramatically and can lead to equilibrium inhibited SO₂ absorption. The SO₂ vapor pressure represents the equilibrium condition between the liquid and gas and for a known flue gas composition one can calculate the theoretical maximum SO₂ removal efficiency. For example, if the flue gas SO₂ concentration is 2000 ppm, and the IFGT operating conditions produce an SO₂ vapor pressure of 60 ppm, then the maximum achievable SO₂ removal efficiency is 97%.

When the scrubbing liquid contains sufficient dissolved alkalinity so that essentially no finite SO₂ liquid vapor pressure exists at any location in the absorber section, the mass transfer occurs under conditions referred to as *Gas Phase Mass-Transfer Limited*. Under these conditions, the SO₂ absorption process is controlled by the diffusion of SO₂ from the bulk gas through the gas film at the liquid surface. The rate of mass transfer (R), then, is directly proportional to the SO₂ concentration in the flue gas [Y_{SO2}].

$$R = k_g a [Y_{SO_2}] \quad (\text{mole/cm}^2\text{-sec}) \quad (8)$$

The term "k_g" is the mass transfer coefficient. The term "a" is the surface area between the gas and liquid. An evaluation of this relationship at various inlet SO₂ concentrations shows that the SO₂ removal *efficiency* remains constant. In practical terms, if the SO₂ concentration is reduced by 50%, the SO₂ absorption *rate* is equally reduced and the SO₂ removal efficiency remains unchanged.

The generation of gas-liquid surface area in the IFGT process is accomplished by:

- 1) initial introduction of the scrubbing liquid through spray nozzles,
- 2) liquid hold up above the last row of tubes,
- 3) liquid passing over tube surfaces,
- 4) liquid drops passing from tube to tube and from the last row of tubes to the sump, and
- 5) liquid flowing down the walls.

At full load conditions, and an L/G (liquid-to-gas ratio) less than approximately 0.13 l/m³ (1.0 gal/1000 ft³), some tube and wall surfaces are not active, and there is no liquid holdup above the last set of tubes. At L/Gs that range from approximately 0.13 to 0.27 l/m³ (1 to 2 gal/1000 ft³), the surface area from droplets increases. At an L/G above approximately 0.27 l/m³ (2 gal/1000 ft³), liquid hold up above the top row of tubes becomes significant. The total surface area is a complex function of L/G, and is difficult to estimate without conducting very specialized tests. Obviously, the surface area increases with L/G and enhances SO₂ removal efficiency.

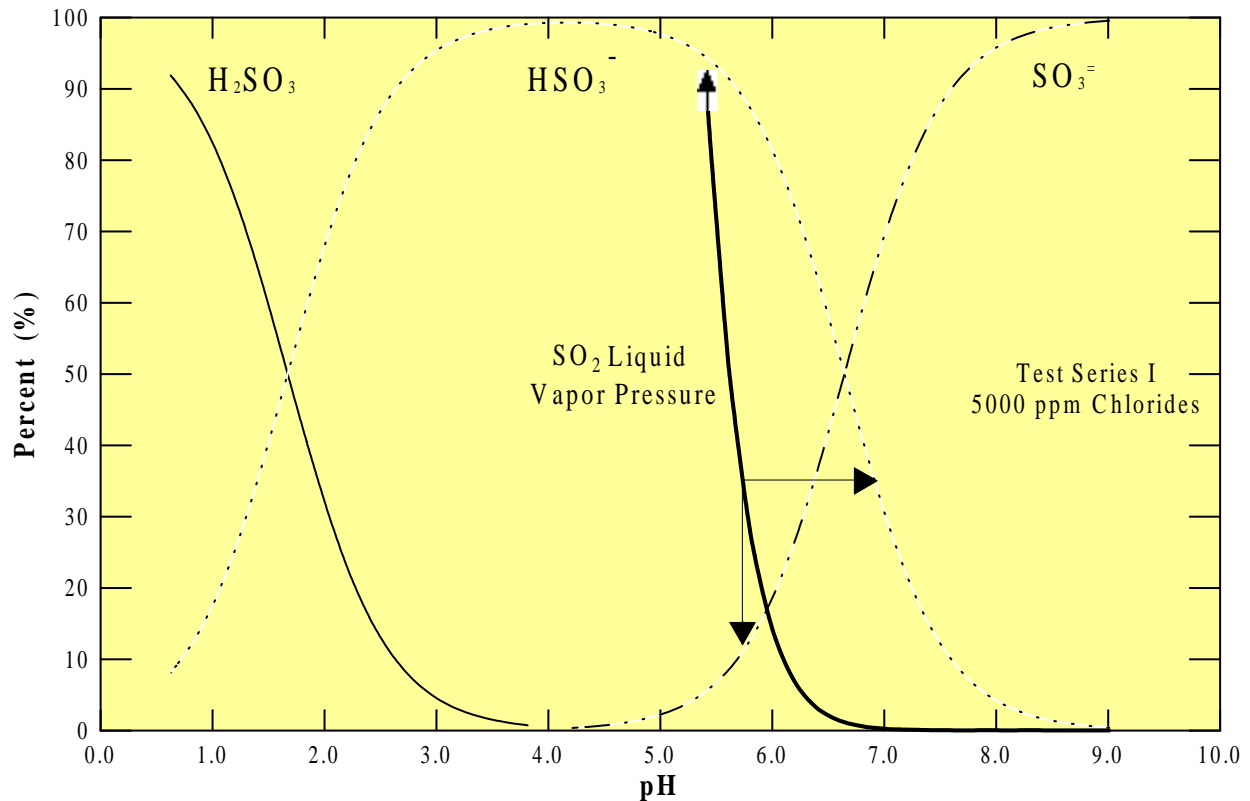


Figure 3.2 Distribution of Total Liquid Phase Sulfite as a Function of pH.

The ability of SO_2 to diffuse from the bulk flue gas through the gas-liquid boundary layer to the liquid surface is primarily controlled by factors that affect the SO_2 diffusion transport properties and the thickness of the gas-liquid boundary layer. The transport properties primarily depend on the type of gases in the system. Within the limits of typical IFGT operating conditions these properties remain essentially unchanged. The thickness of the gas-liquid boundary layer, however, decreases as the relative velocity between the liquid and gas increases. The positive effect is related through the dimensionless Reynolds number and varies approximately with the square root of velocity. Mathematical equations estimating mass transfer rates as a function of velocity for tubes and drops are discussed in Section 5.2.

4.0 TEST DESCRIPTION

4.1 Test Conditions

The experimental test program completed for the SBS/IFGT facilities was designed to investigate the effect of the primary system operating parameters on pollutant removal and is discussed in the following sections. The SBS/IFGT facilities were operated from 5 to 12 days on each coal to characterize the performance of the IFGT system. Four coals were tested that included a 80/20 blend of Ohio #5/Ohio #6 coal (Test I), a Pittsburgh #8 coal that is used at the ECTC (Test II), a Powder River Basin Coal (Test III), and a 80/20 blend of Ohio #6/Ohio #5 coal (Test IV). The composition of these coals are described in Table 4.1. Tests using the ECTC coal provided data that will be directly applicable to the 5.0 MW IFGT tests at the ECTC scheduled for Phase II.

Table 4.1 Coal Analyses

Coal		80% Ohio#5 20% Ohio #6 Test Series I	Pittsburgh # 8 Test Series II	Powder River Basin Test Series III	80% Ohio #6 20% Ohio #5 Test Series IV
C	% by wt.	69.15	75.08	58.74	75.58
H ₂	% by wt.	5.03	5.09	4.05	5.24
S	% by wt.	3.85	2.58	0.44	3.07
O ₂	% by wt.	7.01	5.45	14.48	8.79
N ₂	% by wt.	1.37	1.5	0.96	1.41
H ₂ O	% by wt.	6.93	0.92	15.12	2.83
Ash	% by wt.	6.66	9.38	6.21	5.08
Heating Value - wet basis (Btu/lb)		12538	13438	10049	13320
Arsenic	ppm _m	12.43	7.92	1.59	7.47
Barium	ppm _m	3.24	25.26	493.50	3.85
Beryllium	ppm _m	0.15	0.63	0.11	0.83
Cadmium	ppm _m	0.70	0.05	0.09	0.19
Cobalt	ppm _m	0.78	0.91	1.43	0.53
Chromium	ppm _m	46.58	0.34	9.26	1.23
Manganese	ppm _m	15.75	9.29	28.20	6.19
Nickel	ppm _m	22.11	18.93	13.14	42.70
Lead	ppm _m	5.71	2.58	3.05	6.01
Selenium	ppm _m	1.56	1.17	0.12	1.90
Mercury	ppm _m	0.43	0.10	0.41	0.13
Chlorides	ppm _m	2200	123	134	1900
Fluorides	ppm _m	25.8	<11	46	25.6

Tables 4.2 through 4.5 summarize the completed test matrix for test series I, II, III, and IV. Each matrix is grouped according to the different types of pollutant removal under study. The first three test series evaluated removal efficiencies for various gas phase, and particulate phase species with different coals and sodium carbonate - also known commercially as dense soda ash - reagent. The fourth test series evaluated the ability of the reagents soda ash, lime and mag-lime to capture SO₂, mercury, and heavy metals, and investigated the use of mesh pads for providing fine particulate control. The HCl and HF measurements conducted in test series IV repeated measurements that were made earlier in the program and showed relatively poor HCl removal efficiencies compared to all other test data. Mesh pads were also used in Test Series IV for providing fine (sub-micron) particulate removal. The mesh pads were positioned in the inter-stage of the IFGT system. Particle loading and size distribution measurements were made at the inlet and outlet of the IFGT system.

During each test series, several large samples of blowdown waste water were collected in 35 gallon drums. This condensate waste will be used to evaluate disposal methods in Phase II of the program. Additionally, smaller samples of the blowdown were collected to determine the chemistry of the waste water and to test for mercury, particulate, and other heavy metals.

4.1.1 Acid Gas Pollutant Removal

In these tests, SO₂ and NO_x removal, and HCL and HF removal were evaluated. SO₂, HCl, and HF removal was evaluated during all four test series. A greater or lesser number of tests were conducted on any given coal so that sufficient data was collected to determine the SO₂ and NO_x removal characteristics of the IFGT.

At high liquid pH with Na₂CO₃, or Ca(OH)₂ reagent, the significant resistances to absorption of SO₂ are those affecting mass transfer from the gas phase to the alkaline liquid surface. Above a liquid pH greater than about 6.5, the vapor pressure of SO₂ in the liquid is essentially zero. Under these conditions, the major factors for SO₂ removal performance are the amount of gas-liquid surface area in the 2nd stage of the IFGT and flue gas velocity. When the absorbing reagent liquids pH falls below about 6.5, then the liquid phase SO₂ vapor pressure increases which can contribute to a measurable reduction in the absorption of SO₂. To investigate these effects, the test matrix included conditions at a variety of liquid pH, flue gas inlet velocity, and liquid-to gas ratio (L/G) values. The SO₂ tests were conducted with continuous gas concentration monitors at the IFGT inlet and outlet. Therefore, the test durations were relatively short. Once the inlet and outlet SO₂ levels stabilized, approximately 10 to 20 minutes was required to collect operating data from the Data Acquisition System and other instruments, and to collect process stream samples.

Table 4.2 - Test Series I Completed Test Matrix.

Test ID	pH	Flue Gas Outlet Temperature (°C)	Flue Gas Inlet Velocity (m/s)	Stage 2 L/G Ratio (l/m ³)	Particulate Loading (mg/dscm)	IFGT Inlet NH3 Concentration (ppm _v)	Stage 2 Steam Injection (kg/hr)
---------	----	----------------------------------	-------------------------------	---------------------------------------	-------------------------------	--	---------------------------------

SO₂ and NO_x Removal and Heat Recovery

1	8	Dewpoint	12	0.07	<14 to 420
2	8	Dewpoint	12	0.13	<14 to 420
3	8	Dewpoint	12	0.27	<14 to 420
4	8	Dewpoint	12	0.67	<14 to 420
5	8	Dewpoint	12	1.07	<14 to 420
7	8	Dewpoint	6	2.14	<14 to 420
8	8	Dewpoint	6	0.27	<14 to 420
9	8	Dewpoint	6	0.67	<14 to 420
10	8	Dewpoint	6	1.07	<14 to 420
11	8	Dewpoint - 11	12	0.07	<14 to 420
12	8	Dewpoint - 11	12	0.13	<14 to 420
13	8	Dewpoint - 11	12	0.27	<14 to 420
14	8	Dewpoint - 11	12	0.67	<14 to 420
15	8	Dewpoint - 11	12	1.07	<14 to 420
16	7	Dewpoint	12	0.07	<14 to 420
17	7	Dewpoint	12	0.27	<14 to 420
18	7	Dewpoint	12	1.07	<14 to 420
19	6	Dewpoint	6	0.07	<14 to 420
20	6	Dewpoint	6	0.27	<14 to 420
21	6	Dewpoint	6	1.07	<14 to 420
22	7	Dewpoint - 11	6	1.88	<14 to 420
23	7	Dewpoint - 11	6	1.34	<14 to 420
24	7	Dewpoint - 11	6	0.40	<14 to 420
25	7	Dewpoint - 11	6	0.67	<14 to 420
26	7	Dewpoint - 11	6	1.07	<14 to 420

HCl and HF Removal

4A	8	Dewpoint	12	0.67	420
----	---	----------	----	------	-----

Hg and Heavy Metals Metals Removal

4B	8	Dewpoint	12	0.67	420
4C	8	Dewpoint	12	0.67	<14
14D	8	Dewpoint - 11	6	0.67	420

Ammonia Removal

4	8	Dewpoint	12	0.67	420	50
4F	8	Dewpoint	12	0.67	420	10
14G	8	Dewpoint - 11	12	0.67	420	50

Particulate Removal

4J	8	Dewpoint	12	0.67	0.3	----	45.3
----	---	----------	----	------	-----	------	------

Particulate Removal - Cascade Impactor

4L	8	Dewpoint	12	0.67	0.3	----	0
14M	8	Dewpoint - 11	12	0.67	0.3	----	0
4N	8	Dewpoint	12	0.67	0.3	----	45.3

Table 4.3 Test Series II Completed Test Matrix

Test ID	pH	Flue Gas Outlet Temperature (°C)	Flue Gas Inlet Velocity (m/s)	Stage 2 L/G Ratio (l/m ³)	Particulate Loading (mg/dscm)	IFGT Inlet NH ₃ Concentration (ppm _v)
---------	----	----------------------------------	-------------------------------	---------------------------------------	-------------------------------	--

SO₂ Removal and Heat Recovery

1	8	Dewpoint	12	0.07	<14 to 28
2	8	Dewpoint	12	0.13	<14 to 28
3	8	Dewpoint	12	0.27	<14 to 28
4	8	Dewpoint	12	0.67	<14 to 28
5	8	Dewpoint	12	1.07	<14 to 28
6	8	Dewpoint	6	0.27	<14 to 28
7	8	Dewpoint	6	0.67	<14 to 28
8	8	Dewpoint	6	1.07	<14 to 28
9	6	Dewpoint	12	0.07	<14 to 28
10	6	Dewpoint	12	0.27	<14 to 28
11	6	Dewpoint	12	0.67	<14 to 28
12	7	Dewpoint	12	0.07	<14 to 28
13	7	Dewpoint	12	0.27	<14 to 28
14	7	Dewpoint	12	0.67	<14 to 28
16	6	Dewpoint	6	0.67	<14 to 28
17	6	Dewpoint	6	0.27	<14 to 28
18	6	Dewpoint	6	1.07	<14 to 28
19	6	Dewpoint	6	0.80	<14 to 28
20	7	Dewpoint	6	0.27	<14 to 28
21	7	Dewpoint	6	0.67	<14 to 28
22	7	Dewpoint	6	1.07	<14 to 28
23	7	Dewpoint - 11	6	0.47	<14 to 28
24	7	Dewpoint - 11	6	1.27	<14 to 28
25	7	Dewpoint - 11	6	0.27	<14 to 28
26	7	Dewpoint - 11	6	0.67	<14 to 28
27	7	Dewpoint - 11	6	1.07	<14 to 28

HCl and HF Removal

4B	8	Dewpoint	12	0.67	<14 to 28
----	---	----------	----	------	-----------

Hg and Heavy Metals Metals Removal

4A	8	Dewpoint	12	0.67	<14 to 28
4C	8	Dewpoint	12	0.67	42 to 420

Ammonia Removal

4D	8	Dewpoint	12	0.67	<14 to 28	50
4E	8	Dewpoint	12	0.67	<14 to 28	20
4F	8	Dewpoint - 11	12	0.67	<14 to 28	50

Particulate Removal

4F	8	Dewpoint - 11	12	0.67	<14 to 28	50
----	---	---------------	----	------	-----------	----

Particulate Removal - Cascade Impactor

4G	8	Dewpoint	12	0.67	42 to 420	---
----	---	----------	----	------	-----------	-----

Table 4.4 Test Series III Completed Test Series

Test ID	pH	Flue Gas Outlet Temperature (°C)	Flue Gas Inlet Velocity (m/s)	Stage 2 L/G Ratio (l/m ³)	Particulate Loading (mg/dscm)	IFGT Inlet NH3 Concentration (ppm _v)
---------	----	----------------------------------	-------------------------------	---------------------------------------	-------------------------------	--

SO2 Removal and Heat Recovery

1	NC	Dewpoint	12	0.00	420 to 830
2	NC	Dewpoint	12	0.40	420 to 830
3	4	Dewpoint	12	0.40	420 to 830
4	4	Dewpoint	12	0.20	420 to 830
5	5	Dewpoint	12	0.40	420 to 830
6	5	Dewpoint	12	0.20	420 to 830
7	6.5	Dewpoint	12	0.40	420 to 830
8	6.5	Dewpoint	12	0.20	420 to 830
9	8	Dewpoint	12	0.40	420 to 830
10	8	Dewpoint	12	0.20	420 to 830
11	8	Dewpoint	6	0.80	420 to 830
12	8	Dewpoint	6	0.40	420 to 830
13	5	Dewpoint	6	0.80	420 to 830
14	6.5	Dewpoint	6	0.40	420 to 830
15	nc	Dewpoint - 11	12	0.40	420 to 830
16	6.5	Dewpoint - 11	12	0.40	420 to 830
17	6.5	Dewpoint - 11	12	0.20	420 to 830
15R	NC	Dewpoint - 11	12	0.20	420 to 830

HCl and HF Removal

7A	6.5	Dewpoint	12	0.40	420 to 830
----	-----	----------	----	------	------------

Hg and Heavy Metals Metals Removal (See Note 1)

9A	8	Dewpoint	12	0.40	420 to 830
12A	8	Dewpoint	6	0.40	420 to 830

Ammonia Removal

7B	6.5	Dewpoint	12	0.40	420 to 830	20
9B	8	Dewpoint	12	0.40	420 to 830	50
18	8	Dewpoint - 11	12	0.40	420 to 830	50

Particulate Removal

9B	8	Dewpoint	12	0.40	420 to 830	20
12C	8	Dewpoint	6	0.40	420 to 830	----

Particulate Removal - Cascade Impactor

12B	8	Dewpoint	6	0.40	420 to 830	----
12D	8	Dewpoint	6	0.40	420 to 830	----

Table 4.5 Test Series IV Completed Test Matrix

Test ID	Feed pH	Return pH	Flue Gas Outlet Temperature (°C)	Flue Gas Inlet Velocity (m/s)	Stage 2 L/G Ratio (l/m ³)	Particulate Loading (mg/dscm)	Reagent	Mesh Pad
---------	---------	-----------	----------------------------------	-------------------------------	---------------------------------------	-------------------------------	---------	----------

SO₂ Removal and Heat Recovery

1	8	--	Dewpoint	12	0.53	420 to 830	Sodium Carbonate	
2	8	--	Dewpoint	6	0.53	420 to 830	Sodium Carbonate	
3	8	--	Dewpoint	12	0.80	420 to 830	Hydrated Lime	
4	10	--	Dewpoint	12	1.07	420 to 830	Hydrated Lime	
5	10	--	Dewpoint	12	0.53	420 to 830	Hydrated Lime	
6	8	--	Dewpoint	12	0.53	420 to 830	Hydrated Lime	
7	8	--	Dewpoint	12	1.07	420 to 830	Hydrated Lime	
8	6	--	Dewpoint	12	0.80	420 to 830	Hydrated Lime	
9	6	--	Dewpoint	12	0.53	420 to 830	Hydrated Lime	
10	6	--	Dewpoint	12	1.07	420 to 830	Hydrated Lime	
12	--	8	Dewpoint	12	0.13	420 to 830	Mag-Hydrated Lime	
13	--	8	Dewpoint	12	0.27	420 to 830	Mag-Hydrated Lime	
14	--	7	Dewpoint	12	0.53	420 to 830	Mag-Hydrated Lime	
14R1	--	6	Dewpoint	12	0.53	420 to 830	Mag-Hydrated Lime	
15	--	7	Dewpoint	12	1.07	420 to 830	Mag-Hydrated Lime	
16	--	6	Dewpoint	12	0.27	420 to 830	Mag-Hydrated Lime	

HCl and HF Removal

1A	8	--	Dewpoint	40	0.53	420 to 830	Sodium Carbonate	
----	---	----	----------	----	------	------------	------------------	--

Hg and Heavy Metals Metals Removal

14A	8	7	Dewpoint	12	0.53	420 to 830	Mag-Hydrated Lime	
-----	---	---	----------	----	------	------------	-------------------	--

Particulate Removal

2A	8	--	Dewpoint	6	0.53	420 to 830	Sodium Carbonate	None
----	---	----	----------	---	------	------------	------------------	------

Particulate Removal - Cascade Impactor

1B	8	--	Dewpoint	12	0.53	420 to 830	Sodium Carbonate	Interstage
2B	8	--	Dewpoint	6	0.53	420 to 830	Sodium Carbonate	None

The absorption of NO_x occurs by mechanisms similar to SO₂. However, approximately 95% of NO_x is in the form of NO, and the solubility of NO is less by a factor of about 1300. While some NO is absorbed in the IFGT system, it is estimated that the mass transfer of NO_x will be approximately 1/20th of that for SO₂. These levels of NO_x absorption were not detectable, and NO_x removal was evaluated only during the first test series, as measured NO_x removals were very low.

The test matrix for each test series included one test to investigate HCl and HF removal. The HCl and HF removal efficiency was quantified across the IFGT utilizing EPA methods and required approximately two hours to complete a single test.

4.1.2 Mercury and Heavy Metals Removal

The ability of the IFGT to remove mercury and heavy metals from the flue gas and the fate of the mercury was also determined. A total of eight test conditions were completed. Mercury speciation measurements were also conducted at both the inlet and outlet of the IFGT to quantify total, elemental, and oxidized mercury removal for each of the coals evaluated. Quantifying the individual species is important since each species has different chemical and physical properties. The main forms of mercury emitted in flue gas are elemental (Hg^0) or the oxidized state (Hg^{++} , typically mercuric chloride). Previous SBS measurements indicate that the total mercury emissions were within the expected range of 1-10 $\mu\text{g}/\text{m}^3$ (0.7 - 7 lb/trillion Btu) typical of coal-fired boilers.

Mercury species are removed from the flue gas by either condensation of (Hg^0) or absorption of Hg^{++} into the reagent liquid. Condensation of Hg^0 is usually not complete as the trace metal concentration is relatively low. However, the lower outlet flue gas temperature of the IFGT (35°C, 90°F) over a commercial wet scrubber (50°C, 122°F) may provide for higher levels of elemental mercury removal.

To address the final form of the mercury and to evaluate mercury material balances across the IFGT system, the IFGT liquid condensate, collected particulate and the reagent were analyzed for mercury concentration. Other streams outside of the IFGT system that were also evaluated for mercury content include the coal feed and upstream bag house ash.

To summarize, mercury concentration measurements were conducted on the following process streams:

- coal feed
- IFGT inlet and outlet gas flows and particulate
- IFGT condensate/blowdown
- bag house ash

Under steady-state operating condition, measurements were conducted in triplicate for all eight test conditions to determine the repeatability of the data. Each test required approximately two hours of sample time. Blanks were also run in order to assess the uncertainty in the measurements and to detect unknown sources of contamination.

4.1.3 Ammonia Removal

To determine ammonia removal, ammonia was injected upstream of the IFGT system at a constant measured flow rate. Below 230°C (450°F) ammonia reacts with sulfur trioxide (SO_3) in the flue gas, so that some of the ammonia may be removed from the flue gas upstream of the IFGT. Ammonia removal tests were conducted only during the first three test series. A matrix of 3 tests was completed during each test series for a total of nine tests. For all of these tests, removal efficiency was based on measurements at the inlet and outlet of the IFGT. A Severn Sciences continuous ammonia analyzer was used to sequentially measure the ammonia concentration upstream and downstream of the IFGT. Ammonia concentrations at the inlet and

outlet were also measured using EPA Method 206. Differences between the measured and calculated concentration based on the injection rate of ammonia at the IFGT inlet were used as a measure of the ammonia-sulfur reactions.

4.1.4 Particulate Removal

These tests determined the overall particulate removal efficiency of the IFGT facility and the removal efficiency as a function of particle size. The particulate loading to the IFGT facility consisted of the fugitive emissions from the SBS bag house, and a portion of the flue gas from the SBS that was diverted around the bag house and fed directly to the IFGT. Approximately 20% of the flue gas bypassed the SBS bag house.

A total of eight cascade impactor tests were completed to measure the particulate size distribution. Andersen Mark III cascade plate impactors were utilized for all particulate sizing tests. Additional total particulate measurements were also obtained as part of the sampling for mercury and acid gases. For those measurements, the sampling technique requires collection of particulate as well as the gas sample. Thirty-one total particulate concentration measurements were completed.

The effect of steam injection on particulate removal was also investigated in this test program. It has been proposed that the addition of steam to water saturated flue gas can enhance the removal of fine particulate. Supersaturating the flue gas causes condensation to occur on particulate, resulting in particle growth. As the smaller sub-micron size particles increase in diameter they may become easier to remove from the flue gas stream. Saturated plant steam was injected between the first and second stage of the IFGT and particulate loading measurements were conducted at the inlet and outlet to the IFGT.

The effect of mesh pads on particulate removal was investigated in this test program. Several layers of mesh pads were placed in the horizontal transition just before entering the second stage. The particulate removal efficiency was measured by cascade impactor tests at the 1st stage inlet and outlet. Mesh pads provide a target surface for impaction of fine particulate that passes through the first stage.

4.1.5 Heat Recovery

The heat recovery provided by the IFGT was an integral part of the standard data acquisition, and was recorded continuously for all of the tests. In addition to this standard data, the following tests were conducted to investigate specific heat transfer mechanisms.

- *Onset of 1st Stage Condensation* - For this test, cooling water passed only through the 1st stage heat exchanger. The cooling water flow rate was increased until condensate initially formed on the tubes. The data was compared to heat transfer models to better understand the conditions that initiate condensation.
- *Onset of 1st Stage Measurable Condensate Flow* - This was an extension of the previous test, where the cooling water flow rate is sufficient to produce a continuous

flow of condensate that can be collected and weighed. The data was compared to heat transfer models to better understand the conditions that initiate condensation.

4.1.6 Calcium Reagents

After a preliminary analysis of the data collected through the third test series, the database for a sodium carbonate reagent was deemed sufficient to meet the project goals and objectives. The remaining tests conditions for the fourth test series were modified to include reagents other than sodium carbonate.

Effective reagents for the fourth test series must supply a source of alkalinity in the liquid phase that can then readily react with the SO_2 absorbed from the flue gas. The dissolved alkalinity produced by the reagent defines the SO_2 absorption capacity of the liquor, and includes all dissolved species more alkaline than the bisulfite ion (HSO_3^-). Flue Gas Desulfurization (FGD) systems have primarily relied on highly soluble reagents containing sodium carbonate and slurry reagents containing calcium hydroxide and magnesium hydroxide, or calcium carbonate that slowly dissolve into alkaline anions. The two additional reagents selected for the fourth test series derive their alkalinity from calcium and magnesium hydroxide compounds. The first reagent, calcium hydroxide is widely used in commercial FGD systems and dissolves into highly alkaline hydroxide (OH^-) anions. The second reagent, magnesium promoted calcium hydroxide is also widely used in commercial FGD systems and in addition to (OH^-) anions also produces high dissolved concentrations of alkaline sulfite (SO_3^-) anions. The SO_2 removal performance of the these reagents was expected to be sufficient enough to justify their use in commercial applications. The calcium hydroxide reagent was expected to have lower SO_2 removal capability, as this reagent does not produce as high dissolved alkalinity as sodium carbonate or magnesium promoted calcium hydroxide.

4.2 Sampling

Two types of data were measured during these tests:

- continuous on-line measurements by process instrumentation that monitored the operation of the IFGT facility, and
- grab-samples of the process streams that were then analyzed to determine concentrations of components in the process streams.

Removal efficiencies for the IFGT process reported in this document are based on simultaneous measurements at the inlet and outlet of the facility. The following are descriptions of the primary sampling methods and techniques used in these tests.

NO_x , O_2 , NH_3 , and SO_2 - These gas phase constituents were measured with continuous gas analyzers. Flue gas for NO_x , SO_2 , and O_2 measurements was conveyed from the inlet and outlet flue work of the IFGT facility with heated sample lines and a sample pump maintained at 149°C (300°F). The flue gas was then chilled to about 10°C (50°F) to remove water vapor, and routed to the various gas analyzers. The continuous gas analyzers for measuring the concentration of

these constituent gases were calibrated at regular intervals (1 to 4 hours) using gas standards traceable to the National Institute of Standards and Technology (NIST).

A single gas analyzer was used for on-line measurement of ammonia concentration in the flue gas. The analyzer was equipped with a dedicated glass lined sample probe that was maintained at 260°C (500°F). For these measurements, the ammonia was measured sequentially at the inlet and outlet of the IFGT facility. Verification of the measurements made with the continuous analyzer were obtained by chemical analysis of simultaneous EPA Method 206 sampling at the inlet and outlet of the IFGT system.

Chloride and Fluoride - Chloride and fluoride concentrations were determined using EPA Method 26A. These measurements were conducted simultaneously at the inlet and outlet of the IFGT facility. Typical sample times were two hours. For these tests the sample train probe and particulate filter were maintained at a temperature of 121°C (250°F) at both the inlet and outlet measurement locations. Analysis of the sample train impingers provided gas phase concentration data. The particulate from the probe and filter were also analyzed to determine particle phase chloride and fluoride concentrations.

Mercury and Trace Elements - Gas phase mercury concentrations were measured using draft EPA Method 29 and the Ontario Hydro (B1) sample trains. These two techniques differ in the chemical composition of the liquid in the first three of the six impingers - see Appendix B.

The Ontario Hydro technique requires the addition of a preservative (potassium permanganate) in the first two impingers at the completion of the test. In test series III the permanganate was added within one hour of the completion of sampling, and within 20 minutes for test IV.

At the inlet to the IFGT facility, the probe and filter were maintained at 121°C (250°F), which was the same temperature as the flue gas. At the outlet of the IFGT facility the flue gas temperature was typically 38°C (100°F) and the probe and filter were maintained at a temperature of 121°C (250°F).

Total Particulate - Total particulate at the inlet and outlet of the IFGT facility was measured using EPA Method 5. This EPA Method for sampling particulate is an integral part of EPA Methods 26A, 29, 206 and the Ontario Hydro Method that were used for grab sample gas sampling.

Flue gas sampling was conducted at 102 mm (4 inch) diameter ports in the facility inlet and outlet piping. The pipe at the inlet was horizontal while the outlet pipe was vertical down flow. At each location, a distance of greater than eight diameters of straight length of pipe preceded the sampling location. Measurements showed that the velocity profile at both sampling locations was uniform. Constraints on space permitted only a single sampling traverses across the ducts, which consisted of four points representing equal areas. Each point in the traverse was sampled twice during a test.

Cascade Impactor - Anderson Mark III cascade impactors were used to measure the aerodynamic particle size distribution of the fly ash. The impactors consist of seven separation stages and a

backup filter. With this technique the sampled flue gas is directed through a plate with many small diameter orifices, and onto a filter. The gas velocity and fluid properties determines the aerodynamic size of the particles that impact the filter. An orifice plate and associated filter constitutes one stage of separation. Successive plates contain orifices that are ever smaller in diameter, so that ever smaller particles are collected in each separation stage. Typical aerodynamic particle sizes for the successive stages ranged from about 0.2 μm to 8 μm . The backup filter is equivalent to a Method 5 filter and collects all particulate that remains in the gas after passing through the last stage.

The cascade impactor is housed in a stainless steel cylinder about 76 mm (3 inches) in diameter and 102 mm (4 inches) long. The entire impactor is inserted into the gas stream and permitted to come to thermal equilibrium with the gas stream. Since the gas flow must be maintained constant during a test, the impactor was positioned at the centerline of the flue for the entire test. The iso-kinetic gas sample rate for the test was based on Method 5 measurements that preceded each test.

Solid Samples - Samples of solids were collected primarily to compliment the tests for mercury and trace metals. The samples consisted of pulverized coal, bag house fly ash, and dry reagent. Pulverized coal and bag house fly ash was sampled during each of the triplicate measurements associated with a Method 29 or Ontario Hydro test. Samples were taken at the start, the middle, and end of a triplicate test and composited. Samples from each triplicate test were then composited to obtain a sample for analysis. Not all of the samples collected in this manner were analyzed.

Coal samples were obtained from the coal pipe leading to the burner. Bag house fly ash samples were acquired at the outlet of the rotary valve below the bag house. A dry reagent sample was randomly selected during testing.

Liquid Samples - Samples of liquid streams consisted of the reagent feed, reagent blow down, and the high purity water used as make up water for the reagent feed. The high purity water was sampled only twice during testing as verification of its low trace element content. Single samples of the reagent feed or blow down were taken during a triplicate test. The samples were usually taken at the middle to end of the six-hour test period to ensure that steady-state concentrations had been reached.

Typically, the reagent samples were left intact until analysis was conducted. Some of these samples were immediately filtered to separate the particle and liquid phases. The separated fractions were then retained for analysis.

4.3 Reporting Basis

The concentration of compounds, elements, and particulate in the flue gas are on a dry basis, corrected to 3% excess oxygen. The units used in this report are micrograms per dry standard cubic meter ($\mu\text{g}/\text{dscm}$, 20°C and 1 atmosphere), milligrams per dry standard cubic meter (mg/dscm), and parts per million on a volume basis (ppm_v). The concentration of compounds and elements in the solid phase are reported as parts per million on a mass basis (ppm_m).

5.0 RESULTS AND DISCUSSION

5.1 Heat Recovery

One principal benefit of the IFGT process compared with other gas clean up technologies is the capability to recover waste heat from the flue gas. The heat recovery capability can be a substantial benefit provided there is a use for the recovered heat. The quantity of heat that can be recovered from the flue gas is dependent on several factors including the temperature of the flue gas, the sink temperature for the cooling water, and the flue gas water vapor dew-point temperature. In an open cycle industrial system the heat recovery can amount to 10% to 12% of the furnace heat release.

For coal combustion, the flue gas dew-point temperature is typically about 38°C (100°F), which is substantially less than for oil and gas combustion. In addition, the sink temperature at electric utility generating plants that use a closed steam cycle is typically higher than the sink temperature associated with open cycle processes. The combination of low dew-point temperature and high sink temperature reduces the quantity of heat than can be recovered, but this heat can still have a significant impact on the cost of operation.

5.1.1 Measured Heat Recovery

Temperatures and flows of cooling water and flue gas were monitored continuously during these tests, primarily as a means to control the operating conditions of the IFGT. The flue gas inlet temperature was maintained at 120°C (250°F) for all tests. Flue gas outlet temperature was maintained either at the water vapor dew-point temperature, or 8 to 12°C (14 to 22°F) below the dew-point temperature. The 120°C inlet temperature is lower than the 150°C (300°F) that is typical of the inlet temperature to most flue gas desulfurization systems. At the ARC pilot IFGT, the bag house is limited to a 150°C temperature, and heat loss and air infiltration reduces the temperature to well below 150°C. A 120°C inlet temperature was selected because it was quickly attainable at startup, and could be controlled regardless of the gas flow or ambient conditions.

Since the water and gas-side temperatures and flows were nearly the same for all tests, the heat recovery (as a percentage of furnace heat release) was also nearly the same. Figure 5.1 shows the components of heat recovery expressed as a percentage of the furnace heat release for an outlet flue gas temperature at the dew-point temperature (Test I-5) and 10°C (18°F) below the dew-point temperature (Test I-14D). For a condensing mode of operation, the heat recovery is equally split between the first and second heat exchanger stages, and the latent heat recovery (2%) accounts for about 1/3 of the total heat recovery (6%). In test I-5 (non-condensing) the stage 1 heat recovery is nearly the same as for test I-14D, while the second stage heat recovery is less, because of the absence of condensation.

Although net condensation does not occur in Test I-5, both evaporation and condensation occur in the second heat exchanger stage. The flue gas enters the second stage at a temperature greater than the dew-point temperature by about 17°C (30°F). The flue gas is then evaporatively cooled to the adiabatic saturation temperature. As the flue gas moves through the second stage, the

water initially evaporated to cool the flue gas is condensed as the flue gas temperature is reduced to the original dew-point temperature. This reflux process does not affect the net heat transfer, but it may influence the removal of pollutants.

5.1.2 Predictions of Heat Recovery and Gas Side Pressure Drop

CHXs[®] are sized with the assistance of a computer program that determines the physical size of the heat exchanger for the required gas flow and predicts heat recovery and gas side pressure drop through the unit. Several tests were conducted to determine the accuracy of these predictions.

Heat Recovery - Heat transfer tests were conducted using only the first heat exchanger stage so that the effect of water flow rate and water temperature could be closely controlled, and condensate flow rates could be accurately measured. Table 5.1 lists the operating conditions for these tests, which were designed to vary the condensation in the heat exchanger in a step wise fashion. As shown in Table 5.1, the energy balance for the measured data varied between about $\pm 5\%$.

Figure 5.2 shows the percent error between the measured and predicted heat recovery for the five tests. As shown, the errors are all negative indicating that the model consistently predicts a slightly greater energy recovery than was measured.

Figure 5.3 is a comparison of measured and predicted condensate flows for the five tests. As expected, based on the energy balance error, the program predicts a slightly greater condensate flow rate than was measured. Although the predictions show a fixed bias, the difference between measured and predicted energy recovery are quite small. Likewise, the differences between measured and predicted condensate flows and water and gas temperatures are all on the order of experimental error.

Gas Side Pressure Drop - The gas side pressure drop through the first heat exchanger stage was measured as a function of air flow rate for isothermal operation and is shown in Figure 5.4. Also shown in this Figure, is the predicted gas side pressure drop for the first stage. The predicted pressure drop is less than the measured pressure drop by about 8% over the entire range of flows.

Part of the error in the predicted pressure drop is likely due to differences in the geometry of the pilot CHX[®] unit compared with a full scale unit. The “near wall” area in the pilot unit represents a larger fraction of the total flow area than a commercial sized unit. Pressure drop predictions are based on data for commercial sized units that closely simulate an infinite array of tubes.

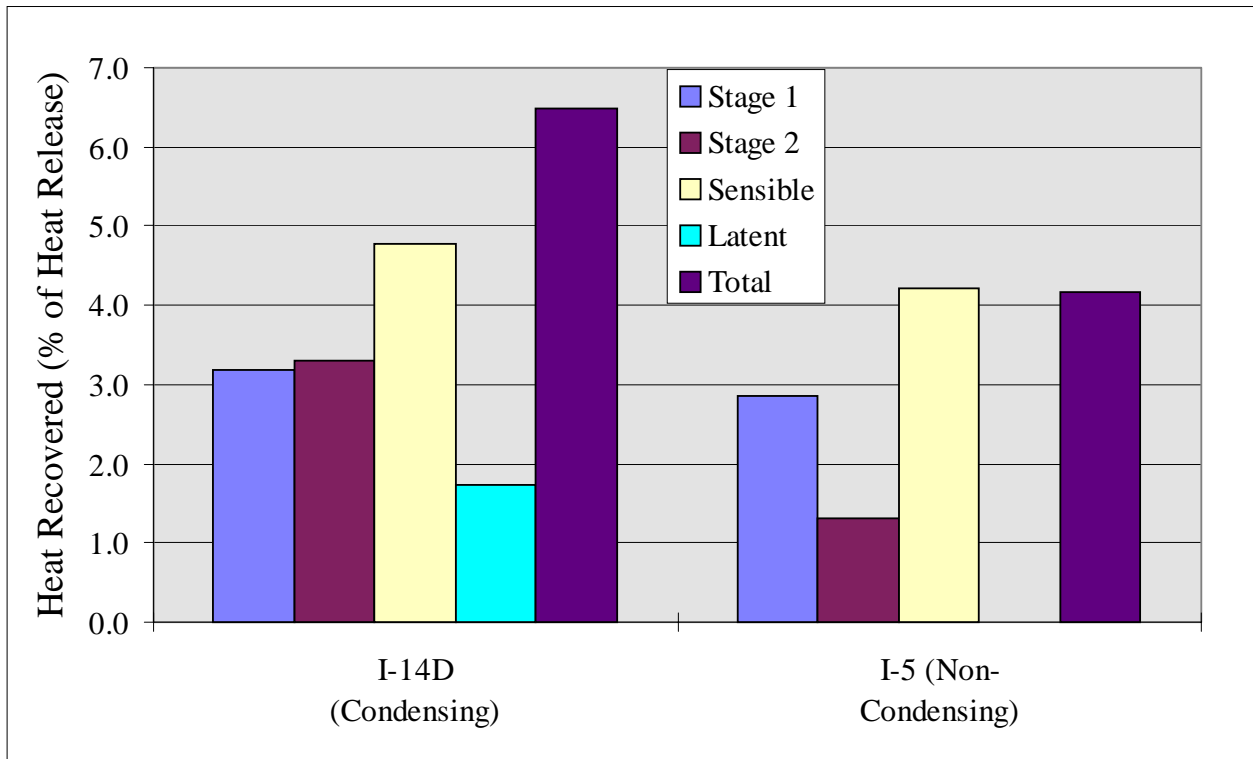


Figure 5.1 Components of Heat Recovery in the IFGT Process

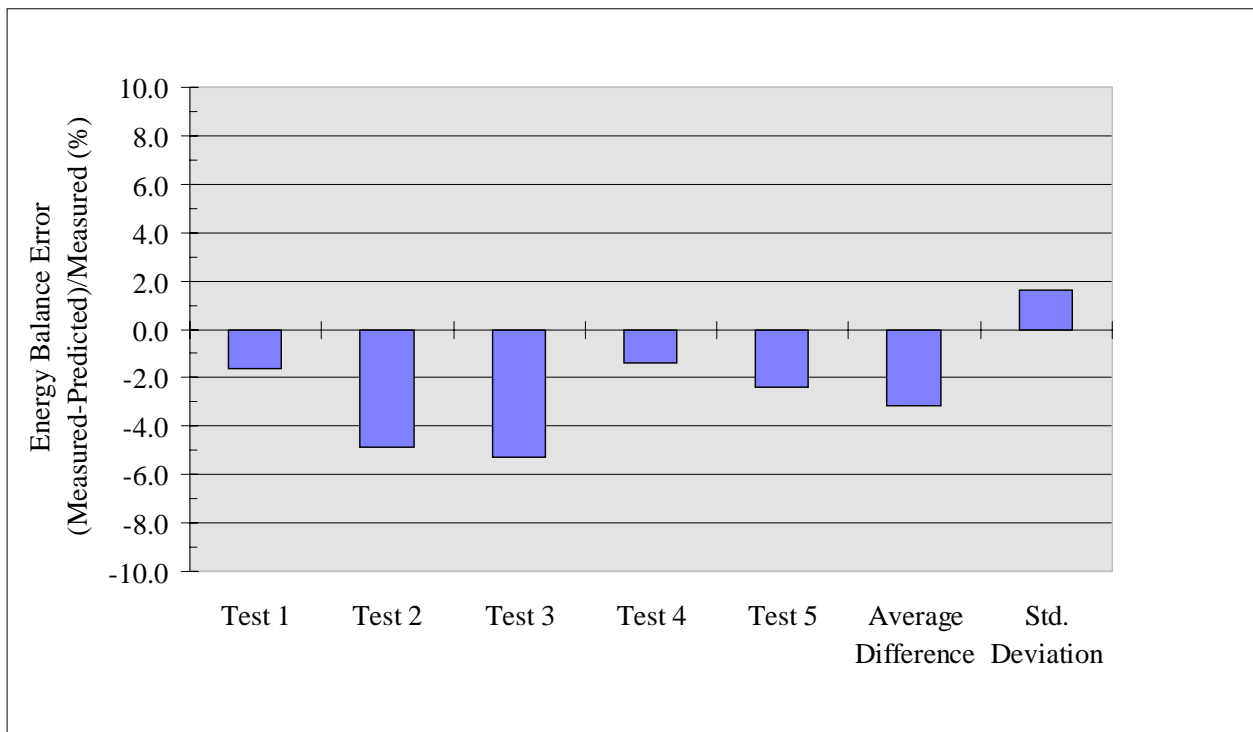


Figure 5.2 Percent Difference Between the Measured and Predicted Heat Recovery for the Five Heat Transfer Tests

Table 5.1 Summary Operating Conditions and Comparison to Predicted Heat Recovery for the Five Heat Transfer Tests

		CASE 1	CASE 2	CASE 3	CASE 4	CASE 5
		II-HX1	II-HX2	II-HX3	II-HX4	II-HX5
Cooling Water Flow Rate (Corr)	(kg/min)	15.7	15.3	22.6	22.9	21.8
Cooling Water Inlet Temperature	(°C)	18.1	12.3	11.3	22.4	11.4
Cooling Water Outlet Temperature	(°C)	62.1	60.0	47.9	54.2	43.6
Water Energy Gain, Stage 1	(kw)	48.3	50.9	57.6	50.9	48.9
Flue Gas Flow (Wet)	(kg/min)	39.2	39.0	39.1	38.8	27.7
Gas Temperature @ Module 1 Inlet	(°C)	120.7	123.3	123.7	124.1	120.9
Inlet Dew Point Temperature	(°C)	35.5	35.3	36.1	36.0	34.5
Humidity at CHX inlet	(gm/gm)	0.036	0.036	0.038	0.037	0.035
Flue Gas Flow (dry)	(kg/min)	37.9	37.6	37.7	37.4	26.8
Gas Temperature @ Module 1 Outlet	(°C)	53.0	51.3	47.7	52.8	41.7
Flue Gas Total Energy Loss	(kw)	48.4	54.4	60.9	49.7	49.6
Condensate Flow Rate	(gm/min)	85.4	165.0	249.9	71.5	293.8
Condensation Heat to Water	(kw)	3.5	6.8	10.3	2.9	12.1
Fraction of Water Energy Gain	%	7.3%	13.3%	17.8%	5.8%	24.7%
Overall Water/Gas Energy Balance	%	-3.3%	3.6%	2.9%	-5.9%	-1.7%
PREDICTIONS						
Predicted Water Energy Gain, Stage 1	(kw)	49.1	53.4	60.7	51.6	50.1
Measured - Predicted	(kw)	-0.8	-2.5	-3.0	-0.7	-1.2
Measured - Predicted	%	-1.65%	-4.89%	-5.29%	-1.39%	-2.42%
Predicted condensate flow	(gm/min)	165.7	202.2	300.8	183.9	312.3
Measured - Predicted	(gm/min)	-80.3	-37.2	-51.0	-112.3	-18.5
Predicted flue gas outlet temperature	(°C)	56.2	53.9	49.6	56.0	40.3
Measured - Predicted	(°C)	-3.2	-2.6	-1.9	-3.3	1.4
Predicted water outlet temperature	(°C)	62.8	62.3	49.8	54.6	44.3
Measured - Predicted	(°C)	-0.7	-2.3	-1.9	-0.4	-0.8

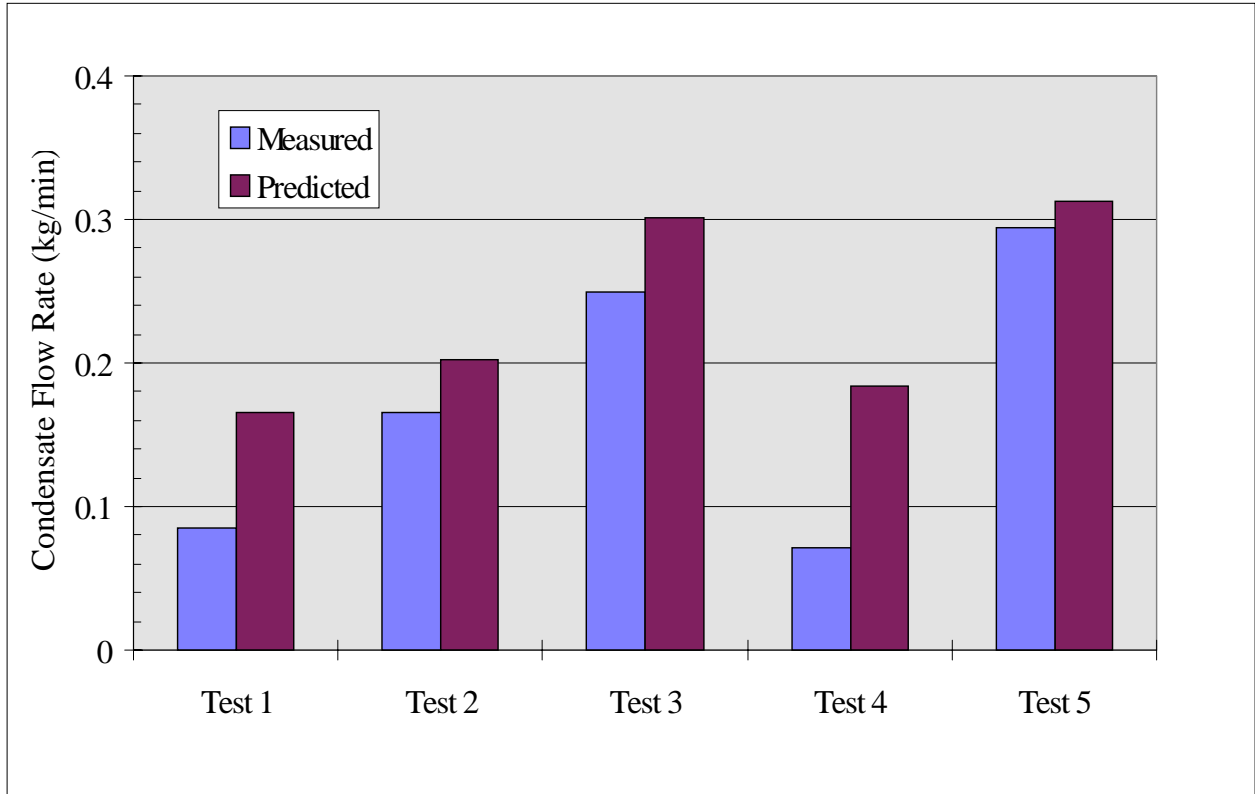


Figure 5.3 Comparison of Measured and Predicted Condensate Flow Rates

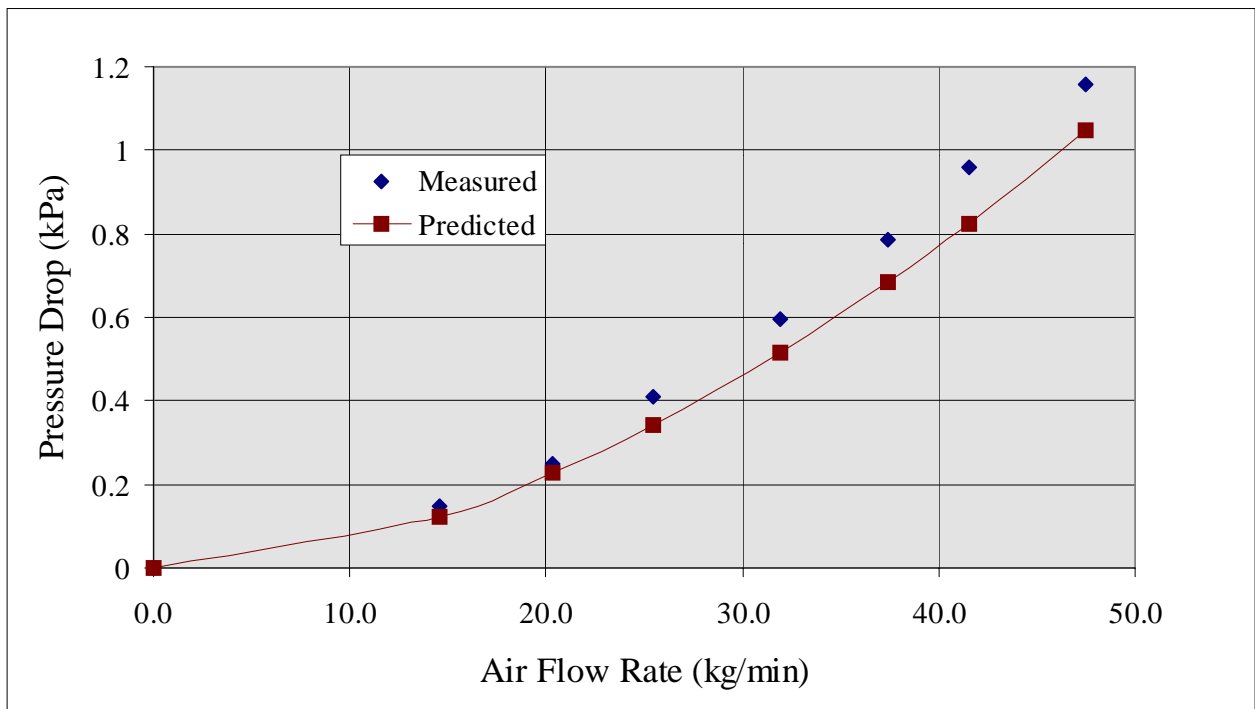


Figure 5.4 Measured and Predicted Pressure Drop Across the First Heat Exchanger Stage as a Function of Air Flow Rate

5.2 SO₂ Removal

SO₂ absorption in the IFGT was studied as a function of L/G, pH, load, reagent type, outlet temperature, and coal type. Overall SO₂ removal performance can be expressed in terms of percent removal or in terms of “number of transfer units”. Although in chemical engineering parlance N_g is defined rigorously as $dN_g = dy/(y-y_i)$, it has become common practice in the FGD industry to define N_g as follows:

$$N_g = -\ln(1-\epsilon)$$

where:

$$\epsilon = 100(1 - y_{outlet}/y_{inlet})$$

ϵ = SO₂ removal efficiency, %

y_{inlet} = Inlet SO₂ concentration (ppm_v)

y_{outlet} = Outlet SO₂ concentration (ppm_v)

y_i = SO₂ vapor pressure at the gas-liquid interface (ppm_v)

Expressing performance in terms of transfer units has two advantages. First, N_g has greater sensitivity to incremental changes than removal percentage when the SO₂ removal efficiency approaches 100%. The effect of operating parameters are more easily visualized in graphical form. Second, transfer units usually produce more linear relationships between SO₂ removal and system parameters. For the plots shown in this section, the left y-axis is given in transfer units and the right y-axis shows the equivalent percent removal.

5.2.1 Test Repeatability

Soda ash reagent testing was carried out for the four test series with 118 individual tests. For selected tests, system operating conditions were repeated to determine the repeatability of SO₂ data. A comparison of the repeatability data for all coals is shown in Table 5.2 below. The measure of repeatability used in Table 5.2 is the standard deviation of the SO₂ removal. Overall, the repeatability was good. The average standard deviation in the measurements was $\pm 0.6\%$, and ranged from 0.2% to 1.4%.

Table 5.2 Repeatability of SO₂ Removal Measurements

Test ID. ¹	Number of Measurements	Average SO ₂ Removal (%)	Standard Deviation (% of Removal)
I-4	7	97.2	0.5
II-4	5	98.3	0.2
III-7	3	97.1	0.5
IV-2	4	87.2	1.4

(1) "I-4" denotes test series I, test condition 4.

5.2.2 Sodium Reagent Test Results

Effect of L/G

The recirculated liquid flow rate is one of the major process operating factors affecting the SO₂ removal efficiency. For all of the figures that follow, the recirculated liquid flow rate is expressed as the ratio of liquid (or slurry) flowing to the top of the 2nd stage of the IFGT to the flue gas flow leaving the top of the 2nd stage. This quantity is generally referred to as the "Liquid-To-Gas Ratio" (L/G) and is considered one of the major process operating factors specified by Flue Gas Desulfurization (FGD) system designers. When the L/G increases, the qualitative effect is to increase the liquid (or dissolved) alkalinity per unit volume of treated gas. When the gas flow is constant and the reagent flow rate is increased, there is usually an increase in the liquid surface area per unit volume of treated gas, an increase in the amount of liquid in the IFGT system (commonly called the "liquid holdup"), and an increase in the turbulence (or agitation) between the gas and liquid. These effects improve the mass transfer characteristics of SO₂ removal.

The major effect of increasing L/G under typical constant load conditions is to increase the exposed surface area for gas absorption, and to increase the rate of absorption by reducing the resistance for SO₂ transport into the liquid. The SO₂ removal efficiency data shown in Figure 5.5 for Test series I, shows the quantitative effect of L/G at full load. At low L/G in the range of 0.07 to 0.27 l/m³ (0.5 to 2.0 gal/1000 ft³), the SO₂ removal efficiency increases rapidly, and reflects the generation of additional surface area from partial to complete liquid coverage of the internal tubes and walls, and an increase in the capacity of the reagent for SO₂ absorption. As the L/G increases above 0.27 l/m³, more surface area is generated by increasing the number of liquid droplets flowing downward between the tubes. The incremental surface area generated for an L/G > 0.27 l/m³ is significantly less, and the SO₂ removal efficiency increases only moderately. The qualitative effect of L/G measured for test series I was consistently evident for all of the coals tested.

The data shown in Figure 5.5 for Test Series I, a high-sulfur Ohio Coal, show that 95% SO₂ removal efficiency can be obtained at an L/G between 0.13 and 0.2 l/m³ (1.0 and 1.5 gal/1000 ft³). Increasing the L/G by a factor of 4 from 0.27 to 1.07 l/m³ (2.0 to 8.0 gal/1000 ft³) only

moderately increases the SO₂ removal efficiency from approximately 96.5% to 98.5%. However, this represents a significant increase in the transfer units from 3.3 N_g to 4.3 N_g .

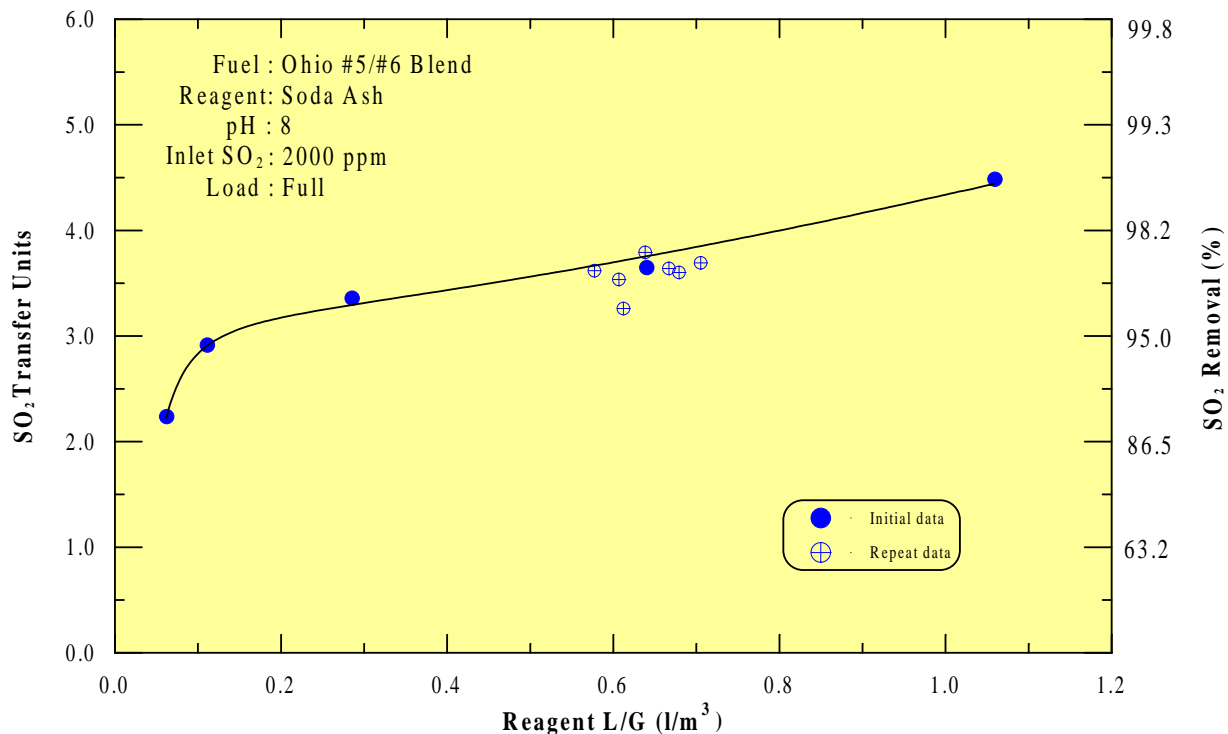


Figure 5.5 Effect of L/G at High pH

Effect of pH

The pH of the recirculating liquid entering the top of the second stage can affect the SO₂ removal efficiency. The effect will only be significant when the pH is sufficiently low that for the specific test conditions, the composition of the liquid flowing down through the IFGT second stage changes significantly. A significant composition change will be evident when the pH of the liquid leaving the bottom of the IFGT is low enough to create significant SO₂ vapor pressure at the gas-liquid interface. When this condition occurs, a sufficient excess of dissolved alkalinity is not present to absorb SO₂ and still maintain the pH at the gas-liquid interface above approximately six. For typical IFGT operating conditions with sodium reagent, operation at a recirculated solution pH greater than approximately 8.0 will usually ensure that the liquid pH leaving the IFGT is above 7.0, with no significant SO₂ vapor pressure. The relationship between the scrubbing solution pH and the SO₂ vapor pressure for soda ash reagent is discussed in Section 3.2, and shown in Figure 3.3.

The SO₂ removal efficiency at a pH of 8 and 7 for Test Series I is shown in Figure 5.6. The SO₂ removal efficiency at a pH of 7 is somewhat lower than with a pH of 8 with good agreement on the incremental effect of L/G. At similar L/Gs, reducing the pH from 8 to 7 lowered the SO₂ removal efficiency by approximately 0.5 transfer units. At the lower pH of 7, the reduced SO₂ removal efficiency reflects sufficient changes in the liquid composition for the generation of a significant SO₂ vapor pressure.

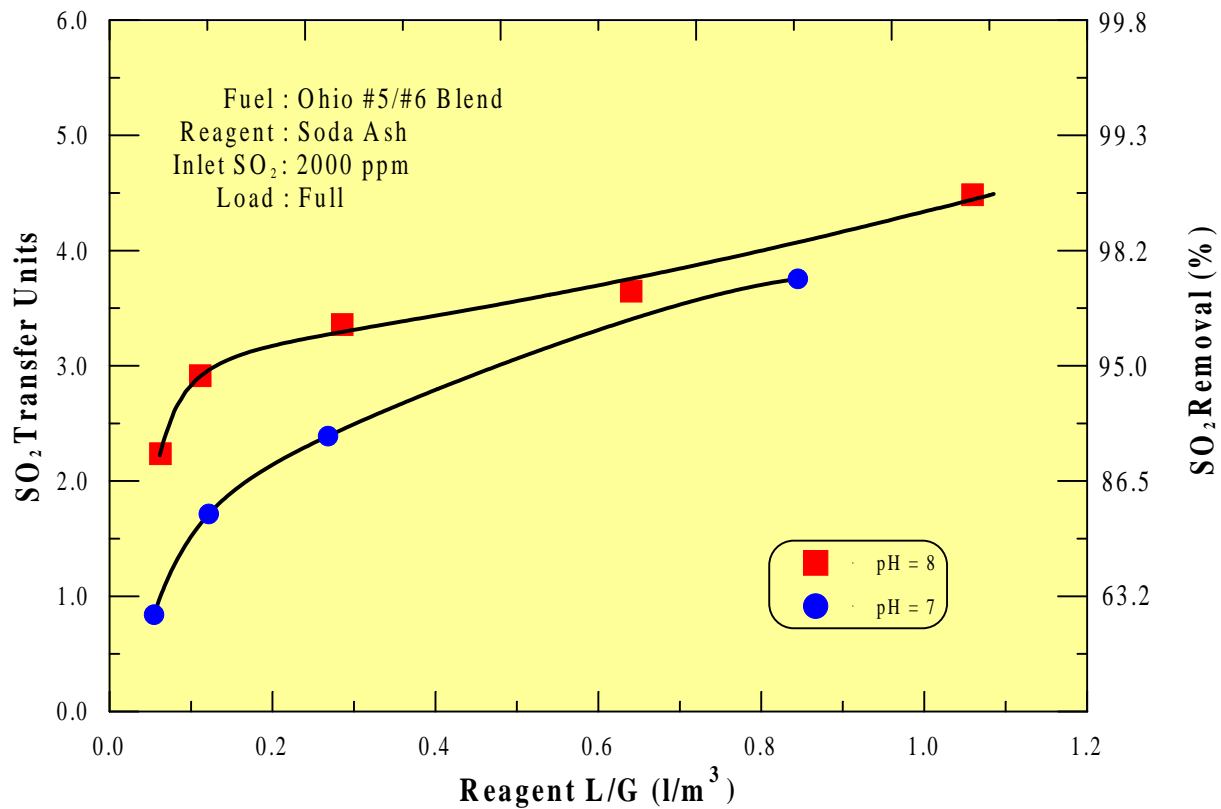


Figure 5.6 SO₂ Removal as a Function of L/G at Two Levels of pH

Effect of Load

The effect of the load on SO₂ removal efficiency is shown in Figure 5.7 along with the effects of L/G and pH. For operation at half load, the SO₂ removal efficiency is significantly less by approximately 1.5 N_g . Two factors are contributing to the reduction in SO₂ removal efficiency at reduced load. First, the reduced load decreases the liquid holdup and its contribution to exposed surface area for gas absorption from droplets traveling downward from tube to tube. Second, is the reduction in turbulence between the liquid and gas. The reduced turbulence decreases the rate of absorption by increasing the resistance in the gas phase for SO₂ transport into the liquid surface.

Effect of Outlet Temperature

The outlet flue gas temperature of the IFGT second-stage is typically adjusted for operation at temperatures ranging from slightly above to several degrees below the dewpoint. The flue gas temperature throughout the IFGT second stage is relatively constant when operating at or below the dewpoint. When the operating temperature of the flue gas within the IFGT second stage changes, physical and mass transfer properties of the flue gas, SO₂, and liquid may also change. The overall effect on the rate of mass transfer is complex, but the net effect on the mass transfer rate may be estimated by combining the individual temperature effects.

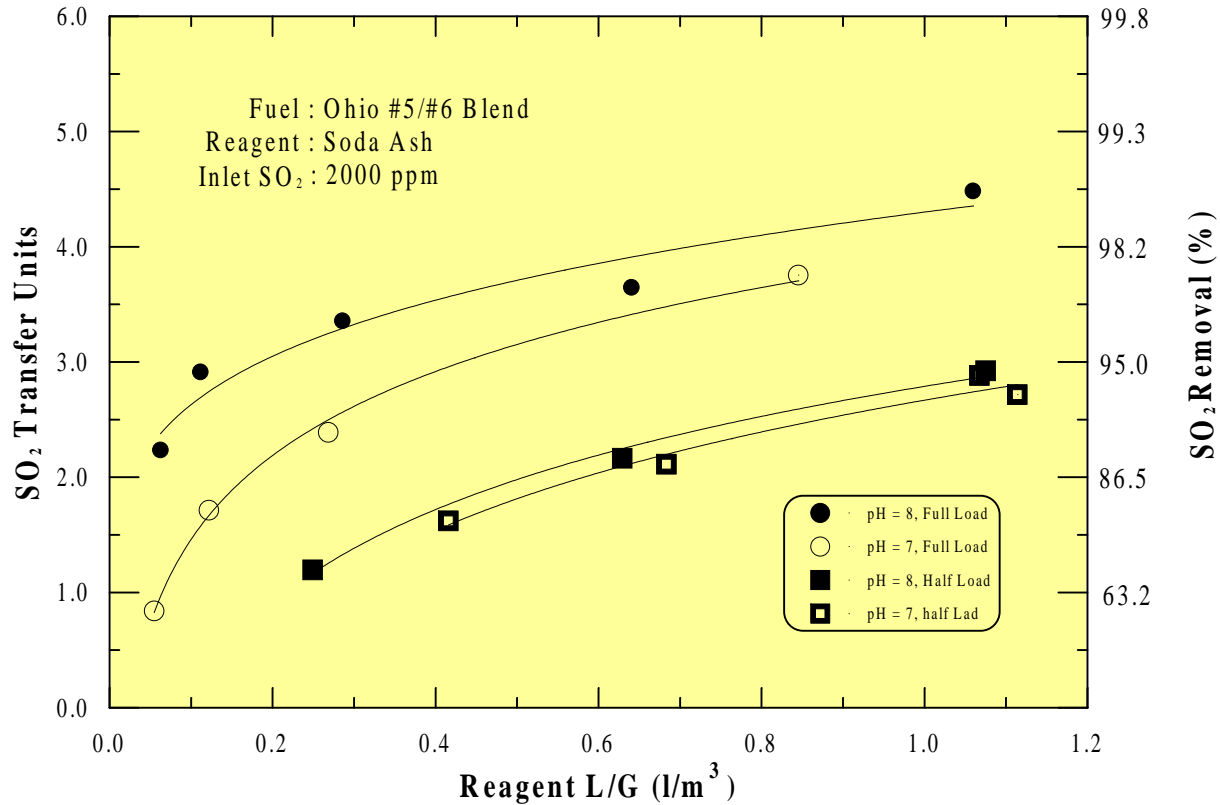


Figure 5.7 Effect of Load SO₂ Removal

The effect of temperature on the mass transfer rate was measured during Test Series I at a pH of 8 at full load and is shown in Figure 5.8. The data suggests that reducing the operating temperature by 9°C (20°F) reduces the mass transfer rate by approximately 3 to 5%. To estimate the observed effect of temperature, dimensionless empirical power law mass transfer correlations for droplets and cylindrical tubes were evaluated for the effect of temperature dependency. In an attempt to simplify the estimate, the analysis was conducted assuming a high pH in which the liquid phase resistance to mass transfer could be considered insignificant. This was confirmed experimentally as increasing the pH above 8 did not change the difference between the reagent feed pH and the pH at the exit of the IFGT second stage. For the droplets falling between the tubes, the following expression for turbulent mass transfer around a sphere applies (ref 1):

$$N_{sh} = 2.0 + 0.55N_{re}^{1/2}N_{sc}^{1/3} \tag{9}$$

where:

- N_{sh} = Sherwood No.
- N_{re} = Reynold's No.
- N_{sc} = Schmidt No.

For the liquid flowing over the tubes the expression for turbulent mass transfer is (ref 2):

$$N_{sh} = 0.25N_{re}^{0.6}N_{pr}^{0.38} \tag{10}$$

For both expressions, the factors that are temperature dependant are the flue gas density, flue gas viscosity, and binary diffusion coefficient for SO₂ in flue gas. The dependency of these

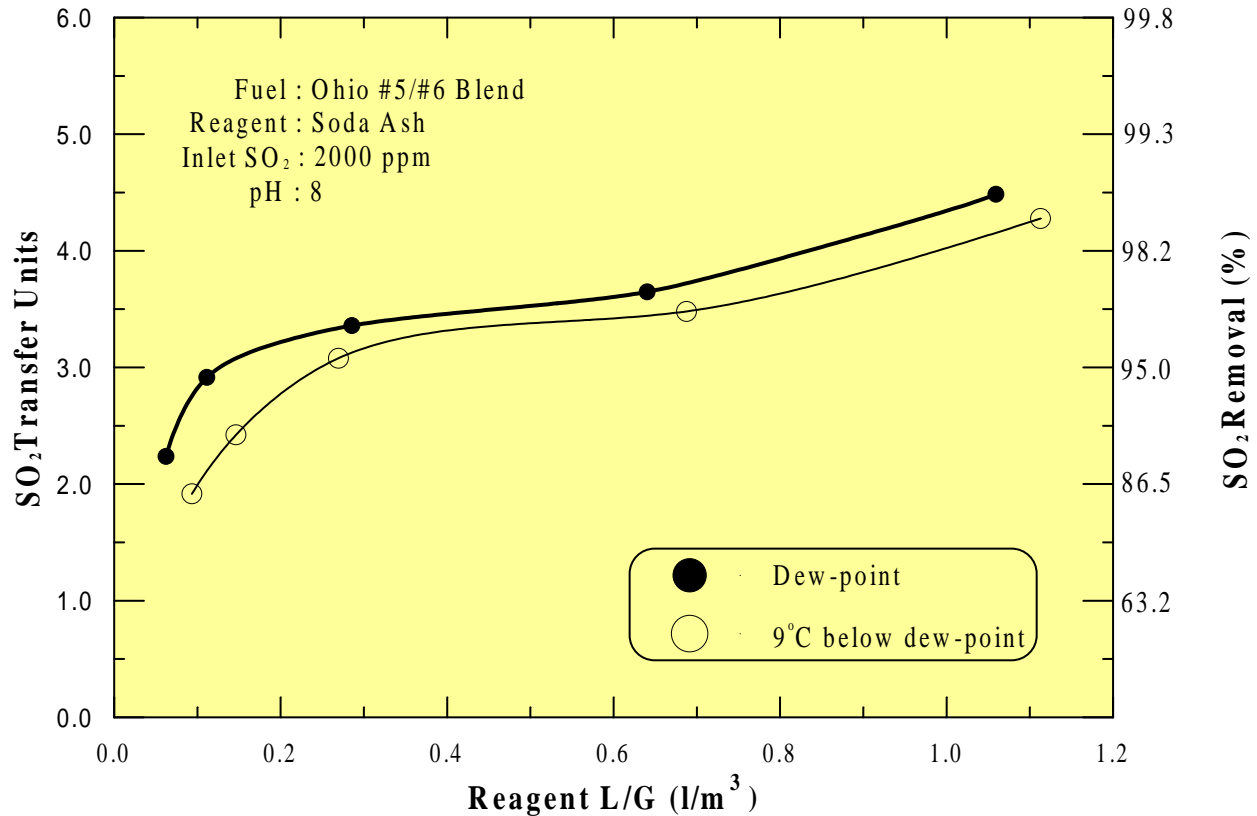


Figure 5.8 - Effect of Outlet Temperature on SO₂ Removal.

parameters on temperature was used in Equations 9 and 10, to determine the overall effect of a 9°C (16°F) temperature decrease on the mass transfer rate. For the droplets, the net effect was a decrease in mass transfer rate of approximately 9%. For the tubes, the net effect was a decrease in mass transfer rate of approximately 10%. The total mass transfer in the IFGT second stage is some combination from the droplets and tubes. As the estimated effect of temperature is essentially identical for both the droplets and tubes, the estimated effect of the temperature reduction is approximately 9%. This is consistent with the measured reduction in transfer units of approximately 3% to 5%.

Effect of Coal Type

The primary effect of the coal type is the variation in the coal sulfur content. The coal ash content and coal ash alkali composition have an insignificant effect as essentially all of the fly ash is collected in the upstream bag house. For the four coals tested, the flue gas SO₂ concentration ranged from approximately 300 ppm_v to 2000 ppm_v. The SO₂ removal efficiency at full load and solution pH of 8 for various L/Gs is shown in Figure 5.9. At these conditions, no clear effect of the coal sulfur content on SO₂ removal efficiency is evident. This is consistent with operation under gas phase mass transfer limited conditions where the SO₂ removal efficiency is unaffected by variations in the inlet SO₂ concentration.

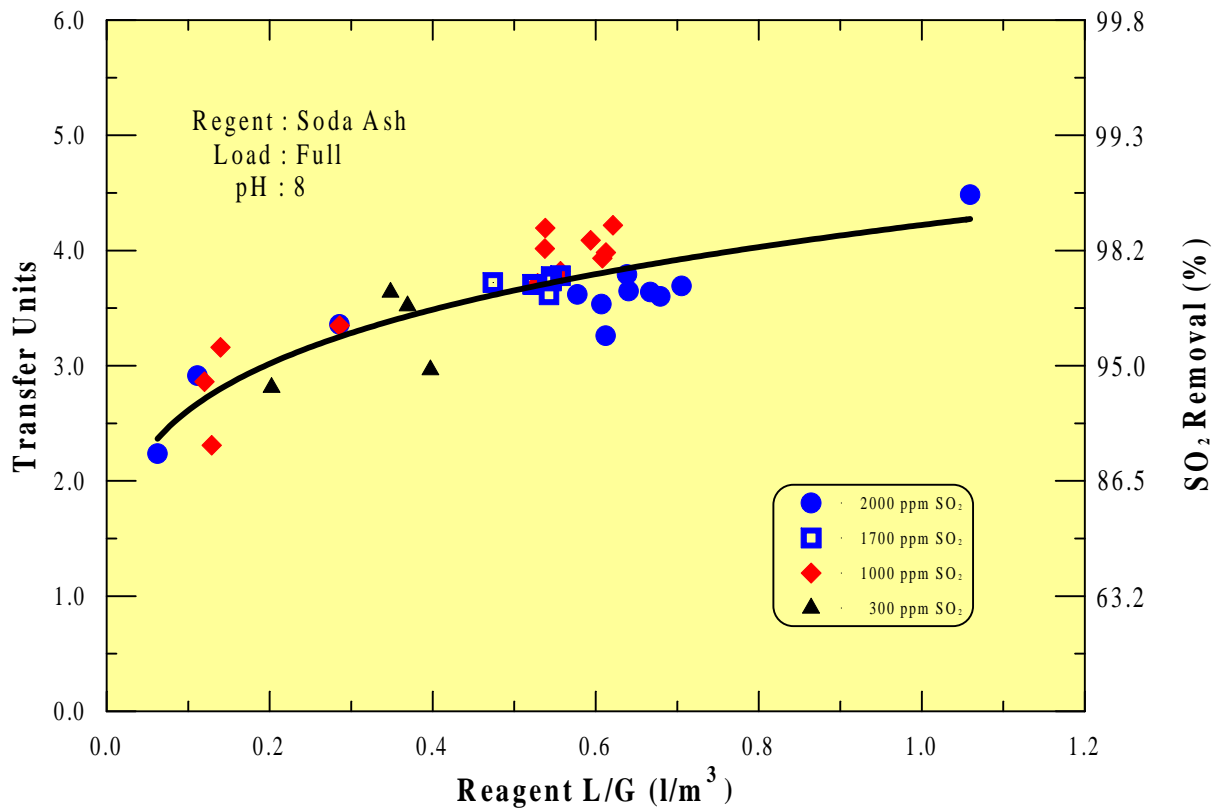


Figure 5.9 Effect of Inlet SO₂ Concentration on SO₂ Removal

As an example, if the inlet SO₂ concentration is reduced by a factor of 2, the SO₂ absorbed will likewise decrease by a factor of 2 and the SO₂ removal efficiency will remain the same (see equation 8, Section 3.2). The SO₂ removal efficiency at half load and reagent feed pH of 7 for various L/Gs is shown in Figure 5.10. At these conditions, there was a noticeable effect of the coal sulfur content on SO₂ removal efficiency. It is generally assumed that at pH of 7 or less there will be significant SO₂ back pressure at the gas-liquid interface, causing some liquid phase mass transfer resistance. Under these conditions, reducing the flue gas SO₂ concentration will contribute to higher SO₂ removal efficiency.

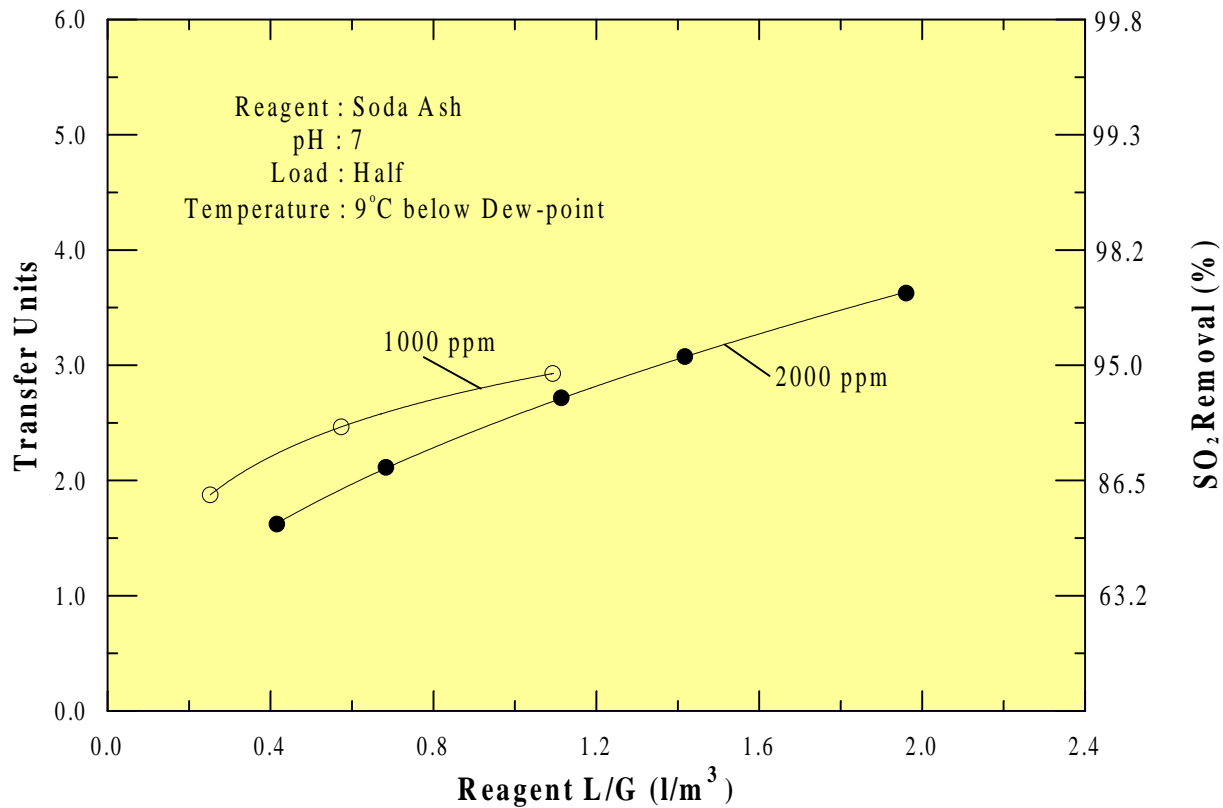


Figure 5.10 Effect of Inlet SO₂ Concentration on SO₂ Removal at Half Load

5.2.3 Lime Reagent

A lime-based reagent differs from soda ash reagent in both the type of alkaline species they generate, and in the amount of dissolved alkaline species produced. With soda ash reagent, the active alkaline species is highly soluble sodium sulfite and bicarbonate. A lime reagent produces relatively low dissolved levels of hydroxide. In a 5% magnesium-95% lime reagent, approximately 5% of the total alkali comes from magnesium sulfite. While the magnesium sulfite is low in total concentration, it is highly soluble and can deliver 10 to 15 times as much dissolved alkalinity as a calcium-based lime reagent.

The effect of reagent type on SO₂ removal efficiency is shown in Figure 5.11 for full load conditions. At an L/G of 0.8 l/m³ (6 gal/1000 ft³), the SO₂ removal efficiency for the sodium reagent was 98%, and for the mag-lime reagent was 83%. For both reagents the pH measured in the scrubbing solution return line was approximately 7.5. While there was a small reduction in reagent pH of 0.5 across the second stage for the sodium reagent, the mag-lime reagent scrubbing solution pH dropped by approximately four. This is consistent with the lower SO₂ removal efficiency, and suggests that the mag-lime has insufficient dissolved alkalinity at an L/G of 0.8 l/m³ to absorb the available SO₂.

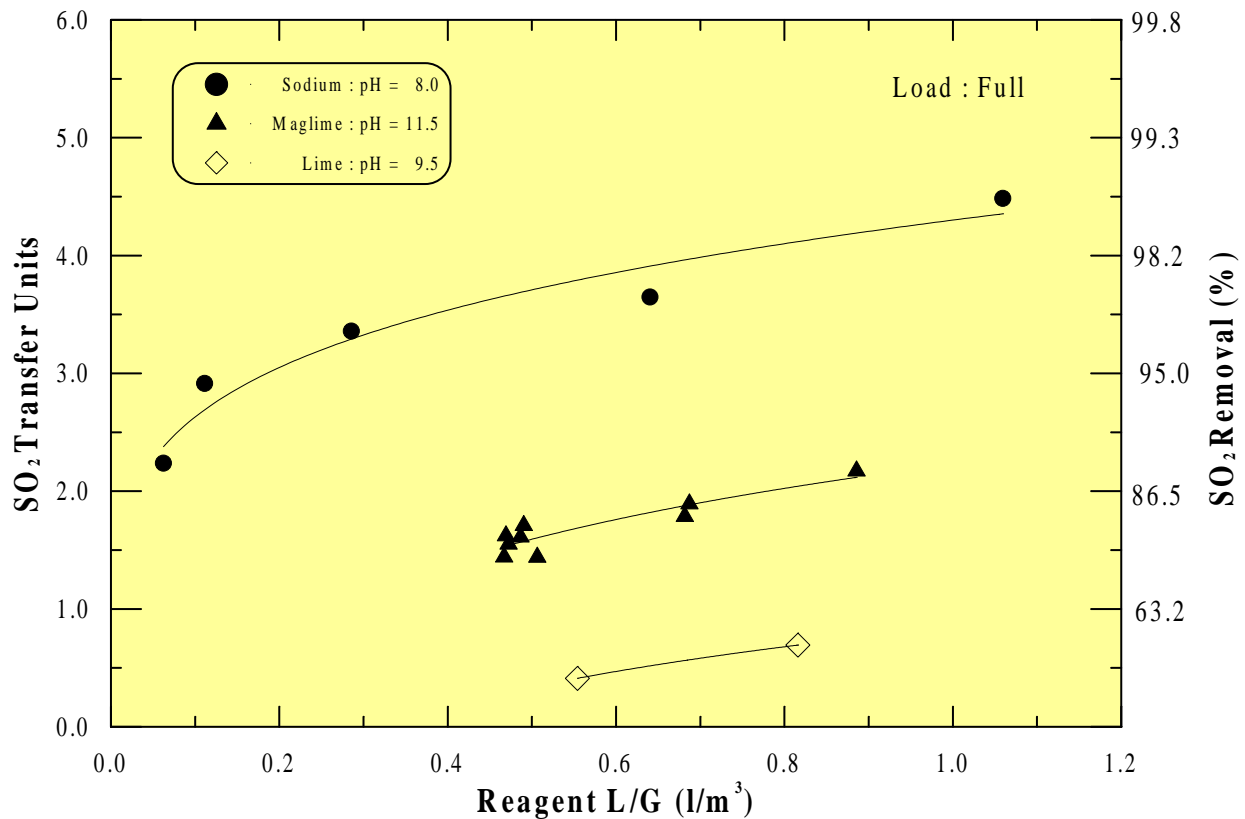


Figure 5.11 Effect of Reagent Type on SO₂ Removal

When planning the mag-lime tests, it was anticipated that a 5% mag-95% lime reagent would give only slightly less SO₂ removal efficiency than soda ash. The results showed a significant drop in SO₂ removal efficiency. Post test analysis indicated that the actual composition of the mag-lime reagent was 12% magnesium hydroxide and 88% calcium hydroxide. The high magnesium concentration should have allowed sufficient buildup of dissolved magnesium sulfite. However, the dissolved solids for the mag-lime test was unexpectedly low, about 0.4 %, and is the cause for the lower than anticipated removal. Allowing more operation time for the magnesium sulfite to dissolve or, higher L/G will be required to approach the performance of a sodium reagent.

For the lime reagent, significantly lower SO₂ removal efficiency was anticipated. At an L/G of 0.8 l/m³ (6 gal/1000 ft³), the SO₂ removal efficiency for the sodium reagent was 98% for a feed pH of 8.0. For the lime reagent at the same L/G, the SO₂ removal efficiency was approximately 50%, for a feed pH of 9.5. There was a significant reduction in the pH of the scrubbing solution (~5.5 pH units) across the second stage. This was expected, as the lime reagent produces very low dissolved alkalinity in the lime slurry.

5.3 Chloride/Fluoride Removal

Chlorine and fluorine are halogens present in coal and released from combustion as the acid gases hydrogen chloride (HCl) and hydrogen fluoride (HF). Of the four halogens - fluorine (F), chlorine (Cl), bromine (Br), and iodine (I) present in coal, chlorine and fluorine are the most abundant and are present in sufficiently high concentrations to be of concern. Some countries currently require emissions control of these halogens, and new regulations are pending in others. The IFGT system has the capability to absorb these acid gases by mechanisms similar to the capture of SO₂. Generally, HCl and HF will be absorbed at levels equal to or greater than SO₂. This section reports the removal efficiencies of HCl and HF measured across the IFGT for various coals for a wide range of combustion emission concentrations. Although some data are inconsistent, high removals were generally obtained for both HCl and HF.

Chlorine

Chloride emissions are a major contributor to man-made atmospheric acidity. Most of the chloride in coal is in the form of NaCl, which is converted essentially 100% to HCl in the combustion process. The HCl passes completely through the combustion process and particulate collection devices as there is little interaction between the HCl and fly ash. Generally, deposition will only occur in the particulate collection device if the flue gas temperature is below the acid dew point for HCl of 60°C (140°F). While SO₂ and NO_x emissions are greater than emissions of HCl, both the absorption rate and solubility of HCl in water is much higher.

The HCl concentration was measured at the inlet and outlet of the IFGT for each coal. Table 5.3 lists the test conditions and indicates how HCl partitioned to the vapor and particulate phases and the removal efficiency for the particulate and gas phases. More than 99.9% of the HCl entering the IFGT was in the vapor phase with concentrations ranging from 22 mg/dscm to 134 mg/dscm. The HCl concentration in the particle phase was generally much lower than in the vapor phase.

Table 5.3 Vapor and Particle Phase Chloride Concentration and Removal Efficiencies

Test	Scrubbing Solution pH	Location	Conc. in Particulate (ppm _v)	Unit Concentrations			Removal Efficiency			on Filter (%)	Percent in Vapor (%)
				Vapor (ug/dscm)	Particulate (ug/dscm)	Total (ug/dscm)	Vapor (%)	Particulate (%)	Total (%)		
I-4A	7.9	Inlet	134	134430	97	134527				0.07	99.9
		Outlet	8080	44709	209	44919	66.7	-116.3	66.6	0.47	99.5
II-4B	8.3	Inlet	16600	184429	26	184455				0.01	100.0
		Outlet	---	1150	---	1207	99.4	---	99.4	0.00	100.0
III-7A	6.5	Inlet	0.26	21997	0.01	21997				0.00	100.0
		Outlet	0.31	551	0.00	551	97.5	90.3	97.5	0.00	100.0
IV-1A	8.0	Inlet	396	156951	15	156966				0.01	100.0
		Outlet	18600	3628	44	3672	97.7	-184.5	97.7	1.20	98.8

As shown in Table 5.3, the HCl concentration in the particulate was generally less than 400 ppm_m. However, for test series II, the HCl concentration in the particulate was very high - 16,600 ppm_m. For test series II, the SBS carbon carryover was also very high, and the bag house was operated without bypass. The relatively high HCl concentration measured in the particulate could be due to either excessive carbon carryover from the furnace adsorbing HCl, or HCl being concentrated in the particulate fines that pass through the bag house. The overall effect indicated an 40-fold increase in the particulate's chloride concentration compared to the other tests.

The HCl removal efficiency for tests I, II, and III, were 66.7%, 99.4%, and 97.5%, respectively. The results for test I, were much lower than anticipated. A review of the analytical methods and procedures followed did not explain the results. The test was repeated in test series IV and the removal efficiency was measured at 97.7%. For test III, the effect of reagent feed pH on HCl removal efficiency was measured by reducing the reagent feed pH from approximately 8.0 to 6.5. The HCl removal efficiency was not significantly reduced and measured 97.5%.

The HCl removal efficiency for the particulate phase indicates large negative efficiencies. This is primarily due to the relatively large measurement uncertainty associated with the small measured concentrations for chloride in the particulate.

Fluorine

Fluoride emissions are a relatively minor component of the acid gases from coal combustion. For the four test series, the concentration of HCl in the flue gas was 40 to 87 times greater than the concentration of HF. Like HCl, the absorption rate and solubility of HF in water is much higher than SO₂ or NO_x. Most of the HF in coal is in the form of the mineral fluorapatite [Ca₅(PO₄)₃(OH,F,Cl)], fluorite (CaF₂), and biotite [K(Mg,Fe)₃(AlSi₃)O₁₀(OH,F)₂]. These fluoride compounds are converted essentially 100% to HF in the combustion process. Like HCl, HF also passes completely through the combustion process and particulate collection devices as there is little interaction between the HF and fly ash.

The HF removal efficiency was measured at the inlet and outlet of the IFGT for each coal with sodium reagent. Table 5.4 lists the test conditions and the vapor and particulate phase concentration and removal efficiency. More than 98% of the HF entering the IFGT was in the vapor phase with concentrations ranging from 0.43 mg/dscm to 4.3 mg/dscm. The HF concentration in the particulate was generally less than 700 ppm_m. However, for test series II, the HF concentration in the particulate was relatively high and measured 49,000 ppm_m. For test series II, the SBS carbon carryover was also very high, and the bag house was operated without bypass. The relatively high HF concentration measured in the particulate could be due to either excessive carbon carryover from the furnace adsorbing HF, or HF being concentrated in the particulate fines that pass through the bag house. The overall effect indicated an 80-fold increase in the particulate's fluoride concentration compared to the other tests.

Table 5.4 Vapor and Particle Phase Fluoride Concentration and Removal Efficiencies

Test	Scrubbing Solution pH	Location	Conc. in Particulate (ppm _v)	Unit Concentrations			Removal Efficiency			Percent on Filter (%)	Percent in Vapor (%)
				Vapor (ug/dscm)	Particulate (ug/dscm)	Total (ug/dscm)	Vapor (%)	Particulate (%)	Total (%)		
I-4A	7.9	Inlet	37	1655	14	1669	96.4	85.6	96.3	0.87	99.1
		Outlet	560	60	2	62				3.35	96.7
II-4B	8.3	Inlet	48800	4184	65	4249	99.5	---	99.5	1.52	98.5
		Outlet	---	22	---	22				0.00	100.0
III-7A	6.5	Inlet	22	431	1	432	82.8	9.5	82.7	0.24	99.8
		Outlet	241	74	1	75				1.25	98.7
IV-1A	8.0	Inlet	610	1859	24	1883	97.8	74.8	97.5	1.27	98.7
		Outlet	2535	42	6	48				12.62	87.4

As shown in Table 5.3, the HCl concentration in the particulate was generally less than 400 ppm_m. However, for test series II, the HCl concentration in the particulate was very high - 16,600 ppm_m. For test series II, the SBS carbon carryover was also very high, and the bag house was operated without bypass. The relatively high HCl concentration measured in the particulate could be due to either excessive carbon carryover from the furnace adsorbing HCl, or HCl being concentrated in the particulate fines that pass through the bag house. The overall effect indicated an 40-fold increase in the particulate's chloride concentration compared to the other tests.

The HF removal efficiency for tests I, II, III, and IV, were 96.3%, 99.2%, 82.7%, and 97.5%, respectively. The results were generally as expected. The HF removal for test III was lower than the other three tests and may be due to the lower reagent pH for this test, or may be due to uncertainty arising from the low concentrations of HF for this test.

5.4 Ammonia Removal

Ammonia has been used extensively in electric utility and industrial catalytic systems to control NO_x emissions. A concern in the operation of these systems is how much ammonia passes through unreacted and is emitted to the atmosphere. These ammonia emissions are commonly referred to as "Ammonia Slip". Currently, the USEPA has not imposed limits on ammonia slip. However, ammonia emission limits have been established by state and local agencies. In California, NO_x emission limits generally range from 2 ppm_v to 10 ppm_v. Operators of NO_x control systems must balance between using sufficient ammonia to meet NO_x emissions without exceeding the ammonia slip limits. Excessive ammonia use can also cause ammonia salt formation, which can cause fouling in air heaters and catalyst deactivation in the NO_x control equipment. The ammonia salts are formed by the reaction of ammonia with SO₃ in the flue gas to form ammonium sulfate compounds (NH₄HSO₄ and [NH₄]₂SO₄). With these concerns in mind, operators of ammonia based NO_x control systems could benefit from an IFGT system if the IFGT could demonstrate the ability to absorb a large amount of ammonia. The NO_x system could then be operated at higher ammonia to NO_x ratios without increasing ammonia slip.

One objective for ammonia testing for Task 2 was to measure ammonia removal through the IFGT system. Ammonia removal was based on measurements at the inlet and outlet of the IFGT. Ammonia was injected at a constant measured flow rate upstream of the IFGT inlet, at the inlet to the SBS system ID fan. The ammonia flow rate was measured by a certified rotameter and manually controlled at the rotameter. A continuous ammonia analyzer was then used to sequentially measure the ammonia concentration upstream and downstream of the IFGT. For selected tests, the measurements of the continuous analyzer were verified using USEPA Method 206.

During each of the first three test series, three ammonia removal tests were conducted. Table 5.5, Section A, summarizes the results for all nine test conditions. The inlet ammonia concentration ranged from 31 ppm_v to 94 ppm_v and removal efficiency ranged from 57% to 93%. All ammonia tests were conducted at full load. For test III-9B, the measured inlet ammonia concentration was inconsistent with previous data and was estimated from the rotameter settings and previously measured reductions from ammonia-sulfur reactions. The ammonia removal efficiency for test III-9B was subsequently adjusted from 24% to 57%. The IFGT system outlet flue gas temperature for tests I-14G, II-4F, III-18 were planned to be at 11 °C (20 °F) below the water vapor dewpoint. However, due to seasonal variations in the process cooling water temperature, the actual outlet temperatures achieved were 9 °C (16 °F), 7 °C (13 °F), and 4 °C (8 °F), respectively, below the water vapor dewpoint.

The ammonia removal data in Table 5.5 indicates that the major factors affecting ammonia removal include the IFGT outlet temperature, L/G, the level of dissolved solids in the recirculating liquid, and liquid pH. The effect of outlet temperature is shown for three pair of data sets in Table 5.5, Section B. As with SO₂, the solubility of ammonia in aqueous solution is strongly affected by temperature. The solubility of ammonia increases as the temperature of the liquid decreases. The equilibrium solubility of ammonia in contact with air containing 100 ppm ammonia is approximately 65 mg/l at 38 °C (100 °F) and increases to 100 mg/l at 27 °C (80 °F).

Table 5.5 Summary of Ammonia Removal Measurements

Section A - Data Summary						
Test	NH ₃ At CHX Inlet (ppm _v , wet)	NH ₃ At CHX Outlet (ppm _v , wet)	NH ₃ Removal (%) / (TU)	Outlet Gas Temp. (°C)	Feed pH	L/G l/m ³
I - 4G	70	5	93 / 2.69	27.2	7.9	0.67
I - 4F	94	22	76 / 1.43	36.1	7.9	0.67
I - 4E	68	16	76 / 1.42	36.1	7.9	0.68
II - 4D	68	12	83 / 1.76	36.0	8.2	0.66
II - 4F	64	7	88 / 2.16	29.3	8.2	0.64
II - 4E	31	8	73 / 1.30	36.3	8.2	0.64
III - 18	84	20	76 / 1.45	38.0	7.9	0.39
III - 9B	70	30	57 / 0.86	42.3	8.2	0.35
III - 7B	31	4	87 / 2.02	42.3	6.8	0.34
Section B - Effect of Lower Outlet Temperature.						
I - 4E	68	16	76 / 1.42	36.1	7.9	0.68
I - 14G	70	5	93 / 2.69	27.2	7.9	0.67
II - 4D	68	12	83 / 1.76	36.0	8.2	0.66
II - 4F	64	7	88 / 2.16	29.3	8.2	0.64
III - 9B	70	30	57 / 0.86	42.3	8.2	0.35
III - 18	84	20	76 / 1.45	38.0	7.9	0.39
Section C - Effect of Lower Inlet NH ₃ Concentration.						
I - 4F	94	22	76 / 1.43	36.1	7.9	0.67
I - 4E	68	16	76 / 1.42	36.1	7.9	0.68
II - 4D	68	12	83 / 1.76	36.0	8.2	0.66
II - 4E	31	8	73 / 1.30	36.3	8.2	0.64
Section D - Effect of Reduced L/G and Total Dissolved Solids.						
I - 4F	94	22	76 / 1.43	36.1	7.9	0.67
III - 18	84	20	76 / 1.45	38.0	7.9	0.39
Section E - Effect of pH.						
III - 9B	70	30	57 / 0.86	42.3	8.2	0.35
III - 7B	31	4	87 / 2.02	42.3	6.8	0.34

On average, the data suggests that the ammonia removal efficiency improved by approximately 0.75 TU (Transfer Units) for a 6°C (10°F) reduction in outlet temperature.

The effect of inlet ammonia concentration is shown for two pair of data sets in Table 5.5, Section C. There was essentially no measured improvement in ammonia removal efficiency in Test Series I, when the inlet ammonia concentration was reduced from 94 ppm_v to 68 ppm_v. In Test Series II the ammonia removal efficiency improved somewhat from 73% to 83% when the inlet ammonia concentration was reduced by almost half from 68 ppm_v to 31 ppm_v.

In the third test series, the reagent feed total dissolved solids, or “TDS”, was reduced from approximately 12% to 4% to reflect the relatively low sulfur content of powder river basin coal. Reducing the TDS reduces the ionic strength in the reagent feed and increases the solubility of ammonia in the liquid. For Test Series III, the lower TDS enhanced the ammonia solubility by approximately 30%. As shown in Table 5.5, Section D, high TDS test (I-4F) is compared to a low TDS test (III-18). The measured ammonia removal efficiency for both tests was 76%. As previously discussed, the slightly lower flue gas ammonia concentration will not significantly affect the ammonia removal efficiency. Therefore, the data suggests that the ammonia removal efficiency can be held constant while reducing the L/G from 0.67 l/m³ (5.0 gal/1000 ft³) to 0.39 l/m³ (2.9 gal/1000 ft³) by lowering the TDS from approximately 12% to 4%.

Ammonia, being an alkaline gas, is better absorbed by liquids with lower pH. The effect of pH on ammonia removal efficiency was investigated in Test Series III, see Table 5.5, Section E. For the indicated tests, two factors were varied. The inlet ammonia concentration was reduced from 70 ppm to 31 ppm, and the reagent feed pH was reduced from 8.2 to 6.8. Based on the previous data, the estimated effect of lowering the inlet ammonia concentration would be a reduction in ammonia removal efficiency of approximately 0.4 TU. However, by also reducing the pH from 8.2 to 6.8, the ammonia removal efficiency **increased** from 57% to 87%, or a net increase of 1.1 TU. These results suggest that for the operating conditions used in test series III, reducing the liquid pH from 8.2 to 6.8 improved the ammonia removal efficiency by approximately 1.5 TU.

Another objective for ammonia testing for Task 2 was to estimate the amount of ammonia that reacts with SO₂ before the IFGT system. Below 230°C (450°F), ammonia reacts with sulfur trioxide (SO₃) in the flue gas, so that some of the gaseous ammonia will be removed from the flue gas upstream of the IFGT. Differences between the measured and calculated ammonia concentration at the IFGT inlet based on the ammonia injection rate determined the amount of the ammonia-sulfur reactions. For the nine completed ammonia tests, the ammonia reduction attributable to ammonia-sulfur reactions ranged from 27% to 45%, and averaged 36%. The ammonia reduction for test III-9B was measured at 75%, and was considered inconsistent with the other test results.

5.5 Particulate Removal

The IFGT system is effective at removing particulate from a flue gas stream because of the serpentine gas flow path around the Teflon[®]-covered tubes in the heat exchangers. The primary removal mechanism is inertial impaction of the larger particles on the tube surface. Previous testing conducted using oil-fired flue gas indicated that removal extends to smaller particles in which inertial effects are minimal.

Although effective at removing particulate, the CHX[®] design is not intended to handle the full particle load from a coal-fired boiler. Collected particulate must be rinsed from the tubes and flushed from the system at regular intervals to prevent plugging between tubes. However, since the measurement of particle loading, particle removal efficiency, and trace element concentrations in particulate are all more easily made if the particle loading to the IFGT inlet is relatively large, the particle loading to the IFGT system inlet was set to about 600 to 900 mg/dscm (0.4 to 0.6 lb/million Btu) for most of the tests. This particle loading represents about 10% of the ash in the coal. In the SBS combustor about 50% of the fly ash is retained in the furnace/convection pass as bottom ash and ash deposits, so the loading to the IFGT system was about 20% of the normal ash loading to the baghouse.

To achieve the targeted particle loading, the baghouse bypass valve was opened so that the baghouse pressure drop was reduced about 20%, indicating a bypass gas flow of about 20%. Once set, the valve position was maintained for the duration of a test. The normal bag cleaning cycle based on baghouse pressure drop was suspended during a test day. Likewise, soot blowing of the convection pass tubes was delayed until the end of a test day. These precautions prevented upsets in the particle loading at the IFGT during testing. Soot blowing and bag cleaning was performed at the end of a test day. Similarly, particulate was permitted to accumulate in the first stage of the IFGT system during a test day and was rinsed after daily testing was completed.

Using this procedure, the particle loading to the IFGT system was lowest at the start of the day when the baghouse pressure drop was lowest. Later in the day, as the filter cake on the bags caused the baghouse pressure drop to increase, a larger fraction of the gas flow was bypassed and so the particle loading at the IFGT system inlet increased. These mild changes in particle loading did not influence the results as the particle loading changed only slowly with time, and removal efficiencies were always based on simultaneous measurements at the inlet and outlet of the IFGT system.

Raw coal for the SBS furnace was crushed, dried and stored in a bunker. The crushed coal was then ground in an MPS pulverizer and stored in a second bunker. All of the coals used on these tests was ground to the same nominal coal fineness of 70% through a 200 mesh screen (70% < 75 micrometers).

The particle size distributions of the fly ash at the inlet to the IFGT system for the four test series are shown in Figure 5.12. The cumulative percent of the mass is shown as a function of the flyash aerodynamic particle size. These size distributions were measured with the cascade

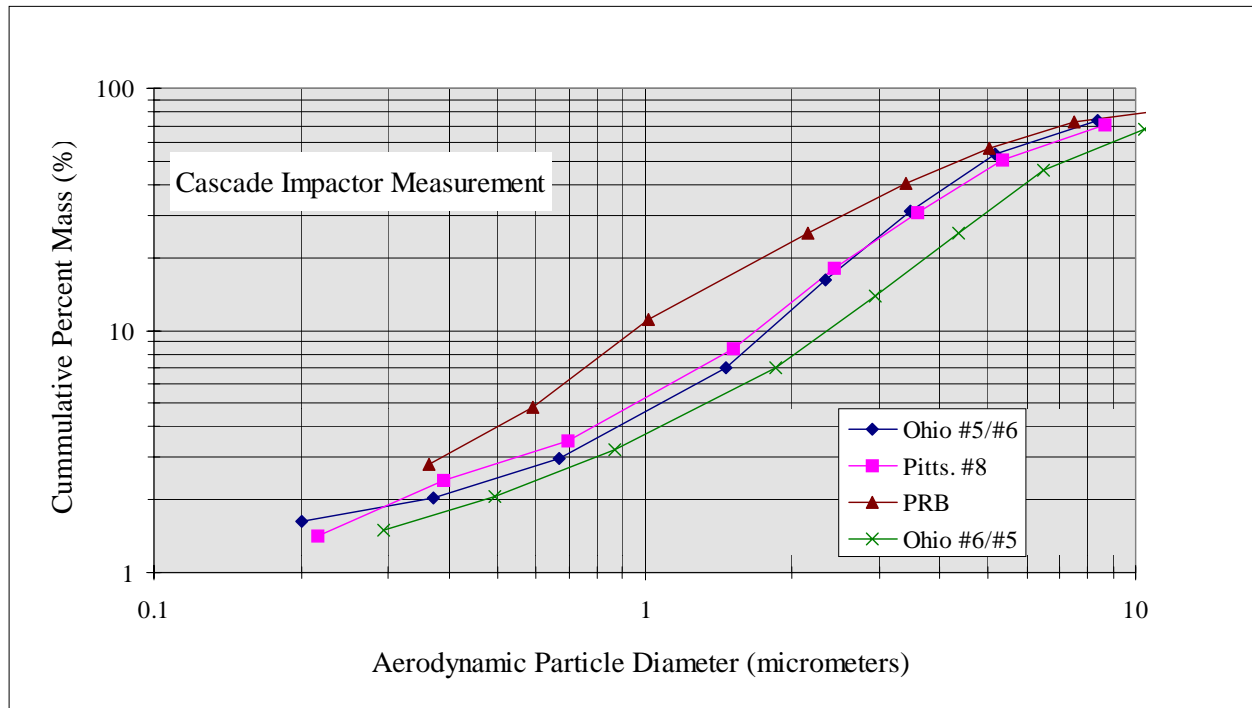


Figure 5.12 Fly Ash Particle Size Distribution at the IFGT Inlet for Each Coal Tested

impactor at the inlet to the IFGT system. As shown in the figure, the flyash size distribution for test series I and II (Ohio 5/6 and Pittsburgh coals) are nearly identical. The size distribution for test series IV (Ohio 6/5) is slightly larger, and the size distribution for test series III, Powder River Basin coal, is smaller. The mass median diameters for the four test series range from 4 μm to about 7 μm , which is in the range of that for coal-fired utility power plants.

5.5.1 Particle Removal Efficiency as a Function of Particle Size

Cascade impactor measurements were made for selected tests to determine the fly ash particle size distribution measurements at the inlet and outlet of the IFGT system. The particle size distribution combined with the measured particle loading at the inlet and outlet was used to determine the particle removal efficiency as a function of particle size.

Removal efficiencies calculated in this manner are subject to errors because of the small amount of mass collected on some of the filters (< 1 mg), and because the different flue gas conditions at the inlet and outlet flues result in slightly different cut sizes for the impactor plates. To minimize these errors, the following approach was used to determine removal efficiencies:

- The aerodynamic particle diameter cut size of the cascade impactor stages were calculated based on the flue gas properties, temperature and sample flow rate through the cascade impactor. The procedure followed was that recommended by Southern Research Institute³.
- The cumulative percent of mass and the particle loading were used along with the calculated particle diameter cut sizes to determine the cumulative mass loading (mg/dscm) as a function of particle size at the inlet and outlet.

- Linear interpolation of the cumulative mass loading data was used to determine the slope of the curve ($dm/d\log[D]$) at a set of diameters, D . Removal efficiency was calculated at each D as the percent change in ($dm/d\log[D]$) from the inlet to the outlet.

Cascade impactor measurements were made for seven different tests which spanned the four test series and included two different inlet gas velocities (loads). Table 5.6 provides a listing of the cascade impactor tests cross referenced to the test at which total removal measurements were also made. Five tests were conducted at full load and two tests were conducted at partial load.

Table 5.6 List of Cascade Impactor Tests

Cascade Impactor Test ID	Total Removal Test ID	Inlet Gas Velocity (m/s)	L/G (l/m³)	Gas Outlet Temperature Difference From Dew-Point (°C)	Comments
I-4L	I-4B	11.77	0.64	0.0	
I-14M	I-14D	12.05	0.70	-9.0	
I-4N	I-4J	11.79	0.64	1.0	Inter-stage Steam Injection
II-4G	II-4C	11.78	0.63	0.0	
III-12B	III-12A	7.10	0.36	0.0	Partial Load
IV-1B	IV-1A	11.14	0.52	0.0	Mesh Pad
IV-2B	IV-2A	7.02	0.47	0.0	Partial Load

Figure 5.13 shows the cumulative mass distribution at the inlet and outlet of the IFGT for test I-14. The data is presented as the cumulative mass as a function of fly ash aerodynamic particle size. The data in this figure shows that the mass median diameter (50% mass) at the inlet to the IFGT is about 5 μm , and is about 1 μm at the outlet.

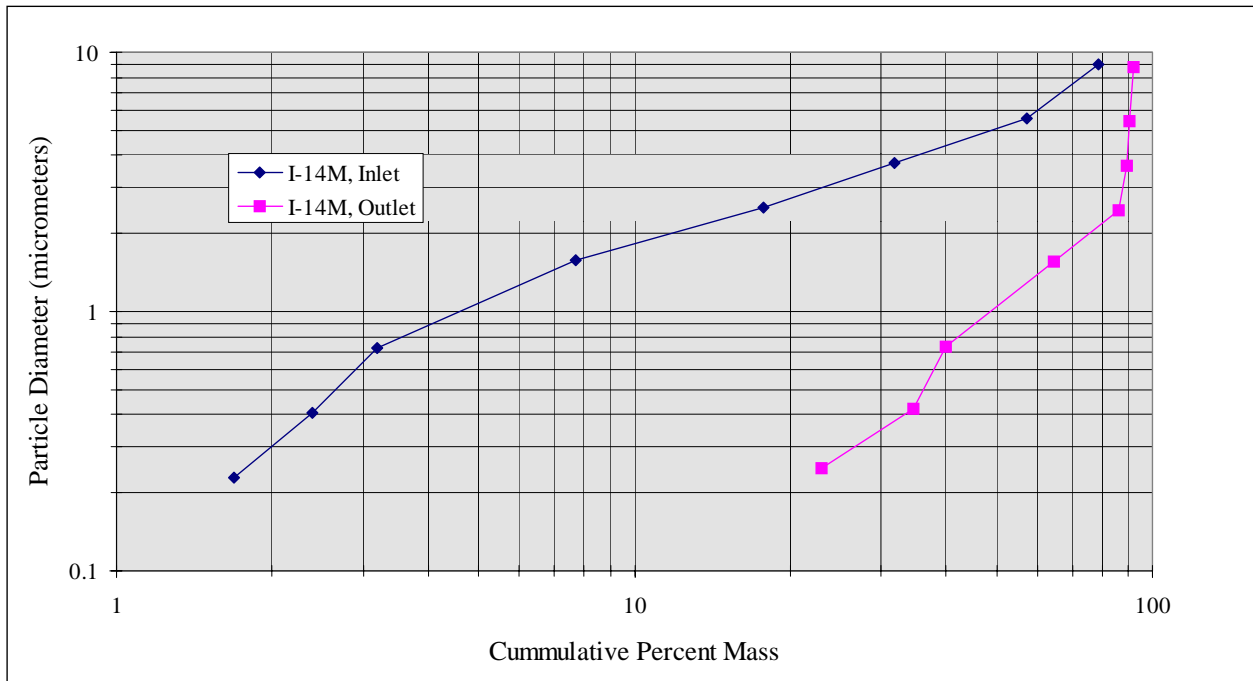


Figure 5.13 Fly Ash Particle Size Distribution at the Inlet and Outlet of the IFGT System for Test I-14M

Figure 5.14 shows the particle removal efficiency as a function of particle size calculated from the data presented in Figure 5.13. This curve has several general characteristics that are evident

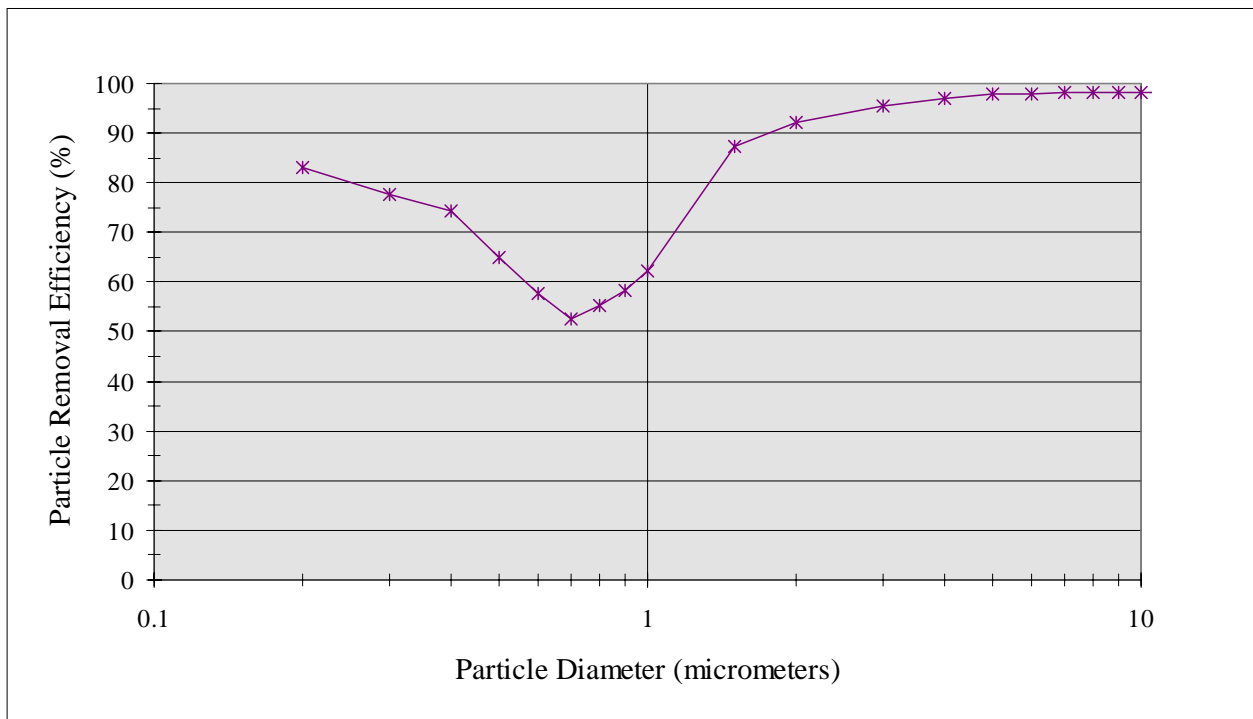


Figure 5.14 Particle Removal Efficiency by Particle Size for the Data in Figure 5.13

in all of the data:

- The removal efficiency is greatest at the largest particle size and then decreases rapidly with particle size below 3 μm .
- The removal efficiency decreases to a minimum value at about 0.6 μm .
- the removal efficiency increases as particle diameter decreases for diameters below about 0.6 μm .

The removal efficiencies for particle sizes greater than 1 μm have the least uncertainty because they represent the greatest amount of mass collected on the filters. Similarly, the removal efficiencies for particulate less than 1 μm have the greatest uncertainty because they represent only a small fraction of the mass collected. Typically, the mass collected on the filters in this size range was less than .5 mg, and represented less than 5% of the total mass collected.

The decrease in removal efficiency with particle size is expected since the primary particle removal mechanism is inertial impaction, which is less effective as particle size decreases. The cause for the increase in removal efficiency for diameters less than $\sim 0.5\mu\text{m}$ is not known. In this size range diffusion and thermophoresis may become important mechanisms and enhance particle removal.

Figure 5.15 shows the removal efficiency as a function of particle size for the five full-load tests, and the average for the five tests. The data show that the average removal efficiency for particles greater than 1 μm is in excess of 90%, while the average removal for particles smaller than 1 μm is about 60%.

The removal efficiency as a function of particle size for the two partial load tests are shown in Figure 5.16. The two data curves have the same general shape as the data for full load, but with lower overall removal efficiencies. This again is not unexpected since the effect of inertial impaction is diminished as gas velocity is decreased.

5.5.2 Total Particle Removal

Particle loading at the inlet and outlet of the IFGT facility was made during all of the sampling for mercury/trace metals, chloride/fluoride, and ammonia, along with several dedicated Method 5 samples.

The only abnormal occurrence in the particle loading data occurred in test series II using the Pittsburgh #8 coal. With Method 5 sampling, the total collected particulate consists of the fly ash collected on a filter (filter particulate) and the fly ash that deposits on the sampling probe surfaces and is collected in a rinse (probe rinse particulate). In test series II, the probe rinse particulate was weighed with a scale of insufficient accuracy and resolution. For the test series II tests, particle removal efficiency was calculated based on the filter weights only. This is a conservative approach since for all tests, the probe rinse is a greater fraction of the total particulate collected at the inlet to the IFGT facility than at the outlet.

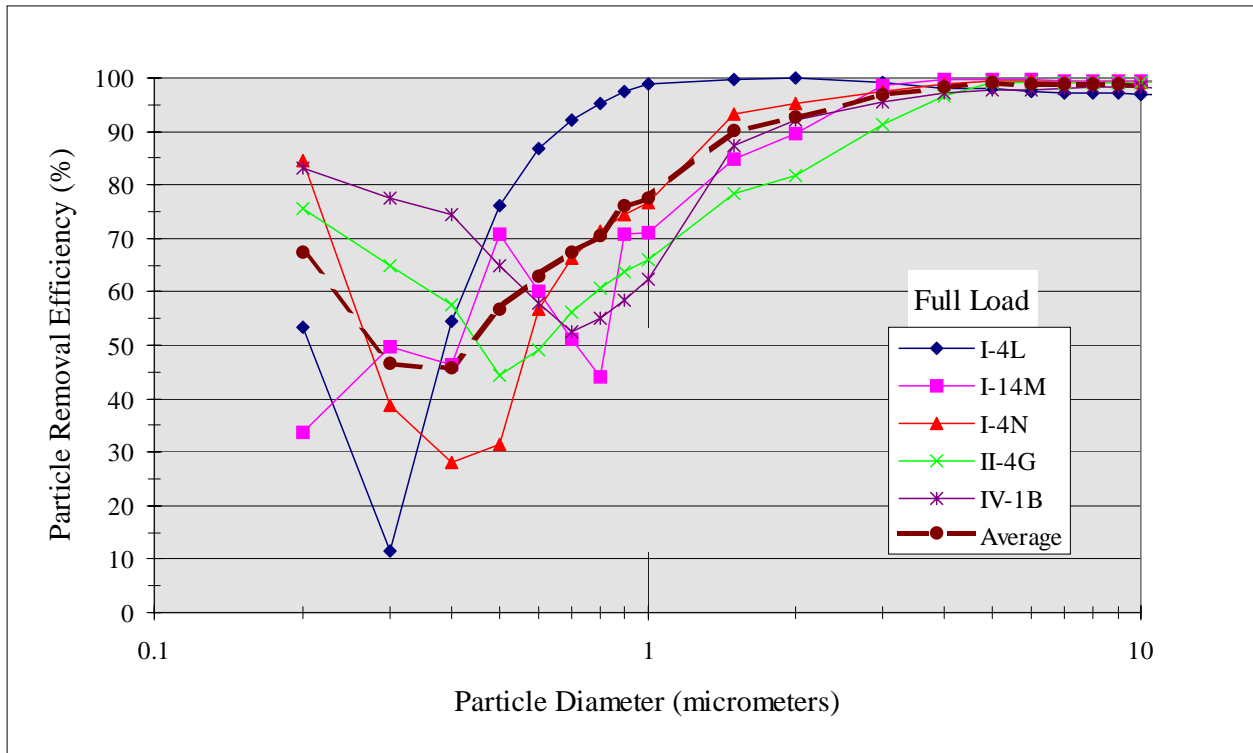


Figure 5.15 Particle Removal Efficiency by Particle Size for All Full Load Tests

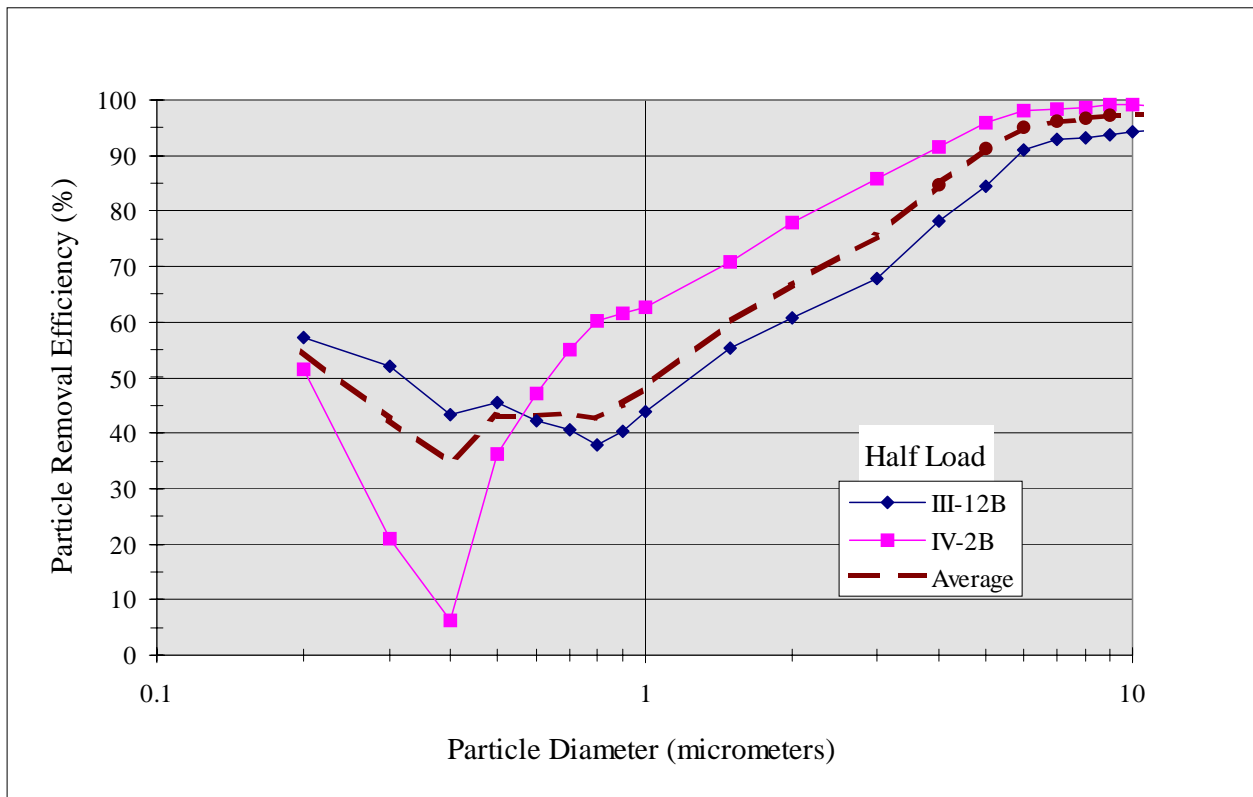


Figure 5.16 Particle Removal Efficiency by Particle Size For Partial Load Tests

The particle removal data are shown in Table 5.7. Along with the particle loading and removal efficiency, this table also provides the type of test, sampling time, gas velocity at the CHX[®] inlet and the reagent liquid-to-gas ratio. For test series I, the particle loading exceeded 400 mg/dscm, and the particle removal efficiency exceeded 95%. For test series II, the inlet particle loading varied from about 0.7 to 400 mg/dscm, and the removal efficiency ranged from 23% to 94%. For tests II-4A and II-4F all of the flue gas was routed through the baghouse. The low inlet particle loadings of 3.6 and 0.7 mg/dscm are the fugitive baghouse emissions and are well below the NSPS limit of 42 mg/dscm (0.03 lb/million Btu).

The removal efficiency for tests III-9A, -9B and -7A averaged about 89%, which is less than other data at comparable particle loadings. The lower overall removal efficiency for these tests is due to the finer fly ash particle size distribution for the Powder River Basin coal and the lower removal efficiency for the fine particulate.

From the data in the table, it is evident that the particle removal efficiency decreases as the particle loading to the CHX[®] is reduced. This is due to the size distribution of the particulate. The other trend in evidence in Table 5.7 is shown by tests III-9B and III-12A which show a decrease in removal efficiency as the gas velocity (i.e., load) is decreased.

In Test IV-2A, the use of wire mesh pads was investigated as a means of fine particulate removal. For this test four layers of mesh pad were located in the inter-stage between the first and second heat exchanger stages. The measured removal efficiency of 93% is substantially greater than the 77.5% removal efficiency for test III-12A which was also conducted at partial load, but without the use of a mesh pad. Although this is a substantial difference, most of the difference may be attributable to differences in the inlet particle size distribution.

With the exception of load (gas velocity) and particle loading, the removal efficiency is insensitive to other operating conditions over the range tested.

Table 5.7 Overall Particulate Removal Data

Test Number	Test Type	Total Sample Time (hrs)	Inlet Gas Velocity (m/s)	Outlet Gas Temperature (°C) ¹	L/G (l/m ³)	Inlet Particle Loading (mg/dscm)	Particle Removal Efficiency (%)
I-14D	M-29 Avg.	6.0	12.05	-9.0	0.70	842.	96.5
I-4A ²	M-26	1.7	11.87	0.0	0.67	722.	96.4
I-4J ³	M-5	2.0	11.79	1.0	0.64	711.	95.2
I-4F	M-5/NH3	2.0	11.95	0.0	0.65	644.	95.6
I-4B	M-29 Avg.	6.0	11.77	0.0	0.64	642.	97.2
I-4C	M-29 Avg.	6.0	11.78	0.0	0.63	401.	95.9
II-4C	M-29 Avg.	6.0	11.87	0.0	0.53	655.	93.9
III-7A	M-26	2.0	11.70	0.0	0.38	482.	88.7
III-9B	M-5NH3	1.3	11.60	1.0	0.35	480.	89.7
III-9A	M-29/OH Avg.	6.0	11.53	0.0	0.36	478.	88.4
IV-14A	M-29/OH Avg.	6.0	11.42	-1.0	0.49	296.	95.1
IV-1A	M-26	2.0	11.14	0.0	0.52	40.2	94.3
II-4A	M-29 Avg.	6.0	11.77	0.0	0.61	3.6	71.9
II-4F	M-5/NH3	2.0	11.94	-8.0	0.64	0.7	23.6
IV-2A	M-5	1.3	7.02	0.0	0.47	444.	93.0
III-12A	M-29/OH Avg.	6.0	7.10	0.0	0.36	384.	77.6

1) Gas Temperature Relative to The Water Vapor Dew Point Temperature

2) Woven Mesh Pad Located in the IFGT Inter-stage

3) Inter-stage Steam Injection

5.6 Mercury Removal

5.6.1 Measurement Methods and Detection Limits

The mercury content of the vapor and particle phases entering the IFGT facility were measured in each of the four test series. Triplicate two hour tests were conducted at each test condition. In the first two test series, mercury concentrations were measured exclusively using EPA Method 29 sample trains. During the third and fourth test series the triplicate measurements consisted of two Ontario Hydro sample trains bracketing a single Method 29 sample train. The sample time for the mercury measurements were two hours for each triplicate test.

The measurement accuracy of speciated forms of mercury using Method 29 and the Ontario Hydro method have not been resolved, and this issue is beyond the scope of this work. Rather, the concentrations of the speciated forms and the total mercury as determined using the Method 29 and Ontario Hydro are presented in this report with the caution that the absolute accuracy of the speciated concentrations are in question.

The concentration of mercury in the recovered impingers (vapor phase) and the concentration of mercury in the digested particulate samples (particle phase) was measured using Cold Vapor Atomic Absorption (CVAA). The detection for mercury measurements in the laboratory using CVAA is 0.1 parts per billion (ppb) for ionic mercury and 0.5 ppb for elemental mercury when measured in a prepared solution. The solution analyzed in the laboratory is prepared from the impinger and washing solutions gathered from the Method 29 and Ontario Hydro sampling trains. Mercury emissions are normally expressed on terms of micrograms per dry standard cubic meter, ($\mu\text{g}/\text{dscm}$). If the laboratory detection limits of 0.1 to 0.5 ppb are transformed to $\mu\text{g}/\text{dscm}$ using typical Method 29 and Ontario Hydro sampling rates and impinger volumes, the detection limits can be compared to actual measurements to insure that these measurements are sufficiently above the detection limits to be meaningful. The estimated detection limits for mercury are summarized in Table 5.8. Also listed in Table 5.8 are the minimum reportable concentrations that have been used in this report. These minimum reportable concentrations take into account the detector's limits as well as triplicate test repeatability.

Table 5.8 Mercury Detection Limits and the Minimum Reportable Concentrations

Mercury Form	Detection Limit in the Flue Gas ($\mu\text{g}/\text{dscm}$)	Minimum Reportable Concentration ($\mu\text{g}/\text{dscm}$)
Ionic Vapor Phase	0.02	0.5
Elemental Vapor Phase	0.20	1.0
Total Vapor Phase	0.22	1.0
Particle Phase	0.01	0.2
Total mercury	0.23	1.0
Mercury in the Coal	2.66	(-)

5.6.2 Mercury Concentration in the Coal

Typically, the concentration of mercury in the coal was determined from grab samples of the pulverized coal in the coal pipe just upstream of the burner. Grab samples were obtained at the start, middle, and end of a two-hour test period. A composite of the grab samples from the triplicate tests was used to obtain a test average coal sample for analysis.

Not all of the collected samples were analyzed for mercury. Rather, the mercury concentration in the coal provided measurement redundancy and a cross check by which the reasonableness of gas and particle phase measurements could be evaluated.

Figure 5.17 shows the concentration of mercury in the flue gas that would result from 100% emission of the mercury contained in the coal for each coal in the four test series. The error bars indicate the range of multiple measurements. The mercury level from the Ohio #5/#6 coal (Test Series I) and the PRB coal are relatively high, while the Pittsburgh #8 and Ohio #6/#5 coal are relatively low*. The coals selected for the pollutant removal tests were based primarily on sulfur content and origin. Within those parameters, coals with high mercury concentrations were desired in order to provide increased measurement accuracy associated with the absolute concentrations and mercury removal. The mercury concentration in the Ohio and Pittsburgh coals are within ranges generally reported in the literature⁴. The concentration of mercury in the PRB coal is higher than typically reported in the literature.

5.6.3 Comparison of Gas Phase Mercury Speciation from Method 29 and the Ontario Hydro Method

Mercury vapor in the flue gas exists in both elemental (Hg^0) and ionic (Hg^{++}) forms. The ionic form is the more reactive of the two, so that ionic mercury is more readily removed in sulfur scrubbing systems. EPA Method 29 sampling has been validated for measuring metals concentration, including mercury, in the vapor state. With this technique, the metal vapors are trapped by the chemical solutions in the sample impinger bottles. The ability of Method 29 to distinguish between the different forms of mercury in the vapor state has been under question, and alternate methodologies (Ontario Hydro, for example) have been proposed to more accurately assess the concentration of the two forms of mercury.

In test series III and IV, triplicate measurements consisted of an EPA Method 29 sample train bracketed by two Ontario Hydro (OH) sample trains. A comparison of the ionic mercury concentration measured with the two techniques at the inlet and outlet of the IFGT facility are shown in Figure 5.18. The OH data are the average of two measurements and the uncertainty bars indicate the data range.

Figure 5.18 shows that at the inlet to the IFGT facility, the OH measurement of Hg^{++} exceeded the M-29 measurement of Hg^- in test III-12, while in test III-9 and IV-14, the M-29 measurement

*Ohio #5/#6 denotes a blend of 80% Ohio #5 and 20% Ohio #6. The Ohio #6/#5 contained 80% #6 and 20% #5.

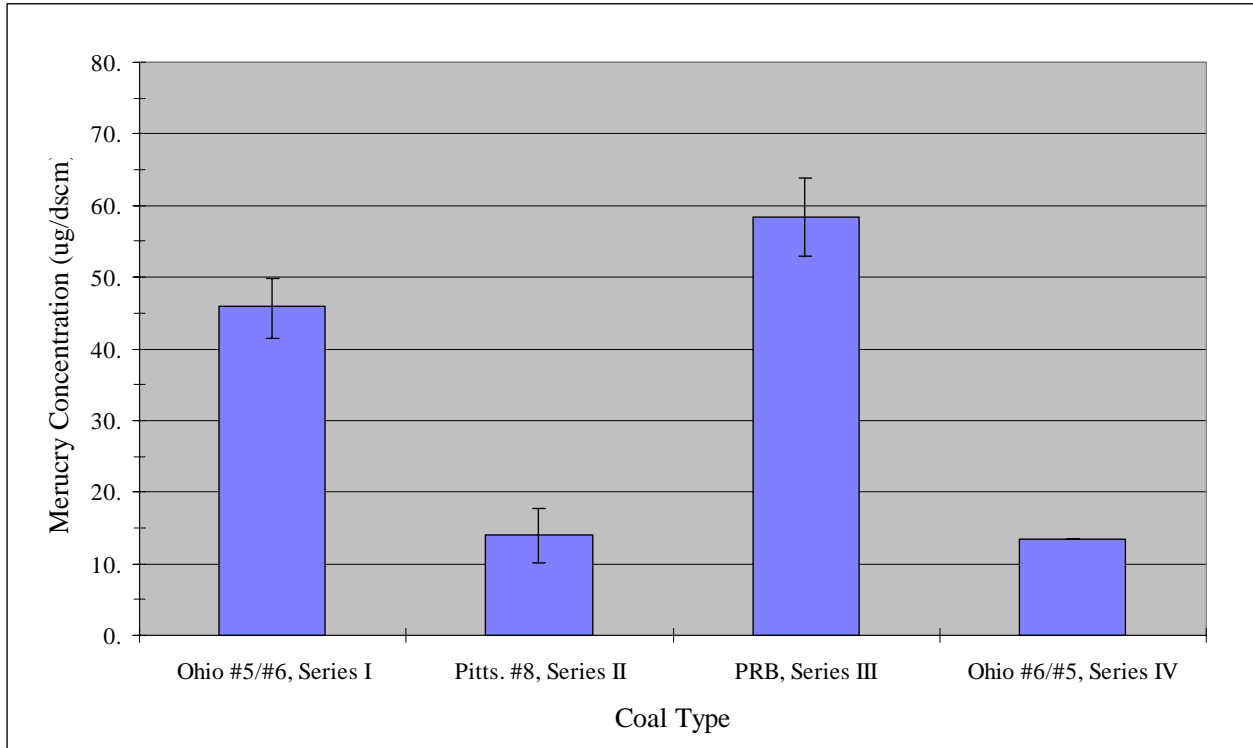


Figure 5.17 Flue Gas Mercury Concentration Resulting From 100% Release of Mercury in the Coal

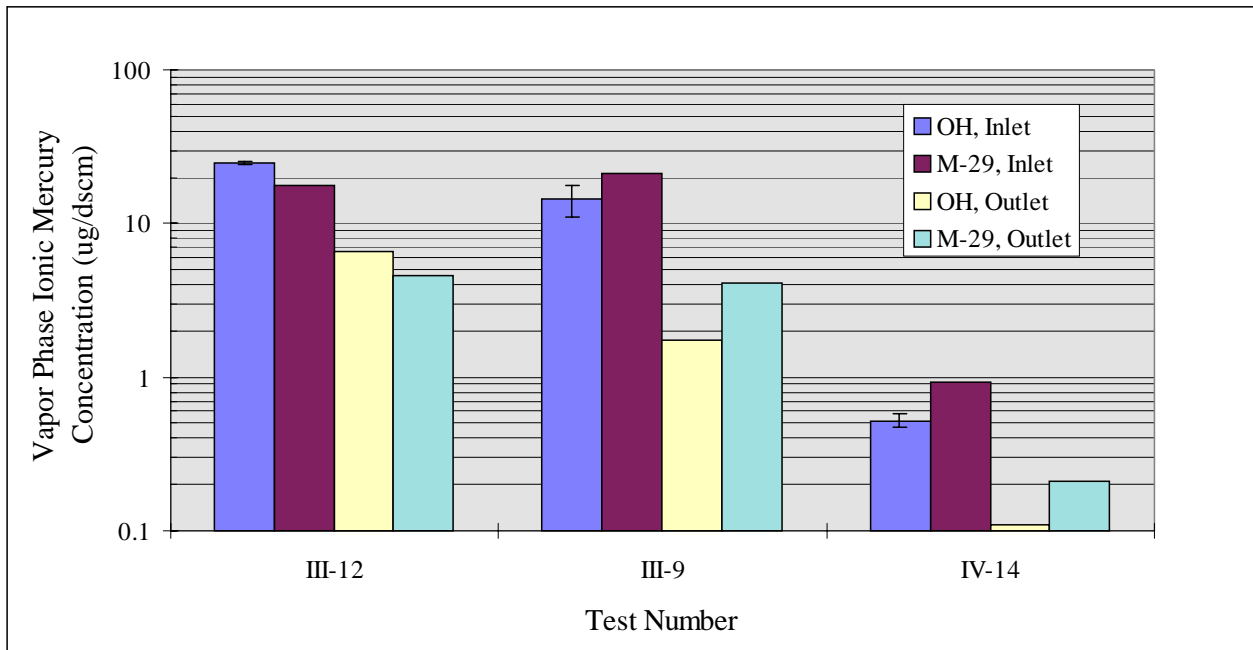


Figure 5.18 Comparison of Vapor Phase Ionic Mercury Measured Using Method 29 (M-29) and Ontario Hydro (OH) Sample Trains

exceeded the OH measurement. In all three tests, the M-29 measurement is outside the range of the OH measurements.

Comparison of the OH and M-29 data at the outlet of the IFGT indicate the same trend, so that the relative change in Hg^- across the IFGT system is nearly the same for either technique. This indicates that the difference between the two measurement techniques may have been due to a real variation in Hg^{++} concentration in the flue gas over the six hour duration of the triplicate tests. The difference in the average ionic mercury concentration between tests series III and IV is due to the coal used for each test. Test III used a PRB coal while test IV used an Ohio coal.

Figure 5.19, is a corresponding comparison of the two measurement techniques for elemental mercury at the inlet and outlet of the IFGT facility. For tests III-12 and III-9 the elemental mercury concentration was quite high and the difference in concentration between the two measurement techniques at the inlet and outlet location are quite small. For test IV-14 the concentration of Hg^0 was very low. The OH method provides a slightly larger measured value of Hg^0 at both the inlet and outlet of the IFGT. The relative difference between the two techniques for this test is greater than for test series III, but the absolute difference is again very small.

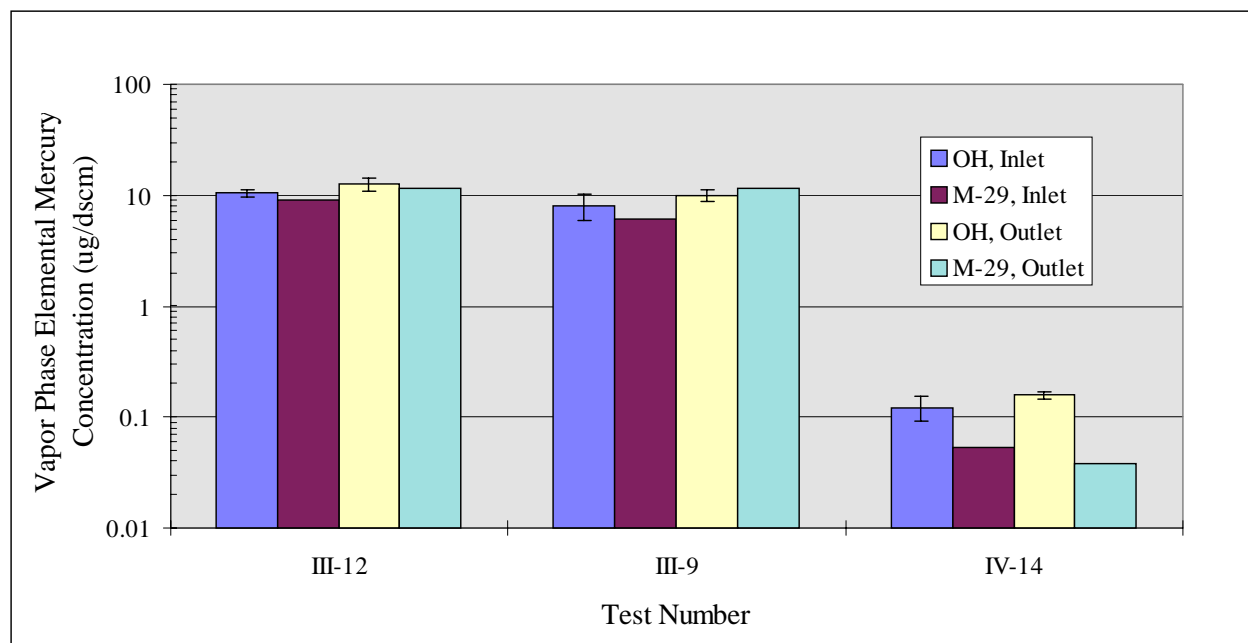


Figure 5.19 Comparison of Vapor Phase Elemental Mercury Measured Using Method 29 and Ontario Hydro Sample Trains

Comparison of the OH and M-29 measurements of elemental and ionic mercury show only relatively small differences, and the difference is consistent at the inlet and outlet measurement locations. For this reason, no further distinction will be made between the two techniques with respect to the total concentration of mercury or the speciated forms of mercury. The data from the two measurement techniques were averaged to determine test average mercury concentrations and removal efficiencies.

5.6.4 Mercury Partitioning

Mercury is a relatively volatile element that can exist in the flue gas as a vapor and can also be attached to particulate carried by the flue gas. Figure 5.20 shows the concentration of mercury in the flue gas at the inlet to the IFGT facility as vapor, and that contained on the particulate, for all of the tests. The particulate and vapor forms are both in the common basis of ug/dscm. Expressed in this form, it is understood that the particle phase mercury concentration in the flue gas depends not only on the mercury concentration in the fly ash, but also the fly ash concentration in the flue gas.

Figure 5.20 shows that for test series I and III most of the mercury is partitioned to the vapor phase and is very repeatable from test to test. In test series II the total vapor phase concentration was below reportable limits, while in test II-4C the particulate concentration is larger than for any other test. In test IV-14 the vapor phase concentration is about the same as the particulate phase. For the data shown in Figure 5.20, the particle loading to the IFGT facility was about the same for all tests.

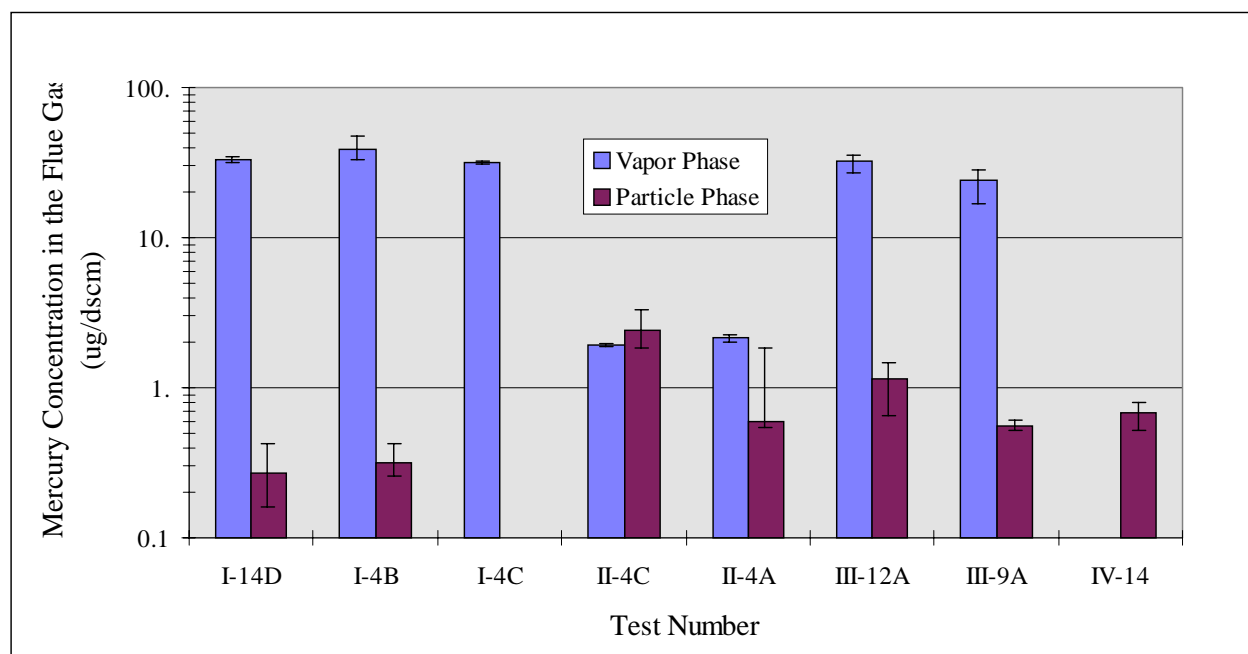


Figure 5.20 Vapor Phase and Particle Phase Concentrations of Mercury in the Flue Gas

The differences in particle phase concentration shown in Figure 5.20 is primarily due to differences in mercury concentration in the fly ash, and not particle loading. The cause of the variation from one test series to the next is not known, but is likely dependent on the coal type. Field measurements of mercury concentrations at utility power plants have traditionally shown wide variation⁵. Precautions were taken during the tests to ensure that combustion conditions were duplicated for each of the four tests. This included the same burner, excess air, load, primary and secondary air temperatures, coal grind (fineness), downstream equipment and operating procedure.

5.6.5 Vapor Phase Mercury Removal

Figure 5.21 shows the triplicate average ionic mercury concentration at the inlet to the IFGT facility and the calculated removal efficiency for each test. The vertical bars on the concentration data indicate the range of the triplicate measurements. The vertical bars on the removal efficiency is the estimated uncertainty based on the standard deviation in the triplicate measurements.

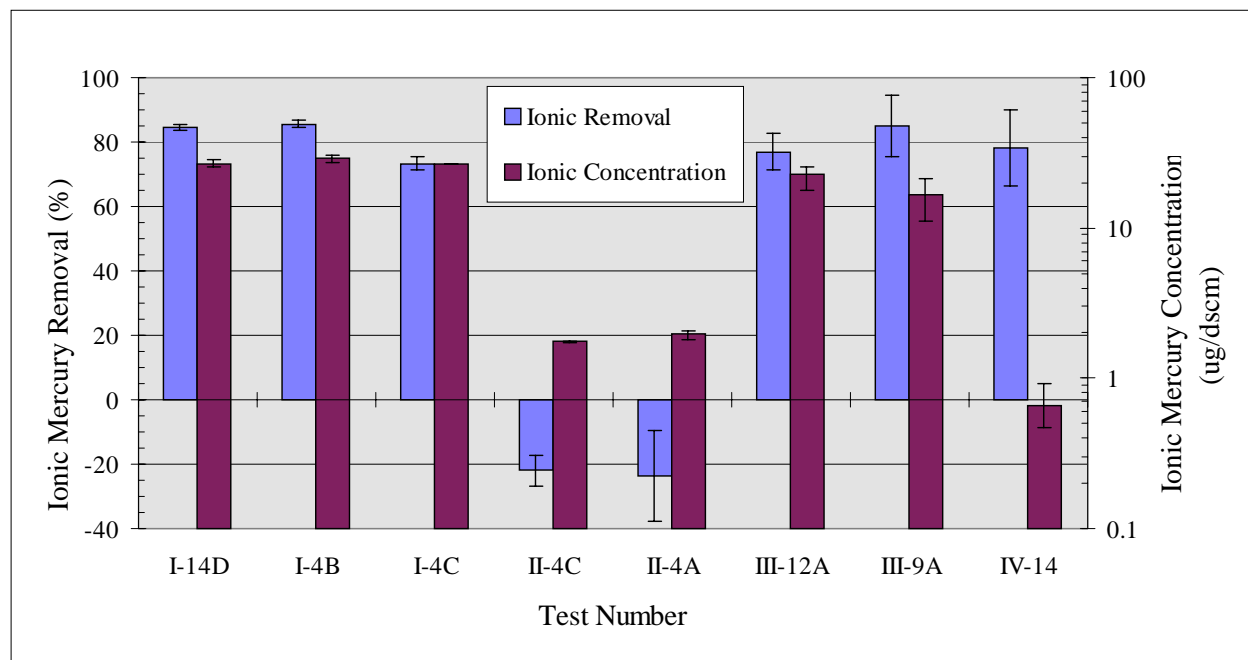


Figure 5.21 IFGT Removal Efficiency for Ionic Mercury (Left y-axis) and Ionic Mercury Concentration (Right y-axis).

For test series I, III, and IV the ionic mercury removal efficiencies ranged from 75% to 85%, while for test series II the removal efficiency averaged less than 0%. Removal efficiencies on the order of 70% to 90% for ionic mercury are to be expected⁶. The measured concentrations for test II are just above reportable limits, and so may be subject to relatively large error. However, the measured concentrations for test IV-14 are similarly low, and are in agreement with the data for test series I and III. The data and analysis procedures from test series II have been reviewed and a cause for the abnormal results could not be found. However, the data are not in agreement with that from the other three test series and are not in agreement with data reported in the literature, and so should be considered questionable.

Figure 5.22 shows the average concentration and removal efficiency of elemental mercury for each test. The removal data averages from about 0% to -35% and is independent of mercury concentration or coal type. Elemental mercury removal data is not presented for test series II as the concentrations were below reportable limits.

The indicated increase in elemental concentration across the IFGT facility was not limited to triplicate averages at the inlet and outlet. Essentially all paired inlet/outlet measurement of

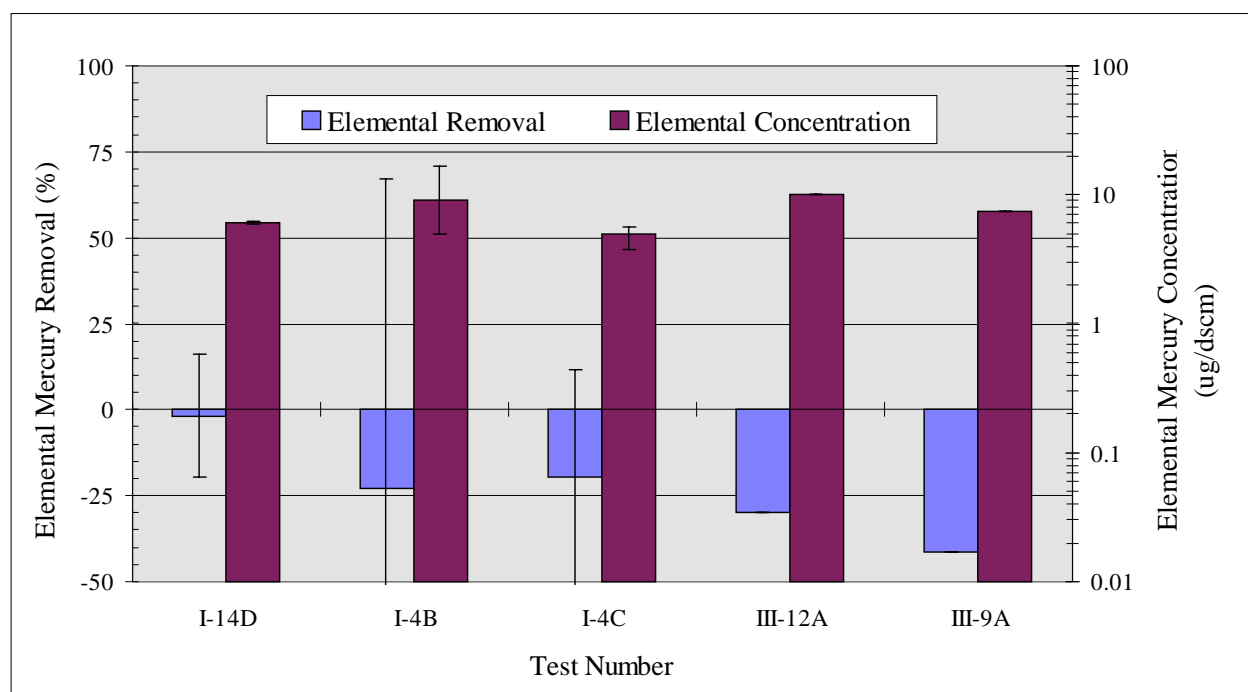


Figure 5.22 IFGT Removal Efficiency for Elemental Mercury (Left y-axis) and Elemental Mercury Concentration (Right y-axis).

elemental mercury indicated some increase in concentration. This effect may be real, if captured ionic mercury is reduced to elemental mercury and subsequently evolved from the scrubbing solution. This effect may also be an artifact of the sample trains used to measure ionic and elemental mercury.

Removal efficiencies of about 0% for elemental mercury are in general agreement with published data for other flue gas treatment equipment, primarily wet scrubbers⁷. An anticipated benefit from low temperature operation of the IFGT facility was not realized. The outlet flue gas temperatures for the data in Figure 5.22 ranged from about 27°C to 37°C (80°F to 98°F), which is well below the normal operating temperature for wet scrubbers.

5.6.6 Particle Phase Mercury Removal

The particle phase mercury concentration and removal efficiency for each of the tests are shown in Figure 5.23. Data are shown only for those tests in which the mercury concentration was above reportable limits. Three of the tests show an average removal efficiency of about 75%. Of the two tests that have lower removal efficiencies, test III-12A was conducted at partial load, and the lower mercury removal (42%) was due to a lower particulate removal efficiency (77%). The cause of the low removal efficiency of test III-9A is unknown. As indicated by the uncertainty limits, the measured concentrations of particulate mercury in the triplicate tests varied significantly.

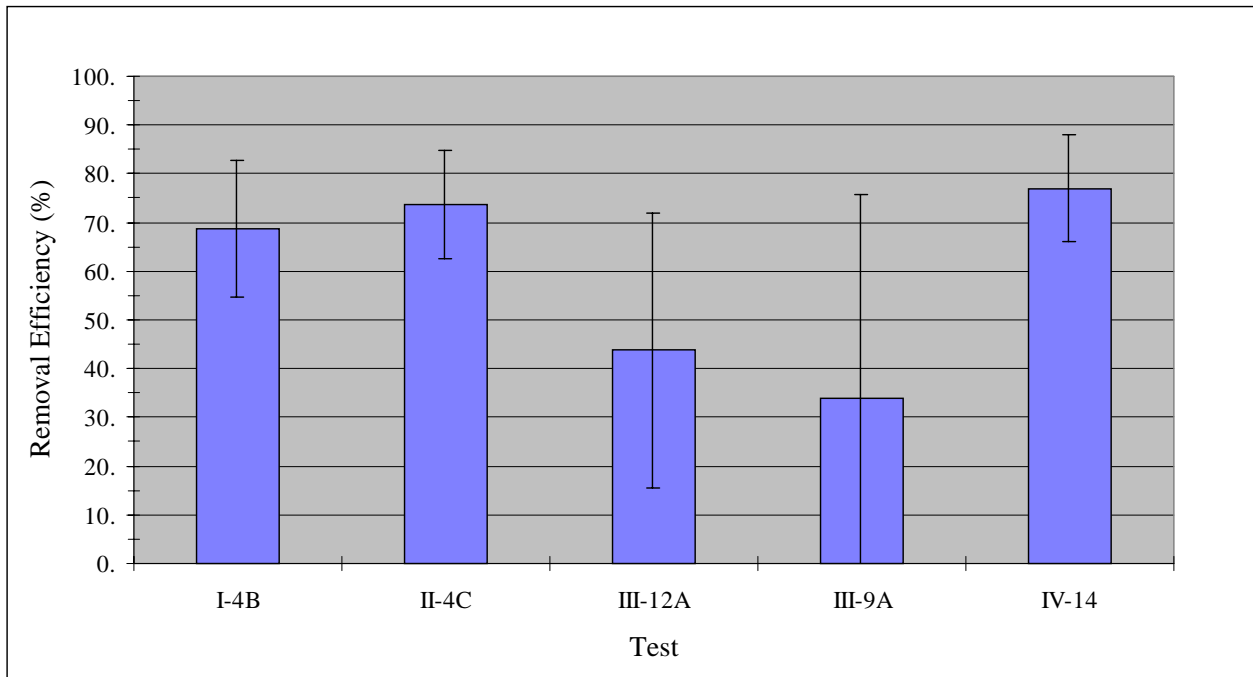


Figure 5.23 Removal Efficiency for Particle Phase Mercury

The particle phase mercury removal is less than the overall particulate removal because the mercury concentration in the particulate at the outlet of the IFGT facility averaged 3 to 5 times greater than at the inlet. This indicates that the mercury tends to be concentrated in the sub-micron particulate, which is less effectively removed by the IFGT process.

5.7 Trace Element Removal

5.7.1 Trace Element Measurement and Detection Limits

The trace element content of the vapor and particle phases entering the CHX[®] were measured in each of the four test series. Triplicate two hour tests were conducted at each test condition. In the first two test series, element concentrations were measured exclusively using EPA Method 29 sample trains. During the third and fourth test series the triplicate measurements consisted of two Ontario Hydro sample trains bracketing a single Method 29 sample train. The sample time for the Method 29 and Ontario Hydro trains were two hours for each of the triplicate tests. The Ontario Hydro sample trains were used primarily to obtain comparative mercury speciation data.

The concentration of trace elements in the recovered impingers and the concentration of trace elements in digested particulate samples were measured using graphite furnace atomic absorption (GFAA). Table 5.9 lists the limits of detection of the trace elements for the gas phase, fly ash, and coal samples that are typical for the four test series for the M-29 sample train. Also shown are the minimum reportable detection limits which have been defined as 10 times the detectable limit or 1.0 ug/dscm, whichever is greater for gas phase concentrations.

Table 5.9 Limits of Detection of the Trace Elements

Element	Vapor Phase Limits		Particle Phase Limits		Coal
	Detection Limit (ug/dscm)	Reporting Limit (ug/dscm)	Detection Limit (ug/dscm)	Reporting Limit (ug/dscm)	
Arsenic	0.117	1.2	0.064	1.0	0.20
Barium	1.173	11.7	0.643	6.4	2.00
Beryllium	0.059	1.0	0.439	4.4	0.10
Cadmium	0.012	1.0	0.026	1.0	0.02
Chromium	0.117	1.2	0.064	1.0	0.40
Cobalt	0.235	2.4	0.161	1.6	0.20
Lead	0.117	1.2	0.142	1.4	0.20
Manganese	0.117	1.2	0.101	1.0	0.40
Nickel	0.235	2.4	0.161	1.6	0.20
Selenium	0.117	1.2	0.142	1.4	0.20

Although Ontario Hydro trains have not been validated for trace elements other than mercury at this time, vapor phase trace elements were also measured in the Ontario Hydro impingers for test series III. The detection limits for vapor phase metals from OH sample trains are about 5 times greater than for the M-29 sample trains shown in Table 5.9. For test series III and IV the vapor phase concentration of all trace elements except mercury were below reportable values for both the OH sampling methods, so that an accurate comparison of the two techniques using this data cannot be made.

5.7.2 Vapor Phase Trace Element Removal

Most of the trace elements are non-volatile and condense to a solid state at relatively high temperatures. Generally, trace elements measured in the vapor phase were below the reportable limits of detection at the inlet to the CHX[®]. This was especially true for the Pittsburgh and PRB coals for which gas phase concentrations of trace elements was very low. The exceptions are arsenic and selenium which occurred in fairly high concentration for several of the coals tested. Significant quantities of lead, nickel, and manganese were occasionally measured, but the repeatability of the concentration data as determined by the triplicate measurements was poor.

Figure 5.24 shows the concentrations and removal efficiency for arsenic for test series I and IV that used the Ohio coals. The uncertainty bars on the concentration represent the range of triplicate measurements, while the uncertainty bars on removal efficiency represents a root mean square (rms) uncertainty based on triplicate concentration measurements. The concentration of arsenic for the Pittsburgh and PRB coals were below reportable limits, and are not shown. For

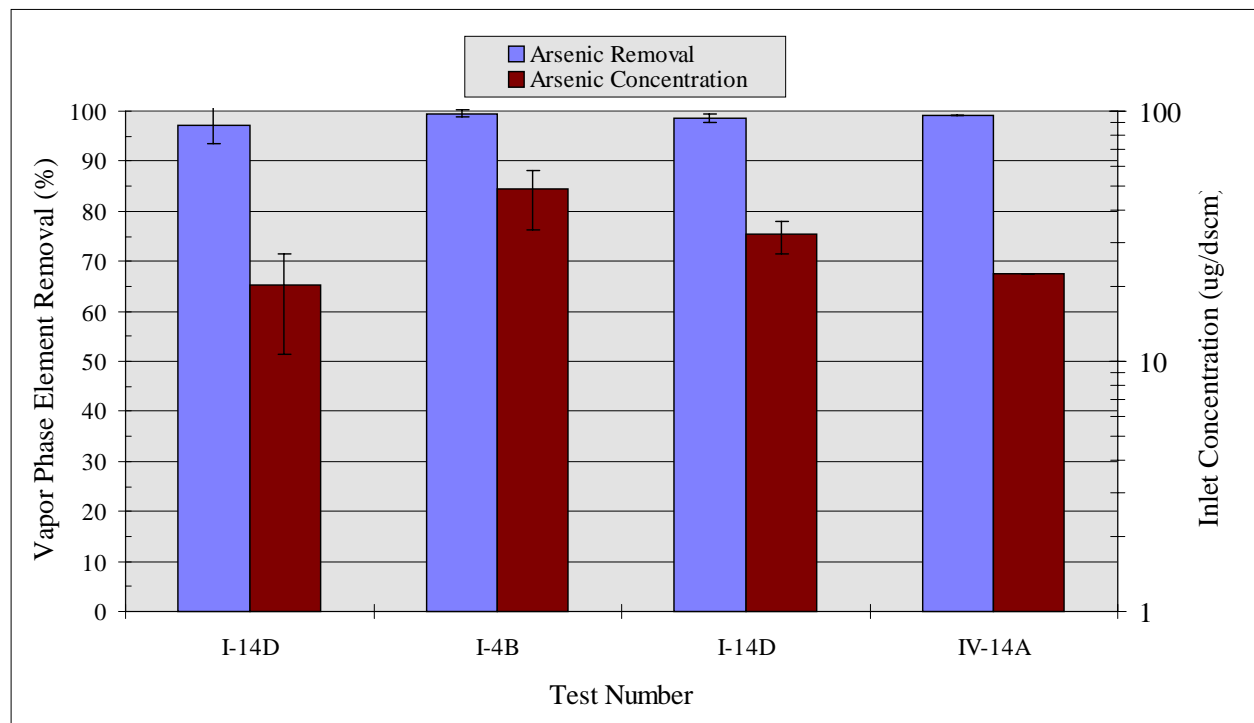


Figure 5.24 IFGT Removal Efficiency for Vapor Phase Arsenic (Left y-axis) and the Inlet Concentration (Right y-axis)

the tests shown in Figure 5.24, the arsenic concentration varied from 20 to 70 ug/dscm, and the removal efficiency was greater than 95%. The removal efficiency for test IV-14A with a mag-lime reagent is no different than for the other tests in which soda ash reagent was used.

Figure 5.25 is a similar figure showing the concentration and removal efficiency for vapor phase selenium. Reportable quantities of selenium were measured in the Pittsburgh coal (series II) as well as for the Ohio coals (series I and IV). For test series I and test II-4C the selenium concentration and removal efficiency are both quite high. For test II-4A, the removal efficiency is about 50%, but the concentration is just above the reportable limit, and the uncertainty in the removal efficiency is quite large.

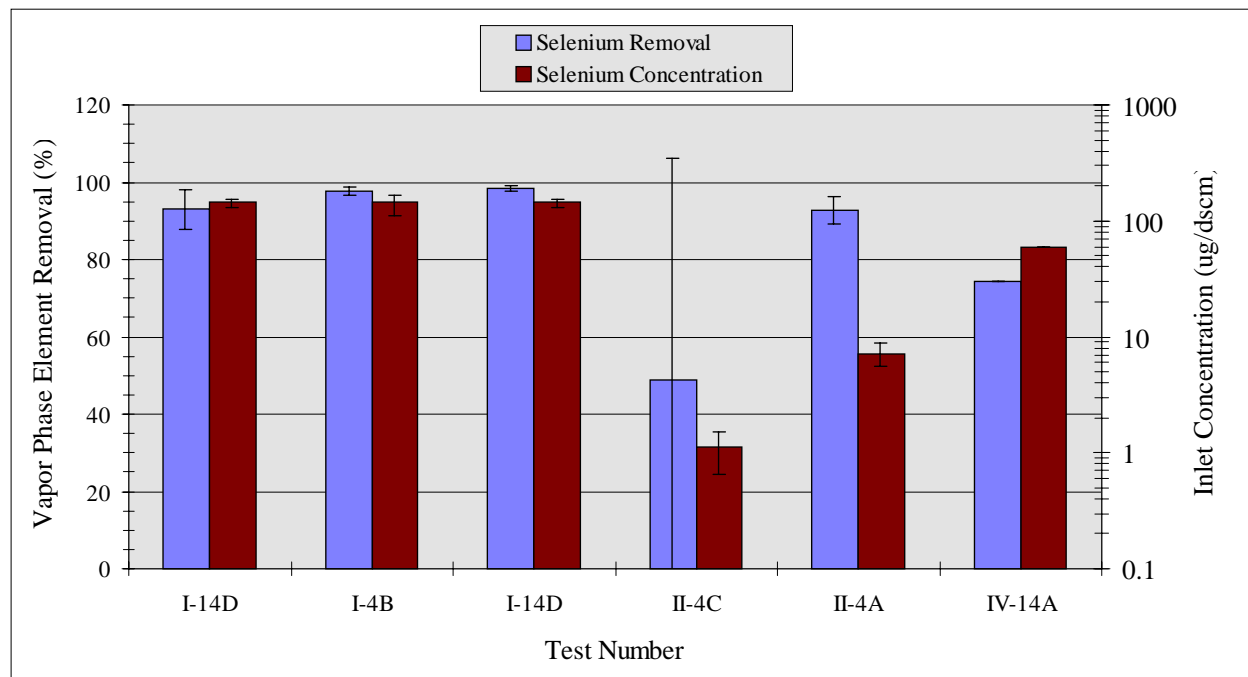


Figure 5.25 IFGT Removal Efficiency for Vapor Phase Selenium (Left y-axis) and the Inlet Concentration (Right y-axis)

Test IV-14A represents a single M-29 sample. The removal efficiency is lower than for tests with comparable concentrations. The lower removal efficiency for this test may be due to the mag-lime reagent that was used. All other tests were conducted with sodium based reagent.

5.7.3 Particle Phase Trace Element Removal

When expressed on a gas phase basis, the concentration of an element contained on particulate depends on both particulate concentration in the flue gas and the element concentration in the particulate. It is the product of these two numbers which represents the total quantity of the element in the fluegas.

Figure 5.26 shows the particle phase concentration of the elements in the flue gas at the inlet for three tests that represent the three different coals. For these three tests the particle loading at the

inlet to the CHX[®] was relatively constant, so most of the test to test variation shown in the figure is due to variation of the elemental concentration in the particulate.

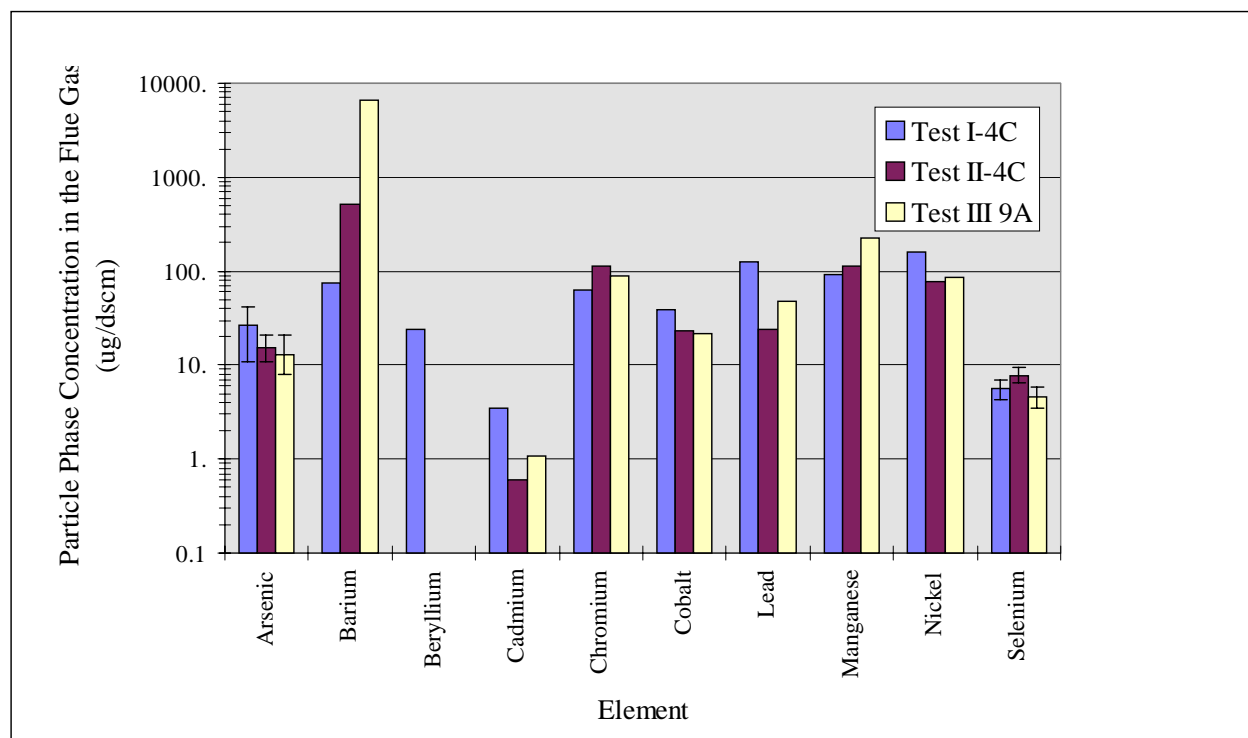


Figure 5.26 Particle Phase Elemental Concentration at the IFGT Inlet

Chromium has the lowest concentration of all of the elements measured, and is just above reportable limits. For most of the elements the variability with coal type (Ohio, Pittsburgh and PRB) is less than the variability from element to element. The exception is barium which had a very high concentration for test series III (PRB coal).

Figure 5.27 shows the element removal efficiency for the particle phase data. Measured data from all full-load tests are included in this figure. The particle phase removal efficiencies range from about 20% for cadmium to 100% for Beryllium. In general, although the concentration of cadmium in the particulate was above reportable limits, the triplicate measurements indicated a large variability.

For all elements except beryllium, the removal efficiency for the element is less than the removal efficiency measured for the particulate. For the tests shown in Figure 5.27, particle removal efficiencies ranged from 87% to 96%. The reduced efficiency for the removal of these elements compared to removal of the total particulate is caused by enrichment in the fine particulate.

With the exception of beryllium, all elements indicated a higher concentration in the fly ash at the outlet of the IFGT system than at the inlet to the IFGT system. This is illustrated by Figure 5.28 which shows the ratio of the element concentration in the particulate at the inlet of the CHX[®] to that at the outlet. As shown, the element concentration in the fly ash at the outlet is generally 2 to 10 times that at the inlet. Since the median particle size of the flyash at the outlet

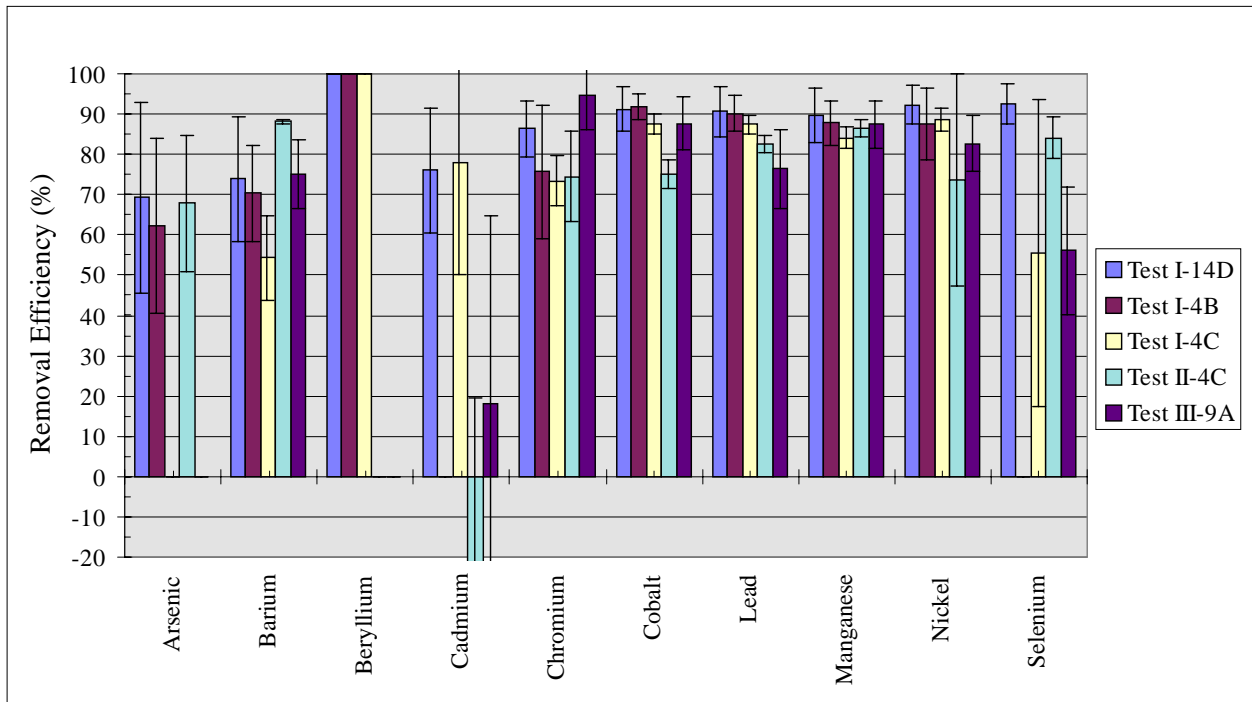


Figure 5.27 Particle Phase Trace Element Removal Efficiency

is about one-fifth of that at the inlet (1 micron vs 5 microns) this indicates that the fine particulate contain proportionately higher concentrations of these elements. The removal of the element is less than the removal of the total particulate because the fine particulate, of which only 60% is removed, contains a disproportionate amount of the element.

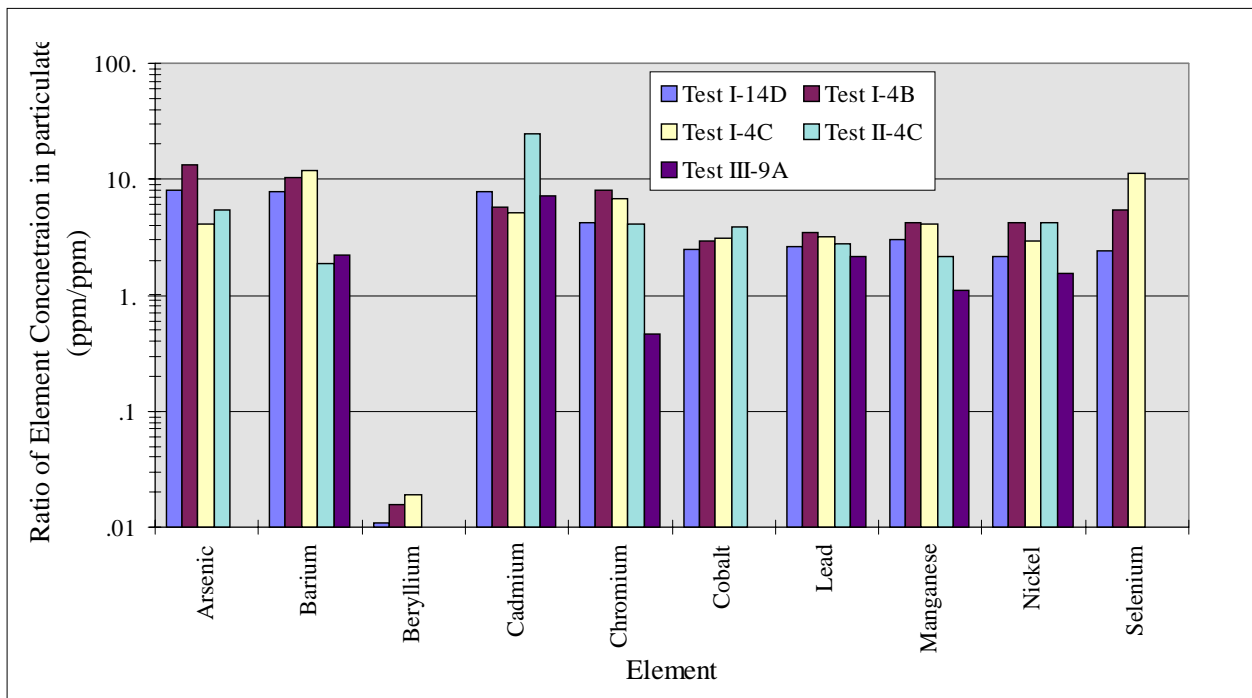


Figure 5.28 Ratio of Element Concentration in the Fly Ash at the IFGT Outlet to the Inlet

5.8 NO_x Removal

NO_x concentrations at the inlet and outlet of the IFGT facility were measured during test series I. Although removal of NO was not anticipated, NO₂ removal with the sodium based reagent was possible. The NO_x measurements in Test Series I were performed to determine if any measurable reduction in NO_x occurred in the IFGT process.

Figure 5.29 shows the calculated NO_x removal efficiencies for all of measured data. Within the experimental error of the measurements, NO_x removal averaged 0% for all of the tests. Based on these results, NO_x measurements were suspended for the remaining tests.

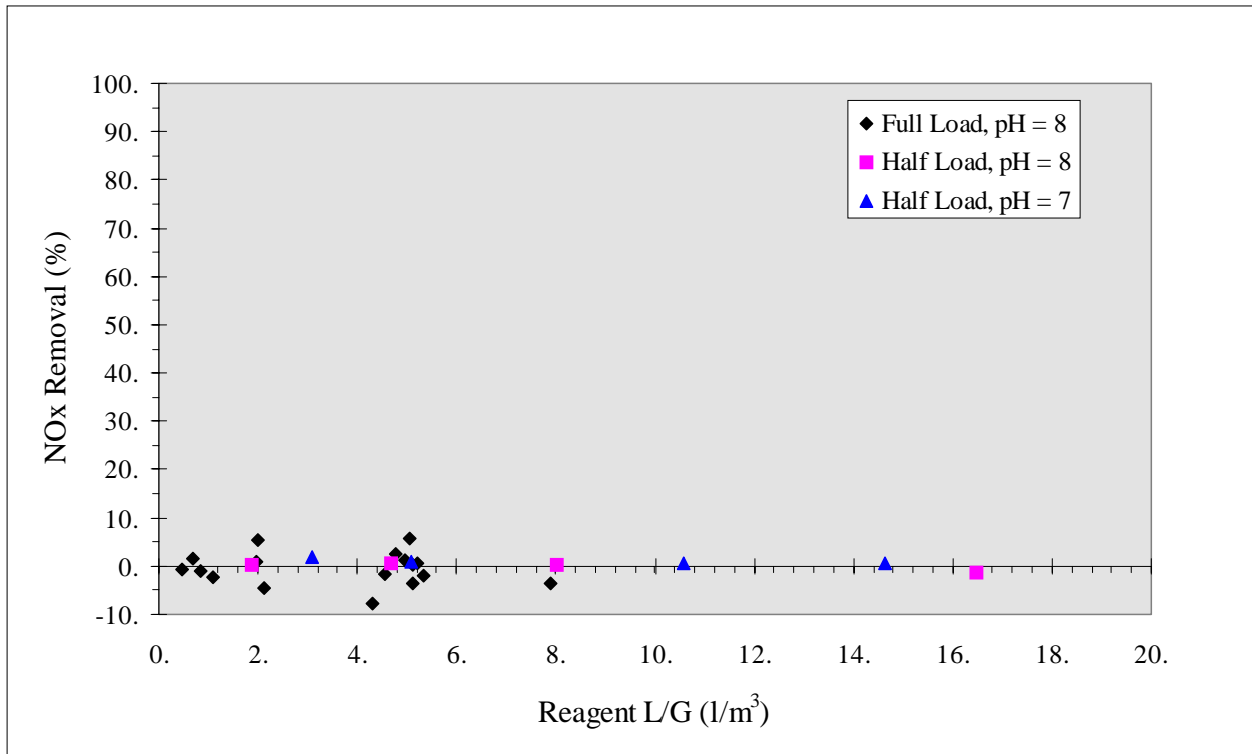


Figure 5.29 Measured NO_x Removal as a Function of L/G for Test Series I

6.0 CONCLUSIONS AND RECOMMENDATIONS

The pollutant removal goals were established with the objective of demonstrating pollutant removal performance that met or exceeded that of conventional flue gas desulfurization. That goal coupled with the economic benefit in the form of recovering waste heat is intended to show the IFGT to be a reliable new FGD technology for the next century.

The Integrated Flue Gas Treatment Process using condensing heat exchangers is effective at removing multiple pollutants from the flue gas of coal combustion. The Task 2 goals for pollutant removal and the actual performance of the IFGT process are summarized below.

SO₂ Removal

The IFGT process has exceeded the goal for SO₂ removal, providing greater SO₂ removal than a conventional wet scrubber operating at similar L/G. SO₂ removal depends on the absorption capacity of the reagent, and the gas-liquid contact area for absorption. The soda ash reagent is highly reactive and has sufficient dissolved alkalinity to remove all of the SO₂ in high sulfur flue gas even at low liquid-to-gas ratios. Greater than 95% removal of SO₂ at these low L/G shows that the surface area of the tubes in the second stage provides more than adequate gas-liquid contact for SO₂ absorption.

The 50% SO₂ removal using lime slurry and the 88% removal efficiency of the mag-lime slurry reflects the diminished absorption capacity of these reagents. These removal efficiencies were achieved with a 1.5 % sulfur coal. The removal efficiencies for coals with lower sulfur content will be greater. The estimated removal efficiencies for a 0.75% sulfur coal are estimated to be approximately 70% for lime and 95% with mag-lime. Without any modification to the current process (higher L/Gs for example) this is sufficiently high to meet the SO₂ removal needs.

The SO₂ removal tests using calcium-based reagents confirm that they are potentially acceptable alternatives to the sodium based reagents. This is significant from the standpoint of operation costs, disposal costs, and environmental issues. Calcium-based byproducts are environmentally benign and are potentially saleable.

The increase in removal efficiency with L/G for the lime and mag-lime slurry is lower than expected and suggests that there is a mal-distribution of the slurry and the gas. For a pilot facility of the size used in these tests, the mal-distribution likely results from wall effects. This effect can be caused by too much slurry on the walls or by too little slurry on the wall. It is nearly always evident in wet scrubber pilot facilities in which the SO₂ removal efficiency of the pilot facility is always less than the full size unit it represents. The magnitude of this effect can be determined only by tests using a larger facility in which the gas flow area associated with the wall is much smaller than the total gas flow area.

Particle Removal

At full load, the particle removal efficiency of the IFGT process exceeded goals. The overall removal efficiency depends on the particle size distribution of the fly ash entering the IFGT

system. Removal efficiency for particulate greater than 2.5 microns averaged 98%. More significantly, the removal efficiency for particulate smaller than 2.5 microns averaged 76%. These fine particulate, referred to as PM_{2.5}, will be regulated in the near future, and while the exact nature of the regulations are not yet defined, the IFGT process provides the capability to address these forthcoming regulations. The test data show that while the removal efficiency is dependent on the size distribution of the coal, it is otherwise independent of coal type.

Particle removal was achieved at an inlet particle loading up to 800 mg/dscm. For a typical utility coal-fired boiler this represents about 10% to 15% of the fly ash removed by particulate clean-up devices. Higher particulate loading is possible, but the point at which high particle loading affects the performance (removal efficiency or cleaning) of the IFGT has not been determined. Although the IFGT process may not be capable of handling the full particulate loading from a boiler, it can provide relief from operational problems and upsets associated with particle removal devices. In the case of an ESP, the IFGT could augment or replace some of the particulate removal capability of the ESP. In the case of a bag house, an IFGT could accommodate an increase in particulate loading due to damaged bags, providing more flexibility to plant operation.

The IFGT system was operated at particle loading up to 800 mg/dscm without problems in handling or disposing of the particulate from the system. The fly ash retained on the heat exchanger tubes was easily rinsed by increasing the flow rate of rinse water above the design value of about 60 l/min.-m² (1.5 gpm/ft²). The design value is based on experience with oil and gas-fired units, and the increase in flow needed for the higher loading of coal fly ash is expected.

Mercury

The goal for vapor phase mercury removal of 90% was not achieved. Measured removal efficiencies for vapor phase mercury ranged from +69% to -23% and was significantly dependent on relative amounts of ionic and elemental mercury. Ionic mercury removal ranged from 75 to 85%. There was no measurable removal of elemental mercury. In fact, some tests indicated an increase in elemental mercury across the IFGT. This result could be an artifact of sampling techniques or could be caused by reduction of ionic mercury in the aqueous phase and subsequent evolution of elemental mercury.

The inability to remove elemental mercury in the IFGT system indicates that flue gas temperature is not a significant factor in the removal of this specie. The flue gas temperatures in the IFGT were about 15°C (27°F) cooler than in wet FGD systems, while the measured removal efficiencies closely parallel results obtained in other studies.

Ionic mercury removal was essentially the same for all tests, and no clear trend with operating condition over the range tested was evident. If the effects of operating conditions are small, they could easily be masked by the overall accuracy of the measurements. The removal efficiency for ionic mercury parallels that obtained in conventional wet FGD systems that operate with different scrubbing chemistry, pH and L/G.

Full-load particulate mercury removal ranged from 55% to 80%. This is less than the total particle removal efficiency. The cause of the difference is the enrichment of mercury in the fine particulate and the fact that the fine particulate removal for the IFGT is less than the overall removal.

Chloride and Fluoride

The goals for chloride and fluoride removal from the flue gas were met with the IFGT system. Except for one outlier (Test I-4A) the chloride removal averaged 98.2% over all tests. Fluoride removal ranged from 83% to 99% for the coals and operating conditions tested. Chloride and fluoride compounds tend to be highly soluble in aqueous solutions and the high measured removal efficiencies were expected.

NO_x

NO_x removal measured in test series I averaged essentially 0%, and so these measurements were suspended for the balance of the tests. Either the sodium reagent was not effective at removing the NO₂, or the NO₂ component of total NO_x was too small to detect any change in concentration of total NO_x.

Ammonia

Ammonia removal ranged from 50% to 90% depending primarily on the scrubbing solution pH, dissolved solids, and the flue gas outlet temperature. Although there are no Federal regulations for ammonia removal, state and local emissions limits typically range from 2 to 10 ppm. The IFGT can effectively remove ammonia to these concentrations, thereby providing the means to more completely remove NO_x with SCR and SNCR systems.

Trace Elements

The test data showed that arsenic and selenium were the only vapor phase trace metals that were consistently detected. Other elements were occasionally detected in reportable quantities but measurement repeatability was poor. The removal efficiencies for arsenic and selenium averaged greater than 95%.

Heat Recovery

Heat recovery averaged 5.0% of furnace heat release with an inlet flue gas temperature of 120°C (250°F), an outlet flue gas temperature of 35°C (95°F) and a cooling water inlet temperature of 30°C (86°F). At these conditions the outlet flue gas temperature is at or above the water vapor dew point and all of the heat recovery is in the form of sensible heat. For inlet flue gas temperatures of 150°C (300°F), which is more typical for back-end gas cleanup, the heat recovery would increase to 6% of the furnace heat release.

For utility power plants, the amount of useable heat that can be recovered from the flue gas will depend on the temperature at which heat is rejected in the power cycle. Typically, this is higher

than the 30°C used in this test, and is closer to 60°C. With this restriction the energy that can be recovered into the power cycle is reduced to about 3% of the furnace heat release.

This energy recovery is significantly less than the 8% to 12% that can be recovered in gas- and oil-fired industrial processes. In industrial processes the cooling water temperature can be as low as 10°C (50°F), the flue gas temperature in excess of 175°C (350°F) and the water vapor dew-point temperature near 60°C (140°F). Still, a 3% energy recovery can provide a 1% increase in generated electricity. For a 100 MW plant this is equivalent to approximately \$.5 million per year. This improvement in efficiency can partially offset the operating cost of the IFGT equipment. **No other commercial flue gas treatment equipment can offer this economic benefit.**

Based on the results of the Task 2 testing we can conclude that the overall objectives of Phase I, Task 2 have been met. Specifically,

- The pollutant removal performance of the IFGT process for pollutants that are currently regulated, or for which regulations are being considered, have been characterized for a range of operating conditions and for a range of coal types.
- Most of the pollutant removal goals for the IFGT process were demonstrated. Removal of vapor phase mercury, and the elemental form of mercury in particular was less than originally expected, but in general agreement with data for other types of flue gas treatment equipment.
- Tests with calcium-based reagents have shown that they are a feasible alternative to sodium reagent for low sulfur coals. Process modifications to permit higher L/Gs or greater dissolved alkalinity in the reagent will likely provide 90%+ SO₂ removal for higher sulfur coals.
- The increase in SO₂ transfer units with L/G for both soda ash and calcium reagents was less than expected, and indicates a possible mal-distribution between the liquid scrubbing solution and the flue gas. This mal-distribution is most likely associated with the region near the walls of the second-stage heat exchanger. This type of wall effect is common in small pilot-scale facilities. Larger test facilities provide performance results more representative of commercial scale equipment.
- The IFGT is an effective particulate removal device, removing over 98% of particulate greater than 2.5 microns and 76% of particulate smaller than 2.5 microns. The removal of the fine particulate is especially important in view of impending regulations on PM 2.5.
- The IFGT is effective at removing vapor phase selenium and arsenic, the only trace elements that were repeatably measured in significant quantities in the flue gas.
- The operating temperatures and water vapor content of the flue gas for utility power boilers will typically limit heat recovery to about 3% of the boiler heat release. This

heat recovery can increase plant efficiency, providing a substantial economic benefit and reducing emission of pollutants on the basis of energy produced.

- The Integrated Flue Gas Treatment process successfully removes multiple pollutants (SO₂, HCl, HF, particulate, ammonia, arsenic, selenium, and mercury) in a single device.

7.0 REFERENCES

- 1 - Fogiel, M., "The Essentials of Transport Phenomena II", The Research and Education Association, 1987.
- 2 - Holman, J.P., "Heat Transfer - Fourth Edition", Mcgraw Hill, 1976.
- 3 - Johnson, J. W., "A Computer-Based Cascade Impactor Data Reduction System", Southern Research Institute, March 1978, EPA-600/7-78-042.
- 4 - U.S. Geological Survey Coal Quality (COALQUAL) Database: Version 1.3, OPEN FILE-REPORT 94-205, 1994.
- 5 - EPRI, Electric Utility Trace Substances Synthesis Report - Volume 3", EPRI TR-104614-V3, 1994.
- 6 - Peterson, J.R., et al, "Mercury Emissions Control By Wet FGD Systems: EPRI Pilot-Scale Results", EPRI, DOE, EPA 1995 SO₂ Control Symposium.
- 7 - Sloss, L.L., "Mercury Emissions and Effects - The Role of Coal", IEA Coal Research Report ISBN 92-9029-258-X, 1995.

8.0 BIBLIOGRAPHY

Danckwerts, P.V., "Gas-Liquid Reactions", McGraw-Hill, 1970.

Jarvis, J.B., et al, "The Effect of High total Dissolved Solids on Wet Lime-Limestone Flue Gas Desulfurization Systems", EPRI TR-100242, 1991.

Zemaitis, J.F., et al, "Handbook of Aqueous Electrolyte Thermodynamics", AICHE, 1986.

9.0 LIST OF ACRONYMS AND ABBREVIATIONS

ARC	Alliance Research Center
B&W Inc.	Babcock and Wilcox Inc.
CHX [®]	Condensing Heat Exchanger (trademarked product name)
ECTC	Environmental Control Technology Center
EPRI	Electric Power Research Institute
FGD	Flue gas desulfurization
IFGT	Integrated flue gas treatment (trademarked product name)
MTI	McDermott Technology Inc.
USDOE	United States Department of Energy
USEPA	United States Environmental Protection Agency

APPENDIX A

DETAILED FACILITY AND INSTRUMENTATION

DETAILED FACILITY AND INSTRUMENTATION

Facility Description

The IFGT is essentially a two-pass counter flow shell and tube heat exchanger - see Figure A.1. The hot flue gas enters at the top and flows downward through the first cooling stage, across a horizontal transition, and then upward through the second cooling stage. The first cooling stage consists of 56 rows of Teflon[®]-covered tubes with 6 tubes in each row. The water flow path through the tubes is counter flow to the gas path. The second cooling stage consists of 64 rows of Teflon[®]-covered tubes.

Each tube in the IFGT system is covered with Teflon[®], which is extruded over the outside of the tube. Since Teflon[®] is hydrophobic, condensation on the surface of the tube occurs in drops rather than as a film. This allows continuous exposure of most of the surface and improves heat transfer. Teflon[®] is also durable and resistant to abrasion by solid particles in the gas. The inside surfaces of the heat exchanger shell are covered with Teflon[®] sheets. During fabrication, the Teflon[®]-covered tubes are pushed through the Teflon[®] tube sheet lining to form a Teflon[®]/Teflon[®] seal, ensuring that all heat exchanger surfaces exposed to the flue gas are protected against acid corrosion. Interconnections between the heat exchanger tubes are made outside the tube sheet and are not exposed to the corrosive flue gas stream.

There are four major sections of the IFGT; the first heat exchanger stage, the inter-stage transition region, the second heat exchanger stage, and the mist eliminator. Most of the sensible heat is removed from the flue gas in the first heat exchanger stage of the IFGT. Condensation can occur within the first heat exchanger stage if the gas temperature at the tube surface is below the dew point. Some flue gas pollutant removal can occur within the first heat exchanger as the particulate impact the tubes and acid gas condensation occurs.

The inter-stage transition provides a gas flow path between the two heat exchanger stages and also acts as a collection sump for reagent/condensate. The transition is equipped with water spray nozzles that can be used to assist in removing pollutants from the flue gas. The transition piece is made of corrosion resistant fiberglass-reinforced plastic.

The second heat exchanger stage is usually operated in the condensing mode, removing both latent and sensible heat from the gas along with pollutants. The flue gas in this stage is flowing upward while the liquid droplets in the gas fall downward. This provides a scrubbing mechanism that enhances particulate and pollutant capture. The dimensions and spacing of the heat exchanger tubes ensure that the larger particulate impact the wet tubes where droplet condensation is taking place. Sub-micron size particles act as condensation sites in the gas and are collected in the condensate stream. The top of the second heat exchanger stage is equipped with an alkali reagent spray system to enhance SO₂ removal. The condensed gases, particulate, and reacted alkali reagent are collected in the transition section. The condensate/alkali reagent solution is recirculated to the spray system to improve the efficiency of the process.

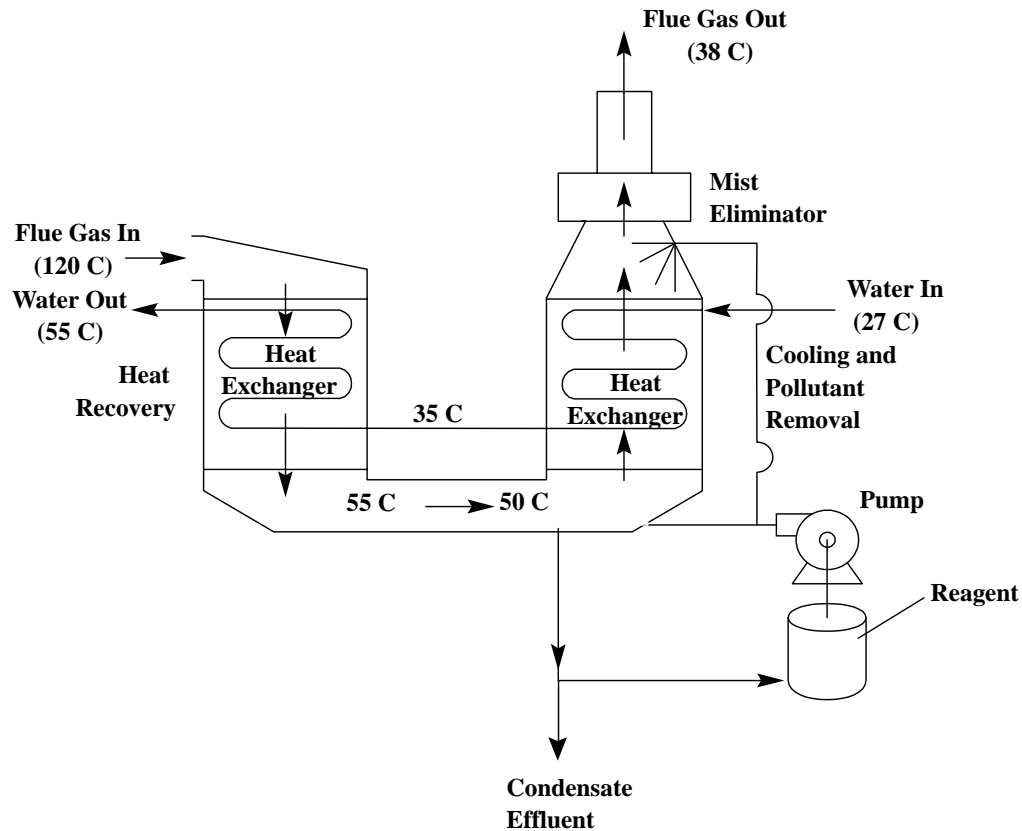


Figure A.1 Process Flow Schematic of the Pilot IFGT Condensing Heat Exchanger

The flue gas outlet of the IFGT system is equipped with a mist eliminator to reduce moisture carryover. The spray/disengagement region consists of three plastic sections installed above the second heat exchanger stage. Each section is about 18 inches in height. The plastic sections contain the second-stage reagent spray nozzles and chevron style mist eliminators. They also provide a disengagement zone for liquid drops entrained in the flue gas as it exits the second heat exchanger stage.

An alkali reagent tank is used to provide the alkali spray for the SO_2 removal tests. Dry powdered reagent is added to the water in the tank either manually or with a feeder controlled by the pH controller. A mixer stirs the solution in the tank to disperse and dissolve the reagent. The spent reagent and condensate collected at the bottom of the transition piece during operation is gravity fed to the reagent tank. The reagent tank is equipped with an overflow drain to accommodate the increase in water/reagent inventory from condensation and the addition of makeup water. Approximately 300 lb/hr of makeup water is added to the system to maintain the reagent feed liquor below 15% dissolved solids.

The reagent spray can be directed to the top of the second stage heat exchanger or to the transition section. The fiberglass transition piece located between the two heat exchanger stages is equipped with six spray nozzles. The six nozzles are aimed to direct the sprays horizontally into the transition region:

- Four spray nozzles are located on the sidewalls. One pair is located on opposite sidewalls directly under the first heat exchanger stage and the other pair is located about midway between the two heat exchanger stages.
- The other two spray nozzles are located in opposite ends of the transition piece. One nozzle is located directly under the first heat exchanger stage and directs the spray in the direction of the gas flow. The second nozzle is located directly below the second heat exchanger stage, with the spray directed against the gas flow stream.

Duct work is installed to bring the exhaust gas from the SBS to the pilot IFGT. The 12-inch insulated duct is tied into the exhaust of the SBS downstream of the baghouse and I.D. fan. The flue gas enters at the top of the first heat exchanger stage and exits out the top of the second heat exchanger stage. A 12-inch non-insulated PVC duct is installed at the exit of the pilot IFGT to an exhaust stack located outside the building.

Gas sampling lines and 4-inch ports for in-situ sampling are located at the inlet and outlet of the IFGT facility. The gas sample lines are used to continuously withdraw flue gas for the on-line gas sample analyzers. One gas sample line is located in the inlet duct just upstream of the first heat exchanger stage. The other gas sample line is located in the PVC outlet duct. Heat-traced lines are used to transport the flue gas samples from the ducts to the gas analyzers. Two four-inch ports are installed both in the inlet and in the outlet flue gas ducts for particulate sampling and other gas sampling as required by the test.

Instrumentation

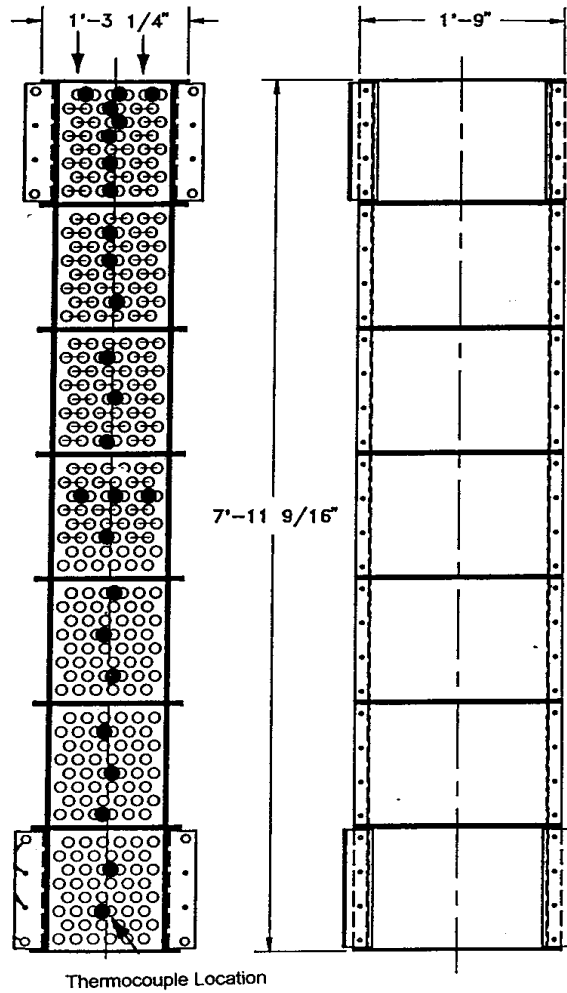
The IFGT facility is equipped with instrumentation to measure process operating conditions including flow rate, temperature, pressure, pH, and flue gas species such as SO₂, O₂, and NO_x. The major process streams are:

- Inlet flue gas
- Makeup water
- Reagent addition to reagent tank
- Inlet cooling water
- Reagent feed to IFGT second stage
- Cooling water to second stage
- Reagent return from IFGT second stage to reagent tank
- Blowdown
- Outlet flue gas
- Outlet cooling water

Most of the IFGT facility operating data was obtained by a computerized data acquisition system. B&W utilized a PC-based computerized Data Acquisition System (DAS) using a Labview platform to monitor and record all instrumentation with an electronic signal output. Table A.1 contains a list of facility monitoring instrumentation used in Task 2. The DAS data was collected and stored for later data reduction approximately every 15 seconds during short-term SO₂ testing and approximately every minute during long-term EPA methods testing. Some of the data, such as ammonia flow rate, and gas side pressure drop was manually recorded.

Temperature data was continuously collected to measure the heat exchanger tubeside water temperature profiles. Figure A.2 shows the location of 26 thermocouples that are connected to the first-stage heat exchanger water tubes. Figure A.3 shows the location of 19 thermocouples placed on the second-stage heat exchanger water tubes. The specific thermocouple locations were chosen after reviewing previous temperature profile measurements in an effort to better measure the vertical temperature profile and the side-to-side water temperature distribution.

This project utilized the R&DD's ISO 9001 Standard Practice Quality Assurance (QA) system. This QA system required that all measuring and test equipment used on this project must be certified or calibrated before and after use to ensure that measurements made are accurate and reproducible in terms of nationally recognized standards. A certified measurement indicates that the performance of the instrument used was documented at predetermined intervals before and after the measurement was obtained. Generally, a certified instruments examination interval is on the order of one year. "Calibrate Before Use" equipment generally requires frequent calibration to an external standard. This equipment has relatively short stability and may require calibration daily. An example of "Calibrate Before Use" equipment used in this project are the reagent feed and reagent return pH transmitters. These instruments were checked, at a minimum, against buffers at the beginning and end of each test day. Other "Calibrate Before Use" instruments such as the inlet and outlet SO₂ flue gas analyzers were checked against calibration gases periodically throughout the test day. The data collected by the SO₂ gas analyzers were corrected of any detected instrument drift.



1st Stage, North Side

Figure A.2 Location Of Thermocouples On The Stage 1 Heat Exchanger

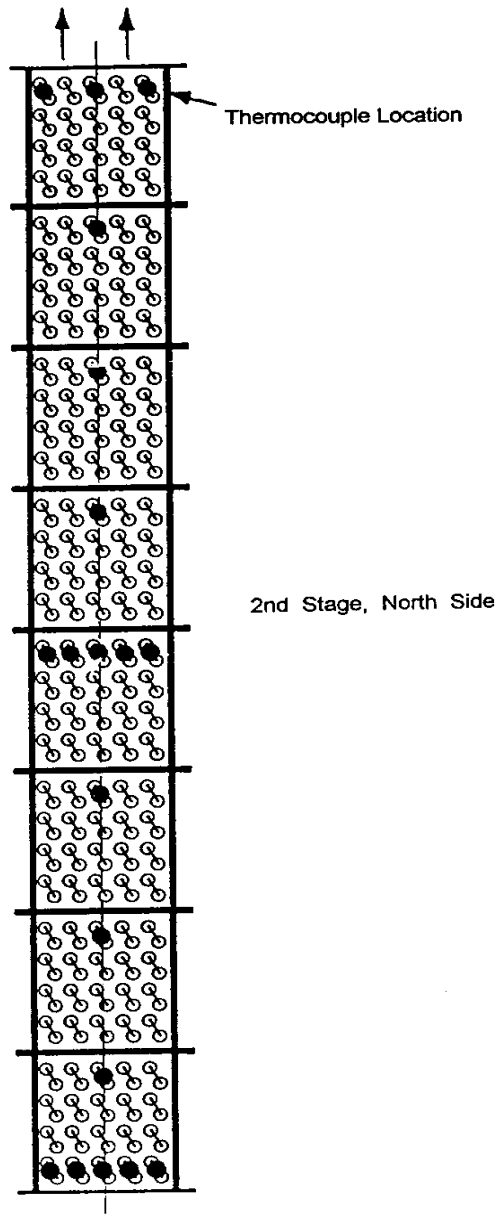


Figure A.3 Location Of Thermocouples On The Stage 2 Heat Exchanger

Table A.1 IFGT Continuous Monitoring Instrumentation List

MEASUREMENT	Type	Units	Method
1st Stage Differential Pressure	Manometer	inches H ₂ O	Manual
1st Stage Inlet Static Pressure	Manometer	inches H ₂ O	Manual
2nd Stage Differential Pressure	Manometer	inches H ₂ O	Manual
2nd Stage Outlet Static Pressure	Manometer	inches H ₂ O	Manual
Ammonia Flow Rate	Rotameter	lb/hr	Manual
Ammonia Flow Temperature	TC - Type K	°F	Manual
Barometric Pressure (Outside)	Electronic	inches Hg	DAS
Cooling Water Flow Rate	Coriolis - Flow	lb/hr	DAS
Cooling Water Inlet Temperature	TC - Type K	°F	DAS
Cooling Water Interstage Temperature	TC - Type K	°F	DAS
Cooling Water Outlet Temperature	TC - Type K	°F	DAS
Flue Gas NH ₃ Conc. at Inlet/Outlet	Electrolytic	ppm _v	DAS
Flue Gas NO _x Conc. At Inlet	Chemolumin	ppm _v	DAS
Flue Gas NO _x Conc. At Outlet	Chemolumin	ppm _v	DAS
Flue Gas O ₂ Conc. At Inlet	Fuel Cell	ppm _v	DAS
Flue Gas O ₂ Conc. At Outlet	Fuel Cell	ppm _v	DAS
Flue Gas SO ₂ Conc. At Inlet	Ultraviolet	ppm _v	DAS
Flue Gas SO ₂ Conc. At Outlet	Ultraviolet	ppm _v	DAS
Gas Flow Orifice Differential Pressure	Manometer	inches H ₂ O	Manual
Gas Flow Orifice Differential Pressure	Press. XMTR	inches H ₂ O	DAS
Gas Flow Orifice Gage Pressure	Manometer	inches H ₂ O	DAS
Gas Flow Orifice Static Pressure	Press. XMTR	inches H ₂ O	DAS
Gas Flow Orifice Temperature	TC - Type K	°F	DAS
Gas Temperature Tdry @ Module 1 out	TC - Type K	°F	DAS
Gas Temperature Twet @ Module 1 out	TC - Type K	°F	DAS
Gas Temperature @ Inlet To Analyzers	TC - Type K	°F	DAS
Gas Temperature @ Module 1 Inlet	TC - Type K	°F	DAS
Gas Temperature @ Module 1 Outlet	TC - Type K	°F	DAS
Gas Temperature @ Module 2 Inlet	TC - Type K	°F	DAS
Gas Temperature @ Module 2 Outlet	TC - Type K	°F	DAS
Gas Temperature @ Outlet Flue	TC - Type K	°F	DAS
Makeup Water Flow Rate	Coriolis - Flow	lb/hr	DAS
pH Buffer Temperature	TC - Type K	°F	DAS
Reagent Blowdown Flow Rate	Coriolis - Flow	lb/hr	DAS
Reagent Flow Density (Micromotion)	Coriolis-density	lb/lb	DAS
Reagent Flow Rate	Coriolis - Flow	lb/hr	DAS
Reagent Nozzle Pressure - Top Spray	Press.-Gage	lb/in ² gage	Manual
Reagent Nozzle Pressure - Transition	Press.-Gage	lb/in ² gage	Manual
Reagent Return pH	Ag/AgCl ₂	-LOG[H+ ACT]	DAS
Reagent Return Temperature	TC - Type K	°F	DAS
Reagent Return Temperature (Micromotion)	RTD - Platinum	°F	DAS
Reagent Supply Ph	Ag/AgCl ₂	-LOG[H+ ACT]	DAS
Room Temperature	TC - Type K	°F	DAS
Steam Plenum Pressure	Pres.-Gage	lb/in ² gage	Manual
Steam Temperature	TC - Type K	°F	DAS

Table A.1 Continued

MEASUREMENT	Type	Units	Method
TC @ Tube Row 01A -Stage 2	TC - Type K	°F	DAS
TC @ Tube Row 01B -Stage 2	TC - Type K	°F	DAS
TC @ Tube Row 01C -Stage 2	TC - Type K	°F	DAS
TC @ Tube Row 01D -Stage 2	TC - Type K	°F	DAS
TC @ Tube Row 01E -Stage 2	TC - Type K	°F	DAS
TC @ Tube Row 03 -Stage 1	TC - Type K	°F	DAS
TC @ Tube Row 06 -Stage 1	TC - Type K	°F	DAS
TC @ Tube Row 07 -Stage 2	TC - Type K	°F	DAS
TC @ Tube Row 09 -Stage 1	TC - Type K	°F	DAS
TC @ Tube Row 12 -Stage 1	TC - Type K	°F	DAS
TC @ Tube Row 15 -Stage 1	TC - Type K	°F	DAS
TC @ Tube Row 15 -Stage 2	TC - Type K	°F	DAS
TC @ Tube Row 18 -Stage 1	TC - Type K	°F	DAS
TC @ Tube Row 21 -Stage 1	TC - Type K	°F	DAS
TC @ Tube Row 23 -Stage 2	TC - Type K	°F	DAS
TC @ Tube Row 24 -Stage 1	TC - Type K	°F	DAS
TC @ Tube Row 27 -Stage 1	TC - Type K	°F	DAS
TC @ Tube Row 30C -Stage 1	TC - Type K	°F	DAS
TC @ Tube Row 30E -Stage 1	TC - Type K	°F	DAS
TC @ Tube Row 30W -Stage 1	TC - Type K	°F	DAS
TC @ Tube Row 31A -Stage 2	TC - Type K	°F	DAS
TC @ Tube Row 31B -Stage 2	TC - Type K	°F	DAS
TC @ Tube Row 31C -Stage 2	TC - Type K	°F	DAS
TC @ Tube Row 31D -Stage 2	TC - Type K	°F	DAS
TC @ Tube Row 31E -Stage 2	TC - Type K	°F	DAS
TC @ Tube Row 33 -Stage 1	TC - Type K	°F	DAS
TC @ Tube Row 36 -Stage 1	TC - Type K	°F	DAS
TC @ Tube Row 39 -Stage 1	TC - Type K	°F	DAS
TC @ Tube Row 39 -Stage 2	TC - Type K	°F	DAS
TC @ Tube Row 42 -Stage 1	TC - Type K	°F	DAS
TC @ Tube Row 45 -Stage 1	TC - Type K	°F	DAS
TC @ Tube Row 47 -Stage 1	TC - Type K	°F	DAS
TC @ Tube Row 47 -Stage 2	TC - Type K	°F	DAS
TC @ Tube Row 49 -Stage 1	TC - Type K	°F	DAS
TC @ Tube Row 51 -Stage 1	TC - Type K	°F	DAS
TC @ Tube Row 53 -Stage 1	TC - Type K	°F	DAS
TC @ Tube Row 54 -Stage 1	TC - Type K	°F	DAS
TC @ Tube Row 55 -Stage 1	TC - Type K	°F	DAS
TC @ Tube Row 55 -Stage 2	TC - Type K	°F	DAS
TC @ Tube Row 56C -Stage 1	TC - Type K	°F	DAS
TC @ Tube Row 56E -Stage 1	TC - Type K	°F	DAS
TC @ Tube Row 56W -Stage 1	TC - Type K	°F	DAS
TC @ Tube Row 63A -Stage 2	TC - Type K	°F	DAS
TC @ Tube Row 63C -Stage 2	TC - Type K	°F	DAS
TC @ Tube Row 63E -Stage 2	TC - Type K	°F	DAS
Transmitter Power Supply Volts	Volts	Volts	DAS

APPENDIX B

DETAILED ANALYSIS METHODS

DETAILED ANALYSIS METHODS

This appendix describes the analytical methods for the determination of elements and compounds present in the IFGT process streams. All of the analytical methods were completed at ARC by MTI personnel. During the test program, various solid and liquid samples were obtained and analyzed to compliment the operating data acquired by the data acquisition system. Solid samples originated from process streams. Liquid samples either originated from process streams, or were generated as impinger solutions from EPA methods testing for mercury and heavy metals. Table B.1 provides the appropriate method of sample acquisition and the method reference.

Before analyses could be performed, most of the samples required some type of sample preparation. The applicable procedures for sample preparation are listed in Table B.2. The mercury and trace metals sampling and analytical techniques selected are those either approved or recommended by the EPA. The applicable detection limits of mercury and heavy metals in the MTI laboratory are listed in Table B.3. Tables B.4, B.5, and B.6 outline the analytical methods to be employed for solid streams (coal, ash, and reagent), flue gas impingers and liquid process streams. Table B.7 summarizes the standard analytical methods used to characterize the coal stream.

Mercury Speciation Measurement

When the project began, EPA Method 29 was the only draft method used. The EPA subsequently finalized the method (dated October, 1996) with essentially no significant revisions. MTI personnel utilized EPA Method 29 with only minor deviations to the stepwise procedures. For example, in Section 5.2.8 the solutions collected in impingers 1, 2, and 3 are collected in a graduated cylinder, and the collected quantity is measured to within 0.5 ml using the graduated cylinder. For these tests, the amount of liquid collected in impingers was collected in a graduated cylinder but measured by weight on a 2 place balance, not by volume in a graduated cylinder.

The U.S. DOE and EPRI are sponsoring efforts to evaluate various measurement techniques for quantifying the relative amount of elemental and non-elemental or oxidized forms of mercury in the flue gas.^[B1] The various techniques can be generally classified as impinger-train or solid-sorption based methods. The on-going work is currently focusing on two impinger train methods - the TRIS buffer method and the Ontario Hydro Method. All of the mercury speciation methods continue to evolve as more field and laboratory experience is gained. There is currently no USEPA validated method for measuring individual mercury species in flue gas.

EPA Method 29 is a validated method for measuring total mercury emissions and is used as a benchmark for comparison of alternative speciation methods. Much of the early field mercury emissions testing was performed using EPA Method 29. However, the method has been shown to report a significant fraction of the elemental mercury as oxidized mercury.^[B1]

B1 - "A State-of-the-Art Review of Flue Gas Mercury Speciation Methods," Energy & Environmental Research Center, EPRI Report No. TR-107080, October, 1996.

Table B.1 IFGT Sampling Methods

Sampling Methods	
Target Substance	Method
Impinger Liquids	
Metals	Draft EPA Method 29
Chloride, Fluoride	EPA Method 26A
Process Liquids	EPRI Method A1
Process Solids	
Coal	ASTM D - 197
Particulate	EPA Method 5 & Anderson Mark III
Reagent	Grab/Composite

Table B.2 IFGT Sample Preparation Techniques

Analytes	Matrix	Preparation Technique	Method Reference
Metals	Coal	Microwave Digestion	ASTM E926-88
Mercury	Coal	Oxygen Bomb	ASTM D3684-78
Chloride, Fluoride	Coal	Oxygen Bomb	ASTM D2361
Metals	Particulate	Microwave Digestion	ASTM E926-88
Mercury	Particulate	Acid Digestion	EPA 7471A
Chloride, Fluoride	Particulate	Acid Digestion	EPA SW3051
Metals	Na ₂ CO ₃	Microwave Digestion	ASTM C-25
Mercury	Na ₂ CO ₃	Acid Digestion	EPA 7471A
Chloride, Fluoride	Na ₂ CO ₃	Acid Digestion	EPA SW3051, mod
Metals	Solids	Microwave Digestion	ASTM E926-88
Mercury	Solids	Acid Digestion	EPA 7471A
Chloride, Fluoride	Solids	Acid Digestion	EPA SW3051, mod
Calcium, Magnesium	Solids	Acid Digestion	ASTM D1971
Metals (As, Se)	Liquid Streams	Acid Digestion	EPA SW3020
Metals (Other)	Liquid Streams	Microwave Digestion	EPA SW3010
Mercury	Liquid Streams	Acid Digestion	EPA 3015
Chloride, Fluoride	Liquid Streams	None	ASTM D2361

Table B.3 Mercury and Heavy Metals Sampling Detection Limits

Heavy Metals

Element	Vapor Phase Limits	Particle Phase Limits	Coal
	(ug/dscm)	(ug/dscm)	(ppm)
Arsenic	0.117	0.064	0.20
Barium	1.173	0.643	2.00
Beryllium	0.059	0.439	0.10
Cadmium	0.012	0.026	0.02
Chromium	0.117	0.064	0.40
Cobalt	0.235	0.161	0.20
Lead	0.117	0.142	0.20
Manganese	0.117	0.101	0.40
Nickel	0.235	0.161	0.20
Selenium	0.117	0.142	0.20

Mercury

Mercury Form	(ug/dscm)
Ionic Vapor Phase	0.02
Elemental Vapor Phase	0.20
Total Vapor Phase	0.22
Particle Phase	0.01
Total mercury	0.23
Mercury in the Coal	2.66

Table B.4 Analytical Methods for Solid Streams

Analytes	Analytical Method	Method Title
Ba, Be, Cd, Cr, Co, Mn, Ni, Pb	GFAAS	Graphite Furnace Atomic Absorption Spectroscopy
As, Se	HGAAS	Hydride Generation Atomic Absorption Spectroscopy
Hg (Coal)	CVAAS ASTM D364-78	Standard Method for Total Mercury in Coal by Oxygen Bomb/Cold Vapor Atomic Absorption Spectroscopy
Hg (Others)	CVAAS SW7471/SW846	Mercury in Solids or Semi Solids Waste/Cold Vapor Atomic Absorption Spectroscopy
Calcium	FAAS	Flame Atomic Absorption Spectroscopy
Magnesium	FAAS	Flame Atomic Absorption Spectroscopy
Sodium	FAAS	Flame Atomic Absorption Spectroscopy
Alkalinity	Titrimetric	EPRI N3
Chloride (Coal)	Oxygen Bomb,	ASTM D4208-88
Fluoride (Coal)	Oxygen Bomb,	ASTM D3761-91
Chloride (Others)	IC	ASTM D4327, modified
Fluoride (Others)	IC	ASTM D4327, modified
Carbon (Coal)	Gravimetric	ASTM D3178-89

Others - Ash, Reagent, Solids

Table B.5 Analytical Methods for Flue Gas Impingers

Analytes	Analytical Method	Method Reference
Ba, Be, Cd, Cr, Co, Mn, Ni, Pb, As	GFAAS	Graphite Furnace Atomic Absorption Spectroscopy
Se	HGAAS	Hydride Generation Atomic Absorption Spectroscopy
Hg, Elemental	CVAAS	Cold Vapor Atomic Absorption Spectroscopy
Hg, Ionic	CVAAS	Cold Vapor Atomic Absorption Spectroscopy
Chloride, Fluoride	IC	Ion Chromatography

Table B.6 Analytical Methods for Liquid Process Streams

Analytes	Analytical Method	Method Reference
Ba, Be, Cd, Cr, Co, Mn, Ni, Pb	GFAAS	Graphite Furnace Atomic Absorption Spectroscopy
As, Se	HGAAS	Hydride Generation Atomic Absorption Spectroscopy
Hg, Total	CVAAS	Cold Vapor Atomic Absorption Spectroscopy
Chloride, Fluoride	IC	Ion Chromatography

Table B.7 Coal Analytical Methods

Analytes	Analytical Method	Method Reference
Moisture	Gravimetric	ASTM D3173-87
Heating Value	Calorimetry	ASTM D2015-19
Ultimate Analysis		
C, H	Gravimetric	ASTM 3178-89
S	Instrumental	ASTM D4239-85, Method C
N	Titrimetric	ASTM 3179-89
Ash	Gravimetric	ASTM 3179-89

The IFGT program has focused on the use of EPA Method 29 and the Ontario Hydro Method for quantifying the total amount of mercury in the flue gas and obtaining a relative measure of the distribution of mercury species. EPA Method 29 also provides quantitative measurement of a number of other trace metals.

EPA Method 29

In EPA Method 29 (Multiple Metals Train), a flue gas sample is withdrawn isokinetically from the process using a glass nozzle and glass lined probe arrangement following the specifications in EPA Method 5. The flue gas is drawn through a glass fiber filter which traps the particulates. The probe and filter are maintained at 120°C (250°F). The gas then passes through a series of impingers containing solutions which absorb mercury and other vapor phase trace elements from the flue gas. The impingers are placed in an ice bath to condense water vapor from the flue gas. The impinger arrangement used is summarized in Table B.8. The flue gas is pulled through a dry gas meter following the impingers to measure the total gas sample volume.

Following a sampling period of two to four hours, the impinger solutions are recovered, digested and analyzed for the various elements. The appropriate fractions are analyzed for mercury using cold vapor atomic absorption spectroscopy (CVAAS). Atomic absorption spectroscopy or inductively coupled plasma (ICP) is used for analysis of the other trace element metals.

Table B.8 EPA Method 29 Impinger Sample Train

Impingers	Initial Impinger Set-up	Purpose
1	Empty	Water vapor condensation
2&3	5% HNO ₃ /10% H ₂ O ₂ (100 ml)	Trace metals collection and SO ₂ neutralization
4	Empty	Separate absorbing solutions
5&6	4% KMnO ₄ /10% H ₂ SO ₄ (100 ml)	Mercury collection
7	Silica gel (200-300 grams)	Final moisture trap

In the IFGT program, EPA Method 29 was selected as a total mercury reference in place of EPA Method 101A, due to concern over the impact of the high SO₂ concentration in the flue gas on the permanganate impingers. SO₂ depletes the permanganate which can result in low mercury capture in the impingers. With EPA Method 29, the peroxide impingers protect the permanganate impingers by removing SO₂ from the flue gas.

EPA Method 29 provides only a general indication of mercury speciation. Oxidized forms of mercury are collected in the HNO₃/H₂O₂ impingers. However, this solution also oxidizes and captures some of the elemental mercury in the flue gas as it bubbles through the impingers. Mercury measured in the combined solutions recovered from impingers 1, 2 and 3 is considered to be oxidized mercury. Mercury in the solution recovered from impinger 4 is also considered to be oxidized mercury. Mercury measured in the KMnO₄/H₂SO₄ impinger solutions and an 8N HCl rinse of impingers 5 and 6 is considered to be elemental mercury. In general, EPA Method 29 under reports the amount of elemental mercury in the flue gas and overstates the amount of oxidized mercury.

Ontario Hydro Method

The Ontario Hydro Method is a modification of EPA Method 29 in which an alternative reagent is used in the initial impingers to prevent the oxidation of elemental mercury. This method uses the same basic hardware as EPA Method 29. The initial impinger solution set-up is summarized in Table B.9.

Table B.9 Ontario Hydro Method Impinger Sample Train

Impingers	Initial Impinger Set-up	Purpose
1&2	1 N KCl (150 ml)	Oxidized mercury collection
3	5% HNO ₃ /10% H ₂ O ₂ (150 ml)	SO ₂ neutralization
4	Empty	Separate absorbing solutions
5&6	4% KMnO ₄ /10% H ₂ SO ₄ (150 ml)	Elemental mercury collection
7	Silica gel (200-300 grams)	Final moisture trap

The solutions recovered from impingers 1 and 2 are combined and stabilized with either dichromate or KMnO₄ to prevent loss of mercury in the analytical work-up procedure. The KCl is a non-oxidizing solution substituted for the HNO₃/H₂O₂ in EPA Method 29 to prevent oxidation of elemental mercury in the flue gas. Mercury measured in these solutions is reported as oxidized mercury. The solutions recovered from impinger 3 and impinger 4 are analyzed for mercury separately and the mercury is considered to have been in the elemental state in the flue gas. The solutions recovered from impingers 5 and 6 are combined for analysis and the mercury content reported as elemental mercury.

In general, the total vapor phase mercury emissions measured by MTI with the Ontario Hydro Method have been lower than those measured with EPA Method 29. For the fourth test series, enhancements to the Ontario Hydro Method were included to address this concern. A KMnO₄/H₂SO₄ solution is added to the KCl impingers immediately following the post-sampling leak check of the impinger train. This stabilizing agent replaces the addition of dichromate in the impinger recovery procedure to prevent the loss of mercury from these impingers during the recovery procedure. This substitution is believed to improve the total mercury recovery using the Ontario Hydro Method.^[B1] It is now recommended that the quartz fiber particulate filter be maintained at the higher of flue gas temperature or a minimum of 120°C (250°F) in the heated filter box rather than 120°C (250°F) as prescribed by EPA Method 29. This temperature change avoids the potential for movement of mercury from the vapor phase to the particulate collected on the filter during the sampling period.

APPENDIX C

**TABULATED DATA FOR
TEST SERIES I, OHIO #5/#6 COAL**

Test Series	I
Fuel Analysis, wt. %	
Sample Number	C-22261
C	69.2
H ₂	5.0
S	3.9
O ₂	7.0
N ₂	1.4
H ₂ O	6.9
Cl, ppm	2200.0
F, ppm	25.8
Ash	6.7
Heating Value - wet basis (J/Kg)	29.14
Heating Value - dry basis (J/Kg)	31.31
Fd (dscm/J)	2.64E-07

Element	Coal Sample Element Concentration in ppm _m							
	C-22290	C-22292	C-22297	C-22298	Average	+ dev.	- dev	det limit
Arsenic	11.40	13.50	12.70	12.10	12.43	1.08	1.03	0.20
Barium	2.22	3.05	4.96	2.74	3.24	1.72	1.02	2.00
Beryllium	0.14	0.14	0.16	0.16	0.15	0.01	0.01	0.10
Cadmium	0.91	0.62	0.63	0.64	0.70	0.21	0.08	0.02
Cobalt	0.69	0.84	0.73	0.85	0.78	0.07	0.09	0.40
Chromium	10.80	45.30	52.50	77.70	46.58	31.13	35.78	0.20
Manganese	17.90	23.10	10.10	11.90	15.75	7.35	5.65	0.20
Nickel	7.74	25.50	23.60	31.60	22.11	9.49	14.37	0.40
Lead	6.82	6.17	5.42	4.43	5.71	1.11	1.28	0.20
Selenium	1.39	1.39	1.75	1.72	1.56	0.19	0.17	0.20
Mercury	0.45	0.48	0.41	0.39	0.43	0.05	0.04	0.02

Test Type		SO ₂	SO ₂	SO ₂	SO ₂	SO ₂	SO ₂	SO ₂	SO ₂	SO ₂
Test ID		I-1	I-11	I-2	I-12	I-13	I-13R	I-3	I-5	I-15
Date		02/08/96	02/13/96	02/08/96	02/13/96	02/12/96	02/13/96	02/08/96	02/13/96	02/13/96
Time		2:52 PM	11:40 AM	2:34 PM	10:54 AM	4:37 PM	10:13 AM	1:54 PM	1:07 PM	9:39 AM
Flue Gas Inlet										
Flow Rate	(kg/min)	39.5	38.1	38.9	37.5	37.8	36.8	38.6	34.9	35.3
Gas Velocity	(m/s)	12.9	12.6	12.7	12.4	12.3	12.2	12.6	11.4	11.6
Temperature	(°C)	123.5	124.8	123.8	124.6	123.6	123.3	124.2	124.4	122.0
O ₂ ⁽¹⁾	(%)	6.32	6.46	6.28	6.49	6.51	6.32	6.33	6.46	5.89
SO ₂ ⁽²⁾	(ppm _v)	2816	2547	2867	2560	2513	2604	2872	2585	2636
NO _x ⁽²⁾	(ppm _v)	572	440	577	482	469	526	389	473	509
Humidity	(gm/gm)	0.038	0.038	0.038	0.038	0.038	0.039	0.038	0.038	0.040
Flue Gas										
Interstage Temperature	(°C)	66.0	56.1	65.8	53.8	51.3	49.5	64.8	52.9	45.5
Outlet Temperature	(°C)	37.3	27.8	37.1	27.0	26.7	26.4	37.1	35.8	26.7
SO ₂ Removal	(%)	89.3	85.3	94.6	91.1	95.8	95.4	96.5	98.9	98.6
NO _x Removal	(%)	-0.84	1.60	-1.16	-2.38	0.91	5.26	-4.43	-3.56	1.20
Cooling Water										
Flow Rate	(kg/min)	34.0	33.5	34.1	33.8	34.1	33.6	33.9	33.3	33.4
Inlet Temperature	(°C)	28.2	6.3	28.2	6.2	6.4	6.1	28.7	27.0	6.2
Interstage Temperature	(°C)	36.7	25.6	36.6	25.0	24.9	24.8	36.6	35.1	24.1
Outlet Temperature	(°C)	51.3	44.6	51.5	44.2	42.0	44.1	51.2	49.0	43.2
Reagent										
L/G Ratio	(l/m ³)	0.062	0.093	0.111	0.146	0.264	0.269	0.285	1.057	1.110
Temperature	(°C)	40.5	38.1	40.4	36.5	34.7	33.8	39.0	37.5	30.5
Supply pH	(-)	7.88	7.84	7.64	7.84	8.03	7.81	7.96	8.02	7.84
Return pH	(-)	6.67	6.48	6.35	6.65	7.02	6.92	7.01	7.80	7.49
Fresh Water Flow	(kg/min)	2.13	1.45	1.61	1.45	1.52	1.35	2.59	2.25	2.01
Blow Down Flow	(kg/min)	1.67	2.24	1.91	2.69	2.25	2.86	2.84	3.09	3.24
Energy										
Stage 1 Recovery	(kw)	34.8	44.3	35.4	45.2	40.8	45.3	34.6	32.4	44.5
Stage 2 Recovery	(kw)	20.2	45.1	19.9	44.4	44.0	43.9	18.6	18.7	41.7
Overall Energy Balance	(%)	11.7	5.9	11.3	5.2	-0.6	5.0	8.8	4.3	5.7

1) Dry basis

2) Dry basis, corrected to 3% O₂

Test Type		SO ₂	SO ₂	SO ₂	SO ₂	SO ₂	SO ₂	SO ₂	SO ₂	SO ₂
Test ID		I-16	I-RTB1	I-17	I-RTB2	I-8	I-9	I-10	I-7	I-24
Date		02/02/96	02/02/96	02/02/96	02/06/96	02/13/96	02/13/96	02/13/96	02/13/96	02/14/96
Time		4:26 PM	3:49 PM	3:33 PM	11:39 AM	3:22 PM	2:15 PM	1:48 PM	4:17 PM	11:12 AM
Flue Gas Inlet										
Flow Rate	(kg/min)	39.6	38.9	38.4	37.0	18.6	18.5	18.5	18.1	19.6
Gas Velocity	(m/s)	12.6	12.3	12.2	11.7	6.2	6.2	6.2	6.1	6.6
Temperature	(°C)	122.1	122.3	122.4	124.0	114.3	114.1	114.5	115.8	120.1
O ₂ ⁽¹⁾	(%)	6.39	6.59	6.70	7.10	7.06	6.89	7.04	7.04	6.84
SO ₂ ⁽²⁾	(ppm _v)	3028	3019	3106	2554	2503	2538	2566	2679	2580
NO _x ⁽²⁾	(ppm _v)	N/A	N/A	N/A	N/A	434	446	456	493	485
Humidity	(gm/gm)	0.037	0.037	0.036	0.035	0.037	0.038	0.037	0.037	0.038
Flue Gas										
Interstage Temperature	(°C)	60.9	59.9	57.0	47.4	53.4	52.3	47.2	47.9	42.4
Outlet Temperature	(°C)	37.5	37.1	37.0	36.5	35.7	37.2	37.3	36.4	23.5
SO ₂ Removal	(%)	56.8	82.0	90.8	97.7	69.8	88.5	94.6	96.3	80.2
NO _x Removal	(%)	N/A	N/A	N/A	N/A	0.15	0.73	0.24	-1.47	1.71
Cooling Water										
Flow Rate	(kg/min)	35.3	35.1	35.1	33.9	17.7	16.8	16.8	17.4	16.6
Inlet Temperature	(°C)	33.3	32.8	33.2	32.8	31.5	34.8	35.1	32.6	7.2
Interstage Temperature	(°C)	36.8	36.8	36.8	36.2	36.1	37.3	37.2	35.9	24.2
Outlet Temperature	(°C)	51.8	51.8	51.7	52.7	49.2	51.1	51.3	48.8	45.4
Reagent										
L/G Ratio	(l/m ³)	0.055	0.122	0.268	0.843	0.248	0.627	1.072	2.203	0.415
Temperature	(°C)	37.2	37.8	37.6	29.3	37.4	37.8	37.8	36.8	30.7
Supply pH	(-)	6.90	6.86	6.71	6.85	7.96	7.89	8.04	8.01	6.95
Return pH	(-)	0.00	0.00	0.00	0.00	7.04	7.57	7.80	7.96	6.58
Fresh Water Flow	(kg/min)	1.33	1.34	1.33	2.25	1.01	0.99	1.00	1.57	0.51
Blow Down Flow	(kg/min)	0.88	0.89	0.82	1.73	1.47	2.03	2.23	1.23	0.72
Energy										
Stage 1 Recovery	(kw)	36.9	36.8	36.5	39.0	16.2	16.1	16.6	15.6	24.5
Stage 2 Recovery	(kw)	8.6	9.7	8.8	8.1	5.7	3.0	2.5	4.1	19.7
Overall Energy Balance	(%)	-4.4	-2.3	-3.1	2.3	0.0	0.7	2.9	-3.3	-6.1

1) Dry basis

2) Dry basis, corrected to 3% O₂

		SO ₂	SO ₂	SO ₂	SO ₂	SO ₂	SO ₂	SO ₂	SO ₂	SO ₂
Test Type	Test ID	I-25	I-RTB3	I-26	I-23	I-22	I-19	I-20	I-19a	I-21
	Date	02/14/96	02/06/96	02/14/96	02/14/96	02/14/96	02/06/96	02/06/96	02/06/96	02/06/96
Flue Gas Inlet	Time	10:35 AM	1:01 PM	10:11 AM	9:33 AM	9:11 AM	3:56 PM	2:54 PM	4:10 PM	2:25 PM
Flow Rate	(kg/min)	19.6	18.6	19.6	19.6	19.6	19.4	19.4	19.3	19.2
Gas Velocity	(m/s)	6.6	6.1	6.6	6.6	6.6	6.4	6.3	6.4	6.3
Temperature	(°C)	119.5	116.4	118.7	117.1	114.7	119.1	118.9	119.1	118.8
O ₂ ⁽¹⁾	(%)	6.61	8.07	6.69	6.61	6.54	7.14	6.85	7.05	7.23
SO ₂ ⁽²⁾	(ppm _v)	2553	2667	2548	2560	2579	2939	2843	2949	2908
NO _x ⁽²⁾	(ppm _v)	459	N/A	N/A	478	466	N/A	N/A	N/A	N/A
Humidity	(gm/gm)	0.038	0.034	0.038	0.038	0.039	0.036	0.037	0.036	0.036

Flue Gas

Interstage Temperature	(°C)	41.1	40.5	40.0	38.5	36.7	48.1	45.4	46.1	42.2
Outlet Temperature	(°C)	23.8	33.6	24.0	24.1	24.7	36.3	36.7	36.5	36.3
SO ₂ Removal	(%)	87.9	94.4	93.4	95.4	97.3	24.1	67.0	75.4	92.3
NO _x Removal	(%)	0.76	N/A	N/A	0.61	0.67	N/A	N/A	N/A	N/A

Cooling Water

Flow Rate	(kg/min)	16.6	19.4	17.3	17.4	17.4	18.2	17.9	18.2	17.9
Inlet Temperature	(°C)	7.1	29.9	7.1	7.3	7.3	35.6	36.6	35.8	36.3
Interstage Temperature	(°C)	23.7	33.6	22.8	22.4	22.3	36.8	37.0	36.5	36.3
Outlet Temperature	(°C)	45.2	49.3	44.2	43.8	43.5	52.9	53.4	52.7	52.6

Reagent

L/G Ratio	(l/m ³)	0.682	1.065	1.111	1.414	1.956	0.096	0.262	0.438	1.093
Temperature	(°C)	29.4	34.6	28.4	27.7	27.4	34.5	35.4	35.2	35.9
Supply pH	(-)	6.93	6.87	6.96	7.01	7.00	5.82	5.87	5.84	5.91
Return pH	(-)	6.65	0.00	6.72	6.78	6.79	0.00	0.00	0.00	0.00
Fresh Water Flow	(kg/min)	0.51	2.25	0.52	0.52	0.52	0.85	0.85	0.81	0.84
Blow Down Flow	(kg/min)	0.60	1.10	0.47	0.12	0.00	0.87	0.88	0.83	0.79

Energy

Stage 1 Recovery	(kw)	24.9	21.3	25.8	26.0	25.7	20.5	20.6	20.6	20.2
Stage 2 Recovery	(kw)	19.1	5.0	18.9	18.3	18.2	1.5	0.5	0.9	0.1
Overall Energy Balance	(%)	-6.4	5.8	-3.0	-3.5	-1.2	-4.6	-8.0	-6.3	-11.2

1) Dry basis

2) Dry basis, corrected to 3% O₂

		Test Type	M-29	M-29	M-29	M-29	M-29	M-29	M-29	M-29	
		Test ID	I-4B1	I-4B2	I-4B3	I-14D1	I-14D2	I-14D3	I-4C1	I-4C2	I-4C3
		Date	02/07/96	02/07/96	02/08/96	02/09/96	02/12/96	02/12/96	02/20/96	02/20/96	02/20/96
		Time	10:40 AM	2:10 PM	10:09 AM	3:54 PM	10:42 AM	2:43 PM	9:56 AM	12:49 PM	3:13 PM
Flue Gas Inlet											
Flow Rate	(kg/min)		36.1	36.0	37.0	37.2	37.3	36.9	36.7	36.6	36.5
Gas Velocity	(m/s)		11.6	11.6	12.2	12.0	12.2	12.0	11.8	11.8	11.7
Temperature	(°C)		123.2	123.0	122.6	122.5	125.0	123.7	124.9	124.0	122.3
O ₂ ⁽¹⁾	(%)		6.38	6.60	6.76	6.55	6.64	6.60	6.44	6.38	6.31
SO ₂ ⁽²⁾	(ppm _v)		2915	2599	2735	2516	2742	2590	2234	2558	2408
NO _x ⁽²⁾	(ppm _v)		N/A	N/A	460	491	557	503	392	418	439
Humidity	(gm/gm)		0.038	0.037	0.037	0.037	0.037	0.037	0.037	0.038	0.038
Flue Gas											
Interstage Temperature	(°C)		53.8	52.7	55.3	49.5	47.7	48.8	52.5	54.3	52.5
Outlet Temperature	(°C)		37.0	36.5	36.0	27.2	26.8	27.1	36.2	36.4	35.9
SO ₂ Removal	(%)		97.1	97.5	96.2	97.3	97.6	95.9	97.3	97.7	97.3
NO _x Removal	(%)		N/A	N/A	-1.58	-3.67	0.61	-1.92	-7.75	2.39	5.82
Cooling Water											
Flow Rate	(kg/min)		33.5	34.1	33.7	33.7	33.8	33.5	32.5	33.2	33.1
Inlet Temperature	(°C)		31.5	29.4	27.2	6.6	6.0	6.3	27.1	26.0	25.0
Interstage Temperature	(°C)		36.7	35.9	35.2	24.5	24.1	24.4	35.2	35.2	34.6
Outlet Temperature	(°C)		52.1	50.5	50.7	42.3	43.6	41.9	51.4	50.7	49.7
Reagent											
L/G Ratio	(l/m ³)		0.605	0.703	0.611	0.685	0.697	0.713	0.576	0.637	0.677
Temperature	(°C)		38.3	37.9	37.9	32.2	31.7	32.0	38.5	38.7	38.2
Supply pH	(-)		7.79	7.92	7.88	7.91	7.92	8.32	8.00	7.96	7.93
Return pH	(-)		0.00	0.00	6.96	7.06	7.38	7.82	7.22	7.24	7.61
Fresh Water Flow	(kg/min)		2.23	2.61	2.40	1.53	2.09	2.10	2.05	1.88	2.24
Blow Down Flow	(kg/min)		1.79	3.20	2.65	1.44	2.66	2.88	2.54	2.30	2.75
Energy											
Stage 1 Recovery	(kw)		36.0	34.6	36.4	41.8	45.8	41.1	36.7	35.9	34.8
Stage 2 Recovery	(kw)		12.0	15.5	18.7	42.1	42.6	42.2	18.5	21.3	22.1
Overall Energy Balance	(%)		4.8	7.1	11.6	3.5	4.9	2.1	8.3	13.2	11.2

1) Dry basis

2) Dry basis, corrected to 3% O2

		Test Type	M-26	NH ₃	NH ₃	NH ₃	NH ₃	NH ₃	NH ₃
		Test ID	I-4A	I-14G-IN	I-14G-OUT	I-4F-IN	I-4F-OUT	I-4E-IN	I-4E-OUT
		Date	02/09/96	02/14/96	02/14/96	02/15/96	02/15/96	02/15/96	02/15/96
Flue Gas Inlet		Time	1:00 PM	4:35 PM	5:25 PM	2:27 PM	5:01 PM	5:52 PM	5:21 PM
Flow Rate	(kg/min)		36.6	37.2	38.2	37.2	37.6	38.2	37.6
Gas Velocity	(m/s)		11.9	12.1	12.4	11.9	12.0	12.1	12.0
Temperature	(°C)		125.4	123.7	123.7	123.2	121.2	120.9	121.2
O ₂ ⁽¹⁾	(%)		6.40	6.15	6.15	6.23	6.39	5.20	5.65
SO ₂ ⁽²⁾	(ppm _v)		2660	2468	1448	2014	2336	2385	1068
NO _x ⁽²⁾	(ppm _v)		478	421	172	355	434	539	481
Humidity	(gm/gm)		0.038	0.039	0.039	0.038	0.037	0.040	0.039

Flue Gas

Interstage Temperature	(°C)	54.6	48.1	49.7	54.6	55.1	55.8	55.1
Outlet Temperature	(°C)	36.3	26.7	27.2	36.4	36.1	36.0	36.0
SO ₂ Removal	(%)	97.4	96.9	27.1	83.3	97.3	68.0	10.3
NO _x Removal	(%)	1.34	-0.50	22.88	5.37	-6.17	7.02	7.15

Cooling Water

Flow Rate	(kg/min)	34.0	35.0	35.3	33.4	33.1	32.4	32.9
Inlet Temperature	(°C)	27.4	6.0	6.4	27.1	25.2	25.2	25.3
Interstage Temperature	(°C)	35.4	23.4	24.1	35.3	35.0	35.0	35.0
Outlet Temperature	(°C)	50.3	39.6	40.1	49.4	48.6	48.4	48.5

Reagent

L/G Ratio	(l/m ³)	0.665	0.699	0.676	0.653	0.674	0.567	0.693
Temperature	(°C)	38.2	31.2	32.0	38.2	38.4	38.3	38.4
Supply pH	(-)	7.92	7.88	7.94	7.95	7.82	7.98	7.86
Return pH	(-)	7.16	7.02	6.99	6.86	7.58	7.63	7.56
Fresh Water Flow	(kg/min)	2.29	2.25	2.04	2.27	2.27	2.27	2.28
Blow Down Flow	(kg/min)	2.57	3.17	3.28	2.62	2.31	3.09	2.30

Energy

Stage 1 Recovery	(kw)	35.6	39.6	39.6	32.8	31.4	30.4	31.0
Stage 2 Recovery	(kw)	18.9	42.4	43.6	19.0	22.6	22.1	22.4
Overall Energy Balance	(%)	7.4	-4.0	-3.4	3.6	7.8	-6.7	0.7

1) Dry basis

2) Dry basis, corrected to 3% O₂

		Test Type	PSD	PSD	M-5	PSD
		Test ID	I-4L	I-14M	I-4J	I-4N
		Date	02/07/96	02/12/96	02/19/96	02/19/96
		Time	4:19 PM	12:45 PM	12:30 PM	2:19 PM
Flue Gas Inlet						
Flow Rate	(kg/min)		36.5	37.4	36.9	37.7
Gas Velocity	(m/s)		11.7	12.2	11.8	12.0
Temperature	(°C)		122.3	124.8	124.2	123.6
O ₂ ⁽¹⁾	(%)		6.97	6.88	6.39	6.74
SO ₂ ⁽²⁾	(ppm _v)		2619	2763	2592	2391
NO _x ⁽²⁾	(ppm _v)		N/A	572	460	473
Humidity	(gm/gm)		0.036	0.037	0.037	0.036

Flue Gas

Interstage Temperature	(°C)		54.3	49.1	56.3	58.9
Outlet Temperature	(°C)		36.2	27.4	36.9	37.2
SO ₂ Removal	(%)		97.4	96.9	99.1	98.5
NO _x Removal	(%)		N/A	0.17	6.76	-0.52

Cooling Water

Flow Rate	(kg/min)		34.0	34.0	33.3	33.5
Inlet Temperature	(°C)		28.4	6.3	16.9	17.1
Interstage Temperature	(°C)		35.5	24.7	34.8	35.1
Outlet Temperature	(°C)		49.6	43.1	49.5	49.5

Reagent

L/G Ratio	(l/m ³)		0.639	0.686	0.639	0.573
Temperature	(°C)		37.8	32.3	41.3	41.4
Supply pH	(-)		7.92	8.09	7.82	7.81
Return pH	(-)		0.00	7.48	7.19	7.21
Fresh Water Flow	(kg/min)		2.63	2.05	1.69	1.86
Blow Down Flow	(kg/min)		3.20	3.41	2.72	3.18

Energy

Stage 1 Recovery	(kw)		33.3	43.7	34.1	33.7
Stage 2 Recovery	(kw)		16.9	43.7	41.6	42.1
Overall Energy Balance	(%)		7.7	6.8	-4.4	-1.5

1) Dry basis

2) Dry basis, corrected to 3% O₂

Test Series I Ammonia Data

Test ID	I-14G-IN	I-14G-OUT	I-4F-IN	I-4F-OUT	I-4E-IN	I-4E-OUT
Date	2/14/96	2/14/96	2/15/96	2/15/96	2/15/96	2/15/96
Time	4:35 PM	5:25 PM	2:27 PM	5:01 PM	5:52 PM	5:21 PM
Gas Temperature @ Module 2 Outlet (°C)	26.9	27.4	36.5	36.1	35.9	36.0
Flue Gas NH ₃ as Particulate (ppm _v , M-26A)			27.0	9.1		
Flue Gas NH ₃ as Vapor (ppm _v , M-26A)			65.9	12.7		
Flue Gas NH ₃ Total (ppm _v , M-26A)			92.9	21.8		
Flue Gas NH ₃ Total (Gas Analyzer, ppm _v)	70.1	4.8	93.9	22.4	67.7	16.3
Flue Gas NH ₃ Injected (ppm _v)	125.2	125.2	169.7	169.7	123.3	123.3
Rotameter Temp (°C)	-2.2	-2.2	-1.0	-1.0	-2.6	-2.6
Rotameter Reading (% Full Scale)	54	54	73.5	73.5	54	54
NH ₃ Flow Rate (kg/hr)	0.159	0.159	0.216	0.216	0.161	0.161

Particulate Loading and Size Distribution Data

Test Date	2/7/96		2/7/96		2/8/96		2/9/96		2/9/96		2/12/96	
Test ID	4B1		4B2		4B3		4A		14D1		14D2	
Test Type	M-29		M-29		M-29		M-26		M-29		M-29	
Location	Inlet	Outlet	Inlet	Outlet	Inlet	Outlet	Inlet	Outlet	Inlet	Outlet	Inlet	Outlet
Sample Volume, DSCF	90.25	83.06	89.4	93.34	95.52	92.3	79.56	79.64	103.1	95.74	103.64	77.8
Sample Time, min	120	120	120	120	120	120	100	100	120	120	120	120
Sample Temp, F	251	98	254	98	253	98	256	98	253	81	256	80
Sample H2O, volume %	6.7	6.2	6.7	7.7	7.1	5.9	7	6.7	6.7	3.6	7.1	3.8
Oxygen Conc., %, dry	6.38	6.58	6.6	6.68	6.76	6.44	6.4	6.55	6.5	6.68	6.64	6.83
Particulate, grams	1.12	0.0469	1.6594	0.03	1.2083	0.0325	1.3178	0.0467	2.5044	0.0266	1.5195	0.0804
Sample Flow, dscf	0.752	0.692	0.745	0.778	0.796	0.769	0.796	0.796	0.859	0.798	0.864	0.648
Particulate, mg/dscm @ 3% O2	539.9	24.9	819.9	14.3	565.1	15.4	721.6	25.8	1065.6	12.3	649.5	46.4
Part. Removal, %		95.4		98.3		97.3		96.4		98.8		92.9

Particulate Loading and Size Distribution Data, Continued

Test Date	2/12/96		2/15/96		2/19/96		2/20/96		2/20/96		2/20/96	
Test ID	14D3		4F		4J		4C1		4C2		4C3	
Test Type	M-29		M-5		M-5		M-29		M-29		M-29	
Location	Inlet	Outlet	Inlet	Outlet	Inlet	Outlet	Inlet	Outlet	Inlet	Outlet	Inlet	Outlet
Sample Volume, DSCF	101.6	93.61	103.06	96.28	109.07	87.87	105.99	100.82	109.09	93.05	108.13	84.76
Sample Time, min	120	120	120	120	120	120	120	120	120	120	120	120
Sample Temp, F	254	81	252	98	253	99	253	98	253	98	249	97
Sample H2O, volume %	6.6	3.5	6.2	6.1	6.2	6.2	7.4	6.3	7.3	6.4	7.4	6.2
Oxygen Conc., %, dry	6.6	6.71	6.23	6.3	6.39	6.62	6.44	6.66	6.38	6.57	6.31	6.48
Particulate, grams	1.8634	0.0612	1.5418	0.0633	1.7822	0.0681	1.0819	0.0292	0.8388	0.0351	1.0579	0.0376
Sample Flow, dscf	0.847	0.78	0.859	0.802	0.909	0.732	0.883	0.84	0.909	0.775	0.901	0.706
Particulate, mg/dscm @ 3% O2	810.2	29.1	644.2	28.4	711.4	34.3	445.9	12.8	334.5	16.6	423.6	19.4
Part. Removal, %		96.4		95.6		95.2		97.1		95		95.4

Particulate Loading and Particle Size Data, Continued

Test Date	2/7/96		2/12/96		2/19/96	
Test ID	4L		14M		4N	
Test Type	Plate PSD		Plate PSD		Plate PSD	
Location	Inlet	Outlet	Inlet	Outlet	Inlet	Outlet
Sample Volume, DSCF	14.94	16.98	12.84	29.9	13.54	27.03
Sample Time, min	15	15	15	30	15	30
Sample Temp, F	257	100	258	82	257	99
Sample H2O, volume %	6.7	7.7	6.6	3.5	6.2	6.2
Oxygen Conc., %, dry	6.97	6.72	6.88	6.91	6.74	6.93
Particulate, grams	0.224	0.0075	0.208	0.025	0.216	0.0205
Sample Flow, dscf	0.996	1.132	0.856	0.997	0.903	0.901
Particulate, mg/dscm @ 3% O2	679.9	19.6	729.8	37.7	711.4	34.3
Part. Removal, %		97.1		94.8		95.2

PSD Catch by Stage, grams

0	0.0379	0.0014	0.0243	0.0009	0.0119	0.0007
1	0.0285	0.001	0.0241	0.0002	0.0082	0.0004
2	0.0316	0.0008	0.0287	0.0001	0.0124	0.0005
3	0.0209	0.0001	0.0158	0.0004	0.0094	0.0014
4	0.0131	0	0.0114	0.0024	0.0145	0.0044
5	0.0058	0.0001	0.0051	0.0028	0.0034	0.0052
6	0.0013	0.0004	0.0009	0.0006	0.0006	0.0023
7	0.0006	0.0008	0.0008	0.0013	0.0008	0.0033
Backup	0.0023	0.001	0.0019	0.0026	0.0028	0.002

Aerodynamic Cut Diameter by Dstage, microns

0	8.34	8.01	8.95	8.73	8.75	9.03
1	5.16	4.96	5.54	5.41	5.42	5.6
2	3.47	3.34	3.72	3.65	3.64	3.77
3	2.34	2.26	2.51	2.47	2.45	2.55
4	1.46	1.42	1.57	1.56	1.54	1.61
5	0.67	0.66	0.73	0.73	0.71	0.76
6	0.37	0.38	0.41	0.42	0.4	0.44
7	0.20	0.21	0.23	0.25	0.22	0.26
Backup	0.10	0.11	0.11	0.13	0.11	0.13

Note; Max collected size = 50 microns at inlet, 25 microns at outlet

Test I-4B - Tabulated Metals data.

Element	Inlet				Outlet				Vapor Phase Removal (%)	Removal Standard Deviation (%)
	Vapor Phase Element in the Inlet Flue Gas (ug/dscm)				Vapor Phase Element in the Outlet Flue Gas (ug/dscm)					
	Average	+ Deviation	-Deviation	RMS Deviation	Average	+ Deviation	-Deviation	RMS Deviation		
Arsenic	48.65	9.56	15.33	13.41	0.23	0.36	0.19	0.31	99.52	0.65
Barium	NR	NR	NR	NR	NR	NR	NR	NR	NR	NR
Beryllium	NR	NR	NR	NR	NR	NR	NR	NR	NR	NR
Cadmium	NR	NR	NR	NR	NR	NR	NR	NR	NR	NR
Chromium	2.80	1.34	0.69	1.16	2.71	1.07	0.76	0.95	3.31	52.44
Cobalt	NR	NR	NR	NR	NR	NR	NR	NR	NR	NR
Lead	2.06	2.02	1.18	1.76	0.48	0.00	0.00	0.00	NR	NR
Manganese	9.27	3.97	7.69	6.66	15.90	2.17	3.46	3.03	NR	NR
Nickel	7.26	4.78	4.40	4.60	1.87	0.10	0.10	0.13	NR	NR
Selenium	143.35	23.70	31.43	28.37	3.49	1.25	1.43	1.35	97.57	1.06
Mercury (Ionic)	29.35	1.32	2.09	1.83	4.21	0.24	0.14	0.21	85.65	1.13
Mercury (Elem.)	9.17	7.33	4.18	6.37	11.29	2.73	2.45	2.60	-23.07	90.05
Mercury (Total)	38.52	8.65	5.24	7.54	15.50	2.59	2.22	2.42	59.77	10.08

Element	Inlet					Outlet					Particle Phase Removal (%)	Removal Standard Deviation (%)
	Average Element in Fly Ash (ppm)	Particle Phase Element in the Flue Gas (ug/dscm)				Average Element in Fly Ash (ppm)	Particle Phase Element in the Flue Gas (ug/dscm)					
		Average	+ Deviation	-Deviation	RMS Deviation		Average	+ Deviation	-Deviation	RMS Deviation		
Arsenic	27.53	17.95	7.49	6.07	6.89	364.00	6.76	3.02	2.80	2.92	62.33	21.75
Barium	174.67	111.11	24.26	21.20	22.89	1814.33	32.95	9.84	12.44	11.36	70.34	11.91
Beryllium	54.33	35.15	11.61	8.68	10.46	0.85	0.02	0.00	0.01	0.01	99.96	0.02
Cadmium	5.22	3.44	1.73	1.72	1.73	30.43	0.54	0.12	0.19	0.16	NR	NR
Chromium	156.00	99.57	23.49	13.06	20.39	1251.33	24.19	15.85	15.72	15.79	75.70	16.62
Cobalt	89.00	57.00	15.20	10.06	13.39	259.33	4.68	1.27	1.51	1.41	91.79	3.13
Lead	403.33	258.00	65.25	35.21	56.56	1392.33	25.63	10.11	9.80	9.96	90.07	4.43
Manganese	217.00	139.09	36.48	23.48	32.03	920.67	16.99	6.96	6.54	6.76	87.79	5.61
Nickel	353.33	229.67	84.55	57.88	74.87	1479.67	28.64	19.76	16.01	18.18	87.53	8.90
Selenium	11.06	7.41	4.57	3.00	4.02	60.13	1.09	0.35	0.31	0.33	NR	NR
Mercury	0.49	0.32	0.11	0.06	0.10	5.36	0.10	0.02	0.04	0.03	68.68	14.07

Test I-14D - Tabulated Metals Data.

Element	Inlet				Outlet				Vapor Phase Removal (%)	Removal Standard Deviation (%)
	Vapor Phase Element in the Inlet Flue Gas (ug/dscm)				Vapor Phase Element in the Outlet Flue Gas (ug/dscm)					
	Average	+ Deviation	-Deviation	RMS Deviation	Average	+ Deviation	-Deviation	RMS Deviation		
Arsenic	20.18	6.53	9.55	8.45	0.56	0.49	0.49	0.69	97.21	3.63
Barium	NR	NR	NR	NR	NR	NR	NR	NR	NR	NR
Beryllium	NR	NR	NR	NR	NR	NR	NR	NR	NR	NR
Cadmium	NR	NR	NR	NR	NR	NR	NR	NR	NR	NR
Chromium	2.58	0.87	0.54	0.76	2.11	0.67	0.67	0.95	18.17	44.21
Cobalt	NR	NR	NR	NR	NR	NR	NR	NR	NR	NR
Lead	NR	NR	NR	NR	NR	NR	NR	NR	NR	NR
Manganese	4.47	8.27	4.22	7.16	13.27	2.03	2.03	2.88	NR	NR
Nickel	26.36	41.88	24.07	36.41	7.03	5.93	5.93	8.39	NR	NR
Selenium	143.80	10.93	12.06	11.54	10.14	5.10	5.10	7.21	92.95	5.04
Mercury (Ionic)	26.90	1.61	1.32	1.49	4.13	0.07	0.07	0.10	84.63	0.93
Mercury (Elem.)	6.11	0.18	0.25	0.23	6.23	0.75	0.75	1.06	-1.83	17.80
Mercury (Total)	33.01	1.35	1.14	1.26	33.01	1.35	1.14	1.26	68.62	3.14

Element	Inlet					Outlet					Particle Phase Removal (%)	Removal Standard Deviation (%)
	Average Element in Fly Ash (ppm)	Particle Phase Element in the Flue Gas (ug/dscm)				Average Element in Fly Ash (ppm)	Particle Phase Element in the Flue Gas (ug/dscm)					
		Average	+ Deviation	-Deviation	RMS Deviation		Average	+ Deviation	-Deviation	RMS Deviation		
Arsenic	28.43	23.98	6.40	5.53	6.01	231.67	7.37	5.27	5.44	5.36	69.26	23.63
Barium	164.00	138.62	41.13	31.39	37.23	1290.33	36.15	19.54	18.56	19.07	73.92	15.44
Beryllium	59.33	50.07	14.13	11.08	12.88	0.64	0.02	0.01	0.01	0.01	99.97	0.02
Cadmium	3.82	3.28	1.82	1.35	1.64	29.97	0.79	0.34	0.31	0.32	76.01	15.55
Chromium	157.67	133.08	31.69	35.60	33.82	675.33	18.21	7.08	8.46	7.86	86.32	6.86
Cobalt	82.67	68.90	10.27	14.32	12.78	206.33	6.13	3.08	4.00	3.63	91.11	5.52
Lead	359.00	303.80	92.07	71.16	83.60	942.33	28.50	13.69	19.86	17.61	90.62	6.34
Manganese	215.67	181.45	43.23	41.73	42.50	652.33	19.05	11.74	11.13	11.44	89.50	6.77
Nickel	407.00	339.72	44.38	82.38	71.42	880.00	26.20	13.52	17.12	15.63	92.29	4.88
Selenium	13.40	11.67	5.67	4.45	5.17	32.07	0.87	0.43	0.41	0.42	92.50	4.88
Mercury	0.31	0.27	0.16	0.11	0.14	6.11	0.14	0.04	0.02	0.04	NR	NR

Test I-4C - Tabulated Metals Data.

Element	Inlet				Outlet				Vapor Phase Removal (%)	Removal Standard Deviation (%)
	Vapor Phase Element in the Inlet Flue Gas (ug/dscm)				Vapor Phase Element in the Outlet Flue Gas (ug/dscm)					
	Average	+ Deviation	-Deviation	RMS Deviation	Average	+ Deviation	-Deviation	RMS Deviation		
Arsenic	32.42	3.73	5.69	5.01	0.47	0.17	0.17	0.24	98.54	0.77
Barium	NR	NR	NR	NR	NR	NR	NR	NR	NR	NR
Beryllium	NR	NR	NR	NR	NR	NR	NR	NR	NR	NR
Cadmium	NR	NR	NR	NR	NR	NR	NR	NR	NR	NR
Chromium	2.04	0.43	0.24	0.37	2.66	0.09	0.15	0.13	-30.28	24.66
Cobalt	NR	NR	NR	NR	NR	NR	NR	NR	NR	NR
Lead	NR	NR	NR	NR	NR	NR	NR	NR	NR	NR
Manganese	7.42	5.58	7.29	6.60	27.87	31.88	16.40	27.61	NR	NR
Nickel	44.13	21.23	38.60	33.48	9.36	8.40	7.14	7.84	NR	NR
Selenium	145.49	9.96	16.90	14.72	2.47	0.68	0.68	0.97	98.30	0.69
Mercury (Ionic)	26.55	0.27	0.18	0.24	7.07	0.64	0.33	0.56	73.39	2.12
Mercury (Elem.)	4.98	0.63	1.17	1.02	5.96	0.85	1.06	0.98	-19.79	31.32
Mercury (Total)	31.53	0.55	0.90	0.78	13.03	0.86	1.37	1.20	58.67	3.95

Element	Inlet					Outlet					Particle Phase Removal (%)	Removal Standard Deviation (%)
	Average Element in Fly Ash (ppm)	Particle Phase Element in the Flue Gas (ug/dscm)				Average Element in Fly Ash (ppm)	Particle Phase Element in the Flue Gas (ug/dscm)					
		Average	+ Deviation	-Deviation	RMS Deviation		Average	+ Deviation	-Deviation	RMS Deviation		
Arsenic	67.93	26.51	14.48	15.71	15.13	282.33	4.36	0.73	0.86	0.80	NR	NR
Barium	187.00	75.46	14.82	17.89	16.57	2205.33	34.52	2.77	1.51	2.40	54.25	10.54
Beryllium	60.67	24.32	2.45	3.57	3.16	1.15	0.02	0.00	0.00	0.00	99.93	0.01
Cadmium	8.45	3.51	1.27	1.77	1.58	43.13	0.77	1.05	0.53	0.91	77.98	27.84
Chromium	157.67	63.54	8.30	13.00	11.40	1074.33	16.90	2.53	2.62	2.57	73.40	6.26
Cobalt	97.67	38.49	1.35	2.35	2.04	301.00	4.74	1.06	0.60	0.92	87.68	2.47
Lead	313.33	125.86	11.88	22.11	19.16	1012.00	15.81	1.68	1.19	1.49	87.44	2.25
Manganese	229.67	92.39	11.87	18.09	15.92	932.00	14.66	0.60	0.68	0.65	84.13	2.82
Nickel	397.67	160.82	35.05	36.98	36.06	1174.33	18.31	1.53	2.79	2.42	88.62	2.96
Selenium	13.83	5.61	1.44	1.39	1.42	154.20	2.50	2.34	1.42	2.04	55.38	38.16
Mercury	0.38	NR	NR	NR	NR	12.71	NR	0.04	0.03	0.04	NR	NR

APPENDIX D

**TABULATED DATA FOR
TEST SERIES II, PITTSBURGH #8 COAL**

Test Series	II
Fuel Analysis, wt. %	
Sample Number	C-22385
C	75.1
H ₂	5.1
S	2.6
O ₂	5.5
N ₂	1.5
H ₂ O	0.9
Cl, ppm	123.0
F, ppm	<11
Ash	9.4
Heating Value - wet basis (J/Kg)	31.23
Heating Value - dry basis (J/Kg)	31.52
Fd (dscm/J)	2.65E-07

Coal Sample Element Concentration in ppm_m

Element	C-22473	C-22474	Average	+ dev.	- dev	det limit
Arsenic	8.38	7.46	7.92	0.46	0.46	0.20
Barium	21.16	29.35	25.26	4.10	4.10	2.00
Beryllium	0.65	0.61	0.63	0.02	0.02	0.10
Cadmium	0.06	0.04	0.05	0.01	0.01	0.02
Cobalt	0.91	0.90	0.91	0.01	0.01	0.40
Chromium	0.34	0.33	0.34	0.01	0.01	0.20
Manganese	8.33	10.24	9.29	0.96	0.96	0.20
Nickel	20.66	17.20	18.93	1.73	1.73	0.40
Lead	1.70	3.46	2.58	0.88	0.88	0.20
Selenium	1.08	1.26	1.17	0.09	0.09	0.20
Mercury	0.13	0.07	0.10	0.03	0.03	0.02

		SO ₂	SO ₂	SO ₂	SO ₂	SO ₂	SO ₂	SO ₂	SO ₂
Test Type		II-1	II-2R	II-2	II-3R2	II-3R1	II-3	II-3R	II-4
Test ID									
Date		04/17/96	04/23/96	04/17/96	04/23/96	04/23/96	04/17/96	04/17/96	04/17/96
Time		10:36 AM	3:56 PM	11:12 AM	4:44 PM	3:19 PM	9:52 AM	11:49 AM	12:15 PM
Flue Gas Inlet									
Flow Rate	(kg/min)	38.9	38.5	37.9	38.1	38.0	37.2	37.4	37.0
Gas Velocity	(m/s)	12.6	12.4	12.3	12.3	12.3	12.0	12.0	11.9
Temperature	(°C)	125.8	125.6	126.2	125.8	125.4	124.6	125.0	124.5
O ₂ ⁽¹⁾	(%)	6.43	6.92	6.28	6.90	6.92	6.49	6.92	6.90
SO ₂ ⁽²⁾	(ppm _v)	1837	1331	1600	1344	1317	2351	1502	1452
Humidity	(gm/gm)	0.038	0.037	0.038	0.037	0.037	0.038	0.037	0.037
Flue Gas									
Interstage Temperature	(°C)	57.1	57.7	57.5	57.8	57.5	55.3	55.1	50.8
Outlet Temperature	(°C)	37.0	36.6	37.2	36.6	36.6	36.5	36.5	36.5
SO ₂ Removal	(%)	72.2	94.3	90.1	95.7	96.5	93.3	96.5	97.4
Cooling Water									
Flow Rate	(kg/min)	34.7	33.5	33.5	33.3	33.4	34.9	33.1	33.1
Inlet Temperature	(°C)	28.7	30.6	30.9	31.2	30.6	29.7	30.5	30.5
Interstage Temperature	(°C)	34.7	35.5	35.8	35.5	35.5	34.9	35.3	35.3
Outlet Temperature	(°C)	54.8	55.2	55.4	55.3	55.2	53.9	54.5	54.1
Reagent									
L/G Ratio	(l/m ³)	0.071	0.120	0.128	0.139	0.193	0.284	0.285	0.506
Temperature	(°C)	37.2	37.8	38.5	38.2	38.6	38.6	38.8	38.2
Supply pH	(-)	8.26	8.19	8.25	8.19	8.19	8.22	8.23	8.22
Return pH	(-)	6.73	7.46	7.09	7.39	7.42	6.38	7.16	6.90
Fresh Water Flow	(kg/min)	1.42	1.10	1.42	1.10	1.02	1.36	1.22	1.22
Blow Down Flow	(kg/min)	1.87	1.15	1.69	0.97	1.06	1.74	1.33	1.31
Energy									
Stage 1 Recovery	(kw)	48.5	46.1	45.8	46.1	45.8	46.1	44.2	43.4
Stage 2 Recovery	(kw)	14.7	11.5	11.3	9.9	11.3	12.7	11.0	11.2
Overall Energy Balance	(%)	16.8	11.9	11.3	10.0	13.1	13.4	8.8	9.3

1) Dry basis

2) Dry basis, corrected to 3% O₂

		SO ₂	SO ₂	SO ₂	SO ₂	SO ₂	SO ₂	SO ₂	SO ₂
Test Type		SO ₂	SO ₂	SO ₂	SO ₂	SO ₂	SO ₂	SO ₂	SO ₂
Test ID		II-5	II-12	II-13	II-14	II-9	II-15	II-10	II-11
Date		05/07/96	04/17/96	04/17/96	04/17/96	04/17/96	04/17/96	04/17/96	04/17/96
Time		3:55 PM	1:58 PM	1:22 PM	12:59 PM	4:15 PM	3:43 PM	3:20 PM	2:57 PM
Flue Gas Inlet									
Flow Rate	(kg/min)	35.5	39.2	37.5	36.9	38.0	37.7	37.5	36.4
Gas Velocity	(m/s)	11.2	12.6	12.0	11.8	12.2	12.1	12.0	11.6
Temperature	(°C)	123.1	123.3	123.6	123.9	122.5	122.6	122.7	122.7
O ₂ ⁽¹⁾	(%)	5.84	7.06	6.94	6.92	6.80	7.16	7.14	7.05
SO ₂ ⁽²⁾	(ppm _v)	1269	1462	1441	1460	1421	1424	1435	1449
Humidity	(gm/gm)	0.039	0.037	0.037	0.037	0.037	0.036	0.036	0.037
Flue Gas									
Interstage Temperature	(°C)	53.4	56.9	54.3	50.2	55.9	54.2	50.2	48.4
Outlet Temperature	(°C)	36.4	36.7	36.4	36.7	36.1	36.0	35.9	35.8
SO ₂ Removal	(%)	98.5	86.1	97.2	97.3	57.7	84.4	92.7	95.4
Cooling Water									
Flow Rate	(kg/min)	32.0	33.1	33.2	33.0	33.4	33.2	33.3	33.3
Inlet Temperature	(°C)	27.5	31.2	30.9	30.9	30.2	30.5	30.4	30.1
Interstage Temperature	(°C)	34.2	35.3	35.2	35.6	35.0	35.1	34.9	34.8
Outlet Temperature	(°C)	49.9	54.5	54.0	54.2	53.5	53.7	53.3	52.9
Reagent									
L/G Ratio	(l/m ³)	0.972	0.064	0.249	0.538	0.099	0.163	0.320	0.681
Temperature	(°C)	38.2	37.8	38.7	38.2	37.3	37.9	37.7	37.3
Supply pH	(-)	8.23	7.23	7.23	7.19	6.21	6.22	6.22	6.17
Return pH	(-)	7.90	6.27	7.05	7.01	4.69	5.12	4.93	6.14
Fresh Water Flow	(kg/min)	0.90	1.22	1.22	1.21	0.93	0.93	0.93	0.92
Blow Down Flow	(kg/min)	1.51	1.24	1.36	1.38	0.93	0.90	1.01	1.21
Energy									
Stage 1 Recovery	(kw)	34.9	44.3	43.4	42.8	43.2	43.2	42.8	42.0
Stage 2 Recovery	(kw)	15.1	9.5	10.1	10.7	11.2	10.7	10.4	10.8
Overall Energy Balance	(%)	2.4	7.0	6.8	10.1	5.0	6.6	5.3	6.4

1) Dry basis

2) Dry basis, corrected to 3% O₂

		SO ₂	SO ₂	SO ₂	SO ₂	SO ₂	SO ₂	SO ₂	SO ₂
Test Type		II-6	II-7	II-8	II-20	II-25	II-23	II-21	II-26
Test ID									
Date		04/18/96	04/18/96	04/18/96	04/18/96	05/09/96	05/09/96	04/18/96	05/09/96
Time		3:39 PM	2:54 PM	2:32 PM	12:53 PM	1:02 PM	12:25 PM	1:23 PM	1:40 PM
Flue Gas Inlet									
Flow Rate	(kg/min)	17.4	17.3	17.4	17.3	19.1	18.9	17.4	19.1
Gas Velocity	(m/s)	5.8	5.8	5.8	5.8	6.2	6.2	5.8	6.3
Temperature	(°C)	118.1	118.5	118.5	119.6	118.8	118.2	119.3	119.1
O ₂ ⁽¹⁾	(%)	6.63	6.69	6.72	6.48	5.97	5.85	6.42	5.81
SO ₂ ⁽²⁾	(ppm _v)	1362	1343	1345	1365	1245	1249	1342	1266
Humidity	(gm/gm)	0.039	0.038	0.038	0.038	0.040	0.040	0.038	0.040
Flue Gas									
Interstage Temperature	(°C)	45.2	43.8	42.5	47.7	47.0	46.4	46.9	46.8
Outlet Temperature	(°C)	35.3	35.0	35.0	37.7	28.9	28.9	36.5	30.0
SO ₂ Removal	(%)	80.7	94.2	95.7	84.7	83.6	89.3	91.5	92.2
Cooling Water									
Flow Rate	(kg/min)	17.9	18.7	18.7	18.6	16.5	16.6	18.9	16.5
Inlet Temperature	(°C)	32.0	30.8	30.8	35.5	13.7	13.6	32.2	14.0
Interstage Temperature	(°C)	34.2	34.0	33.8	36.7	29.5	28.9	35.4	29.4
Outlet Temperature	(°C)	51.1	50.6	50.6	52.9	50.0	49.6	52.5	50.1
Reagent									
L/G Ratio	(l/m ³)	0.245	0.741	1.091	0.251	0.288	0.452	0.572	0.701
Temperature	(°C)	37.1	36.6	36.4	38.7	37.7	36.2	38.1	36.1
Supply pH	(-)	8.26	8.22	8.20	7.11	7.14	7.13	7.15	7.12
Return pH	(-)	7.39	7.81	7.85	6.87	6.95	7.06	6.98	7.05
Fresh Water Flow	(kg/min)	0.71	0.71	0.71	0.71	0.00	0.00	0.71	0.00
Blow Down Flow	(kg/min)	0.73	0.65	0.74	0.69	0.33	0.26	0.61	0.24
Energy									
Stage 1 Recovery	(kw)	21.2	21.7	21.9	21.0	23.8	24.0	22.5	23.8
Stage 2 Recovery	(kw)	2.7	4.2	4.0	1.6	18.2	17.6	4.2	17.8
Overall Energy Balance	(%)	0.3	6.3	7.1	13.6	6.9	6.8	19.7	9.2

1) Dry basis

2) Dry basis, corrected to 3% O₂

		SO ₂	SO ₂	SO ₂	SO ₂	SO ₂	SO ₂	SO ₂
Test Type		SO ₂	SO ₂	SO ₂	SO ₂	SO ₂	SO ₂	SO ₂
Test ID		II-22	II-27	II-24	II-17	II-16	II-19	II-18
Date		04/18/96	04/18/96	05/09/96	04/18/96	04/18/96	04/18/96	04/18/96
Time		2:00 PM	4:45 PM	2:31 PM	12:01 PM	11:08 AM	10:24 AM	9:40 AM
Flue Gas Inlet								
Flow Rate	(kg/min)	17.3	17.4	19.0	17.4	17.3	17.3	17.3
Gas Velocity	(m/s)	5.8	5.8	6.2	5.7	5.7	5.7	5.7
Temperature	(°C)	119.0	117.9	119.8	118.9	118.1	116.9	115.4
O ₂ ⁽¹⁾	(%)	6.55	6.57	5.55	6.51	6.47	6.68	6.60
SO ₂ ⁽²⁾	(ppm _v)	1350	1325	1252	1362	1334	1319	1295
Humidity	(gm/gm)	0.039	0.039	0.040	0.038	0.038	0.037	0.037
Flue Gas								
Interstage Temperature	(°C)	42.9	36.6	44.5	47.9	45.6	44.0	43.6
Outlet Temperature	(°C)	35.5	24.8	30.7	37.7	37.9	37.9	37.8
SO ₂ Removal	(%)	94.6	95.0	96.3	77.1	88.4	90.8	93.2
Cooling Water								
Flow Rate	(kg/min)	18.5	17.1	16.4	18.5	17.7	17.1	16.7
Inlet Temperature	(°C)	31.2	11.2	14.2	35.7	36.7	37.4	37.7
Interstage Temperature	(°C)	34.3	24.3	29.6	37.2	36.8	36.4	36.1
Outlet Temperature	(°C)	51.0	45.5	50.1	53.3	53.2	53.2	52.8
Reagent								
L/G Ratio	(l/m ³)	1.090	1.160	1.320	0.244	0.654	0.849	1.276
Temperature	(°C)	36.7	28.8	34.8	38.4	38.4	38.0	37.9
Supply pH	(-)	7.16	7.20	7.14	6.07	6.03	6.05	6.00
Return pH	(-)	7.08	7.09	7.09	5.70	5.88	5.89	5.87
Fresh Water Flow	(kg/min)	0.71	0.63	0.00	0.71	0.52	0.52	0.68
Blow Down Flow	(kg/min)	0.81	0.97	0.44	0.77	0.43	0.44	0.70
Energy								
Stage 1 Recovery	(kw)	21.6	25.2	23.5	20.7	20.3	20.0	19.4
Stage 2 Recovery	(kw)	4.1	15.6	17.7	1.9	0.2	-1.2	-1.8
Overall Energy Balance	(%)	8.2	1.9	10.7	14.5	10.3	6.8	1.8

1) Dry basis

2) Dry basis, corrected to 3% O₂

		Test Type	M-29	M-29	M-29	M-29	M-29	M-29
		Test ID	II-4A1	II-4A2	II-4A3	II-4C1	II-4C2	II-4C3
		Date	04/23/96	04/23/96	04/24/96	05/07/96	05/07/96	05/09/96
		Time	10:29 AM	1:34 PM	10:14 AM	10:05 AM	2:35 PM	10:15 AM
Flue Gas Inlet								
Flow Rate	(kg/min)		36.6	36.6	36.3	37.8	37.3	36.9
Gas Velocity	(m/s)		11.8	11.8	11.7	12.0	11.9	11.8
Temperature	(°C)		124.7	125.1	126.1	124.6	123.8	125.0
O ₂ ⁽¹⁾	(%)		6.69	6.53	5.83	5.93	5.83	5.59
SO ₂ ⁽²⁾	(ppm _v)		1315	1362	1276	1283	1264	1244
Humidity	(gm/gm)		0.038	0.038	0.039	0.038	0.039	0.039
Flue Gas								
Interstage Temperature	(°C)		52.6	52.6	52.6	55.0	58.2	55.4
Outlet Temperature	(°C)		36.1	36.6	36.5	36.7	36.7	36.8
SO ₂ Removal	(%)		98.0	98.1	98.5	98.5	97.6	98.2
Cooling Water								
Flow Rate	(kg/min)		33.8	33.4	33.9	32.7	32.0	33.8
Inlet Temperature	(°C)		28.6	30.2	29.5	28.4	27.7	25.3
Interstage Temperature	(°C)		34.7	35.3	35.4	34.7	34.7	34.7
Outlet Temperature	(°C)		53.6	54.4	54.0	52.0	50.8	51.4
Reagent								
L/G Ratio	(l/m ³)		0.607	0.611	0.620	0.537	0.527	0.536
Temperature	(°C)		38.2	38.0	38.1	38.6	38.9	39.6
Supply pH	(-)		8.21	8.19	8.09	8.15	8.26	8.00
Return pH	(-)		7.64	8.43	7.26	7.45	7.35	7.13
Fresh Water Flow	(kg/min)		0.96	1.05	1.16	0.98	0.97	0.85
Blow Down Flow	(kg/min)		1.23	1.27	1.37	1.21	1.17	1.21
Energy								
Stage 1 Recovery	(kw)		44.7	44.5	44.1	39.3	35.8	39.3
Stage 2 Recovery	(kw)		14.5	11.8	14.0	14.3	15.7	22.3
Overall Energy Balance	(%)		15.4	13.8	9.9	3.3	1.0	16.4

1) Dry basis

2) Dry basis, corrected to 3% O₂

		Test Type	M-26	NH ₃	NH ₃	NH ₃	NH ₃	NH ₃	PSD
		Test ID	II-4B	II-4D-IN	II-4D-OUT	II-4E-OUT	II-4E-IN	II-4F	II-4G
		Date	04/24/96	05/02/96	05/02/96	05/02/96	05/02/96	05/02/96	05/07/96
		Time	3:19 PM	12:26 PM	1:17 PM	1:42 PM	2:07 PM	4:11 PM	12:12 PM
Flue Gas Inlet									
Flow Rate	(kg/min)		36.0	37.3	37.2	37.2	37.0	37.3	37.4
Gas Velocity	(m/s)		11.6	11.9	11.8	11.8	11.8	11.9	11.9
Temperature	(°C)		124.9	123.6	123.2	123.4	123.2	123.9	124.5
O ₂ ⁽¹⁾	(%)		5.65	6.38	6.60	6.28	6.31	6.16	5.82
SO ₂ ⁽²⁾	(ppm _v)		1296	1334	1171	1308	1295	1250	1266
Humidity	(gm/gm)		0.039	0.038	0.037	0.038	0.038	0.038	0.039
Flue Gas									
Interstage Temperature	(°C)		52.2	52.9	51.9	51.7	52.6	47.5	56.5
Outlet Temperature	(°C)		36.7	36.1	35.9	35.9	36.5	29.1	36.4
SO ₂ Removal	(%)		98.3	98.9	99.3	99.0	98.8	98.4	97.8
Cooling Water									
Flow Rate	(kg/min)		33.9	33.9	33.7	33.8	33.6	34.3	32.1
Inlet Temperature	(°C)		28.4	28.1	27.8	27.7	29.4	12.4	27.7
Interstage Temperature	(°C)		35.2	34.4	33.9	34.1	34.4	26.6	34.2
Outlet Temperature	(°C)		53.6	53.0	52.6	52.5	52.9	46.0	50.9
Reagent									
L/G Ratio	(l/m ³)		0.592	0.673	0.654	0.662	0.634	0.637	0.555
Temperature	(°C)		38.9	38.1	37.8	37.8	38.0	33.2	38.4
Supply pH	(-)		8.26	8.23	8.21	8.21	8.22	8.20	8.45
Return pH	(-)		7.63	7.55	7.52	7.72	7.69	7.65	7.44
Fresh Water Flow	(kg/min)		0.93	0.89	0.88	0.88	0.88	0.74	0.99
Blow Down Flow	(kg/min)		1.26	1.12	1.11	1.10	1.09	1.41	1.24
Energy									
Stage 1 Recovery	(kw)		43.6	44.0	44.0	43.5	43.3	46.4	37.2
Stage 2 Recovery	(kw)		16.2	14.9	14.3	14.9	11.7	33.9	14.6
Overall Energy Balance	(%)		15.2	12.6	11.9	9.8	9.8	2.0	-1.9

1) Dry basis

2) Dry basis, corrected to 3% O₂

Test Type HEAT TR. HEAT TR. HEAT TR. HEAT TR. HEAT TR.

Test ID		II-HX1	II-HX2	II-HX3	II-HX4	II-HX5
Date		04/15/96	04/15/96	04/15/96	04/15/96	04/15/96
Time		12:48 PM	2:01 PM	2:37 PM	3:35 PM	4:49 PM
Flue Gas Inlet						
Flow Rate	(kg/min)	39.2	39.0	39.1	38.8	27.7
Gas Velocity	(m/s)	12.6	12.6	12.7	12.6	9.2
Temperature	(°C)	120.7	123.3	123.7	124.1	120.9
O ₂ ⁽¹⁾	(%)	6.19	6.57	6.56	6.67	9.58
SO ₂ ⁽²⁾	(ppm _v)	-26	2122	2157	2196	2153
Humidity	(gm/gm)	0.037	0.037	0.038	0.038	0.036

Flue Gas

Interstage Temperature	(°C)	49.1	49.1	44.7	48.1	38.1
Outlet Temperature	(°C)	39.1	38.4	37.0	39.1	34.7
SO ₂ Removal	(%)	N/A	98.5	98.5	98.5	-8.0

Cooling Water

Flow Rate	(kg/min)	15.9	15.5	22.8	23.2	22.0
Inlet Temperature	(°C)	31.3	34.3	33.2	33.0	32.6
Interstage Temperature	(°C)	18.1	12.3	11.3	22.4	11.4
Outlet Temperature	(°C)	62.1	60.0	47.9	54.2	43.6

Reagent

L/G Ratio	(l/m ³)	0.425	0.406	0.411	0.420	1.640
Temperature	(°C)	40.0	38.8	37.6	39.2	34.6
Supply pH	(-)	7.01	7.06	7.00	7.03	7.00
Return pH	(-)	5.21	6.88	6.75	6.74	6.94
Fresh Water Flow	(kg/min)	0.07	1.89	1.90	1.89	1.89
Blow Down Flow	(kg/min)	0.00	0.88	1.64	1.22	2.47

Energy

Stage 1 Recovery	(kw)	48.8	51.5	58.2	51.5	49.4
Stage 2 Recovery	(kw)	0.0	0.0	0.0	0.0	0.0
Overall Energy Balance	(%)	11.3	10.7	16.0	12.3	27.5

1) Dry basis

2) Dry basis, corrected to 3% O₂

Test Series II Ammonia Data

Test ID	II-4D-IN	II-4D-OUT	II-T4E-OUT	II-4E-IN	II-4F-IN	II-4F-OUT
Date	5/2/96	5/2/96	5/2/96	5/2/96	5/2/96	5/2/96
Time	12:10 PM	12:35 PM	1:17 PM	1:42 PM	2:50 PM	4:17PM
Gas Temperature @ Module 2 Outlet (°C)	36.16	35.91	35.96	36.59	29.44	29.25
Flue Gas NH ₃ as Particulate (ppm _v , M-26A)					19.1	2.5
Flue Gas NH ₃ as Vapor (ppm _v , M-26A)					44.4	4.8
Flue Gas NH ₃ Total (ppm _v , M-26A)					63.5	7.4
Flue Gas NH ₃ Total (Gas Analyzer, ppm _v)	67.7	11.6	8.5	31.1	82.1	0.0
Flue Gas NH ₃ Injected (ppm _v)	113.4	113.4	47.2	47.5	113.2	113.2
Rotameter Temp (°C)	15.0	19.4	19.0	21.3	20.4	21.1
Rotameter Reading (% Full Scale)	50	50	20	20	50	50
NH ₃ Flow Rate (kg/hr)	0.145	0.144	0.060	0.060	0.144	0.144

Particulate Loading and Particle Size Data

Test Date	4/23/96		4/23/96		4/24/96		4/24/96	
Test ID	4A1		4A2		4A3		4B	
Test Type	M-29		M-29		M-29		M-26	
Location	Inlet	Outlet	Inlet	Outlet	Inlet	Outlet	Inlet	Outlet
Sample Volume, DSCF	101.19	95.46	103.02	85.99	99.77	79.23	83.95	71.7
Sample Time, min	120	120	120	120	120	120	100	100
Sample Temp, F	252	98	250	99	255	98	252	99
Sample H2O, volume %	7.3	6.2	6.6	6.3	6.7	6.3	6.9	6.4
Oxygen Conc., %, dry	6.7	6.7	6.61	6.53	5.83	5.83	5.76	5.65
Particulate, grams	0.0095	0.0007	0.0078	0.0006	0.0081	0.0046	0.003	ND
Sample Flow, dscf	0.843	0.796	0.859	0.717	0.831	0.66	0.84	0.717
Particulate, mg/dscm @ 3% O2	4.2	0.3	3.3	0.3	3.4	2.4	1.5	0
Part. Removal, %		92.2		90.8		28.5		---

Particulate Loading and Particle Size Data, Continued

Test Date	5/2/96		5/7/96		5/7/96		5/8/96	
Test ID	4F		4C1		4C2		4C3	
Test Type	M-5		M-29		M-29		M-29	
Location	Inlet	Outlet	Inlet	Outlet	Inlet	Outlet	Inlet	Outlet
Sample Volume, DSCF	139.98	122.18	102.15	94.87	105.24	90.77	106.68	88.04
Sample Time, min	120	120	120	120	120	120	120	120
Sample Temp, F	254	84	251	99	250	102	253	106
Sample H2O, volume %	5.6	4.1	6.5	6.2	6.4	7	7.2	6.3
Oxygen Conc., %, dry	6.15	6.15	5.96	5.93	5.89	5.83	5.63	5.59
Particulate, grams	0.0024	0.0016	1.6445	0.0842	1.2165	0.0851	2.058	0.0905
Sample Flow, dscf	1.167	1.018	0.851	0.791	0.877	0.756	0.889	0.734
Particulate, mg/dscm @ 3% O2	0.7	0.6	680.8	37.5	486.5	39.3	798.2	42.4
Part. Removal, %		23.6		94.5		91.9		94.7

Particle Loading and Particle Size Data, Continued

Test Date	5/7/96	
Test ID	4G	
Test Type	Plate PSD	
Location	Inlet	Outlet
Sample Volume, DSCF	14.01	23.67
Sample Time, min	15	30
Sample Temp, F	254	99
Sample H2O, volume %	6.5	6.2
Oxygen Conc., %, dry	5.84	5.82
Particulate, grams	0.195	0.0217
Sample Flow, dscf	0.934	0.789
Particulate, mg/dscm @ 3% O2	583.7	38.4
Part. Removal, %		93.4

PSD Catch by Stage, grams

0	0.0356	0.0009
1	0.024	0.0006
2	0.024	0.0007
3	0.0152	0.0036
4	0.0116	0.0082
5	0.006	0.0077
6	0.0013	0.0031
7	0.0012	0.0014
Backup	0.0017	0.0014

Aerodynamic Cut Diameter by Dstage, micr

0	8.64	9.71
1	5.35	6.02
2	3.59	4.06
3	2.42	2.75
4	1.52	1.74
5	0.7	0.82
6	0.39	0.48
7	0.22	0.29
Backup	0.11	0.15

Note; Max collected size = 50 microns at inlet, 25 microns at

Test II-4C - Tabulated Metals Data.

Element	Inlet				Outlet				Vapor Phase Removal (%)	Removal Standard Deviation (%)
	Vapor Phase Element in the Inlet Flue Gas (ug/dscm)				Vapor Phase Element in the Outlet Flue Gas (ug/dscm)					
	Average	+ Deviation	-Deviation	RMS Deviation	Average	+ Deviation	-Deviation	RMS Deviation		
Arsenic	NR	NR	NR	NR	NR	NR	NR	NR	NR	NR
Barium	NR	NR	NR	NR	NR	NR	NR	NR	NR	NR
Beryllium	NR	NR	NR	NR	NR	NR	NR	NR	NR	NR
Cadmium	NR	NR	NR	NR	NR	NR	NR	NR	NR	NR
Chromium	NR	NR	NR	NR	NR	NR	NR	NR	NR	NR
Cobalt	NR	NR	NR	NR	NR	NR	NR	NR	NR	NR
Lead	NR	NR	NR	NR	NR	NR	NR	NR	NR	NR
Manganese	NR	NR	NR	NR	NR	NR	NR	NR	NR	NR
Nickel	NR	NR	NR	NR	NR	NR	NR	NR	NR	NR
Selenium	1.13	0.37	0.48	0.43	0.58	0.43	0.43	0.61	48.91	57.21
Mercury (Ionic)	1.75	0.03	0.05	0.04	2.14	0.05	0.05	0.07	-22.00	4.91
Mercury (Elem.)	NR	NR	NR	NR	NR	0.01	0.01	0.02	NR	NR
Mercury (Total)	1.92	0.03	0.05	0.04	1.92	0.03	0.05	0.04	-21.46	4.02

Element	Inlet					Outlet					Particle Phase Removal (%)	Removal Standard Deviation (%)
	Average Element in Fly Ash (ppm)	Particle Phase Element in the Flue Gas (ug/dscm)				Average Element in Fly Ash (ppm)	Particle Phase Element in the Flue Gas (ug/dscm)					
		Average	+ Deviation	-Deviation	RMS Deviation		Average	+ Deviation	-Deviation	RMS Deviation		
Arsenic	22.88	15.17	5.87	4.35	5.27	124.87	4.88	2.25	1.17	1.95	67.81	17.04
Barium	820.27	517.71	20.64	11.57	17.92	1547.35	61.43	2.76	1.78	2.43	88.13	0.62
Beryllium	0.21	NR	NR	NR	NR	2.03	NR	NR	NR	NR	NR	NR
Cadmium	0.94	0.61	0.13	0.08	0.11	23.41	0.93	0.42	0.41	0.41	-54.47	73.82
Chromium	182.33	114.86	7.25	3.77	6.28	740.05	29.32	14.80	8.36	12.85	74.48	11.27
Cobalt	36.71	23.12	1.94	2.24	2.11	144.38	5.75	0.69	0.50	0.62	75.13	3.51
Lead	38.86	24.36	0.30	0.43	0.38	106.47	4.24	0.31	0.58	0.50	82.60	2.06
Manganese	176.08	111.68	10.42	9.09	9.83	378.85	14.94	1.18	2.30	1.99	86.62	2.14
Nickel	119.63	76.44	6.99	7.86	7.46	504.46	20.18	21.83	17.60	20.05	73.60	26.35
Selenium	12.02	7.60	2.01	1.15	1.74	30.63	1.21	0.31	0.21	0.27	84.08	5.12
Mercury	3.66	2.39	0.95	0.57	0.82	15.78	0.63	0.17	0.12	0.15	73.58	11.09

Test II-4A - Tabulated Test Data.

Element	Inlet				Outlet				Vapor Phase Removal (%)	Removal Standard Deviation (%)
	Vapor Phase Element in the Inlet Flue Gas (ug/dscm)				Vapor Phase Element in the Outlet Flue Gas (ug/dscm)					
	Average	+ Deviation	-Deviation	RMS Deviation	Average	+ Deviation	-Deviation	RMS Deviation		
Arsenic	NR	NR	NR	NR	NR	NR	NR	NR	NR	NR
Barium	NR	NR	NR	NR	NR	NR	NR	NR	NR	NR
Beryllium	NR	NR	NR	NR	NR	NR	NR	NR	NR	NR
Cadmium	NR	NR	NR	NR	NR	NR	NR	NR	NR	NR
Chromium	NR	NR	NR	NR	NR	NR	NR	NR	NR	NR
Cobalt	NR	NR	NR	NR	NR	NR	NR	NR	NR	NR
Lead	NR	NR	NR	NR	NR	NR	NR	NR	NR	NR
Manganese	1.50	0.62	0.62	0.88	1.09	0.06	0.06	0.09	NR	NR
Nickel	1.44	0.02	0.02	0.03	1.90	0.04	0.05	0.04	-32.21	4.45
Selenium	7.17	1.65	1.65	2.34	0.52	0.18	0.19	0.18	92.80	3.48
Mercury (Ionic)	1.97	0.10	0.15	0.14	2.44	0.25	0.17	0.22	-23.71	14.11
Mercury (Elem.)	NR	NR	NR	NR	NR	0.01	0.01	0.01	NR	NR
Mercury (Total)	2.16	0.09	0.15	0.13	2.66	0.26	0.18	0.23	-23.04	13.07

Element	Inlet					Outlet					Particle Phase Removal (%)	Removal Standard Deviation (%)
	Average Element in Fly Ash (ppm)	Particle Phase Element in the Flue Gas (ug/dscm)				Average Element in Fly Ash (ppm)	Particle Phase Element in the Flue Gas (ug/dscm)					
		Average	+ Deviation	-Deviation	RMS Deviation		Average	+ Deviation	-Deviation	RMS Deviation		
Arsenic	450.05	1.67	0.60	0.65	0.63	2854.18	0.97	1.49	0.84	1.29	41.59	80.58
Barium	523.83	NR	NR	NR	NR	1079.77	NR	NR	NR	NR	NR	NR
Beryllium	18.12	NR	NR	NR	NR	160.56	NR	NR	NR	NR	NR	NR
Cadmium	64.21	0.24	0.09	0.15	0.13	1354.96	0.48	0.26	0.31	0.29	NR	NR
Chromium	3318.50	11.90	2.61	1.38	2.26	78101.77	28.38	27.27	14.29	23.63	-138.52	203.69
Cobalt	125.05	NR	NR	NR	NR	2387.07	NR	NR	NR	NR	NR	NR
Lead	622.32	2.18	1.03	0.91	0.98	3815.94	1.35	1.41	0.79	1.22	38.16	62.62
Manganese	2372.54	8.31	6.56	3.97	5.72	10469.49	3.67	3.88	2.25	3.37	NR	NR
Nickel	1003.89	3.80	2.35	3.38	3.00	420110.21	0.49	0.03	0.03	222.75	NR	NR
Selenium	112.54	NR	NR	NR	NR	1264.97	NR	NR	NR	NR	NR	NR
Mercury	164.22	0.59	1.23	0.05	0.71	1935.52	0.81	0.18	0.22	0.21	NR	NR

APPENDIX E

**TABULATED DATA FOR
TEST SERIES III, POWDER RIVER BASIN COAL**

Test Series	III
Fuel Analysis, wt. %	
Sample Number	C-22625
C	58.7
H ₂	4.1
S	0.4
O ₂	14.5
N ₂	1.0
H ₂ O	15.1
Cl, ppm	134.0
F, ppm	46.0
Ash	6.2
Heating Value - wet basis (J/Kg)	23.35
Heating Value - dry basis (J/Kg)	27.51
Fd (dscm/J)	2.63E-07

Coal Sample Element Concentration in ppm_m

Element	M-55194	M-55195	Average	+ dev.	- dev	det limit
Arsenic	1.76	1.41	1.59	0.18	0.18	0.20
Barium	519.00	468.00	493.50	25.50	25.50	2.00
Beryllium	0.08	0.13	0.11	0.03	0.03	0.10
Cadmium	0.10	0.08	0.09	0.01	0.01	0.02
Cobalt	1.50	1.36	1.43	0.07	0.07	0.40
Chromium	9.56	8.96	9.26	0.30	0.30	0.20
Manganese	25.80	30.60	28.20	2.40	2.40	0.20
Nickel	17.00	9.27	13.14	3.87	3.87	0.40
Lead	2.74	3.35	3.05	0.31	0.31	0.20
Selenium	0.11	0.13	0.12	0.01	0.01	0.20
Mercury	0.45	0.37	0.41	0.04	0.04	0.02

		SO ₂	SO ₂	SO ₂	SO ₂	SO ₂	SO ₂	SO ₂	SO ₂
Test Type		III-1	III-9	III-10	III-17	III-15R	III-16	III-8	III-7
Test ID									
Date		09/04/96	09/04/96	09/04/96	09/06/96	09/10/96	09/06/96	09/04/96	09/04/96
Time		10:53 AM	5:16 PM	5:41 PM	4:35 PM	9:36 AM	4:14 PM	4:25 PM	3:44 PM
Flue Gas Inlet									
Flow Rate	(kg/min)	38.3	35.6	34.9	39.0	38.2	37.0	35.5	34.8
Gas Velocity	(m/s)	12.4	11.5	11.2	12.6	12.3	11.9	11.5	11.3
Temperature	(°C)	124.9	123.9	123.5	123.2	120.3	123.1	125.2	125.8
O ₂ ⁽¹⁾	(%)	7.20	6.98	6.77	6.71	7.03	6.49	6.86	6.69
SO ₂ ⁽²⁾	(ppm _v)	293	359	332	360	354	354	359	355
Humidity	(gm/gm)	0.050	0.051	0.052	0.052	0.051	0.053	0.051	0.052
Flue Gas									
Interstage Temperature	(°C)	62.1	56.4	56.0	63.6	57.2	55.7	57.8	56.1
Outlet Temperature	(°C)	42.3	40.8	40.9	38.9	38.1	38.4	40.8	41.1
SO ₂ Removal	(%)	-13.7	94.0	94.8	71.8	15.3	97.8	35.1	67.7
Cooling Water									
Flow Rate	(kg/min)	34.0	33.6	33.6	34.2	34.8	34.0	33.7	33.7
Inlet Temperature	(°C)	31.1	33.8	33.8	23.3	22.5	23.3	34.0	34.0
Interstage Temperature	(°C)	39.1	39.9	39.9	36.3	34.8	36.6	40.0	40.3
Outlet Temperature	(°C)	56.6	55.0	54.8	52.9	52.6	52.6	55.5	55.7
Reagent									
L/G Ratio	(l/m ³)	0.001	0.202	0.396	-0.002	0.043	0.169	0.186	0.365
Temperature	(°C)	25.2	42.6	42.7	44.5	23.6	43.7	42.3	42.7
Supply pH	(-)	7.59	8.22	8.28	6.75	6.40	6.69	6.72	6.71
Return pH	(-)	2.68	7.16	7.61	5.07	3.36	6.14	4.45	4.48
Fresh Water Flow	(kg/min)	0.00	0.76	0.76	0.00	0.00	0.01	0.76	0.76
Blow Down Flow	(kg/min)	0.21	0.72	0.72	0.32	0.51	0.00	0.70	0.76
Energy									
Stage 1 Recovery	(kw)	41.5	35.6	34.9	39.4	43.2	38.0	36.4	36.2
Stage 2 Recovery	(kw)	18.9	14.2	14.3	31.2	29.8	31.6	14.2	14.7
Overall Energy Balance	(%)	26.7	1.4	2.0	7.6	12.0	7.3	0.3	3.6

1) Dry basis

2) Dry basis, corrected to 3% O₂

		SO ₂	SO ₂	SO ₂	SO ₂	SO ₂	SO ₂	SO ₂	SO ₂
Test Type									
Test ID		III-15	III-14	III-6	III-5	III-4	III-3	III-2	III-11
Date		09/06/96	09/12/96	09/04/96	09/04/96	09/04/96	09/04/96	09/04/96	09/11/96
Time		3:55 PM	5:16 PM	3:08 PM	2:33 PM	1:51 PM	1:06 PM	12:10 PM	4:25 PM
Flue Gas Inlet									
Flow Rate	(kg/min)	36.5	20.7	35.0	35.7	35.9	35.1	35.3	20.9
Gas Velocity	(m/s)	11.8	6.9	11.3	11.5	11.6	11.4	11.4	7.0
Temperature	(°C)	123.2	123.4	125.3	124.5	124.5	125.5	125.9	126.2
O ₂ ⁽¹⁾	(%)	6.63	7.06	6.80	7.36	6.86	6.70	6.75	6.77
SO ₂ ⁽²⁾	(ppm _v)	349	420	338	328	349	376	416	421
Humidity	(gm/gm)	0.052	0.052	0.051	0.050	0.051	0.052	0.051	0.053
Flue Gas									
Interstage Temperature	(°C)	55.3	56.4	55.9	59.4	57.2	55.4	55.3	54.1
Outlet Temperature	(°C)	38.4	41.0	41.0	41.0	41.1	41.5	41.7	40.3
SO ₂ Removal	(%)	99.3	90.7	46.2	45.6	41.0	37.9	21.5	96.8
Cooling Water									
Flow Rate	(kg/min)	34.3	17.8	33.7	33.5	33.8	33.8	33.7	16.8
Inlet Temperature	(°C)	23.3	36.4	33.9	34.5	33.8	34.2	33.9	34.1
Interstage Temperature	(°C)	36.4	38.7	40.3	40.2	40.4	40.5	40.4	39.0
Outlet Temperature	(°C)	52.3	58.5	55.5	55.8	56.1	56.4	56.6	59.9
Reagent									
L/G Ratio	(l/m ³)	0.445	0.463	0.371	0.186	0.195	0.374	0.385	0.789
Temperature	(°C)	42.3	41.7	42.4	42.2	42.5	42.8	42.7	39.6
Supply pH	(-)	6.63	7.16	5.56	5.39	4.15	3.90	3.73	8.20
Return pH	(-)	6.34	6.70	3.47	3.03	2.79	2.73	2.07	7.31
Fresh Water Flow	(kg/min)	0.01	0.41	0.73	0.72	0.70	0.69	0.72	2.79
Blow Down Flow	(kg/min)	0.36	0.30	0.67	0.66	0.73	0.67	0.82	0.23
Energy									
Stage 1 Recovery	(kw)	38.1	24.6	35.7	36.4	37.0	37.4	38.1	24.5
Stage 2 Recovery	(kw)	31.4	2.9	15.0	13.2	15.5	15.0	15.3	5.8
Overall Energy Balance	(%)	9.3	0.3	3.1	4.7	6.8	9.9	13.4	-5.1

1) Dry basis

2) Dry basis, corrected to 3% O₂

Test Type		M-26	OH	M-29	OH	OH	M-29	OH
Test ID		III-7A	III-9A1	III-9A2	III-9A3	III-12A1	III-12A2	III-12A3
Date		09/06/96	09/05/96	09/05/96	09/06/96	09/11/96	09/12/96	09/12/96
Time		2:14 PM	11:40 AM	4:46 PM	10:36 AM	11:44 AM	11:33 AM	2:39 PM
Flue Gas Inlet								
Flow Rate	(kg/min)	36.4	36.0	35.6	36.2	21.6	21.0	21.5
Gas Velocity	(m/s)	11.7	11.5	11.5	11.6	7.2	7.0	7.1
Temperature	(°C)	124.2	121.7	124.3	123.9	123.4	121.2	121.2
O ₂ ⁽¹⁾	(%)	6.77	6.82	6.77	6.47	7.14	7.00	7.22
SO ₂ ⁽²⁾	(ppm _v)	370	308	338	329	418	423	411
Humidity	(gm/gm)	0.051	0.051	0.051	0.052	0.052	0.052	0.052
Flue Gas								
Interstage Temperature	(°C)	56.5	55.9	57.7	55.6	56.2	53.9	55.8
Outlet Temperature	(°C)	41.7	42.6	42.1	41.8	41.9	40.9	41.2
SO ₂ Removal	(%)	96.4	97.4	99.7	97.0	91.6	88.2	89.6
Cooling Water								
Flow Rate	(kg/min)	33.4	34.7	35.5	33.6	16.8	17.7	17.7
Inlet Temperature	(°C)	34.7	37.7	33.4	34.3	37.5	36.1	36.3
Interstage Temperature	(°C)	40.3	41.3	40.7	40.5	40.0	38.9	39.4
Outlet Temperature	(°C)	55.9	56.5	55.3	56.4	61.0	58.5	58.8
Reagent								
L/G Ratio	(l/m ³)	0.384	0.347	0.367	0.368	0.355	0.355	0.364
Temperature	(°C)	43.0	43.6	44.1	43.4	41.8	41.4	41.8
Supply pH	(-)	6.54	8.27	8.28	8.24	8.19	8.26	8.25
Return pH	(-)	6.16	7.78	7.55	7.72	7.89	7.04	7.30
Fresh Water Flow	(kg/min)	0.72	0.72	0.72	0.73	0.37	0.41	0.40
Blow Down Flow	(kg/min)	0.68	0.62	0.76	0.84	0.35	0.46	0.44
Energy								
Stage 1 Recovery	(kw)	36.1	36.7	36.1	37.4	24.6	24.2	23.9
Stage 2 Recovery	(kw)	13.3	8.8	18.0	14.4	3.0	3.5	3.7
Overall Energy Balance	(%)	7.0	14.3	20.5	10.6	6.7	1.2	3.4

1) Dry basis

2) Dry basis, corrected to 3% O₂

		Test Type	NH ₃	NH ₃	NH ₃	NH ₃	NH ₃	PSD
		Test ID	III-18-IN	III-18-OUT	III-7B-IN	III-7BOUT	III-9B	III-12B
		Date	09/10/96	09/10/96	09/10/96	09/10/96	09/10/96	09/11/96
		Time	12:42 PM	1:08 PM	2:59 PM	2:34 PM	4:05 PM	2:39 PM
Flue Gas Inlet								
Flow Rate	(kg/min)		36.0	35.9	36.3	36.5	36.2	21.1
Gas Velocity	(m/s)		11.5	11.5	11.6	11.7	11.6	7.1
Temperature	(°C)		121.9	122.0	122.4	122.1	122.6	125.3
O ₂ ⁽¹⁾	(%)		6.38	6.59	6.80	6.98	7.10	6.91
SO ₂ ⁽²⁾	(ppm _v)		364	374	386	393	409	416
Humidity	(gm/gm)		0.053	0.052	0.051	0.051	0.050	0.052
Flue Gas								
Interstage Temperature	(°C)		54.0	53.6	59.5	58.2	59.1	57.7
Outlet Temperature	(°C)		38.1	38.0	42.5	42.4	42.4	41.8
SO ₂ Removal	(%)		100.7	102.8	97.2	97.7	100.2	93.7
Cooling Water								
Flow Rate	(kg/min)		35.3	35.6	33.8	33.7	33.8	18.1
Inlet Temperature	(°C)		22.9	23.0	36.9	36.9	36.8	36.7
Interstage Temperature	(°C)		35.9	35.9	41.2	41.0	41.1	40.3
Outlet Temperature	(°C)		52.4	52.2	57.1	57.1	57.0	59.9
Reagent								
L/G Ratio	(l/m ³)		0.398	0.370	0.331	0.338	0.346	0.439
Temperature	(°C)		42.4	42.3	43.2	42.9	43.1	42.5
Supply pH	(-)		7.98	7.92	6.95	6.78	8.22	8.21
Return pH	(-)		7.25	7.37	6.33	6.35	7.90	7.43
Fresh Water Flow	(kg/min)		0.00	0.00	0.77	0.77	0.77	0.37
Blow Down Flow	(kg/min)		0.45	0.44	0.76	0.71	0.75	0.36
Energy								
Stage 1 Recovery	(kw)		40.6	40.6	37.6	37.8	37.4	24.8
Stage 2 Recovery	(kw)		32.1	32.1	10.2	9.7	10.1	4.6
Overall Energy Balance	(%)		12.1	12.4	15.4	15.6	16.9	8.7

1) Dry basis

2) Dry basis, corrected to 3% O₂

Test Series III Ammonia Data

Test ID	III-18-IN	III-18-OUT	III-7B-OUT	III-7B-IN	III-9B-IN	III-9B-OUT
Date	9/10/96	9/10/96	9/10/96	9/10/96	9/10/96	9/10/96
Time	12:42 PM	1:08 PM	2:34 PM	2:59 PM	3:44 PM	4:26 PM
Gas Temperature @ Module 2 Outlet (°C)	38.13	37.95	42.27	42.34	42.34	42.18
Flue Gas NH ₃ as Particulate (ppm _v , M-26A)	83.8	19.7	4.1	30.8	27.9	0.0
Flue Gas NH ₃ as Vapor (ppm _v , M-26A)					0.1	0.3
Flue Gas NH ₃ Total (ppm _v , M-26A)					38.5	29.2
Flue Gas NH ₃ Total (Gas Analyzer, ppm _v)					38.6	29.5
Flue Gas NH ₃ Injected (ppm _v)	114.3	114.3	46.5	46.5	112.7	112.7
Rotameter Temp (°C)	24.9	26.8	25.7	33.6	30.2	29.0
Rotameter Reading (% Full Scale)	50	50	20	20	50	50
NH ₃ Flow Rate (kg/hr)	0.142	0.142	0.059	0.058	0.141	0.141

Particle Loading and Particle Size Data

Test Date	9/5/96		9/5/96		9/6/96		9/6/96		9/10/96	
Test ID	9A1		9A2		9A3		7A		9B	
Test Type	M-OH		M-29		M-OH		M-26		M-5	
Location	Inlet	Outlet	Inlet	Outlet	Inlet	Outlet	Inlet	Outlet	Inlet	Outlet
Sample Volume, DSCF	84.61	88.54	87.98	91.46	87.26	89.58	87.48	92.76	55.82	58.41
Sample Time, min	120	120	120	120	120	120	120	120	80	80
Sample Temp, F	246	110	252	108	252	107	251	109	247	109
Sample H2O, volume %	8.7	8.7	8.5	9	9	8.4	8.5	8.4	8.4	8.5
Oxygen Conc., %, dry	6.66	6.81	6.68	6.75	6.34	6.47	6.6	6.7	7	7
Particulate, grams	0.9606	0.1121	0.9642	0.1214	0.8892	0.1019	0.9549	0.1134	0.59	0.0636
Sample Flow, dscf	0.705	0.738	0.733	0.762	0.727	0.747	0.729	0.773	0.698	0.73
Particulate, mg/dscm @ 3% O2	503.6	56.8	486.8	59.3	442.1	49.8	482.2	54.4	480.3	49.5
Part. Removal, %		88.7		87.8		88.7		88.7		89.7

Particle Loading and Particle Size Data, Continued

Test Date	9/11/96		9/11/96		9/12/96		9/12/96	
Test ID	12C		12A1		12A2		12A3	
Test Type	M-5, INT		M-OH		M-29		M-OH	
Location	Inter	Outlet	Inlet	Outlet	Inlet	Outlet	Inlet	Outlet
Sample Volume, DSCF	42.5	---	55.83	56.38	52.73	59.87	61.83	61.75
Sample Time, min	120	---	120	120	120	120	120	120
Sample Temp, F	129	---	254	108	254	106	254	107
Sample H2O, volume %	9.1	---	8.6	8.3	9	8	8.5	8.1
Oxygen Conc., %, dry	7	---	6.95	7.1	6.77	6.97	7.01	7.22
Particulate, grams	0.1142	---	0.5008	0.1201	0.4358	0.1012	0.5116	0.1122
Sample Flow, dscf	0.354	---	0.465	0.47	0.439	0.499	0.515	0.515
Particulate, mg/dscm @ 3% O2	122.1	---	406.2	97.5	369.5	76.6	376.3	83.9
Part. Removal, %		---		76		79.3		77.7

Particle Loading and Particle Size Data, Continued

Test Date	9/11/96		9/11/96		9/11/96	
Test ID	12D-1		12D-2		12B	
Test Type	Plate PSD, INT		Plate PSD, INT		Plate PSD	
Location	Inlet	Inter	Inter	Outlet	Inlet	Outlet
Sample Volume, DSCF	20.404	25.665	25.665	33.45	20.404	33.45
Sample Time, min	45	60	60	70	45	70
Sample Temp, F	250	141	141	108	250	108
Sample H2O, volume %	8.6	8.6	8.6	8.3	8.6	8.3
Oxygen Conc., %, dry	6.7	6.7	6.7	6.9	6.7	6.9
Particulate, grams	0.186	0.0704	0.07	0.0723	0.186	0.0723
Sample Flow, dscf	0.453	0.428	0.428	0.478	0.453	0.478
Particulate, mg/dscm @ 3% O2	406.2	122.1	122.1	97.5	406.2	97.5
Part. Removal, %		69.9		20.1		76

PSD Catch by Stage, grams

0	0.017	0.0147	0.0147	0.0015	0.017	0.0015
1	0.0097	0.0064	0.0064	0.0013	0.0097	0.0013
2	0.0151	0.0057	0.0057	0.0026	0.0151	0.0026
3	0.0158	0.0081	0.0081	0.0075	0.0158	0.0075
4	0.015	0.0119	0.0119	0.0125	0.015	0.0125
5	0.0136	0.0124	0.0124	0.0144	0.0136	0.0144
6	0.006	0.0082	0.0082	0.009	0.006	0.009
7	0.002	0.0033	0.0033	0.0029	0.002	0.0029
Backup	0.0027	0.0034	0.0034	0.003	0.0027	0.003

Aerodynamic Cut Diameter by Dstage, microns

0	12.06	12.85	12.85	12.25	12.06	12.25
1	7.48	7.98	7.98	7.61	7.48	7.61
2	5.04	5.39	5.39	5.13	5.04	5.13
3	3.41	3.66	3.66	3.48	3.41	3.48
4	2.15	2.32	2.32	2.21	2.15	2.21
5	1.02	1.11	1.11	1.06	1.02	1.06
6	0.59	0.66	0.66	0.63	0.59	0.63
7	0.36	0.42	0.42	0.4	0.36	0.4
Backup	0.18	0.21	0.21	0.2	0.18	0.2

Note; Max collected size = 50 microns at inlet, 25 microns at outlet

Test III-12A Tabulated Metals Data.

Element	Inlet				Outlet				Vapor Phase Removal (%)	Removal Standard Deviation (%)
	Vapor Phase Element in the Inlet Flue Gas (ug/dscm)				Vapor Phase Element in the Outlet Flue Gas (ug/dscm)					
	Average	+ Deviation	-Deviation	RMS Deviation	Average	+ Deviation	-Deviation	RMS Deviation		
Arsenic	NR	NR	NR	NR	NR	NR	NR	NR	NR	NR
Barium	NR	NR	NR	NR	NR	NR	NR	NR	NR	NR
Beryllium	NR	NR	NR	NR	NR	NR	NR	NR	NR	NR
Cadmium	NR	NR	NR	NR	NR	NR	NR	NR	NR	NR
Chromium	NR	NR	NR	NR	NR	NR	NR	NR	NR	NR
Cobalt	NR	NR	NR	NR	NR	NR	NR	NR	NR	NR
Lead	NR	NR	NR	NR	NR	NR	NR	NR	NR	NR
Manganese	NR	NR	NR	NR	NR	NR	NR	NR	NR	NR
Nickel	NR	NR	NR	NR	NR	NR	NR	NR	NR	NR
Selenium	NR	NR	NR	NR	NR	NR	NR	NR	NR	NR
Mercury (Ionic)	22.58	2.94	4.71	4.12	5.19	0.64	0.64	0.91	77.00	5.82
Mercury (Elem.)	9.99	1.14	0.90	1.04	12.96	1.23	1.23	1.74	-29.68	22.09
Mercury (Total)	32.57	2.92	5.61	4.86	32.57	2.92	5.61	4.86	44.27	11.64

Element	Inlet					Outlet					Particle Phase Removal (%)	Removal Standard Deviation (%)
	Average Element in Fly Ash (ppm)	Particle Phase Element in the Flue Gas (ug/dscm)				Average Element in Fly Ash (ppm)	Particle Phase Element in the Flue Gas (ug/dscm)					
		Average	+ Deviation	-Deviation	RMS Deviation		Average	+ Deviation	-Deviation	RMS Deviation		
Arsenic	21.60	7.46	1.30	1.27	1.29	40.77	3.64	1.62	2.81	2.44	51.16	33.79
Barium	14193.33	4845.99	399.35	281.10	355.30	23348.33	2011.17	280.57	203.57	251.08	58.50	6.01
Beryllium	0.17	NR	NR	NR	NR	0.73	NR	NR	NR	NR	NR	NR
Cadmium	2.51	0.85	0.04	0.05	0.05	9.67	0.82	0.09	0.06	0.08	4.15	10.76
Chromium	225.67	71.37	38.40	22.30	33.40	162.67	13.70	5.32	5.22	5.27	80.81	11.63
Cobalt	54.60	18.51	0.25	0.29	0.27	62.19	5.38	0.91	1.04	0.98	70.93	5.31
Lead	129.21	43.75	0.13	0.20	0.17	256.53	21.99	1.26	1.62	1.47	49.73	3.37
Manganese	463.00	158.10	17.48	9.03	15.14	524.00	45.32	9.82	5.13	8.51	71.33	6.04
Nickel	365.00	112.44	85.14	49.52	74.06	1034.33	92.80	69.32	39.65	60.24	NR	NR
Selenium	11.10	3.56	1.48	0.86	1.28	19.88	1.68	0.15	0.20	0.18	52.83	17.76
Mercury	3.17	1.14	0.33	0.49	0.43	7.33	0.64	0.17	0.24	0.21	43.82	28.20

Test III-9A - Tabulated Metals Data.

Element	Inlet				Outlet				Vapor Phase Removal (%)	Removal Standard Deviation (%)
	Vapor Phase Element in the Inlet Flue Gas (ug/dscm)				Vapor Phase Element in the Outlet Flue Gas (ug/dscm)					
	Average	+ Deviation	-Deviation	RMS Deviation	Average	+ Deviation	-Deviation	RMS Deviation		
Arsenic	NR	NR	NR	NR	NR	NR	NR	NR	NR	NR
Barium	NR	NR	NR	NR	NR	NR	NR	NR	NR	NR
Beryllium	NR	NR	NR	NR	NR	NR	NR	NR	NR	NR
Cadmium	NR	NR	NR	NR	NR	NR	NR	NR	NR	NR
Chromium	NR	NR	NR	NR	NR	NR	NR	NR	NR	NR
Cobalt	NR	NR	NR	NR	NR	NR	NR	NR	NR	NR
Lead	NR	NR	NR	NR	NR	NR	NR	NR	NR	NR
Manganese	1.46	NR	NR	NR	0.23	NR	NR	NR	84.26	NR
Nickel	NR	NR	NR	NR	NR	NR	NR	NR	NR	NR
Selenium	1.29	NR	NR	NR	2.18	NR	NR	NR	-69.46	NR
Mercury (Ionic)	16.69	4.44	5.60	5.12	2.52	1.56	1.08	1.39	84.89	9.51
Mercury (Elem.)	7.39	2.76	1.49	2.39	10.44	1.06	1.74	1.52	-41.35	50.16
Mercury (Total)	24.08	3.92	7.09	6.15	12.97	2.63	2.82	2.73	46.16	17.82

Element	Inlet					Outlet					Particle Phase Removal (%)	Removal Standard Deviation (%)
	Average Element in Fly Ash (ppm)	Particle Phase Element in the Flue Gas (ug/dscm)				Average Element in Fly Ash (ppm)	Particle Phase Element in the Flue Gas (ug/dscm)					
		Average	+ Deviation	-Deviation	RMS Deviation		Average	+ Deviation	-Deviation	RMS Deviation		
Arsenic	26.68	13.12	7.46	5.20	6.62	19.61	1.03	0.94	0.85	0.90	NR	NR
Barium	13228.00	6538.57	773.71	1224.21	1072.45	29298.67	1631.72	565.55	288.05	489.81	75.04	8.54
Beryllium	0.13	NR	NR	NR	NR	0.78	NR	NR	NR	NR	NR	NR
Cadmium	2.18	1.08	0.14	0.21	0.19	15.71	0.88	0.55	0.30	0.48	18.27	46.42
Chromium	177.67	88.01	22.31	13.70	19.49	82.67	4.82	8.34	4.76	7.25	94.52	8.32
Cobalt	44.16	21.84	2.89	3.74	3.39	48.78	2.70	1.36	1.38	1.37	87.64	6.57
Lead	95.84	47.38	3.27	5.92	5.14	204.22	11.22	3.57	5.03	4.48	76.33	9.80
Manganese	463.67	229.34	31.10	48.73	42.74	517.33	28.78	13.50	10.43	12.26	87.45	5.83
Nickel	170.67	84.53	20.75	14.16	18.37	261.33	14.67	3.11	5.71	4.95	82.64	6.96
Selenium	9.37	4.64	1.19	1.14	1.17	37.18	2.03	0.31	0.61	0.53	56.13	15.84
Mercury	1.12	0.55	0.06	0.04	0.05	6.78	0.36	0.20	0.25	0.23	33.85	41.95

APPENDIX F

**TABULATED DATA FOR
TEST SERIES IV, OHIO #6/#5 COAL**

Test Series	IV
Fuel Analysis, wt. %	
Sample Number	C-22882
C	75.6
H ₂	5.2
S	3.1
O ₂	8.8
N ₂	1.4
H ₂ O	2.8
Cl, ppm	1900.0
F, ppm	25.6
Ash	5.1
Heating Value - wet basis (J/Kg)	30.96
Heating Value - dry basis (J/Kg)	31.86
Fd (dscm/J)	2.67E-07

Coal Sample Element Concentration in ppm_m

Element	C-22911	det limit
Arsenic	7.47	0.20
Barium	3.85	2.00
Beryllium	0.83	0.10
Cadmium	0.19	0.02
Cobalt	0.53	0.40
Chromium	1.23	0.20
Manganese	6.19	0.20
Nickel	42.70	0.40
Lead	6.01	0.20
Selenium	1.90	0.20
Mercury	0.13	0.02

		LIME							
		SO ₂	SO ₂	SO ₂	SO ₂	SO ₂	SO ₂	SO ₂	SO ₂
		IV-9	IV-8	IV-10	IV-6	IV-3	IV-7	IV-5	IV-4
		03/04/97	03/04/97	03/04/97	03/04/97	03/04/97	03/04/97	03/04/97	03/04/97
Flue Gas Inlet	Test Type								
	Test ID								
	Date								
	Time								
Flow Rate	(kg/min)	35.9	36.5	36.1	36.2	36.5	37.1	33.9	39.3
Gas Velocity	(m/s)	11.3	11.6	11.4	11.5	11.6	11.8	10.8	12.5
Temperature	(°C)	117.5	123.2	121.6	123.7	123.7	124.1	124.0	124.6
O ₂ ⁽¹⁾	(%)	6.92	6.87	7.00	7.01	7.16	6.96	7.32	6.78
SO ₂ ⁽²⁾	(ppm _v)	2174	2349	2295	2311	2311	2349	2246	2214
Humidity	(gm/gm)	0.033	0.033	0.033	0.033	0.033	0.033	0.033	0.033
Flue Gas									
Interstage Temperature	(°C)	51.8	49.8	48.9	52.8	49.4	49.3	50.1	50.2
Outlet Temperature	(°C)	35.8	35.6	35.1	33.7	33.9	33.0	33.4	34.9
SO ₂ Removal	(%)	19.5	33.7	40.8	25.5	34.1	40.0	33.7	50.0
Cooling Water									
Flow Rate	(kg/min)	32.2	32.5	32.6	33.2	33.0	33.3	33.1	33.0
Inlet Temperature	(°C)	23.6	21.8	21.1	16.1	17.6	15.5	15.7	18.7
Interstage Temperature	(°C)	33.5	33.3	32.9	31.5	31.3	30.3	31.3	32.8
Outlet Temperature	(°C)	50.6	51.3	50.4	50.2	50.1	49.1	49.4	50.7
Reagent									
L/G Ratio	(l/m ³)	0.469	0.668	0.908	0.506	0.703	0.863	0.552	0.812
Temperature	(°C)	39.2	38.9	38.7	38.8	38.1	36.9	38.2	38.4
Supply pH	(-)	6.29	6.24	6.26	7.64	8.03	7.86	9.73	9.33
Return pH	(-)	3.61	3.71	3.67	3.57	3.73	3.86	3.82	3.92
Fresh Water Flow	(kg/min)	0.00	0.46	0.00	0.42	0.41	0.80	0.81	0.79
Blow Down Flow	(kg/min)	0.29	0.84	0.34	0.92	1.09	2.65	3.22	3.17
Energy									
Stage 1 Recovery	(kw)	38.4	40.8	39.8	43.3	43.2	43.8	41.7	41.2
Stage 2 Recovery	(kw)	22.3	26.0	26.9	35.7	31.7	34.4	35.9	32.5
Overall Energy Balance	(%)	33.1	32.3	32.3	33.4	30.9	27.8	36.4	28.0

1) Dry basis

2) Dry basis, corrected to 3% O₂

Test Type Test ID Date Time		MAG-LIME							
		SO ₂	SO ₂	SO ₂	SO ₂	SO ₂	M-29/OH	M-29/OH	M-29/OH
		IV-14R1	IV-15	IV-16	IV-13	IV-12	IV-14A1	IV-14A2	IV-14A3
		03/10/97	03/10/97	03/10/97	03/10/97	03/10/97	03/07/97	03/07/97	03/10/97
Flue Gas Inlet									
Flow Rate	(kg/min)	36.7	37.5	37.3	36.8	34.8	35.5	36.1	36.9
Gas Velocity	(m/s)	11.5	11.8	11.7	11.6	10.9	11.2	11.4	11.7
Temperature	(°C)	117.2	119.1	118.9	118.8	118.3	123.9	122.6	122.6
O ₂ ⁽¹⁾	(%)	7.47	7.47	7.36	7.63	7.13	6.65	6.76	6.87
SO ₂ ⁽²⁾	(ppm _v)	2172	2191	2188	2207	2125	2194	2236	2307
Humidity	(gm/gm)	0.032	0.032	0.032	0.032	0.033	0.034	0.033	0.033
Flue Gas									
Interstage Temperature	(°C)	52.1	50.4	48.7	51.3	54.1	56.3	58.2	53.5
Outlet Temperature	(°C)	33.8	34.0	33.4	33.8	34.1	33.9	33.6	34.0
SO ₂ Removal	(%)	76.3	83.2	88.6	84.9	80.0	81.9	80.2	76.3
Cooling Water									
Flow Rate	(kg/min)	32.4	32.4	32.4	32.4	32.4	32.6	33.0	32.7
Inlet Temperature	(°C)	25.6	25.7	24.6	25.4	25.4	23.8	23.0	24.4
Interstage Temperature	(°C)	32.0	32.2	31.2	32.2	32.4	32.3	32.0	32.3
Outlet Temperature	(°C)	48.0	47.9	46.9	48.0	48.2	49.7	48.7	49.5
Reagent									
L/G Ratio	(l/m ³)	0.465	0.679	0.882	0.684	0.484	0.488	0.467	0.504
Temperature	(°C)	35.0	35.0	34.7	35.2	35.0	35.9	35.8	35.6
Supply pH	(-)	11.25	11.24	11.53	11.53	11.39	11.51	11.60	11.65
Return pH	(-)	5.71	6.89	6.47	7.89	8.91	6.33	6.78	6.56
Fresh Water Flow	(kg/min)	1.46	1.42	1.46	1.42	1.42	1.49	1.30	1.48
Blow Down Flow	(kg/min)	2.18	2.17	2.54	2.01	1.85	2.04	1.86	2.11
Energy									
Stage 1 Recovery	(kw)	36.3	35.4	35.5	35.6	35.6	39.7	38.6	39.3
Stage 2 Recovery	(kw)	14.5	14.7	14.9	15.5	15.8	19.3	20.7	18.0
Overall Energy Balance	(%)	7.4	3.2	-0.4	6.5	11.9	11.9	10.8	8.4

1) Dry basis

2) Dry basis, corrected to 3% O₂

		SODIUM				
		M-26	M-5	PSD	PSD	
		Test ID	IV-1A	IV-2A	IV-1B	IV-2B
		Date	02/27/97	02/28/97	02/27/97	02/28/97
Flue Gas Inlet		Time	1:15 PM	11:05 AM	4:30 PM	1:55 PM
Flow Rate	(kg/min)	35.4	21.6	34.8	22.2	
Gas Velocity	(m/s)	11.1	7.0	11.0	7.2	
Temperature	(°C)	117.5	123.0	116.6	123.5	
O ₂ ⁽¹⁾	(%)	7.41	7.17	7.33	7.33	
SO ₂ ⁽²⁾	(ppm _v)	2285	2364	2250	2283	
Humidity	(gm/gm)	0.032	0.033	0.033	0.033	

Flue Gas

Interstage Temperature	(°C)	47.6	55.7	46.7	58.5
Outlet Temperature	(°C)	33.9	34.0	33.5	34.2
SO ₂ Removal	(%)	97.5	88.6	97.6	85.8

Cooling Water

Flow Rate	(kg/min)	32.3	17.2	32.9	17.4
Inlet Temperature	(°C)	25.6	19.2	26.2	19.1
Interstage Temperature	(°C)	32.4	33.2	31.4	33.7
Outlet Temperature	(°C)	49.1	58.2	47.8	57.2

Reagent

L/G Ratio	(l/m ³)	0.522	0.466	0.543	0.463
Temperature	(°C)	37.5	38.5	36.8	38.6
Supply pH	(-)	8.00	7.96	8.05	8.37
Return pH	(-)	7.38	7.25	7.37	7.60
Fresh Water Flow	(kg/min)	1.41	0.68	1.53	0.98
Blow Down Flow	(kg/min)	1.61	0.91	2.01	1.20

Energy

Stage 1 Recovery	(kw)	37.8	30.0	37.6	28.5
Stage 2 Recovery	(kw)	15.3	16.8	11.9	17.7
Overall Energy Balance	(%)	14.3	36.4	5.7	35.0

1) Dry basis

2) Dry basis, corrected to 3% O₂

Particulate Loading and Particle Size Data

Test Date	2/27/97		2/28/97		2/28/97		2/28/97		2/28/97	
Test ID	1A		2A		14A1		14A2		14A3	
Test Type	M-26		M-5		M-OH		M-29		M-OH	
Location	Inlet	Outlet	Inlet	Outlet	Inlet	Outlet	Inlet	Outlet	Inlet	Outlet
Sample Volume, DSCF	83.07	87.51	50.66	44.21	89.9	92.05	91.12	90.46	91.14	89.85
Sample Time, min	120	123	80	80	120	120	120	120	120	120
Sample Temp, F	239	96	253	95	252	95	250	67	250	95
Sample H2O, volume %	6.21	5.43	6.2	5.2	6.27	5.46	6.2	5.49	6.26	5.64
Oxygen Conc., %, dry	7.4	7.4	6.2	6.2	6.65	6.65	6.76	6.76	6.87	6.87
Particulate, grams	0.0714	0.0043	0.5229	0.0318	0.5833	0.0338	0.6353	0.0318	0.5863	0.0225
Sample Flow, dscf	0.692	0.711	0.633	0.553	0.749	0.767	0.759	0.754	0.76	0.749
Particulate, mg/dscm @ 3% O2	40.2	2.3	443.6	30.9	287.6	16.3	311.5	15.7	289.6	11.3
Part. Removal, %		94.3		93		94.3		95		96.1

Particulate Loading and Particle Size Data, Continued

Test Date	2/27/97		2/28/97	
	1B		2B	
	Plate PSD		Plate PSD	
Location	Inlet	Outlet	Inlet	Outlet
Sample Volume, DSCF	41.65	43.65	37.76	33.89
Sample Time, min	60	60	60	60
Sample Temp, F	243	95	255	95
Sample H2O, volume %	6.2	5.4	6.2	5.2
Oxygen Conc., %, dry	7.6	7.2	7.1	7.1
Particulate, grams	0.035	0.0022	0.366	0.0229
Sample Flow, dscf	0.694	0.728	0.629	0.565
Particulate, mg/dscm @ 3% O2	40.2	2.3	443.6	30.9
Part. Removal, %		94.3		93

PSD Catch by Stage, grams

0	0.01392	0.00123	0.08405	0.00134
1	0.01281	0.00078	0.05619	0.00067
2	0.01457	0.00118	0.05338	0.00141
3	0.00677	0.00093	0.02912	0.00405
4	0.00434	0.00109	0.01789	0.00532
5	0.00159	0.00129	0.0098	0.00537
6	0.002	0.00332	0.00304	0.00201
7	0.00131	0.00116	0.00145	0.00158
Backup	0.00213	0.00143	0.00385	0.00327

Aerodynamic Cut Diameter by Dstage, microns

0	10.02	10.12	10.44	11.56
1	6.21	6.28	6.47	7.18
2	4.18	4.23	4.35	4.84
3	2.82	2.87	2.94	3.29
4	1.77	1.81	1.85	2.08
5	0.83	0.86	0.87	1
6	0.47	0.5	0.49	0.59
7	0.28	0.31	0.29	0.37
Backup	0.14	0.15	0.15	0.19

Note; Max collected size = 50 microns at inlet, 25 microns at

Test IV-14A - Tabulated Metals Data

Element	Inlet				Outlet				Vapor Phase Removal (%)	Removal Standard Deviation (%)
	Vapor Phase Element in the Inlet Flue Gas (ug/dscm)				Vapor Phase Element in the Outlet Flue Gas (ug/dscm)					
	Average	+ Deviation	-Deviation	RMS Deviation	Average	+ Deviation	-Deviation	RMS Deviation		
Arsenic	22.38	NR	NR	NR	0.20	NR	NR	NR	99.09	NR
Barium	NR	NR	NR	NR	NR	NR	NR	NR	NR	NR
Beryllium	NR	NR	NR	NR	NR	NR	NR	NR	NR	NR
Cadmium	NR	NR	NR	NR	NR	NR	NR	NR	NR	NR
Chromium	9.41	NR	NR	NR	0.22	NR	NR	NR	97.65	NR
Cobalt	NR	NR	NR	NR	NR	NR	NR	NR	NR	NR
Lead	NR	NR	NR	NR	NR	NR	NR	NR	NR	NR
Manganese	2.26	NR	NR	NR	2.13	NR	NR	NR	5.72	NR
Nickel	NR	NR	NR	NR	NR	NR	NR	NR	NR	NR
Selenium	58.54	NR	NR	NR	15.00	NR	NR	NR	74.37	NR
Mercury (Ionic)	0.66	0.27	0.19	0.24	0.14	0.07	0.03	0.06	78.23	11.92
Mercury (Elem.)	NR	NR	NR	NR	NR	0.05	0.08	0.07	NR	NR
Mercury (Total)	NR	NR	NR	NR	NR	NR	NR	NR	NR	NR

Element	Inlet					Outlet					Particle Phase Removal (%)	Removal Standard Deviation (%)
	Average Element in Fly Ash (ppm)	Particle Phase Element in the Flue Gas (ug/dscm)				Average Element in Fly Ash (ppm)	Particle Phase Element in the Flue Gas (ug/dscm)					
		Average	+ Deviation	-Deviation	RMS Deviation		Average	+ Deviation	-Deviation	RMS Deviation		
Arsenic	360.00	111.72	NR	NR	NR	2140.00	33.49	NR	NR	NR	70.03	NR
Barium	361.00	112.03	NR	NR	NR	4.09	0.06	NR	NR	NR	99.94	NR
Beryllium	0.02	NR	NR	NR	NR	0.82	NR	NR	NR	NR	NR	NR
Cadmium	1.47	0.46	NR	NR	NR	15.40	0.24	NR	NR	NR	47.18	NR
Chromium	211.00	65.48	NR	NR	NR	14000.00	219.06	NR	NR	NR	-234.54	NR
Cobalt	41.60	12.91	NR	NR	NR	3.14	0.05	NR	NR	NR	99.62	NR
Lead	104.00	32.28	NR	NR	NR	421.00	6.59	NR	NR	NR	79.59	NR
Manganese	310.00	96.21	NR	NR	NR	9120.00	142.70	NR	NR	NR	-48.33	NR
Nickel	279.00	86.58	NR	NR	NR	1690.00	26.44	NR	NR	NR	69.46	NR
Selenium	18.90	5.87	NR	NR	NR	92.00	1.44	NR	NR	NR	75.46	NR
Mercury	2.55	0.69	0.11	0.17	0.15	11.70	0.16	0.05	0.08	0.07	76.95	10.99

MULTIPLE POLLUTANT REMOVAL USING THE CONDENSING HEAT EXCHANGER

Phase I Final Report

Addendum II

Task 3 Topical Report: Long Term Wear Test

Start Date: November, 1995

End Date: June, 1997

Issue Date: June, 1998

This report contains no trade secret information

Principal Author

G. A. Kudlac

McDermott Technology, Inc.
1562 Beeson Street
Alliance, Ohio 44601

This project was sponsored by the U. S. Department of Energy,
the Ohio Coal Development Office (Department of Development, State of Ohio),
the Electric Power Research Institute, and Babcock & Wilcox

US DOE-FETC Contract:

DE-AC22-95PC95255

Ralph T. Bailey

OCDO Grant Agreement:

CDO/D-94-1

FAX: 330-829-7283

McDermott Technology, Inc. Contract: CRD 1337

Phone: 330-829-7353

Disclaimer

“This report was prepared as an account of work sponsored by the United States Government and the Ohio Coal Development Office (OCDO). Neither the United States, any agency thereof, the State of Ohio, any agency thereof, or Babcock & Wilcox, nor any of their employees, makes any warranty, express or implied, or assumes any legal liabilities or responsibility for the accuracy, completeness or usefulness of any information, apparatus, product, or process disclosed, or represents that its use would not infringe privately owned rights. Reference herein to any specific commercial product, process, or service, by trade name, mark, manufacturer, or otherwise, does not necessarily constitute or imply its endorsement, recommendation, or favoring by the United States, the State of Ohio, or any agency thereof. The views and opinions of authors expressed herein do not necessarily state or reflect those of the United States Government or any agency thereof.”

ABSTRACT

Long-term operation of a condensing heat exchanger under typical coal-fired flue gas conditions was investigated in Phase I, Task 3 of the "Multiple Pollutant Removal Using the Condensing Heat Exchanger" test program. The program was conducted under contract to the United States Department of Energy's Fossil Energy Technology Center (DOE-FETC) and was supported by the Ohio Coal Development Office (OCDO) within the Ohio Department of Development, Electric Power Research Institute's Environmental Control Technology Center (EPRI-ECTC) and Babcock and Wilcox - a McDermott Company (B&W).

The specific goal of this task was to determine the amount of wear, if any, on the Teflon[®]-covered heat transfer tubes in a condensing heat exchanger. A pilot-scale single-stage condensing heat exchanger (CHX[®]) was operated under typical coal-fired flue gas conditions on a continuous basis for a period of approximately 10 months. Operating conditions and particulate loadings for the test unit were monitored, Teflon[®] film thickness measurements were conducted, and surface replications (which duplicate the surface finish at the microscopic level) were taken at various times during the test.

Data from the test indicate that virtually no decrease in Teflon[®] thickness was observed for the coating on the first two rows of heat exchanger tubes, even at high inlet particulate loadings (400 mg/dscm [0.35 lb/10⁶ Btu]). Evidence of wear was present only at the microscopic level, and even then was very minor in severity. Operation at high inlet particulate loadings resulted in accumulated ash deposits within the heat exchanger. Installation of a modified (higher flow rate) wash nozzle manifold substantially reduced subsequent deposit formation.

TABLE OF CONTENTS

<u>Section</u>	<u>Page</u>
1.0 EXECUTIVE SUMMARY	1-1
2.0 INTRODUCTION	2-1
3.0 FACILITIES AND INSTRUMENTATION	3-1
4.0 TEST DESCRIPTION	4-1
4.1 Unit Operation	4-1
4.2 Inspection Measurements	4-2
5.0 RESULTS AND DISCUSSION	5-1
5.1 Operation Summary and Discussion	5-1
5.2 Wear Performance Discussion	5-6
5.2.1 Teflon® Film Thickness Measurements	5-6
5.2.2 Teflon® Surface Replications	5-9
6.0 CONCLUSIONS AND RECOMMENDATIONS	6-1

APPENDICES

Appendix

A Tabulated Data - Teflon® Film Thickness Measurements, Data Set 1 - 3/12/96	A-1
B Tabulated Data - Teflon® Film Thickness Measurements, Data Set 2 - 4/29/96	B-1
C Tabulated Data - Teflon® Film Thickness Measurements, Data Set 3 - 7/9/96	C-1
D Tabulated Data - Teflon® Film Thickness Measurements, Data Set 4 - 9/12/96	D-1
E Tabulated Data - Teflon® Film Thickness Measurements, Data Set 5 - 1/20/97	E-1
F Tabulated Data - Teflon® Film Thickness Measurements, Data Set 6 - 3/21/97	F-1
G Graphical Data - Change in Teflon® Film Thickness as a Function of Time	G-1

LIST OF TABLES

Table

1.1 Summary of CHX® Operating Conditions at the ECTC	1-2
3.1 CHX® Wear Test Instrumentation List	3-5
4.1 Design Operating Conditions for the CHX® Pilot Unit -- One Year Wear Test	4-1
5.1 Summary of CHX® Operating Conditions at the ECTC	5-1

TABLE OF CONTENTS (Cont'd)
LIST OF FIGURES

<u>Figure</u>	<u>Page</u>
1.1 Cumulative Change in Teflon® Film Thickness as a Function of Time for Tubes 1 through 6	1-3
1.2 Cumulative Change in Teflon® Film Thickness as a Function of Time for Tubes 7 through 12	1-3
3.1 Gas Flow Schematic of the ECTC Facility	3-2
3.2 CHX® Pilot Unit at the ECTC	3-3
3.3 Top View of the Pilot CHX® Unit Heat Exchanger	3-4
4.1 Location of Film Thickness and Surface Replication Measurements	4-2
5.1 P-5A Measurements of Particulate Concentration During the One Year Test	5-2
5.2 Top of CHX® Heat Exchanger Prior to Washing	5-3
5.3 Top of CHX® Heat Exchanger After Washing	5-3
5.4 Flyash Deposits on the Tubes of the CHX® Heat Exchanger	5-4
5.5 Wash Water Solids Concentration	5-5
5.6 Differential Pressure Across the CHX® Unit as a Function of Time	5-6
5.7 Cumulative Change in Teflon® Film Thickness as a Function of Operating Hours for Tubes 1 through 6	5-7
5.8 Cumulative Change in Teflon® Film Thickness as a Function of Operating Hours for Tubes 7 through 12	5-7
5.9 Cumulative Change in Teflon® Film Thickness as a Function of Operating Hours and Angular Position -- Tube 1	5-8
5.10 Cumulative Change in Teflon® Film Thickness as a Function of Operating Hours and Angular Position -- Tube 5	5-9
5.11 Microphotograph of Clean Tube Surface	5-10
5.12 Microphotograph of Tube 1 -- End of Test	5-11
5.13 Microphotograph of Tube 6 -- End of Test	5-11
G.1 Cumulative Change in Teflon® Film Thickness as a Function of Operating Time and Angular Position -- Tube 2	G-1
G.2 Cumulative Change in Teflon® Film Thickness as a Function of Operating Time and Angular Position -- Tube 3	G-1
G.3 Cumulative Change in Teflon® Film Thickness as a Function of Operating Time and Angular Position -- Tube 4	G-2
G.4 Cumulative Change in Teflon® Film Thickness as a Function of Operating Time and Angular Position -- Tube 6	G-2

1.0 EXECUTIVE SUMMARY

This is the Task 3 Topical Report for “Multiple Pollutant Removal Using the Condensing Heat Exchanger,” conducted by McDermott Technology Inc., Research & Development Division under contract to the United States Department of Energy, Fossil Energy Technology Center. The work was jointly sponsored by the Department of Energy’s Fossil Energy Technology Center (DOE-FETC), the Ohio Coal Development Office (OCDO) within the Ohio Department of Development, the Electric Power Research Institute’s Environmental Control Technology Center (EPRI-ECTC), and Babcock & Wilcox - a McDermott Company (B&W). The guidance and support of the project managers from the sponsoring organizations, Thomas J. Feeley III of DOE-FETC, Richard Chu of the OCDO, and Gerry B. Maybach of the EPRI-ECTC, is gratefully acknowledged.

The purpose of Phase I of this contract was to determine the pollutant removal performance and the anticipated wear life of an Integrated Flue Gas Treatment system using flue gas from coal combustion. Integrated Flue Gas Treatment uses two Condensing Heat Exchangers (CHXs[®]) to remove a variety of pollutants from combustion flue gas. The Teflon[®]-covered internals of the CHX[®] also permit heat recovery at temperatures below the acid dew point of the flue gas.

Condensing Heat Exchangers using Teflon[®]-covered heat exchanger tubes have long been used in the industrial market to recover energy from flue gas, thereby improving the overall thermal efficiency of the combustion process. More than 110 commercial units are in service, with operating lifetimes up to 14 years. These industrial installations have been exclusively gas and oil-fired installations. Prior to this work, only limited data existed on the pollutant removal efficiency of the IFGT process, and the effects of long-term exposure to abrasive flyash on the integrity of the Teflon[®]-covered heat exchanger tubes was unknown.

The objective of Task 3 was to demonstrate long-term operation of a condensing heat exchanger for coal-fired conditions. The specific goal of the task was to determine the amount of wear, if any, on the Teflon[®]-covered internals of the heat exchanger.

Task 3 Overview

Task 3 of this contract was conducted at the Electric Power Research Institute's Environmental Control Technology Center in Barker, New York. A single-stage CHX[®] unit was installed downstream of the ECTC electrostatic precipitator. The unit was operated as a heat recovery unit to determine the effects of long-term exposure to flyash under typical flue gas conditions.

Standard operating parameters (flue gas flows and temperatures, cooling water temperatures, etc.) were monitored and recorded by the ECTC data acquisition system over the course of the program. In addition, periodic visual inspections and Teflon[®] film thickness measurements were performed to determine the amount of wear. Finally, replications of the Teflon[®] film surface were made to both document the general physical condition of the Teflon[®] surface and allow for detection of wear at the microscopic level. Surface replications are made by moistening a strip of cellulosic film in acetone, laying the strip on the tube surface, and allowing to dry. The physical characteristics of the tube surface are thus exactly duplicated on the cellulosic film.

The wear test unit was operated for over 6,200 hours during the test program. A summary of the operating conditions is shown in Table 1.1.

Table 1.1 Summary of CHX[®] Operating Conditions at the ECTC

Time of Operation	6,240 hours
Inlet Gas Flow	1,275 scmh (750 scfm)
Inlet Gas Temperature	150°C (300°F)
Inlet Water Temperature	55 to 60°C (130 to 140°F)
Outlet Gas Temperature	82 to 93°C (180 to 200°F)
Outlet Water Temperature	76 to 80°C (170 to 175°F)
Inlet Particulate Loading (average)	25. mg/dscm (0.022 lb/10 ⁶ Btu) 2,060 hours 400. mg/dscm (0.35 lb/10 ⁶ Btu) 4,180 hours
Tube Wash Cycle	20 minutes every 8 hours

Five inspection trips were made over the course of the test program. During each trip, visual inspections, Teflon[®] thickness measurements and surface replications were performed.

No visible signs of wear were evident over the course of the test program. Minor amounts of fly ash deposition, not removed by the normal wash cycle, were detected after 5,000 hours of operation. These deposits were located several rows down from the top of the tube manifold and were attributed to inadequate wash water flowrates. A new wash nozzle manifold (3 nozzles vs. 1 nozzle) was installed following the 5,000 hour inspection. The end of test inspection revealed virtually no ash deposition.

Data from the Teflon[®] thickness measurements indicated no significant decrease in the tube film thickness. Measurements were made at several locations on each of the tubes in the top two rows of the tube bank. Over the course of the test program, the Teflon[®] film thickness increased approximately 7-10% (30.5 to 50.8 μm [1.2 to 2.0 mils] of a nominal 508 μm [20 mil] film) after roughly 2,000 hours of operation then showed no subsequent signs of decrease. This initial thickness increase has been attributed to a relaxation of surface stresses in the Teflon[®]. These surface stresses are a result of the manufacturing process, and stress relaxation occurs when the Teflon[®] film is heated. A graphical summary of the Teflon[®] thickness measurements is given in Figures 1.1 and 1.2.

Evaluation of the film surface replications revealed no significant wear damage to the Teflon[®] covering. Very minor wear damage was visible on tube 6, which was subject to the highest flue gas flow rate. This damage, however, was on the μm scale and is of the same magnitude as the surface striations created during manufacture and should pose no problems for extended operation.

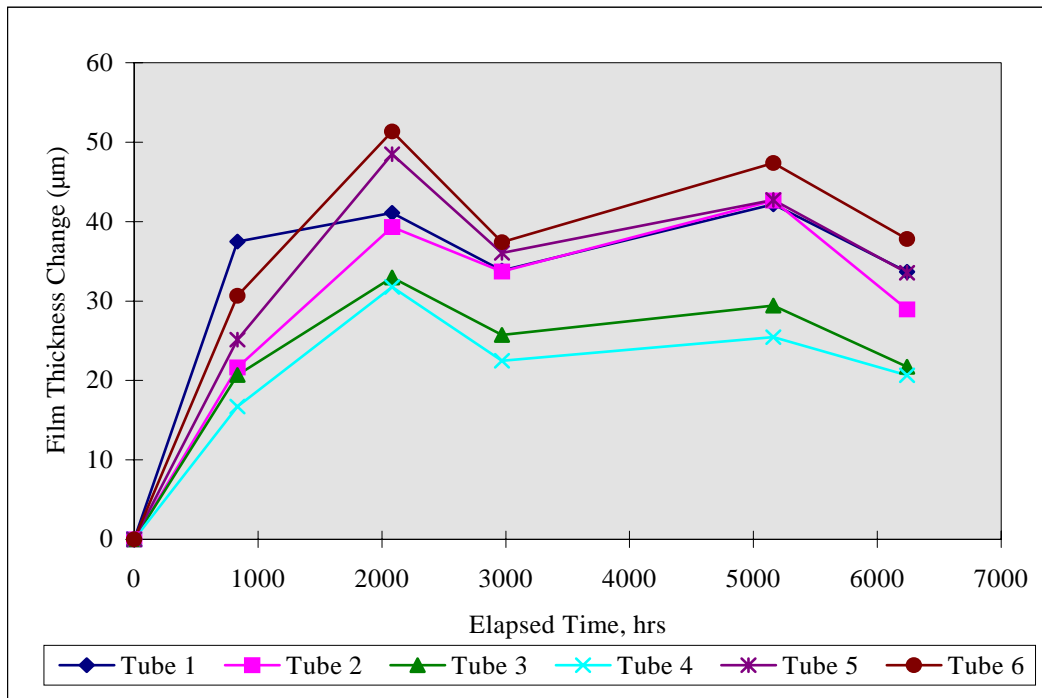


Figure 1.1 Cumulative Change in Teflon® Film Thickness as a Function of Time for Tubes 1 through 6

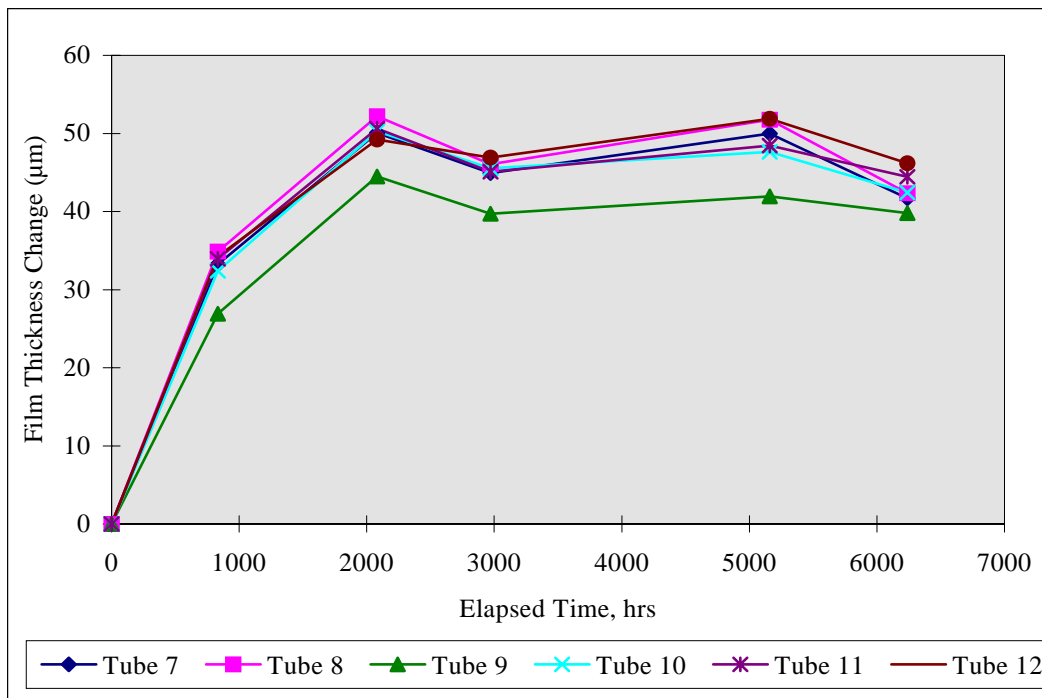


Figure 1.2 Cumulative Change in Teflon® Film Thickness as a Function of Time for Tubes 7 through 12

Task 3 Conclusions and Recommendations

Based on the operational and inspection data collected over the course of the test program, the following conclusions and recommendations can be made:

- No significant wear was observed for any of the Teflon[®] tube coverings. Minor microscopic wear detected on some tubes is insignificant and should pose no problems for extended operation.
- Particulate deposition can be a problem, especially at higher particulate loadings and insufficient wash water flows. Increasing the wash water flow rate by modifying the wash nozzle manifold essentially eliminated particulate deposition.
- Teflon[®] life expectancy should be greater than 10 years. Tube replacement will more likely be required due to operational problems other than abrasive wear.

2.0 INTRODUCTION

The 1990 Clean Air Act Amendments address the need to reduce the quantity of pollutants released to the atmosphere. Some pollutants are currently regulated and additional species are targeted for control in the near future. The emission of SO₂ and particulate from electric utilities is currently regulated under the Phase I and Phase II requirements defined in Title IV. An additional 189 substances, classified as hazardous air pollutants, have been identified for regulation under Title III of the Clean Air Act Amendment. The Title III requirements will be imposed across approximately 750 source categories. Cluster rules are also being established to set emission standards for specific industries. Many state and local agencies are already imposing stringent regulations on hazardous pollutants, such as mercury. There is a need for equipment to remove the pollutants of concern in a cost-effective manner. Most of the commercial pollutant removal equipment suffer from three major drawbacks:

- Commercially available pollution removal equipment is parasitic, that is, they consume energy during operation. A typical coal-fired power plant will have a 2-4% or more reduction in power generation capacity when commercial SO₂ and particulate removal equipment is added for gas clean up.
- Commercially available flue gas clean up equipment generally treats only one pollutant at a time. Separate units are installed for each of the pollutants to be removed.
- Most of the commercial flue gas clean up equipment used in the electric utility industry can not be economically scaled down for industrial coal-fired applications. The capital cost and operating cost of these units are often prohibitive for the smaller energy producer.

An untapped source of energy from coal-fired units is the waste heat in the flue gas released to the stack. The efficiency of a boiler can be significantly increased by decreasing the flue gas exit temperature. One means of lowering the exit temperature is to use a condensing heat exchanger to recover both sensible and latent heat from the flue gas. Condensing Heat Exchangers (CHX[®]) using Teflon[®]-covered internals are widely used to recover waste heat from flue gases. The Teflon[®] covering protects the heat exchanger components from corrosion as the temperature of the flue gas drops below the acid dew point. The most common applications to date are boilers firing oil or natural gas. Single-stage commercial condensing heat exchangers have provided satisfactory performance and lifetimes for more than one hundred industrial installations for the past fourteen years.

A recent innovation to the commercial condensing heat exchanger design, called the Integrated Flue Gas Treatment (IFGT) system, exhibits improved pollutant removal from the flue gas while recovering waste heat. The IFGT system is a two-stage condensing heat exchanger. Most of the sensible heat is removed from the gas in the first heat exchanger stage. The second heat exchanger stage can be operated in a condensing mode, recovering latent heat from the gas while removing pollutants. The top of the second heat exchanger stage is equipped with an alkali reagent spray system to enhance SO₂ and particulate removal. Pollutant removal mechanisms in

the IFGT include condensing (for water, some organic compounds, and some acid gases and trace metals), impaction (for particulates), and gas absorption (for removal of SO₂ and other acid gases). In an IFGT, several pollutants are treated using a single device - while recovering waste heat. Because of its modular design, it can be easily built for a wide range of size applications. An additional benefit realized by using the condensing heat exchanger is the proportional reduction in carbon dioxide released per MW of generated electricity because of the increase in plant efficiency.

One of the major questions that must be addressed before the IFGT can be considered viable for coal-fired applications is the expected material lifetime for the Teflon[®] covering on the tubes. Commercial condensing heat exchangers with Teflon[®]-covered parts have exhibited lifetimes of over 14 years, but these have been clean fuel (oil or natural gas) applications. Tests on coal-fired units have been limited in duration.

To address the material lifetime issue for coal-fired applications, a long-term wear test was included in Phase I of this project as Task 3 -- "Long-Term Wear Testing". The specific goal of this task was to determine the amount of wear, if any, on the Teflon[®]-covered internals of the heat exchanger. The location of maximum material wear in an IFGT will be at the inlet of the first heat exchanger stage. This is where the flue gas and Teflon[®] coverings are the hottest, the flue gas velocity and particulate loading the highest, and where the particulates first impact the Teflon[®]-covered tubes. It is expected that the top rows of tubes in an IFGT will experience the maximum wear due to fly ash abrasion. A single-stage condensing heat exchanger unit was used for the material lifetime demonstration since the inlet conditions will be the same as for an IFGT. Visual and physical examinations were performed on the top rows of tubes at periodic intervals during the one-year demonstration.

3.0 FACILITIES AND EQUIPMENT

The Environmental Control Technology Center (ECTC) was used to provide the flue gas to the wear test CHX[®] unit for this test program. The ECTC is a comprehensive test facility for evaluating advanced emissions control technologies applied to high sulfur coals. The test facility utilizes about one percent of the flue gas available from the 662 MW Kintigh Station, a pulverized coal boiler operated by the New York State Electric and Gas Corporation (NYSEG) in Barker, New York.

A flow schematic of the ECTC facility is shown in Figure 3.1. The facility is operated 24 hours a day, allowing long-term continuous tests to be performed. The pilot CHX[®] unit was installed in the mini-pilot wet scrubber sub-loop of the ECTC. This loop has a flue gas flow capacity of 2040-2550 acmh (1200-1500 acfm), sufficient to provide the "design" flue gas velocity of 12.2 m/sec (40 ft/sec) between the tubes at the inlet of the heat exchanger. To reproduce expected commercial conditions, the unit used a slipstream from the flue gas after it exits the electrostatic precipitator (ESP). The pilot CHX[®] test unit was located downstream of the ESP in place of the mini-pilot wet scrubber.

The CHX[®] unit used for the wear test is a skid-mounted, single-stage unit as shown in Figure 3.2. In addition to the heat exchanger, the unit is also equipped with a flue gas inlet control damper, water pump, and water circulation tank. Figure 3.3, is a top view drawing of the heat exchanger module of the CHX[®] pilot test unit. The internal dimensions of the heat exchanger are 30.87 cm by 36.51 cm (12 5/32 inches by 14 3/8 inches). There are six heat exchanger tubes in each row and 32 rows of tubes. The heat exchanger tube rows are staggered from each other (triangular pitch) so that there is no open line of sight from the top to the bottom of the heat exchanger. The CHX[®] pilot heat exchanger is operated with countercurrent flow, with the flue gas entering the top of the heat exchanger and exiting at the bottom, and the cooling water entering the bottom row of tubes and exiting the top row. The flue gas inlet plenum is removable, allowing access to the top of the heat exchanger for inspection of the Teflon[®] film on the top rows of tubes.

Data from the CHX[®] pilot test unit and ECTC equipment was collected and recorded by the ECTC data acquisition system. In addition, ECTC personnel maintained an hourly log of the major test parameters, including gas and water flows and temperatures, and ESP operating conditions. A list of the measured operating parameters and instruments used for the wear test is provided in Table 3.1.

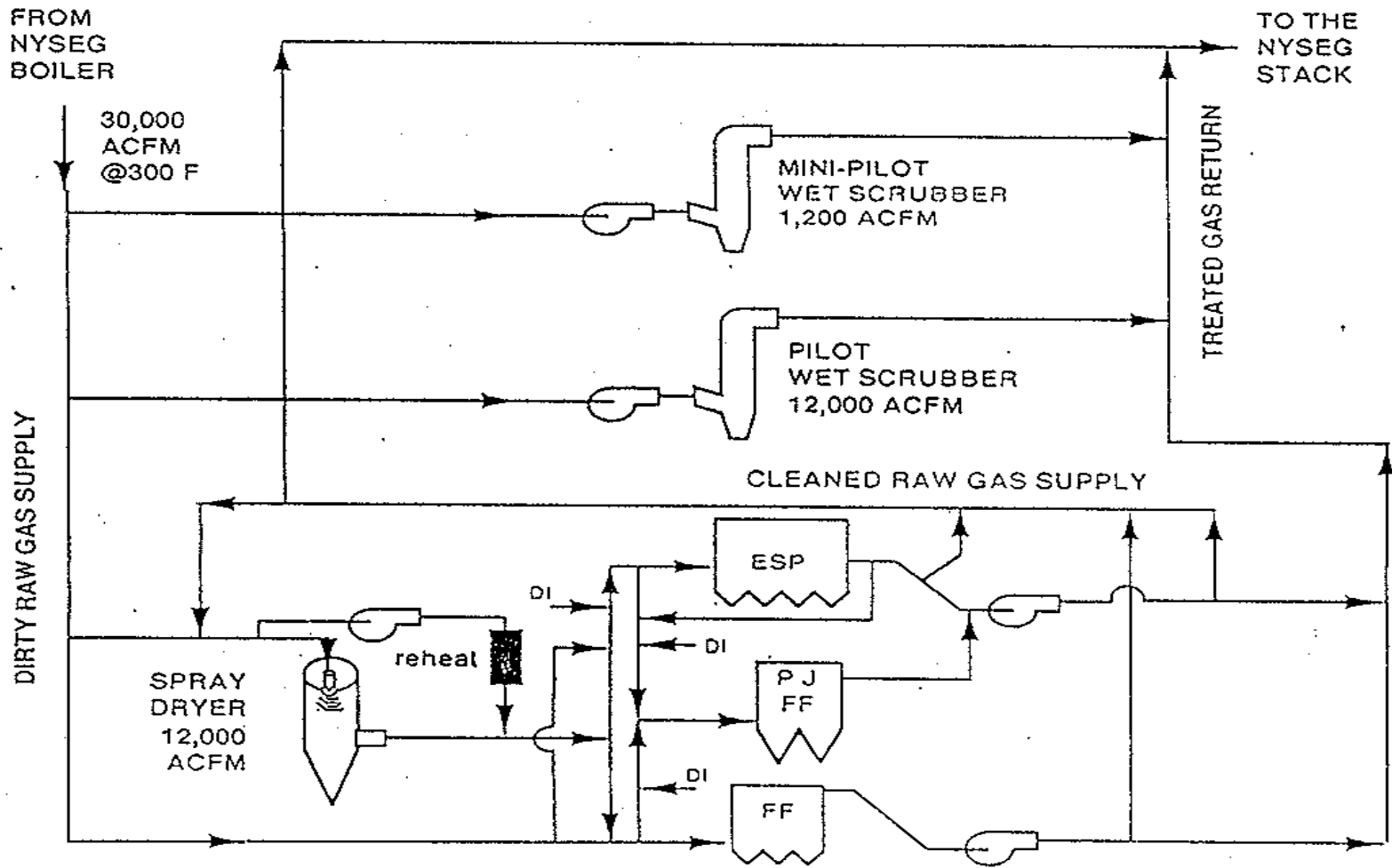


Figure 3.1 Gas Flow Schematic of the ECTC Facility

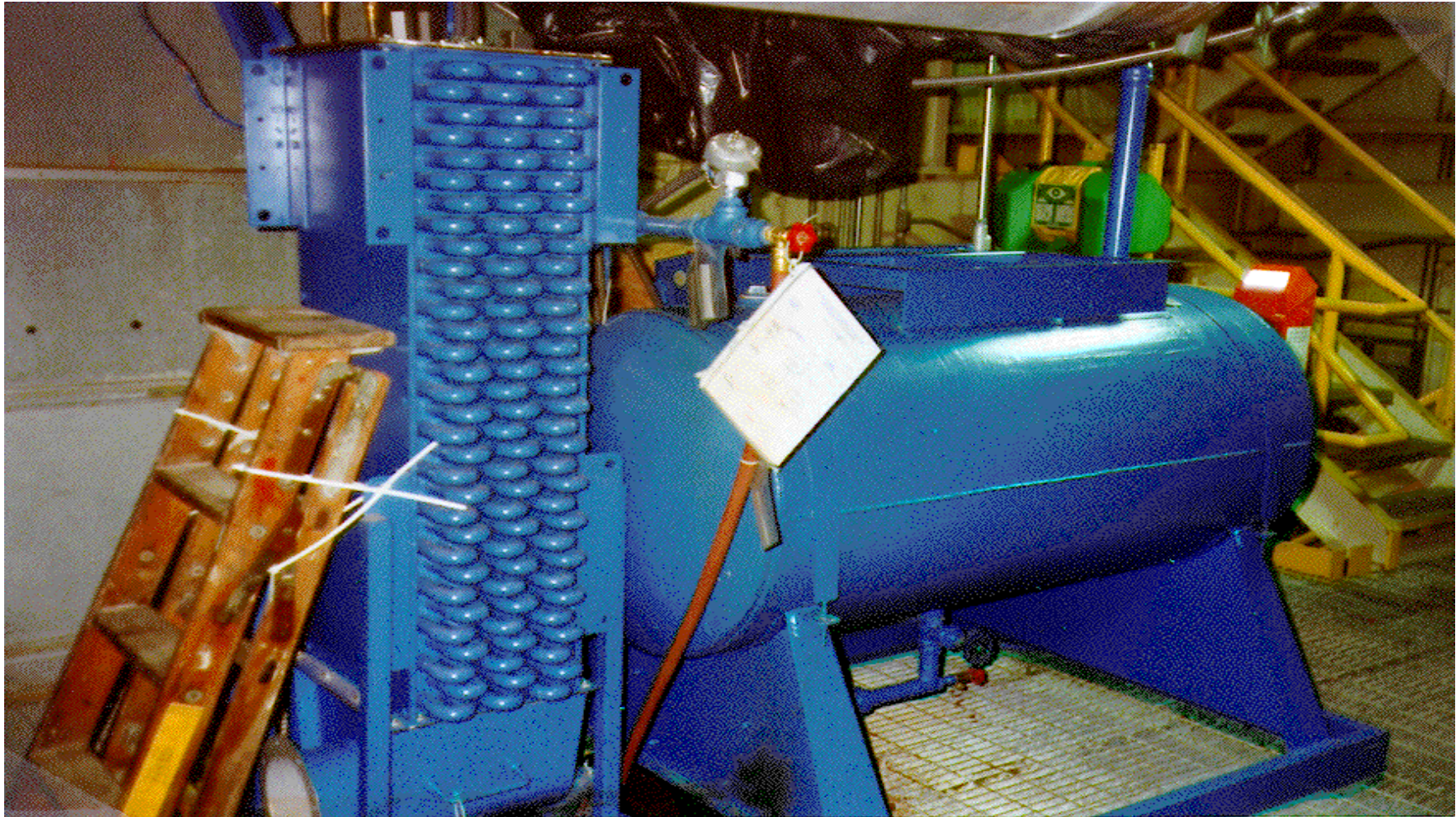


Figure 3.2 CHX[®] Pilot Unit at the ECTC

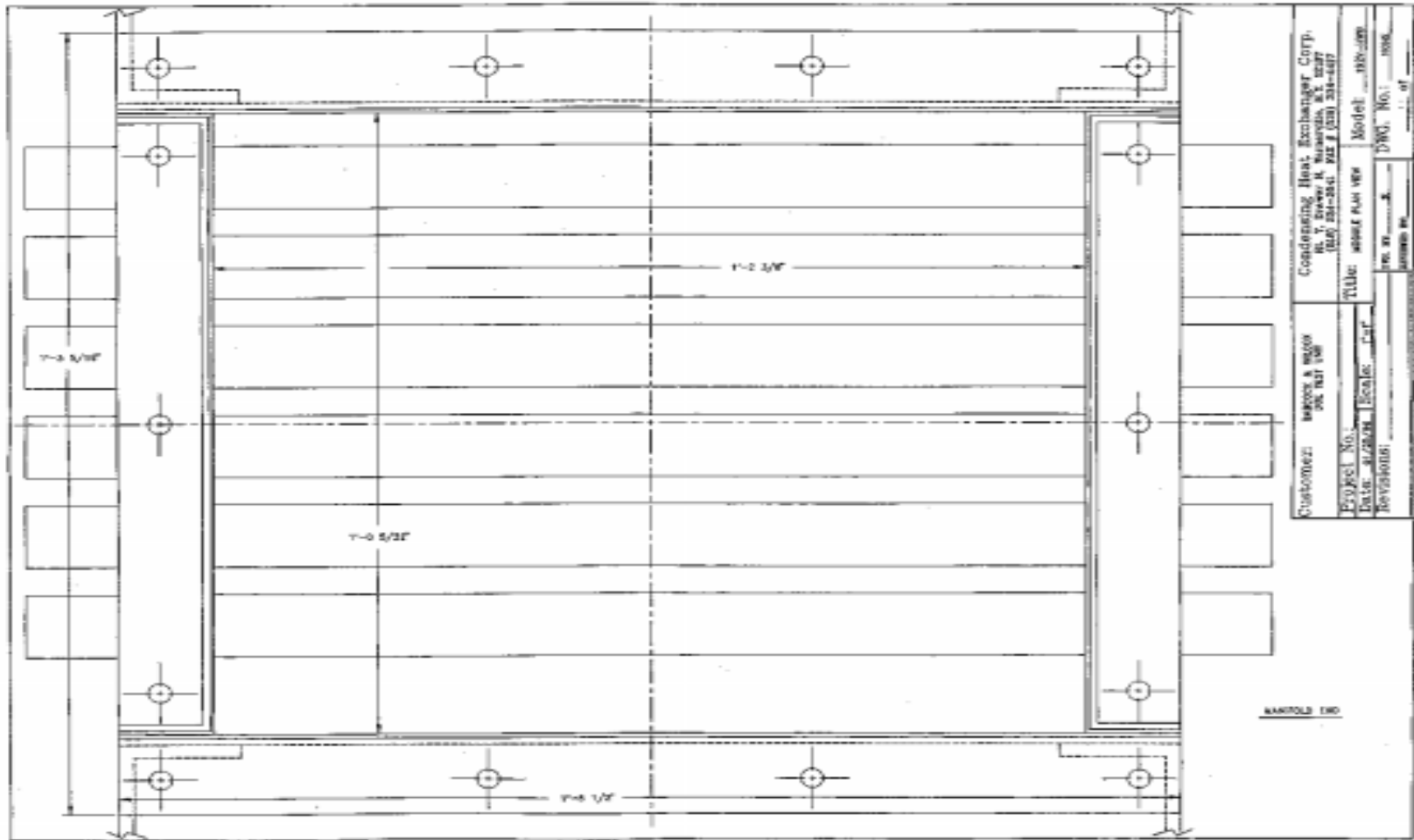


Figure 3.3 Top View of the Pilot CHX[®] Unit Heat Exchanger

Table 3.1 CHX[®] Wear Test Instrumentation List

Measurement Parameter	Instrument	Provided By	Calibration Frequency	Measurement Frequency
Inlet water temperature	Type K Thermocouple	B&W	NA	Continuous DAS
Outlet water temperature	Type K Thermocouple	B&W	NA	Continuous DAS
Inlet gas temperature	Type K Thermocouple	B&W	NA	Continuous DAS
Outlet gas temperature	Type K Thermocouple	B&W	NA	Continuous DAS
Particle loading EPA Method 5		Parsons Power	NA	Periodic
Opacity	opacity meter	Parsons Power	weekly	Continuous DAS
Gas flow across orifice pressure diff. pressure temperature	pressure trans diff pressure trans Type K TC	Parsons Power	semi-annually semi-annually NA	Continuous DAS
Pressure at CHX [®] inlet	pressure transmitter	Parsons Power	semi-annually	Continuous DAS
Pressure drop across CHX [®]	differential pressure transmitter	Parsons Power	semi-annually	Continuous DAS
CHX [®] exposure time	clock	Parsons Power	NA	Continuous
Teflon [®] wear tube dimension surface profile thickness	micrometer profilometer eddy current	B&W	annually NA during use	Periodic
Sulfur dioxide	SO ₂ analyzer	Parsons Power	daily	Continuous DAS
Oxygen	O ₂ analyzer	Parsons Power	daily	Continuous DAS

4.0 TEST DESCRIPTION

4.1 Unit Operation

The ECTC pilot facility and the condensing heat exchanger were operated so that the wear test was conducted under conditions representative of commercial operation at the flue gas inlet of an IFGT condensing heat exchanger. Specifically, this required:

- A flue gas with a representative particulate loading, temperature, and flow for a commercial coal-fired application. For example, the inlet particulate loading was to be maintained at 34 mg/dscm (0.03 lbs/10⁶ Btu) or greater during the test period.
- Controlling the temperature and flow rate of the cooling water for the condensing heat exchanger to provide the Teflon[®] film temperature expected at the flue gas inlet of a full-scale IFGT unit.
- Operation of the CHX[®] unit on a continuous basis, whenever possible, to maximize the Teflon[®] exposure to flue gas.

The design operating conditions used as a basis for operation of the CHX[®] pilot unit are shown in Table 4.1. All major operating parameters (see Table 3.1) were monitored by ECTC personnel (and recorded by the ECTC data acquisition system) to ensure that the CHX[®] test unit was operating within the desired conditions.

Table 4.1 Design Operating Conditions for the CHX[®] Pilot Unit -- One Year Wear Test

Parameter	Nominal Value	Range
Inlet Flue Gas Temperature	160 °C (320 °F)	+/- 17 °C (30 °F)
Outlet Water Temperature	77 °C (170 °F)	+/- 11 °C (20 °F)
Cooling Water Supply	11.4 lpm {3.0 gpm (est.)}	---
Flue Gas Velocity, between tubes	12.2 m/sec (40 ft/sec)	+/- 1.5 m/sec (5 ft/sec)
Inlet Flue Gas Flow	1,275 scmh (750 scfm)	+85 -0 scmh (+50 -0 scfm)
Inlet Particulate Loading	representative of poor to good particulate cleanup from a commercial cleanup device.	34 to 340 mg/dscm (0.03 to 0.3 lbs/10 ⁶ Btu)

To achieve the desired particulate loading (~34 mg/dscm [0.03 lbs/10⁶ Btu] or greater) at the inlet to the condensing heat exchanger, the test unit was located downstream of the ECTC ESP. An opacity meter was used to monitor the flue gas particulate loading downstream of the ESP. In addition to the opacity meter, an Environmental Systems P-5A *in-situ* particulate monitor was used as a qualitative indicator for the particulate loading level to aid ECTC personnel in

maintaining a steady particulate loading. Finally, EPA Method 5 particulate loading measurements were made at various times during the test to confirm the opacity readings and the particulate loading to the unit.

4.2 Inspection Measurements

In order to determine the amount of wear, if any, on the Teflon[®] covered internals of the heat exchanger, and specifically the tubes, three types of measurements, in addition to a visual inspection, were performed during each of the five inspection trips conducted during the course of the test program. These measurements included:

- Vertical and horizontal tube dimensions
- Eddy current Teflon[®] film thickness determination
- Teflon[®] film surface replications

A fourth type of surface measurement utilizing a surface profilometer, which was originally specified as a test program measurement, was not used due to damage to the Teflon[®] film caused by the profilometer probe during use.

Each measurement was performed at several locations on the top two rows of tubes. A graphical representation of the measurement locations is shown in Figure 4.1. Tubes 1 through 6 are located in the top row of the heat exchanger and tubes 7 through 12 in the second row. Flue gas

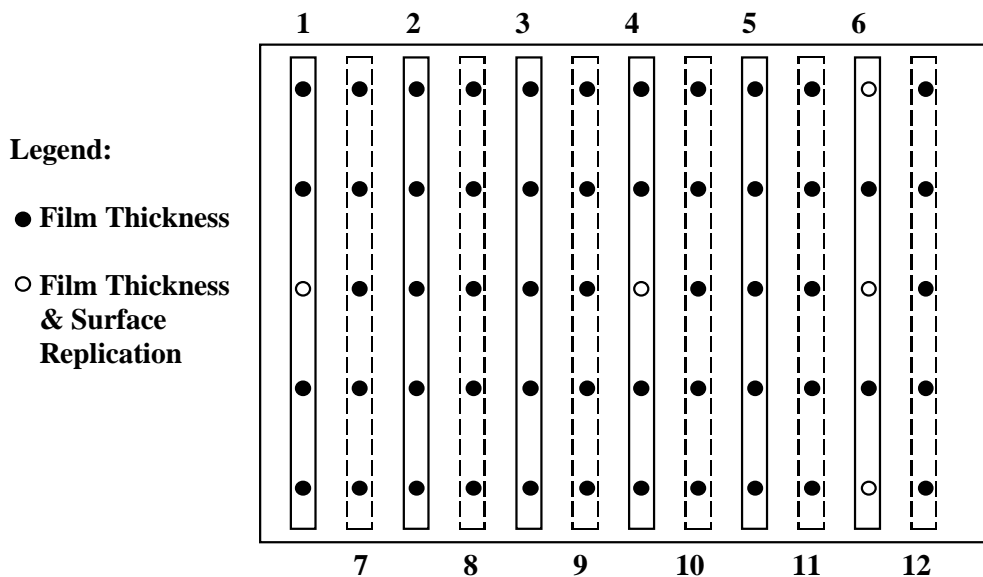


Figure 4.1 Location of Film Thickness and Surface Replication Measurements

flow with respect to the diagram is from the left and then into the page. Each of the dimensional measurements (horizontal, vertical, and film thickness) were performed in triplicate at each location and the values averaged. These location values were then averaged to obtain an average

tube value. Single surface replications were made at each of the indicated locations. Three replications were performed on tube 6 since the greatest potential for abrasive wear was expected on this tube. Descriptive summaries of each of the three measurement techniques may be found in the following paragraphs:

Tube Dimensions: Micrometers were used to measure the top-to-bottom and side-to-side dimensions of the top row of tubes at each of the locations shown in Figure 4.1 (locations labeled "Film Thickness" on tubes 1 through 6). A digital caliper micrometer was used for the horizontal diameter measurements and a standard micrometer was used for the vertical diameter measurements. The overall accuracy of the horizontal diameter measurement was 25.4 μm (0.001 inches) and the overall accuracy of the vertical diameter measurement was 12.7 μm (0.0005 inches). After two sets of dimensional measurements were obtained, it was discovered that the Teflon[®] tube surfaces were being damaged by the micrometers. This was most likely due to the tight tube spacing, which complicated the insertion and removal of the calipers. Evaluation of the two sets of measurements indicated that any change in film thickness would be more evident from the eddy current measurements, so this procedure was dropped from subsequent inspection trips.

Film Thickness: An Elcometer 300 Coating Thickness Gage, which uses an eddy current measurement principle, was used to make the film thickness measurements. The instrument has a range of 25.4 to 1,016 μm {0.001 to 0.040 inches (1 to 40 mils)} and an accuracy of $\pm 1\%$ of its reading. Teflon[®] thickness measurements were made for the top surface of the first and second row of heat exchanger tubes. Thickness measurements were also made at specified angles from vertical (0 + 45 and 0 - 45 degrees) for the top row of tubes. In relation to the diagram in Figure 4.1, "vertical" may be thought of as a line coming straight out of the paper, "+45" angled towards tube 1 and "-45" angled towards tube 6. Thickness measurements could not be made for these angles for the second row of tubes because of the staggered array (overlap of the tubes for adjacent rows) of the tubes. Measurements were made at the locations indicated in Figure 4.1. As mentioned above, these measurements were made in triplicate at each location and angle and then averaged. These location average values were then averaged for each tube to obtain a tube average. Each data set was then normalized based on 1) the calibration data for that particular set, and 2) the film thickness data from a "reference" tube measured at the same time using the same calibration as the inspection.

Surface Roughness: A cellulosic film surface replication technique was used to obtain a physical replicate of the Teflon[®] tube surfaces. The goal of making the surface replications was to record and observe any microscopic changes to the Teflon[®] tube surface. The replications were made during each inspection trip at the locations indicated in Figure 4.1. After cleaning the Teflon[®] tube surfaces, a strip of cellulosic film tape was moistened with acetone and laid on the surface of the tube. Upon drying, the tape was lifted from the tube and mounted on a glass slide, replicate side up. This procedure was then repeated for the remaining sample locations. The tapes were then viewed under a microscope and photographed at magnifications of 25X and 200X for comparison with the replications made prior to exposing the heat exchanger to flue gas.

5.0 RESULTS AND DISCUSSION

5.1 Operation Summary and Discussion

Over the course of Task 3, the CHX[®] pilot test unit was operated "at conditions" for 6,240 hours. During this time, all major design conditions operating ranges were met and maintained. A summary of the major operating conditions and the actual operating ranges is given in Table 5.1.

Table 5.1 Summary of CHX[®] Operating Conditions at the ECTC

Operating Parameter	Range or Value
Inlet Gas Flow	1275 scmh (750 scfm)
Inlet Gas Temperature	150°C (300°F)
Inlet Water Temperature	55 to 60°C (130 to 140°F)
Outlet Gas Temperature	82 to 93°C (180 to 200°F)
Outlet Water Temperature	76 to 80°C (170 to 175°F)
Inlet Particulate Loading (EPA M5 average)	25. mg/dscm (0.022 lb/10 ⁶ Btu) 2,060 hours 400. mg/dscm (0.35 lb/10 ⁶ Btu) 4,180 hours
Tube Wash Cycle	20 minutes every 8 hours

The particulate loading to the inlet of the CHX[®] test unit is reported as an average unit because the loading was increased partway through the test. The above value represents an average of the measured values after the change in particulate loading. A graphical summary of the CHX[®] inlet particulate loading over the course of the test program is shown in Figure 5.1. The particulate loading data presented in Figure 5.1 was obtained using an Environmental Systems P-5A *in situ* particulate monitor. The P-5A monitor was operated on a continuous basis and served as a qualitative indicator for the particulate loading level to aid ECTC personnel in maintaining a steady particulate loading to the CHX[®]. EPA Method 5 particulate sample trains were performed periodically to confirm the particulate loading. Particulate loadings from the EPA Method 5 sample trains are considered to be the official particulate loading data for Task 3.

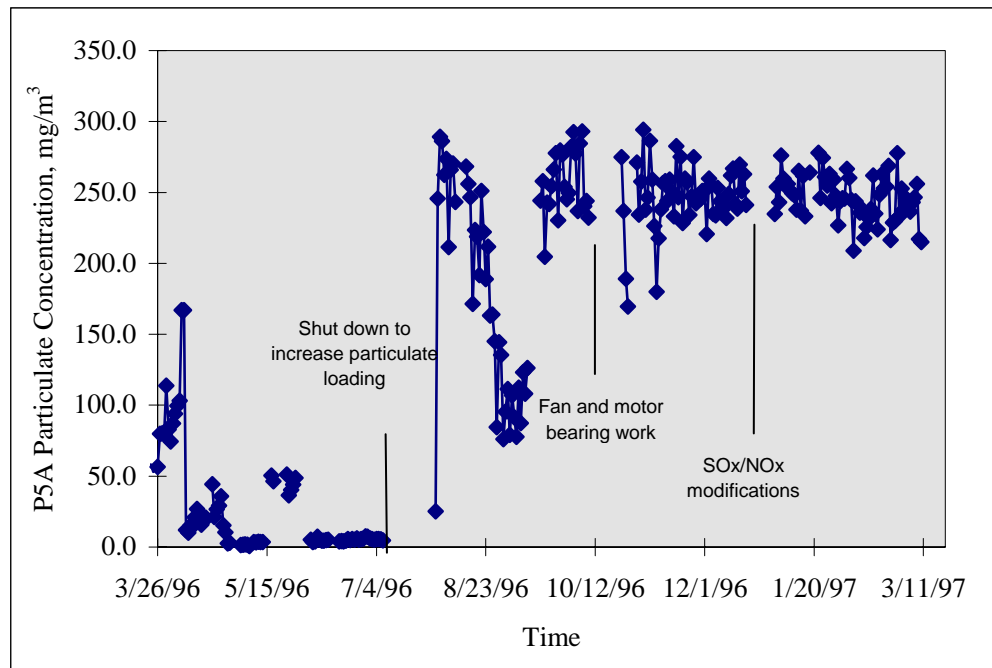


Figure 5.1 P-5A Measurements of Particle Concentration During the One Year Test

Visual inspections of the top surface of the CHX[®] heat exchanger were made both before and after scheduled tube washings during each inspection trip. In every case, the "dirty" inspection revealed a uniform coating of fly ash on each tube with no apparent bias from one tube to another. This coating covered the top (leading) half of each tube. Minimal fly ash was found on the bottom (trailing) half. After washing, the "clean" inspection revealed essentially complete removal of the fly ash coating, with only isolated areas (<5% total visible surface area) retaining some of the fly ash. Photographs of typical "dirty" and "clean" tubes may be found in Figures 5.2 and 5.3, respectively. The clean area in the center of Figure 5.2 is due to inadvertent contact with the tube surface prior to being photographed.

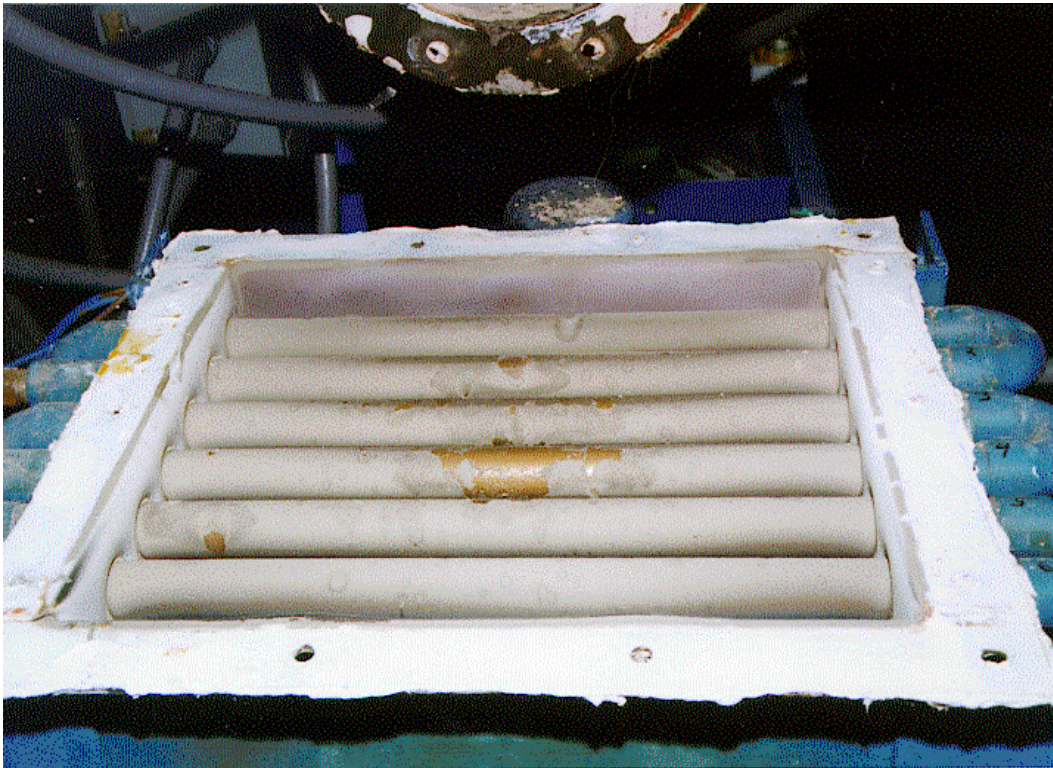
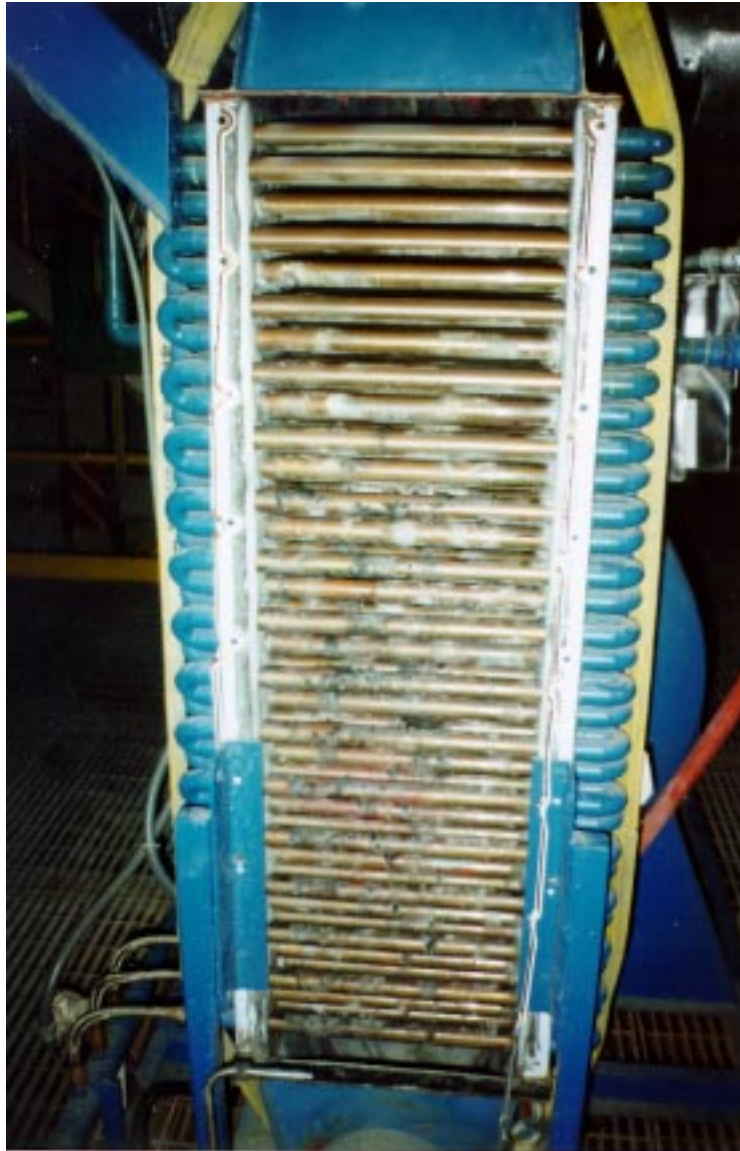


Figure 5.2 Top of CHX[®] Heat Exchanger Prior to Washing



Figure 5.3 Top of CHX[®] Heat Exchanger After Washing

After approximately 5,000 hours of operation, several fly ash deposits were found in the heat exchanger which were unaffected by the wash cycle. These deposits began approximately halfway down the heat exchanger, on the tubes closest to the walls, and continued to the bottom of the heat exchanger. These deposits can be seen in Figure 5.4. The most likely cause for these



**Figure 5.4 Flyash Deposits on the Tubes
Of the CHX[®] Heat Exchanger**

deposits is inadequate wash water flow rate. The initial wash water setup consisted of one (1) spray nozzle with a nominal flow rate of 3.8 lpm (1 gpm) which operated for 20 minutes every 8 hours. This is the standard wash cycle for oil-fired applications. While the top few rows of tubes were effectively cleaned, being subjected to the most energetic cleaning, the tubes further down in the heat exchanger were essentially cleaned by wash water dripping from the tubes above. Any deposits which were not removed, but only wetted, then served as sites for additional fly ash deposition. Based on these findings, a new wash nozzle manifold, consisting of three (3) equally spaced 3.8 lpm (1 gpm) nozzles, was installed for the remainder of the test. This new manifold was also operated for 20 minutes, effectively tripling the wash water flow rate.

The effect of the modified wash water manifold can be seen in Figures 5.5 and 5.6. In Figure 5.5, the percent solids of the wash water effluent is shown for the two manifold setups. For the original setup (1 nozzle), it can be seen that the percent solids concentration levels off at the end of the wash cycle, indicating that less than complete solids removal is occurring. With the modified manifold (3 nozzles), not only is the percent solids concentration continually decreasing, the initial and final concentrations are higher (and lower, respectively), indicating more complete solids removal.

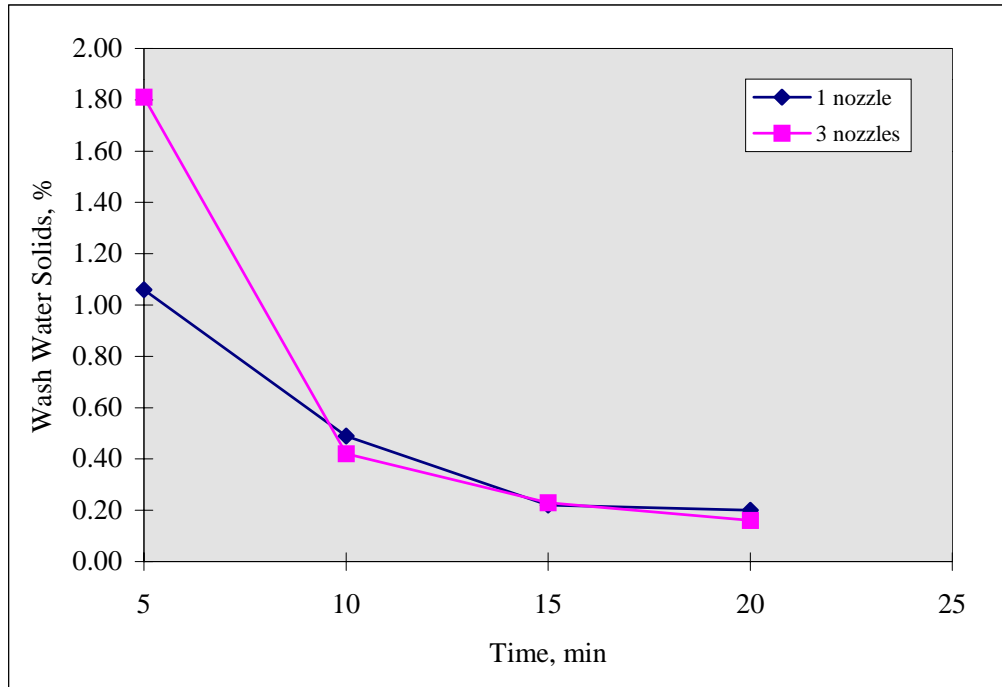


Figure 5.5 Wash Water Solids Concentration

In Figure 5.6, the heat exchanger differential pressure drop is shown as a function of time for the last four extended operating periods. The first three periods were conducted with one wash nozzle in service, the last with the three-nozzle manifold. In each of the first three operating periods, the differential pressure drop increased by approximately 100 Pa (0.4 in. H₂O) and was increasing, while the pressure drop increase for the last period was approximately 50 Pa (0.2 in. H₂O) and essentially steady.

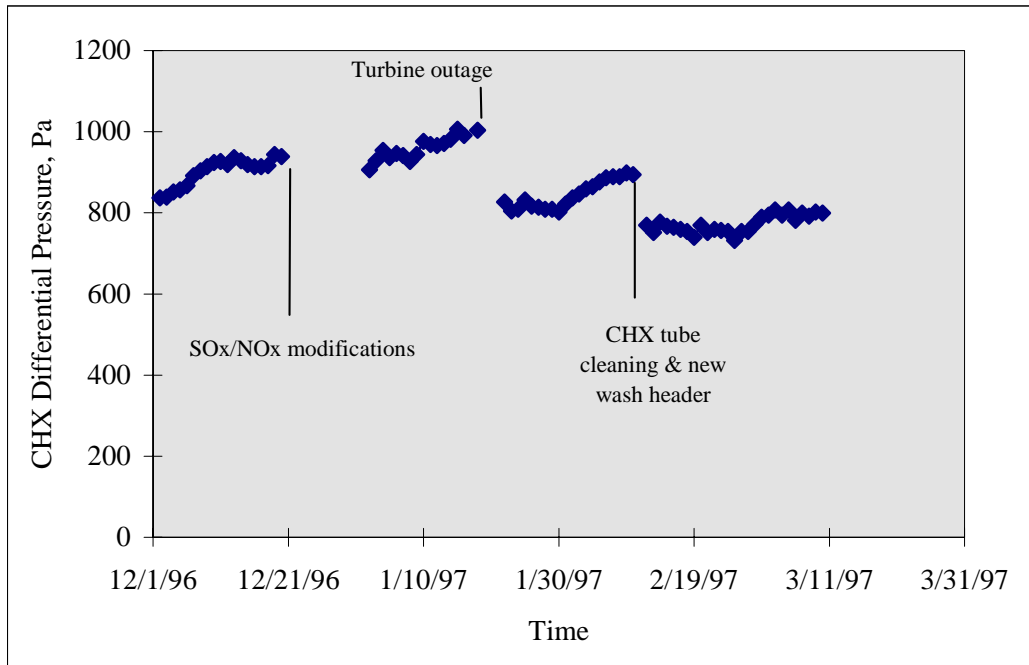


Figure 5.6 Differential Pressure Across the CHX[®] Unit as a Function of Time

5.2 Wear Performance Discussion

The primary goal of Task 3 was to determine the amount of wear, if any, incurred by the Teflon[®] internals of the CHX[®] pilot unit's heat exchanger (specifically the heat exchanger tube surfaces), while operating under typical flue gas conditions. As mentioned in Section 4.2, three measurement techniques were employed in an effort to determine the amount and type of wear. This section will focus on the results from two of the techniques (eddy current film thickness and surface replication). The third technique (vertical and horizontal tube dimensions) is not included in this discussion for the reasons outlined in Section 4.2.

5.2.1 Teflon[®] Film Thickness Measurements

Six complete sets (including measurements taken prior to flue gas exposure) of film thickness measurements were obtained during the course of the test program. Each set consists of 90 data points for the top row of tubes (3 angles * 6 tubes * 5 locations) and 30 data points for the second row of tubes (1 angle * 6 tubes * 5 locations). Tabular summaries of each of the data sets are located in Appendix A through F. All film thickness data presented in graphical and tabular form have been normalized.

Results of the film thickness measurements indicated that no significant reduction in tube film thickness occurred during the course of the test program. Figures 5.7 and 5.8 illustrate this finding. The data presented in Figures 5.7 and 5.8 represent the average tube values for measurements taken in the vertical position for tubes 1 through 6 and tubes 7 through 12, respectively.

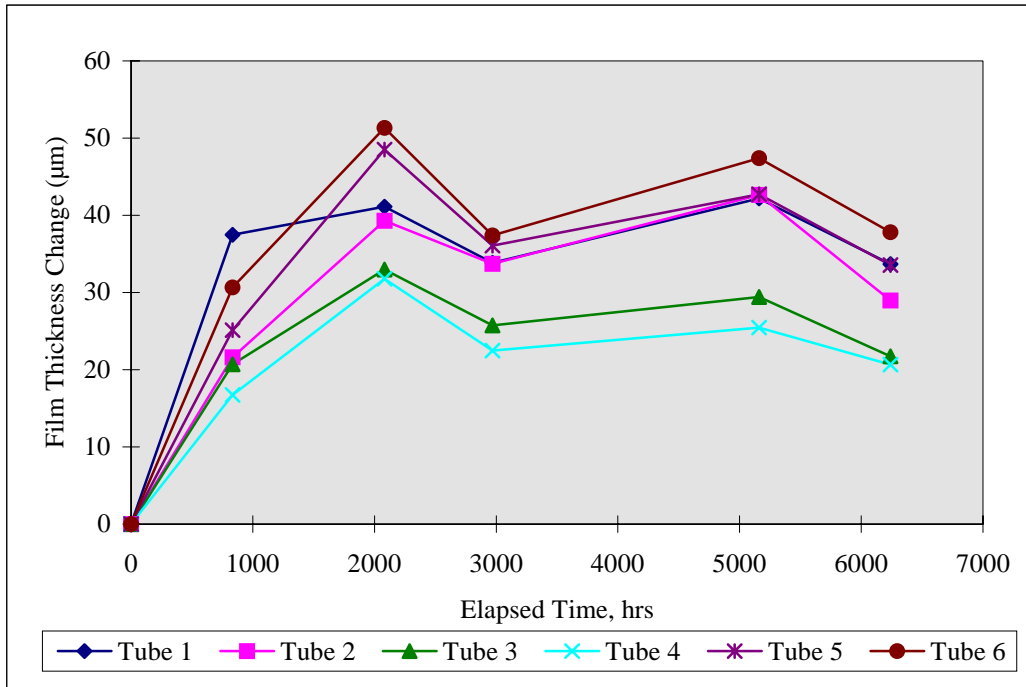


Figure 5.7 Cumulative Change in Teflon® Film Thickness as a Function of Operating Hours for Tubes 1 through 6

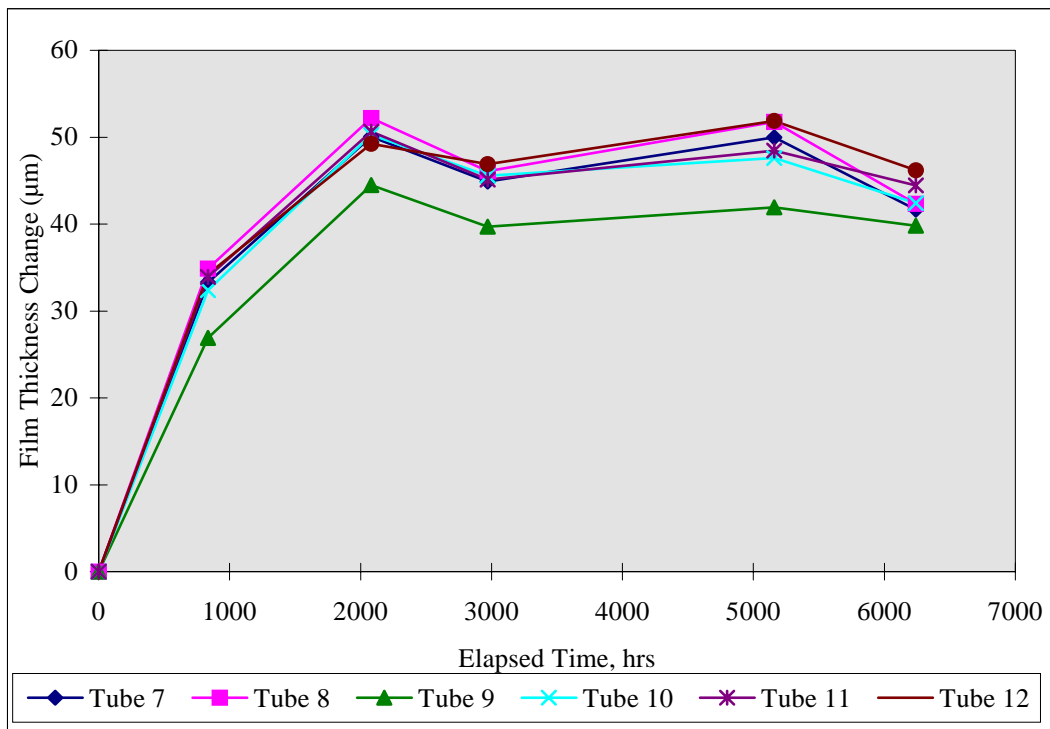


Figure 5.8 Cumulative Change in Teflon® Film Thickness as a Function of Operating Hours for Tubes 7 through 12

As illustrated in the two figures, after an initial increase in film thickness, no significant decrease was observed on any of the tubes measured. The increase in film thickness observed during the first two inspection trips is most likely due to the relaxation of surface stresses in the Teflon[®] film. These surface stresses result from the manufacturing process, and stress relaxation occurs when the Teflon[®] film is heated. The amount of increase ranged from 30.5 to 50.8 μm (1.2 to 2.0 mils), representing a 7 to 10% increase for a nominal 508 micron (20 mil) film.

As mentioned in Section 4.2, thickness measurements were also obtained for angles of +45° and -45° from the vertical at each of the measurement locations. These off-angle measurements were conducted to expand the amount of film surface being inspected and thus offer a more complete picture of any potential wear patterns and tendencies. In addition, the flue gas velocity at these locations was higher, creating the potential for greater abrasive wear than on the top surface of the tubes. In Figures 5.9 and 5.10, film thickness data is plotted as a function of both time and measurement angle for tubes 1 and 5, respectively. Due to the flue gas flow pattern from the inlet plenum to the first row of tubes, tubes 1 and 5, respectively, were chosen as representative of minimal and maximal potential wear sites. Tube 6, having the greatest potential for wear in the top row, was not chosen for this comparison due to instrument positioning problems during inspection, resulting in greater measurement variation. Plots for the other 4 tubes from the top row may be found in Appendix G.

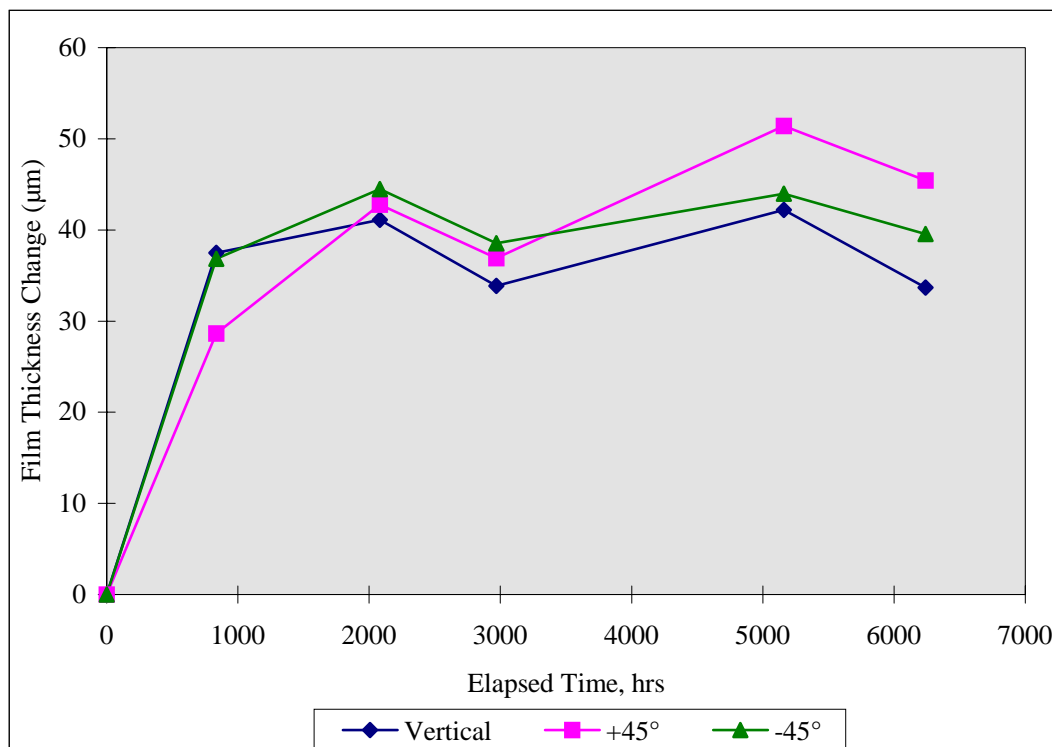


Figure 5.9 Cumulative Change in Teflon[®] Film Thickness as a Function Of Operating Hours and Angular Position -- Tube 1

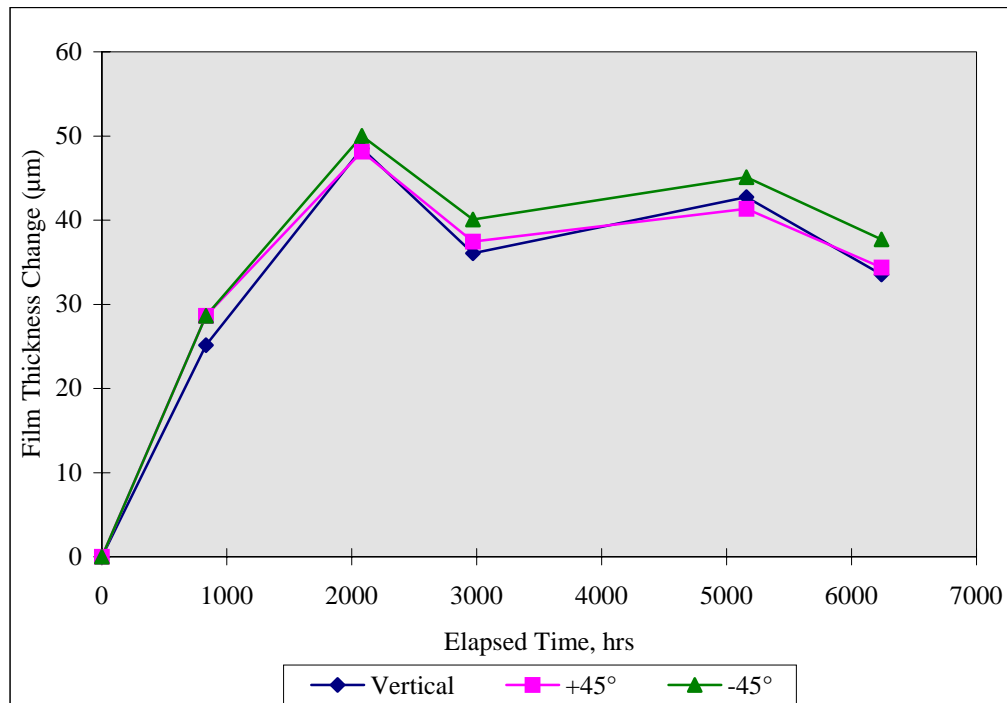


Figure 5.10 Cumulative Change in Teflon® Film Thickness as a Function of Operating Hours and Angular Position -- Tube 5

In each of the figures it can be seen that there were no significant differences in film thickness changes as a function of angular position, suggesting that high flue gas velocity areas, such as those between tubes, do not incur increased amounts of abrasive wear. Similar results were observed for the other 4 tubes in the top row of the heat exchanger. Although there appears to be a slight (10.2 µm [0.4 mil]) decrease in film thickness for tube 5, this amount is within the absolute accuracy range (+/- 1% of reading) of the thickness gage for a nominal 508 µm (20 mil) film.

5.2.2 Teflon® Surface Replications

Six sets (including replications made prior to flue gas exposure) of film surface replications were obtained during the course of the test program. Each set consists of 5 film replications made in the locations shown in Figure 4.1. The goal of making the surface replications was to record and observe any microscopic changes to the Teflon® tube surface which may not be evident to the naked eye or detected with the eddy current film thickness technique. As mentioned in Section 4.2, each replication was inspected under a microscope and then photographed at two different magnifications (25X and 200X). Comparisons were then made between the pre-test, intermediate and post-test replications to determine the location and amount of microscopic surface wear. Representative examples of the surface replications are shown in Figures 5.11 through 5.13. Figure 5.11 represents a typical tube surface prior to exposure to flue gas, Figure 5.12 shows the surface of tube 1, and Figure 5.13 the surface of tube 6, both at the conclusion of

the test program. The microphotographs in each of the three figures were taken at a magnification of 200X.

In Figure 5.11 the surface of the Teflon[®] film is extremely smooth, with only minor striations running axially (lengthwise). These striations result from the manufacturing process. In Figure 5.12 (tube 1), minimal surface damage is visible. This is not unexpected in that the predicted flue gas flow pattern to the top row of tubes has a region of low flow at this tube. The vertical

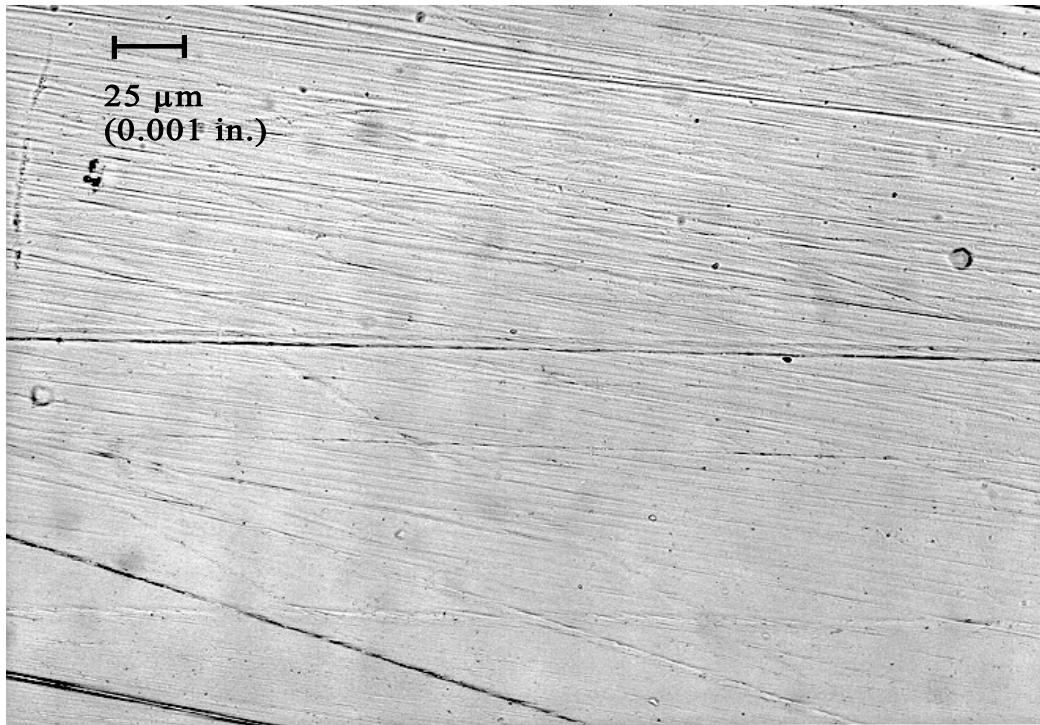


Figure 5.11 Microphotograph of Clean Tube Surface

marks running from the lower right to upper left are cuts in the surface made by the calipers used to make the tube dimensional measurements (see Section 4.2). In Figure 5.13 (tube 6) some minor wear damage is visible. This also is not unexpected, since this tube was expected to see the most flue gas (and fly ash). The wear damage appears to be very fine and uniform, but very small (μm range), resembling small, circular depressions. Typically, details for any given object are visible to the naked eye down to about $200\ \mu\text{m}$ (8 mils). At a magnification of 200X, this translates to a size of approximately 38.1 mm (1.5 inches) on the microphotograph. For comparison, the dark oval in the center of the Figure 5.13 is approximately 12.7 mm (0.5 inches) long, or approximately $63\ \mu\text{m}$ (2.5 mils).

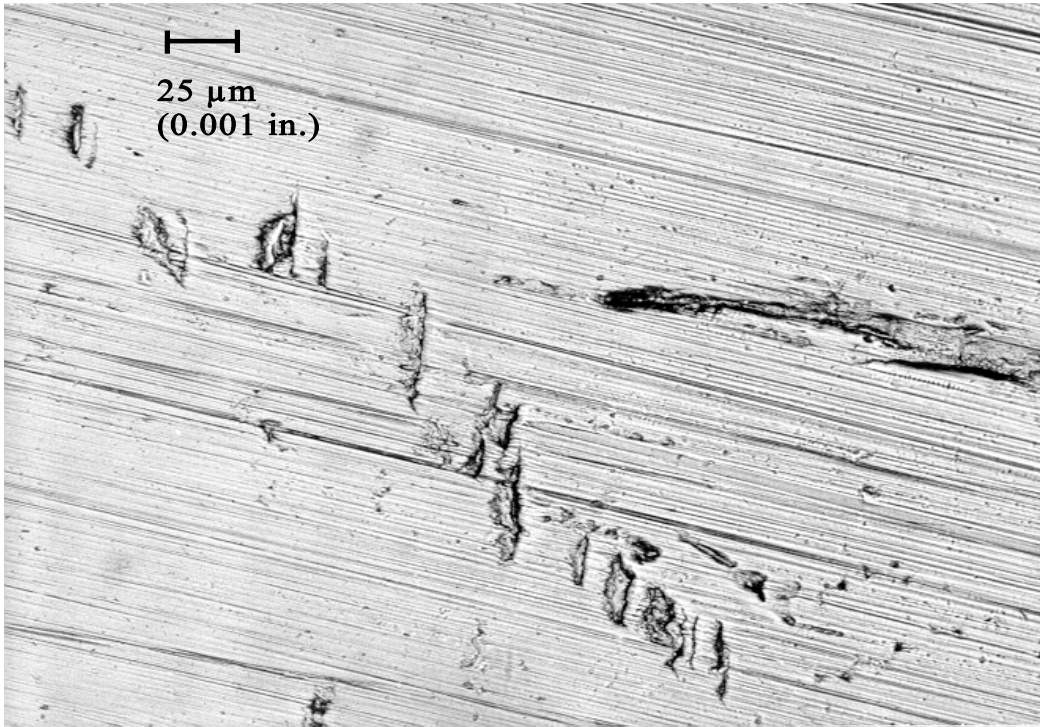


Figure 5.12 Microphotograph of Tube 1 -- End of Test

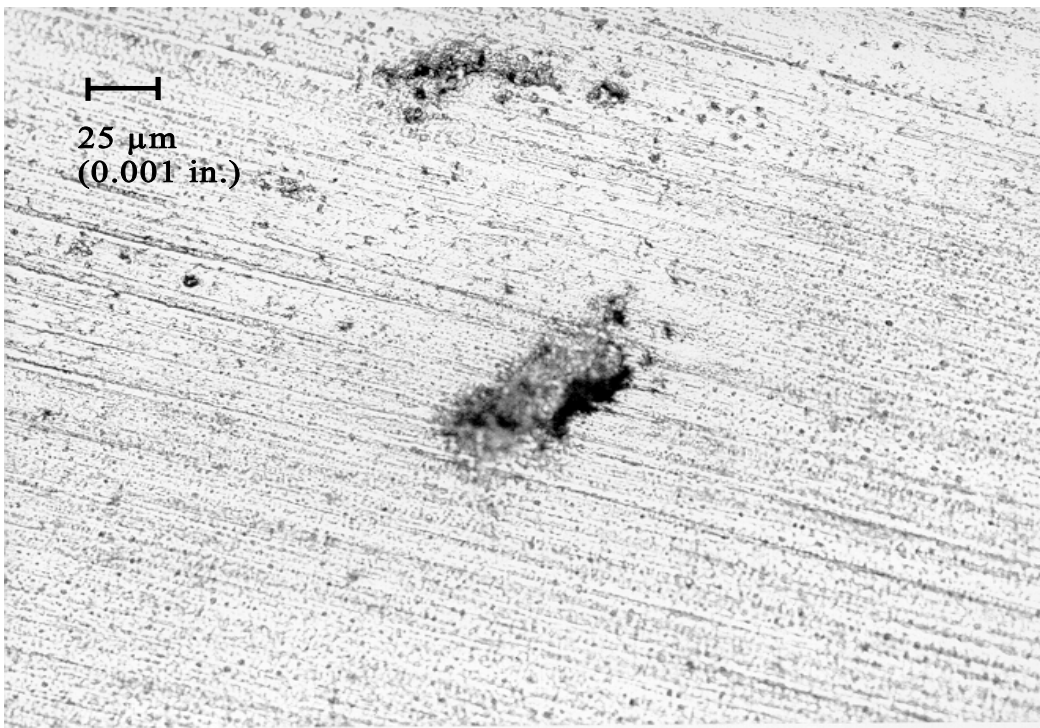


Figure 5.13 Microphotograph of Tube 6 -- End of Test

6.0 CONCLUSIONS AND RECOMMENDATIONS

The objective of Task 3 was to demonstrate long-term operation of a condensing heat exchanger for coal-fired conditions. The specific goal of the task was to determine the amount of wear, if any, on the Teflon[®]-covered internals of the heat exchanger. A single-stage pilot CHX[®] unit was installed at the ECTC and operated at typical flue gas conditions for over 6,200 hours. Visual inspections, film thickness measurements, and film surface replications were performed at various times during the test program. No significant wear was detected on any of the tube surfaces. Specific conclusions and recommendations include the following:

- Particulate Deposition: At higher particulate loadings, deposition can be a problem, particularly if inadequate wash water flow rates are used. Wetted ash surfaces which are not removed during washing become sites for additional ash deposition, resulting in increases in heat exchanger pressure drop. Installation of the modified, 3-nozzle manifold (and subsequent increase in flow rate) seemed to alleviate this problem. For oil applications, the "design" wash schedule is 40.75 lpm/m² (1 gpm/ft²) for 10 minutes. Based on the results from this test program, this rate will need to be increased for higher particulate loadings such as coal-fired utility applications.
- Film Thickness: No significant decrease in film thickness was detected during the course of the test program. After an initial increase in film thickness resulting from surface stress relaxation during heating, film thicknesses remained essentially constant. Some locations exhibited a slight decrease (0.4 mils) in thickness, but this amount is within the absolute accuracy range (+/- 1% of reading) of the thickness gage. Measurements at various angular positions around the circumference of the tubes also showed no significant wear, even in areas of high flue gas velocity.
- Film Surface: Surface replications taken during the course of the test program revealed only minor, microscopic wear damage to the surface of the Teflon[®] film, and only on tubes subjected to the highest flue gas flow rates. The wear damage appeared to be on the μm level and was very fine and uniform, resembling round depressions in the film surface. At this scale, this type of wear damage should pose no problems for long-term operation of a large-scale unit.
- Predicted Teflon[®] Film Life: Based on the measurement data, the Teflon[®] covering on the heat exchanger tubes should have a life expectancy of greater than 10 years. If the 0.4 mil decrease observed for some tube locations is correct, 10 years of operation would yield an approximate decrease in film thickness of 4 mils from a nominal film thickness of 20 mils. It would be more probable that any tube replacement would be due to other operational problems (e.g., scale buildup, temperature excursions due to cooling water failure, etc.). For comparison, operation at a particulate loading of 400 mg/dscm (0.35 lb/10⁶ Btu) for 6 months is equivalent to 10 years at 20 mg/dscm (0.017 lb/10⁶ Btu).

**Appendix A: Tabulated Data - Teflon[®] Film Thickness Measurements
Data Set 1 - 3/12/96**

Project No. 43456-300

One Year CHX Life Test at the ECTC

MEASUREMENT: Teflon Thickness (Top of Tube), millimeters							
Tube Location	Measurement Number	TUBE NUMBER					
		1	2	3	4	5	6
A	1	0.508	0.506	0.467	0.479	0.557	0.513
	2	0.513	0.496	0.455	0.481	0.554	0.510
	3	0.515	0.510	0.459	0.481	0.554	0.508
	Average	<i>0.512</i>	<i>0.504</i>	<i>0.460</i>	<i>0.480</i>	<i>0.555</i>	<i>0.510</i>
B	1	0.501	0.523	0.518	0.552	0.557	0.525
	2	0.518	0.523	0.493	0.508	0.554	0.525
	3	0.508	0.523	0.523	0.491	0.554	0.523
	Average	<i>0.509</i>	<i>0.523</i>	<i>0.511</i>	<i>0.517</i>	<i>0.555</i>	<i>0.524</i>
C	1	0.489	0.481	0.489	0.510	0.535	0.515
	2	0.493	0.472	0.484	0.476	0.547	0.523
	3	0.491	0.469	0.503	0.486	0.537	0.520
	Average	<i>0.491</i>	<i>0.474</i>	<i>0.492</i>	<i>0.491</i>	<i>0.540</i>	<i>0.519</i>
D	1	0.518	0.501	0.459	0.469	0.523	0.527
	2	0.498	0.510	0.459	0.467	0.518	0.520
	3	0.508	0.510	0.464	0.464	0.520	0.525
	Average	<i>0.508</i>	<i>0.507</i>	<i>0.461</i>	<i>0.467</i>	<i>0.520</i>	<i>0.524</i>
E	1	0.496	0.518	0.459	0.489	0.530	0.518
	2	0.498	0.513	0.472	0.498	0.540	0.554
	3	0.496	0.513	0.469	0.496	0.549	0.535
	Average	<i>0.497</i>	<i>0.514</i>	<i>0.467</i>	<i>0.494</i>	<i>0.540</i>	<i>0.536</i>
	Tube Average	0.503	0.504	0.478	0.490	0.542	0.523
Hrs. Operation: 0		25.4 mm = 1 inch					
Temperature: 51 F							
Date: 3/12/96							
Recorded by: KHS							

Project No. 43456-300

One Year CHX Life Test at the ECTC

MEASUREMENT: Teflon Thickness (Top of Tube), millimeters																			
Tube Location	Measurement Number	TUBE NUMBER																	
		7	8	9	10	11	12												
A	1	0.527	0.569	0.498	0.513	0.527	0.518												
	2	0.527	0.569	0.486	0.513	0.527	0.513												
	3	0.527	0.569	0.486	0.515	0.525	0.513												
	Average	<i>0.527</i>	<i>0.569</i>	<i>0.490</i>	<i>0.514</i>	<i>0.527</i>	<i>0.514</i>												
B	1	0.527	0.559	0.503	0.518	0.520	0.506												
	2	0.515	0.564	0.506	0.515	0.525	0.501												
	3	0.515	0.564	0.506	0.515	0.523	0.501												
	Average	<i>0.519</i>	<i>0.562</i>	<i>0.505</i>	<i>0.516</i>	<i>0.523</i>	<i>0.502</i>												
C	1	0.510	0.540	0.479	0.520	0.523	0.506												
	2	0.518	0.547	0.476	0.520	0.525	0.498												
	3	0.520	0.549	0.472	0.520	0.523	0.498												
	Average	<i>0.516</i>	<i>0.545</i>	<i>0.476</i>	<i>0.520</i>	<i>0.523</i>	<i>0.501</i>												
D	1	0.523	0.532	0.476	0.518	0.525	0.506												
	2	0.527	0.535	0.476	0.520	0.525	0.506												
	3	0.520	0.537	0.476	0.523	0.518	0.506												
	Average	<i>0.523</i>	<i>0.535</i>	<i>0.476</i>	<i>0.520</i>	<i>0.523</i>	<i>0.506</i>												
E	1	0.523	0.542	0.523	0.513	0.518	0.513												
	2	0.523	0.537	0.520	0.510	0.518	0.513												
	3	0.523	0.532	0.523	0.510	0.518	0.513												
	Average	<i>0.523</i>	<i>0.537</i>	<i>0.522</i>	<i>0.511</i>	<i>0.518</i>	<i>0.513</i>												
	Tube Average	0.522	0.550	0.494	0.516	0.523	0.507												
<table style="width: 100%; border: none;"> <tr> <td style="width: 30%;">Hrs. Operation:</td> <td style="width: 30%;">0</td> <td style="width: 40%; text-align: right;">25.4 mm = 1 inch</td> </tr> <tr> <td>Temperature:</td> <td>51 F</td> <td></td> </tr> <tr> <td>Date:</td> <td>3/12/96</td> <td></td> </tr> <tr> <td>Recorded by:</td> <td>KHS</td> <td></td> </tr> </table>								Hrs. Operation:	0	25.4 mm = 1 inch	Temperature:	51 F		Date:	3/12/96		Recorded by:	KHS	
Hrs. Operation:	0	25.4 mm = 1 inch																	
Temperature:	51 F																		
Date:	3/12/96																		
Recorded by:	KHS																		

Project No. 43456-300

One Year CHX Life Test at the ECTC

MEASUREMENT: Teflon Thickness (Top + 45°), millimeters							
Tube Location	Measurement Number	TUBE NUMBER					
		1	2	3	4	5	6
A	1	0.552	0.525	0.510	0.513	0.574	0.566
	2	0.542	0.508	0.554	0.544	0.574	0.569
	3	0.537	0.535	0.557	0.518	0.566	0.554
	Average	<i>0.544</i>	<i>0.523</i>	<i>0.540</i>	<i>0.525</i>	<i>0.571</i>	<i>0.563</i>
B	1	#N/A	0.510	0.540	0.525	0.561	0.569
	2	#N/A	0.508	0.578	0.506	0.581	0.569
	3	#N/A	0.506	0.542	0.513	0.549	0.574
	Average	#N/A	<i>0.508</i>	<i>0.553</i>	<i>0.514</i>	<i>0.564</i>	<i>0.570</i>
C	1	0.547	0.501	0.510	0.508	0.530	0.564
	2	0.535	0.498	0.515	0.510	0.530	0.574
	3	0.544	0.493	0.513	0.508	0.535	0.574
	Average	<i>0.542</i>	<i>0.497</i>	<i>0.513</i>	<i>0.509</i>	<i>0.531</i>	<i>0.570</i>
D	1	0.540	0.506	0.506	0.510	0.530	0.557
	2	0.552	0.506	0.506	0.506	0.530	0.564
	3	0.544	0.503	0.503	0.508	0.540	0.569
	Average	<i>0.545</i>	<i>0.505</i>	<i>0.505</i>	<i>0.508</i>	<i>0.533</i>	<i>0.563</i>
E	1	0.549	0.530	0.508	0.549	0.537	0.537
	2	0.549	0.530	0.508	0.554	0.537	0.540
	3	0.559	0.527	0.510	0.561	0.542	0.520
	Average	<i>0.553</i>	<i>0.529</i>	<i>0.509</i>	<i>0.555</i>	<i>0.539</i>	<i>0.532</i>
	Tube Average	0.546	0.512	0.524	0.522	0.548	0.560
Hrs. Operation: 0 Temperature: 51 F Date: 3/12/96 Recorded by: KHS		25.4 mm = 1 inch					

Project No. 43456-300

One Year CHX Life Test at the ECTC

MEASUREMENT: Teflon Thickness (Top - 45°), millimeters							
Tube Location	Measurement Number	TUBE NUMBER					
		1	2	3	4	5	6
A	1	0.527	0.547	0.474	0.527	0.569	0.530
	2	0.520	0.547	0.469	0.491	0.566	0.496
	3	0.518	0.544	0.469	0.489	0.566	0.532
	Average	<i>0.522</i>	<i>0.546</i>	<i>0.471</i>	<i>0.502</i>	<i>0.567</i>	<i>0.519</i>
B	1	0.506	0.544	0.481	0.489	0.571	0.484
	2	0.508	0.549	0.491	0.496	0.564	0.506
	3	0.506	0.552	0.484	0.496	0.566	0.481
	Average	<i>0.506</i>	<i>0.548</i>	<i>0.485</i>	<i>0.493</i>	<i>0.567</i>	<i>0.490</i>
C	1	0.518	0.537	0.491	0.489	0.559	0.501
	2	0.506	0.542	0.503	0.496	0.564	0.474
	3	0.510	0.540	0.501	0.496	0.564	0.474
	Average	<i>0.511</i>	<i>0.540</i>	<i>0.498</i>	<i>0.493</i>	<i>0.562</i>	<i>0.483</i>
D	1	0.535	0.554	0.484	0.486	0.564	0.476
	2	0.535	0.554	0.489	0.498	0.559	0.503
	3	0.532	0.554	0.486	0.496	0.559	0.491
	Average	<i>0.534</i>	<i>0.554</i>	<i>0.486</i>	<i>0.493</i>	<i>0.561</i>	<i>0.490</i>
E	1	0.513	0.566	0.474	0.510	0.569	0.508
	2	0.513	0.554	0.472	0.508	0.566	0.476
	3	0.513	0.569	0.472	0.506	0.569	0.481
	Average	<i>0.513</i>	<i>0.563</i>	<i>0.472</i>	<i>0.508</i>	<i>0.568</i>	<i>0.489</i>
	Tube Average	0.517	0.550	0.483	0.498	0.565	0.494
Hrs. Operation: 0 Temperature: 51 F Date: 3/12/96 Recorded by: KHS		25.4 mm = 1 inch					

**Appendix B: Tabulated Data - Teflon[®] Film Thickness Measurements
Data Set 2 - 4/29/96**

Project No. 43456-300

One Year CHX Life Test at the ECTC

MEASUREMENT: Teflon Thickness (Top of Tube), millimeters							
Tube Location	Measurement Number	TUBE NUMBER					
		1	2	3	4	5	6
A	1	0.548	0.523	0.484	0.503	0.584	0.538
	2	0.550	0.523	0.484	0.513	0.587	0.543
	3	0.540	0.526	0.496	0.508	0.582	0.545
	Average	<i>0.546</i>	<i>0.524</i>	<i>0.488</i>	<i>0.508</i>	<i>0.584</i>	<i>0.542</i>
B	1	0.543	0.523	0.506	0.503	0.570	0.555
	2	0.530	0.523	0.511	0.513	0.584	0.575
	3	0.540	0.530	0.508	0.503	0.584	0.555
	Average	<i>0.538</i>	<i>0.526</i>	<i>0.508</i>	<i>0.507</i>	<i>0.580</i>	<i>0.562</i>
C	1	0.540	0.503	0.511	0.499	0.555	0.545
	2	0.526	0.499	0.501	0.503	0.550	0.550
	3	0.540	0.503	0.506	0.501	0.555	0.550
	Average	<i>0.535</i>	<i>0.502</i>	<i>0.506</i>	<i>0.501</i>	<i>0.553</i>	<i>0.548</i>
D	1	0.540	0.526	0.491	0.503	0.555	0.562
	2	0.545	0.548	0.503	0.499	0.550	0.553
	3	0.550	0.526	0.503	0.496	0.548	0.557
	Average	<i>0.545</i>	<i>0.533</i>	<i>0.499</i>	<i>0.499</i>	<i>0.551</i>	<i>0.557</i>
E	1	0.543	0.548	0.494	0.518	0.565	0.557
	2	0.540	0.545	0.494	0.513	0.565	0.557
	3	0.535	0.545	0.491	0.521	0.570	0.557
	Average	<i>0.539</i>	<i>0.546</i>	<i>0.493</i>	<i>0.517</i>	<i>0.566</i>	<i>0.557</i>
	Tube Average	0.541	0.526	0.499	0.507	0.567	0.553
Hrs. Operation:		834		25.4 mm = 1 inch			
Temperature:		62 F					
Date:		4/29/96					
Recorded by:		KHS					

Project No. 43456-300

One Year CHX Life Test at the ECTC

MEASUREMENT: Teflon Thickness (Top of Tube), millimeters							
Tube Location	Measurement Number	TUBE NUMBER					
		7	8	9	10	11	12
A	1	0.560	0.604	0.516	0.545	0.560	0.548
	2	0.557	0.597	0.511	0.540	0.555	0.550
	3	0.557	0.594	0.513	0.543	0.557	0.548
	Average	<i>0.558</i>	<i>0.598</i>	<i>0.513</i>	<i>0.543</i>	<i>0.557</i>	<i>0.548</i>
B	1	0.553	0.594	0.526	0.548	0.555	0.535
	2	0.548	0.584	0.530	0.540	0.555	0.528
	3	0.553	0.584	0.528	0.543	0.553	0.528
	Average	<i>0.551</i>	<i>0.588</i>	<i>0.528</i>	<i>0.544</i>	<i>0.554</i>	<i>0.530</i>
C	1	0.548	0.587	0.506	0.565	0.565	0.526
	2	0.543	0.587	0.501	0.550	0.555	0.533
	3	0.550	0.577	0.503	0.553	0.557	0.533
	Average	<i>0.547</i>	<i>0.584</i>	<i>0.503</i>	<i>0.556</i>	<i>0.559</i>	<i>0.530</i>
D	1	0.565	0.577	0.506	0.555	0.555	0.543
	2	0.560	0.577	0.506	0.553	0.550	0.545
	3	0.560	0.577	0.506	0.555	0.555	0.548
	Average	<i>0.562</i>	<i>0.577</i>	<i>0.506</i>	<i>0.554</i>	<i>0.553</i>	<i>0.545</i>
E	1	0.557	0.567	0.555	0.548	0.562	0.545
	2	0.560	0.580	0.550	0.548	0.560	0.555
	3	0.555	0.580	0.553	0.545	0.553	0.557
	Average	<i>0.557</i>	<i>0.575</i>	<i>0.553</i>	<i>0.547</i>	<i>0.558</i>	<i>0.553</i>
	Tube Average	0.555	0.584	0.521	0.549	0.556	0.541
Hrs. Operation:		834		25.4 mm = 1 inch			
Temperature:		62 F					
Date:		4/29/96					
Recorded by:		KHS					

Project No. 43456-300

One Year CHX Life Test at the ECTC

MEASUREMENT: Teflon Thickness (Top + 45°), millimeters							
Tube Location	Measurement Number	TUBE NUMBER					
		1	2	3	4	5	6
A	1	0.584	0.535	0.518	0.528	0.604	0.580
	2	0.567	0.538	0.533	0.557	0.597	0.575
	3	0.570	0.530	0.521	0.533	0.599	0.580
	Average	<i>0.574</i>	<i>0.535</i>	<i>0.524</i>	<i>0.539</i>	<i>0.600</i>	<i>0.578</i>
B	1	0.562	0.530	0.533	0.550	0.584	0.580
	2	0.570	0.540	0.548	0.535	0.589	0.577
	3	0.570	0.543	0.545	0.535	0.582	0.575
	Average	<i>0.567</i>	<i>0.538</i>	<i>0.542</i>	<i>0.540</i>	<i>0.585</i>	<i>0.577</i>
C	1	0.577	0.540	0.538	0.540	0.557	0.589
	2	0.580	0.533	0.540	0.538	0.557	0.604
	3	0.584	0.543	0.543	0.540	0.553	0.589
	Average	<i>0.580</i>	<i>0.539</i>	<i>0.540</i>	<i>0.539</i>	<i>0.556</i>	<i>0.594</i>
D	1	0.584	0.533	0.545	0.550	0.560	0.580
	2	0.577	0.533	0.538	0.538	0.562	0.584
	3	0.575	0.530	0.540	0.545	0.562	0.572
	Average	<i>0.579</i>	<i>0.532</i>	<i>0.541</i>	<i>0.544</i>	<i>0.562</i>	<i>0.579</i>
E	1	0.572	0.567	0.550	0.543	0.582	0.577
	2	0.570	0.562	0.548	0.545	0.580	0.550
	3	0.575	0.567	0.540	0.553	0.575	0.557
	Average	<i>0.572</i>	<i>0.566</i>	<i>0.546</i>	<i>0.547</i>	<i>0.579</i>	<i>0.562</i>
	Tube Average	0.576	0.542	0.539	0.542	0.576	0.578
Hrs. Operation:		834		25.4 mm = 1 inch			
Temperature:		62 F					
Date:		4/29/96					
Recorded by:		KHS					

Project No. 43456-300

One Year CHX Life Test at the ECTC

MEASUREMENT: Teflon Thickness (Top - 45°), millimeters							
Tube Location	Measurement Number	TUBE NUMBER					
		1	2	3	4	5	6
A	1	0.560	0.584	0.511	0.528	0.611	0.533
	2	0.562	0.582	0.501	0.523	0.609	0.523
	3	0.557	0.589	0.501	0.526	0.614	0.523
	Average	<i>0.560</i>	<i>0.585</i>	<i>0.504</i>	<i>0.526</i>	<i>0.611</i>	<i>0.526</i>
B	1	0.543	0.584	0.523	0.528	0.602	0.518
	2	0.543	0.589	0.523	0.526	0.604	0.508
	3	0.538	0.589	0.526	0.526	0.604	0.501
	Average	<i>0.541</i>	<i>0.588</i>	<i>0.524</i>	<i>0.526</i>	<i>0.603</i>	<i>0.509</i>
C	1	0.543	0.584	0.513	0.526	0.582	0.511
	2	0.550	0.580	0.526	0.511	0.582	0.511
	3	0.550	0.580	0.530	0.513	0.577	0.513
	Average	<i>0.548</i>	<i>0.581</i>	<i>0.523</i>	<i>0.517</i>	<i>0.580</i>	<i>0.512</i>
D	1	0.575	0.587	0.508	0.516	0.584	0.533
	2	0.577	0.589	0.516	0.508	0.582	0.518
	3	0.577	0.589	0.518	0.511	0.584	0.518
	Average	<i>0.576</i>	<i>0.589</i>	<i>0.514</i>	<i>0.512</i>	<i>0.584</i>	<i>0.523</i>
E	1	0.540	0.597	0.506	0.535	0.587	0.521
	2	0.545	0.597	0.496	0.530	0.587	0.503
	3	0.550	0.602	0.501	0.530	0.594	0.526
	Average	<i>0.545</i>	<i>0.598</i>	<i>0.501</i>	<i>0.532</i>	<i>0.589</i>	<i>0.517</i>
	Tube Average	0.554	0.588	0.513	0.522	0.594	0.517
Hrs. Operation:		834		25.4 mm = 1 inch			
Temperature:		62 F					
Date:		4/29/96					
Recorded by:		KHS					

**Appendix C: Tabulated Data - Teflon[®] Film Thickness Measurements
Data Set 3 - 7/9/96**

Project No. 43456-300

One Year CHX Life Test at the ECTC

MEASUREMENT: Teflon Thickness (Top of Tube), millimeters							
Tube Location	Measurement Number	TUBE NUMBER					
		1	2	3	4	5	6
A	1	0.543	0.543	0.502	0.522	0.607	0.589
	2	0.548	0.550	0.504	0.520	0.604	0.594
	3	0.556	0.548	0.502	0.517	0.607	0.563
	Average	<i>0.549</i>	<i>0.547</i>	<i>0.502</i>	<i>0.520</i>	<i>0.606</i>	<i>0.582</i>
B	1	0.543	0.535	0.512	0.522	0.604	0.571
	2	0.543	0.538	0.514	0.522	0.620	0.574
	3	0.553	0.535	0.512	0.517	0.612	0.571
	Average	<i>0.546</i>	<i>0.536</i>	<i>0.513</i>	<i>0.520</i>	<i>0.612</i>	<i>0.572</i>
C	1	0.532	0.512	0.517	0.507	0.574	0.561
	2	0.538	0.517	0.527	0.517	0.574	0.558
	3	0.535	0.520	0.512	0.507	0.571	0.571
	Average	<i>0.535</i>	<i>0.516</i>	<i>0.519</i>	<i>0.510</i>	<i>0.573</i>	<i>0.563</i>
D	1	0.548	0.561	0.504	0.517	0.568	0.574
	2	0.556	0.538	0.514	0.538	0.576	0.579
	3	0.553	0.535	0.520	0.522	0.579	0.584
	Average	<i>0.552</i>	<i>0.544</i>	<i>0.513</i>	<i>0.526</i>	<i>0.574</i>	<i>0.579</i>
E	1	0.538	0.576	0.525	0.535	0.589	0.574
	2	0.538	0.576	0.507	0.530	0.581	0.574
	3	0.545	0.574	0.496	0.532	0.589	0.576
	Average	<i>0.540</i>	<i>0.575</i>	<i>0.509</i>	<i>0.532</i>	<i>0.586</i>	<i>0.574</i>
	Tube Average	0.544	0.544	0.511	0.522	0.590	0.574
Hrs. Operation: 2082		25.4 mm = 1 inch					
Temperature: 73 F							
Date: 7/9/96							
Recorded by: KHS							

Project No. 43456-300

One Year CHX Life Test at the ECTC

MEASUREMENT: Teflon Thickness (Top of Tube), millimeters							
Tube Location	Measurement Number	TUBE NUMBER					
		7	8	9	10	11	12
A	1	0.584	0.625	0.525	0.563	0.579	0.568
	2	0.579	0.628	0.527	0.558	0.576	0.563
	3	0.579	0.622	0.527	0.561	0.574	0.563
	Average	<i>0.580</i>	<i>0.625</i>	<i>0.526</i>	<i>0.561</i>	<i>0.576</i>	<i>0.565</i>
B	1	0.574	0.617	0.553	0.566	0.581	0.550
	2	0.576	0.620	0.550	0.566	0.574	0.543
	3	0.563	0.620	0.550	0.576	0.571	0.548
	Average	<i>0.571</i>	<i>0.619</i>	<i>0.551</i>	<i>0.569</i>	<i>0.575</i>	<i>0.547</i>
C	1	0.563	0.599	0.517	0.576	0.579	0.545
	2	0.563	0.602	0.517	0.576	0.579	0.548
	3	0.556	0.592	0.514	0.574	0.579	0.548
	Average	<i>0.561</i>	<i>0.598</i>	<i>0.516</i>	<i>0.575</i>	<i>0.579</i>	<i>0.547</i>
D	1	0.571	0.594	0.525	0.566	0.566	0.556
	2	0.571	0.579	0.520	0.568	0.566	0.558
	3	0.568	0.581	0.520	0.566	0.566	0.558
	Average	<i>0.570</i>	<i>0.585</i>	<i>0.521</i>	<i>0.567</i>	<i>0.566</i>	<i>0.557</i>
E	1	0.584	0.581	0.581	0.561	0.571	0.566
	2	0.574	0.584	0.574	0.561	0.568	0.566
	3	0.574	0.584	0.574	0.561	0.571	0.566
	Average	<i>0.577</i>	<i>0.583</i>	<i>0.576</i>	<i>0.561</i>	<i>0.570</i>	<i>0.566</i>
	Tube Average	0.572	0.602	0.538	0.567	0.573	0.556
Hrs. Operation: 2082		25.4 mm = 1 inch					
Temperature: 73 F							
Date: 7/9/96							
Recorded by: KHS							

Project No. 43456-300

One Year CHX Life Test at the ECTC

MEASUREMENT: Teflon Thickness (Top + 45°), millimeters							
Tube Location	Measurement Number	TUBE NUMBER					
		1	2	3	4	5	6
A	1	0.602	0.540	0.532	0.556	0.622	0.589
	2	0.586	0.550	0.538	0.553	0.622	0.592
	3	0.586	0.540	0.532	0.553	0.620	0.589
	Average	<i>0.592</i>	<i>0.544</i>	<i>0.534</i>	<i>0.554</i>	<i>0.622</i>	<i>0.590</i>
B	1	0.581	0.548	0.558	0.550	0.607	0.607
	2	0.581	0.548	0.553	0.550	0.625	0.607
	3	0.584	0.540	0.553	0.556	0.604	0.610
	Average	<i>0.582</i>	<i>0.545</i>	<i>0.555</i>	<i>0.552</i>	<i>0.612</i>	<i>0.608</i>
C	1	0.586	0.548	0.556	0.566	0.561	0.592
	2	0.589	0.543	0.553	0.538	0.566	0.610
	3	0.589	0.543	0.548	0.548	0.566	0.607
	Average	<i>0.588</i>	<i>0.544</i>	<i>0.552</i>	<i>0.550</i>	<i>0.564</i>	<i>0.603</i>
D	1	0.594	0.548	0.556	0.556	0.581	0.615
	2	0.586	0.540	0.550	0.553	0.576	0.594
	3	0.584	0.543	0.548	0.550	0.574	0.612
	Average	<i>0.588</i>	<i>0.544</i>	<i>0.551</i>	<i>0.553</i>	<i>0.577</i>	<i>0.607</i>
E	1	0.592	0.586	0.553	0.561	0.607	0.574
	2	0.594	0.586	0.550	0.574	0.602	0.574
	3	0.594	0.576	0.550	0.576	0.604	0.574
	Average	<i>0.593</i>	<i>0.583</i>	<i>0.551</i>	<i>0.570</i>	<i>0.604</i>	<i>0.574</i>
	Tube Average	0.590	0.552	0.549	0.556	0.596	0.596
Hrs. Operation: 2082 Temperature: 73 F Date: 7/9/96 Recorded by: KHS		25.4 mm = 1 inch					

Project No. 43456-300

One Year CHX Life Test at the ECTC

MEASUREMENT: Teflon Thickness (Top - 45°), millimeters							
Tube Location	Measurement Number	TUBE NUMBER					
		1	2	3	4	5	6
A	1	0.589	0.597	0.558	0.535	0.622	0.540
	2	0.568	0.607	0.514	0.530	0.622	0.545
	3	0.568	0.599	0.509	0.532	0.630	0.538
	Average	<i>0.575</i>	<i>0.601</i>	<i>0.527</i>	<i>0.532</i>	<i>0.625</i>	<i>0.541</i>
B	1	0.540	0.602	0.522	0.540	0.625	0.535
	2	0.545	0.599	0.522	0.548	0.630	0.517
	3	0.540	0.599	0.522	0.540	0.622	0.530
	Average	<i>0.542</i>	<i>0.600</i>	<i>0.522</i>	<i>0.543</i>	<i>0.626</i>	<i>0.527</i>
C	1	0.563	0.592	0.530	0.527	0.610	0.512
	2	0.558	0.599	0.522	0.525	0.594	0.522
	3	0.556	0.592	0.522	0.525	0.594	0.525
	Average	<i>0.559</i>	<i>0.594</i>	<i>0.525</i>	<i>0.526</i>	<i>0.599</i>	<i>0.520</i>
D	1	0.581	0.607	0.527	0.525	0.607	0.520
	2	0.581	0.617	0.525	0.530	0.604	0.514
	3	0.576	0.610	0.525	0.530	0.615	0.517
	Average	<i>0.580</i>	<i>0.611</i>	<i>0.526</i>	<i>0.528</i>	<i>0.609</i>	<i>0.517</i>
E	1	0.553	0.612	0.504	0.558	0.617	0.499
	2	0.556	0.610	0.504	0.545	0.617	0.504
	3	0.550	0.610	0.504	0.543	0.615	0.504
	Average	<i>0.553</i>	<i>0.610</i>	<i>0.504</i>	<i>0.549</i>	<i>0.616</i>	<i>0.502</i>
	Tube Average	0.562	0.603	0.521	0.535	0.615	0.521
Hrs. Operation: 2082 Temperature: 73 F Date: 7/9/96 Recorded by: KHS		25.4 mm = 1 inch					

**Appendix D: Tabulated Data - Teflon[®] Film Thickness Measurements
Data Set 4 - 9/12/96**

Project No. 43456-300

One Year CHX Life Test at the ECTC

MEASUREMENT: Teflon Thickness (Top of Tube), millimeters							
Tube Location	Measurement Number	TUBE NUMBER					
		1	2	3	4	5	6
A	1	0.551	0.531	0.501	0.516	0.599	0.546
	2	0.541	0.531	0.496	0.511	0.607	0.551
	3	0.541	0.529	0.493	0.511	0.604	0.546
	Average	<i>0.545</i>	<i>0.530</i>	<i>0.497</i>	<i>0.513</i>	<i>0.603</i>	<i>0.548</i>
B	1	0.541	0.554	0.521	0.511	0.584	0.564
	2	0.539	0.546	0.521	0.524	0.581	0.564
	3	0.539	0.546	0.508	0.516	0.584	0.564
	Average	<i>0.539</i>	<i>0.549</i>	<i>0.517</i>	<i>0.517</i>	<i>0.583</i>	<i>0.564</i>
C	1	0.529	0.508	0.508	0.503	0.561	0.554
	2	0.526	0.511	0.508	0.506	0.561	0.556
	3	0.529	0.508	0.508	0.506	0.561	0.561
	Average	<i>0.528</i>	<i>0.509</i>	<i>0.508</i>	<i>0.505</i>	<i>0.561</i>	<i>0.557</i>
D	1	0.544	0.549	0.501	0.503	0.566	0.566
	2	0.534	0.546	0.496	0.503	0.561	0.566
	3	0.534	0.546	0.503	0.503	0.566	0.569
	Average	<i>0.537</i>	<i>0.547</i>	<i>0.500</i>	<i>0.503</i>	<i>0.565</i>	<i>0.567</i>
E	1	0.539	0.551	0.503	0.526	0.581	0.564
	2	0.536	0.561	0.496	0.524	0.574	0.566
	3	0.536	0.554	0.493	0.521	0.576	0.564
	Average	<i>0.537</i>	<i>0.555</i>	<i>0.498</i>	<i>0.524</i>	<i>0.577</i>	<i>0.565</i>
	Tube Average	0.537	0.538	0.504	0.512	0.578	0.560
Hrs. Operation: 2970		25.4 mm = 1 inch					
Temperature: 78 F							
Date: 9/12/96							
Recorded by: GAK							

Project No. 43456-300

One Year CHX Life Test at the ECTC

MEASUREMENT: Teflon Thickness (Top of Tube), millimeters							
Tube Location	Measurement Number	TUBE NUMBER					
		7	8	9	10	11	12
A	1	0.574	0.617	0.524	0.556	0.566	0.556
	2	0.569	0.619	0.524	0.554	0.566	0.556
	3	0.566	0.614	0.526	0.556	0.569	0.556
	Average	<i>0.570</i>	<i>0.617</i>	<i>0.524</i>	<i>0.555</i>	<i>0.567</i>	<i>0.556</i>
B	1	0.579	0.617	0.551	0.566	0.574	0.561
	2	0.576	0.617	0.549	0.569	0.574	0.556
	3	0.576	0.617	0.549	0.569	0.571	0.556
	Average	<i>0.577</i>	<i>0.617</i>	<i>0.550</i>	<i>0.568</i>	<i>0.573</i>	<i>0.558</i>
C	1	0.554	0.591	0.511	0.564	0.571	0.536
	2	0.556	0.586	0.508	0.564	0.566	0.536
	3	0.554	0.591	0.508	0.564	0.566	0.536
	Average	<i>0.555</i>	<i>0.590</i>	<i>0.509</i>	<i>0.564</i>	<i>0.568</i>	<i>0.536</i>
D	1	0.561	0.576	0.513	0.559	0.559	0.554
	2	0.564	0.579	0.511	0.559	0.559	0.551
	3	0.561	0.571	0.511	0.561	0.559	0.549
	Average	<i>0.562</i>	<i>0.576</i>	<i>0.512</i>	<i>0.560</i>	<i>0.559</i>	<i>0.551</i>
E	1	0.566	0.581	0.576	0.564	0.571	0.571
	2	0.571	0.581	0.566	0.561	0.571	0.566
	3	0.571	0.576	0.574	0.561	0.571	0.569
	Average	<i>0.570</i>	<i>0.580</i>	<i>0.572</i>	<i>0.562</i>	<i>0.571</i>	<i>0.569</i>
	Tube Average	0.567	0.596	0.533	0.562	0.568	0.554
Hrs. Operation: 2970		25.4 mm = 1 inch					
Temperature: 78 F							
Date: 9/12/96							
Recorded by: GAK							

Project No. 43456-300

One Year CHX Life Test at the ECTC

MEASUREMENT: Teflon Thickness (Top + 45°), millimeters							
Tube Location	Measurement Number	TUBE NUMBER					
		1	2	3	4	5	6
A	1	0.576	0.544	0.534	0.551	0.614	0.589
	2	0.576	0.541	0.534	0.551	0.617	0.586
	3	0.576	0.541	0.531	0.551	0.614	0.586
	Average	<i>0.576</i>	<i>0.542</i>	<i>0.533</i>	<i>0.551</i>	<i>0.615</i>	<i>0.587</i>
B	1	0.581	0.539	0.536	0.536	0.589	0.604
	2	0.584	0.536	0.539	0.534	0.589	0.607
	3	0.581	0.534	0.541	0.536	0.591	0.607
	Average	<i>0.582</i>	<i>0.536</i>	<i>0.539</i>	<i>0.535</i>	<i>0.590</i>	<i>0.606</i>
C	1	0.586	0.529	0.549	0.551	0.556	0.591
	2	0.586	0.531	0.549	0.554	0.551	0.594
	3	0.591	0.529	0.549	0.549	0.551	0.591
	Average	<i>0.588</i>	<i>0.529</i>	<i>0.549</i>	<i>0.551</i>	<i>0.553</i>	<i>0.592</i>
D	1	0.581	0.541	0.539	0.561	0.581	0.584
	2	0.584	0.541	0.544	0.559	0.569	0.581
	3	0.584	0.541	0.544	0.559	0.576	0.589
	Average	<i>0.583</i>	<i>0.541</i>	<i>0.542</i>	<i>0.560</i>	<i>0.576</i>	<i>0.585</i>
E	1	0.586	0.579	0.556	0.554	0.594	0.561
	2	0.584	0.576	0.551	0.554	0.594	0.561
	3	0.581	0.571	0.551	0.564	0.589	0.556
	Average	<i>0.584</i>	<i>0.576</i>	<i>0.553</i>	<i>0.557</i>	<i>0.592</i>	<i>0.560</i>
	Tube Average	0.583	0.545	0.543	0.551	0.585	0.586
Hrs. Operation: 2970 Temperature: 78 F Date: 9/12/96 Recorded by: GAK		25.4 mm = 1 inch					

Project No. 43456-300

One Year CHX Life Test at the ECTC

MEASUREMENT: Teflon Thickness (Top - 45°), millimeters							
Tube Location	Measurement Number	TUBE NUMBER					
		1	2	3	4	5	6
A	1	0.561	0.594	0.506	0.529	0.619	0.531
	2	0.569	0.599	0.508	0.526	0.619	0.524
	3	0.571	0.599	0.511	0.526	0.622	0.524
	Average	<i>0.567</i>	<i>0.597</i>	<i>0.508</i>	<i>0.527</i>	<i>0.620</i>	<i>0.526</i>
B	1	0.536	0.591	0.513	0.519	0.604	0.521
	2	0.539	0.594	0.516	0.521	0.604	0.519
	3	0.536	0.594	0.513	0.519	0.604	0.516
	Average	<i>0.537</i>	<i>0.593</i>	<i>0.514</i>	<i>0.519</i>	<i>0.604</i>	<i>0.519</i>
C	1	0.551	0.597	0.524	0.526	0.591	0.526
	2	0.549	0.597	0.526	0.521	0.602	0.513
	3	0.551	0.591	0.529	0.524	0.602	0.526
	Average	<i>0.550</i>	<i>0.595</i>	<i>0.526</i>	<i>0.524</i>	<i>0.598</i>	<i>0.522</i>
D	1	0.574	0.609	0.511	0.526	0.594	0.511
	2	0.576	0.604	0.513	0.534	0.599	0.513
	3	0.579	0.599	0.516	0.529	0.597	0.516
	Average	<i>0.576</i>	<i>0.604</i>	<i>0.513</i>	<i>0.529</i>	<i>0.597</i>	<i>0.513</i>
E	1	0.546	0.607	0.506	0.539	0.604	0.539
	2	0.549	0.604	0.506	0.536	0.607	0.524
	3	0.549	0.604	0.508	0.539	0.609	0.536
	Average	<i>0.548</i>	<i>0.605</i>	<i>0.507</i>	<i>0.538</i>	<i>0.607</i>	<i>0.533</i>
	Tube Average	0.556	0.599	0.514	0.527	0.605	0.523
Hrs. Operation: 2970		25.4 mm = 1 inch					
Temperature: 78 F							
Date: 9/12/96							
Recorded by: GAK							

**Appendix E: Tabulated Data - Teflon[®] Film Thickness Measurements
Data Set 5 - 1/20/97**

Project No. 43456-300

One Year CHX Life Test at the ECTC

MEASUREMENT: Teflon Thickness (Top of Tube), millimeters							
Tube Location	Measurement Number	TUBE NUMBER					
		1	2	3	4	5	6
A	1	0.557	0.549	0.504	0.517	0.614	0.560
	2	0.555	0.547	0.506	0.520	0.611	0.560
	3	0.557	0.547	0.504	0.520	0.611	0.563
	Average	<i>0.556</i>	<i>0.547</i>	<i>0.505</i>	<i>0.519</i>	<i>0.612</i>	<i>0.561</i>
B	1	0.547	0.549	0.514	0.517	0.595	0.571
	2	0.547	0.549	0.517	0.517	0.595	0.576
	3	0.549	0.552	0.520	0.517	0.595	0.579
	Average	<i>0.547</i>	<i>0.550</i>	<i>0.517</i>	<i>0.517</i>	<i>0.595</i>	<i>0.575</i>
C	1	0.533	0.514	0.517	0.509	0.565	0.560
	2	0.538	0.517	0.517	0.506	0.565	0.565
	3	0.536	0.517	0.517	0.506	0.565	0.563
	Average	<i>0.536</i>	<i>0.516</i>	<i>0.517</i>	<i>0.507</i>	<i>0.565</i>	<i>0.563</i>
D	1	0.541	0.552	0.501	0.504	0.568	0.576
	2	0.544	0.555	0.501	0.506	0.568	0.576
	3	0.544	0.552	0.501	0.506	0.568	0.576
	Average	<i>0.543</i>	<i>0.553</i>	<i>0.501</i>	<i>0.505</i>	<i>0.568</i>	<i>0.576</i>
E	1	0.547	0.571	0.498	0.528	0.587	0.576
	2	0.544	0.568	0.498	0.528	0.581	0.576
	3	0.544	0.568	0.498	0.528	0.581	0.576
	Average	<i>0.545</i>	<i>0.569</i>	<i>0.498</i>	<i>0.528</i>	<i>0.583</i>	<i>0.576</i>
	Tube Average	0.545	0.547	0.508	0.515	0.585	0.570
<p>Hrs. Operation: 5160 25.4 mm = 1 inch</p> <p>Temperature:</p> <p>Date: 1/20/97</p> <p>Recorded by: GAK</p>							

Project No. 43456-300

One Year CHX Life Test at the ECTC

MEASUREMENT: Teflon Thickness (Top of Tube), millimeters							
Tube Location	Measurement Number	TUBE NUMBER					
		7	8	9	10	11	12
A	1	0.581	0.624	0.530	0.565	0.576	0.565
	2	0.584	0.627	0.533	0.565	0.579	0.568
	3	0.581	0.624	0.530	0.563	0.579	0.565
	Average	<i>0.582</i>	<i>0.625</i>	<i>0.531</i>	<i>0.564</i>	<i>0.578</i>	<i>0.566</i>
B	1	0.571	0.614	0.547	0.563	0.571	0.549
	2	0.568	0.614	0.544	0.563	0.568	0.547
	3	0.571	0.616	0.547	0.560	0.571	0.544
	Average	<i>0.570</i>	<i>0.614</i>	<i>0.546</i>	<i>0.562</i>	<i>0.570</i>	<i>0.547</i>
C	1	0.563	0.597	0.512	0.568	0.571	0.544
	2	0.563	0.595	0.512	0.568	0.571	0.541
	3	0.563	0.595	0.512	0.568	0.571	0.541
	Average	<i>0.563</i>	<i>0.596</i>	<i>0.512</i>	<i>0.568</i>	<i>0.571</i>	<i>0.542</i>
D	1	0.568	0.581	0.517	0.565	0.565	0.560
	2	0.568	0.587	0.514	0.565	0.568	0.565
	3	0.568	0.587	0.517	0.565	0.568	0.563
	Average	<i>0.568</i>	<i>0.585</i>	<i>0.516</i>	<i>0.565</i>	<i>0.567</i>	<i>0.563</i>
E	1	0.576	0.587	0.571	0.557	0.571	0.581
	2	0.576	0.587	0.576	0.557	0.568	0.576
	3	0.576	0.587	0.573	0.565	0.571	0.576
	Average	<i>0.576</i>	<i>0.587</i>	<i>0.573</i>	<i>0.560</i>	<i>0.570</i>	<i>0.578</i>
	Tube Average	0.572	0.601	0.536	0.564	0.571	0.559
<p>Hrs. Operation: 5160 25.4 mm = 1 inch</p> <p>Temperature:</p> <p>Date: 1/20/97</p> <p>Recorded by: GAK</p>							

Project No. 43456-300

One Year CHX Life Test at the ECTC

MEASUREMENT: Teflon Thickness (Top + 45°), millimeters							
Tube Location	Measurement Number	TUBE NUMBER					
		1	2	3	4	5	6
A	1	0.600	0.547	0.536	0.544	0.616	0.605
	2	0.600	0.549	0.536	0.547	0.624	0.603
	3	0.597	0.549	0.533	0.552	0.627	0.605
	Average	<i>0.599</i>	<i>0.548</i>	<i>0.535</i>	<i>0.547</i>	<i>0.622</i>	<i>0.605</i>
B	1	0.605	0.541	0.557	0.541	0.603	0.592
	2	0.603	0.544	0.557	0.541	0.597	0.595
	3	0.603	0.541	0.557	0.544	0.600	0.592
	Average	<i>0.604</i>	<i>0.542</i>	<i>0.557</i>	<i>0.542</i>	<i>0.600</i>	<i>0.593</i>
C	1	0.595	0.538	0.552	0.538	0.560	0.597
	2	0.597	0.538	0.552	0.538	0.560	0.600
	3	0.597	0.538	0.555	0.538	0.563	0.605
	Average	<i>0.597</i>	<i>0.538</i>	<i>0.553</i>	<i>0.538</i>	<i>0.561</i>	<i>0.601</i>
D	1	0.595	0.544	0.547	0.544	0.571	0.595
	2	0.584	0.547	0.549	0.544	0.571	0.597
	3	0.587	0.547	0.549	0.544	0.573	0.595
	Average	<i>0.589</i>	<i>0.546</i>	<i>0.548</i>	<i>0.544</i>	<i>0.572</i>	<i>0.596</i>
E	1	0.603	0.576	0.547	0.552	0.589	0.584
	2	0.597	0.576	0.547	0.552	0.589	0.584
	3	0.595	0.576	0.547	0.555	0.592	0.584
	Average	<i>0.598</i>	<i>0.576</i>	<i>0.547</i>	<i>0.553</i>	<i>0.590</i>	<i>0.584</i>
	Tube Average	0.596	0.550	0.548	0.545	0.589	0.596
<p>Hrs. Operation: 5160 25.4 mm = 1 inch</p> <p>Temperature:</p> <p>Date: 1/20/97</p> <p>Recorded by: GAK</p>							

Project No. 43456-300

One Year CHX Life Test at the ECTC

MEASUREMENT: Teflon Thickness (Top - 45°), millimeters							
Tube Location	Measurement Number	TUBE NUMBER					
		1	2	3	4	5	6
A	1	0.573	0.603	0.509	0.528	0.627	0.517
	2	0.571	0.605	0.509	0.525	0.627	0.520
	3	0.571	0.605	0.509	0.525	0.624	0.522
	Average	<i>0.572</i>	<i>0.605</i>	<i>0.509</i>	<i>0.526</i>	<i>0.626</i>	<i>0.520</i>
B	1	0.538	0.597	0.517	0.530	0.619	0.501
	2	0.541	0.597	0.520	0.530	0.619	0.504
	3	0.538	0.597	0.520	0.533	0.619	0.504
	Average	<i>0.539</i>	<i>0.597</i>	<i>0.519</i>	<i>0.531</i>	<i>0.619</i>	<i>0.503</i>
C	1	0.549	0.589	0.522	0.512	0.595	0.506
	2	0.552	0.589	0.525	0.512	0.595	0.504
	3	0.552	0.589	0.522	0.512	0.595	0.504
	Average	<i>0.551</i>	<i>0.589</i>	<i>0.523</i>	<i>0.512</i>	<i>0.595</i>	<i>0.505</i>
D	1	0.576	0.603	0.514	0.514	0.597	0.506
	2	0.579	0.605	0.514	0.514	0.597	0.509
	3	0.581	0.605	0.514	0.514	0.597	0.512
	Average	<i>0.579</i>	<i>0.605</i>	<i>0.514</i>	<i>0.514</i>	<i>0.597</i>	<i>0.509</i>
E	1	0.563	0.632	0.504	0.552	0.611	0.512
	2	0.568	0.632	0.506	0.552	0.614	0.509
	3	0.565	0.630	0.506	0.552	0.616	0.514
	Average	<i>0.565</i>	<i>0.631</i>	<i>0.505</i>	<i>0.552</i>	<i>0.614</i>	<i>0.512</i>
	Tube Average	0.561	0.605	0.514	0.527	0.610	0.510
<p>Hrs. Operation: 5160 25.4 mm = 1 inch</p> <p>Temperature:</p> <p>Date: 1/20/97</p> <p>Recorded by: GAK</p>							

**Appendix F: Tabulated Data - Teflon[®] Film Thickness Measurements
Data Set 6 - 3/21/97**

Project No. 43456-300

One Year CHX Life Test at the ECTC

MEASUREMENT: Teflon Thickness (Top of Tube), millimeters							
Tube Location	Measurement Number	TUBE NUMBER					
		1	2	3	4	5	6
A	1	0.546	0.530	0.492	0.510	0.595	0.548
	2	0.543	0.530	0.489	0.510	0.595	0.546
	3	0.538	0.530	0.489	0.510	0.595	0.546
	Average	<i>0.542</i>	<i>0.530</i>	<i>0.490</i>	<i>0.510</i>	<i>0.595</i>	<i>0.547</i>
B	1	0.538	0.533	0.507	0.510	0.587	0.566
	2	0.538	0.533	0.507	0.510	0.587	0.566
	3	0.538	0.530	0.507	0.510	0.587	0.566
	Average	<i>0.538</i>	<i>0.532</i>	<i>0.507</i>	<i>0.510</i>	<i>0.587</i>	<i>0.566</i>
C	1	0.530	0.510	0.513	0.505	0.559	0.556
	2	0.530	0.507	0.513	0.505	0.559	0.556
	3	0.530	0.507	0.510	0.505	0.559	0.556
	Average	<i>0.530</i>	<i>0.508</i>	<i>0.512</i>	<i>0.505</i>	<i>0.559</i>	<i>0.556</i>
D	1	0.536	0.536	0.495	0.502	0.561	0.566
	2	0.536	0.538	0.495	0.502	0.561	0.566
	3	0.536	0.538	0.495	0.502	0.559	0.566
	Average	<i>0.536</i>	<i>0.537</i>	<i>0.495</i>	<i>0.502</i>	<i>0.560</i>	<i>0.566</i>
E	1	0.538	0.559	0.497	0.525	0.577	0.569
	2	0.538	0.559	0.495	0.525	0.577	0.566
	3	0.538	0.559	0.495	0.525	0.577	0.566
	Average	<i>0.538</i>	<i>0.559</i>	<i>0.495</i>	<i>0.525</i>	<i>0.577</i>	<i>0.567</i>
	Tube Average	0.537	0.533	0.500	0.510	0.575	0.561
<p>Hrs. Operation: 6240 end of test 25.4 mm = 1 inch</p> <p>Temperature:</p> <p>Date: 3/21/97</p> <p>Recorded by: GAK</p>							

Project No. 43456-300

One Year CHX Life Test at the ECTC

MEASUREMENT: Teflon Thickness (Top of Tube), millimeters							
Tube Location	Measurement Number	TUBE NUMBER					
		7	8	9	10	11	12
A	1	0.566	0.607	0.525	0.556	0.577	0.564
	2	0.566	0.610	0.525	0.556	0.571	0.564
	3	0.566	0.607	0.525	0.554	0.574	0.564
	Average	<i>0.566</i>	<i>0.608</i>	<i>0.525</i>	<i>0.555</i>	<i>0.574</i>	<i>0.564</i>
B	1	0.559	0.607	0.543	0.556	0.569	0.543
	2	0.561	0.605	0.543	0.556	0.569	0.543
	3	0.559	0.607	0.543	0.556	0.566	0.541
	Average	<i>0.559</i>	<i>0.606</i>	<i>0.543</i>	<i>0.556</i>	<i>0.568</i>	<i>0.542</i>
C	1	0.556	0.589	0.513	0.566	0.569	0.543
	2	0.556	0.589	0.513	0.566	0.569	0.543
	3	0.556	0.589	0.515	0.566	0.571	0.543
	Average	<i>0.556</i>	<i>0.589</i>	<i>0.513</i>	<i>0.566</i>	<i>0.570</i>	<i>0.543</i>
D	1	0.566	0.577	0.515	0.561	0.561	0.551
	2	0.566	0.577	0.515	0.561	0.561	0.551
	3	0.564	0.577	0.515	0.561	0.564	0.551
	Average	<i>0.565</i>	<i>0.577</i>	<i>0.515</i>	<i>0.561</i>	<i>0.562</i>	<i>0.551</i>
E	1	0.569	0.579	0.569	0.554	0.561	0.566
	2	0.569	0.579	0.571	0.554	0.561	0.566
	3	0.571	0.579	0.571	0.556	0.561	0.566
	Average	<i>0.570</i>	<i>0.579</i>	<i>0.571</i>	<i>0.554</i>	<i>0.561</i>	<i>0.566</i>
	Tube Average	0.563	0.592	0.534	0.559	0.567	0.553
<p>Hrs. Operation: 6240 end of test 25.4 mm = 1 inch Temperature: Date: 3/21/97 Recorded by: GAK</p>							

Project No. 43456-300

One Year CHX Life Test at the ECTC

MEASUREMENT: Teflon Thickness (Top + 45°), millimeters							
Tube Location	Measurement Number	TUBE NUMBER					
		1	2	3	4	5	6
A	1	0.597	0.538	0.528	0.538	0.610	0.587
	2	0.595	0.538	0.528	0.538	0.610	0.587
	3	0.589	0.538	0.525	0.538	0.607	0.584
	Average	<i>0.594</i>	<i>0.538</i>	<i>0.527</i>	<i>0.538</i>	<i>0.609</i>	<i>0.586</i>
B	1	0.587	0.541	0.551	0.538	0.584	0.589
	2	0.579	0.541	0.551	0.538	0.584	0.587
	3	0.587	0.541	0.548	0.538	0.584	0.587
	Average	<i>0.584</i>	<i>0.541</i>	<i>0.550</i>	<i>0.538</i>	<i>0.584</i>	<i>0.588</i>
C	1	0.587	0.533	0.551	0.538	0.556	0.592
	2	0.592	0.533	0.548	0.538	0.556	0.592
	3	0.587	0.533	0.548	0.538	0.556	0.592
	Average	<i>0.589</i>	<i>0.533</i>	<i>0.549</i>	<i>0.538</i>	<i>0.556</i>	<i>0.592</i>
D	1	0.595	0.541	0.546	0.543	0.571	0.597
	2	0.597	0.541	0.546	0.543	0.571	0.595
	3	0.592	0.541	0.546	0.543	0.571	0.597
	Average	<i>0.595</i>	<i>0.541</i>	<i>0.546</i>	<i>0.543</i>	<i>0.571</i>	<i>0.596</i>
E	1	0.595	0.577	0.546	0.554	0.589	0.574
	2	0.597	0.574	0.546	0.554	0.589	0.577
	3	0.595	0.574	0.546	0.554	0.589	0.574
	Average	<i>0.595</i>	<i>0.575</i>	<i>0.546</i>	<i>0.554</i>	<i>0.589</i>	<i>0.575</i>
	Tube Average	0.593	0.545	0.544	0.542	0.582	0.587
<p>Hrs. Operation: 6240 end of test 25.4 mm = 1 inch Temperature: Date: 3/21/97 Recorded by: GAK</p>							

Project No. 43456-300

One Year CHX Life Test at the ECTC

MEASUREMENT: Teflon Thickness (Top - 45°), millimeters							
Tube Location	Measurement Number	TUBE NUMBER					
		1	2	3	4	5	6
A	1	0.569	0.605	0.510	0.530	0.620	0.528
	2	0.569	0.605	0.510	0.530	0.620	0.528
	3	0.569	0.605	0.510	0.530	0.620	0.528
	Average	<i>0.569</i>	<i>0.605</i>	<i>0.510</i>	<i>0.530</i>	<i>0.620</i>	<i>0.528</i>
B	1	0.541	0.597	0.518	0.528	0.610	0.505
	2	0.541	0.597	0.518	0.528	0.610	0.505
	3	0.543	0.597	0.518	0.525	0.610	0.502
	Average	<i>0.542</i>	<i>0.597</i>	<i>0.518</i>	<i>0.527</i>	<i>0.610</i>	<i>0.504</i>
C	1	0.548	0.584	0.518	0.513	0.589	0.507
	2	0.548	0.584	0.518	0.513	0.589	0.507
	3	0.548	0.584	0.520	0.513	0.589	0.507
	Average	<i>0.548</i>	<i>0.584</i>	<i>0.518</i>	<i>0.513</i>	<i>0.589</i>	<i>0.507</i>
D	1	0.571	0.600	0.513	0.515	0.592	0.507
	2	0.571	0.597	0.513	0.515	0.592	0.507
	3	0.571	0.597	0.513	0.513	0.592	0.507
	Average	<i>0.571</i>	<i>0.598</i>	<i>0.513</i>	<i>0.514</i>	<i>0.592</i>	<i>0.507</i>
E	1	0.554	0.610	0.500	0.536	0.602	0.502
	2	0.554	0.607	0.500	0.536	0.602	0.502
	3	0.554	0.607	0.502	0.536	0.602	0.502
	Average	<i>0.554</i>	<i>0.608</i>	<i>0.501</i>	<i>0.536</i>	<i>0.602</i>	<i>0.502</i>
	Tube Average	0.557	0.598	0.512	0.524	0.603	0.510
<p>Hrs. Operation: 6240 end of test 25.4 mm = 1 inch</p> <p>Temperature:</p> <p>Date: 3/21/97</p> <p>Recorded by: GAK</p>							

Appendix G: Graphical Data - Change in Teflon[®] Film Thickness as a Function of Time

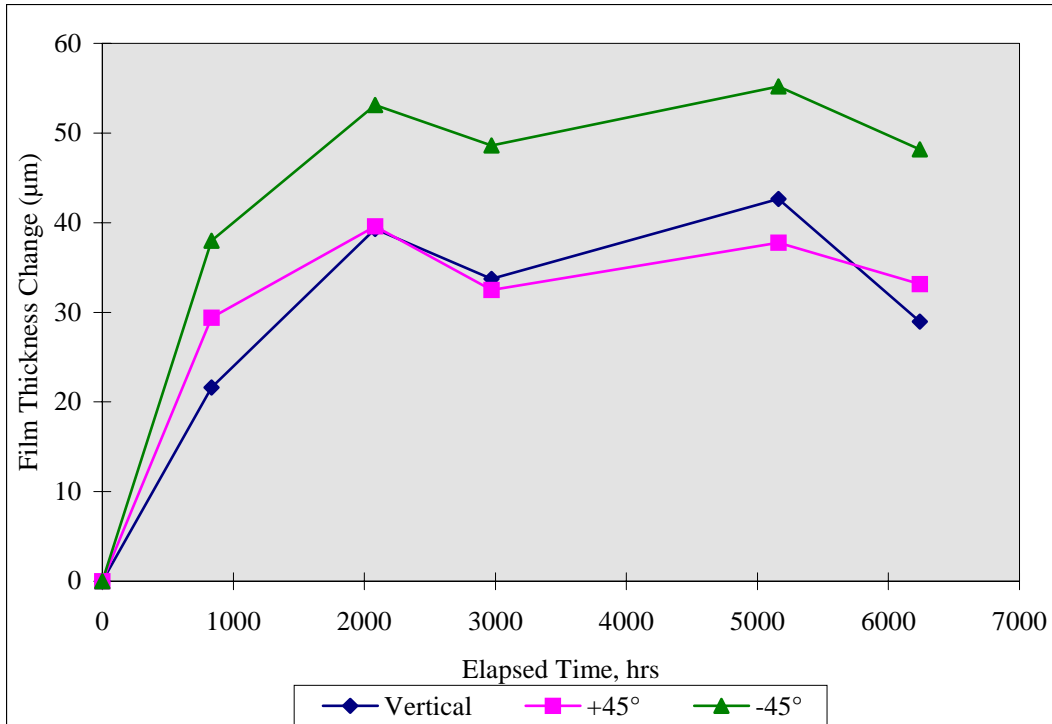


Figure G.1 Cumulative Change in Teflon® Film Thickness as a Function of Operating Time and Angular Position -- Tube 2

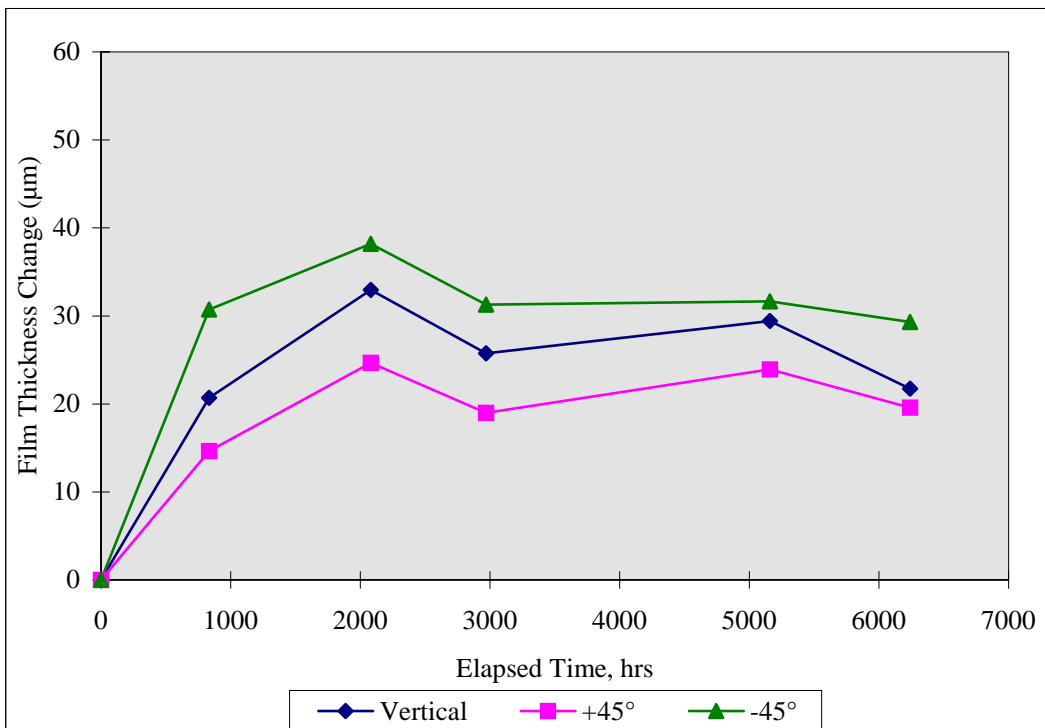


Figure G.2 Cumulative Change in Teflon® Film Thickness as a Function of Operating Time and Angular Position -- Tube 3

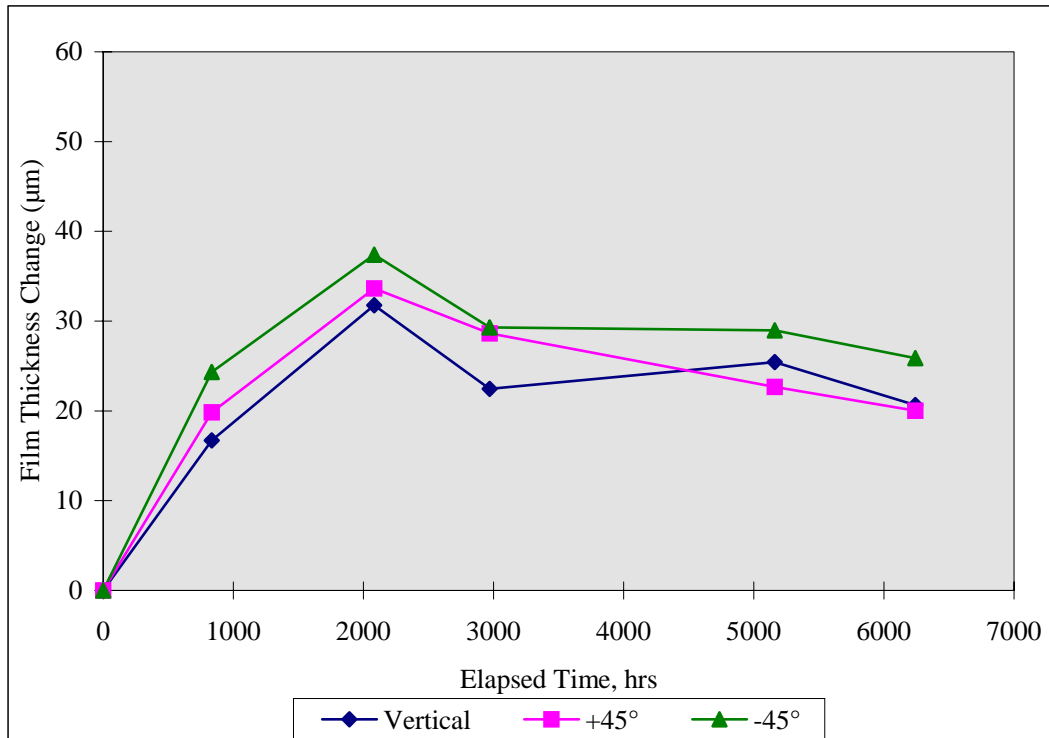


Figure G.3 Cumulative Change in Teflon® Film Thickness as a Function Of Operating Time and Angular Position -- Tube 4

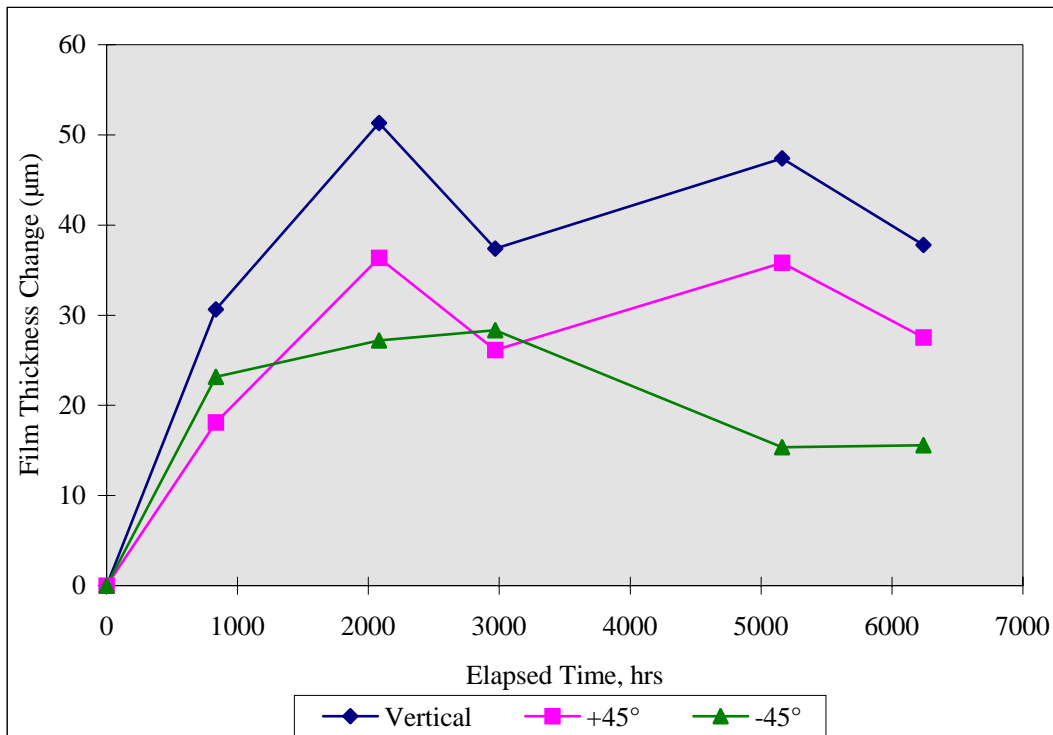


Figure G.4 Cumulative Change in Teflon® Film Thickness as a Function of Operating Time and Angular Position -- Tube 6